U.S. DEPARTMENT OF INTERIOR

U.S. GEOLOGICAL SURVEY

GEOLOGIC CONTROLS AND RESOURCE POTENTIAL OF NATURAL GAS IN DEEP SEDIMENTARY BASINS IN THE UNITED STATES

Edited by

T.S. Dyman[1]

Open-File Report 92-524

1. Denver, CO 80225

GEOLOGIC CONTROLS AND RESOURCE POTENTIAL OF NATURAL GAS IN DEEP SEDIMENTARY BASINS IN THE UNITED STATES

FINAL REPORT

(November 1, 1990 - May 1, 1992)

Prepared by

Thaddeus S. Dyman

U.S. Geological Survey

P.O. Box 25046, MS 934

Denver Federal Center

Denver, CO 80225

For

GAS RESEARCH INSTITUTE

Contract No. 5090-260-2040

GRI Project Manager

Paul A Westcott

Basic Research, Geosciences

May 1992

GRI DISCLAIMER

50272-101

REPORT DOCUMENTATION PAGE	1. REPORT NO. GRI- 92/0276	2.	3. Recipient's Accession No

4. Title and Subtitle
Geologic Controls and Resource Potential of Natural Gas in Deep Sedimentary Basins in the United States

5. Report Date
May 1992 Date of Issue

6.

7. Author(s)
Thaddeus S. Dyman

8. Performing Organization Rept. No

9. Performing Organization Name and Address
Branch of Petroleum Geology
U.S. Geological Survey
Box 25046, MS 934
Denver Federal Center
Denver, CO 80225

10. Project/Task/Work Unit No

11. Contract(C) or Grant(G) No.
(C) 5090-260-2040
(G)

12. Sponsoring Organization Name and Address
Gas Research Institute
8600 West Bryn Mawr Ave.
Chicago, Illinois 60631

13. Type of Report & Period Covered

14.

15. Supplementary Notes

16. Abstract (Limit: 200 words)

An empirical framework for predicting the porosity range of sandstones was developed. The presence of hydrocarbons (HC's) flattens the porosity-R_o curve and is the fundamental reason for porosity preservation at depth and an important factor in the presence of deep natural gas resources. Measurement of capillary pressure under confining stress suggests that constriction of pore throats is the controlling mechanism effecting fluid flow at reservoir conditions in the samples examined. Sequential northeastward partitioning of the Rocky Mountain foreland during Late Cretaceous may be critical to the entrapment of deep natural gas in that region. The presence of geochemically identified source beds of Middle Proterozoic age, active (HC) seeps, and favorable thermal maturities for generating and preserving natural gas, indicate a source rock potential adequate for economic gas accumulations in flanking basins of the Midcontinent Rift System. High-rank methane generation (from thermal decomposition of C_{15+} HC's) takes place at much higher maturation ranks than previously thought to be the case. Abundant non HC gases in carbonate reservoirs and the presence of H_2S indicates that thermochemical sulfate reduction and oxidation of HC's to CO_2 may be the dominant control on gas composition in these reservoirs. Review and analysis of resource appraisal methodologies and approaches has allowed tentative identification of methodologies for dealing with the more common types of deep gas occurrences.

17. Document Analysis a. Descriptors
Petroleum geology, natural gas, resources, gas reservoirs, tectonics, geochemistry

b. Identifiers/Open-Ended Terms
Earth sciences and natural resources - Geology and geophysics - Natural resources and energy - Fuels

c. COSATI Field/Group

18. Availability Statement	19. Security Class (This Report)	21. No. of Pages
Release unlimited	UNCLASSIFIED	296
	20. Security Class (This Page) UNCLASSIFIED	22. Price

RESEARCH SUMMARY

Title: Geologic controls and resource potential of natural gas in deep sedimentary basins in the United States.

Contractor: U.S. Geological Survey
GRI Contract Number 5090-260-2040

Principal Investigator: T.S. Dyman

Report Period: November 1, 1990 - May 1, 1992
Final Report

Objective: The purpose of the research is to determine the geologic factors that control deep gas accumulations in sedimentary basins as a means of locating exploration targets and to develop methodologies that improve the accuracy of assessing the resource potential of deep gas accumulations.

Technical Perspective: Deep sedimentary basins in the U.S. are known to contain large accumulations of natural gas but the distribution and character of potential deep gas accumulations needs to more accurately defined. In order to achieve this understanding, the geological and geochemical variables controlling deep gas accumulations are defined and quantified, and methodologies by which accumulations can be assessed are evaluated. Deep natural gas accumulations are defined arbitrarily for this report as those occuring below 4,270 m (14,000 ft).

Results: An empirical framework for predicting the porosity range of sandstones in Rocky Mountain basins was developed and broadly applied to deeply buried sandstone in general. The presence of hydrocarbons (HC's) flattens the porosity-R_o curve and is the fundamental reason for porosity preservation at depth and an important factor in the presence of deep natural gas resources.

For Ro >1.1%, the rate of porosity decrease as thermal maturity increases for Anadarko basin non-reservoir sandstones is less rapid than that of sandstones in general. Similar slopes of the porosity trends of reservoir and non-reservoir sandstones suggest that sandstones of the central and southern Anadarko basin may retain sufficient porosity for economic accumulations of HC's, even at high thermal maturities.

Small pore throats (<0.1um), common in fine to very fine grained clastic rocks, are very sensitive to confining stress, and probably act as limiting factors controlling the flow of gas to the well bore. Small pore throats are also very sensative to the presence of formation fluids, which reduce their effective diameter. Measurement of capillary pressure under confining stress suggests that constriction of pore throats is the controlling mechanism effecting fluid flow at reservoir conditions in the samples examined.

Three hundred sixty three significant reservoirs (reservoirs with cumulative production greater than 6 Bcf of gas) in the U.S. produce from depths greater than 4,270 m (14,000 ft). Most deep significant reservoirs (249) are classified as gas producers (66%). Of the total cumulative natural gas production in the U.S. (698 Tcf, 1989), deep reservoirs account for 8% (50 Tcf) of the total, and significant deep reservoirs account for nearly half (21.5 Tcf) of the deep reservoir total.

In the Rocky Mountain region, structural partitioning prior to thrusting in selected basins, and sequential northeastward partitioning of the Rocky Mountain foreland during Late Cretaceous may be critical to the entrapment of natural gas. Undiscovered structurally-trapped deep gas may still be found in parts of the Wind River and Hanna basins.

The presence of Middle Proterozoic source rocks, active HC seeps, and favorable thermal maturities for generating and preserving natural gas, indicate a potential for economic gas accumulations in flanking basins of the Midcontinent Rift System and in the Grand Canyon region.

High-rank methane generation (from thermal decomposition of C_{15+} HC's) takes place at higher maturation ranks than previously thought.

The occurrence of significant non-HC gases in deep carbonate reservoirs and the presence of H_2S indicates that thermochemical sulfate reduction and simultaneous oxidation of HC's to CO_2 may be the dominant control on non-HC gas composition in these reservoirs. Giant quartz-vein systems in convergent, transpressive plate margin basins may be associated with major gas accumulations as in the deep Anadarko and Arkoma basins.

Where sufficient information is available concerning the geologic characteristics of known or suspected deposits of deep gas, a deposit simulation based on a geologic model of reservoir volumes is the most appropriate assessment methodology. This method is based on measurement of known or estimated physical properties of traps, reservoir rocks and fluids, and the host environment in terms of temperatures, pressures and fluid dynamics.

Technical Approach:

Data for significant reservoirs were retrieved from the NRG-Associates Significant Field File of field and reservoir data. Topical and areal research studies were carried out on the geochemistry of source rocks, diagenesis of deep reservoirs, and structural geology of deep natural gas traps. An analysis of the geological factors controlling the origin and distribution of deep natural gas accumulations was conducted in order to evaluate appropriate methodologies used to assess this resource.

Project Implications: This report concludes an avenue of research initiated by GRI four years ago. Funding and a portion of the original objectives are being abandoned at the stage of development presented in this report. Since starting this research, GRI has gained the perception that high accuracy resource assessments only occur in hindsight. Some quantitative arguments are presented in this report that show why reserve potential estimates must range through orders of magnitude until real data from drilling and production are available. Consistent with this view, the new knowledge and quantitative tools gained through this research are expected to have greater application for exploration and production purposes than for improving total gas-in-place assessment predictions. The multiple avenues of research conducted at the U.S. Geological Survey include: porosity prediction, time/ temperature and pressure effects on maturation, and some preliminary evaluations of good prospects for deep gas plays within the U.S.

TABLE OF CONTENTS

INTRODUCTION

Objective

The purpose of the research is to determine the geologic factors that control deep natural gas accumulations in sedimentary basins as a means of locating exploration targets and to develop methodologies that improve the accuracy of assessing the resource potential of deep gas accumulations. The ongoing work is subdivided into eight tasks. The first seven are related to understanding the geologic factors controlling deep gas. The eighth task is related to developing methodologies to assess resource potential of deep gas accumulations.

Project Description

The basic tasks to be performed were to:

(1) Develop and quantify rules-of-thumb for estimating the distribution of porosity in sedimentary rocks as a function of time-temperature exposure, and extrapolate these findings as predictive equations for deep portions of sedimentary basins.

(2) Determine pore-throat entry size, as well as porosity and permeability, and capillary pressure response, under ambient and in situ conditions in order to better understand the behavior of deep clastic reservoirs, and determine generalized petrophysical properties of deep reservoirs.

(3) Analyze the relation between geologic characteristics and drilling and production data for deep wells and reservoirs in order to (a) describe success of deep drilling, and (b) identify conditions favorable for deep gas accumulations and production.

(4) Determine the structural setting and trapping mechanisms of deep gas accumulations in different types of sedimentary basins in order to relate the structural setting and trapping mechanisms to modern tectonic concepts and styles.

(5) Determine the source-rock potential of Precambrian sedimentary rocks which floor many deep basins. Precambrian outcrop and well samples from the Midcontinent Rift System, the Grand Canyon, and the Uinta Mountains will be collected, and analyzed to determine amounts, type, and thermal maturity of organic matter.

(6) Describe the thermal destruction of C_{15+} HC's by conversion to high-rank methane, and investigate the loss of HC-generating potential with increasing thermal maturity for different types of organic matter.

(7) Investigate the occurrence, geologic setting, and geochemical controls of non-HC gases, such as carbon dioxide, hydrogen sulfide, and nitrogen, which can dilute and destroy deep natural gas accumulations.

(8) Develop quantitative methods and assessment models for resource estimation of deep gas accumulations based on geologic models of occurrence. Assessment methodology development and testing will be based on stochastic, probabilistic, and statistical approaches using geologic information developed by tasks 1-7 of this project.

Rationale for undertaking project

This project evolved as an outgrowth of work in part funded by Gas Research Institute (contract 5087-260-1607) entitled "Distribution of Natural Gas and Reservoir Properties in the Continental Crust of the U.S" (Rice, 1989). During this work, problem areas were identified that were not addressed by the initial research including (1) identifying geologic characteristics responsible for the distribution of natural gas in deep basins, (2) compiling geologic and production data summaries for large, significant reservoirs in the U.S., (3) analyzing and interpreting well data (including location, identification, test, and production data) in order to define the spatial distribution of deep drilling and the distribution of pressure data from deep wells, (4) identifying the geochemical controls and geologic setting of non-HC gases, (5) defining the occurrence and controls of unusually high porosity in deeply buried clastic and carbonate rocks, and (6) conducting laboratory simulation experiments from deeply-buried source rocks to define the range of generating potential of kerogen at high levels of maturation.

The problem of assessing volumes of natural gas in deep sedimentary basins was considered as the next phase of work after the geologic parameters controlling the distribution of gas were defined and analyzed. Assessment here is based on natural gas "plays" that define unique geologic characteristics and often are basin-wide as compared to "prospects" which are identified for exploration. Assessment methodologies are evaluated, assessments are presented for hypothetical plays, and geologic parameters are modelled in order to show the range of results under different conditions.

Acknowledgements

We wish to acknowledge the careful and critical reviews of this manuscript by Paul A. Westcott, Gas Research Institute, and Dudley D. Rice, Mahlon M. Ball, Jerry L. Clayton, and Michael D. Lewan, U.S. Geological Survey.

Ronald R. Charpentier retrieved reservoir data from the NRG Associates file of all fields having both pressure data and a depth to the top of the reservoir of 4,270 m (14,000 ft) or deeper.

RESULTS

Major results of contract work are subdivided into (1) identification and explanation of major deep natural gas resources based on comprehensive retrievals of published well and reservoir data bases, (2) a detailed discussion of the major geologic controls affecting the distribution of natural gas in deep sedimentary basins, and (3) an evaluation of resource assessment methodologies which can be used to assess deep natural gas resources. The following discussion of results is based on detailed discussions of Task results (Tasks 1 through 8) in Appendices 1 through 8 of this report.

Identification of known resources--significant reservoirs

Deep natural gas resources are distributed throughout many U.S. basins and occur in widely different geologic environments. Three hundred seventy eight significant reservoirs (reservoirs with total cumulative production

greater than 1 million barrels of equivalent--BOE or 6 Bcf) in the U.S. produce from depths greater than 4,270 m (14,000 ft) according to NRG Associates (1988). Of these 378, 256 produce from depths greater than 4,572 m (15,000 ft). These reservoirs occur primarily in the Gulf Coast, Permian, Anadarko, Williston, and Rocky Mountain basins (Fig. 1). Table 1 contains a brief summary of the main geologic and production characteristics of these regions. Appendix 3a contains tables of geologic and production data and a list of the geologic factors controlling deep natural gas production derived from the NRG Associates field file, Petroleum Information Corporation's Well History Control System (Petroleum Information Corporation, 1988, 1991), and the published literature. Other U.S. sedimentary basins contain additional deep gas reservoirs below 4,270 m (14,000 ft), but these reservoirs do not meet the minimum qualifications for entry into the NRG Associates data base.

According to Dwight's Energy Data (1985) 1,998 total reservoirs occurred below 4,572 m (15,000 ft) in the U.S. at the end of 1985. Of the total cumulative natural gas production in the U.S. (698 Tcf; Mast and others, 1989), deep reservoirs account for 8% (50 Tcf) of the total, and significant deep reservoirs (NRG reservoirs) account for nearly half (21.5 Tcf; Fig. 3) of the deep reservoir total (Dyman and others, 1989). When the Nation is taken as a whole, deep gas reservoirs account for only a small portion of the total production. The percentage rises when recent production is considered, but the total cumulative production is still low. Based on work presented in this report and previous work by Rice and others (1989), additional significant quantities of deep natural gas remain to be found in U.S. sedimentary basins. One goal of this contract is to identify geologic conditions which may help to identify these resources.

Deep reservoirs are defined arbitrarily as those occurring below 4,572 m (15,000 ft). However, a single producing horizon may extend both above and below 4,572 m (15,000 ft). For this reason, NRG retrievals were selected for all reservoirs below 4,270 m (14,000 ft) in order to capture all reservoirs occurring at approximately 4,572 m (15,000) ft depth.

Most deep significant reservoirs (249) are classified as gas producers (66%). An additional 25 reservoirs are classified as oil and gas producers. Sixty eight percent of the reservoirs are classified as structural or combination (combined structural and stratigraphic) traps. Fifty percent of these reservoirs (188 reservoirs) produce from Mesozoic or younger rocks, and 58% (221 reservoirs) produce from clastic rocks of any age. As expected, the number of reservoirs decreases with increasing depth, but more than one quarter (26%) of the total significant deep reservoirs occur below 5,180 m (17,000 ft).

Of the 378 deep reservoirs, 174 (or 46%) occur in the Gulf Coast basin. More than 6 Tcf of natural gas have been produced from significant reservoirs in the Gulf Coast basin. Reservoirs occur primarily in Tertiary clastic rocks and deeper mixed carbonate-clastic rocks of Mesozoic age. Forty percent of the known recoverable natural gas resources (13.7 Tcf; Table 1; Fig. 3) in deep significant (NRG) reservoirs occurs in the Gulf Coast basin.

The Permian basin contains 24% of the deep reservoirs (89 of 378) in the U.S. with more than 12.4 Tcf of natural gas produced. Reservoirs occur in Silurian and Devonian carbonate rocks. Seventy five percent of the Permian basin reservoirs are developed in Devonian or older rocks. Forty five percent of the known recoverable natural gas resources (15.1 Tcf; Table 1; Fig. 3) in the U.S. occurs in the Permian basin.

The Anadarko basin contains 22% of the deep reservoirs (85 of 378) in the U.S. with 2.4 Tcf of natural gas produced (Table 1; Fig. 3). Deep reservoirs in the Anadarko basin are primarily clastic (65% of the total reservoirs in the basin) with subordinate production from Cambrian through Silurian carbonate rocks.

Rocky Mountain basins are grouped together because of their similar origin and geographic distribution (Table 1; Fig. 3). These basins have produced 0.4 Tcf of gas from Jurassic and Cretaceous clastic reservoirs and Paleozoic mixed clastic-carbonate reservoirs. Variations in the thermal histories and the Late Cretaceous through Tertiary deformational sequence resulting in basin evolution (Appendices 3 and 4) control the distribution of and tendency toward natural gas or oil in the basins.

The above 4 regions account for 355 of the 378 significant reservoirs. Only two deep significant reservoirs occur in California in the Ventura and San Joachin basins; they produce primarily oil from Tertiary clastic rocks. Only one reservoir occurs in Alaska in the Cook Inlet area; it produces primarily gas from Tertiary clastic rocks at approximately 4,510 m (14,800 ft). Five deep significant reservoirs occur in the Williston basin. They produce oil and gas from the Ordovician Red River Formation.

Large volumes of deeply buried sedimentary rocks occur in other basins in the U.S. where no significant gas production now exists. Recent work by Palacas (Appendix 5) indicates that portions of the Midcontinent rift system may contain source rocks capable of generating natural gas below 4,572 m (15,000 ft). Other deep Rocky Mountain basins (Fig. 1) including the Raton, Albuquerque, and Crazy Mountains basins have been sparsely drilled and the recoverable natural gas resource is unknown. Furthermore, drilling data analyzed by Wandrey and Vaughan (Plates 1 through 9) show that many deeper parts of productive basins have not been adequately drilled even where source- and reservoir-rock conditions are appropriate. For the last U.S. Geological Survey national petroleum assessment, 59 of approximately 250 petroleum plays assessed contained reservoir rocks at least in part buried below 4,572 m (15,000 ft) (Mast and others, 1989).

Identification of known significant deep natural gas resources--deep well distribution

A series of maps showing wells drilled deeper than 4,572 m (15,000 ft) was created using Petroleum Information Corporation's Well History Control System (WHCS) current to December 1991 (Petroleum Information Corporation, 1991). These maps can be used in conjunction with discussions in this report to identify the distribution of deep wells in the U.S. See Appendix 3c, for detailed discussion of work of Wandrey and Vaughan.

Four maps showing non-producing wells grouped by the age of the oldest rocks penetrated (Plates 1-4). Non-producing means that HC's could not be economically recovered at the time drilling was completed. Shows of oil and/or gas may have been recorded but were insufficient to warrant production, or completion problems may have precluded production. Four additional maps show wells that have produced HC's grouped by the age of the producing rocks (Plates 5-9).

Of the 6,178 wells that produce or have produced HC's from depths greater than 4,572 m (15,000 ft), 4,547 are gas or gas and condensate wells. Only two areas contain significant numbers of deep oil wells (Uinta and Gulf Coast basins); wells are producing from relatively young rocks. It is likely that

source rocks, which are still producing oil at these depths, have been buried deeply for only a short period of time.

Geologic controls affecting the distribution of natural gas in deep basins:

Task 1a. Distribution of porosity in sedimentary rocks as a function of time-temperature exposure--Rocky Mountain basins

One of the factors that has limited deep drilling for sandstone reservoirs is the knowledge that porosity and permeability can be too low to sustain economic HC production. Better predictive relationships for determining the porosity and porosity range of sandstones are presented by J.W. Schmoker (Appendix 1a) for risk evaluation and reduction in deep-drilling programs based on an empirical approach to porosity trends as related to thermal maturity.

Porosity trends are developed as functions of thermal maturity, as represented by vitrinite reflectance (R_o). In this context, R_o serves as a generalized index of burial history. The porosity range at a given level of thermal maturity is predicted also, and is investigated as a function of rock properties such as clay content, carbonate cementation, grain size, and HC generation. Examples are drawn from Cretaceous sandstones of the Rocky Mountain region, with emphasis on the Lower Cretaceous J sandstone (Muddy Sandstone) of the Denver basin, Colorado and Upper Cretaceous sandstones of the Mesaverde Group of the Piceance and Uinta basins, Colorado and Utah. Figure 1-11 (Appendix 1a, Schmoker) illustrates the range of depths encountered for a particular thermal maturity value based on the data from this study.

The range of porosity at a given level of thermal maturity is not obscured by averaging but is depicted by porosity-R_o trends representing the 10th, 25th, 50th, 75th, and 90th porosity percentiles. Effects upon porosity of variations in rock properties are thus taken into account.

An empirical approach for estimating the porosity and the porosity range of Cretaceous sandstones in Rocky Mountain basins is shown (Figs. 1-18A and 1-18B, Appendix 1a) where the predictive porosity framework is composed of two elements (or models A and B), in an effort to represent the porosity-R_o data better than regression lines fit to the entire R_o range. For R_o less than 0.9%, trend lines of A and B are identical and represent all data. Model A applies to strata in which porosity continues to decrease at a uniform rate as R_o increases above 0.9%. Model B applies to strata in which the rate of porosity loss becomes more gradual as R_o increases above 0.9%. Models A and B do not directly reflect variability in rock properties such as grain size and sorting, shale content, and composition of framework grains. The effects upon porosity of these factors are already incorporated in the porosity range defined by the 10th through 90th porosity percentiles. Rather, models A and B are interpreted as representing sandstones in which porosity evolution follows one of two fundamentally different pathways. Models A and B are derived from observation of porosity-R_o crossplot patterns and represent a working hypothesis that, because of a paucity of data, is at present supported only by circumstantial evidence.

The line segments of Figure 1-18B change slope as R_o increases. Such porosity models implicitly assume that the net effect upon porosity of various diagenetic processes varies as different processes wax and wane during burial.

The choice of diagenetic pathway (model A versus model B) is important for sandstone porosity prediction in deep portions of Rocky Mountain basins. At R_o= 2.0%, for example, model A predicts median porosities of about 2% and 90th-percentile porosities of only 4%; in contrast, model B predicts median porosities of about 5% and 90th-percentile porosities of 8%. Extrapolating beyond the data to R_o=3.0%, model A predicts 10th- through 90th-percentile porosities to all be less than 3%, whereas model B predicts some porosities of 6-7%. Maximum depths of economic production predicted by model A in a given area of a basin would be thousands of feet less than those predicted by model B.

The particular strata of the data set which conform to model B are from the Almond Formation in the Green River basin and the Mesaverde Group (marine and nonmarine) in the Piceance basin. Low-permeability sandstones in both formations are commonly overpressured, at R_o greater than 0.9%, due to HC generation. It is thus possible that some Cretaceous sandstones of Rocky Mountain basins do not follow "normal" diagenetic pathways (Fig. 1-18A) because of the effects upon diagenesis of HC generation from adjacent and intercalated coals and organic-rich shales.

As is apparent from the porosity comparisons, the hypothesis that porosity evolution can follow distinctly different pathways as R_o increases above 0.9% has significant implications for the economic production of deeply buried HC's. An understanding as to which sandstones follow models analogous to A and which follow models analogous to B is important. However, such understanding is uncertain, and a discussion of cause and effect is speculative.

Hydrocarbon generation in overpressured non-subsiding basins of the Rocky Mountain region has the potential to retard porosity loss as R_o increases in at least three ways: (1) HC's can inhibit cementation by displacing pore water, (2) carbon dioxide and organic acids produced by the thermal breakdown of kerogen can create secondary porosity by dissolving cements and framework grains, and (3) overpressuring can slow pressure solution and associated porosity decrease by reducing the lithostatic load on grain contacts. Overpressuring can also reduce cementation by developing a fluid-flow system characterized by expulsion, rather than exchange, of liquids. Although the relative importance of these three reasons is difficult to define, the presence of HC's flattens the porosity-R_o curve and is the fundamental reason for porosity preservation at depth and an important factor in the presence of deep natural gas resources.

If HC generation is indeed the primary underlying process causing some sandstones to deviate from porosity-R_o trends similar to those of Figure 1-18A and follow instead trends similar to those of Figure 1-18B, then the results and discussion of this section are not restricted to Rocky Mountain Cretaceous sandstones but are applicable to other deep sedimentary basins in the U.S.

Task 1b. Distribution of porosity in sandstones as a function of time-temperature exposure--Anadarko basin

The goal of Task 1b (see T.C. Hester, Appendix 1b) was to characterize Anadarko basin sandstone-porosity trends with respect to thermal maturity in order to predict locations for new future reservoirs based on porosity prediction models. Three R_o data sets were compiled-- two data sets representing Anadarko basin reservoir and non reservoir sandstones, and one composite data set from many basins (excluding the Anadarko basin) representing sandstones in general. The first data set provides a porosity-Ro trend typical of Anadarko basin HC-bearing sandstone reservoirs. Non-reservoir sandstones in the second data set are defined as those typical of the Anadarko basin and may be reservoir sandstones at other locations. Non-reservoir sandstones provide a background by which to compare other sandstones. The third data set represents a sample of sandstones of diverse ages, diagenetic facies, and thermal histories exclusive of the Anadarko basin.

Non-reservoir sandstones

A least-squares fit to the porosity-R_o data for non-reservoir sandstones of the central and southern Anadarko basin shows that sandstone porosity generally declines with increasing thermal maturity. However, the data appear to consist of two separate populations--a less thermally mature population represented by R_o <1.1% and a more thermally mature population represented by R_o >1.1%. Correlation coefficients of the least-squares fit to each population shows a much stronger dependence of porosity on R_o for the less mature trend of non-reservoir sandstones than for these sandstones taken as a whole. The improved correlation of the less mature trend over that of the data set taken as a whole suggests that the two data populations might best be considered as separate trends. The two trends probably overlap to some extent as the more mature diverges from the less mature. Nevertheless, for the purposes of this report, a single preliminary boundary separating the two trends is placed at about R_o =1.1%. Additional porosity data might show the rapid porosity loss of the less mature trend continuing beyond R_o=1.1%. Ro of 1.1% approximately corresponds to a depth of 3,444 m (11,300 ft) based on an R_o-depth curve for measurements from wells throughout the Anadarko basin within Pennsylvanian rocks (T.C. Hester, unpublished data).

In both populations, porosity generally declines as a power function of increasing thermal maturity. The least-squares fit to the data show that for R_o <1.1%, the rate of porosity decrease with increasing R_o for non-reservoir sandstones is more rapid than that of the average trend of the porosity-R_o framework representing sandstones in general. For R_o >1.1%, the rate of porosity decrease for non-reservoir sandstones is less rapid than that of sandstones in general.

Sufficient data to substantiate a probable cause for the change of slope of the porosity trend of Anadarko basin non-reservoir sandstones are not yet available. However, the two populations of non-reservoir sandstone-porosity data (apparent in Fig. 1-21, Appendix 1b) may represent sandstones from different geographic areas, depositional environments, or subsurface pressure regimes, or sandstones with different burial or cementation histories. Identification and stratigraphic correlation of the non-reservoir sandstones, with the addition of petrographic information, are suggested here as a first approach to examining the nature of the two populations of Anadarko basin non-reservoir sandstones.

Reservoir sandstones

The porosity-R_o trend of Anadarko basin HC-reservoir sandstones follows a different pattern. Their least-squares fit shows that the rate of porosity loss for reservoir sandstones is much slower than that of both non-reservoir sandstones of the central and southern Anadarko basin, and sandstones in general (Fig. 1-22, Appendix 1b). This relatively slow rate of porosity decline with increasing R_o could be due to geologic factors such as overpressuring or the inhibiting effects of early HC emplacement on sandstone diagenesis, and/or to economic factors such as the bias inherent in the selection of sandstone HC reservoirs.

As R_o increases from low levels to about 1.1%, the porosity trends of Anadarko basin reservoir and non-reservoir sandstones cross. Thus, as thermal maturity increases, the porosity of reservoir sandstones becomes increasingly restricted to the upper range of porosity percentiles of non-reservoir sandstones. If these trends were to continue diverging, porosity sufficient for commercial sandstone HC reservoirs would become extremely rare at only moderate levels of thermal maturity. At about R_o =1.1%, however, the slope of the porosity trend for Anadarko basin non-reservoir sandstones levels off. The average porosity of Anadarko basin reservoir sandstones then remains within about the upper 10% of the porosity range of non-reservoir sandstones. As thermal maturity levels increase above about 1.1% R_o, the similar slopes of the porosity trends of reservoir and non-reservoir sandstones suggest that sandstones of the central and southern Anadarko basin may retain sufficient porosity for economic accumulations of HC's, even at high thermal maturities.

Task 2. Pore throats, capillary pressures, porosity, and permeability of clastic reservoirs in the Uinta, Wind River, and Anadarko basins

The primary goal of Task 2 was to document the effects of confining stress on pore geometry, as well as on porosity and permeability in clastic reservoirs at various depths (C.W. Keighin, Appendix 2). We wish to understand pore structures and how these structures are generated and modified with depth and burial history. Almost no data are available documenting the effects of confining stress on pore-throat size distribution based on mercury injection/capillary pressure when the sample is under confining stress. Nineteen samples from three basins (Uinta, Wind River, and Anadarko basins; Fig. 1), from different depths, and with different diagenetic histories, were examined. The samples vary primarily in the relative abundance of quartz, feldspar, and rock fragments; carbonate cements are locally abundant.

Porosity and permeability of these samples show a wide range of values, although porosity is typically less than 8% and Klinkenberg permeability below 0.1md for all samples examined. Cross plots of these data indicate a generally close correlation between porosity and permeability. As expected, there is a general decrease in porosity and permeability with depth, but depth is not the only factor affecting the decrease of both. Nor is the decrease in porosity with depth uniform. Examination of thin sections indicates that while compaction due to increasing depth of burial appears to be a factor, the degree of compaction is greatly influenced by lithology, especially the presence and quantity of labile rock fragments. Cementation, either by silica or carbonate minerals, acts to reduce both porosity and permeability, as well as significantly modifying pore structure.

The relative abundance of rock fragments may have a significant effect on both macro and micro porosity, both macro and micro, and permeability. Compression of labile rock fragments reduces intergranular porosity and

creates intergranular pseudomatrix porosity; both reduce effective permeability. Partial dissolution of rock fragments commonly creates microporosity; micropores introduce micro-pore-throats which restrict fluid migration.

Data show that confining stress has a varying effect on permeability. Relationships between capillary pressure and wetting phase saturation (i.e., air), and pore-size distribution for a range of porosity and permeability values suggest that some samples are very porous and have large visible pores. Plots of pore size frequency versus pore entry/throat diameter, however, reveal that pore throats in these samples are most frequently in the 10um range, significantly smaller than the pores visible in thin section. The plots also show that pore throats are constricted by increased confining stress, although not as dramatically as in samples with lower initial porosity and permeability, and smaller measured pore throats. Data indicate that for samples more typically fitting the "tight" sand designation, pore throats are more typically in the <0.1um size range, and that these already small pores are further reduced by confining stress. Thus, even though pores visible in thin section may be relatively large, all pores must be accessed through pore throats, which are smaller - often much smaller - than the pores. The data also suggest that pore throats, rather than stress-relief micro fractures, are indeed being closed with increasing confining stress for the samples studied.

As more data become available, contoured maps quantifying the pore-throat character and resulting variations in permeability could be used to define "sweet spots" targeting exploration strategies.

Task 3. Summary of deep natural gas reservoir pressures and initial-potential test data in U.S.

A study of available deep (4,572 m-->15,000 ft) reservoir pressures was conducted as a part of Task 3 (C.W. Spencer and C.J. Wandrey, Appendix 3b) because: (1) abnormally high pore pressure may reduce the rate of porosity and permeability loss with increasing burial depth, and (2) gas reservoirs with high pore pressure will have more gas-in-place than low-pressure reservoirs at the same temperature and porosity owing to the high compressibility of natural gas. An important aspect of this work was to define the aerial distribution of major pressure regimes from computer data files and to summarize reasons for overpressuring in different regions.

Pressure data for this study were obtained from two sources: (1) the drillstem test (DST) reports in Petroleum Information's Well History Control System and (2) reservoir-pressure data compiled in the NRG Associates Significant Oil and Gas Fields of the U.S. file (NRG Associates, 1991). The NRG file is updated to July 1991 and contains data on about 10,000 fields of which about 250 are deeper than 4,270 m (14,000 ft) and have some form of reservoir pressure data recorded.

Shallow (2,440 m--<8,000 ft) reservoirs are usually normally pressured or underpressured, whereas deep (4,572 m-->15,000 ft) hot reservoirs may have normal to above normal pressures. In order to determine the general distribution of abnormally high pressures and predict their distribution in undrilled areas, it is helpful to consider possible causes of high pore pressure and the distribution of pressure regimes in the geologic environment based on available data.

There is no single cause that can adequately explain **all** occurrences of above normal pressures. However, most proposed mechanisms require that semi-isolated or fairly well sealed reservoirs be present in order to maintain abnormal pressure. Some of the more commonly accepted causes of overpressuring are dewatering of shales owing to compaction, clay mineral transformations that release water, active hydrocarbon generation, and aquathermal pressuring caused by thermal expansion of water.

Normal pressures range from 0.43 to 0.465 psi/ft depending on reservoir salinity and other factors. Overpressured deep "significant" gas reservoirs are present in the Rocky Mountain region in the Wind River and Greater Green River basins (Fig. 2). This region also contains overpressured shallower reservoirs in the depth range from 3,200 m (10,500 ft) to more than 3,960 m (13,000 ft). Most of the overpressured gas-bearing rocks are of Tertiary and Cretaceous age and the overpressuring is caused by active HC generation.

The Anadarko basin contains overpressured Permian, Pennsylvanian, Mississippian-Devonian, and Ordovician sandstones, carbonates, and shales in the deep parts of the basin. This overpressuring may be related to HC generation.

The Permian basin has overpressuring in about 35% of the >4,270 m-deep (>14,000 ft-deep_ significant reservoirs in the NRG Associates Significant Field File. Most of the overpressuring occurs in rocks of Wolfcampian, Morrowan, Atokan, and Mississippian age. Dominant reservoir lithologies are sandstone, limestone, and dolostone. Minor overpressuring occurs in Devonian limestone. The origin of this overpressuring is not well defined at the present time but may be caused by the thermal conversion of previously migrated oil to gas plus some active generation of gas from deep basin source beds.

The Gulf Coast region has extensive overpressured reservoirs. The overpressuring in younger Miocene and Oligocene sandstones and shales is part caused by undercompaction. Overpressuring in Cretaceous and Jurassic sandstones and carbonates in the eastern Gulf may be caused by several mechanisms, and more study needs to be done to allow better prediction of the overpressuring because its distribution is highly variable.

An additional study was made of the initial potential tests (IP's) of all wells completed in the U.S. at depths greater 4,572 m (15,000 ft) using Petroleum Information Corporation's Well History Control System (WHCS). Preliminary plots of initial-potential gas versus depth do not identify specific trends and several factors may be responsible for the distribution of these data (Figs. 3-2A through 3-2H, Appendix 3b). Deep wells tend to have lower matrix permeabilities and the degree and openness of natural fractures is a controlling factor influencing individual well productivity. Second, many of the wells were artificially stimulated with acid and/or hydraulic fracturing. It is well known that the success of these techniques varies considerably throughout the U.S. Through time, completion techniques can improve in a given basin, and in some basins, rocks of similar ages and lithologies dominate the data set, whereas in other areas, diverse ages and lithologies are combined in a single plot.

The Uinta basin shows a wide range of IP values at all depths but none of the wells are very high volume (maximum IP equals about 2.75 million cubic ft/day at about 16,000 ft--4,870 m). A nearly random scatter occurs but the majority of data points are less than 1 MMcf. These reservoirs are dominantly sandstone and are Early Tertiary in age. Natural fractures are causing the

variability of these low permeability reservoirs (Spencer, 1989). Wind River basin deep IP tests are all from Cretaceous sandstones except for IP's at about 7,310 m (24,000 ft) which represent completions in Mississippian dolomite; they are high CO_2 gas. The Anadarko basin shows a wide range in variability of IP results. Data show some very high volume wells (above 200 MMcf) but most are in the less than 5 MMcf range.

Task 4. Deep gas-prone basins of the Rocky Mountain region

The purpose of Task 4 (W.J. Perry, Jr., Appendix 4) was to identify the structural setting and trapping mechanisms of deep gas accumulations in different sedimentary basins in the Rocky Mountain region in order to relate these factors to undiscovered natural gas resources. Selected deep basins were studied in detail and used as models from which to compare the structural characteristics of other deep basins. Also, the timing and structural style of Rocky Mountain basins was studied in order to determine the evolution of deformation and subsequent entrapment of gas.

Several sedimentary basins in the central Rocky Mountains have substantial volumes of sedimentary rock at depths greater than 4,572 m (15,000 ft); the largest being the Green River and Uinta basins, respectively north and south of the Uinta uplift (Figs 1 and 2). These basins initially developed during Cretaceous time as foredeeps in front of the eastward prograding Wyoming and Utah salients of the Cordilleran thrust belt. A southeastward progression of major uplift and consequent basin development in the Rocky Mountain foreland began in extreme southwestern Montana during Cenomanian-Turonian time (Fig. 2).

The Late Cretaceous eastward progradation of the Laramide deformation front reached the Colorado Front Range (central Colorado, Fig. 2) by 69 Ma. In support of this contention, no evidence of Campanian or older Cretaceous Laramide-style deformation is present in the Rocky Mountain foreland east or southeast of the Blacktail-Snowcrest and Wind River uplifts (Fig. 4-1), based on available palynostratigraphic dating of preorogenic and synorogenic sediments. Such dating reveals that growth of the Front Range uplift culminated in exposure of the crystalline basement by early Paleocene time. Subsequent Laramide deformation spread northeastward from the Granite Mountains-Shirley Mountains uplift in south-central Wyoming; the Laramide deformation front reachied the Black Hills by late Paleocene time, creating first, the Wind River and then the Powder River basins, partitioning these basins from an earlier continuous foreland basin with minor welts. These broad structural welts of low relief, such as the San Rafael swell in eastern Utah, had begun to grow in the Rocky Mountain foreland by mid-Cretaceous time.

South of the major east-west crustal discontinuity along the Wyoming-Colorado border, which separates Archean basement rocks on the north from Proterozoic basement rocks to the south, Laramide deformation proceeded from east to west, culminating along and defining the eastern boundary of the Colorado Plateau in late Eocene, chiefly Green River time.

Economic implications of this new model of deformation of the Rocky Mountain foreland include progressive opening and subsequent blockage of migration paths for HC's generated from source rocks in southeastern Idaho, southwestern Montana, Wyoming, Colorado, and eastern Utah.

Hanna basin

The Hanna basin in southern Wyoming contains more than 9,140 m (30,000 ft) of Phanerozoic sedimentary rocks of which more than 4,572 m (15,000 ft) are Upper Cretaceous and predominantly marine. Latest Cretaceous (?) and Paleocene nonmarine rocks (the Ferris and Hanna Formations) are nearly 4,572 m (15,000 ft) thick. The nonmarine formations penetrated are gas-prone, and these shallow rocks are being exploited for coal-bed methane.

The sequence of structural events in the Hanna basin in southern Wyoming region are: **first,** development of the Hanna trough sequence of thick marine Upper Cretaceous rocks which trends east-west across southern Wyoming; **second,** isolation of the Hanna basin by early Paleocene growth of the Granite Mountains-Shirley Mountains transpressive zone to the north and Rawlins uplift to the west; **third,** southward tilting, probably in mid-Paleocene time concurrent with early growth of the Sweetwater uplift and then development of the Shirley thrust along the northern margin of the basin subsequent to Hanna deposition. The last phase of structural growth, uplift of the Medicine Bow Mountains concurrent with development of the Arlington thrust, appears to have been initiated in late Paleocene time. The geometry suggests major gas possibilities in the undrilled northern part of the basin beneath the Shirley thrust provided that gas generation continued during and after thrusting.

It would appear that much deep gas remains to be found in deep Rocky Mountain foreland basins if the scenario shown in the Hanna basin is found to be correct and this type of tilting prior to thrusting can be demonstrated in other areas. Because of the high vitrinite reflectance values at depths of greater than 3,050 m (10,000 ft), discussed above, the deeper Cretaceous units should also yield natural gas. However, only one small gas field has been developed -- on the northwest flank of the basin. Very few deep wells have been drilled in the Hanna Basin, unlike other basins to the west and north. Substantial amounts of deep gas may yet be found in this basin.

Wind River basin

The Wind River basin, northwest of the Hanna basin, is separated from the latter by the Granite Mountains-Sweetwater uplift which may have begun to grow during the mid-Cretaceous and was a positive element in the Campanian. Late Cretaceous rocks thicken southeastward in the Wind River basin to greater than 5,490 m (18,000 ft). The Bull Frog field developed in Cretaceous Frontier sandstones (>5,700 m-->18,700 ft) in this part of the basin contains the deepest producing Cretaceous gas reservoir in the Rocky Mountain region. Other significant nearby fields include West Poison Spider and Tepee Flats, the latter beneath the lip of the Casper arch, from which it is separated by a major basement-involved thrust system which dips northeastward beneath and is responsible for the arch.

The Deep Madden gas field, in the northern part of the Wind River basin lies in front of (south of) the Owl Creek thrust which bounds the northern margin of the basin and is likely continuous with that under the lip of the Casper arch. The Madden anticline, the locus of this growing giant gas field, is cored by a thrust wedge, and the north-bounding Owl Creek thrust has more than 10,670 m (35,000 ft) of structural relief, comparable in size to the Wichita frontal fault system along the southern margin of the Anadarko basin.

The Wind River basin is bounded on two sides by thrust faults whereas the Hanna basin is bounded on all four sides by inward facing thrusts. The Wind River basin was partitioned from the remainder of the Rocky Mountain foreland in the late Paleocene by growth of the Casper arch which led to internal drainage as represented by Lake Walton and isolation from long-distance

migration of HC's from previously down-dip areas to the west and southwest. The Wind River basin occupies a critical position with respect to the sequential development of Laramide structure in Wyoming because cessation of major Laramide deformation in the area occurred during early Eocene. Sedimentation rates are consistent with relatively late Laramide strike-slip dominated transpressional deformation along the northern margin of the Wind River basin, similar to the earlier Laramide transpressional boundary along the northern margin of the Hanna basin to the south. Undiscovered structurally trapped deep gas may still be found north and northwest of the Madden anticline in the northern part of the Wind River basin.

Task 5. Source-rock potential of Precambrian rocks in selected basins of the U.S

The goal of Task 6 (J.G. Palacas, Appendix 5) was to determine the source-rock potential of Proterozoic unmetamorphosed sedimentary rocks in selected basins of the U.S. Proterozoic rocks are widely distributed in the U.S. and commonly occur in the deeper parts of basins. Their petroleum source-rock potential, however, is poorly known. These rocks may have generated and expelled petroleum which was subsequently trapped in Precambrian and/or younger overlying Phanerozoic rocks.

The reason for assigning a petroleum potential to Precambrian rocks in the U.S. is influenced by the actual production of commercial oil and gas derived from Precambrian rocks in other parts of the world. This report emphasizes the source rock evaluation of Proterozoic rocks in two regions of the U.S., the Midcontinent Rift System (MRS) and the Grand Canyon area, northern Arizona and vicinity.

Midcontinent Rift System

Rocks of the Midcontinent Rift System (MRS), delineated by strong gravimetric and magnetic anomalies, are exposed in the Lake Superior district of Michigan, northern Wisconsin, and Minnesota and extend in the subsurface into Minnesota, Iowa, Nebraska and northeastern Kansas (Fig. 5-1). The 1,570-km-long (940-mile-long) MRS is a failed rift characterized by a series of asymmetric basins filled with clastic rocks, in places up to 9,750 m (32,000 ft) in thickness. The rocks belong to the Middle Proterozoic, Keweenawan Supergroup, comprised of the Bayfield Group above and the Oronto Group below. The MRS is conveniently divided into four geographically identifiable segments: Lake Superior, Minnesota, Iowa, and Kansas.

Lake Superior region

The potential for petroleum reserves in the Midcontinent Rift System has long been recognized because of the active crude oil seeps emanating from the ~1.1 billion-year-old Nonesuch Formation at the White Pine Mine locality, Lake Superior region (Fig. 5-1). In this region, the Nonesuch Formation consists of interbedded dark grayish to greenish sandstones, siltstones and silty shales with poor source-rock potential. However, for finely laminated calcareous and noncalcareous silty shales that occur in thin intervals, TOC contents range from 0.25 to 2.8%. Should thicker sections of these HC-generating shales occur downdip from the outcrop belt and be subjected to higher levels of thermal maturation (but still within the wet gas to dry gas window; Rice, 1989), the gas source potential for the Lake Superior and the adjoining area in northern Wisconsin should be considered good.

Minnesota segment

The source rock potential of the Minnesota segment of the MRS is evaluated from examination of Keweenawan Solor Church Formation rocks as sampled in the Lonsdale 65-1 borehole, Rice county, Minnesota. The formation consists principally of interbedded conglomerate, sandstone, siltstone, and shale or mudstone. Analyses of core samples, mainly from the bottom 20% of the core, show TOC contents ranging from 0.01 to 1.77% and averaging 0.24%, indicating an overall poor source rock potential for oil or gas for the entire formation. A very low average genetic potential is largely attributed to the advanced level of thermal maturation. Based on maturity evaluations of basins worldwide, the Solor Church organic matter at the Lonsdale 65-1 locality has advanced to the transition stage between the wet gas and dry gas generating zones. The gas source potential of the Precambrian Solor Church Formation rocks, in the vicinity of the Lonsdale well and presumably in the neighboring areas, is poor.

Iowa segment

The Iowa segment of the MRS is unique in that the HC source rock assessment has been made of the thickest section (4,541 m--14,898 ft) of Precambrian sedimentary rock sampled by drilling from anywhere throughout the 940-mile-long structure. Assessment is based on analysis of core and cuttings samples from the 5,441-m-deep (17,851-ft-deep) Amoco M. G. Eischeid #1 well, drilled in 1987 in an asymmetric half-graben-like basin northwest of the Iowa Horst, Carroll County, Iowa (Fig. 5-1). Most of the Keweenawan sedimentary rocks, composed of red and red-brown sandstones, siltstones, and silty shales, are oxidized and have no source rock potential. However, at depths between 4,572 m (15,000 ft) and 5,006 m (16,425 ft), a conspicuous darker colored section of rock, possibly equivalent to the Nonesuch Formation of the Lake Superior region, contains a cumulative thickness of 60 to 90 m (200 to 300 ft) of gray to black, pyrite-bearing, organic-rich laminated shales. T_{max} values strongly indicate that the shales are thermally overmature and in the transitional zone between wet gas and dry gas, similar to the findings for the Solor Church Formation in southeastern Minnesota. The laminated shales have little remaining capacity for HC generation but may have generated significant amounts of gas in the geologic past. Equivalent laminated shale facies, as those observed in the Eischeid well, might have fair to good HC source potential if present at shallower depths of burial, under lower levels of thermal stress, along basin flanks, away from the frontal fault zone of the medial horst.

Kansas segment

The Kansas segment of the MRS is evaluated on the basis of examination of cuttings samples from two boreholes in northeastern Kansas: the Texas Poersche #1 well and the Producers Engineering Finn #1 well (Fig. 5-1). The two wells exhibit remarkably different lithologies, probably reflecting different structural, stratigraphic, and/or depositional regimes. Hence, the two sections of rock may belong to two different subbasins. This is in agreement with the findings provided by geophysical and borehole data that the MRS segment in northeastern Kansas is divided into small subbasins that probably are only a few tens of square miles in extent.

The Poersche well, drilled to a total depth of 3,440 m (11,300 ft), penetrated 2,846 ft of Phanerozoic rock and 2,580 m (8,454 ft) of Precambrian (Keweenawan) rock, the latter of which is comprised of nearly equal successions of highly oxidized arkosic sandstones and siltstones and mafic volcanic and intrusive rocks. No organic matter was noted in any of the oxidized sedimentary rocks, unequivocally indicating no source rock potential.

The Producers Engineering Finn #1 well showed some minor gas source potential in a 91-m (300-ft) section of gray siltstones directly beneath the Paleozoic-Precambrian unconformity. Thermal maturity values contrast dramatically with the much higher maturity values observed in the Minnesota and Iowa segments of the MRS, but demonstrate that some gas source potential is present. Because of the structural complexity and abrupt facies changes, it appears that individual subbasins need to be examined before complete source rock evaluation be made of the Kansas portion of the rift system.

Grand Canyon area, northern Arizona

The Late Proterozoic Chuar Group is exposed in the eastern portion of the Grand Canyon. It is composed of a 1,640-m-thick (5,370-ft-thick) succession of predominantly very fine grained siliciclastic rocks that contains thin sequences of sandstone and stromatolitic and cryptalgal carbonate rocks. More than half the succession consists of organic-rich gray to black mudstone (or shale) and siltstone.

Geochemical analyses indicate that the 280-m-thick (922-ft-thick) Walcott Member, the uppermost unit of the Kwagunt Formation, has good to excellent petroleum source rock potential. The lower half of the Walcott is characterized by total organic carbon (TOC) contents as much as 10.0%, , hydrogen indices as much as 204 mgHC/g TOC, genetic potentials (S_1 + S_2) of nearly 16,000 ppm, and extractable organic matter (EOM) as much as 4,000 ppm. Preliminary ata for the upper Walcott suggest that these rocks are as rich or richer than the lower Walcott. Maturity assessment indicates that source rocks of the Walcott are within the oil generation window.

Strata of the underlying thermally mature Awatubi Member of the Kwagunt and the thermally mature to overmature Galeros Formation are, in general, rated as poor oil sources with genetic potentials generally less than 1,000 ppm, but they appear to be acceptable to good source rocks for gas generation.

Chuar Group strata may be potential sources for economic accumulations of gas and oil in upper Proterozoic or lower Paleozoic reservoir rocks in northwest Arizona and Utah. The relative proportion of gas or oil in any one area will depend in large part upon the degree of thermal maturation.

Task 6. C15+ Hydrocarbon Thermal Destruction as Related to high-rank, deep-basin gas resource bases

The purpose of Task 6 (L.C. Price, Appendix 6) was to describe the thermal destruction of C_{15+} HC's by conversion to high-rank methane, and investigate the loss of HC-generating potential with increasing thermal maturity for different types of organic matter.

The data from this study demonstrate that C_{15+} HC's are thermally stable to **very high** maturation ranks. In fact: (1) C_{15+} HC's are thermally stable to ranks as high as R_o = 7.0-8.0% in deep, unsheared petroleum basins. (2) C_{2+} HC's are thermally stable to even higher ranks, well into true rock metamorphism. (3) Methane is stable probably into mantle conditions.

The evidence for C_{15+} HC thermal stability comes from: (1) petroleum-geochemical analyses of ultra-deep (4-6 mi), high-rank (R_o = 2.0-8.0%), fine-grained rocks, analyses which demonstrate that moderate to high concentrations of C_{15+} HC's survive to these ranks; (2) compositional changes in both the saturated and aromatic HC's in the approach to and during C_{15+} HC thermal

destruction, changes which have been only occasionally observed in the deepest rocks of sedimentary basins; (3) long-established physical-chemical laws which demonstrate that C_{15+} saturated, and especially aromatic, HC's are thermally stable species with high bond energies; (4) published data which demonstrate that low concentrations of C_{15+} HC's persist into conditions of true rock metamorphism and other high temperature settings; (5) "oils" of normal (moderate) maturities (as determined by biomarker analyses) entrained in very low concentrations (by gas solution) in dry "high-rank" gas accumulations; (6) a lack of high-temperature assemblages of saturated and aromatic HC's in "high-rank" gas accumulations; (7) the rare occurrences of high-rank oil accumulations that do exist, and (8) the lack of the expected methane carbon-isotopic compositions versus depth in the high-rank, dry gas deposits of the Anadarko basin, if such gas deposits indeed originated by thermal destruction of C_{15+} HC's.

The controlling parameters of organic matter (OM) metamorphism are considered to be burial temperature and geologic time (e.g. - first-order reaction kinetics). These controlling parameters predict C_{15+} HC thermal destruction by R_o = 1.35%. This prediction is in strong contrast with observed C_{15+} HC thermal stability to R_o = 7.0-8.0%. Furthermore, no *solid* evidence exists which indicates that OM metamorphism follows first-order reaction kinetics. Thus it is concluded that the controlling parameters of OM metamorphism, according to present-day petroleum-geochemical paradigms, must be at least partially in error.

Increase in burial temperature is the principal cause for OM metamorphic reactions. Other controlling parameters and characteristics of OM metamorphic reactions are hypothesized to be: (1) increases in static fluid pressures retard all aspects of OM metamorphism; (2) the presence of water enriches (hydrogenates) kerogen and suppresses HC thermal destruction; (3) open or closed reaction sites: open reaction sites (product escape) promotes OM metamorphism, closed reaction sites (product retention) retards OM metamorphism; (4) OM metamorphic reactions are not first-order reactions, but are higher-ordered reactions; and (5) the reactivities of the different kerogen (OM) types vary, increasing with increase in sulphur content and decreasing with increase in hydrogen content. Thus Type II-S OM reacts before Type III OM which reacts before Type II OM which reacts before Type I OM.

Evidence for deep-basin HC destruction has been attributed to the lack of deep-basin oil accumulations and strong basinal HC zonations: dry gas only in the deep basin, oil on the shelves with both gas-oil-ratios and API gravities decreasing with decreasing burial. However, these two HC distribution patterns (no deep-basin oil and strong basinal HC zonations) can also be explained by: (1) emplacement processes during migration (oil emplaced mostly at shallow depths during vertical migration); and (2) condensation, buoyancy, migration, and "flushing" processes (Gussow, 1954) which also apply to the C_2-C_4 HC gases in the deep basin).

Because of their high aqueous solubilities, both CO_2 and H_2S are quickly (10^4-10^5 years) dissolved in water-bearing deep gas accumulations. Thus the presence of either of these two gases in deep-basin gas accumulations dictates that such gas accumulations: (1) contain no water; and (2) are closed systems with regard to fluid migration. The probability of water-free, deep-basin gas reservoirs carry strong implications for: (1) enhanced thermal destruction of C_{15+} HC's; and (2) possible formation (skin) damage around the wellbore during drilling, completion, and stimulation procedures.

Some gas accumulations show by methane-isotopic, compositional, and geologic evidence that they have had a high temperature (400°-1200°C?) origin, involving C_{15+} HC thermal destruction. However, such gas deposits appear to be unusual, based on existing data. Most high-rank, deep-basin, dry gas accumulations have probably not originated by an in-reservoir thermal destruction of C_{15+} HC's. Such methane accumulations are believed to largely be made up of methane cogenerated with C_{15+} HC's during both the intense and late stages of C_{15+} HC generation from kerogen. Condensation and buoyancy processes combined with Gussow's (1954) principal of differential entrapment, are believed to lead to an expulsion of all C_{2+} HC's (and perhaps water) from deep-basin gas traps.

Faulting and fracturing are probably necessary for highly efficient primary migration of gases from source rocks. Thus deep-basin gas accumulations should nearly always be associated with faulting. Normal and extensional faulting would be most favorable for migration because of voids along the fault zones. Later evolution to compressional (high-angle reverse) faulting (such as occurred in the Anadarko basin in southern Oklahoma) would be favorable for preservation of deep-basin gas deposits over geologic time. The existence of cracks, fractures, parting laminae and other such voids in deep-basin rocks may help offset a general trend of decreasing porosity with increase in maturation rank in deep petroleum basins. Basinal structural styles evolve through geologic time. For example, the depocenter and southernmost margin of the Anadarko basin, although previously an extensional wrench fault regime, later evolved into a compressional tectonic regime, characterized by numerous, large, high-angle reverse faults. Migration of HC fluids could occur during periods of normal or extensional faulting and later evolution to a compressional tectonic regime might be quite favorable to preserving deep, high-rank gas deposits over geologic time by minimizing loss by leakage up these "tight" compressional systems.

Very large, in-place, non-conventional gas-resource bases exist, among which are: basin-centered gas deposits, coal-gas, tight-gas, black-shale gas, and Gulf Coast overpressured-geothermal gas. It is hypothesized that the existence of such unconventional gas-resource bases are primarily due to, and are direct evidence of, highly restricted fluid flow and inefficient primary HC migration in deep sedimentary basins. Much of the rock volume of deep sedimentary basins is perceived to be an essentially closed system with respect to significant fluid flow once basinal evolution goes beyond the youthful stage to the mature stage with a corresponding decline in geothermal gradients.

Task 7. Migration of 10's to 100's of TCF of Hydrocarbon and non-Hydrocarbon Gases from the Deep Crust: Composition, Flux, and Tectonic Setting

The purpose of Task 7 (R.C. Burruss, Appendix 7) was to investigate the occurrence, geologic setting, and geochemical controls of non-HC gases (NHCG), such as carbon dioxide, hydrogen sulfide, and nitrogen, which dilute and can contribute to the destruction of deep gas accumulations.

Comparison of gas compositions in deep reservoirs with the compositions of gases generated in the deep crust yields three types of information: (1) similarities between the gases in the two crustal regimes; (2) evidence for volumetric fluxes of non-HC and HC gases in metamorphic rocks presently exposed at the surface that can be used to estimate the potential flux of gases to shallow crustal levels accessible to the drill; and (3)

identification of crustal environments (tectonic and metamorphic terranes) that generate significant quantities of gas that can be coupled with analysis of basin structural style and setting to identify basins where deep crustal sources may have contributed to the HC resource base.

Analysis of trends in gas composition versus depth and reservoir lithology were performed on available gas data in the NRG Associates Significant Field File for 120 U.S. reservoirs at depths of 4,270 m (14,000 ft) or greater. When the fraction of total NHCG is plotted as a function of reservoir temperature (to eliminate significant variations in geothermal gradient) two trends are apparent. One trend of gradually increasing NHCG with depth up to about 10% is common to both carbonate and sandstone reservoirs from all basins. The first trend is due to fluid-rock interactions involving organic matter and dissolution and reprecipitation of carbonate cements. A second trend, of rapidly increasing NHCG with depth is present in a small number of reservoirs, all but two of which are in carbonate rocks. The second trend occurs in carbonate reservoirs of the Permian basin (Ellenberger Formation) and carbonate and sandstone reservoirs in the Smackover Formation and related strata (Norphlet Formation) of the Gulf Coast. Although the dominant NCHG in these reservoirs is CO_2, H_2S is also important (up to 25%). The occurrence of these high NHCG gases in carbonate reservoirs and the presence of H_2S indicates that thermochemical sulfate reduction and simultaneous oxidation of HC's to CO_2 may be the dominant control on gas composition in these reservoirs.

Most of the evidence for the composition of fluids in the deep crust comes from observations on fluid inclusions in metamorphic and igneous rocks. Metasedimentary rocks which contain graphitic carbon and carbonate minerals can act as a source of carbon bearing gas components, CH_4 and CO_2. An additional source of information on fluids in crustal rocks is fluid inclusions in quartz veins associated with ore mineralization. Recent information from ore deposits is important because it records the flux of fluids from deep to shallower levels of the crust and provides a basis for quantitative estimates of the flux of gases to shallow crustal levels as discussed in the following section.

The trends in NHCG content of natural gases shown in deep sedimentary basins can be extended to deeper crustal levels by including data from fluid inclusions in rocks of well constrained depth of burial. Individual localities may show a significant range in composition, but even the highest temperature rocks still contain some methane and the compositions tend to lie along the extension of the first trend identified above for sedimentary basins. Clearly, the "early burnout" of HC gases that one would predict from the second trend of rapidly increasing NHCG's, for carbonate reservoirs, does not occur in all crustal rocks. Work on a siliceous marble that equilibrated at 800^{o}C documents the occurrence of about 1 mole % methane in carbon dioxide at this temperature showing that methane is stable to great depths in the crust.

Metamorphic rocks that contain more than about 10 mole percent methane in fluid inclusions tend to be graphite bearing. The compositions of the inclusions tend to be generally consistent with calculated compositions of aqueous fluids in equilibrium with graphite , especially when the possibility of hydrogen diffusion from inclusions is taken into account. This observation plus the textural evidence for precipitation of graphite from fluids clearly documents the generation and migration of methane and carbon dioxide bearing fluids in the deep crust. This also suggests that identification of geologic environments where carbon-rich sediments have been incorporated into

metamorphic rocks will help define areas where there is the greatest probability of deep crustal sources contributing to shallower natural gas resources.

Estimates of the flux of gases from the deep crust are based on the measured solubility of quartz in water as a function of temperature, pressure, and salinity which can be translated into a quantity of quartz precipitated per volume of water in a vein system at a given depth. From the volume of quartz veins that can be measured in the field, we can estimate the volume of water necessary to form the vein system. The ratio of HC and non-HC gases to water can be determined from fluid inclusion measurements. Therefore we can estimate the volume of gases transported with the water necessary to form quartz veins at depth in a given tectonic setting.

Studies have documented the geochemical processes and tectonic setting of formation of "giant quartz-vein systems" which in many cases have associated gold mineralization (Kerrick and Feng, 1992; Appendix 7). In one example of a giant vein system, it has been estimated that 6 X 10^{18} g of aqueous fluid (6 X10^3 km^3) deposited about 6 X 10^{15} g of quartz and in the process transported 3 X 10^{15} g of CO_2. This is 1,500 trillion cubic feet (Tcf) of CO_2. Based on the range of methane/carbon dioxide ratios observed in fluid inclusions in quartz from one of these giant vein systems (1:3 to 1:40), **a single giant vein system may transport on the order of 50 to 500 TCF of CH_4 to shallow crustal levels.** Twelve giant vein systems have been documented in the Canadian, European, and Australian shields (Kerrick and Feng, 1992).

Giant quartz-vein systems are an important component of any consideration of deep crustal sources of HC and non-HC gases for several reasons. First, quartz veins are direct evidence of focused flow of fluids from deep to shallow crustal levels. Second, the systems occur at convergent plate margins, especially those associated with transpressive tectonic regimes, a geologic environment with major HC accumulations. Giant vein systems may be the best evidence to support earlier suggestions of natural gas accumulations in "accretionary" terranes.

On the negative side, convergent, transpressive tectonic regimes tend to have a component of very active vertical tectonics. This can lead to rapid erosional exhumation of potential reservoir rocks and loss of accumulations. For example, there is a large amount of fluid inclusion evidence for methane generation and transport through the European quartz veins, but any sedimentary cover that could have provided reservoirs has been stripped off this young terrane.

Task 8. Resource assessment methodology for deep natural gas resources

The primary goal of Task 8 (G.L. Dolton and R.A. Crovelli, Appendix 8) was to identify and develop quantitative resource assessment methods and models for evaluation of undiscovered deep gas resources, based on geologic models of occurrence and information developed by Tasks 1-7 of this project.

Review and analysis of resource appraisal methodologies and approaches allow identification of methods for dealing with deep gas accumulations. These methods are ultimately dependent upon the level of geologic and engineering data available and understanding of the geologic model for the

specific deep gas occurrence. One or more may be appropriate in a given case, and multiple approaches are desirable as independent checks. The methods of assessment which appear most appropriate to assessment of undiscovered resources of deep gas are: (1) deposit simulation, (2) reservoir performance, (3) analog, (4) discovery process and finding rate models, (5) mass balance calculations, and (6) volumetric and areal yield determinations.

Geologic information in our companion studies indicates that many deep gas occurrences should be treated at a play level (see Mast and others, 1989 and Appendix 8) and with a method that will provide information on the size of the accumulations and their geologic characteristics, as well as a total resource value, so that economic and supply studies can be made. Several of the preceding methods meet criterion for evaluation of undiscovered deep gas resources. Where sufficient information is available concerning the geologic characteristics of known or suspected deposits of deep gas, a **volumetric calculation of resources** is appropriate. This method is based on measurement of known or estimated physical properties of the traps, reservoir rocks and fluids and of the host environment in terms of temperatures, pressures and fluid dynamics. It has the advantage of working with the basic geologic properties of the accumulations and dealing with them in a rigorous, quantitative mode and allows for simulation of the HC deposit(s) through estimation of properties where data are lacking or incomplete.

The calculation of gas resources is based on a fundamental reservoir volume engineering formula. Simulation of properties of the accumulation or an aggregate of accumulations requires that reservoir volume parameters are represented as estimates expressed as ranges of values, accompanied by probabilities of occurrence, representing the natural geologic variability of geologic characteristics and our uncertainty about them. The model can be used both at the scale of a single prospect or for an aggregate of prospects within a common geologic setting or play.

A hypothetical case of deep gas occurrence is applied for a population of drillable prospects, which have been identified geologically or geophysically or are hypothesized to exist, and which bear common geologic characteristics. For instance, we may estimate that we are dealing with a sandstone reservoir lying in structural traps at depths ranging from 18,000 to 22,000 ft. In this case, we assume that the various play attributes for HC occurrence have been met, hence no risk has been assigned.

Results from calculation of the modeled play are shown in Table 8-1 (Appendix 8). Several interesting relationships emerge from this calculation. First, is the relatively modest amount of gas calculated, considering the prospect areal size. This is largely the function of small amounts of effective matrix porosity. Should porosity of less than 5% contribute gas to the reservoir, then the cut-off value should reflect this so that it is included. In any case, the diminished pore space is viewed as a significant factor in many deep gas reservoirs. It effects not only the amount of resource present but also production. In many cases, the presence of natural fractures is necessary for economic production. In such instances, adjustment of reservoir porosity values must be made to accommodate fracture porosity. Special situations do occur, where porosity is retained at great depth, as in some overpressured reservoirs, and need to be considered in exploration, development and assessment scenarios.

Alternatively, if we assume better reservoir conditions as occur in many of the clastic reservoirs of the Gulf Coast, and overpressuring, and use these variables in place of the original data set (Table 8-1, Appendix 8), recoverable resources increase significantly. For this more optimistic case, we assumed a average reservoir porosity of 18%, and a pressure gradient of 0.75 psi/ft (clearly an overpressured reservoir as is commonly associated with deep natural gas accumulations). In the first case, the mean resource value in these prospects contained 298 Bcf. In the second, more optimistic case, the prospects contained 1,017 Bcf of gas, a three-fold increase. In this instance, the increase in recoverable gas was due to the increase in porosity and pressure. Other variables which particularly affect the overall reservoir volume include reservoir thickness and size of prospects

This volumetric method is flexible in that it permits the geologist to model the geologic conditions controlling the resource. This allows for a wide range of resource values for a wide range of geologic conditions.

CONCLUSIONS

(1) An empirical framework for predicting the porosity range of sandstones in Rocky Mountain basins is developed. The concept is broadly applied to deeply buried sandstone in general. For vitrinite reflectance (Ro) >1.1%, the rate of porosity decrease as thermal maturity increases for Anadarko basin reservoir and non-reservoir sandstones is less rapid than that of sandstones in general. The similar slopes of porosity trends suggest that sandstones of the central and southern Anadarko basin may retain sufficient porosity for economic accumulations of HC's, even at high thermal maturities.

(2) Pore throats are controlling factors in the flow of fluids through pore networks. Data show that they are typically smaller than pores visible in thin section, or apparent in hand specimen. Pore throats, especially small (<0.1um) pore throats, common in fine to very fine grained clastic rocks, are very sensitive to confining stress, and probably act as limiting factors controlling the flow of gas to the well bore. Small pore throats are also very sensitive to the presence of formation fluids, which reduce their effective diameter. Measurement of capillary pressure under confining stress suggests that constriction of pore throats is the controlling mechanism effecting fluid flow at reservoir conditions in the samples examined.

These data aid in defining reservoir properties under in situ conditions, and are valuable for reservoir descriptions and in simulation studies.

(3) Three sixty three significant deep reservoirs occur primarily in the Gulf Coast, Permian, Anadarko, Williston, and Rocky Mountain basins; California and Alaska basins together contribute three reservoirs. Analysis of drilling, geologic, and production data for significant reservoirs indicates that a complex interplay of geological and geochemical factors controls the distribution of deep natural gas in sedimentary basins.

(4) In the Rocky Mountain region, structural partitioning prior to thrusting in selected basins, and sequential southeastward and later northeastward

partitioning of the Rocky Mountain foreland during Late Cretaceous may be critical to the entrapment of natural gas resources. Economic implications of this new model of deformation of the Rocky Mountain foreland include progressive opening and subsequent blockage of migration paths for HC's generated from source rocks in southeastern Idaho, southwestern Montana, Wyoming, Colorado, and eastern Utah.

(5) The presence of geochemically identified source beds of Middle Proterozoic age, active (HC) seeps, and favorable thermal maturities for generating and preserving natural gas, indicate a source rock potential adequate for economic gas accumulations in flanking basins of the Midcontinent Rift System and the Grand Canyon region.

(6) High-rank methane generation (from thermal decomposition of C_{15+} HC's) takes place at very high maturation ranks. Data demonstrate that C_{15+} HC's (HC's) are thermally stable to very high maturation ranks. In fact: (1) C_{15+} HC's are thermally stable to ranks as high as R_o = 7.0-8.0% in deep, unsheared petroleum basins. (2) C_{2+} HC's are thermally stable to even higher ranks, well into true rock metamorphism. (3) Methane is stable probably into mantle conditions.

(7) The occurrence of significant nonhydrocarbon gases in carbonate reservoirs and the presence of H_2S indicates that thermochemical sulfate reduction and simultaneous oxidation of HC's to CO_2 may be the dominant control on gas composition in these reservoirs.

Giant quartz-vein systems in convergent, transpressive plate margin basin systems may be associated with major deep gas accumulations such as in the deep Anadarko and Arkoma basins. Based on the range of methane/carbon dioxide ratios observed in fluid inclusions in quartz from one of these giant vein systems (1:3 to 1:40), a single giant vein system may transport on the order of 50 to 500 Tcf of CH_4 to shallow crustal levels.

(8) Review and analysis of resource appraisal methodologies and approaches has allowed identification of methodologies for dealing with deep gas occurrences. Modelling of assessment methodologies supports the possibility of large volumes of natural gas resources in deep sedimentary basins. Where sufficient information is available concerning the geologic characteristics of known or suspected deposits of deep gas, a volumetric calculation of resources is appropriate. This method is based on measurement of known or estimated physical properties of the traps, reservoir rocks and fluids and of the host environment in terms of temperatures, pressures and fluid dynamics. It has the advantage of working with the basic geologic properties of the accumulations and dealing with them in a rigorous, quantitative mode and allows for simulation of the HC deposit(s) through estimation of properties where data are lacking or incomplete.

RECOMMENDATIONS FOR FUTURE RESEARCH

In any scientific investigation, many new problems and opportunities for research are identified. Much of the following research could be conducted by the U.S. Geological Survey in part because of ongoing research objectives and because of state-of-the-art laboratory facilities and experience. The U.S. Geological Survey routinely assesses both conventional and unconventional petroleum resources as mandated by Congress.

The following new scientific investigations could add greatly to our knowledge of deep natural gas resources:

(1) Create additional thermal maturation profiles of deep basins in the U.S. to add to the existing models developed for Task 1 of this report. Further investigate the geological and geochemical variables controlling the porosity variations at depth under specific thermal maturity regimes. Determine how far the model proposed for Rocky Mountain basins extends in other parts of the U.S.? Determine why the thermal profiles for the Rocky Mountain basins and the Anadarko basin change at different reflectance values? What are the controlling mechanisms behind this change? How is permeability related to these trends?

(2) Investigate initial potential (IP) volume data from available data bases more thoroughly to determine the controlling mechanisms behind the expected IP volumes under different conditions. Determine how the volumes can be improved by fracture enhancement on a regional basis and can these improvements be predicted? More clearly define pressure compartments and determine their role in this change?

(3) More precisely determine the role of diagenesis in pore-throat character under different compositional conditions for clastic reservoir rocks and analyze additional samples using Hg-injection capillary-pressure measurements to determine the role of pore-throats in fluid migration. What are the roles of pore throats in pressure compartment systems?

(4) Investigate the role of fracture systems in leaky reservoirs and in production of deep natural gas in different basins. Answer how these fracture systems relate to major faults (which may be the pathways for fluid migration and loss)? What are the spatial configuration systems by which these fracture systems are developed? Model the distribution of fracture systems using fractal functions.

(5) Investigate the recovery technologies available for deep natural gas reservoirs and further model the assessment procedures to better define the range of recoverable resources under different geological and geochemical conditions.

(6) Conduct geochemical studies of quartz-vein systems in different regimes in basement rocks of deep sedimentary basins Can we clearly identify a crustal component of the dry gas in old (mature) sedimentary basins? Analyze carbon-isotope data from fluid inclusions to more precisely define the origin of methane and carbon dioxide. Can the isotopic signature of methane and carbon dioxide from both sedimentary and crustal regimes be identified?

(7) It is suggested in this study that non-conventional gas-resource accumulations may be both larger and of a higher grade than previously believed. Research to identify these accumulations should include geologically-based engineering studies to determine appropriate recovery techniques. A further need also exists for more extensive chemical analyses and characterization of high-rank methane to better understand the origin of these gases in order to predict recovery.

References Cited

Dwights Energy Data, 1985, Petroleum Data System (through 1985): Available from Dwights Energy Data Corp., Oklahoma City, OK 73108.

Gussow, W.C., 1954, Differential entrapment of oil and gas.- a fundamental principle: American Association Petroleum Geologists Bulletin, v. 38, p. 816-853.

Kerrich, R., and Feng, R., 1992, Archean geodynamics and the Abitibi-Pontiac collision: implications for advection of fluids at transpressive collisional boundaries and the origin of giant quartz vein systems, Earth-Science Reviews, v. 32, p. 33-60.

Martin, P.E., Cooke, L.W., Carpenter, G.B., Pecora, W.C., and Rose M.B., 1989, Estimates of undiscovered conventional oil and gas resources in the United States-A part of the Nation's energy endowment: U.S. Geological Survey and Minerals Management Service special publication, 44 p.

NRG Associates Inc., 1988, The significant oil and gas fields of the United states (through December 31, 1988): Available from Nehring Associates, Inc., P.O. Box 1655, Colorado Springs, CO 80901.

NRG Associates Inc., 1991, The significant oil and gas fields of the United states (through December 31, 1991): Available from Nehring Associates, Inc., P.O. Box 1655, Colorado Springs, CO 80901.

Petroleum Information Corporation, 1988, Well History Control System (through December 1988): Available from Petroleum Information Corporation, 4100 East Dry Creek Road, Littleton, CO 80122.

Petroleum Information Corporation, 1991, Well History Control System (through December 1991): Available from Petroleum Information Corporation, 4100 East Dry Creek Road, Littleton, CO 80122.

Rice, D.D., 1989, Distribution of natural gas and reservoir properties in the continental crust of the U.S.: Gas Research Institute Final Report GRI-89/0188, 132 p.

Spencer, C.W., 1989, Review of characteristics of low-permeability gas reservoirs in Western United States: American Association of Petroleum geologists Bulletin, v. 73, p. 613-629.

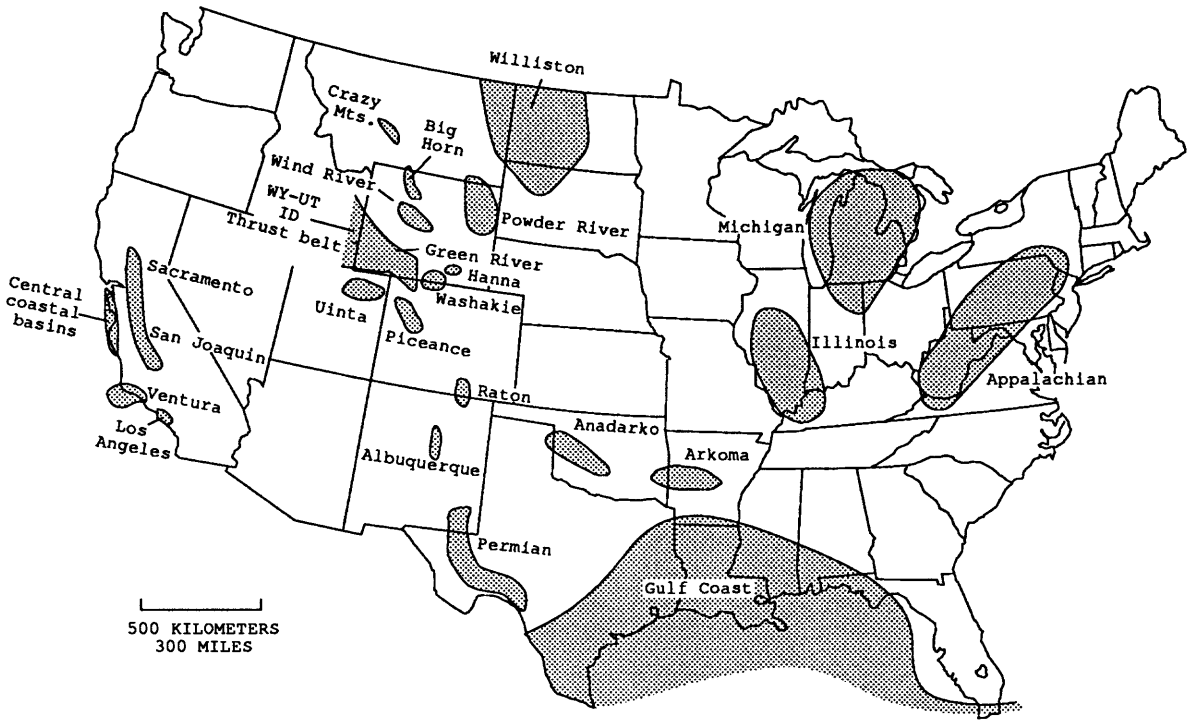

Figure 1. Map of continuous U.S. showing basins containing sediments greater than 15,000 ft deep.

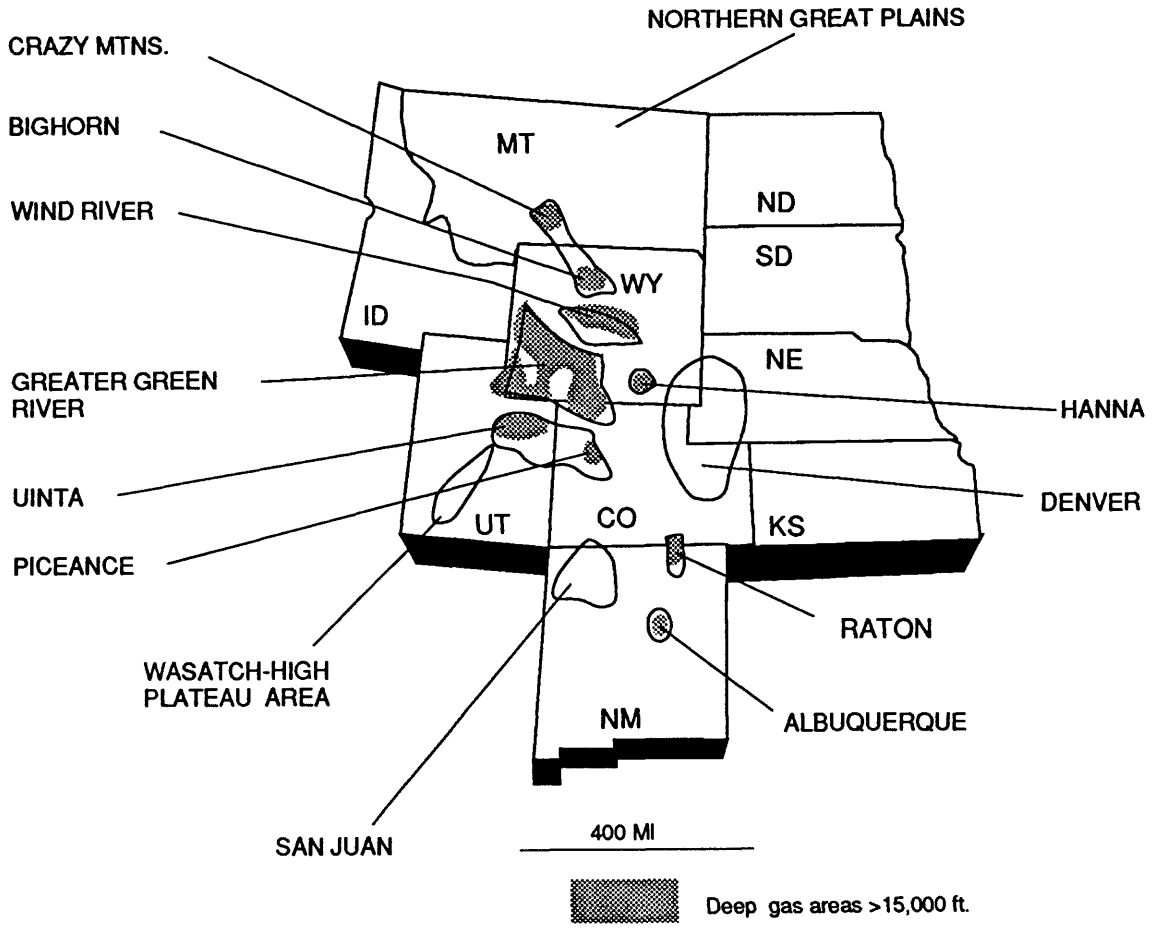

Figure 2. Map of Rocky Mountain region showing basins where deep (greater than 15,000 ft) natural gas is interpreted to occur on the basis of gas shows, formation tests, geology, and known production. Deep gas is being produced in the Wind River basin and from a few structural traps in the Greater Green river basin and the thrust belt in southwest Wyoming and northern Utah.

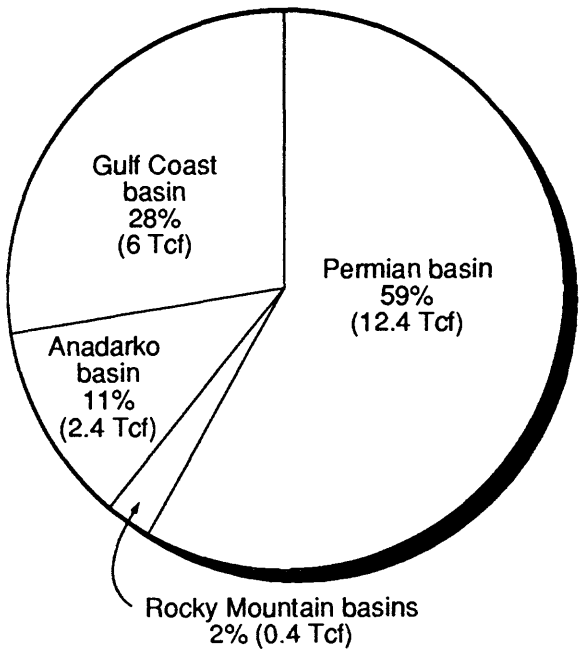

Figure 3. Pie chart illustrating the percent distribution of total cumulative production by region in the U.S. from significant reservoirs deeper than 14,000 ft. Total deep significant production equals 21.2 Tcf. Based on data from NRG Associates Inc. (1988).

Table 1. Reservoir summary for significant reservoirs in major deep basin areas of U.S. Based on data from NRG Associates Significant Field file (NRG Associates, 1988). Eight reservoirs from Williston basin and Pacific region not included. Rec.= recoverable; Res.= reservoirs; total of 378 reservoirs used for U.S.

Basin/region	Number of reservoirs and percent of total	Cumulative gas and percent of total gas	Known rec. gas and percent of total gas	Stratigraphic and lithologic information	Number fields discovered prior to 1970 and % of total	Comments
Gulf Coast	174/363= 46%	6.2/21.5= 29%	13.3/33.7= 40%	Tertiary reservoirs mostly clastic; Jurassic and Cretaceous reservoirs mixed carbonate/clastic.	64/174= 37%	37% of deep reservoirs are Tertiary.
Permian	89/363= 24%	12.4/21.5=58%	15.1/33.7= 45%	Middle Paleozoic mixed clastic/carb. reservoirs and Silurian/Devonian mostly carbonate res.	32/174=36%	67/89 res. occur in Devonian or older rks. Permian res. strat. trapped.
Anadarko	85/363= 22%	2.4/21.5= 11%	2.8/33.7= 8%	Mostly a clastic basin. Some Cambrian-Silurian carbonate production.	25/85= 29%	65% of res. produce from Pennsylvanian strata.
Rocky Mt. basins	22/363=6%	0.4/21.5= 2%	2.2/33.7= 7%	Jurassic and Cretaceous clastic res. and Paleozoic mixed carb./clastic res.	9/22= 41%	Deep gas mostly from Utah-Wyoming thrust belt. Potential from Hanna, Wind River, Piceance, Green River, Uinta, Crazy Mts., Big Horn, and Raton.

Appendix 1a--Distribution of porosity in sedimentary rocks as a function of time-temperature exposure

by J.W. Schmoker

INTRODUCTION

The first goal of Task 1 was to develop "rules of thumb" to use as empirical predictive models for the modification of sandstone porosity during burial. To this end, a generalized framework data set of sandstone porosity-vitrinite reflectance (R_O) data was developed. The Rocky Mountain Cretaceous porosity-R_O data set is now prepared as a digital data base.

The second goal of Task 1 was to develop approaches to treating the effects upon porosity of the petrographic variability of particular formations, within an overall thermal maturity framework. The Lower Cretaceous J (Muddy) sandstone of the Denver basin and the Upper Cretaceous sandstones of the Mesaverde Group of the Piceance and Uinta basins, Colorado and Utah, have been used as a case history.

The technology for drilling below 4,572 m (15,000 ft) ("deep") is well developed, and the ability to detect traps at these depths has improved steadily over the years. Nevertheless, in some deep basins of the U.S., relatively few wells penetrate below 4,572 m (15,000 ft), and deeply buried sandstones in these basins are sparsely explored.

One of the factors that has limited deep drilling for sandstone reservoirs is the knowledge that porosity can be too low to sustain economic HC production. Better predictive methods for the porosity and porosity range of sandstones are needed for risk evaluation and reduction in deep-drilling programs, as well as for regional assessment of deep HC resources.

An empirical approach to porosity prediction in deeply-buried sandstones is discussed here. Porosity trends are developed as functions of thermal maturity, as represented by vitrinite reflectance (R_O). The porosity range at a given level of thermal maturity is predicted also, and is investigated as a function of rock properties such as clay content, carbonate cementation, and grain size, and as a possible function of HC generation.

Examples are drawn from Cretaceous sandstones of the Rocky Mountain region, with emphasis on the Lower Cretaceous J sandstone (Muddy Sandstone) of the Denver basin, Colorado, and Upper Cretaceous sandstones of the Mesaverde Group of the Piceance and Uinta basins, Colorado and Utah. This paper is not intended as a report on the geology of these units. Rather, the J and Mesaverde sandstones serve to illustrate an approach to porosity prediction that has broad applicability to deeply buried sandstones. Cretaceous sandstones of Rocky Mountain basins are themselves not deeply buried in many of the areas studied, but are chosen as analogs because of the availability of porosity, vitrinite-reflectance, and petrographic data.

APPROACH TO POROSITY PREDICTION

Predictive sandstone porosity models should account for effects of both rock properties and burial history upon porosity. Relating porosity to rock properties alone, as is sometimes done in petrographic and core studies, may yield descriptive data that are difficult to generalize into regional predictive models.

The influence of burial history upon porosity has commonly been represented by plots of porosity versus depth (e.g., Athy, 1930; Maxwell, 1964; Baldwin and Butler, 1985). However, apparent relations between porosity and depth have come under critical review in recent years (van de Kamp, 1976; Lyons, 1978, 1979; Cassan and others, 1981; Siever, 1983; Scherer, 1987; Schmoker and Gautier, 1988, 1989; Keighin and others, 1989; Bloch, 1991). The point made in many of these papers is that processes of porosity modification during burial are strongly influenced by time and temperature.

By plotting porosity against vitrinite reflectance, which is a measure of time-temperature exposure, effects of temporal and spatial variations in thermal gradient, subsidence, uplift, and erosion are normalized. Also, the duration of a given set of burial conditions is empirically taken into account.

Porosity-maturity relations, like porosity-depth curves, do not provide much insight into the actual processes causing porosity change in the subsurface. The influence upon porosity of factors such as grain size and sorting, clay matrix, framework composition, early cementation, overpressuring, proximity to unconformities, dissolution (secondary porosity), and coating of framework grains is empirically taken into account by developing porosity-R_o trends that represent the 10th, 25th, 50th, 75th, and 90th porosity percentiles of data sets (Fig. 1-1).

The 90th porosity percentile, for example, represents strata of the data set that have rock properties relatively favorable for porosity preservation or development; in contrast, the 10th porosity percentile represents intervals of the data set with properties that result in low porosities at similar levels of thermal maturity. By depicting porosity using the 10th through 90th porosity percentiles (Fig. 1-1), the porosity range at a given R_o is taken into account. If porosity was reported only as an average, information significant for risk assessment, reservoir-engineering models, and volumetric calculations would be lost.

Schmoker and Gautier (1988, 1989) found that the dependence of sandstone porosity upon vitrinite reflectance can often be represented by a power function of the form $=A(R_o)^B$, where A and B (a negative number) are constants. Such trends graph as straight-line segments on log-log plots.

PREDICTIVE POROSITY TRENDS FOR J SANDSTONE

Introduction

The Lower Cretaceous J sandstone of the Denver basin (Fig. 1-2) was deposited in nearshore-marine, deltaic, and fluvial-estuarine (valley-fill) settings. The J is correlative to other Lower Cretaceous Dakota Group sandstones of the Rocky Mountain region (Coalson, 1989). Approximately 90 percent of the oil and gas extracted from the Denver basin has been produced from the J sandstone (Land and Weimer, 1978; Tainter, 1984).

The maximum depth of the J sandstone in the wells of this study (Fig. 1-2) is only 2,665 m (8,745 ft), which at first consideration seems insufficient for the development of deep-sandstone porosity models. However, a good suite of porosity, vitrinite-reflectance, and thin-section data (Schmoker and Higley, 1991) makes the J sandstone a useful formation for developing

approaches to porosity prediction. Such approaches might then be applied to sandstones in general.

This section focusing on the J sandstone is based upon work of Schmoker and Higley (1991), who presented complete tables of the data used here.

Porosity-Maturity Trends

Core-plug porosity data from productive and nonproductive sandstones from 31 wells in the Denver basin (Fig. 1-2) are used for the porosity-vitrinite reflectance plots of Figures 1-3 and 1-4. R_o values were measured in each well by M.J. Pawlewicz, U.S. Geological Survey, using material from shales within and adjacent to the J sandstone. Because formation thickness does not exceed 45 m (150 ft) and is generally less than 30 m (100 ft), the thermal maturity of the J sandstone interval in an individual well does not vary significantly.

For the J sandstone, as well as for the other examples of this report, the porosity data of a given measurement suite (such as data from a particular well) are grouped into a histogram and represented by the 10th, 25th, 50th, 75th, and 90th porosity percentiles, as previously discussed (Fig. 1-1). The porosity of the J sandstone is characterized by 31 such histograms.

Figure 1-3 shows the 50th (median) percentiles of the 31 J sandstone porosity histograms, plotted as a function of vitrinite reflectance. A least-squares power-law regression line with R_o as the independent variable is fit to the data of this figure. Similar plots have been made for the 10th, 25th, 75th, and 90th porosity percentiles. The porosity-R_o regression lines of these five plots are assembled in Figure 1-4 and documented in Table 1-1. Correlation coefficients range between -0.76 and -0.88. For 31 data points, a correlation coefficient of -0.42 would be significant at the one-percent level (Till, 1974).

A power-function relation of porosity to R_o explains roughly three-fourths of the porosity variance of the 50th, 75th, and 90th J sandstone porosity percentiles (Table 1-1). For these sandstones, the effect of thermal maturity upon porosity change in the subsurface is considerably larger than that of all other factors combined.

The five regression lines of Figure 1-4 each show a decrease of porosity with increasing thermal maturity. Although the 10th through 90th porosity-percentile trends represent different combinations of diagenetic processes and geologic factors, the negative correlation between porosity and time-temperature exposure is characteristic of each case.

The trend lines of Figure 1-4 provide an empirical framework for estimating both the porosity and the porosity range of the J sandstone within the Denver basin. It is important to note, however, that the concept behind Figure 1-4 is broader than a study of a particular sandstone in a particular basin. Figure 1-4 illustrates a sound general approach to empirical porosity prediction in sandstones.

Porosity Range at a Given R_o

The predictive porosity model of Figure 1-4 incorporates the porosity range at a given level of thermal maturity. Although a substantial porosity range at a given R_o is typical of sandstones in general, the particular causal

factors are varied and cannot be specified independently of observation. Examination of thin sections reveals that the petrographic factors that most affect J sandstone porosity variability at a given R_o are carbonate cementation and clay content. These two factors are discussed briefly in the following paragraphs, as examples of the links between empirical porosity percentiles and causal geologic elements.

Carbonate cement, where present, reduces porosity. In addition, corroded and embayed quartz edges show that carbonate cement was formerly more widespread. Such cement, prior to its dissolution, could protect the pore network from burial diagenesis, relative to uncemented intervals. Thus, direct and indirect effects of carbonate cementation are responsible for a portion of the porosity range at a given R_o shown in Figure 1-4.

Abundant clay reduces J sandstone porosity by occupying pores and deforming during burial to fill pore networks. Low clay content is also observed to reduce porosity of the J sandstone probably because inhibiting effects of clay upon quartz cementation are largely absent. Thus, the higher J sandstone porosities at a given R_o tend to be associated with intervals of intermediate clay content: that is, a clay content sufficient to retard quartz cementation, yet low enough to minimize the mechanical clogging of pores (Fig. 1-5). The clay content associated with maximum porosity percentile is roughly 12% in the J sandstone (Fig. 1-5).

An important aspect of Figure 1-5 that extends beyond the characterization of the J sandstone, is that the vertical axis (porosity percentile) represents porosity adjusted for the level of thermal maturity, rather than porosity on an absolute scale. This technique permits the crossplotting of porosity and petrographic measurements from rocks of different thermal-maturity levels. The influence of geologic elements upon porosity evolution in the subsurface can thus be isolated from the influence of burial history as represented by time-temperature exposure.

PREDICTIVE POROSITY TRENDS FOR MESAVERDE GROUP SANDSTONES

Introduction

Upper Cretaceous, undifferentiated, predominantly nonmarine sandstones of the Mesaverde Group in the Piceance and Uinta basins contain large volumes of natural gas. Economically successful exploration in these low permeability rocks has proven difficult, however. In large portions of the two basins, the Cretaceous section is sparsely drilled, and patterns of deposition, fracturing, and reservoir quality are not well known.

The maximum depth of Mesaverde sandstones in the wells of this study (Fig. 1-6) in the Piceance basin is 2,225 m (7,300 ft). In the Uinta basin, the Mesaverde is deeper than 4,572 m (15,000 ft) in one well. As in the preceding J sandstone example, the exercise of developing predictive porosity models for Mesaverde sandstones is intended to illustrate approaches that can be applied to sandstones in general.

This section focusing on Mesaverde sandstones is based upon work of Schmoker and others (1992), who documented more fully the data used here.

Porosity-Maturity Trends

Core-plug porosity data from 14 wells (11 locations) in the Piceance and Uinta basins (Fig. 1-6) are used for the porosity-vitrinite reflectance plots

of Figures 1-7 and 1-8. R_o values were estimated in each well, based on core-plug depths, by interpolating from a variety of published and unpublished sources (Schmoker and others, 1992). The merging of data from the Piceance and Uinta basins is rationalized on the basis that Mesaverde rocks of both basins are temporally and depositionally similar (Keighin and Fouch, 1981). As in the case of the J sandstone, the porosity distribution of a given measurement suite is represented by porosity percentiles (Fig. 1-1). The porosity of predominantly nonmarine Mesaverde sandstones is characterized by 31 such histograms.

Figure 1-7 shows the 25th and 75th percentiles (connected by vertical lines) of the 31 Mesaverde porosity histograms, plotted as a function of vitrinite reflectance. These data depict the middle range of porosity measurements and thus define an envelope of typical or normal porosities.

Porosity-R_o trend lines representing composites of other formations are also shown in Figure 1-7. The dashed line labeled "type curve" was presented by Schmoker and Gautier (1989) as a typical porosity-thermal maturity curve for clastic rocks. The dashed lines labeled "10th percentile" and "90th percentile" are from Schmoker and Hester (1990) and form an envelope which encompasses 80% of their porosity data from various basins and formations. These three trend lines provide a reference framework against which to compare Mesaverde porosities.

Porosities of predominantly nonmarine Mesaverde sandstones are sometimes subjectively described as low. However, comparison to the reference lines of Figure 1-7 demonstrates that this is not the general case if levels of time-temperature exposure (R_o) are taken into consideration. In sharp contrast to J sandstone porosities, which decrease systematically as R_o increases (Figs. 1-3, 1-4), the middle porosity range of Mesaverde sandstones does not show an overall porosity decrease between R_o of 0.7% and 1.8% (Fig. 1-7). These R_o levels approximate the window of active HC generation (Tissot and Welte, 1984) for the type III kerogen present in nonmarine portions of the Mesaverde Group. Between R_o of 0.7% and 1.8%, Mesaverde sandstones have typical porosities in the 5% to 8% range (Fig. 1-7).

Figure 1-8 shows the 75th percentiles and the single highest measurements (connected by vertical lines) of the 31 Mesaverde porosity histograms, plotted as a function of R_o. These data depict the upper quartile of porosity measurements and thus define an envelope of above-average porosities. Two reference lines (dashed) are also shown in Figure 1-8. One marks the 8% porosity level, which is sometimes taken as an arbitrary lower cutoff for sandstone reservoirs. The other approximates the high-porosity limit of the data set.

The trends of above-average porosities (Fig. 1-8) parallel those of typical porosities (Fig. 1-7). For R_o between 0.7% and 1.8%, Mesaverde sandstones are likely to have some intervals in which porosity is greater than 8%; the maximum porosity in this thermal-maturity range is about 13% (Fig. 1-8).

Models for the porosity and porosity range of the J and Mesaverde sandstones predict quite different responses of porosity to increasing thermal maturity (Figs. 1-4, 1-7, and 1-8). However, both models result from the same empirical method of porosity prediction. This method is robust and offers a

sound general approach to the problem of porosity prediction in deeply buried sandstones.

Porosity Range at a Given R_o

The predictive porosity model of Figures 1-7 and 1-8 incorporates the porosity range at a given level of thermal maturity. Petrographic data reveal that factors favoring higher porosities in Mesaverde sandstones include proximity to the unconformity at the top of the Mesaverde Group, dissolution of early carbonate cement, larger grain size, and lower clay-matrix content. These factors are discussed as additional examples of the links between empirical porosity percentiles and causal geologic elements.

Hansley and Johnson (1980) noted that secondary porosity appears best developed immediately below the Tertiary-Cretaceous unconformity at the top of the Mesaverde Group. They associated enhanced dissolution with surface weathering. The unconformity might also have enhanced later-stage dissolution, in the subsurface, by focusing the flow of basin waters.

Porosities of Mesaverde sandstones greater than a few percent are unlikely if carbonate-cement percentage (as determined from point counts of thin sections) exceeds about 12%. As in the case of the J sandstone, carbonate cement might formerly have been widespread in intervals that have little such cement at present. Early carbonate cement could preserve the pore network from mechanical and chemical compaction during burial, compared to uncemented intervals; subsequent carbonate-cement dissolution could then create relatively high, secondary porosity.

Grain size can influence the rate and extent of burial diagenesis (Houseknecht, 1984, and references therein). Data to test for a relation between grain size and porosity in Mesaverde sandstones are plotted in Figure 1-9. The porosity ranges associated with the different grain-size categories are large and overlap. However, the midpoint porosity of each porosity range increases as grain size increases. These data (Fig. 1-9) indicate a weak relation between grain size and porosity, with porosity tending to be higher in sandstones of larger grain size.

Data to test for a relation between clay-matrix content and porosity in Mesaverde sandstones are plotted in Figure 1-10. Pseudomatrix and authigenic clays resulting from matrix recrystallization are included, to some extent, in the category of clay-matrix content. In direct contrast to the J sandstone (Fig. 1-5), Figure 1-10 shows no evidence of an association between optimum porosities and intermediate clay content. Although a predictive relation between clay-matrix content and porosity cannot be proposed, maximum porosity decreases systematically as matrix content increases (Fig. 1-10). Porosities greater than a few percent are improbable if clay-matrix content exceeds 8%.

The examples of the J and Mesaverde sandstones show how effects of geologic factors upon porosity range can be incorporated within a thermal-maturity framework.

PREDICTIVE POROSITY TRENDS FOR UNDIFFERENTIATED CRETACEOUS SANDSTONES OF ROCKY MOUNTAIN REGION

Introduction

In this section, porosity and vitrinite-reflectance data from Cretaceous sandstones of Rocky Mountain basins are combined in order to develop generic,

regional models for porosity as a function of R_o. As in the examples of preceding sections, the development of a predictive porosity model for Cretaceous sandstones of the Rocky Mountain region is intended primarily to illustrate approaches that can be applied to sandstones in general and deeply buried sandstones in particular.

The Cretaceous data set described in Table 1-2 represents formations in five different basins, a variety of geologic settings, and a wide range of thermal maturities and depths. The J sandstone and Mesaverde Group measurement suites of the preceding sections make up 57% of the combined data set.

Ideally, the measurement suites assembled here would represent a comprehensive sampling of all Rocky Mountain Cretaceous sandstones. In reality, the data set is limited (Table 1-2). Furthermore, wells in these basins are drilled according to specific selection criteria and do not provide an unbiased sampling of the subsurface. Nevertheless, the data set is thought to be sufficient to illustrate characteristics of generic, regional models for porosity and porosity range, in which porosity is based on the level of time-temperature exposure.

Porosity-Maturity Trends

Because R_o is proportional to integrated time-temperature history, which strongly influences burial diagenesis (Siever, 1983), porosity data from basins with different thermal and burial histories can be combined using R_o as the independent variable of comparison. Depth is sometimes used as the comparison variable, on the implicit assumption that depth is a direct measure of thermal and burial history. Although this assumption is valid for some geologic settings, it is invalid for Rocky Mountain basins. As shown in Figure 1-11, time-temperature exposure (R_o) cannot be accurately predicted on the basis of present depth within and between Rocky Mountain basins. Present depth is not a good measure of thermal and burial history in these basins and is therefore not a good parameter for combining the diverse Cretaceous sandstone porosity data of this study.

The 10th, 25th, 50th, 75th, and 90th percentiles (Fig. 1-1) of 107 porosity histograms, representing Cretaceous sandstones in the Denver, Green River, Powder River, Uinta, and Piceance basins (Table 1-2), are plotted against R_o in Figures 1-12 through 1-16. For each porosity percentile, an overall decrease of porosity with increasing R_o is apparent. Least-squares power-law regression lines with R_o as the independent variable are fit to the data of Figures 1-12 through 1-16 (Table 1-3). Correlation coefficients range between -0.60 and -0.76. These correlation coefficients (Table 1-3) are somewhat lower than those for the J sandstone data set (Table 1-1), as might be expected because of the greater geologic diversity and thermal-maturity range of the regional Cretaceous data set. For 107 data points, a correlation coefficient of -0.22 would be significant at the one-percent level (Till, 1974).

The fraction of the total variance explained by the regression lines of Figures 1-12 through 1-16 increases from 0.36 for the 10th porosity percentile to 0.58 for the 90th percentile (Table 1-3). The higher porosity percentiles are thus modeled with more confidence than the lower percentiles. A power-function relation of porosity to R_o explains slightly more than one-half of the porosity variance of the 50th, 75th, and 90th percentiles (Table 1-3).

For these diverse Rocky Mountain Cretaceous sandstones, the effect of time-temperature history upon porosity change in the subsurface is at least equal to that of all other factors combined.

The porosity-R_o regression lines of Figures 1-12 through 1-16 together provide a possible empirical framework for estimating the porosity and the porosity range of Cretaceous sandstones in Rocky Mountain basins. The Cretaceous sandstone porosity model (Fig. 1-17) is analogous in concept and similar in overall appearance to the J sandstone porosity model (Fig. 1-4). However, the two porosity models differ in detail.

First, the five regression-line slopes of the Cretaceous sandstone porosity model are equal, within error limits, whereas those of the J sandstone porosity model decrease systematically as porosity percentile increases. Second, the 50th-percentile regression-line slope of the Cretaceous sandstone porosity model is less steep than that of the J sandstone porosity model. As illustrated by comparison to a "type curve" (Fig. 1-17), this slope is also less steep than is typical of other sandstone data sets.

Examination of the relation between the regression lines of Figures 1-12 through 1-16 and the data points from which they are derived reveals the principal reason for the differences between the J sandstone (Fig. 1-4) and Rocky Mountain Cretaceous sandstone (Fig. 1-17) porosity models. For R_o less than about 0.7% and greater than about 1.2%, the regression lines systematically underestimate the actual porosity values; between R_o of roughly 0.7 and 1.2%, the regression lines systematically overestimate the actual porosity values. Thus, variations about the regression lines are not random. Although the correlation coefficients are fairly high, single regression lines fit to the entire R_o range do not reflect the internal structure of the Rocky Mountain Cretaceous sandstone data set.

Alternative Porosity Model

A second possible empirical approach for estimating the porosity and the porosity range of Cretaceous sandstones in Rocky Mountain basins is shown in Figure 1-18. This alternative predictive porosity framework is composed of two elements, in an effort to represent the porosity-R_o data better than regression lines fit to the entire R_o range (Fig. 1-17). The trend lines of models A (Fig. 1-18A) and B (Fig. 18B) are subjectively drawn to fit the data of Figures 1-12 through 1-16.

Model A applies to strata in which porosity continues to decrease at a uniform rate as R_o increases above 0.9%. Model B applies to strata in which the rate of porosity loss becomes more gradual as R_o increases above 0.9%. (The change in slope may be more gradational than is shown in Figure 1-18B.) For R_o less than 0.9%, models A and B are identical.

Models A and B do not directly reflect variability in rock properties such as grain size and sorting, shale content and composition of framework grains. The effects upon porosity of these factors are already incorporated in the porosity range defined by the 10th through 90th porosity percentiles. Rather, models A and B are interpreted as representing sandstones in which porosity evolution follows one of two fundamentally different pathways. Models A and B are derived from observation of porosity-R_o crossplot patterns and represent a working hypothesis that, because of a paucity of data, is at present supported only by circumstantial evidence.

The predictive porosity models of Figure 1-17 and Figure 1-18A are conceptually similar in that each line segment spans the entire thermal-maturity range. Such models implicitly assume that the net effect upon porosity of various diagenetic processes, operative at different levels of thermal maturity, can be approximated by single power functions over a large R_o range. This assumption does not seem obvious, but is empirically supported by a number of published data sets (Schmoker and Gautier, 1988, 1989; Schmoker and Hester, 1990; Schmoker and Higley, 1991). A single porosity-R_o power function spanning a large R_o range is analogous to a single porosity-depth exponential function spanning a large depth range (Schmoker and Gautier, 1988). Such porosity-depth exponential curves are common in the literature, although the underlying assumptions are rarely discussed.

The line segments of Figure 1-18B change slope as R_o increases. Such porosity models implicitly assume that the net effect upon porosity of various diagenetic processes varies as different processes wax and wane during burial. Figure 1-18B could not be depicted by a single exponential curve in the porosity-depth domain.

The choice of diagenetic pathway (model A versus model B) is important for sandstone porosity prediction in deep portions of Rocky Mountain basins. At R_o= 2.0%, for example, model A predicts median porosities of about 2% and 90th-percentile porosities of only 4%; in contrast, model B predicts median porosities of about 5% and 90th-percentile porosities of 8%. Extrapolating beyond the data to R_o=3.0%, model A predicts 10th- through 90th-percentile porosities to all be less than 3%, whereas model B predicts some porosities of 6-7%. Reference to Figure 1-11 shows that maximum depths of economic production predicted by model A in a given area of a basin would be thousands of ft less than those predicted by model B.

As is apparent from the foregoing porosity comparisons, the hypothesis that porosity evolution can follow distinctly different pathways as R_o increases above 0.9% has significant implications for the economic production of deeply buried HC's. An understanding as to which sandstones follow models analogous to A and which follow models analogous to B is important. At this point, however, such understanding is uncertain, and the following discussion of cause and effect is speculative.

The particular strata of the data set which conform to model B are from the Almond Formation in the Green River basin and the Mesaverde Group (marine and nonmarine) in the Piceance basin (Table 1-2). Low-permeability sandstones in both formations are commonly overpressured at R_o greater than 0.9% due to HC generation (Spencer, 1987). It is thus possible that some Cretaceous sandstones of Rocky Mountain basins do not follow "normal" diagenetic pathways (Fig. 1-18A) because of the effects upon diagenesis of HC generation from adjacent and intercalated coals and organic-rich shales.

Hydrocarbon generation, of which overpressuring in the non-subsiding basins of the Rocky Mountain region is evidential (Spencer, 1987), might retard porosity loss as R_o increases (Fig. 1-18B) in at least three ways. First, HC's can inhibit cementation by displacing pore water. Second, carbon dioxide (Schmidt and McDonald, 1979) and organic acids (Surdam and others, 1989) produced by the thermal breakdown of kerogen can create secondary porosity by dissolving cements and framework grains. Third, overpressuring can slow pressure solution and associated porosity decrease by reducing the

lithostatic load; overpressuring can also reduce cementation by developing a fluid-flow system characterized by expulsion, rather than exchange, of liquids.

If HC generation is indeed the primary underlying process causing some sandstones to deviate from porosity-R_o trends similar to those of Figure 1-18A and follow instead trends similar to those of Figure 1-18B, then the results and discussion of this section are not restricted to Rocky Mountain Cretaceous sandstones.

SUMMARY AND CONCLUSIONS

This paper describes empirical porosity trends in sandstones. Empirical descriptions are of limited value, however, if progress is not made toward predictive models. Sandstone porosity is linked here with thermal maturity, rock properties, and HC generation. These parameters are useful in predictive porosity models because they can often be anticipated in advance of the drill.

The overall decrease of sandstone porosity during burial is treated as a function of thermal maturity as represented by vitrinite reflectance. In this context, R_o serves as a generalized index of burial history rather than as a specialized indicator of kerogen decomposition. Complicating the picture, however, the data show that the response of sandstone porosity to increasing thermal maturity may depend in part on the presence or absence of HC generation and overpressuring.

The range of porosity at a given level of thermal maturity is not obscured by averaging but is depicted by porosity-R_o trends representing the 10th, 25th, 50th, 75th, and 90th porosity percentiles. Effects upon porosity of variations in rock properties are thus taken into account.

Data from Cretaceous sandstones of Rocky Mountain basins are used to illustrate and test methods for predicting the porosity and porosity range of sandstones. Most of these Cretaceous sandstones are not deeply buried, but the availability of porosity, vitrinite-reflectance, and rock-property data makes them useful formations for developing approaches to porosity prediction. These approaches can be applied to deeply buried sandstones in general.

REFERENCES CITED

Athy, L.F., 1930, Density, porosity, and compaction of sedimentary rocks: American Association of Petroleum Geologists Bulletin, v. 14, no. 1, p. 1-24.

Baldwin, Brewster, and Butler, C.O., 1985, Compaction curves: American Association of Petroleum Geologists Bulletin, v. 69, no. 4, p. 622-626.

Bloch, S., 1991, Empirical prediction of porosity and permeability in sandstones: American Association of Petroleum Geologists Bulletin, v. 75, no. 7, p. 1145-1160.

Cassan, J.P., Garcia-Palacios, M.C., Fritz, Bertrand, and Tardy, Yves, 1981, Diagenesis of sandstone reservoirs as shown by petrographical and geochemical analysis of oil bearing formations in the Gabon basin: Bulletin des Centres de Recherches Exploration-Production Elf-Aquitaine, Pau, France, v. 5, no. 1, p. 113-135.

Cleveland, W.S., 1985, The elements of graphing data: Monterey, California, Wadsworth Advanced Books and Software, 323 p.

Coalson, E.B., ed., 1989, Petrogenesis and petrophysics of selected sandstone reservoirs of the Rocky Mountain region: Rocky Mountain Association of Geologists, Denver, 353 p.

Hansley, P.L., and Johnson, R.C., 1980, Mineralogy and diagenesis of low-permeability sandstones of Late Cretaceous age, Piceance Creek basin, northwestern Colorado: The Mountain Geologist, v. 17, no. 4, p. 88-106.

Higley, D.K., and Schmoker, J.W., 1989, Influence of depositional environment and diagenesis on regional porosity trends in the Lower Cretaceous "J" sandstone, Denver basin, Colorado, *in* Coalson, E.B., ed., Petrogenesis and petrophysics of selected sandstone reservoirs of the Rocky Mountain region: Rocky Mountain Association of Geologists, Denver, p. 183-196, 334-335.

Houseknecht, D.W., 1984, Influence of grain size and temperature on intergranular pressure solution, quartz cementation, and porosity in a quartzose sandstone: Journal of Sedimentary Petrology, v. 54, no. 2, p. 348-361.

Keighin, C.W., and Fouch, T.D., 1981, Depositional environments and diagenesis of some nonmarine Upper Cretaceous reservoir rocks, Uinta basin, Utah, *in* Ethridge, F.G., and Flores, R.M., eds., Recent and ancient nonmarine depositional environments: Models for exploration: Society of Economic Paleontologists and Mineralogists Special Publication No. 31, p. 109-125.

Keighin, C.W., Law, B.E., and Pollastro, R.M., 1989, Petrology and reservoir characteristics of the Almond Formation, greater Green River basin, Wyoming, *in* Coalson, E.B., ed., Petrogenesis and petrophysics of selected sandstone reservoirs of the Rocky Mountain region: Rocky Mountain Association of Geologists, Denver, p. 281-298, 344-347.

Land, C.B., and Weimer, R.J., 1978, Peoria field, Denver basin, Colorado--J sandstone distributary channel reservoir, *in* Pruit, J.D., and Coffin, P.E., eds., Energy resources of the Denver basin: Rocky Mountain Association of Geologists, Denver, p. 81-104.

Lyons, D.J., 1978, Sandstone reservoirs: Petrography, porosity-permeability relationship, and burial diagenesis: Report 8, Technology Research Center, Japan National Oil Corporation, Tokyo, December, p. 1-69.

Lyons, D.J., 1979, Organic metamorphism and sandstone porosity prediction from acoustic data: Report 9, Technology Research Center, Japan National Oil Corporation, Tokyo, March, p. 1-51.

Maxwell, J.C., 1964, Influence of depth, temperature, and geologic age on porosity of quartzose sandstone: American Association of Petroleum Geologists Bulletin, v. 48, no. 5, p. 697-709.

Pitman, J.K., Anders, D.E., Fouch, T.D., and Nichols, D.J., 1986, Hydrocarbon potential of nonmarine Upper Cretaceous and Lower Tertiary rocks, eastern Uinta basin, Utah, *in* Spencer, C.W., and Mast, R.F., eds., Geology of tight gas reservoirs: American Association of Petroleum Geologists Studies in Geology No. 24, p. 235-252.

Pitman, J.K., Franczyk, K.J., and Anders, D.E., 1987, Marine and nonmarine gas-bearing rocks in Upper Cretaceous Blackhawk and Neslen Formations,

eastern Uinta basin, Utah: Sedimentology, diagenesis, and source rock potential: American Association of Petroleum Geologists Bulletin, v. 71, no. 1, p. 76-94.

Pitman, J.K., Franczyk, K.J., and Anders, D.E., 1988, Diagenesis and burial history of nonmarine Upper Cretaceous rocks in the central Uinta basin, Utah: U.S. Geological Survey Bulletin 1787-D, 24 p.

Scherer, M., 1987, Parameters influencing porosity in sandstones: A model for sandstone porosity prediction: American Association of Petroleum Geologists Bulletin, v. 71, no. 5, p. 485-491.

Schmidt, Volkmar, and McDonald, D.A., 1979, The role of secondary porosity in the course of sandstone diagenesis, *in* Scholle, P.A., and Schluger, P.R., eds., Aspects of diagenesis: Society of Economic Paleontologists and Mineralogists Special Publication No. 26, p. 175-207.

Schmoker, J.W., and Gautier, D.L., 1988, Sandstone porosity as a function of thermal maturity: Geology, v. 16, no. 11, p. 1007-1010.

Schmoker, J.W., and Gautier, D.L., 1989, Compaction of basin sediments: Modeling based on time-temperature history: Journal of Geophysical Research, v. 94(B), no. 6, p. 7379-7386.

Schmoker, J.S., and Hester, T.C., 1990, Regional trends of sandstone porosity versus vitrinite reflectance--a preliminary framework, *in* Nuccio, V.F., and Barker, C.E., eds., Applications of thermal maturity studies to energy exploration: Rocky Mountain Section-SEPM, Denver, p. 53-60.

Schmoker, J.W., and Higley, D.K., 1991, Porosity trends of the Lower Cretaceous J sandstone, Denver basin, Colorado: Journal of Sedimentary Petrology, v. 61, no. 6, p. 909-920.

Schmoker, J.W., Nuccio, V.F., and Pitman, J.K., 1992, Porosity trends in predominantly nonmarine sandstones of the Upper Cretaceous Mesaverde Group, Uinta and Piceance basins, Utah and Colorado, *in* Fouch, T.D., Nuccio, V.F., and Chidsey, T.C., eds., Hydrocarbon and mineral resources of the Uinta basin, Utah and Colorado: Utah Geological Association Guidebook 21, in press.

Siever, Raymond, 1983, Burial history and diagenetic reaction kinetics: American Association of Petroleum Geologists Bulletin, v. 67, no. 4, p. 684-691.

Spencer, C.W., 1987, Hydrocarbon generation as a mechanism for overpressuring in Rocky Mountain region: American Association of Petroleum Geologists Bulletin, v. 71, no. 4, p. 368-388.

Spencer, C.W., and Keighin, C.W., eds., 1984, Geologic studies in support of the U.S. Department of Energy Multiwell Experiment, Garfield County, Colorado: U.S. Geological Survey Open-File Report 84-757, 134 p.

Surdam, R.C., Crossey, L.J., Hagen, E.S., and Heasler, H.P., 1989, Organic-inorganic interactions and sandstone diagenesis: American Association of Petroleum Geologists Bulletin, v. 73, no. 1, p. 1-23.

Tainter, P.A., 1984, Stratigraphic and paleostructural controls on hydrocarbon migration in Cretaceous D and J sandstones of the Denver basin, *in*

Woodward, Jane, Meissner, F.F., and Clayton, J.L., eds., Hydrocarbon source rocks of the greater Rocky Mountain region: Rocky Mountain Association of Geologists, Denver, p. 339-354.

Till, Roger, 1974, Statistical methods for the earth scientist: New York, John Wiley and Sons, 154 p.

Tissot, B.P., and Welte, D.H., 1984, Petroleum formation and occurrence, second edition: New York, Springer-Verlag, 699 p.

van de Kamp, P.C., 1976, Inorganic and organic metamorphism in siliciclastic rocks (abs): American Association of Petroleum Geologists Bulletin, v. 60, no. 4, p. 729.

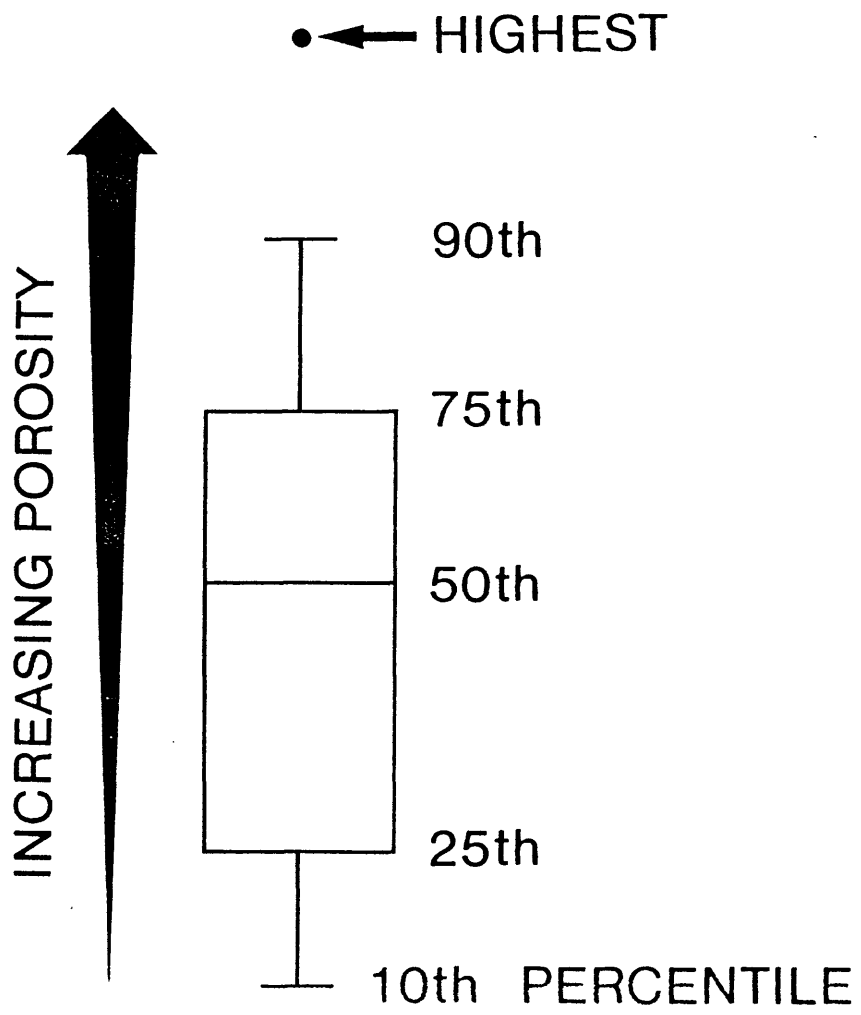

Figure 1-1. Box diagram (described by Cleveland, 1985) illustrating data format used to develop porosity-R_o trends. Porosity distribution of each measurement suite is represented by 10th, 25th, 50th, 75th, and 90th porosity percentiles, as well as by single highest porosity measurement.

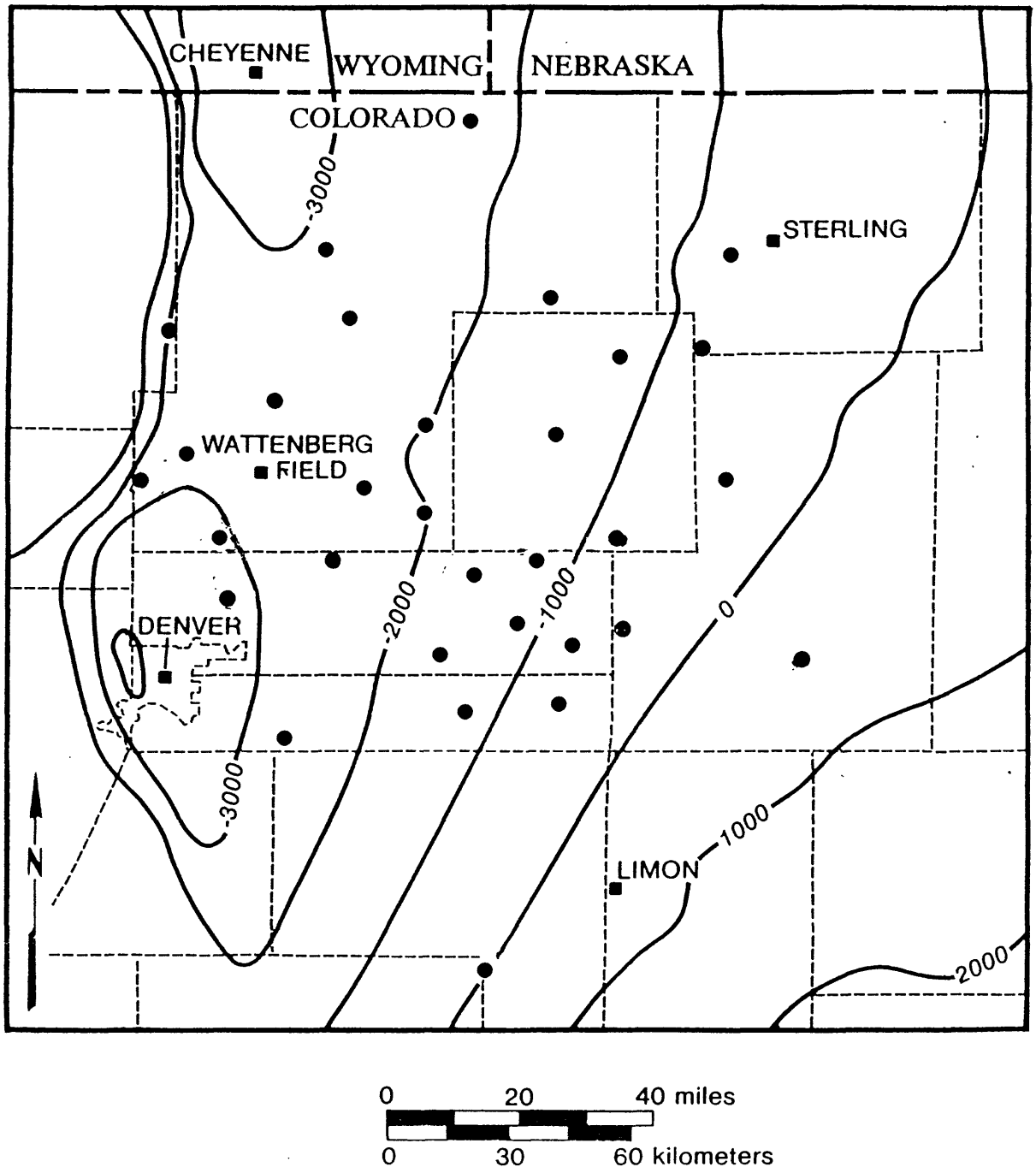

Figure 1-2. Map of study area in Denver basin showing location of wells from which J sandstone porosity and vitrinite-reflectance data were obtained. Contours map structure on top of J sandstone using sea-level datum (after Higley and Schmoker, 1989). Contour interval is 1,000 ft (300 m).

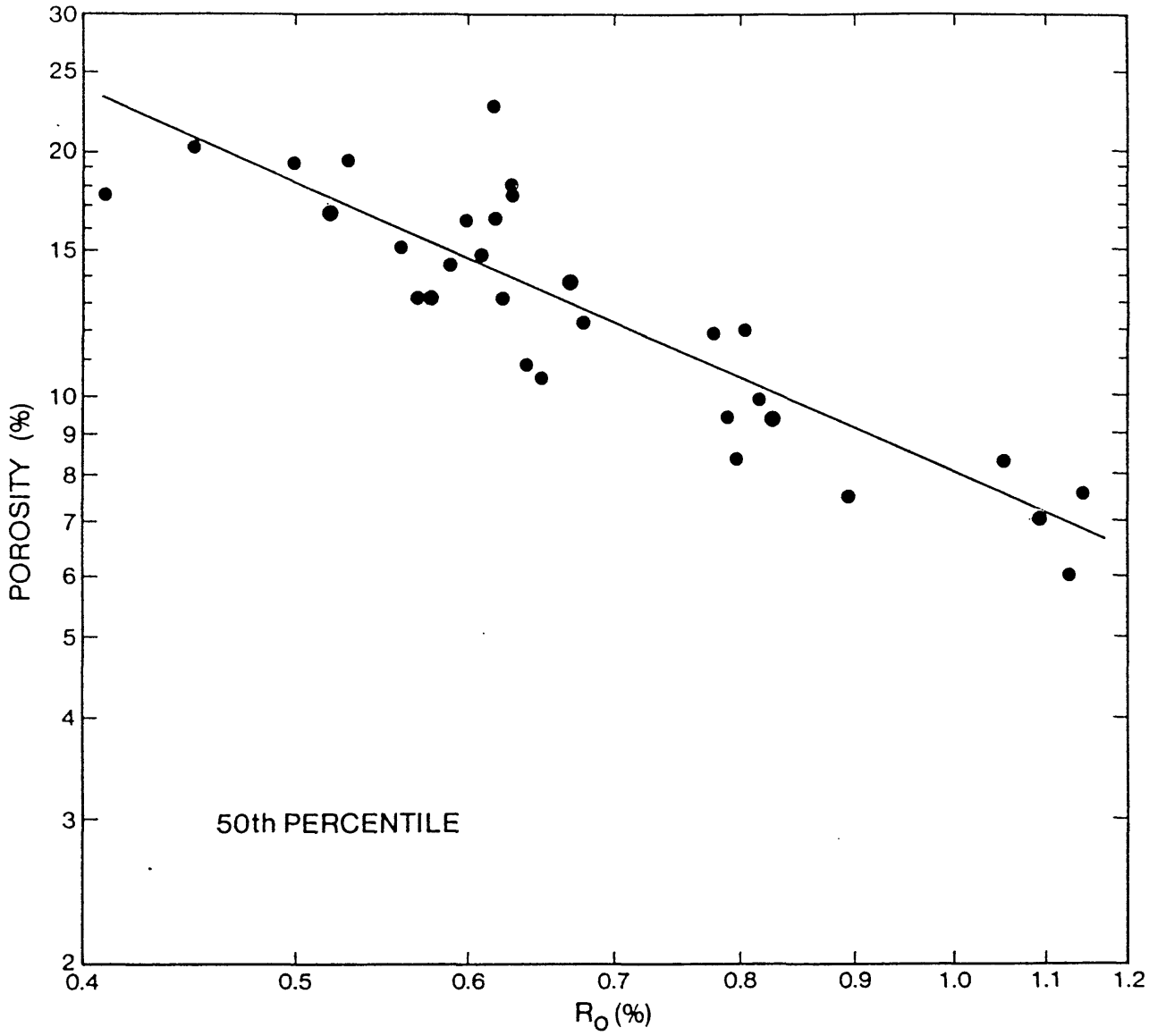

Figure 1-3. Example showing porosity versus vitrinite reflectance for 50th percentile of J sandstone porosity distributions, 31 wells (Fig. 2) of Denver basin. Coefficients for least-squares fit to data (line) are given in Table 1-1.

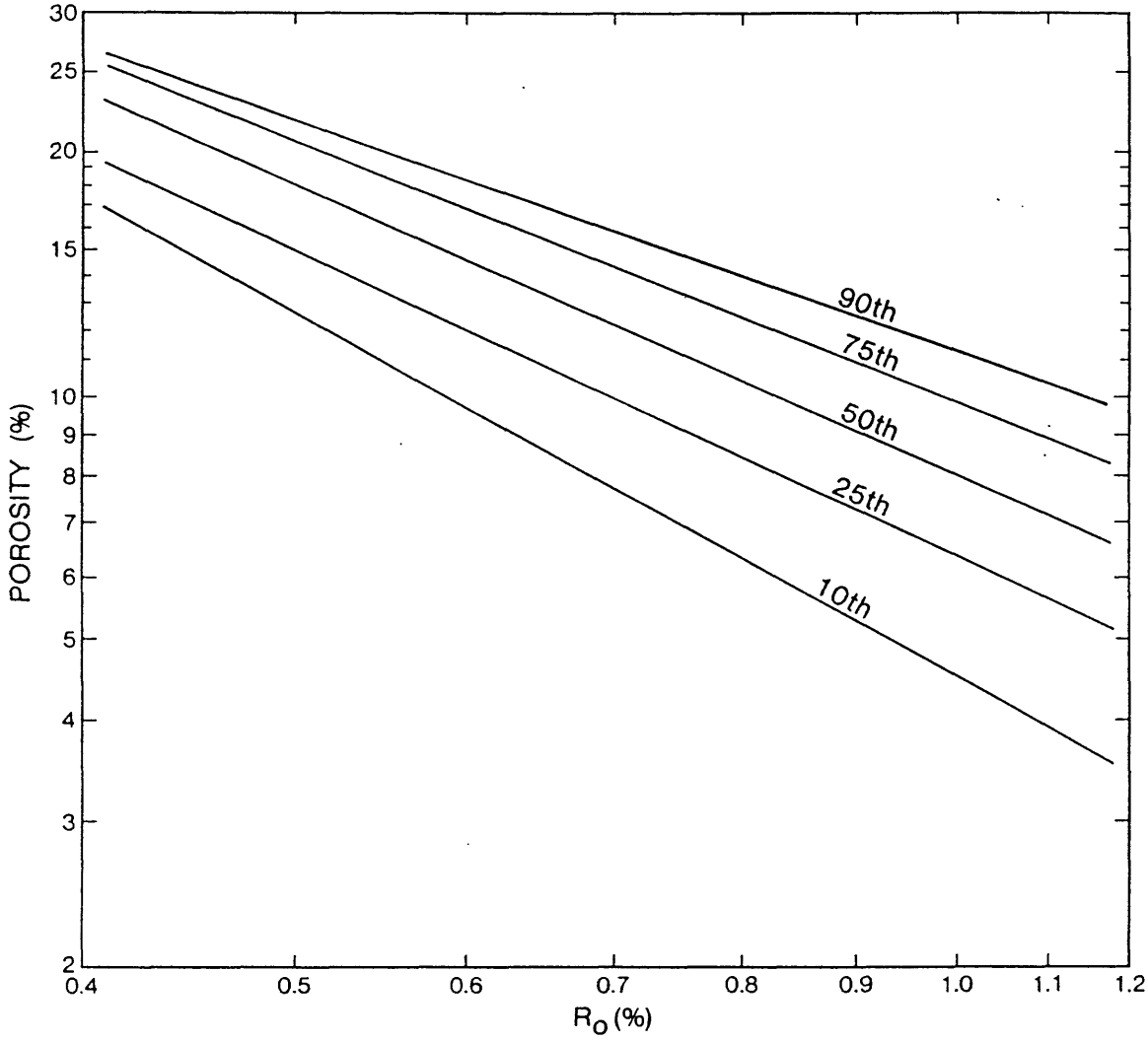

Figure 1-4. Porosity-vitrinite reflectance regression lines (as illustrated by example of Figure 3) representing 10th, 25th, 50th, 75th, and 90th porosity percentiles, J sandstone, Denver basin. Regression lines are documented in Table 1-1. These trend lines constitute an empirical, predictive porosity model for the J sandstone.

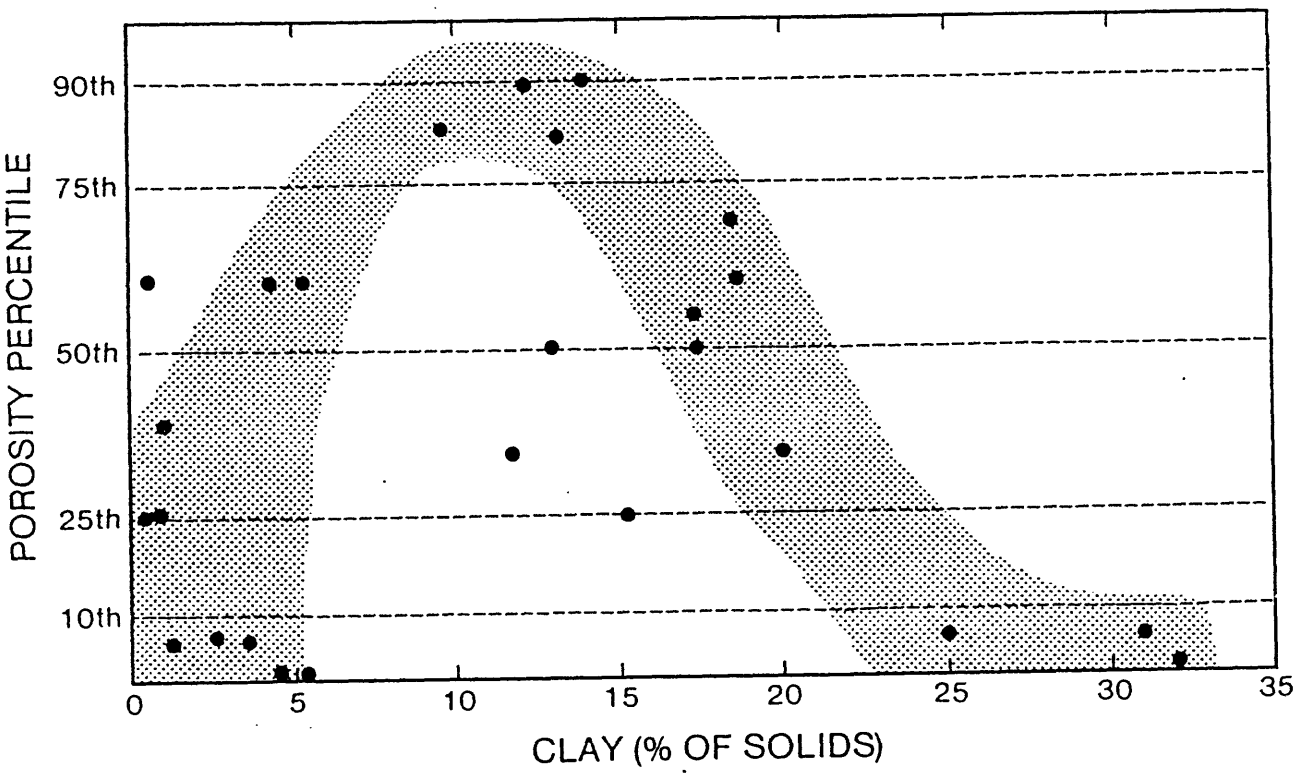

Figure 1-5. Point-count porosity, expressed relative to porosity-percentile trend lines of Figure 1-4, versus clay content, J sandstone, Denver basin. Interpretation of basic trend is shaded. For purposes of this figure, clay is defined as mudstone clasts, detrital clay, and authigenic illite/smectite and chlorite.

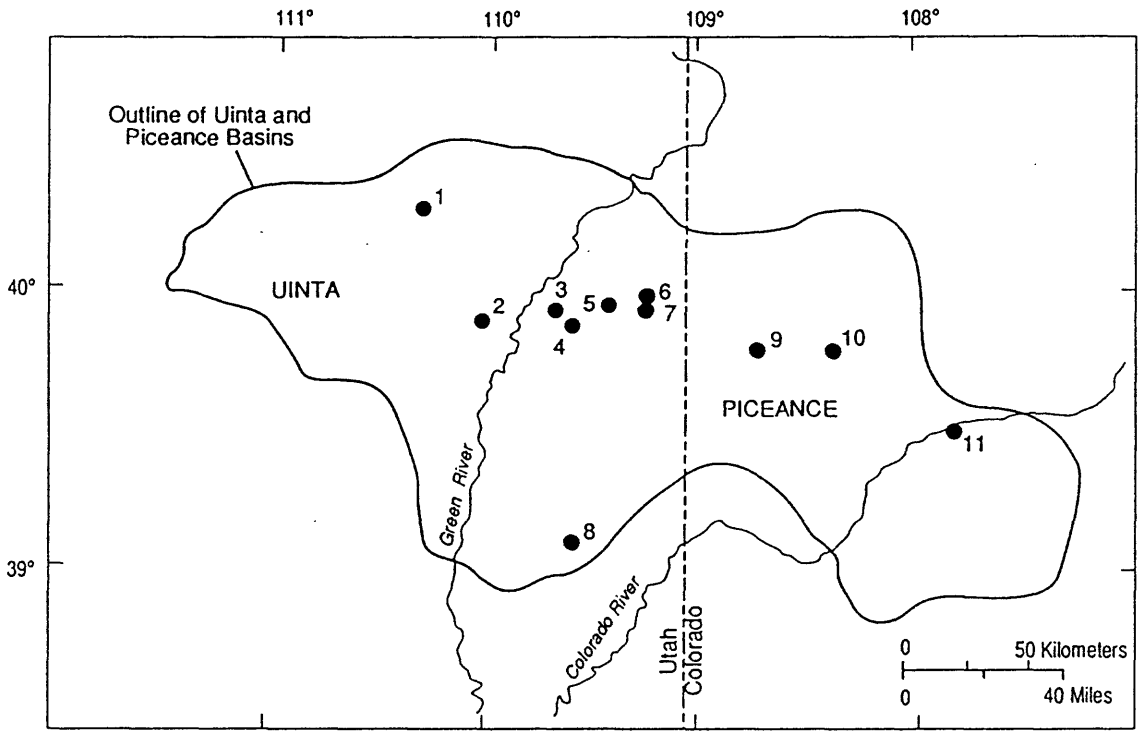

Figure 1-6. Map of study area in Piceance and Uinta basins showing location of wells from which porosity data representing sandstones of Mesaverde Group are obtained.

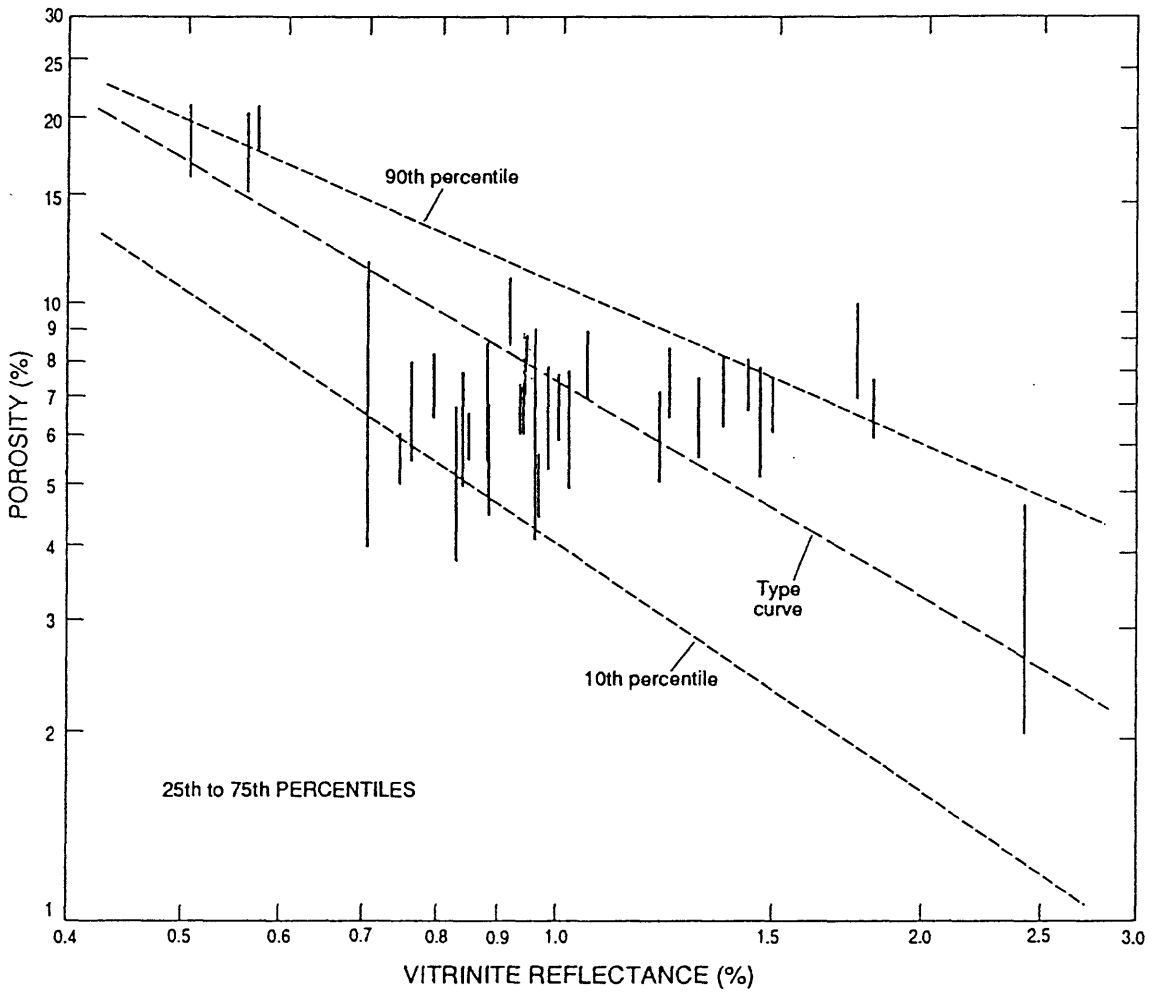

Figure 1-7. Porosity versus vitrinite reflectance for 25th and 75th percentiles (connected by vertical lines) of Mesaverde porosity distributions, 11 locations (Fig. 1-6) in Piceance and Uinta basins. "Type curve", "10th percentile", and "90th percentile" dashed lines provide a reference framework that represents sandstones in general (Schmoker and Gautier, 1989; Schmoker and Hester, 1990).

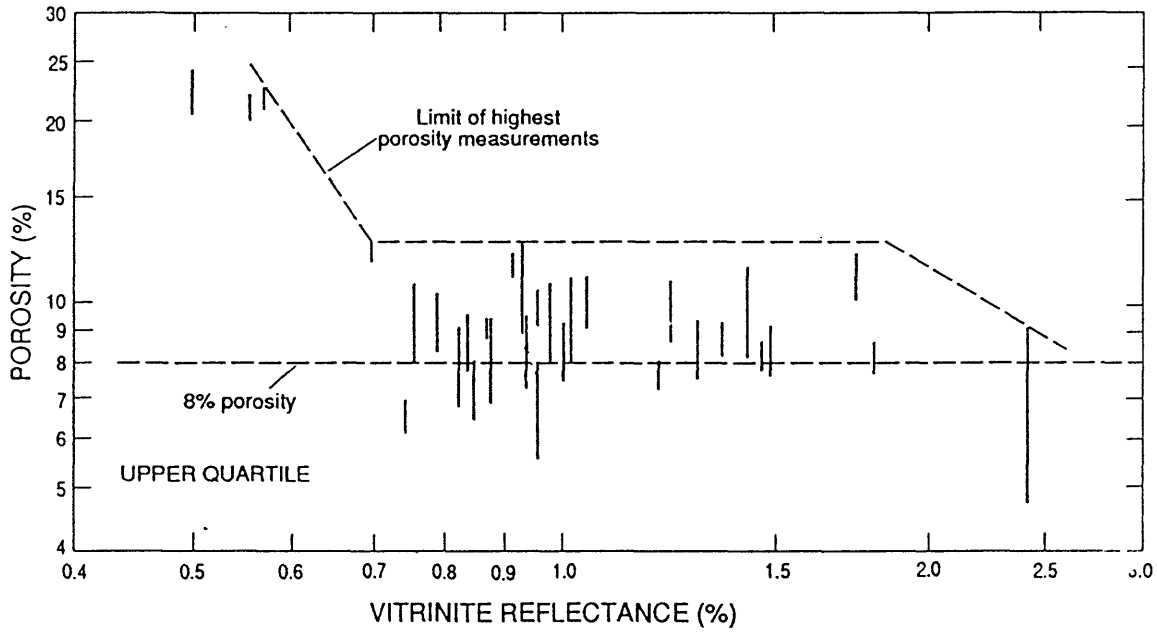

Figure 1-8. Porosity versus vitrinite reflectance for 75th percentiles and single highest measurements (connected by vertical lines) of Mesaverde porosity distributions, 11 locations (Fig. 1-6) in Piceance and Uinta basins.

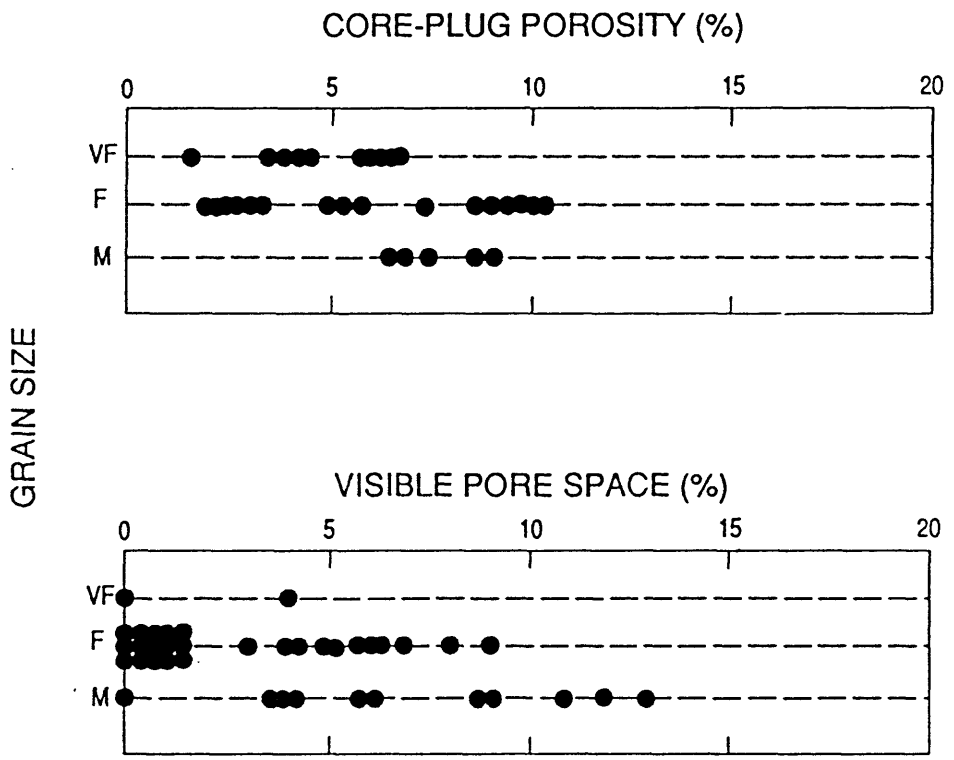

Figure 1-9. Core-plug porosity and visible pore space (determined from point counts) as a function of grain size, Mesaverde sandstones. Data are from Colorado Interstate Gas Exploration Natural Buttes 21 well, 15-T10S-R22E, Uintah Co., Utah (number 5 of Fig. 1-6) (Pitman and others, 1986, 1987). Very fine (VF) = 62-125 microns; fine (F) = 125-250 microns; medium (M) = 250-500 microns.

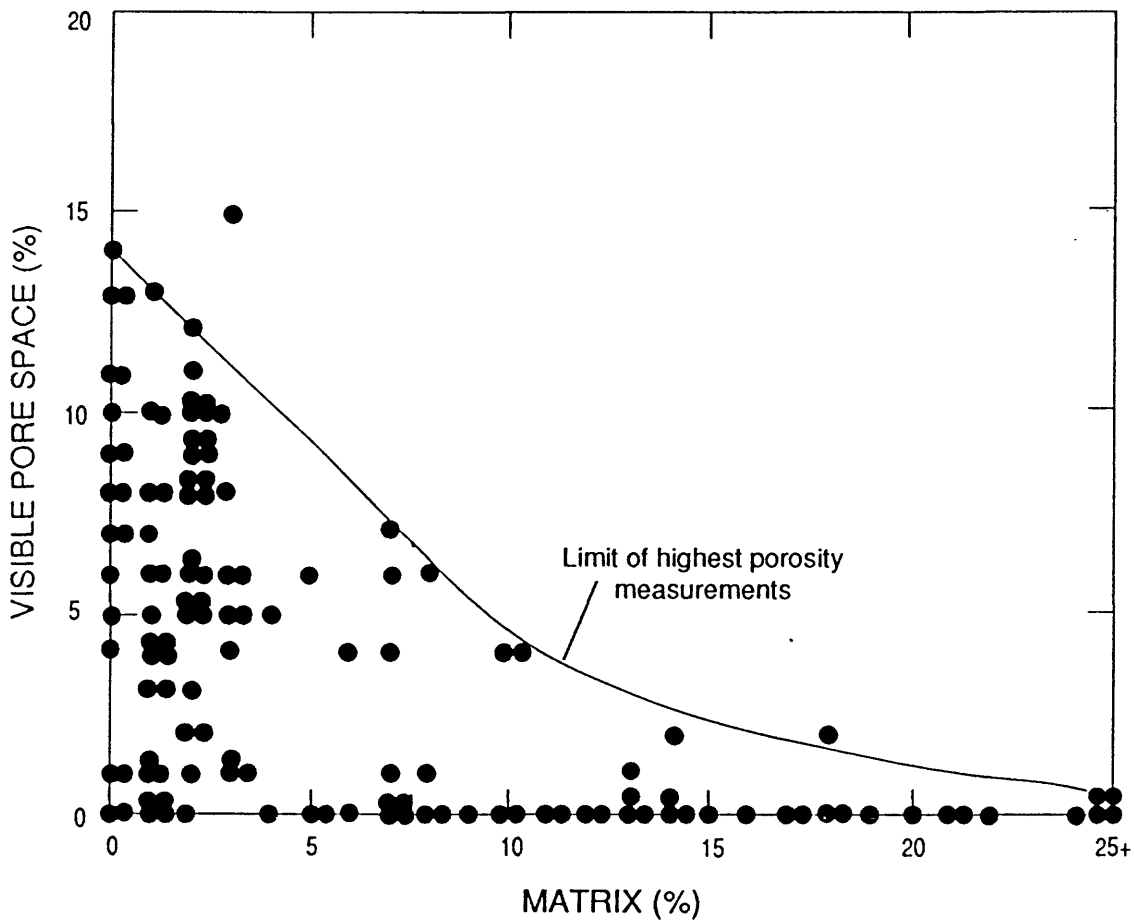

Figure 1-10. Point-count data showing visible pore space as a function of clay-matrix content, Mesaverde sandstones. Data are from Natural Buttes 21 well (see Figure 9 caption) and Exxon Wilkin Ridge 1 well, 29-T10S-R17E, Duchesne Co., Utah (number 2 of Fig. 1-6) (Pitman and others, 1988). Mesaverde R_o values in these two wells are similar (0.75-0.95%).

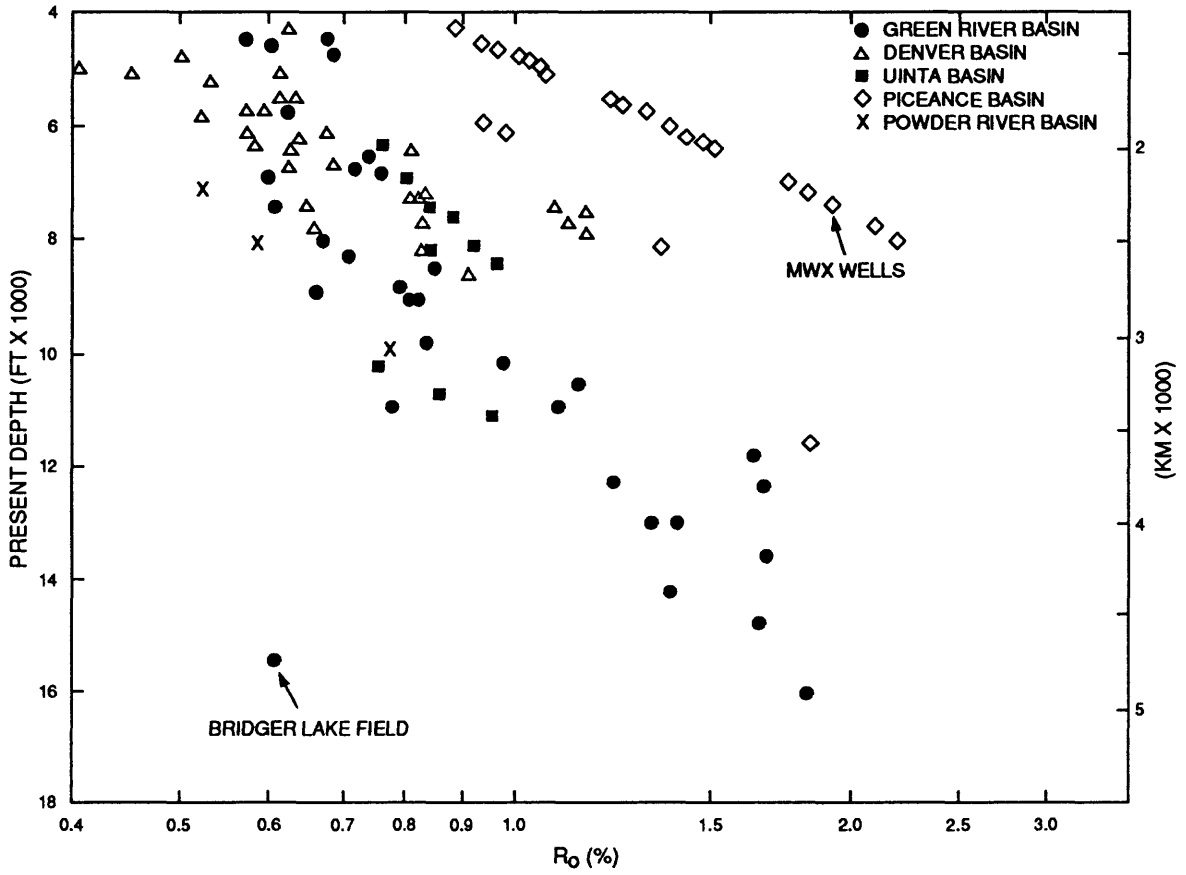

Figure 1-11. Present depth versus vitrinite reflectance for rocks of Cretaceous sandstone data set, Rocky Mountain basins (Table 1-2). Trend labeled "MWX wells" refers to U.S. Department of Energy Multiwell Experiment, Garfield County, Colorado (Spencer and Keighin, 1984). Present depth of rocks at a given R_o can vary by many thousands of feet because of intra- and interbasinal variations in thermal and burial histories.

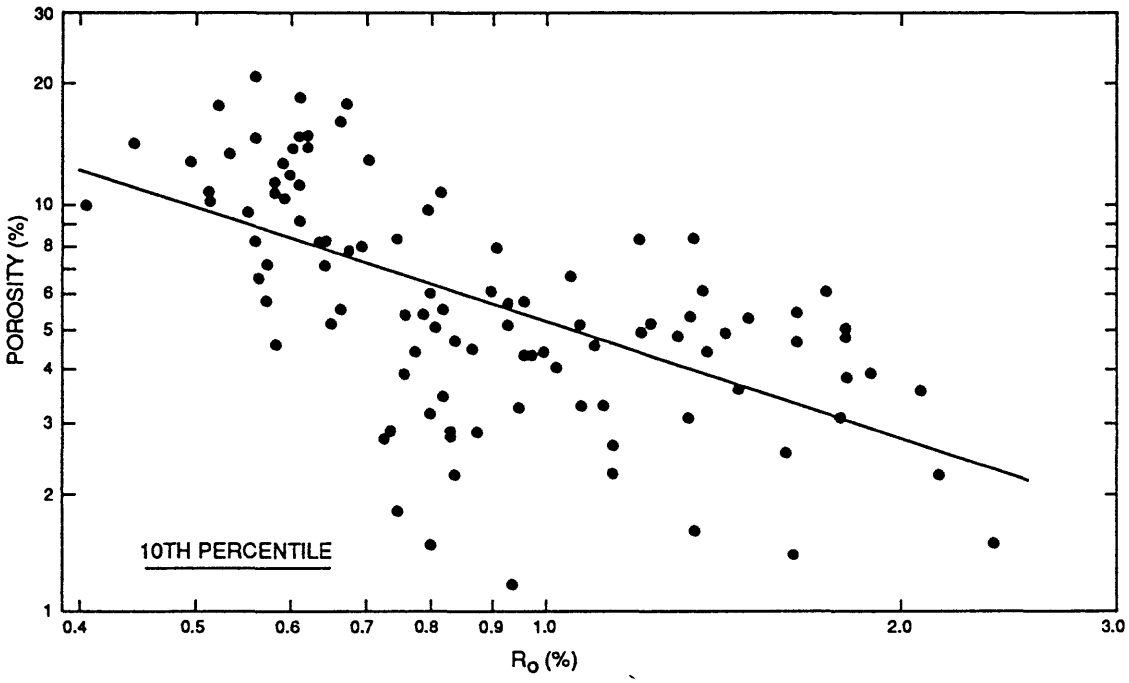

Figure 1-12. Porosity versus vitrinite reflectance for 10th percentile of Cretaceous sandstone data set, Rocky Mountain basins (Table 1-2). For Figures 1-12 through 1-16, parameters for least-squares fit to data (line) are given in Table 1-3.

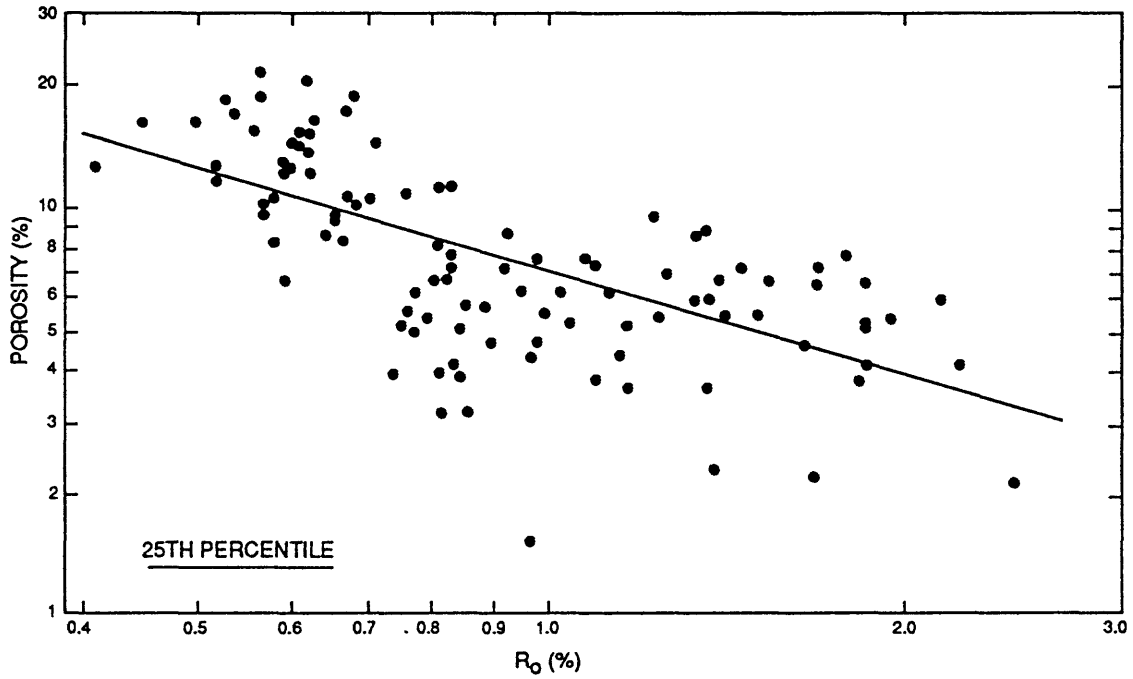

Figure 1-13. Porosity versus vitrinite reflectance for 25th percentile of Cretaceous sandstone data set, Rocky Mountain basins (Table 1-2).

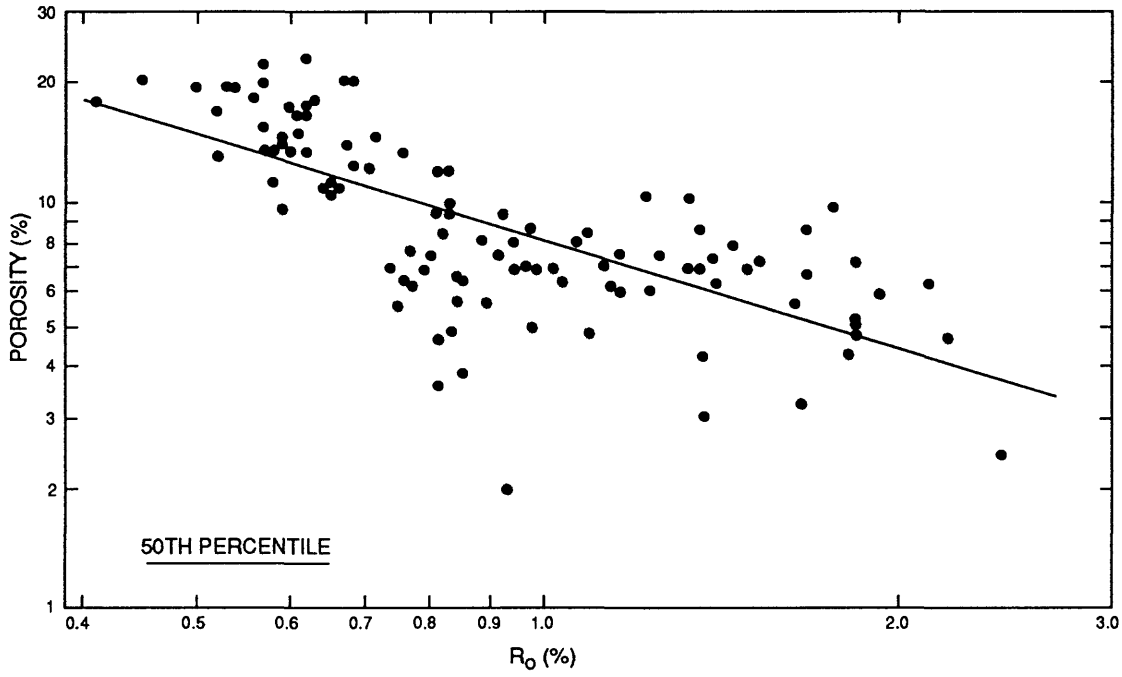

Figure 1-14. Porosity versus vitrinite reflectance for 50th percentile of Cretaceous sandstone data set, Rocky Mountain basins (Table 1-2).

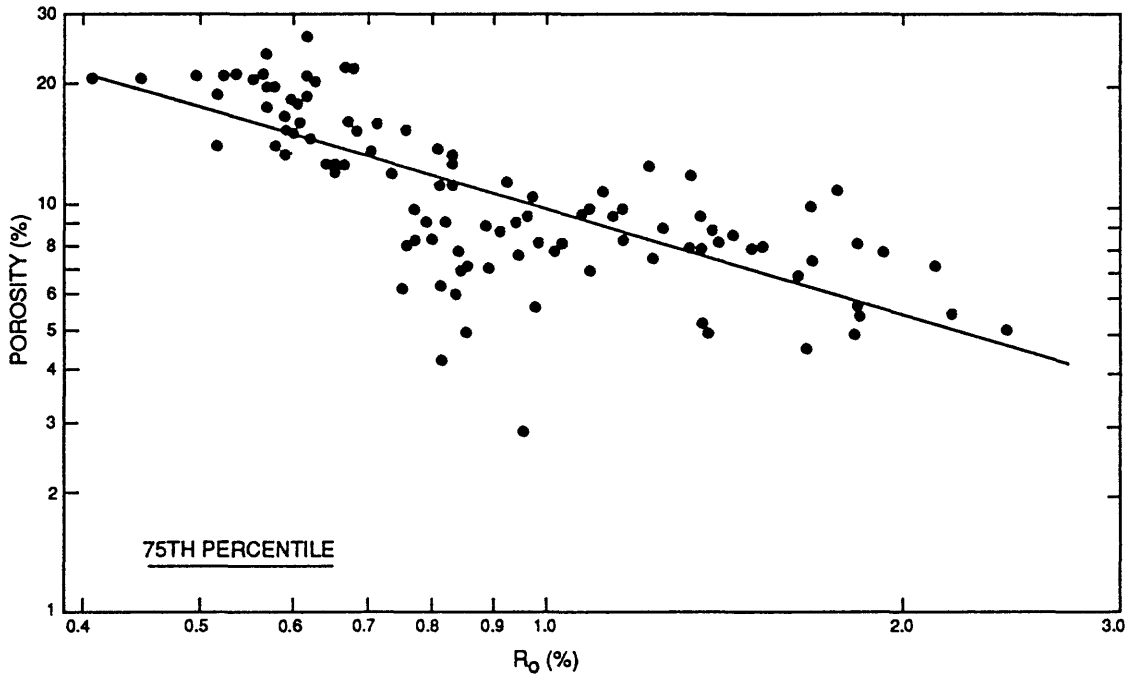

Figure 1-15. Porosity versus vitrinite reflectance for 75th percentile of Cretaceous sandstone data set, Rocky Mountain basins (Table 1-2).

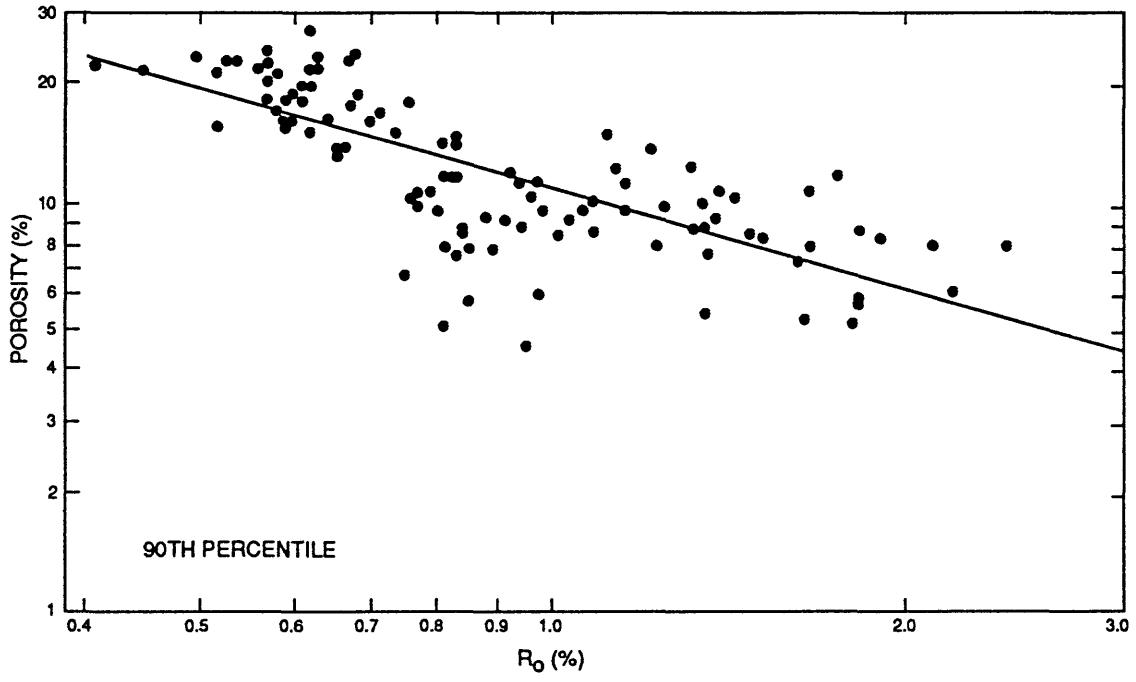

Figure 1-16. Porosity versus vitrinite reflectance for 90th percentile of Cretaceous sandstone data set, Rocky Mountain basins (Table 1-2).

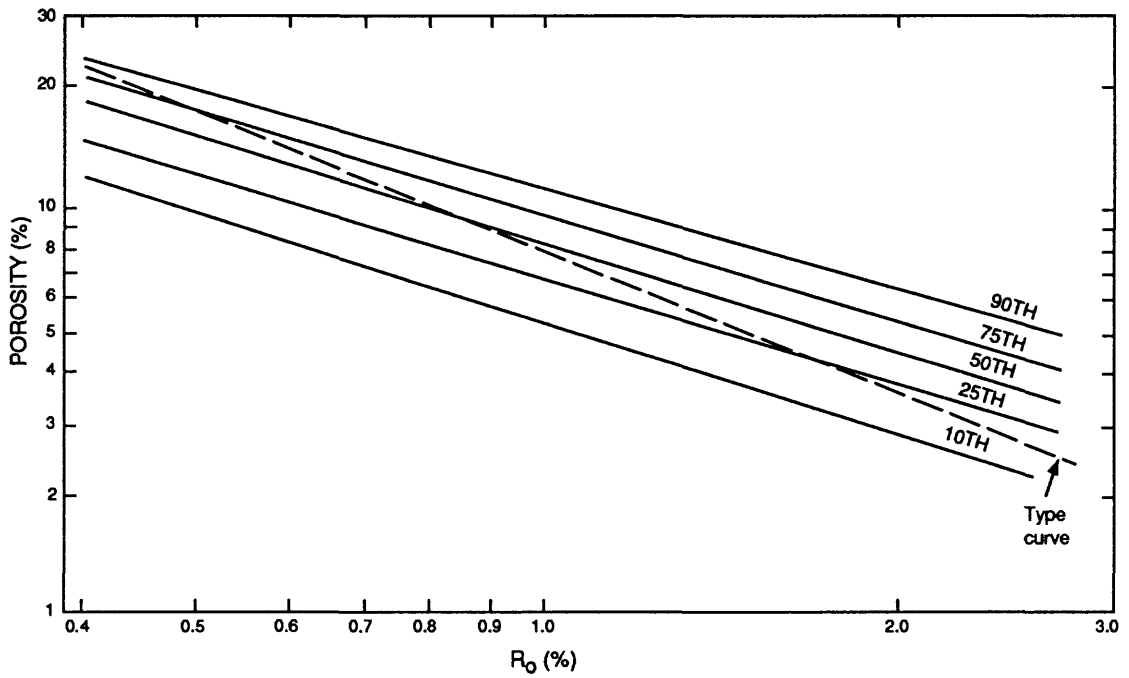

Figure 1-17. Summary figure showing regression lines representing 10th, 25th, 50th, 75th, and 90th porosity percentiles (Figs. 1-12 thropugh 1-16), Cretaceous sandstone data set, Rocky Mountain basins. These trend lines constitute a possible empirical, predictive porosity model for Cretaceous sandstones of the Rocky Mountain region. An alternative model is presented in Figure 1-18. Dashed "type curve" (also shown in Figures 1-7 and 1-18) provides a reference line that represents sandstones in general (Schmoker and Gautier, 1989).

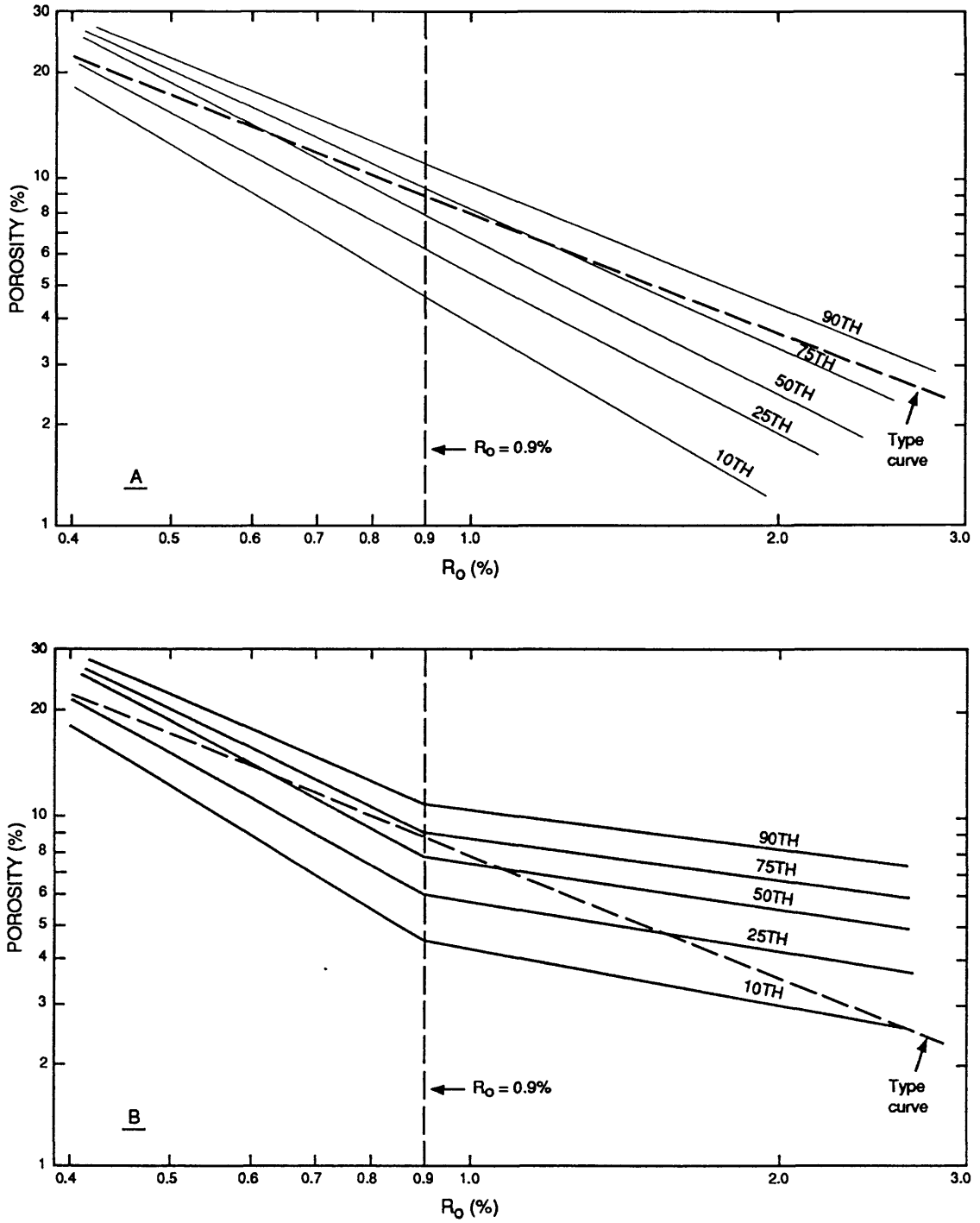

Figure 1-18. Subjectively drawn trend lines representing 10th, 25th, 50th, 75th, and 90th porosity percentiles, Cretaceous sandstone data set, Rocky Mountain basins. These trend lines constitute an alternative predictive porosity model to the set of regression lines of Figure 1-17. Dashed "type curve" (also shown in Figures 1-7 and 1-17) provides a reference line that represents sandstones in general (Schmoker and Gautier, 1989). For R_O less than 0.9%, trend lines of A and B are identical and represent all data (Figs. 1-12 through 1-16). For R_O greater than 0.9%, trend lines of A represent strata in which porosity continues to decrease at a uniform rate; trend lines of B represent strata in which the rate of porosity loss becomes more gradual as R_O increases above 0.9%.

Table 1-1. Power-law regression lines fit to J sandstone porosity-vitrinite reflectance data (Fig. 4). 68-percent confidence intervals are shown for A and B.

Porosity percentile	$= A(R_o)^B$ A	B	Correlation coefficient (r)	Variance (r^2)
10th	4.6 ± 0.5	-1.46 ± 0.23	-0.76	0.58
25th	6.4 ± 0.5	-1.23 ± 0.17	-0.81	0.66
50th	8.1 ± 0.5	-1.18 ± 0.12	-0.88	0.77
75th	9.9 ± 0.5	-1.05 ± 0.12	-0.86	0.75
90th	11.4 ± 0.6	-0.94 ± 0.12	-0.83	0.69

Table 1-2. Description of Cretaceous sandstone data set, Rocky Mountain basins.

Basin	Identification, source	No. of core-plug porosity measurements	No. of measurement suites	Vitrinite-reflectance, percent	Depth 1000' of ft
Denver	J sandstone (Schmoker and Higley, 1991)	963	31*	0.41-1.14	4.3-8
Green River	Dakota Sandstone of Bridger Lake field (Ben E. Law, pers. comm., 1987)	326	1	0.59	15.5
	Undifferentiated Cretaceous strata of El Paso Wagon Wheel #1 well (author's data)	442	7	0.66-1.78	8.1-1
	Almond Formation (Ben E. Law, pers. comm., 1988)	811	24	0.57-1.64	4.5-1
Powder River	Sussex Sandstone Member of Cody Shale (Debra K. Higley, pers. comm., 1991)	632	3	0.52-0.76	7.2-1
Uinta	Predominantly nonmarine sandstones of Mesaverde Group (Schmoker and others, 1992)	318	13*	0.56-2.40	0.7-1
Piceance	Predominantly nonmarine sandstones of Mesaverde Group (Schmoker and others, 1992)	741	18*	0.54-1.80	1.1-7
	Predominantly marine sandstones of Mesaverde Group (author's data; Schmoker and others, 1992)	162	6	1.33-2.16	7.5-8
	"B" zone of Mancos Shale (author's data)	67	4	1.80	11.8
		4,462	107		

*Data used in sections on porosity trends for J or Mesaverde Group sandstones.

Table 1-3. Power-law regression lines fit to combined Rocky Mountain porosity-vitrinite reflectance data (Figs. 12-16). 68-percent confidence intervals are shown for A and B.

Porosity percentile	$= A(R_o)^B$ A	B	Correlation coefficient (r)	Variance (r^2)
10th	5.0 ± 0.3	-0.92 ± 0.12	-0.60	0.36
25th	6.5 ± 0.3	-0.90 ± 0.10	-0.66	0.44
50th	7.9 ± 0.3	-0.93 ± 0.09	-0.72	0.52
75th	9.3 ± 0.3	-0.88 ± 0.08	-0.74	0.55
90th	10.5 ± 0.3	-0.85 ± 0.07	-0.76	0.58

Appendix 1b: Trends of sandstone porosity in the Anadarko basin by T.C. Hester

The goal of Task 1 was to characterize Anadarko basin sandstone-porosity trends with respect to thermal maturity in order to predict locations for new future reservoirs based on porosity prediction models. Three R_O data sets were compiled-- two data sets representing Anadarko basin reservoir and non reservoir sandstones, and one composite data set from many basins (excluding the Anadarko basin) representing sandstones in general. The first data set provides a porosity-Ro trend typical of Anadarko basin HC-bearing sandstone reservoirs. Non-reservoir sandstones in the second data set are defined as those typical of the Anadarko basin and may be reservoir sandstones at other locations. Non-reservoir sandstones provide a background by which to compare other sandstones. The third data set represents a sample of sandstones of diverse ages, diagenetic facies, and thermal histories exclusive of the Anadarko basin.

INTRODUCTION

This report relates porosity and thermal maturity for sandstones of the Anadarko basin, Oklahoma (Hester and Schmoker, 1990). Treating porosity as a function of thermal maturity normalizes the overprint of burial history on porosity evolution, allowing porosity data from basins with different thermal histories to be merged and/or compared in the same context (Schmoker and Hester, 1990).

To best characterize sandstone-porosity trends in the Anadarko basin, three data sets have been compiled--two data sets representing Anadarko basin reservoir and non-reservoir sandstones, and one composite data set of sandstones from numerous basins exclusive of the Anadarko representing sandstones in general. Each data set consists of many sandstone porosity-vitrinite reflectance (R_O) pairs that provide trends representative of that particular subset of sandstones. Porosity-R_O trends of Anadarko basin reservoir and non-reservoir sandstones are each compared to a set of porosity-R_O trends representing sandstones from basins other than the Anadarko, and the two are also compared to each other. Anadarko basin sandstone-porosity trends are thus evaluated relative to a framework of sandstones in general (Schmoker and Hester, 1990).

The data presented here are useful in the following ways: (1) They provide a means of estimating sandstone porosity in the deep relatively unexplored parts of the Anadarko basin; (2) they provide comparative insights into porosity trends of reservoir and non-reservoir sandstones; and (3) they provide a standard with which to identify Anadarko basin sandstones of anomalously high or low porosity for further study.

DATA SETS

The first data set provides a porosity-R_O trend typical of Anadarko basin non-reservoir sandstones, that is, Anadarko basin sandstones in general. The porosity data consist of about 800 measurements representing more than 2,130 net m (7,000 net ft) of Paleozoic-age sandstone from 33 well locations (Fig. 1-19; Table 1-4) in the central and southern Anadarko basin. Sandstones are identified in each well, using compensated-neutron and formation-density logs run on limestone matrix, and are then subdivided into intervals of uniform log character. The neutron and density porosities of each interval (1.2 or more m

thick--4 or more ft) are averaged and the true porosity determined using standard neutron-density crossplots. R_o values for Anadarko basin non-reservoir sandstone intervals are calculated using an empirical R_o-depth relationship developed for the Anadarko basin by Schmoker (1986). In this report, the term "non-reservoir" indicates only that the porosity data were taken directly from well logs, and thus represent a sampling of Anadarko basin sandstones as a whole; the term does not necessarily preclude the presence of HC's.

The second data set provides a porosity-R_o trend typical of Anadarko basin HC-bearing sandstone reservoirs. The porosity data consist of averaged measurements of 104 Paleozoic-age sandstone oil and gas reservoirs of the Anadarko basin (Fig. 1-19; Table 1-5) from published oil- and gas-field compilations (Cramer and others, 1963; Berg and others, 1974; Pipes, 1980; Harrison and Routh, 1981). The term "reservoir" indicates only that R_o values are calculated as in the previous data set (Schmoker, 1986). Porosity data were taken from published descriptions of known reservoirs, and thus represent a sampling of Anadarko basin reservoir sandstones.

The third data set represents a sampling of sandstones of diverse ages, geologic settings, diagenetic facies, and thermal histories, and provides a framework of porosity-R_o trends typical of sandstones in general (Schmoker and Hester, 1990) with which to compare both Anadarko basin non-reservoir and reservoir sandstone-porosity data. The framework data consist of many thousands of individual porosity and R_o measurements from Cenozoic and Mesozoic sandstones in 27 locations in the Northern Hemisphere, exclusive of the Anadarko basin. The framework data presented in this report incorporate published core-plug porosity and R_o measurements in addition to those of Schmoker and Hester (1990), and are represented here by least-squares regression lines fit to the 10th, 25th, 50th, 75th, and 90th porosity percentiles of the framework data set.

POROSITY-R_o TRENDS

A least-squares fit to the porosity-R_o data for non-reservoir sandstones of the central and southern Anadarko basin shows that non-reservoir sandstone porosity generally declines with increasing thermal maturity (Fig. 1-20). However, the data appear to consist of two separate populations--a less thermally mature population represented by R_o <1.1% and a more thermally mature population represented by R_o >1.1%. Correlation coefficients (r^2) of the least-squares fit to each of the two data populations (Fig. 1-21) show a much stronger dependence of porosity on R_o for the less mature trend of non-reservoir sandstones (where R_o <1.1%, r^2 =.40) than for non-reservoir sandstones taken as a whole (Fig. 1-20, r^2 =.15). The improved correlation of the less mature trend over that of the data set taken as a whole suggests that the two data populations might best be considered, as two separate trends. The two trends probably overlap to some extent as the more mature diverges from the less mature trend. Nevertheless, for the purposes of this report, a single preliminary boundary separating the two trends is placed at about R_o =1.1%. Additional porosity data might show the rapid porosity loss of the less mature trend continuing beyond R_o =1.1% (Fig. 1-21).

In both populations of points shown in Figure 1-21, porosity generally declines as a power function (Schmoker and Hester, 1990, eq. 1) of increasing

thermal maturity. The least-squares fit to the data shows that for R_o <1.1%, the rate of porosity decrease with increasing R_o for non-reservoir sandstones is more rapid than that of the average trend of the porosity-R_o framework representing sandstones in general. For R_o >1.1%, the rate of porosity decrease for Anadarko basin non-reservoir sandstones is less rapid than that of sandstones in general.

For this report, sufficient data to substantiate a probable cause for the change of slope of the porosity trend of Anadarko basin non-reservoir sandstones are not yet available. To speculate, the two populations of non-reservoir sandstone-porosity data (apparent in Figures 1-20 through 1-23) may represent sandstones from different depositional environments, or subsurface pressure regimes, or sandstones with different burial or cementation histories. Identification and stratigraphic correlation of the non-reservoir sandstones, with the addition of petrographic information, are suggested here as a first approach to examining the nature of the two populations of Anadarko basin non-reservoir sandstones.

The porosity-R_o trend of Anadarko basin HC-reservoir sandstones (Fig. 1-22) follows a different pattern. Their least-squares line shows that the rate of porosity loss for reservoir sandstones is much slower than that of both non-reservoir sandstones of the central and southern Anadarko basin (for R_o <1.1%, Fig. 1-22), and sandstones in general (Fig. 1-23). This relatively slow rate of porosity decline with increasing R_o could be due to geologic factors such as overpressuring, the inhibiting effects of early HC emplacement on sandstone diagenesis, and/or to economic factors inherent in the selection of sandstone HC reservoirs.

As R_o increases from to about 1.1%, the porosity trends of Anadarko basin reservoir and non-reservoir sandstones cross (Fig. 1-22). Thus, as thermal maturity increases, the porosity of reservoir sandstones becomes increasingly restricted to the upper range of porosity percentiles of non-reservoir sandstones. If these trends were to continue diverging, porosity sufficient for commercial sandstone HC reservoirs would become extremely rare at only moderate levels of thermal maturity. At about R_o =1.1%, however, the slope of the porosity trend for Anadarko basin non-reservoir sandstones levels off (Figs. 1-21 through 1-23). The average porosity of Anadarko basin reservoir sandstones then remains within about the upper 10% of the porosity range of non-reservoir sandstones. As thermal maturity levels increase above about 1.1% R_o, the similar slopes of the porosity trends of Anadarko basin reservoir and non-reservoir sandstones suggest that sandstones of the central and southern Anadarko basin may retain sufficient porosity for economic accumulations of HC's, even at high thermal maturities and great depths.

REFERENCES CITED

Berg, O.R.; Koinm, D.N.; and Richardson, D.E. (eds.), 1974, Oil and gas fields of Oklahoma: Oklahoma City Geological Society Reference Report Supplement I, 54 p.

Cramer, R.D.; Gatlin, Leroy; and Wessman H.G. (eds.), 1963, Oil and gas fields of Oklahoma: Oklahoma City Geological Society Reference Report Volume I, 200 p.

Harrison, W.E.; and Routh, D.L. (compilers), 1981, Reservoir and fluid characteristics of selected oil fields in Oklahoma: Oklahoma Geological Survey Special Publication 81-1, 317 p.

Hester, T.C.; and Schmoker, J.W., 1990, Porosity trends of non-reservoir and reservoir sandstones, Anadarko basin, Oklahoma [abstract]: American Association of Petroleum Geologists Bulletin, v. 75, no. 3, p. 594.

Pipes, P.B. (ed.), 1980, Oil and gas fields of Oklahoma: Oklahoma City Geological Society Reference Report Supplement II, 30 p.

Schmoker, J.W., 1986, Oil generation in the Anadarko basin, Oklahoma and Texas: Modeling using Lopatin's method: Oklahoma Geological Survey Special Publication 86-3, 40 p.

Schmoker, J.W.; and Hester, T.C., 1990, Regional trends of sandstone porosity versus vitrinite reflectance--a preliminary framework, *in* Nuccio, V.F.; and Barker, C.E. (eds.), Applications of thermal maturity studies to energy exploration: Rocky Mountain Section of the Society of Economic Paleontologists and Mineralogists, Denver, p. 53-60.

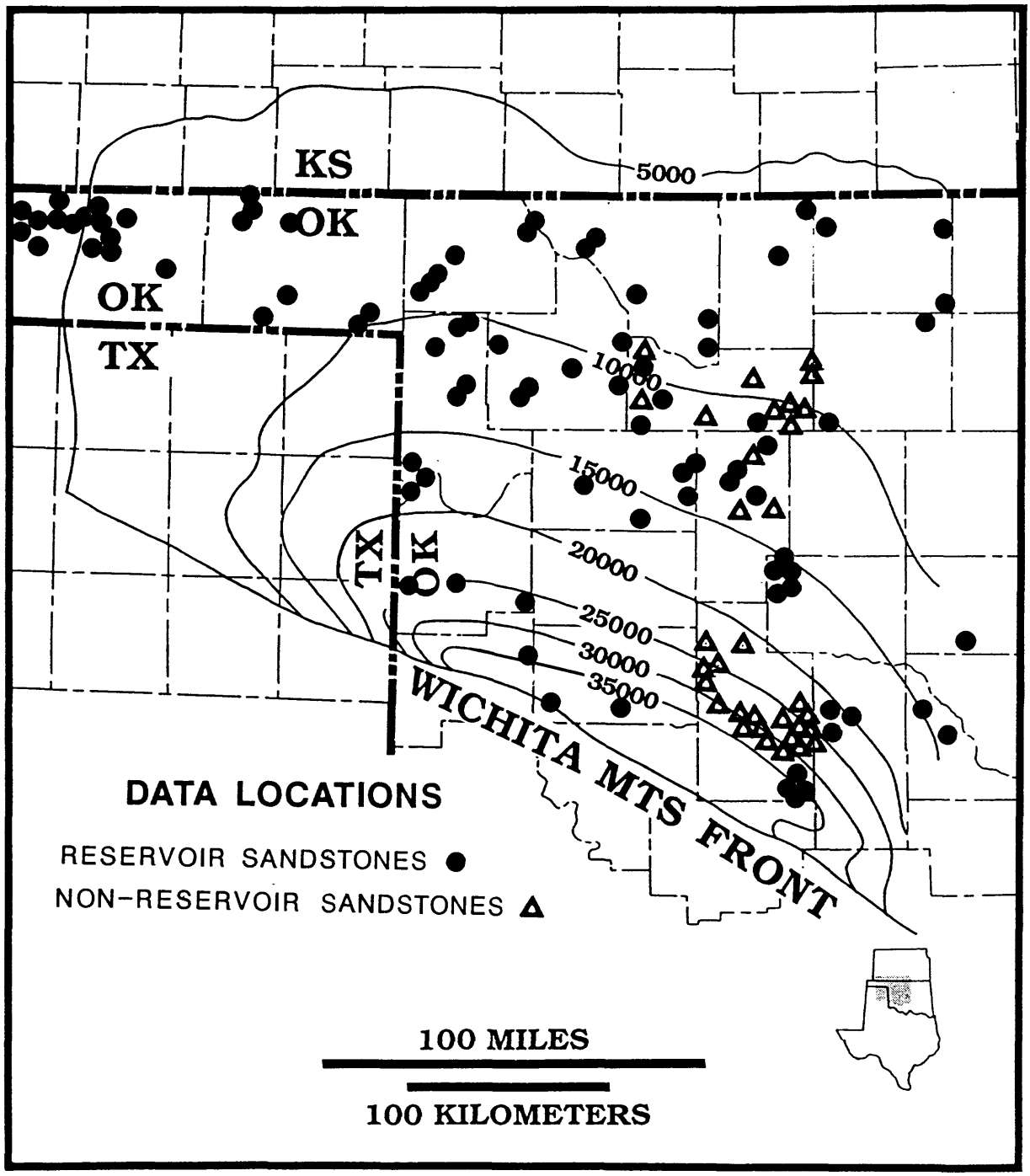

Figure 1-19. Map showing Anadarko basin total-sediment isopachs (ft), and data locations.

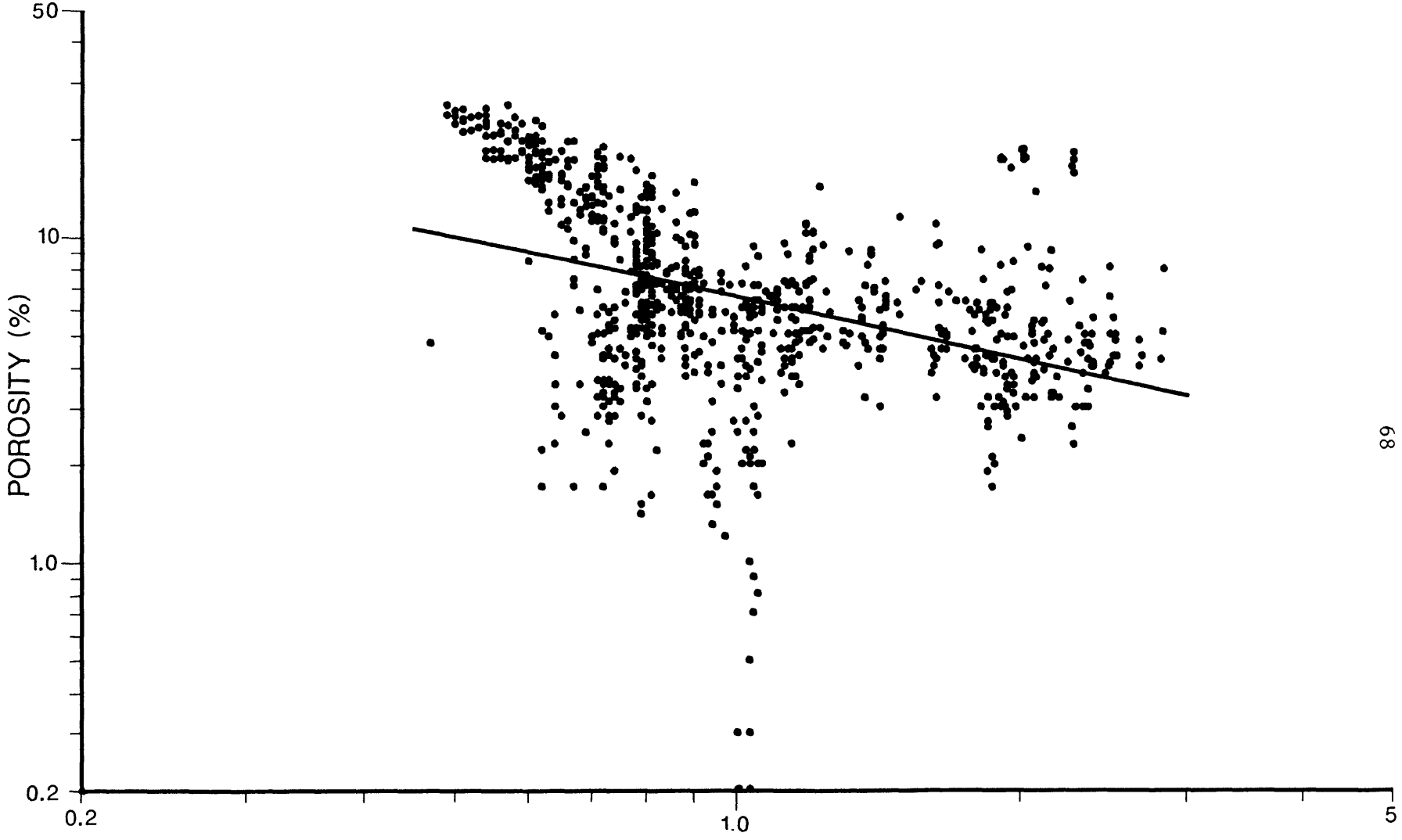

Figure 1-20. Porosity of Anadarko basin non-reservoir sandstones versus vitrinite reflectance (R_o) plotted with least-squares regression line.

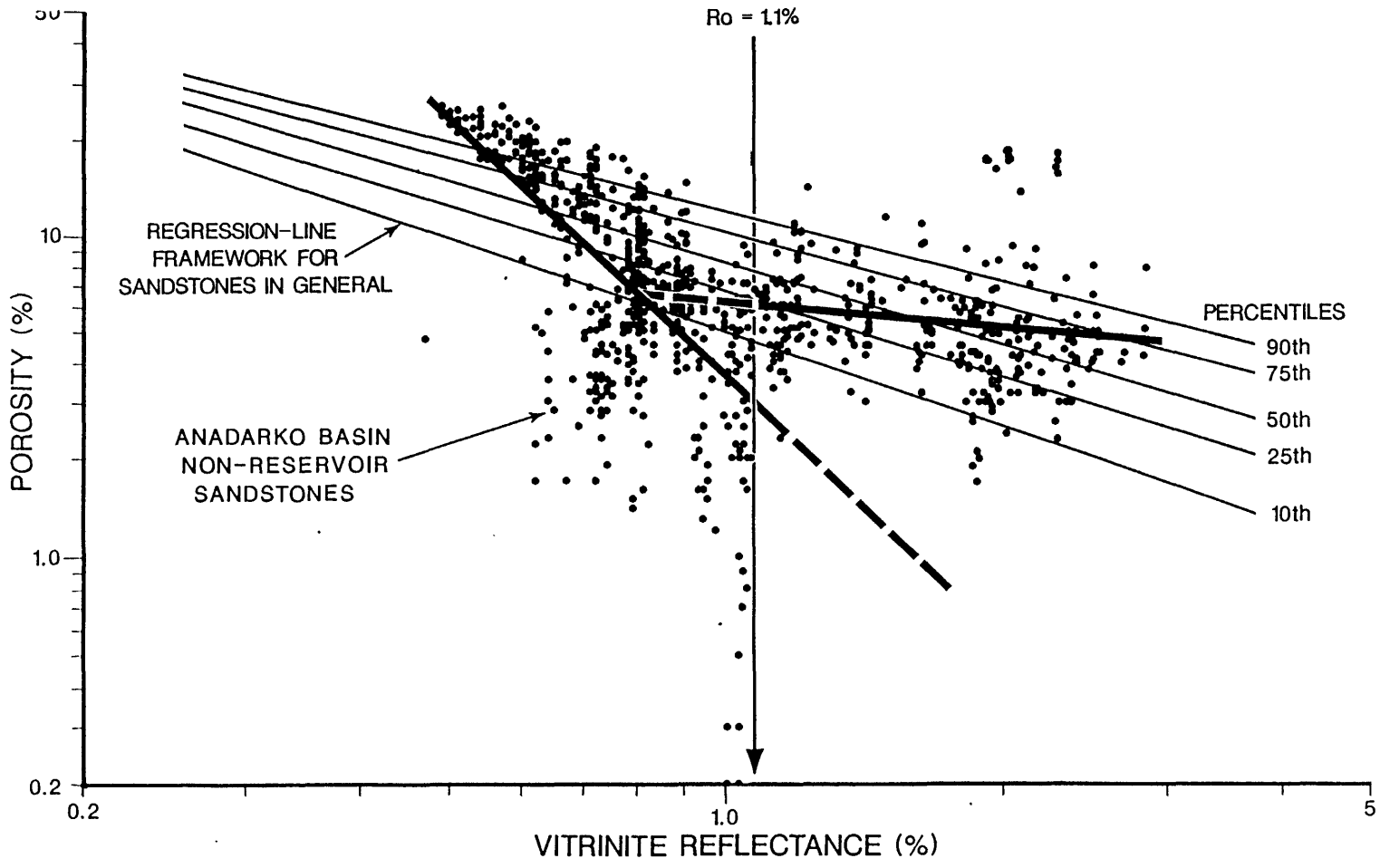

Figure 1-21. Porosity of Anadarko basin non-reservoir sandstones versus vitrinite reflectance (R_o) plotted with least-squares regression lines fit to each of two non-reservoir sandstone data populations separated at R_o =1.1% (dashed where inferred). Also plotted are least-squares regression lines fit to 10th, 25th, 50th, 75th, and 90th porosity percentiles of the framework data set representing sandstones in general (Schmoker and Hester, 1990).

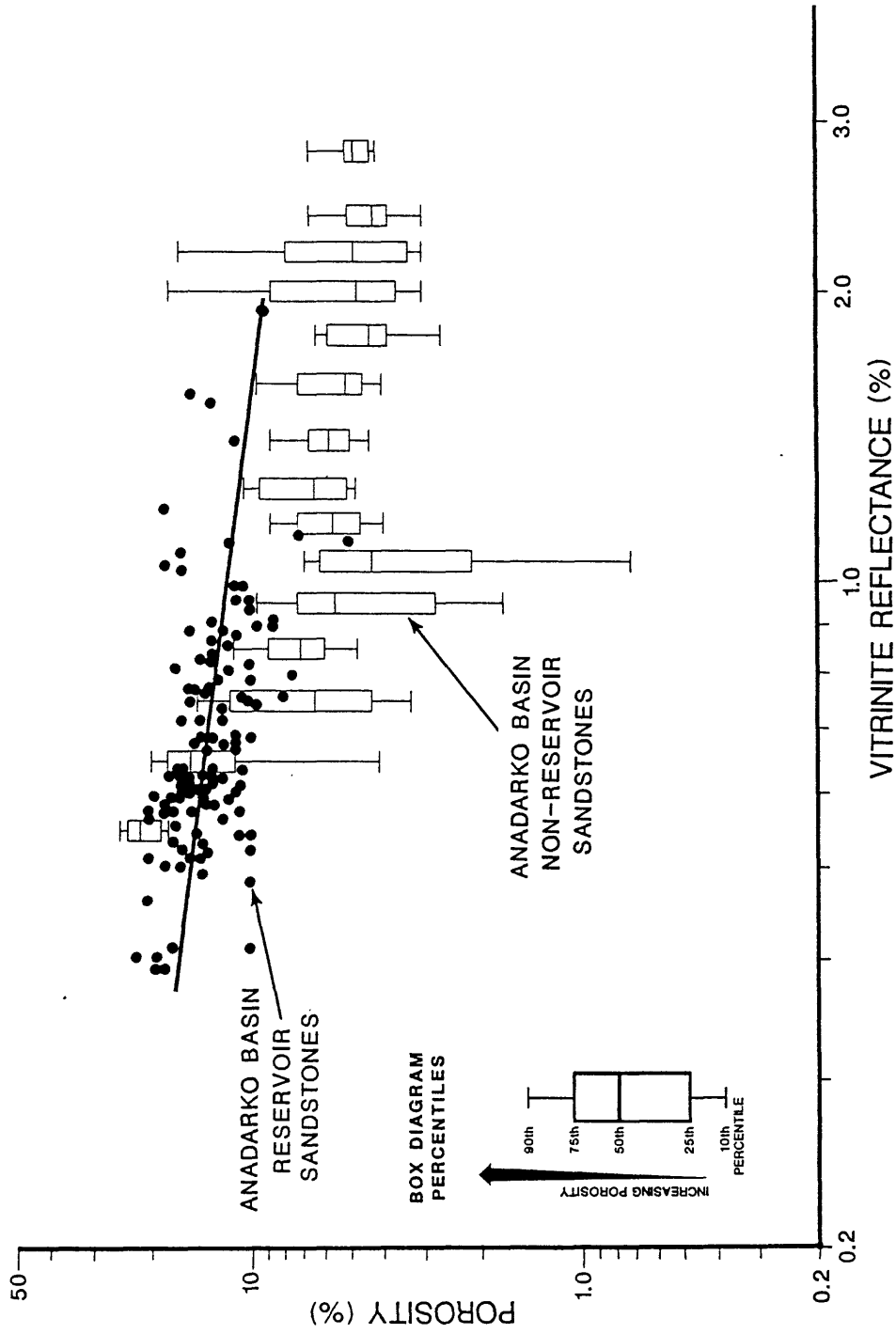

Figure 1-22. Porosity of Anadarko basin reservoir sandstones versus vitrinite reflectance (R_o) plotted with least-squares regression line. Also plotted are box-diagram percentiles representing Anadarko basin non-reservoir sandstone data.

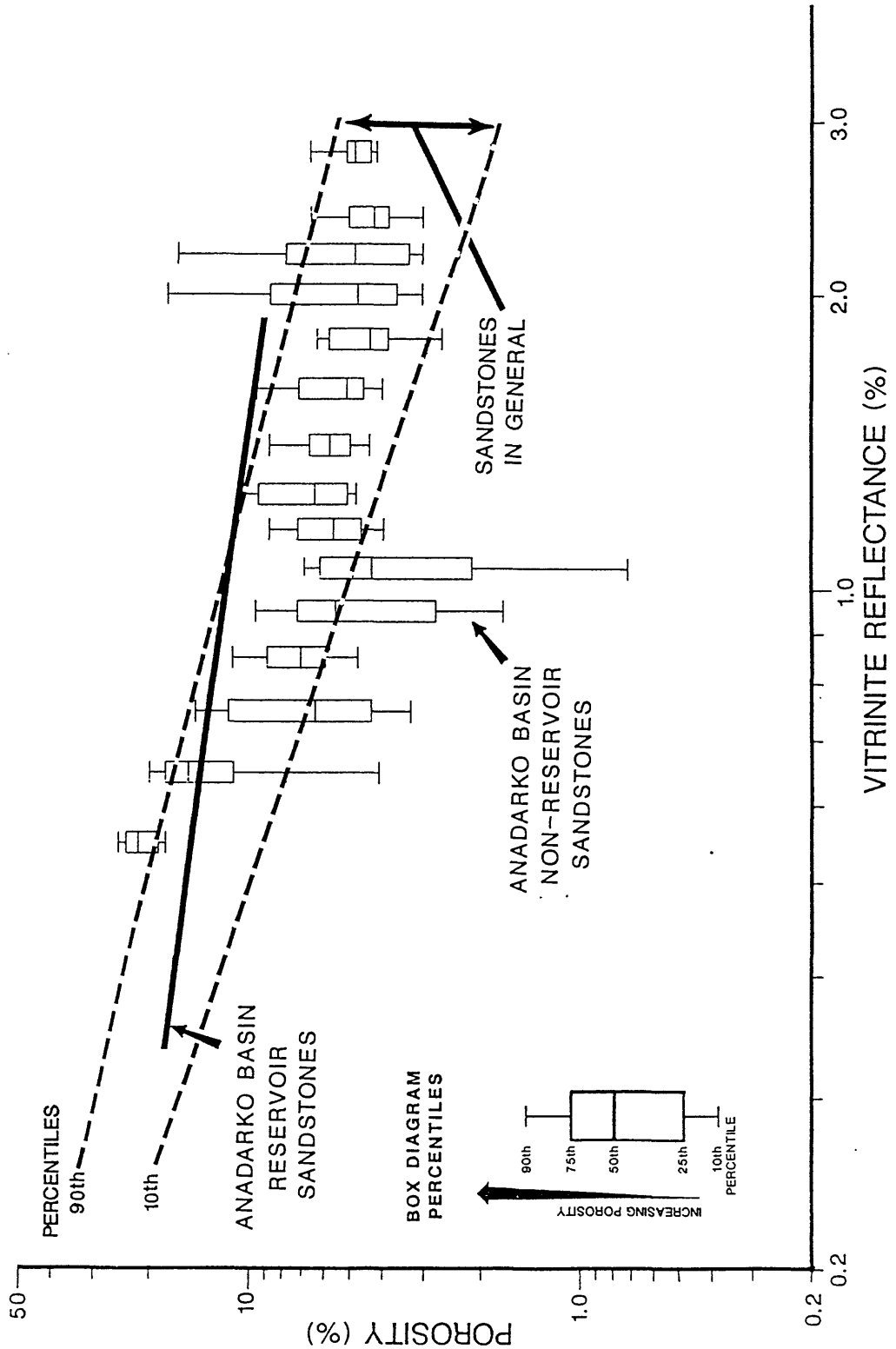

Figure 1-23. Summary diagram showing least-squares regression line for Anadarko basin reservoir sandstones, box-diagram percentiles for Anadarko basin non-reservoir sandstones, and porosity-R_o envelope bounded by least-squares regression lines fit to the 10th and 90th porosity percentiles of the framework data set representing sandstones in general (Schmoker and Hester, 1990).

Table 1-4. List of wells used in this study. [Location (section, township, and range), operator, and well name are as shown on well-log headers.]

Location	Operator	Well Name
Sec.21,T.8N.,R.12W.	Sohio Petroleum	1-21 Stockton
Sec.1,T.7N.,R.12W.	Sohio Petroleum	1-1 Cay
Sec.24,T.10N.,R.13W.	Helmerich and Payne	1 Phifer
Sec.32,T.8N.,R.9W.	Sohio Petroleum	1-32 Harper
Sec.29,T.7N.,R.9W.	Shell Oil	1-29 Bruer
Sec.25,T.7N.,R.11W.	Helmerich and Payne	1-25 C. Adams
Sec.18,T.9N.,R.13W.	L.G. Williams Inc	1-18 Allred
Sec.19,T.10N.,R.13W.	Hadson Petroleum Corp	1-19 Adams
Sec.10,T.8N.,R.13W.	Dyco Petroleum Corp	1-10 M. Caley
Sec.6,T.7N.,R.9W.	Cotton Petroleum Corp	1 Mary
Sec.18,T.8N.,R.9W.	Cotton Petroleum Corp	1-A Cox
Sec.28,T.8N.,R.11W.	GHK	1-28 Didier
Sec.33,T.8N.,R.10W.	Sanguine LTD	1 Griffitis
Sec.13,T.7N.,R.10W.	Shell Oil	1-13 Moore
Sec.26,T.7N.,R.9W.	Sanguine LTD	1 Mae West
Sec.4,T.7N.,R.11W.	Sohio Petroleum	1-4 Nikkel
Sec.10,T.7N.,R.9W.	Cotton Petroleum Corp	1-10 Kvasnica
Sec.26,T.7N.,R.10W.	Davis Oil	1-26 J.D.Miles
Sec.19,T.11N.,R.13W.	Lear Pet. Expl. Inc	1-19 Horn
Sec.25,T.11N.,R.12W.	Cotton Petroleum Corp	1-A Dorsey
Sec.10,T.16N.,R.12W.	Davis Oil	1 Pickett
Sec.7,T.16N.,R.10W.	Bogert Oil	1-7 Bernhardt
Sec.4,T.18N.,R.11W.	Bogert Oil	1-4 Henry
Sec.34,T.22N.,R.9W.	Arapaho Petroleum	2-34 Cottons
Sec.3,T.21N.,R.9W.	Berry Petroleum	1-3 Perry
Sec.19,T.20N.,R.9W.	Western Pacific Pet.	1-1 Patterson
Sec.16,T.21N.,R.11W.	Ladd Petroleum Corp	4 Shiddell
Sec.31,T.20N.,R.13W.	Nobel Operating Inc	2 Sholters
Sec.25,T.20N.,R.10W.	Bogert Oil	1-25 Frank
Sec.36,T.20N.,R.10W.	Cuesta Energy Corp	1-36 Seelke
Sec.28,T.20N.,R.10W.	Prime Energy Corp	1-28 Bierig
Sec.21,T.22N.,R.16W.	Shell Oil	2-21 Foster
Sec.16,T.20N.,R.16W.	TXO Production Corp	1-A Hoskins

Table 1-5. List of oil and/or gas reservoirs used in this study.
[Field and reservoir-formation names are from oil- and gas-field compilations cited in this report.]

Approximate Location	Field Name	Reservoir Formation
T.27N.,R.18W.	Avard, N.W.	Tonkawa
T.27N.,R.18W.	Avard, N.W.	Des Moinesian
T.10N.,R.10W.	Binger, East Binger	Middle Marchand
T.10N.,R.10W.	Binger-Cogar	Lower Marchand
T.10N.,R.10W.	Binger, East	Upper Marchand
T.17N.,R.26W.	Bishop	Tonkawa
T.16N.,R.26W.	Bishop	Tonkawa
T.1N.,R.22ECM	Camrick Area	Morrow
T.12N.,R.21W.	Carpenter	Morrow
T.5N.,R.11ECM	Carthage Dist., N.E.	Morrow
T.5N.R.11ECM	Carthage Gas Area	Morrow
T.23N.,R.17W.	Cedardale, N.E.	Missouri
T.22N.,R.17W.	Cedardale	Cottage Grove
T.5N.,R.9W.	Cement (all areas)	Fortuna
T.5N.,R.9W.	Cement (all areas)	Noble Olson
T.6N.,R.9W.	Cement (all areas)	Fortuna
T.5N.,R.9W.	Cement (all areas)	Hoxbar Group
T.5N.,R.9W.	Cement (all areas)	Fortuna
T.5N.,R.9W.	Cement (all areas)	Noble Olson
T.5N.,R.9W.	Cement (all areas)	Wade
T.5N.,R.9W.	Cement (all areas)	Medrano
T.6N.,R.9W.	Cement (all areas)	Wolfcamp
T.6N.,R.9W.	Cement (all areas)	Missouri
T.13N.,R.10W.	Calumet	Morrow
T.18N.,R.14W.	Canton, S.W.	Morrow
T.18N.,R.12W.	Carleton, N.E.	Atoka-Morrow
T.18N.,R.12W.	Carleton, N.E.	Morrow
T.23N.,R.25W.	Catesby-Chaney	Morrow
T.27N.,R.9W.	Cherokita Trend	Cherokee
T.27N.,R.10W.	Cherokee, N.E.	Cherokee
T.23N.,R.13W.	Cheyenne Valley	Des Moinesian
T.21N.,R.15W.	Cheyenne Valley	Red Fork
T.13N.,R.24W.	Cheyenne, West	Upper Morrow
T.8N.,R.8W.	Chickasha, N.W.	Missouri
T.5N.,R.3W.	Criner-Payne	Bromide
T.7N.,R.3W.	Dribble, North	Red Fork
T.10N.,R.21W.	Elk City	Missouri
T.2N.,R.23ECM	Elmwood	Morrow
T.4N.,R.10ECM	Eva, N.W.	Cherokee
T.5N.,R.23ECM	Forgan, South	Morrow

Table 1-5. (continued)

Approximate Location	Field Name	Reservoir Formation
T.21N.,R.24W.	Gage, South	Morrow
T.20N.,R.24W.	Gage, South	Morrow
T.13N.,R.10W.	Geary	Morrow
T.8N.,R.17W.	Gotebo Area, North	Springer
T.6N.,R.21ECM	Greenough, West	Des Moinesian
T.3N.,R.17ECM	Hardest, North	Morrow
T.18N.,R.26W.	Higgins, South	Morrow
T.17N.,R.11W.	Hitchcock	Atoka
T.24N.,R.4W.	Hunter, South	Layton
T.24N.,R.4W.	Hunter, South	Misener
T.5N.,R.9ECM	Keys Area	Morrow
T.5N.,R.9ECM	Keys	Keys
T.26N.,R.25W.	Laverne	Hoover
T.26N.,R.25W.	Laverne	Tonkawa
T.26N.,R.25W.	Laverne	Morrow
T.18N.,R.18W.	Lenora	Morrow
T.5N.,R.21ECM	Light Gas Area	Upper Morrow
T.5N.,R.21ECM	Light Gas Area	Basal Morrow
T.1N.,R.26ECM	Logan, South	Morrow
T.1N.,R.26ECM	Logan, South	Tonkawa
T.28N.,R.21W.	Lovedale	Morrow
T.28N.,R.21W.	Lovedale	Tonkawa
T.24N.,R.24W.	Luther Hill	Lower Tonkawa
T.24N.,R.24W.	Luther Hill	Lower Morrow
T.28N.,R.3W.	Mayflower, N.W.	Red Fork
T.8N.,R.7W.	Minco, S.W.	Springer
T.27N.,R.24W.	Mocane-Laverne	Morrow
T.5N.,R.15ECM	Mouser	Morrow
T.7N.,R.8W.	Norge and Verden, N.W.	Marchand
T.24N.,R.13W.	Oakdale, N.W.	Redfork
T.17N.,R.14W.	Oakwood, North	Morrow
T.18N.,R.14W.	Oakwood, N.W.	Morrow
T.15N.,R.7W.	Okarche, North	Manning
T.20N.,R.11W.	Okeene, N.W.	Redfork
T.19N.,R.11W.	Okeene, N.W.	Redfork
T.11N.,R.2W.	Oklahoma City	Prue
T.11N.,R.2W.	Oklahoma City	Wilcox
T.5N.,R.13ECM	Postle	Morrow
T.5N.,R.13ECM	Postle	Cherokee
T.4N.,R.13ECM	Postle-Hough	Upper Cherokee

Table 1-5. (continued)

Approximate Location	Field Name	Reservoir Formation
T.5N.,R.13ECM	Postle-Hough	Upper Morrow
T.4N.,R.14ECM	Postle-Hough	Upper Morrow
T.4N.,R.14ECM	Postle-Hough	Morrow Group
T.16N.,R.16W.	Putnam	Des Moinesian
T.13N.,R.26W.	Reydon, W. and N.W.	Upper Morrow
T.25N.,R.4W.	Rich Valley	Simpson
T.25N.,R.4W.	Rich Valley Area	Wilcox
T.5N.,R.12ECM	Richland, Central, N.	Morrow
T.25N.,R.3W.	Saltfork, S.E.	Skinner
T.20N.,R.16W.	Seiling, N.E.	Cottage Grove
T.8N.,R.20W.	Sentinel, West	Granite Wash
T.21N.,R.21W.	Sharon, West	Morrow
T.21N.,R.21W.	Sharon, West	Sharon
T.20N.,R.8W.	Sooner Trend	Des Moinesian
T.5N.,R.10ECM	Sturgis, East	Morrow
T.23N.,R.22W.	Tangier	Morrow
T.28N.,R.8W.	Wakita Trend	Cherokee
T.8N.,R.4W.	Washington, E.	Osborne
T.14N.,R.10W.	Watonga-Chickasha	Morrow
T.14N.,R.10W.	Watonga-Chickasha	Springer
T.14N.,R.10W.	Watonga-Chickasha	Atoka
T.25N.,R.16W.	Waynoka, N.E.	Cottage Grove
T.22N.,R.19W.	Woodward, S.E.	Morrow
T.29N.,R.17W.	Yellowstone	Simpson

Appendix 2: Pore throats, capillary pressures, porosity, and permeability, by C.W. Keighin

INTRODUCTION

The primary goal of Task 2 is to document the effects of confining stress on pore geometry, as well as on porosity and permeability in clastic rocks at various depths. Although studies documenting the effects of confining stress on porosity and permeability in clastic rocks are available, almost no data exist documenting the effects of confining stress on pore-throat size distribution determined by mercury injection/capillary pressure with the sample under confining stress. Nineteen samples from three basins, from different depth ranges, and with different diagenetic histories, were examined. General geographic sample locations are given in Table 2-1; sample depths and a summary of modal analyses and porosity/permeability values are listed in Table 2-2.

DATA INTERPRETATION

The data in Table 2-2 show a wide range in porosity and permeability values, although porosity is typically below 8% and Klinkenberg permeability below 0.1 md. Klinkenberg (1941), showed that, especially in low-permeability media, permeability to a gas is a function of the mean free path of the gas molecules. When gas flows through capillaries with diameters small enough to be comparable to the mean free path of the gas, as is typically the case in low-permeability media, discrepancies appear between gas and liquid permeabilities in the porous media. He introduced the concept of "slip", and the following equation to correct apparent gas permeability (K_g), of a gas flowing at a mean pore pressure ($\bar{P}$), to the true permeability of the porous medium (see also Sampath and Keighin, 1982).

$$K_g = K_\infty (1 = b/\bar{P})$$

Cross plots of these data are shown in Figure 2-1, and indicate a generally close correlation between porosity and permeability. As expected, there is a general decrease in porosity and permeability with depth, but depth is not the only factor to consider in the decrease of either porosity or permeability. Schmoker (1988; and Schmoker, Appendix 1a this volume) considered porosity-reducing diagenetic reactions in the subsurface to be dependent on time-temperature exposure of the formation, and further, that depth may or may not be a good measure of thermal exposure. Nor is decrease in porosity with depth uniform (Atkins and McBride, 1992, their Fig. 9). Examination of thin sections indicates that while compaction due to increasing depth of burial sometimes appears to be a factor, the degree of compaction is greatly influenced by lithology, especially the presence and quantity of labile rock fragments (Dutton and Diggs, 1992). Cementation, either by silica or carbonate minerals, acts to reduce both porosity and permeability, as well as significantly modifying pore structure.

In this report we are particularly interested in pore structure, and, necessarily in how these structures are generated and modified. It would be especially useful to be able to accurately predict porosity and pore-throat structure, and the various mechanisms responsible for modifying porosity, and pore structure. An important aspect of the overall pore structure is the interconnection between pores--the pore throat. Pore throats control fluid flow between pores, and are typically smaller than pores. In part because of

their size, they are more sensitive to diagenetic modifications, whether physical compaction or chemical reactions (dissolution or precipitation of newly formed minerals). Research to date has not completely answered these questions (Bloch, 1991; Bachu and Underschultz, 1992; Harrison, 1989; Surdam and others, 1989). The samples examined in this investigation vary primarily in the relative abundance of quartz, feldspar, and rock fragments (Table 2-2); carbonate cements are locally abundant. Appearance of selected samples is shown in Figure 2-2; petrologic data related to additional samples from the Anadarko basin may be found in Keighin and Flores, 1989. The relative abundance of rock fragments may have a significant effect on porosity, both macro and micro, and permeability. Compression of labile rock fragments reduces intergranular porosity and creates intergranular pseudomatrix; both reduce effective permeability (McBride and others, 1991). Partial dissolution of rock fragments often creates microporosity; micropores introduce micro-pore-throats which may restrict or improve fluid migration depending on the overall history of the rock environment.

Examination of the porosity and permeability data in Table 2-2 shows a wide variation in measured values; the data also show wide variations in the effects of confining stress on permeability. Relationships between capillary pressure and wetting phase (e.g. air) saturation, and pore-size distribution for a range of porosity and permeability values are shown in Figure 2-3 (see also McCreesh and others, 1991). The samples illustrated in Figure 2-3, A and B, are among the most porous of the samples investigated, and, in thin section, have the largest visible pores. Plots of pore-size frequency versus pore entry/throat diameter, however, reveal that pore throats in these samples are most frequently in the 10μm range, significantly smaller than the pores visible in thin section. The plots also show that pore throats are constricted by increased confining stress, although not as dramatically as in samples with lower initial porosity and permeability, and smaller measured pore throats. Data plotted in Figure 2-3C and 2-3D, indicate that for samples more typically fitting the "tight" (i.e permeability <0.1md) sand designation, pore throats are more typically in the <0.1 μm size range, and that these already small pore throats are further reduced by confining stress. Thus, even though pores visible in thin section may be relatively large, all pores must be accessed through pore throats, which are smaller (often much smaller) than the pores themselves. The data also suggest that pore throats, rather than stress-relief micro fractures, are indeed being closed.

These data show that pore throats, controlling factors in flow of fluids through a pore network, are typically smaller than pores visible in thin section, or apparent in hand specimen. Pore throats, especially small (<0.1μm) pore throats, common in fine to very fine grained clastic rocks, are very sensitive to confining stress, and probably act as limiting factors controlling the flow of gas to the well bore. Small pore throats are also very sensitive to the presence of formation fluids, which reduce their effective diameter. Measurement of capillary pressure under confining stress suggests that constriction of pore throats is the controlling mechanism effecting fluid flow at reservoir conditions in the samples examined. These data aid in defining reservoir properties under in situ conditions, and are valuable for reservoir description and in simulation studies. More accurate predictions will be possible when additional data become available.

REFERENCES CITED

Atkins, J.E., and E. F. McBride, 1992, Porosity and packing of Holocene river, dune, and beach sands, American Association of Petroleum Geologists Bulletin, v. 76, no. 3, p. 339-355.

Dutton, S.P., and T.N. Diggs, 1992, Evolution of porosity and permeability in the Lower Cretaceous Travis Peak Formation, East Texas: American Association of Petroleum Geologists Bulletin, v. 76, no. 2, p. 252-269.

Harrison, W.J., 1989, Modeling fluid/rock interactions in sedimentary basins: in T.A. Cross (ed.), Quantitative Dynamic Stratigraphy, Prentice Hall, p. 195-231.

Keighin. C.W., and R.M. Flores, 1989, Depositional facies , petrofacies, and diagenesis of siliciclastics of Morrow and Springer rocks, Anadarko basin, Oklahoma: Oklahoma Geological Survey Bulletin 90, p. 147-161.

Klinkenberg, L.J., 1941, The permeability of porous media to liquids and gases: American Petroleum Institute, Drilling and Production Practice, p. 200-213.

McBride, E.F., T.N. Diggs, and J.C. Wilson, 1991, Compaction of Wilcox and Carrizo sandstones (Paleocene-Eocene) to 4420 m, Texas Gulf Coast: Journal of Sedimentary Petrology, v. 61, no. 1, p. 73-85.

McCreesh, C.A., R. Ehrlich, and S.J. Crabtree. 1991, Petrography and reservoir physics II: Relating thin section porosity to capillary pressure, the association between pore types and throat size: Association of Petroleum Geologists Bulletin, v. 75, no. 10, p. 1563-1578.

Sampath, K., and Keighin, C.W., 1982, Factors affecting slippage in tight sandstones of Cretaceous age in the Uinta basin: Journal of Petroleum Technology, v. 34, no. 11, p. 2715-2720.

Schmoker, J.W., and Gautier, D.L., 1988, Sandstone porosity as a function of thermal maturity: Geology, v. 16, p. 1007-1010.

Surdam, R.S., T.L. Dunn, D.B. MacGowan, and H.P. Heasler, 1989, Conceptual models for the prediction of porosity evolution with an example from the Frontier Formation, Bighorn Basin, Wyoming: *in* E.B. Coalson and others (eds), Petrogenesis and Petrophysics of Selected Sandstone Reservoirs of the Rocky Mountain Region, Rocky Mountain Association of Geologists, p. 7-28.

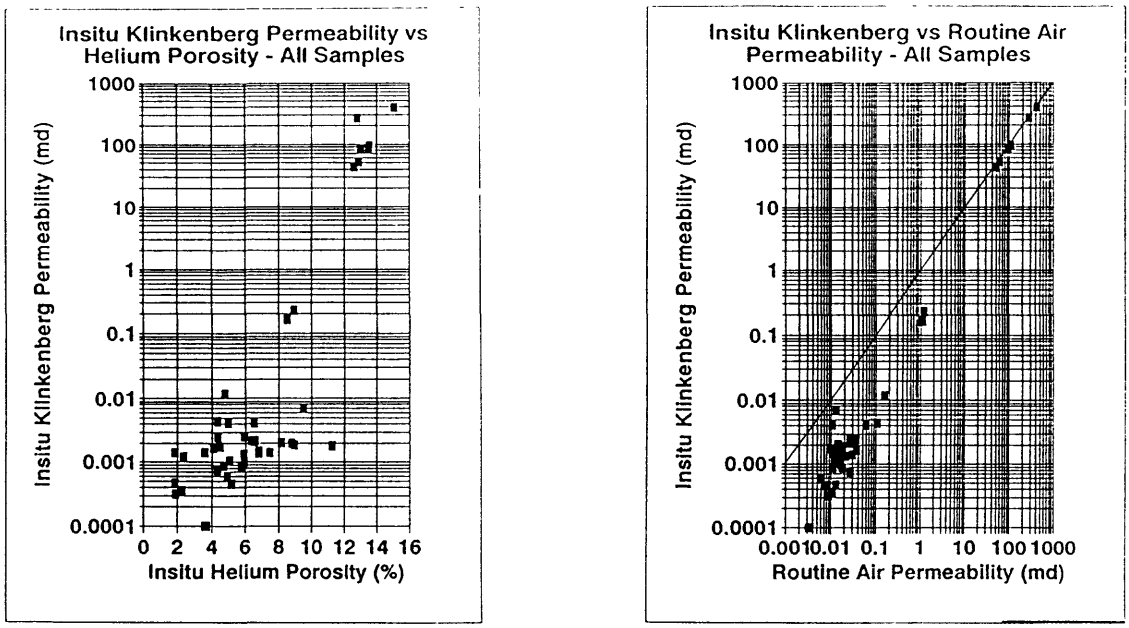

Figure 2-1. Cross plots of insitu Klinkenberg permeability versus insitu helium porosity and insitu Klinkenberg permeability versus routine air permeability for samples from core samples from the Anadarko, Uinta, and Wind River basins.

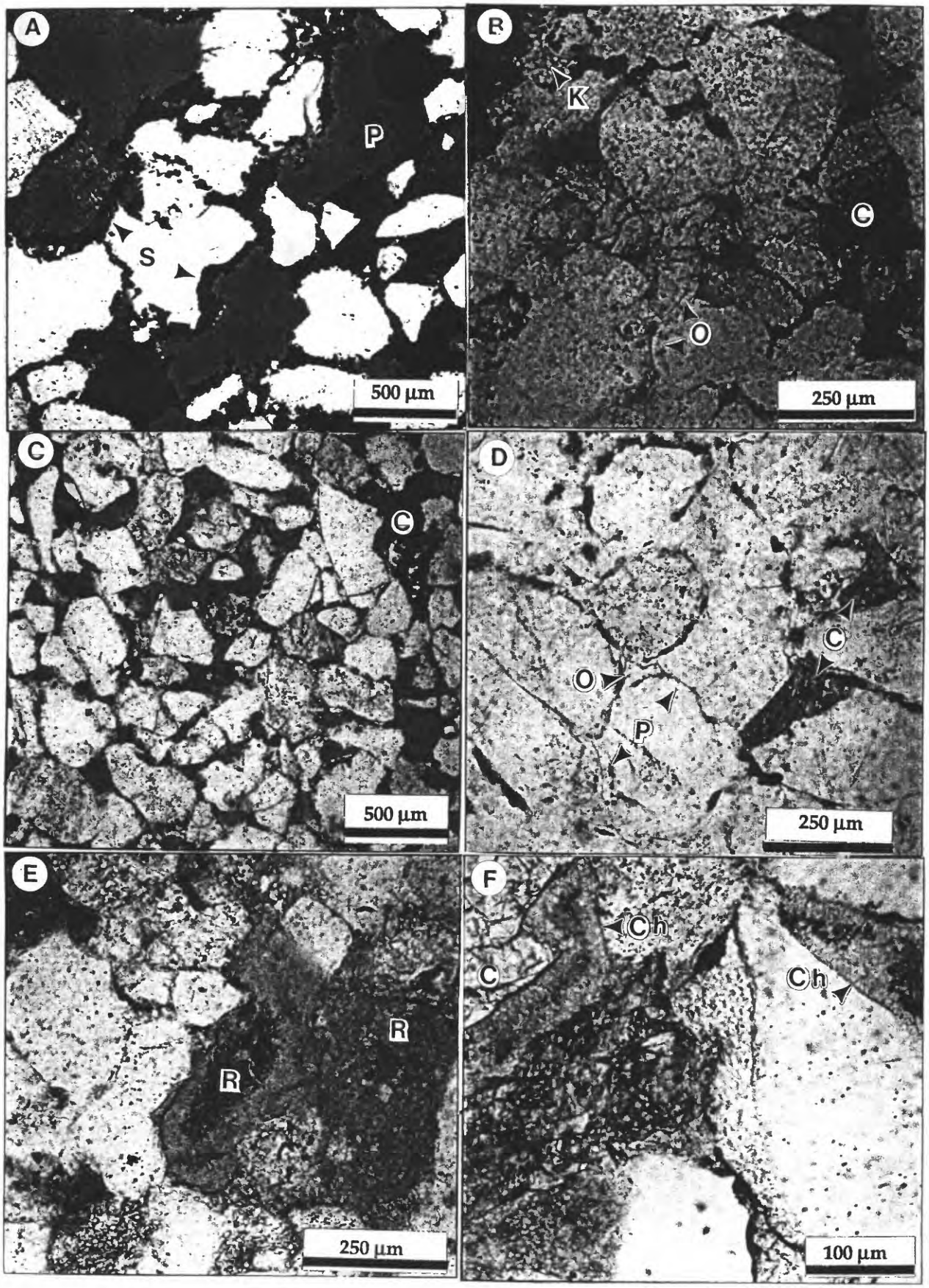
A
P
S
500 µm
B
K
C
O
250 µm
C
C
500 µm
D
C
O
P
250 µm
E
R
R
250 µm
F
Ch
C
Ch
100 µm

Figure 2-2 Photomicrographs of thin sections prepared from plugs on which porosity-permeability and mercury-injection determinations were made. Geographic location of samples is given in Table 1; porosity, permeability, and modal analysis results are listed in Table 2. All photos are taken in plane polarized light. (A). Sample OK-7, depth - 7,096 ft (2,163 m); ϕ_h : 16%; k_{is} : 330 md. Good porosity and permeability created by large, open pores [P]; pores are generally clay-free, but are typically lined by wheat-grain siderite [S]. Neither porosity nor permeability have been reduced by compaction or chemical cementation in this sample. (B). Sample OK-8, depth - 7,198 ft (2,194 m); ϕ_h : 14.1%; k_{is} : 47.7 md. Sample is poorly sorted, but clean (few rock fragments); pores are relatively clean and open, although some are filled with kaolinite [K]. Authigenic quartz overgrowths [O] and carbonate cement [C] occur, but neither porosity nor permeability have been significantly reduced by chemical cementation. (C). Sample OK-3, depth - 11,960 ft (3,645m); ϕ_h :14.3%; k_{is} : 86.6 md. Sandstone is moderately sorted, fine grained, and relatively clean; pores are typically open and clay-free, although iron-bearing carbonate cement [C] is sometimes present. (D). Sample OK-1, depth - 18,076 ft (5,510 m); ϕ_h : 2.1% ; k_{is} : 0.0010 md. Sandstone is well sorted and clean, but porosity and permeability have been significantly reduced by compaction, quartz overgrowths [O] (silica cementation), and pore-filling carbonate [C]. Intergranular pores [P] exist, but are typically very thin [< 5μm]. (E). Sample WY-8, depth - 12,097.5 ft (3,687 m); ϕ_h : 6.9%; k_{is} : 0.0022 md. Moderately sorted medium gained sandstone containing both compacted and partially dissolved rocks fragments [R]; some porosity is microporosity due to partial dissolution of rock fragments; few pores are clean (i.e., free from clays or authigenic cements). Authigenic cements include silica overgrowths and intergranular carbonates. (F). Sample WY-35, depth - 13,631 ft (4,155 m); ϕ_h :7%; k_{is} : 0.0024 md. Medium grained, moderately sorted sandstone rich in rock fragments [R]. Most pores are lined with authigenic chlorite [Ch], and many are filled with other authigenic clays. Porosity has also been reduced by precipitation of intergranular carbonate [C].

ϕ_h = helium porosity k_{is} = insitu permeability

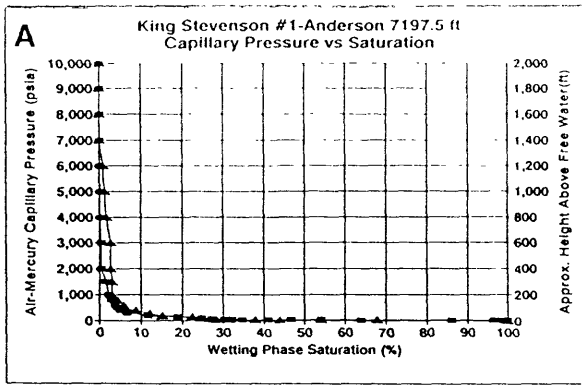
A
King Stevenson #1-Anderson 7197.5 ft
Capillary Pressure vs Saturation
Air-Mercury Capillary Pressure (psia)
Approx. Height Above Free Water(ft)
Wetting Phase Saturation (%)

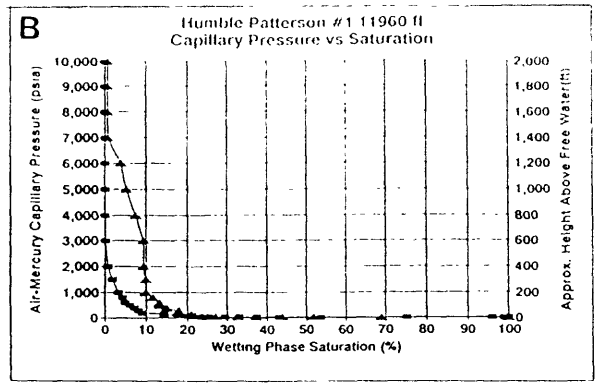
B
Humble Patterson #1 11960 ft
Capillary Pressure vs Saturation
Air-Mercury Capillary Pressure (psia)
Approx. Height Above Free Water(ft)
Wetting Phase Saturation (%)

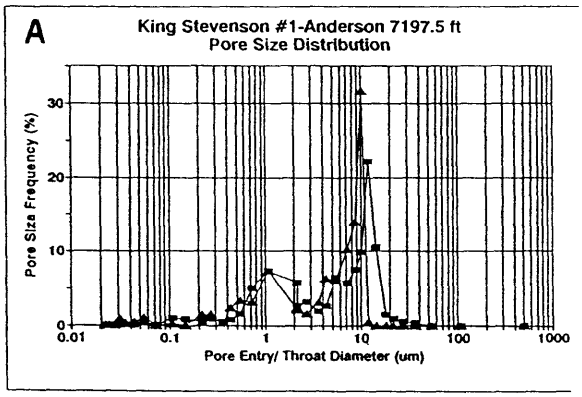
A
King Stevenson #1-Anderson 7197.5 ft
Pore Size Distribution
Pore Size Frequency (%)
Pore Entry/ Throat Diameter (um)

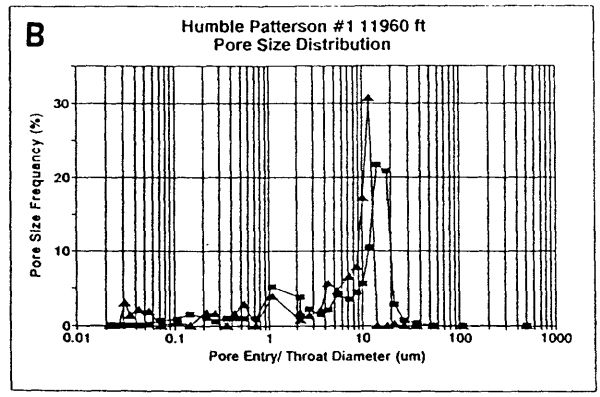
B
Humble Patterson #1 11960 ft
Pore Size Distribution
Pore Size Frequency (%)
Pore Entry/ Throat Diameter (um)

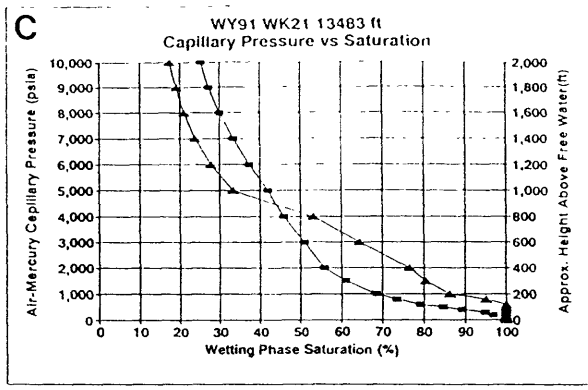
C
WY91 WK21 13483 ft
Capillary Pressure vs Saturation
Air-Mercury Capillary Pressure (psia)
Approx. Height Above Free Water(ft)
Wetting Phase Saturation (%)

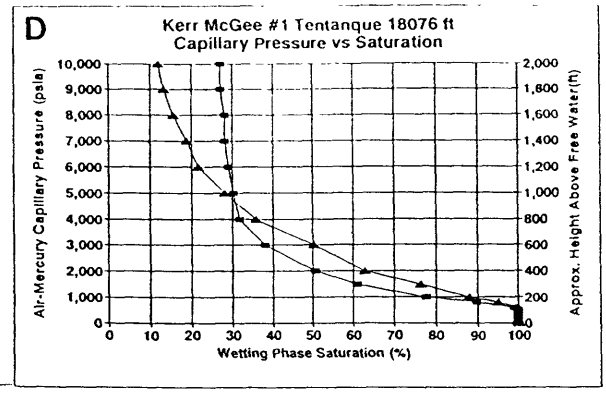
D
Kerr McGee #1 Tentanque 18076 ft
Capillary Pressure vs Saturation
Air-Mercury Capillary Pressure (psia)
Approx. Height Above Free Water(ft)
Wetting Phase Saturation (%)

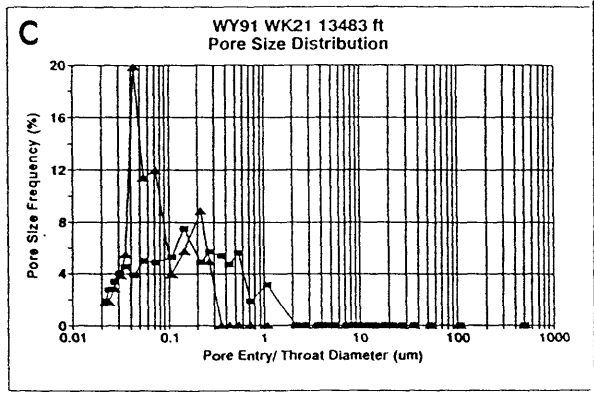
C
WY91 WK21 13483 ft
Pore Size Distribution
Pore Size Frequency (%)
Pore Entry/ Throat Diameter (um)

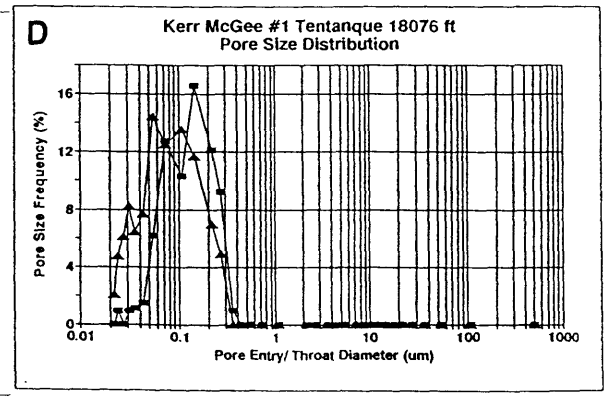
D
Kerr McGee #1 Tentanque 18076 ft
Pore Size Distribution
Pore Size Frequency (%)
Pore Entry/ Throat Diameter (um)

Figure 2-3. Plots illustrating capillary pressure versus wetting phase (i.e., air) saturation and pore size distribution for samples at ambient and under insitu stress conditions. Measurements under ambient conditions are represented by [■]; insitu measurements are represented by [▲]. The values of porosity and permeability which follow are insitu values. (A). Sample OK-8; porosity - 12.8%; permeability 47.65 md; depth 7197.5 ft. Shape and configuration of the capillary pressure vs. saturation curve indicates that mercury entered pores at relatively low pressure, and essentially complete saturation occurred at approximately 7,000 psia. Although the larger pores visible in figure 2B are approximately 50 x 100μm, measured pore-size distribution shows the majority of pore throats to be smaller than approximately 15μm. (B). Sample OK-3; porosity - 13.3%; permeability - 89.6md; depth 11,960 ft. Measured porosity and visible pores in figure 2C suggest properties very similar to those of sample OK-8. The capillary pressure vs. saturation curve indicates that more pore throats are being constricted by application of confining stress. The pore size distribution curves reveal a slightly higher proportion of larger pores (although still in the 20μm size range) in this sample compared to OK-8; pore throats under confining stress are typically smaller than 15μm. (C). Sample WY-21; porosity - 5.9%; permeability - 0.0010md; depth 13,483 ft. Capillary pressure vs. saturation curves show that mercury saturation of pore space is not accomplished, even at 10,000 psia, and that entry into pores is significantly restricted with increasing confining stress. Pore size distribution curves reveal that unconfined pore throats are typically smaller than approximately 1μm; when under confining stress, pore throats are reduced significantly in size and are typically less than 0.05μm. (D). Sample OK-1; porosity - 2.0%; permeability - 0.0010md; depth 18,076 ft. Physical appearance of the sample (see figure 2D) suggests very low porosity and permeability (due, at least in part, to compaction and cementation by carbonate and silica overgrows). Examination of the thin section illustrated in figure 2D suggests that the "thin-film' intergranular pores may be 1-2μm across. Pore size distribution curves, however, show that pore throats are most often <0.2 μm (unconfined) to 0.04 - 0.1μm (confined).

Table 2-1. General geographic location of samples examined in this investigation.

#	Sample	Well	Location				Formation
			County	Sec.	Twp.	Rng.	
		Uinta	**basin**	**UT**			
1	Ch 1-35	Shell-Christenson 1-33-A5	Duchesne	33	1S	5W	Green River
2	Ch 1-35	"	"	"	"	"	"
		Anadardo	**basin**	**OK**			
3	OK-1	Kerr-McGee #1 Tentanque	Cado	35	5N	10W	Springer
4	OK-2	Texaco #1 Carr	Cado	36	5N	11W	Springer
5	OK-3	Humble #1 Patterson	Grady	23	5N	6W	Springer
6	OK-4	"	"	"	"	"	"
7	OK-5	Chevron 1 Berta B Lay	Grady	8	3N	7W	"
8	OK-6	Edwin Cox 1 Miller	Canadian	26	14N	10W	Morrow
9	OK-7	King Stevenson 1 Anderson	Woodward	26	25N	20W	Morrow
10	OK-8	"	"	"	"	"	"
11	OK-9	Odessa Nat. Gas 1 Milstead	"	33	20N	21W	Morrow
		Wind River	**basin**	**WY**			
12	WY-8	Monsanto 1-35 Dolis	Fremont	35	39N	91W	Lance
13	WY-10	"	"	"	"	"	"
14	WY-20	"	"	"	"	"	"
15	WY-21	"	"	"	"	"	"
16	WY-25	"	"	"	"	"	"
17	WY-27	"	"	"	"	"	"
18	WY-31	"	"	"	"	"	"
19	WY-35	"	"	"	"	"	"

Table 2-2. Sample depths, and summary of data from modal analyses, and measured porosity and permeability.

#	Sample	Depth (ft)	Modal analysis* (vol. %)			Properties ** (see below)			Porosity (%)		Permeability^{X} (md)		Perm. (%) (Insitu÷Ambient)
			Q	F	R	Size	Sort	Ang.	Helium$^{\bullet}$	Modal	Ambient	Insitu	
1	Ch 1-35	11852	91.3	2 5	6.2	165	0 7	3.5	2.2	3	0.0065	0.0004	6.15
2	Ch 1-35	11932	93.1	3.1	3.8	193	0 8	2.1	4.0	7.6	0.0165	0.0018	10.9
3	OK-1	18076	100	- -	-.-	207	0.4	3.5	2.0	0 8	0 0050	0.0010	20.
4	OK-2	16078	98.1	0 8	1.1	148	0.4	2.9	4.9	8.5	0.0729	0.0078	10.69
5	OK-3	11960	99.6	0 4	-.-	210	0.9	2.0	13.3	24	95.466	89.6	93.39
6	OK-4	12072	100	-.-	-.-	156	0 4	2.0	4.3	6	0.0477	0.0026	5.45
7	OK-5	16626	99.5	0.5	-.-	140	1.0	2.5	8.8	10.8	0.5185	0.1975	38.09
8	OK-6	10161	98.7	0.9	0.4	166	0.5	3.6	ND	15 4	ND	ND	
9	OK-7	7096	91.4	1.0	7.6	321	0.4	3.8	14.	25	343.75	330.20	96.06
10	OK-8	7197 5	99.6	0.4	-.-	209	1.7	3.8	12.8	22	50.75	47.65	93.89
11	OK-9	10378	98 7	0.65	0.65	101	1.5	0.6	9.6	4.8	0.0078	0.0032	41.03
12	WY-8	12097.5	85.5	2.0	12.5	317	0.7	1.5	6.5	12.2	0.0157	0.0022	14.01
13	WY-10	12111	85.2	0.5	14.3	162	0.5	1.5	8.2	9.5	0.0077	0.0017	22.07
14	WY-20	12709.4	75.8	2.4	21.8	255	0.8	2	5.5	6.1	0.0106	0.0012	10.85
15	WY-21	13483	60.4	3.9	35.7	330	1.0	1.8	5.9	5.7	0.0133	0.0010	7.52
16	WY-25	13517.3	69.7	4.3	26.	226	1.2	1.2	3.7	4.1	0.0012	0.0001	8.33
17	WY-27	13527	77.8	3.9	18.3	317	0.8	1.5	5.2	3.3	0.0052	0.0005	9.62
18	WY-31	13602.5	80	10.9	18.3	397	0.5	2.1	4.7	4.9	0.0051	0.0011	21.57
19	WY-35	13631	62.1	15.9	22	272	0.5	2.2	6.7	7.2	0.0065	0.0024	36.92

*: Content of quartz (Q), feldspar (F), and lithic fragments (R), normalized to 100% ND: Not determined

$^{\bullet}$: Insitu values of helium porosity are listed

^{X}: Permeability values were measured to correct for Klinkenberg effect; listed are averages of two or more determinations.

** Properties

Grain Size		Sorting		Angularity	
Size (in μm)	Wentworth size	Visual estimate	Degree of sorting	Class interval	Grade term
550-250	Medium sand	0-0.35	Very well sorted	2.0 - 3.0	Subangular
250-125	Fine sand	0.35-0.5	Well sorted	3.0 - 4.0	Subrounded
125.-62.5	Very fine sand	0.5-1.0	Moderately sorted	4.0 - 5.0	Rounded
		1.0-2.0	Poorly sorted		

Appendix 3. Geologic characteristics of deep natural gas resources

Introduction

The primary objective of this task was to identify geologic conditions or variables (lithology, structure, pressure, etc.) favorable for natural gas accumulations in deep sedimentary basins. In order to meet this goal, deep basins were studied in terms of their geologic characteristics and comparisons were made between basins. Geologic data were taken primarily from computerized data bases including the NRG Associates Inc. Field File (NRG) (NRG Associates Inc., 1988) and the Petroleum Information Corporation's Well History Control System (WHCS) (Petroleum Information Corporation, 1988). NRG contains geologic, production, and engineering data for all reservoirs (or fields) with one million barrels of equivalent (BOE) or 6 Bcf of gas ultimate recoverable. WHCS contains geologic and drilling information for approximately 2 million wells drilled in the U.S.; of these, 16,500 wells were drilled deeper than 4,572 m (15,000 ft). Experts in the U.S. Geological Survey were consulted on specific problems in basins and for their knowledge about the geologic history of appropriate regions. We wish to acknowledge the help of Christopher Schenk, Mahlon Ball, Keith Robinson, and Richard Powers for their help.

Deep reservoirs and wells are defined arbitrarily as those occurring below 4,572 m (15,000 ft). However, a single producing horizon may extend both above and below 4,572 m (15,000 ft). For this reason, NRG retrievals were selected for all reservoirs below 4,270 m (14,000 ft) in order to capture all reservoirs occurring at approximately 4,572 m (15,000 ft) depth.

During the project, three separate subtasks were undertaken for Task 3: (1) tabulation and interpretation of NRG summaries of significant reservoirs in each deep sedimentary basin in the U.S., (2) preparation of maps illustrating the distribution of deep wells in the U.S. by geologic age, and (3) compilation of formation test data for deep producing wells in the U.S. in order to determine pressure regimes by depth for key reservoirs. The purpose of the regional compilations is to examine relationships in the distribution of deep producing wells and reservoirs in order to define geologic factors which control the distribution of deep natural gas resources in each region. Data for each region are compiled in a national summary (see RESULTS section above) in order to determine controlling factors for deep basin gas that are common to all deep producing areas.

Appendix 3, Subtask 1: Geologic characteristics of deep natural gas resources based on data from significant fields and reservoirs by T.S. Dyman, C.W. Spencer, J. Baird, R. Obuch, and D. Nielsen.

Data summaries from the NRG file and interpretations are presented for the Midcontinent, Rocky Mountain, Gulf Coast, and Permian basin regions. Data summaries are listed for the Williston basin and West Coast region but only 8 total reservoirs are identified as deep and no geologic controls are listed. Geologic and production data for all NRG-included reservoirs in the U.S. deeper than 4,270 m (14,000 ft) (see Introduction above for discussion) were extracted from the data base. Numbers of deep significant fields and reservoirs in the entire U.S. are as follows:

Rocky Mountains--	**19 fields,**	**22 reservoirs**
Permian basin--	**68 fields,**	**89 reservoirs**
Midcontinent--	**76 fields,**	**85 reservoirs**
West Coast--	**3 fields,**	**3 reservoirs**
Gulf Coast--	**160 fields,**	**174 reservoirs**
Williston basin--	**5 fields,**	**5 reservoirs**

Total-- 331 fields, 378 reservoirs

Reservoir data are presented below by region beginning with the Midcontinent (Data Set 1). Geologic conditions or variables favorable for deep gas accumulations are presented following each data set. English units used in table where one meter equals 3.28 ft.

Data Set 1-- Summary of significant fields and reservoirs occurring below 4,270 m (14,000 ft) in the **Midcontinent region** U.S. from The Significant Oil and Gas Fields of the U.S. (NRG Associates Inc., 1988). All deep fields and reservoirs occur in the **Anadarko basin** of Oklahoma and Texas. Refer also to Hugman and Vidas (1988) for field and reservoir data for the Midcontinent region. English units used in table where one meter equals 3.28 ft.

Numbers of deep fields/reservoirs in Anadarko basin of Oklahoma and Texas:
76 fields, 85 reservoirs.

Numbers of deep fields/reservoirs by state in Anadarko basin:
Texas-- 19 fields, 22 reservoirs.
Oklahoma-- 57 fields, 63 reservoirs.

Numbers of deep fields in Anadarko basin by discovery year:

1926-1959-- 6	
1960-- 1	1974-- 5
1961-- 1	1975-- 3
1962-- 4	1976-- 4
1963-- 1	1977-- 7
1964-- 2	1978-- 3
1966-- 2	1979-- 5
1967-- 2	1980-- 7
1969-- 2	1981-- 10
1970-- 4	
1971-- 2	**TOTAL-- 76**
1972-- 2	
1973-- 2	

Field classification in Anadarko basin:
Of 76 fields, 22 gas, and 54 blank (unknown).

Trapping mechanisms in Anadarko basin:
Of 85 reservoirs, 11 are structurally trapped, 14 are stratigraphically trapped, 16 are combination structural and stratigraphic, and 44 are unknown.

Data Set 1 (Anadarko basin) continued:

Numbers of deep reservoirs in Anadarko basin by location and depth:

Location by county and state	Depth in intervals of 1000 ft (14= 14,000-15,000 ft)									
	14	15	16	17	18	19	20	21	22	23
Cooke County, TX	1									
Hemphill County, TX	2	2	1	1		2	1			
Wheeler County, TX	4	2	2		2		1		1	
Carter County, OK			1							
Comanche County, OK					1	1				
Grady County, OK	1	3	3							
Beckham County, OK	1	2	3	3	2			1	1	1
Caddo County, OK	1	2	1	4	1		1			
Custer County, OK	5	4	1							
Washita County, OK	1	1	2							
Roger Mills Co., OK	3	3	2	2					1	
Dewey County, OK		1	1							
TOTALS	19	20	17	10	6	3	3	1	3	1

Deep reservoirs in Anadarko basin by formation and lithology (names are taken directly from NRG and may or may not represent formal stratigraphic units):

Unit	Age	Lithology	Number
Oil Creek	Ordovician	clastic	1
Goddard	Mississippian	clastic	2
Simpson	Ordovician	clastic	1
Bromide	Ordovician	clastic	1
Morrow	Pennsylvanian	clastic	28
Arbuckle	Cambrian	carbonate	2
Springer	Mississippian	clastic	13
Hunton	Silurian	carbonate	14
Morrow-Springer	Miss-Penn	clastic	1
Cottingham	Pennsylvanian	clastic	2
Atoka	Pennsylvanian	clastic	8
Ellenberger	Ordovician	carbonate	1
Henryhouse	Silurian	carbonate	1
Red Fork	Pennsylvanian	clastic	1
Boatwright	Pennsylvanian		1
Puryear	Pennsylvanian		1
Unknown			4

Data Set 1 (Anadarko basin) continued:

Deepest reservoir in Anadarko basin :
New Liberty Southwest, Hunton reservoir
Depth to production equals 23,920 ft
No production data reported in NRG file

Total cumulative production, proven reserves, and known recoverable gas and oil for reservoirs in Anadarko basin. Data represent maximum values because production totals are only available for fields in the state of Oklahoma. Some fields contain no data. Oil in thousands of barrels. Gas in millions of cubic ft. Cum prod= cumulative production; proven res= proven reserves; known res= known recovery.

	cum prod	proven res	known rec
Oil fields	2,332	253	2,585
Gas fields	2,378,997	418,933	2,784,300

Distribution of non-HC gases in the deep Anadarko basin:
Methane values in the Anadarko basin are high when compared to other deep basins in the U.S. (range 80.4 to 97.3%). He, H_2S, and CO_2 values are low.

Distribution of porosity in the the deep Anadarko basin:
Porosity values exhibit a wide range of distribution in the Anadarko basin (Fig. 3-1). The highest porosity values generally occur in clastic reservoirs. All significant reservoirs below 18,000 ft are fractured carbonate reservoirs and have porosities of less than 12%.

Geologic controls of deep gas production based on reservoir and published data for Anadarko basin:

(1) The Anadarko basin accounts for all of the deep gas (and oil) production in the Midcontinent region. Other Midcontinent petroleum-producing basins such as the Arkoma basin contain deep reservoirs, but significant production as defined in the NRG file (at least one million barrels of equivalent--BOE ultimate recoverable oil, or 6 Bcf of gas) does not occur yet. The deep Anadarko basin contains significant reserves of natural gas. The largest reservoirs occur in structural and combination traps along the southern margin of the basin in Oklahoma and the Texas panhandle.

(2) Structural traps within the Anadarko basin are generally thrust-bounded anticlinal closures in an overall transpressional setting. Anticlines are generally northwest- or west-trending and evolved through time such that updip stratigraphic pinchouts created combination structural and stratigraphic traps (Note: The recent Arbuckle discovery in the Criner Hills area of Oklahoma by Consolidated Natural Gas is a thrust-closure trap).

(3) Lower than normal thermal gradients may occur locally along the thrust-faulted margins of the Anadarko basin. Oil might then occur at deeper-than-normal conditions due to inferred downward flow of meteoric water along faults and fracture systems associated with the deep basin margin.

Mills Ranch and Eola Fields possibly illustrate these thermal conditions. An analog in the Rocky Mountain region occurs at Bridger Lake Field, located just north of the Uinta Mountains in Utah.

(4) The Morrow-Springer interval in the deep Anadarko basin is internally sourced and overpressured where rocks lower in the stratigraphic column such, as the Hunton, are normally pressured. The Morrow-Springer high-pressure compartmentalization is enigmatic. It seemingly could not be due to undercompaction as a result of burial. Near-maximum burial depths were reached in the basin at the end of the Permian. Thermogenic reactions involving HC generation are the most likely cause of overpressuring today.

(5) The Woodford Shale of the Anadarko basin is not significantly overpressured, in contrast to the similar Bakken Shale of the Williston basin. HC's are no longer being generated from kerogen at rates which exceed leakage rates in the deeper parts of the Anadarko basin. If gas is now being generated in the deep Woodford, and if the Woodford is not overpressured, the natural gas may be migrating into the Hunton.

(6) Two opposing views are suggested about the quality of source rocks in the Arbuckle Group:

(a) The Arbuckle Group may prove to be disappointing as a major, deep, natural gas producer in the Anadarko basin because it lacks suitable internal source rocks. Additionally, anhydrite in the Arbuckle reacts with methane to produce significant amounts of non-HC gases such as carbon dioxide (from the thermal degradation of carbonates--dilutes methane) and hydrogen sulfide (from thermochemical sulfate reduction of anhydrite--destroys methane). The Hunton contains less anhydrite, allowing methane to be stable at depth.

(b) The Arbuckle has undergone high thermal stress and for the most part displays minimum TOC values. However, higher TOC values in the geologic past, combined with the oil-prone nature of the organic matter (type II-I), could have enabled at least portions of the Arbuckle to generate petroleum. Smackover carbonates, which are also very mature to overmature in the deeper portions of the basin, also exhibit generally low TOC content-- an average of 0.5% (Palacas, in press). Yet, these carbonates are known to be the source of giant oil and gas accumulations. Alternatively, the Arbuckle problem may be simply a matter of not locating and analyzing the right organic-rich sections of rock. Palacas (in press), in summarizing Trask and Patnode's (1942) studies, showed that out of 178 subsurface Arbuckle samples from 18 wells in the Anadarko basin, approximately 46% contained TOC contents ranging from 0.4 to 1.4%. Carbonate rocks with such values can be considered adequate source beds for petroleum.

(7) Large volumes of gas in Pennsylvanian clastic reservoirs were sourced by Upper Mississippian and Pennsylvanian shales. The high percentage of Pennsylvanian stratigraphic traps in clastic reservoirs suggests generation and entrapment close to source.

(8) The Anadarko basin is unlike other deep basins in that HC's have been generated in an unusually long and continuous history that has contributed to the oil and gas productivity in this Paleozoic province. Time-Temperature Index computations indicate that the oil window has migrated upward through time (Schmoker, 1986). Oil may have been generated in the deepest parts of the southern Oklahoma aulacogen as long

as 350 m.y. during the Pennsylvanian and Permian when large volumes of sediment entered the zone of oil generation. Natural gas is very hard to trap. Known discoveries may have been generated during the last 60 million years.

Data Set 2-- Summary of significant fields and reservoirs occurring below 14,000 ft in the **Rocky Mountain region** U.S. from The Significant Oil and Gas Fields of the U.S. (NRG Associates Inc., 1988). English units used in table where one meter equals 3.28 ft.

Numbers of significant fields/reservoirs in deep basins of the Rocky Mountain region:
19 fields, 22 reservoirs.

Numbers of significant fields/reservoirs in deep basins of the Rocky Mountain region by state:
Wyoming-- 16 fields, 19 reservoirs.
Utah-- 1 field, 1 reservoir.
Colorado-- 2 fields, 2 reservoirs.

Numbers of significant fields in deep basins of the the Rocky Mountain region by discovery year:

1926-1959-- 5	1980-- 1
1965-- 1	1981-- 1
1966-- 3	1982-- 3
1972-- 1	1985-- 1
1977-- 1	**TOTAL-- 19**
1979-- 2	

Field classification for significant deep reservoirs in the Rocky Mountain region:
Of 22 reservoirs, 6 oil, 13 gas, and 3 oil and gas.

Trapping mechanisms for significant deep reservoirs in the Rocky Mountain region:
Of 22 reservoirs, 8 are structurally trapped, 9 are combination structural and stratigraphic, and 5 are unknown.

Structurally trapped significant deep reservoirs in the Rocky Mountain region:

Reno, Johnson Co., WY	Oil	Powder River basin
Reno east, Johnson Co. WY	Oil	Powder River basin
Poison Spider West, Natrona Co., WY	Oil	Wind River basin
Butcher Knife Springs, Uinta Co., WY	Gas	Thrust belt
Whitney Canyon, Uinta Co., WY	Gas	Thrust belt
Anschutz Ranch east, Uinta Co., WY	Gas/oil	Thrust belt
Session Mountain, Uinta Co., WY	Gas	Thrust belt
Chicken Creek, Uinta Co., WY	Gas/oil	Thrust belt

Geographic distribution, reservoir classification, and API gravity of significant deep reservoirs in the Rocky Mountain region:

Powder River basin	4 res	(oil)	API grav= 35
Moxa arch	2 res	(oil/gas)	API grav= 40
Wind River basin	2 res	(oil/gas)	API grav= 46
Sand Wash basin	2 res	(gas)	
WY thrust belt	7 res	(oil/gas)	API grav= 51
Washakie basin	5 res	(gas)	

Data Set 2 (Rocky Mountain region) continued:

Significant deep reservoirs in the Rocky Mountain region by formation and lithology:

Minnelusa-- 4 res (mixed) Penn-Perm
Nugget-- 6 res (clastic) Jurassic
Dakota-- 3 res (clastic) Cretaceous
Frontier-- 2 res (clastic) Cretaceous
Madison-- 2 res (carb) Miss.
Bighorn-- 3 res (carb) Ordov.
Weber-- 1 res (clastic) Penn-Perm
Morgan-- 1 res (carb) Penn

Significant reservoirs in the Rocky Mountain region by depth:

14,000-15,000 ft	9 reservoirs
15,000-16,000 ft	8
16,000-17,000 ft	0
17,000-18,000 ft	2
18,000-19,000 ft	3

Deepest significant reservoir in the Rocky Mountain region:
Bull Frog Field, Natrona County, WY with 18,792 ft reservoir
Gas from Frontier Formation; 2,320 proven acres
Field discovered in 1979

Total cumulative production, proven reserves, and known recoverable gas and oil for deep significant reservoirs in the Rocky Mountain region. Data represent minimum values. Some fields contain no data. Oil in thousands of barrels. Gas in millions of cubic ft. Cum prod= cumulative production; proven res= proven reserves; known res= known recovery; blank equals no data.

Oil	Total	Clastic	Carbonate	Chert	Blank
Known rec	45,100	45,100	--	---	---
Proven res	14,400	14,400	--	---	---
cum prod	30,400	30,400	--	---	---

Gas	Total	Clastic	Carbonate	Chert	Blank
Known rec	2,192,600	836,000	1,356,600	---	---
Proven res	1,782,900	595,200	1,187,700	---	---
cum prod	436,400	300,600	135,800	---	---

Distribution of non-HC for significant deep reservoirs in the Rocky Mountain region:
Methane ranges from 22.0 to 94.7%. The lowest value (22.0%) occurs at the LaBarge deep Madison Limestone reservoir in Lincoln County, Wyoming. All Rocky Mountain reservoirs have He values less than 0.5%. Generally the highest H_2S values occur in fields with high CO_2 content. The highest CO_2 values occur in limestone reservoirs.

Distribution of porosity for significant deep reservoirs in the Rocky Mountain region:
Only sparse porosity-depth data are available from the NRG file for the Rocky Mountain region (Fig. 3-1). Of the few reservoirs represented, clastic reservoirs generally exhibit the highest porosities.

Geologic controls of deep gas production based on reservoir data for Rocky Mountain basins:

(1) Of the 22 significant reservoirs in the Rocky Mountain region, 19 are in Wyoming. The total (22) includes 7 in the Wyoming thrust belt; 2 each in the Wind River basin, Moxa arch, and Sand Wash basins; 4 in the Powder River basin; and 5 in the Washakie basin. Deep production in the Rocky Mountain region is dominantly natural gas, gas condensate, and high-gravity oil in the Utah-Wyoming thrust belt. Significant reservoirs in the thrust belt produce primarily from Cretaceous, Jurassic, and Triassic sandstones (Frontier and Nugget) and Permian-Pennsylvanian mixed clastic/carbonate sequences (Weber and Minnelusa) in primarily structural traps. Source rocks for deep reservoirs are primarily organic-rich Cretaceous shales in fault contact with older reservoir rocks.

(2) Significant deep oil production occurs in conventional reservoirs in Rocky Mountain basins. Reservoir rocks are primarily Cretaceous sandstones and Permian-Pennsylvanian sandstones and carbonates. These reservoirs are located in deep areas of abnormally low subsurface temperatures and low thermal maturation, probably caused by cool meteoric water penetrating deep into the basin along bounding faults (Law and Clayton, 1988). The deep western part of the Powder River basin has below normal temperatures, possibly as a result of meteoric waters recharged from outcrops along the western margin of the basin.

(3) Significant deep Mississippian production in the Rocky Mountain region is from limestones and dolomites. These reservoirs have a high productive capacity (> 20 MMcf per day per well) and commonly contain significant amounts of non-HC gases such as H_2S and CO_2. Reservoirs are primarily found in large structures.

(4) Most significant deep reservoirs in the Rocky Mountain region are associated with structural or combination structural and stratigraphic trapping mechanisms. Structural traps in Rocky Mountain basins are directly related to the tectonic evolution of the Rocky Mountain foreland province. According to W.J. Perry, Jr. (Appendix 4, this volume), initial southeastward progression of uplift and basin development from southwest Montana southeastward during the mid Cretaceous established timing limits on petroleum migration and trapping trends. Rocky Mountain foreland development reached the position of the Colorado Front Range by latest Maastrichtian time. Subsequent Laramide deformation spread northeastward during the latest Cretaceous and Paleocene establishing first the Wind River basin and then the Powder River basin. The Laramide deformation front reached the Black Hills by late Paleocene time..

Economic implications of this new model of deformation of the Rocky Mountain foreland include progressive opening and subsequent blockage of migration paths for HC's generated from Paleozoic source rocks in southeastern Idaho, southwestern Montana, Wyoming, Colorado, and eastern Utah. Deep natural gas, generated during the Tertiary, has likely migrated from the deeper parts of these foreland basins into structural traps formed during Laramide deformation.

Data Set 3-- Summary of significant fields and reservoirs occurring below 14,000 ft in the deep **Permian basin region** U.S.. From The Significant Oil and Gas Fields of the U.S. (NRG Associates Inc., 1988). Deep Permian basin here includes primarily reservoirs in the Delaware basin of west Texas and southeast New Mexico. English units used in table where one meter equals 3.28 ft.

Numbers of significant fields/reservoirs in the deep Permian basin:
68 fields, 89 reservoirs.

Number of significant fields in the deep Permian basin by discovery year:

1948 - 1	1963 - 1	1970 - 2	1977 - 5
1955 - 1	1964 - 1	1971 - 3	1978 - 1
1956 - 1	1965 - 2	1972 - 2	1979 - 4
1958 - 2	1966 - 4	1973 - 7	1980 - 1
1960 - 3	1967 - 1	1974 - 1	1981 - 3
1961 - 2	1968 - 5	1975 - 5	1982 - 1
1962 - 2	1969 - 3	1976 - 1	1983 - 1
			Total- 68

Field classification for all significant reservoirs in the deep Permian basin by state and county:

	Oil and Gas	Gas	Total
New Mexico			
Eddy		3	3
Lea	1	8	9
Texas			
Culberson		1	1
Loving		11	11
Pecos		16	16
Reeves		14	14
Terrel		1	1
Ward		20	20
Winkler		14	14
TOTAL	1	88	89

Data Set 3 (Permian basin) continued:

Classification of significant reservoirs in the deep Permian basin by depth and county:

	Depth (ft X 1000)								
County	14	15	16	17	18	19	20	21	22
Eddy Co., NM	3								
Lea Co., NM	8	1							
Culberson Co., TX		1							
Loving Co., TX	1	4	2		1		1	2	
Pecos Co., TX	2	5		1	2	1	2	3	
Reeves Co., TX	1	1	6	1	2	1	2		
Terrel Co., TX	1								
Ward Co., TX	2	2	3	6	3	4			
Winkler Co., TX	3	1	1	2	2	2	1	2	
TOTAL	21	15	12	10	10	8	6	7	

Data Set 3 (Permian basin) continued:

Classification of significant reservoirs in the deep Permian basin by reservoir type and depth:

[c = carbonate; cl = clastic; ch = chert; b = blank]

Location	Depth in intervals of 1,000 feet (14,000-15,000 ft)															
	14				15				16				17			
	c	cl	ch	b	c	cl	ch	b	c	cl	ch	b	c	cl	ch	b
Eddy County, NM	3															
Lea County, NM	4	3	1		1											
Culberson County, TX					1											
Loving County, TX	1				1	1		2			2					
Pecos County, TX		2			3	1		1						1		
Reeves County, TX	1				1				4	2			1			
Terrell County, TX	1															
Ward County, TX	2				2				3				6			
Winkler County, TX	1	1		1	1				1				2			
Totals	21				15				12				10			

Location	18				19				20				21			
	c	cl	ch	b	c	cl	ch	b	c	cl	ch	b	c	cl	ch	b
Eddy County, NM																
Lea County, NM																
Culberson County, TX																
Loving County, TX	1								1				2			
Pecos County, TX	2				1				2				3			
Reeves County, TX	2				1				2							
Terrell County, TX																
Ward County, TX	3				4											
Winkler County, TX	2				2				1				2			
Totals	10				8				6				7			

Data Set 3 (Permian basin) continued:

Numbers of significant reservoirs in the deep Permian basin by geologic age, formation, and lithology:

Age	Formation/unit	Number of Res	Reservoir type
Permian	Wolfcampian	2	(blank)
Pennsylvanian	Pennsylvanian	1	(blank)
Pennsylvanian	Strawn	3	carbonate
Pennsylvanian	Atoka	5	clastic/carb
Pennsylvanian	Morrow	10	clastic
Mississippian	Mississippian	1	carbonate
Devonian	Lower Devonian	5	chert
Siluro-Devonian	Siluro-Devonian	3	carbonate
Silurian	Silurian	4	carbonate
Silurian	Fusselman	10	carbonate
Silurian	Fusselman Dol	12	carbonate
Ordovician	Ellenberger	33	carbonate
TOTAL		89	

Number of significant reservoirs in the deep Permian basin by trap type and depth (blank indicates no trap identified):

Depth	Trap type			
	Stratigraphic	Structural	Combination	Blank
14-15	3	7	8	3
15-16	1	6	4	4
16-17	1	7	3	1
17-18		5	5	1
18-19		6	2	1
19-20		2	4	2
20-21		4	1	1
21-22		3	3	1
TOTAL	5	40	30	14

Total cumulative production, proven reserves, and known recoverable gas and oil for significant reservoirs in the deep Permian basin. Data represent minimum values. Some fields contain no data. Oil in thousands of barrels. Gas in millions of cubic ft. Cum prod= cumulative production; proven res= proven reserves; known res= known recovery.

Oil	Total	Clastic	Carbonate	Chert	Blank
Known rec	8,075	---	8,075	---	---
Proven res	939	---	939	---	---
cum prod	7,136	---	7,136	---	---

Gas	Total	Clastic	Carbonate	Chert	Blank
Known rec	15,127,180	566,030	13,766,982	709,530	84,638
Proven res	2,713,874	157,053	2,481,937	49,970	24,914
cum prod	12,413,306	408,977	11,285,045	659,560	59,724

Data Set 3 (Permian basin) continued:

Distribution of non-HC gases for significant reservoirs in the Permian basin:
Methane ranges from 47.0 to 97.7% in the deep Permian basin but averages approximately 90%. The 3 lowest methane values occur in Ellenberger (carbonate) reservoirs (Brown Bassett, Mi Vida, and Moore-Hooper-Vermejo fields) in the Texas part of the deep basin. Each of these reservoirs have high CO_2 values (34.8 to 53.8%). He and H_2S values are very low in the deep Permian basin.

Distribution of porosity for significant deep reservoirs in the deep Permian basin:
Reservoir porosity systematically decreases with depth in the Permian basin (Fig. 3-1). Generally, significant reservoirs below 16,000 ft are carbonate reservoirs. Below 19,000 ft these reservoirs exhibit porosities below 5%. Of the shallower reservoirs (less than 16,000 ft), clastic reservoirs average higher porosities than carbonate reservoirs.

Geologic controls of deep gas production based on reservoir data for Permian basin:

(1) Deep production in the Permian basin is predominantly gas from carbonate reservoirs in the western and southern parts of the greater Permian basin in what is commonly referred to as the Delaware basin. Some deep gas was generated directly from mature source rocks, while additional gas has been generated by the conversion of oil to gas. Most oil fields in equivalent rocks occur on the periphery of the greater Permian basin, on the north and east margins, supporting this theory of a thermal conversion process.

(2) The volume of available reservoir rocks decreases with depth in the greater Permian basin because the basin area decreases with depth. As a result, finding new, good quality, deep gas reservoirs increases with depth. However, increased pressures with depth result in an increase in gas stored within a given volume of reservoir rock.

(3) Lithologically, shallower reservoirs in the Delaware basin (14,000 to 17,000 ft) are mixed carbonate and clastic reservoirs (but mostly carbonate) including some Pennsylvanian- and Permian-aged rocks. They are located in Lea County, NM and Loving County, TX on the margin of the deep basin. The deepest reservoirs are composed predominantly of carbonate rocks of lower Paleozoic age from the central part of the Delaware basin. Thirty-three deep reservoirs occur in the Ordovician Ellenberger alone.

(4) The deep Ellenberger of the Permian basin is similar to the Arbuckle of the Anadarko basin in that it may not be internally sourced (see item 6, Anadarko basin; and Palacas, in press). Ellenberger HC's are predominantly derived from younger rocks including the Woodford Shale where these rocks have been down-faulted during compression or extension. Gas was probably emplaced in Ellenberger reservoirs after structures were established during Pennsylvanian and Permian time. These Upper Paleozoic collisional structures were formed prior to peak gas generation.

(5) All of the deep stratigraphically trapped reservoirs (five in the NRG data file) occur at shallower depths (14,000 to 17,000 ft) in the youngest reservoir strata of Permian age. The post Wolfcampian Permian basin is a sedimentary rather than a structural basin and traps are facies-controlled in these younger rocks.

(6) The total gas column in Ellenberger reservoirs is very thick reaching more than 3,500 ft in the Gomez Field. Vertical, interconnected fractures occur in some areas. These fracture systems are associated with huge transpressional structures along the eastern margin of the Delaware basin.

(7) Matrix porosity is as high as 5% at depths greater than 19,000 ft (Fig. 3-1) in the deep Permian basin. Fractures are common and result in greatly enhanced permeability and increased deliverability from prospective reservoirs. Poor porosities can result at any depth, but the best porosities decrease with depth at a predictable rate. Limestone reservoirs tend to produce economic volumes of HC's at lower porosities than dolomite. The highest porosities at these depths occur in dolomite reservoirs although NRG data are limited.

(8) Source-rock type becomes less important with respect to the presence of oil and gas with increasing depth because thermal cracking converts oil to gas and condensate at depth. Normal pressure gradients typify deep reservoirs in large fields in the Permian basin. No evidence exists for overpressurized compartments in the significant fields of the NRG data file (published field data).

Data Set 4-- Summary of significant fields and reservoirs occurring below 14,000 ft in the **Pacific region** U.S. from The Significant Oil and Gas Fields of the U.S. (NRG Associates Inc., 1988). Data for the Pacific region in NRG are summarized briefly because only three significant fields with deep reservoirs occur there. English units used in table where one meter equals 3.28 ft.

Number of significant deep fields and reservoirs in Pacific region:
3 reservoirs and 3 fields; 2 in California and one in Alaska.

Field discovery year for significant fields with deep reservoirs in the Pacific region:
Fillmore field discovered 1954, Ventura Co., CA
Rio Viejo field discovered 1975, Kern Co., CA
Beaver Creek field discovered 1967, Kenai Quad, AK

Final field classification for all significant deep reservoirs by State in the Pacific region:
Both California fields have multiple reservoirs and are classified as oil fields. Beaver Creek field, Alaska is classified as a gas field.

Reservoir classification by depth for significant deep reservoirs in the Pacific region:
Rio Viejo field occurs at 14,100 ft and Fillmore field occurs at 14,250 ft. Beaver Creek field occurs at 14,800 ft.

Significant reservoir summary by primary reservoir lithology and depth for Pacific region:
All 3 reservoirs produce from sandstone between 14,000 and 15,000 ft.

Numbers of significant deep reservoirs by rock unit and geologic age, and primary lithology for the Pacific region:
Rio Viejo field 654 Stevens Sandstone
Fillmore field 655 Pico Sandstone
Beaver Creek field 654 Tyonek Sandstone

Numbers of significant deep reservoirs by trap type and depth in Pacific region:
Both California reservoirs are defined as stratigraphic. The Alaska reservoir is classified as structurally trapped.

Data Set 4 (Pacific region) continued:

Known recovery, proven reserves, and cumulative production for significant deep reservoirs in the Pacific region by major lithology:
Known recov.= known recoverable resources; proven res.= proven reserves; and cum. prod.= cumulative production. Gas in millions of cubic ft (MMcf); oil in millions of barrels (MMbls).

	Major reservoir lithology		
	Total	**Clastic**	**Carbonate**
Gas (MMcf)			
Known recov.	264,900	264,900	--
Proven res.	179,912	179,912	--
Cum. prod.	84,988	84,988	--
Oil (MMbls)			
Known recov.	27,650	27,650	--
Proven res.	5,067	5,067	--
Cum. prod.	22,583	22,583	--

Distribution of porosity for significant deep reservoirs in the in the Pacific region:
Both California reservoirs have average reservoir porosities of 31% (Fig. 3-1). The Alaska reservoir has an average porosity of 28%.

Distribution of non-HC gases for significant deep reservoirs in the Pacific region:
Data not available of Pacific region reservoirs.

Geologic controls not presented for Pacific region because only three reservoirs identified.

Data Set 5-- Summary of significant fields and reservoirs occurring below 14,000 ft in the **Williston basin region** U.S. from The Significant Oil and Gas Fields of the U.S. (NRG Associates Inc., 1988). Data for the Williston basin in NRG are summarized briefly because only five significant fields with deep reservoirs occur in the region. These data are listed separately because significant differences exist with data from the Rocky Mountain and Midcontinent regions. English units used in table where one meter equals 3.28 ft.

Number of significant deep fields and reservoirs in the Williston basin:
Five fields containing 5 deep reservoirs. All are located in McKenzie Co., ND.

Field discovery year for significant fields with deep reservoirs in the Williston basin:
Discovery years for fields range from 1952 (Croff field) to 1981 (Poe field).

Final field classification for all significant deep reservoirs by State in the Williston basin:
Croff and Bear Den fields are oil fields and North Fork, Cherry Creek, and Poe fields are classified as oil and gas fields.

Field classification by depth for significant deep reservoirs in the Williston basin:
All reservoirs are located between 14,003 and 14,188 ft.

Summary of significant deep reservoirs by primary reservoir lithology and depth for Williston basin:
All reservoirs produce from the dolomites in the Ordovician Red River Formation.

Numbers of significant deep reservoirs by trap type and depth in Williston basin:
All reservoirs are classified as structural or combination structural and stratigraphic trap types.

Known recovery, proven reserves, and cumulative production for significant deep reservoirs in the Williston basin by major lithology:
Known recov.= known recoverable resources; proven res.= proven reserves; and cum. prod.= cumulative production. Gas in millions of cubic ft (MMcf); oil in millions of barrels (MMbls).

	Major reservoir lithology		
	Total	**Clastic**	**Carbonate**
Gas (MMcf)			
Known recov.	38,142	--	38,142
Proven res.	25,334	--	25,334
Cum. prod.	12,808	--	12,808

Data Set 5 (Williston basin) continued:

	Major reservoir lithology		
	Total	**Clastic**	**Carbonate**
Oil (MMbls)			
Known recov.	1,945	--	1,945
Proven res.	1,014	--	1,014
Cum. prod.	931	--	931

Distribution of porosity for significant deep reservoirs in the Williston basin:
Only one porosity value (10% for Cherry Creek field-- Red River reservoir; Fig. 3-1) was recorded in the NRG file for Williston basin significant reservoirs.

Distribution of non-HC gases for significant deep reservoirs in the Williston basin:
Ordovician, Pennsylvanian, and Triassic reservoirs have tested high percentages of Nitrogen from several wells in the basin.

Geologic controls not identified for Williston basin because only three reservoirs identified.

Data Set 6-- Summary of significant fields and reservoirs occurring below 14,000 ft in the **Gulf Coast basin**, U.S. from the Significant Oil and Gas Fields of the U.S. (NRG Associates Inc., 1988). For Texas and Louisiana, deep natural gas production is a maximum value because shallower reservoirs are included in production totals. English units used in table where one meter equals 3.28 ft.

Number of significant deep fields and reservoirs Gulf Coast basin: 160 fields, 174 reservoirs (total Gulf Coast basin); 14 fields and 16 reservoirs offshore Texas and Louisiana; 45 fields and 48 reservoirs Tertiary onshore; and 101 fields and 110 reservoirs Mesozoic onshore.

Field discovery year for significant fields with deep reservoirs in the Gulf Coast basin.

Year--	Number	Year--	Number	Year--	Number
1942--	2	1961--	2	1976--	8
1943--	1	1962--	2	1977--	8
1944--	1	1964--	2	1978--	8
1945--	1	1965--	3	1979--	12
1948--	1	1966--	4	1980--	7
1949--	1	1967--	2	1981--	8
1951--	1	1968--	6	1982--	6
1952--	1	1969--	8	1983--	4
1954--	2	1970--	12	1984--	10
1956--	1	1971--	5	1985--	1
1957--	4	1972--	7	**TOTAL--**	**160 fields**
1958--	2	1973--	4		
1959--	3	1974--	4		
1960--	2	1975--	4		

Final field classification for significant deep reservoirs by State in the Gulf Coast basin:

	Classification			
State	Oil	Gas	Oil and gas	
Louisiana	5	49	11	
Texas	--	22	1	
Mississippi	21	40	3	
Alabama	11	5	3	
Florida	3	--	--	
Total	40	116	18	= 174 reservoirs

Data Set 6 (Gulf Coast basin) continued:

Classification of significant deep reservoirs by depth for in the Gulf Coast basin:
Depth in intervals of 1,000 ft; LA= Louisiana; TX= Texas; MS= Mississippi; AL= Alabama; FL= Florida.

Depth	Classification: Oil					Gas					Oil and gas				
	LA	TX	MS	AL	FL	LA	TX	MS	AL	FL	LA	TX	MS	AL	FL
14-15	1		12	2		19	12	14			2	1	1		
15-16			3	4	3	13	5	13	1		4	2	2		
16-17	2		3	2		7	4	6	1		4			1	
17-18	1		1			4	1	2			1				
18-19	1		1	3		3		1							
19-20			1			3		2							
20-21									2						
21-22									1						
22-23								1							
23-24								1							
Total	5		21	11	3	49	22	40	5		11	3	3	1	

Reservoir summary by primary reservoir lithology and depth for significant deep reservoirs in the Gulf Coast basin:
Depth in intervals of 1,000 ft; C= carbonate reservoirs; Cl= clastic reservoirs.

	Lithology by state: Louisiana		Texas		Mississippi		Alabama		Florida	
Depth	C	Cl	C	Cl	C	Cl	C	Cl	C	Cl
14-15		22	3	10	6	20	1	1		
15-16		17	2	3	2	16	5	2	2	1
16-17	1	12	3	1	1	8	4			
17-18		6		1	1	3				
18-19		4				2	3			
19-20		3			2	1				
20-21								2		
21-22								1		
22-23					1					
23-24					1					
Total	1	64	8	15	14	50	13	6	2	1

Data Set 6 (Gulf Coast basin) continued:

Numbers of significant deep reservoirs by rock unit and geologic age, and primary lithology for Gulf Coast basin:
Lithology may vary locally due to facies and depositional variations. Stratigraphic names as used in this chart are taken directly from the NRG data file. No attempt is made to differentiate between (a) formal stratigraphic nomenclature and informal drillers terms, (b) and the use of stratigraphic hierarchy such as group versus formation names. Unless rock names are labelled with a (c) = carbonate or (c-cl) = mixed carbonate and clastic, they are considered clastic reservoirs.

	Reservoir depth interval (14= 14,000-15,000 ft interval)										
Rock unit	14	15	16	17	18	19	20	21	22	23	24
Tertiary											
Robulus	2										
Frio	7										
Miocene	15	10	6	3							
Anahuac		3	1								
Bolivina mex.	1										
Discorbis B	1										
Wilcox	2	2		1							
Textularia	2										
Yegu	1										
Planulina		1									
Camerina		1									
Woodburn		1									
Pliocene			1	1	1						
Pleistocene		1									
Bigerina hum.			1								
Cretaceous											
Austin (c)	1										
Tuscaloosa	1	2	3	2	3	3					
Edwards(c)	1		1								
Hosston	3	12	5								
Sligo(c-cl)	4	5	1								
James(c)	1										
Mooringsport	1										
Paluxy	1										
Red	3										
Jurassic											
Buckner(c)	1										
Black River					1						
Cotton Valley	8	1	3	1		1					
Norphlet	3	3		2			2	1			
Smackover(c)	5	9	6	1	4	2			1	1	
Total (=174)	64	51	28	11	9	6	2	1	1	1	

Data Set 6 (Gulf Coast basin) continued:

Numbers of significant deep reservoirs by trap type and depth in Gulf Coast basin:
R= structural trap; S= stratigraphic trap; C= combination structural and stratigraphic trap; B= Blank and indicates no trap type identified in NRG file. Depth in intervals of 1,000 ft.

Trap type by State

	Mississippi				Florida				Texas				Louisiana				Alabama			
	R	S	C	B	R	S	C	B	R	S	C	B	R	S	C	B	R	S	C	B
Depth																				
14-15	21	1	3	1					4	4	3	4	18			2	1		1	
15-16	13		4	1	2		1		2	3		1	9		1	7	2		2	3
16-17	6		3						1		1	1	7		1	5	3			1
17-18	3		1						1				4			2				
18-19	2												2		1	1			2	1
19-20	2	1											1		1	1				
20-21																	2			
21-22																	1			
22-23	1																			
23-24	1																			
24-25																				
Total (=174)	49	2	11	2	2		1		8	7	4	6	41		4	18	9		5	5

Known recovery, proven reserves, and cumulative production for significant deep reservoirs and fields in the Gulf Coast basin by major lithology:
Known recov.= known recoverable resources; proven res.= proven reserves; and cum. prod.= cumulative production. Gas in millions of cubic ft (MMcf); oil in millions of barrels (MMbls).

Major reservoir lithology

	Total	Clastic	Carbonate	Mixed
Gas (MMcf)				
Known recov.	13,262,291	11,110,291	1,679,000	473,000
Proven res.	6,628,587	5,676,587	719,000	233,000
Cum. prod.	6,192,094	4,993,094	960,000	239,000
Oil (Mmbls)				
Known recov.	881,805	330,805	551,000	--
Proven res.	128,226	56,226	72,000	--
Cum. prod.	590,579	111,579	479,000	--

Data Set 6 (Gulf Coast basin) continued:

Distribution of non-HC gases for significant deep reservoirs in the Gulf Coast basin:
Methane ranges from 35-94% for Mesozoic gas reservoirs. The lowest value (35%) occurs at Flomation field, Escambia County, Alabama, in the Norphlet reservoir, which contains 45% carbon dioxide. Methane ranges from 79 to 94% and averages about 90% for Tertiary reservoirs. Carbon dioxide is low (less than 9%) for other reservoirs. The highest hydrogen sulfide value (26%) for significant deep Gulf Coast basin reservoirs occurs at Johns Field, Rankin County, Mississippi, in the Smackover reservoir.

Distribution of porosity for significant deep reservoirs in the Gulf Coast:
A systematic decrease in average porosity occurs with increasing depth for all significant deep reservoirs, although the range of porosity values at a particular depth varies significantly (Fig. 3-1). The approximate rate of decrease in porosity with increasing depth appears to change at about 17,000 ft. Although exceptions exist, porosity values below 17,000 ft appear higher than expected based on the distribution of points above 17,000 ft (Norphlet and Tuscaloosa reservoirs included here). An explanation for this change in rate of porosity decrease is not established here, but the data suggest that porosities high enough for commercial production of gas may occur at depths greater than expected. No significant difference exists between the range of clastic versus carbonate porosities using the NRG data set.

Geologic controls of deep gas production based on reservoir data for Gulf Coast basin:

(1) The two oldest fields containing deep reservoirs are the Lake de Cade field in Terrebonne Parish, Louisiana and the Thornwell South field in Jefferson Davis Parish Louisiana. The fields were discovered in 1942 although the deeper reservoirs were discovered later. The deep reservoirs produce from immediately below 14,000 ft in Tertiary sandstones. Generally, the oldest fields occur in Louisiana and Mississippi. Fields in Texas were discovered from the 1940's through the 1980's. Fields in Florida were discovered in the early 1970's, and fields in Alabama were discovered in the 1960's. More fields with deep reservoirs were discovered during the 1970's (72) than in any other decade. The number of field discoveries in this category approximately doubled with each succeeding decade (1940's= 7; 1950's= 14; 1960's= 31; 1970's= 72; data for 1980's incomplete).

(3) Sixty-seven percent of the significant deep reservoirs are classified as gas producing. More than 40% of the gas (49) reservoirs are located in Louisiana. Of all of the Gulf Coast states, Louisiana, Texas, and Mississippi contain more gas than oil reservoirs (Sassen, 1990). Of the 16 significant deep offshore reservoirs, 15 are gas producers. Of the 110 significant deep Mesozoic reservoirs onshore, 64 are gas producers and an additional 9 are classified as oil and gas producing.

(4) For all states combined, the number of significant deep reservoirs decreases with increasing depth. The deepest reservoirs occur in Alabama and Mississippi. The Jurassic Smackover gas reservoir in the Harrisville field in Simpson County Mississippi is the deepest significant reservoir in the Gulf Coast basin. The reservoir has an average producing depth of

23,007 ft and an average reservoir thickness of 618 ft. Only two other reservoirs listed in the NRG file have greater average thicknesses. The shallower nature of Florida and Texas deep reservoirs is due to the shallow depth of equivalent Mesozoic reservoir rocks. Of the 16 significant reservoirs in offshore Texas and Louisiana, the deepest is 18,895 ft. Most offshore reservoirs produce from less than 16,000 ft.

(5) For all depths together, 79% of the reservoirs are clastic reservoirs. By depth interval, (1) only 16% of the total reservoirs are carbonate reservoirs in the 14,000 to 15,000 ft depth interval, and (2) 30% of the total reservoirs are carbonate reservoirs in the 16,000 to 17,000 ft depth interval. The representation of carbonate reservoirs in the 14,000 to 15,000 ft depth interval is low, and correspondingly more clastic lithologies of the Tertiary sequence are present. In both Florida and Texas, all significant Mesozoic reservoirs are in carbonate rocks. In Louisiana, nearly all significant Mesozoic reservoirs are in clastic rocks. Alabama and Mississippi display more intermediate reservoir facies. All of the offshore Texas and Louisiana reservoirs are classified as sandstone.

(6) The distribution of reservoirs by geologic age is approximately equal with 65 Tertiary, 53 Cretaceous reservoirs, and 56 Jurassic reservoirs present. The largest number of reservoirs occur in the Tertiary Miocene (34), Jurassic Smackover Formation (29), and Cretaceous Hosston Formation (20). All Tertiary reservoirs occur in clastic rocks; whereas, 54% of Jurassic reservoirs (30 reservoirs of 56 total) occur in carbonate rocks (primarily Smackover Formation). Although not identified in this table, approximately 50% of the carbonate reservoirs are defined as dolomite in the NRG data file. Jurassic reservoirs are generally found deeper than Cretaceous and Tertiary reservoirs in the Gulf Coast basin. All offshore Texas and Louisiana reservoir rocks are Tertiary.

(7) Reservoirs in the Gulf Coast Mesozoic basin are primarily structurally trapped. Only 9 reservoirs are identified as stratigraphically trapped, 5 of which occur in Upper Cretaceous or Tertiary rocks. Stratigraphically-trapped reservoirs and reservoirs classified as combination trapped appear to be relatively shallow (less than 20,000 ft). Stratigraphically-trapped reservoirs are controlled by facies variations in marine and nonmarine Upper Cretaceous and Tertiary clastic rocks. All offshore Texas and Louisiana reservoirs are structurally trapped.

(8) More than 6.1 Tcf of gas have been produced from significant deep reservoirs in the Gulf Coast basin. Of this, 2.6 Tcf of gas have been produced from Tertiary reservoirs, and 0.6 MMcf of gas have been produced from offshore Texas and Louisiana Tertiary reservoirs. Clastic reservoirs have produced approximately 5 times as much gas as carbonate reservoirs.

REFERENCES CITED

Hugman, R.H., and Vidas, E.H., 1988, Oil and gas resources of the Midcontinent region--an update of the resource base in the HC supply model: GAs Research Institute Final Report Contract 5087-800-1475.

Law, B.E., and Clayton, J.L., 1987, The role of thermal history in the preservation of oil at the south end of the Moxa arch, Utah and Wyoming--implications for the oil potential of the southern Green river basin [abs.], *in* Carter, L.M.H., ed., U.S. Geological Survey Research on energy resources- 1988, Program and Abstracts: U.S. Geological Survey Circular 1025, p. 27.

NRG Associates Inc., 1988, The significant oil and gas fields of the United states (through December 31, 1988): Available from Nehring Associates, Inc., P.O. Box 1655, Colorado Springs, CO 80901.

Palacas, J.G., in press, Can carbonate rocks be sources of commercial petroleum deposits? *in*, Johnson, K.S., and Cardott, B.J., eds., Source rocks in the southern Midcontinent, 1990 symposium: Oklahoma Geological Survey Circular 93, 29 p.

Petroleum Information Corporation, 1988, Well History Control System (through December 1988): Available from Petroleum Information Corporation, 4100 East Dry Creek Road, Littleton, CO 80122.

Petroleum Information Corporation, 1991, Well History Control System (through December 1991): Available from Petroleum Information Corporation, 4100 East Dry Creek Road, Littleton, CO 80122.

Schmoker, J.W., 1986, Oil generation in the Anadarko basin, Oklahoma and Texas: modelling using Lopatin's method: Oklahoma Geological Survey Special Publication No. 86-3, 40 p.

Trask, P.D., and Patnode, H.W., 1942, Source beds of petroleum: American Association of Petroleum Geologists, Tulsa, OK, 566 p.

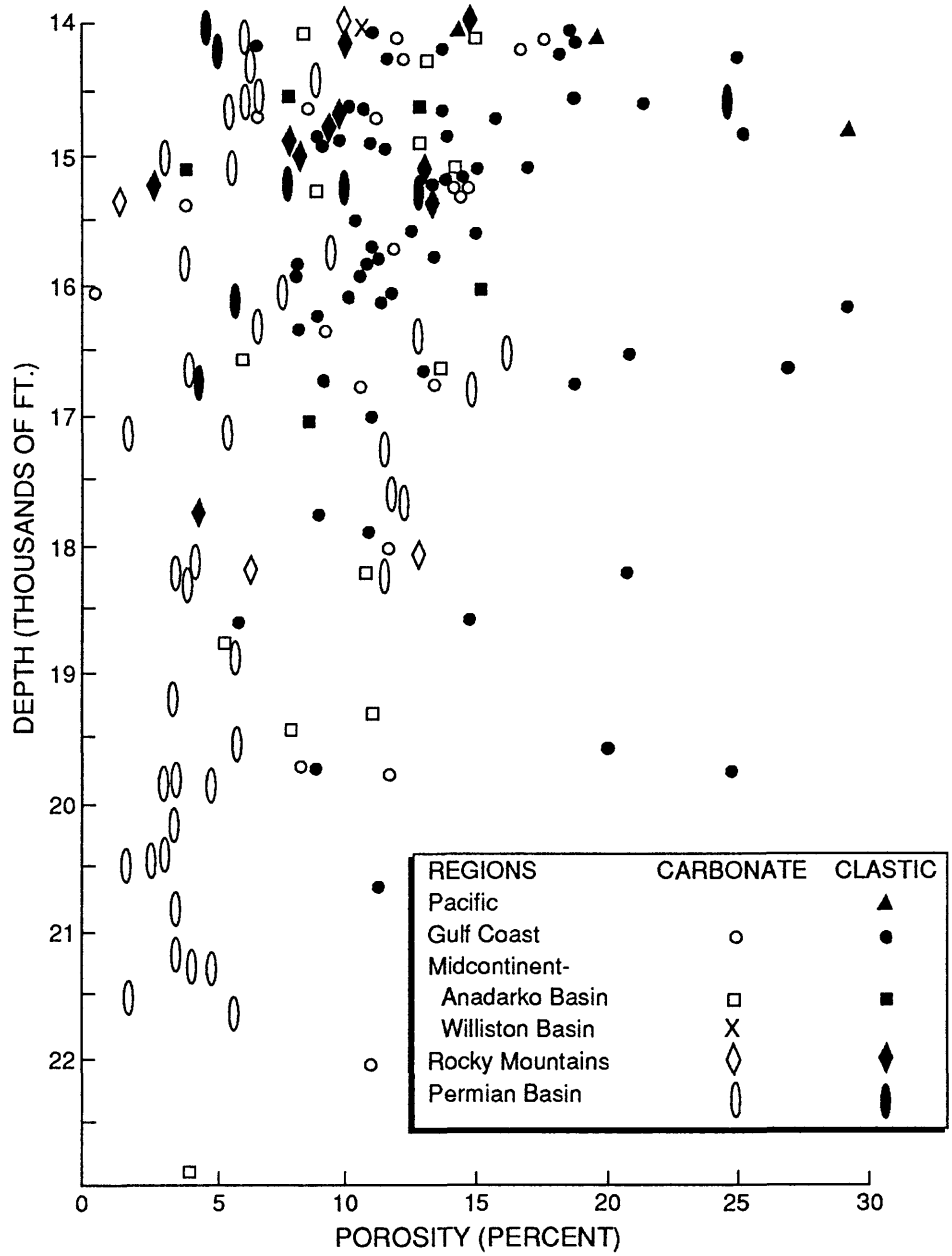

Figure 3-1. Porosity-depth plot for significant deep reservoirs in the U.S. All reservoirs below 4,270 m (14,000 ft included. Data from NRG Associates File of Significant Fields in U.S. Depth in thousands of feet; porosity in percent. Data available for 157 significant reservoirs from the Gulf Coast basin, Midcontinent, Permian basin, Rocky Mountain, and Pacific regions.

Appendix 3, Subtask 2: Maps illustrating the distribution of deep wells in the U.S. by geologic age, by C.J. Wandrey and D. Vaughan

A series of maps showing wells drilled deeper than 4,572 m (15,000 ft) was created using Petroleum Information Corporation's Well History Control System (WHCS) files current to June 1991. While these files are current they are not always complete or entirely accurate. Various methods were used to ensure accuracy and completeness. Some of these methods are discussed below.

The first part of this series consists of four maps showing wells that have produced HCs from depths of 4,572 m (15,000) ft or greater, grouped by geologic age of the producing rocks (Plates 1-4). Since various parts of the WHCS files are incomplete, several cross checks were made to ensure that these wells did in fact produce from depths greater than 4,572 m (15,000 ft). Often the records show that a well produced and was drilled to greater than 4,572 m (15,000 ft) but the depth of production was not indentified in the file. In these cases, the wells are cross checked against subsurface geologic maps and formation top depth and initial-potential files. Information on individual wells in the Gulf Coast region was particularly misleading or lacking. In many cases these wells were drilled to salt domes created by flowage of salt from older deeper salt beds up into younger rocks and the age of the salt rather than the surrounding rocks was identified.

Of the 6,178 wells that produce or have produced HCs from depths greater than 4,572 m (15,000 ft) 4,547 are gas or gas and condensate wells (Table 3-1). The Uinta basin and the Gulf Coast basin, the two areas where there are significant numbers of deep oil wells, are producing from relatively young rocks. It is likely that source rocks which are still producing oil at these depths have been buried deeply for only a short duration or have been overpressured for the greater portion of the time spent in the oil and gas windows. The most likely scenario is a combination of these influences.

The success ratio of approximately 46% for these deep wells is high and may be due to a variety of factors including: (1) greater investment is likely made in preparatory exploration of the prospect to reduce the financial risk, and (2) there appear to be fewer true wildcats (most wells are production wells drilled in proven areas resulting in a better success rate).

The total wells column does not always equal the sum of the other three columns because some wells produced both oil and gas and were therefore listed twice. Some wells lacked final well class information indicating the type of production and in still other cases there was insufficient location information to determine the correct basin. More than two hundred of these wells were not posted on the maps because the well class and location problems could not be resolved. No age was recorded for many offshore wells in the Gulf of Mexico, but their approximate ages were determined by comparing the total depths to neighboring wells with age information. Wells outside the shaded areas (areas with sedimentary rocks at depths of 4,572 m--15,000 ft or greater) may have inaccurate location data or the shaded area may not have been extended far enough due to lack of data.

The second part of the series consists of 5 maps showing non-producing wells grouped by the age of the oldest rocks penetrated (Plates 5-9). Non-producing means that hydrocarbons could not be economically produced at the time drilling was completed. Shows of oil and/or gas may have been present but were insufficient to warrant production, or completion problems may have precluded production. Some of these wells may not be truly "dry" holes in the conventional sense of the term. Since the WHCS file uses the same code for

dry holes and abandoned producers there may be a few wells displayed as dry holes that in fact produced in the past or are temporarily shut-in until pipelines or production facilities are completed. While the number of wells that produced at one time or are still producing is relatively accurate, dry-hole estimates may be high.

The shaded portions of the maps identify areas with sedimentary rocks at depths of 4,572 m (15,000 ft) or greater. Sedimentary thickness data were compiled using a sedimentary rock depth contour map of the continental U.S. (Frezon and Finn, 1983), an unpublished basement map of the southwestern U.S. (W.C. Butler, personal communication, 1992), and well log and seismic data for the Midcontinent Rift system (Anderson, 1990).

Bibliography:

Anderson, R.R., ed., 1990, The AMOCO M.G, Eischeid #1 deep Petroleum test Carroll County, Iowa preliminary investigations: Energy and Geological Resources Division Geological Survey Bureau.

Frezon, Sherwood E., Finn, Thomas M., Lister, Jean H., 1983, Total thickness of sedimentary rocks in the conterminous United States: U.S. Geological Survey Open-file 83-920.

Table 3-1. Total wells, producing wells by production category (oil, gas, and oil and gas), and tectonic regime by basin for selected basins in the U.S. Data from Well History Control System (Petroleum Information Corporation, 1991).

Basin or province	Total	oil	gas	oil and gas	Basin type
Anadarko	1258	41	1231	1	foreland
Ardmore	10	0	10	0	foreland
Arkoma	6	1	10	0	foreland
Bighorn	4	0	4	0	foreland
Green River	107	24	81	0	foreland
Gulf region	3465	999	2411	35	passive margin
Marietta	14	3	11	0	foreland
Permian	873	22	793	2	cont. marg., rift
Piceance	2	1	1	0	foreland
Powder River	32	31	0	0	foreland
San Joaquin	6	5	0	0	foreland
Uinta	154	152	2	0	foreland
Ventura	6	4	2	0	transpressive
Wind River	72	6	65	0	foreland

Note that the total wells column does not always equal the sum of the other three columns because some wells produced both oil and gas and were therefore listed twice. Note also that the total wells column does not equal the the 6,178 wells discussed in the text. Some wells lacked final well-class information indicating the type of production, and in still other cases, location information was insufficient to determine the correct basin. Approximately 169 of these wells were not posted on the maps because well classification and location problems could not be resolved.

Appendix 3, Subtask 3: Deep gas reservoir pressure and initial potential test data, U.S., by C.W. Spencer and C.J. Wandrey

INTRODUCTION

A study of available deep (> 4,572 m--15,000 ft) reservoir pressures was conducted because: (1) abnormally high pore pressure (>0.55 psi/ft) may reduce the rate of porosity and permeability loss with increasing burial depths and (2) gas reservoirs with high pore pressure will have more gas-in-place than low-pressure reservoirs at the same temperature and porosity owing to the high compressability of natural gas. Shallow (< 2,40 m--8,000 ft) reservoirs are usually normally pressured (0.465 psi/ft) or underpressured (<0.43 psi/ft) , whereas deep (> 4,572 m--15,000 ft) hot reservoirs may have normal to above normal pressures. In order to determine the general distribution of abnormally high pressures and predict their occurrence in undrilled areas, it is helpful to consider possible causes of high pore pressures.

There is no single cause that can adequately explain **all** occurrences of above normal pressures. However, most proposed mechanisms require that semi-isolated or fairly well sealed reservoirs be present in order to maintain abnormal pressure. Some of the more commonly accepted causes of overpressuring are dewatering of shales owing to compaction, clay mineral transformations that release water, and aquathermal pressuring caused by thermal expansion of water.

The physical dewatering of clayey sediments and shales by compaction caused by weight of overburden is a widely accepted mechanism (Dickenson, 1953; Morgan and others, 1968; Chapman, 1980; Chiarelli and Duffaud, 1980). This origin of overpressuring is most likely in depocenters characterized by geologically young, rapidly deposited sediments.

Diagenetic alteration of smectite-bearing shales and claystones to a more stable mixed-layer illite/smectite or illitic shale releases water. This is a popular mechanism to explain overpressuring in the U.S. Gulf Coast basin (Powers, 1967; Burst, 1969; Bruce, 1984).

Aquathermal pressuring was proposed by Barker (1972) as the cause of some of the high pore pressure present along the northern coast of the Gulf of Mexico. In his model, the reservoirs must be essentially isolated from pressure bleed-off. If the temperature of a reservoir rock enclosed in excellent seals is increased, the thermal expansion of pore water will cause an increase in reservoir pressure. Magara (1975) suggested that aquathermal pressuring is responsible for reservoir pressures in the Gulf Coast that exceed the weight of overburden. Daines (1982) concluded that aquathermal pressuring could occur at shallow depth in impermeable sediments in areas of high geothermal gradients. However, he concluded that even good clay shales will, over geologic time, bleed off the pressure caused by the relatively small water volume increase caused by thermal expansion. Barker (1972, p. 2068) noted that aquathermal pressuring might not be the only mechanism for abnormal pressure in a given area, but could add to the reservoir pressure caused by other mechanisms.

Other mechanisms for overpressuring are discussed by Fertl (1976) and Gretner (1981). They noted additional proposed causes of abnormally high pressure such as tectonic loading (stress), osmosis, chemical changes such as conversion of gypsum to anhydrite, pressure transfer up faults, salt diapirism, secondary cementation of pores, long HC columns, and thermal conversion of organic matter to oil and gas.

Active or recently active (last few million years) HC generation is a likely explanation for overpressuring in basins where (1) rich source beds are present at high temperature (generally >100° C), (2) the pressuring phase is oil or gas, and (3) the sediments are well compacted (Spencer, 1987).

DATA ANALYSIS

Pressure data for this study were obtained from two main sources: (1) the drillstem test (DST) reports in Petroleum Information's Well History Control System computer files and (2) reservoir-pressure data compiled in the NRG Associates Significant Oil and Gas Fields of the U.S. file (NRG Associates, 1991). The NRG file is updated to July 1991 and contains data on about 10,000 fields of which about 250 are deeper than 4,270 m (14,000 ft) and have some form of reservoir pressure data recorded. A "significant" field is one that has more than 1 million barrels of recoverable oil or more than 6 billion cubic ft (6 Bcf) of recoverable gas.

NRG Associates Significant Field File

The definition of normal pressure varies somewhat among different basins but usyally ranges from 0.43 to 0.465 psi/ft depending on reservoir salinity and other factors. Overpressured deep "significant" gas reservoirs are present in the Rocky Mountain region in the Wind River and Greater Green River basins (Figs. 1 and 2, RESULTS section). This region also contains overpressured shallower reservoirs in the depth range from 3,200 m (10,500 ft) to more than 3,960 m (13,000 ft), but are not part of this study. Most of the overpressured gas-bearing rocks are of Tertiary and Cretaceous age and the overpressuring is caused by active HC generation (Spencer, 1987).

The Anadarko basin (Fig. 1, RESULTS section) contains overpressured Permian, Pennsylvanian, Mississippian-Devonian, and Ordovician sandstones, carbonates, and shales in the deep parts of the basin. The origin of this overpressuring is not known at this time, but may be related to HC generation.

The Permian basin (Fig. 1, see Results section above) has overpressuring in about 35% of the >4,270-m-deep (>14,000 ft-deep) significant reservoirs in the NRG Associates Significant Field File. Most of the overpressuring occurs in rocks of Permian Wolfcampian, Pennsylvanian Morrowan and Atokan, and Mississippian age. Dominant reservoir lithologies are sandstone, limestone, and dolostone. Minor overpressuring occurs in Devonian limestone. The origin of the overpressuring is not well defined but may be caused by the thermal conversion of previously migrated oil to gas plus some active generation of gas from deep basin source beds. More research in this area is needed.

The Gulf Coast region (Fig. 1, RESULTS section) has extensive overpressured, or overpressured reservoirs. The geopressuring in younger Miocene and Oligocene sandstones and shales is probably caused mostly by undercompaction (Dickenson, 1953; Chapman, 1980). These undercompacted, geopressured gas areas have been studied in recent years as part of the U.S. Department of Energy's Geopressured-Geothermal Energy program. Overpressuring in Cretaceous and Jurassic sandstones and carbonates in the eastern Gulf may be caused by several mechanisms, and more study needs to be done to allow better prediction of the overpressuring because its distribution is highly variable.

Well History Control System--initial potentials

Even though initial potentials (IP) of wells cannot be used to define overpressuring, a study was made to analyze expected deep well productivity using (IP's) of all wells completed in the U.S. at depths greater than or equal to 4,572 m (15,000 ft) using Petroleum Information Corporation's Well History Control System (WHCS). Table 3-2 contains drillstem test summaries for deep wells from the WHCS file. Preliminary plots of initial-potential gas production versus depth do not permit a delineation of discrete trends (Figs. 3-2A through 3-2G). Several factors may affect the distribution of data on these plots. Foremost, deep wells tend to have lower matrix permeabilities and the degree and openness of natural fractures is a controlling factor influencing individual well productivity. Second, many of the wells were artificially stimulated with acid and/or hydraulic fracturing. The success of these techniques varies considerably throughout the U.S. Third, is some basins, rocks of similar ages and lithologies dominate the data set, while in other areas, diverse ages and lithologies are combined on a single plot.

Four examples of initial-potential production versus depth (Figs. 3-2A through 3-2D) illustrate the variability of initial potentials at depths of 4,572 m (15,000 ft) or greater across the U.S.

The Uinta basin data set (Figs. 3-2A) shows a wide range of IP values at all depths but none of the wells are very high volume (maximum IP equals about 2.75 million cubic ft/day at about 4,880 m--16,000 ft). Nearly random scatter occurs but the majority of data points are less than 1 MMcf. These reservoirs are dominantly sandstone and Tertiary in age. Natural fractures are causing the variability (scatter) of these low permeability reservoirs. This anlaysis indicates that the deep Uinta basin is not a good place to drill high-volume gas wells.

The Wind River basin data set (Figs. 3-2B) are all from Cretaceous sandstones with the exception of the IP's at about 7,315 m (24,000 ft) which are completions in Mississippian dolomite and are high CO_2 gas.

Figures 3-2C illustrates the wide range in variability of Anadarko basin IP's. Data show some very high volume wells (above 200 MMcf) but most are in the less than 5 MMcf range (Fig. 3-2G). Some of the very high values may be due to data errors in the WHCS data file.

Figure 3-2D illustrates the variability of IP test results in the Gulf Coast basin for the Smackover Formation excluding Texas. The log plots cluster the data by field. The cluster of data at 4,720 to 4,880 m (15,500 to 16,000 ft) represents wells predominantly in Big Escambia, Jay, and Blackjack Creek fields. The cluster of wells from 5,490 to 5,640 m (18,000 to 18,5000 ft) represents wells mostly in Chunchula, Hatters Pond, and Cold Creek fields.

More refinements in these cross plots are necessary to define subtle variations in IP data with depth of test. Data need to be correlated with artificial fracturing techniques in new studies.

REFERENCES CITED

Barker, Colin, 1972, Aquathermal pressuring--Role of temperature in development of abnormal pressure zones: American Association of Petroleum geologists Bulletin, v. 56, p. 2068-2071.

Bruce, C.H., 1984, Smectite dehydration--Its relation to structural development and hydrocarbon accumulation in northern Gulf of Mexico

basin: American Association of Petroleum geologists Bulletin, v. 68, p. 673-683.

Burst, J.F., 1969, Diagenesis of Gulf Coast clayey sediments and its possible relation to petroleum migration: American Association of Petroleum geologists Bulletin, v. 53, p. 73-93.

Chapman, R.E., 1980, Mechanical versus thermal cause of abnormally high pore pressures in shales: American Association of Petroleum geologists Bulletin, v. 64, p. 2179-2183.

Cheney, P.E., 1949, Abnormal pressures, lost circulation Gulf Coast's top drilling problem: The Oil and Gas Journal, v. 47, p. 210-215.

Chiarelli, A., and Duffaud, F., 1980, Pressure origin and distribution in Jurassic of Viking basin (United Kingdom-Norway): American Association of Petroleum geologists Bulletin, v. 64, p. 1245-1250

Daines, S.R., 1982, Aquathermal pressuring and geopressure evaluation: American Association of Petroleum geologists Bulletin, v. 66, p. 931-939.

Dickenson, George, 1953, Geological aspects of abnormal reservoir pressures in Gulf Coast Louisiana: American Association of Petroleum geologists Bulletin, v. 37, p. 410-432.

Fertl, W.H., 1976, Abnormal formation pressure environments, *in* Fertl, F.H., Abnormal formation pressures, Developments in Petroleum Science, 2, Chapter 1: New York, American Elsevier, p. 1-48.

Gretner, P.E., 1981, Pore pressure-fundamentals, general ramifications and implications for structural geology (revised): American Association of Petroleum geologists Continuing Education Course Note Series #4, 131 p.

Magara, Kinji, 1975, Importance of aquathermal pressuring effect in Gulf Coast: American Association of Petroleum geologists Bulletin, v. 59, p. 2037-2045.

Morgan, J.P., Coleman, J.M., and Gagliano,. S.M., 1968, Mudlumps--Diapiric structures in Mississippi delta sediments, *in* Brawnstein, Jules, and O'Brien, G.D., eds., Diapirism and diapirs: American Association of Petroleum geologists Memoir 8, p. 145-161.

NRG Associates Inc., 1988, The significant oil and gas fields of the United states (through July, 1991): Available from Nehring Associates, Inc., P.O. Box 1655, Colorado Springs, CO 80901.

Petroleum Information Corporation, 1991, Well History Control System (through November 1991): Available from Petroleum Information Corporation, 4100 East Dry Creek Road, Littleton, CO 80122.

Powers, M.C., 1967, Fluid release mechanisms in compacting marine mudrocks and their importance in oil exploration: American Association of Petroleum geologists Bulletin, v. 51, p. 1240-1254.

Spencer, C.W., 1987, Hydrocarbon generation as a mechanism for overpressuring in the Rocky Mountain region: American Association of Petroleum geologists Bulletin, v. 71, p. 368-388.

Spencer, C.W., 1989, Review of characteristics of low-permeability gas reservoirs in Western United States: American Association of Petroleum geologists Bulletin, v. 73, p. 613-629.

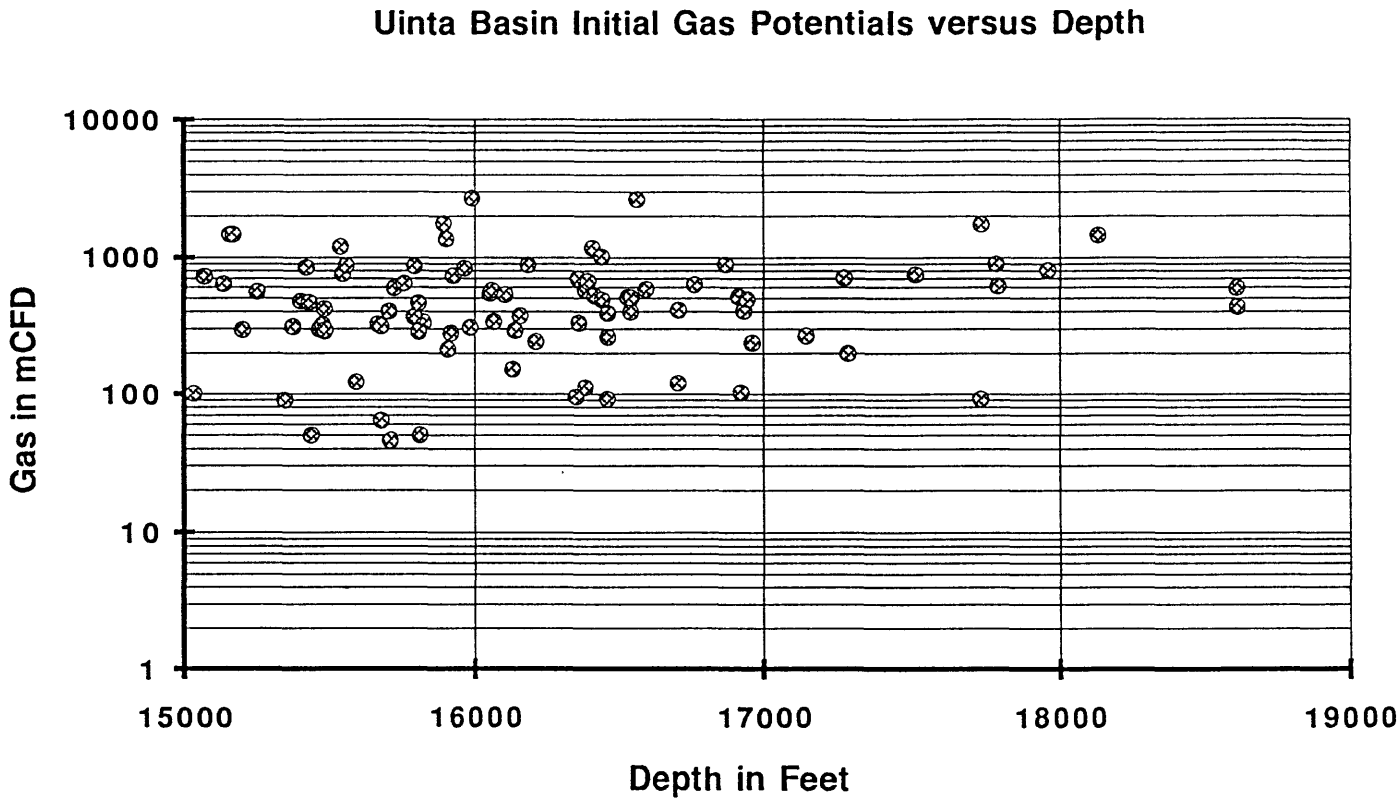

Figure 3-2A. Plot of initial-potential tests and depths for deep wells in Uinta basin. Data from Petroleum Information Corporation (1991).

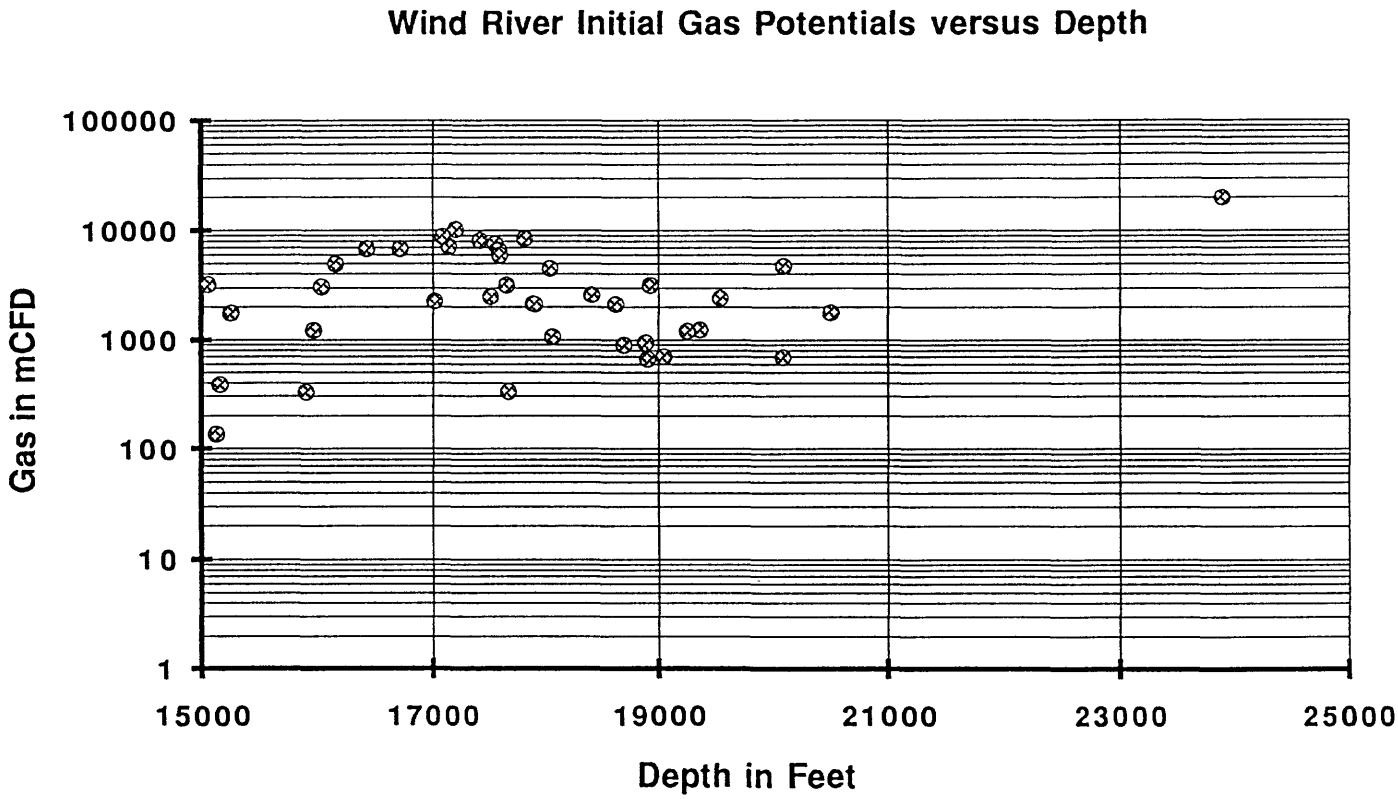

Figure 3-2B. Plot of initial-potential tests and depths for deep wells in Wind River basin. Data from Petroleum Information Corporation (1991).

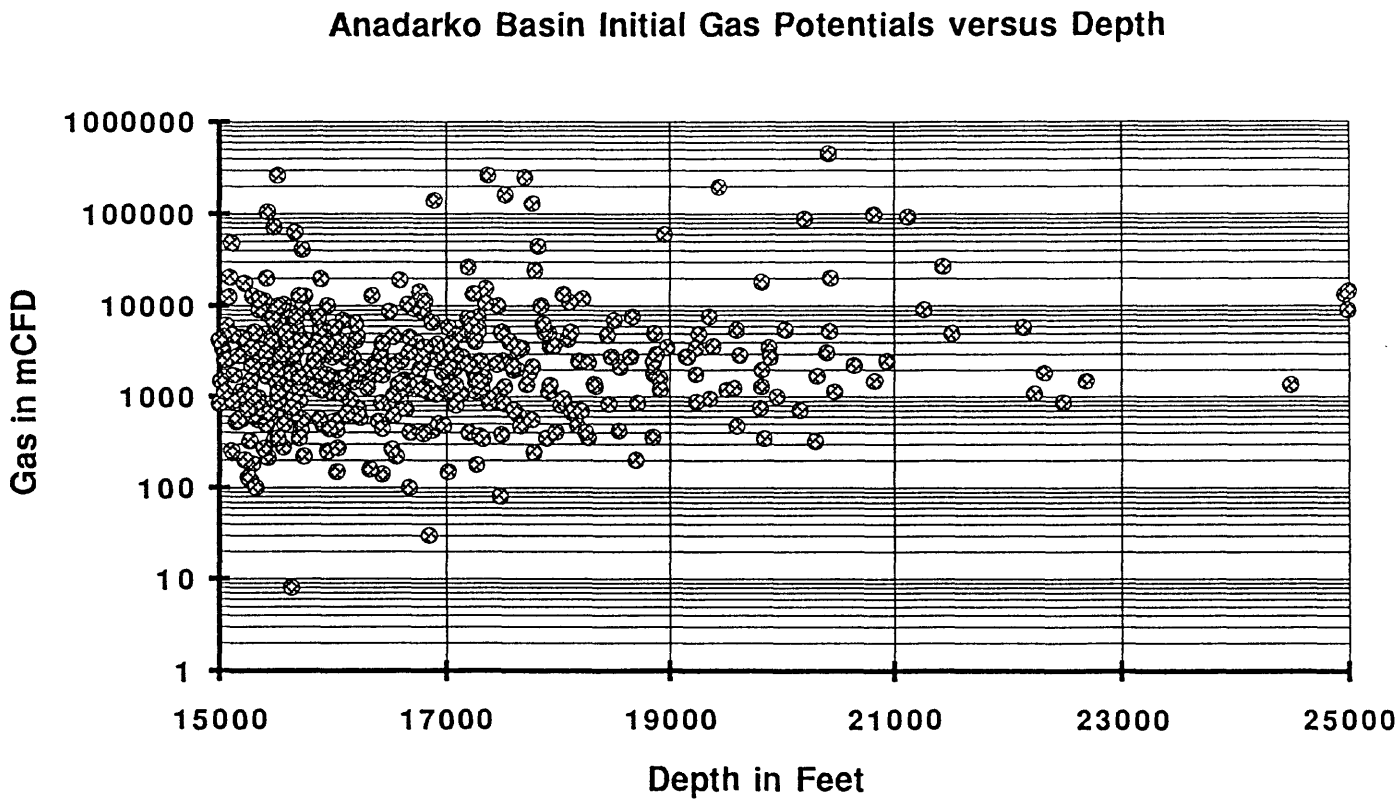

Figure 3-2C. Plot of initial-potential tests and depths for deep wells in Anadarko basin, Oklahoma. Data from Petroleum Information Corporation (1991).

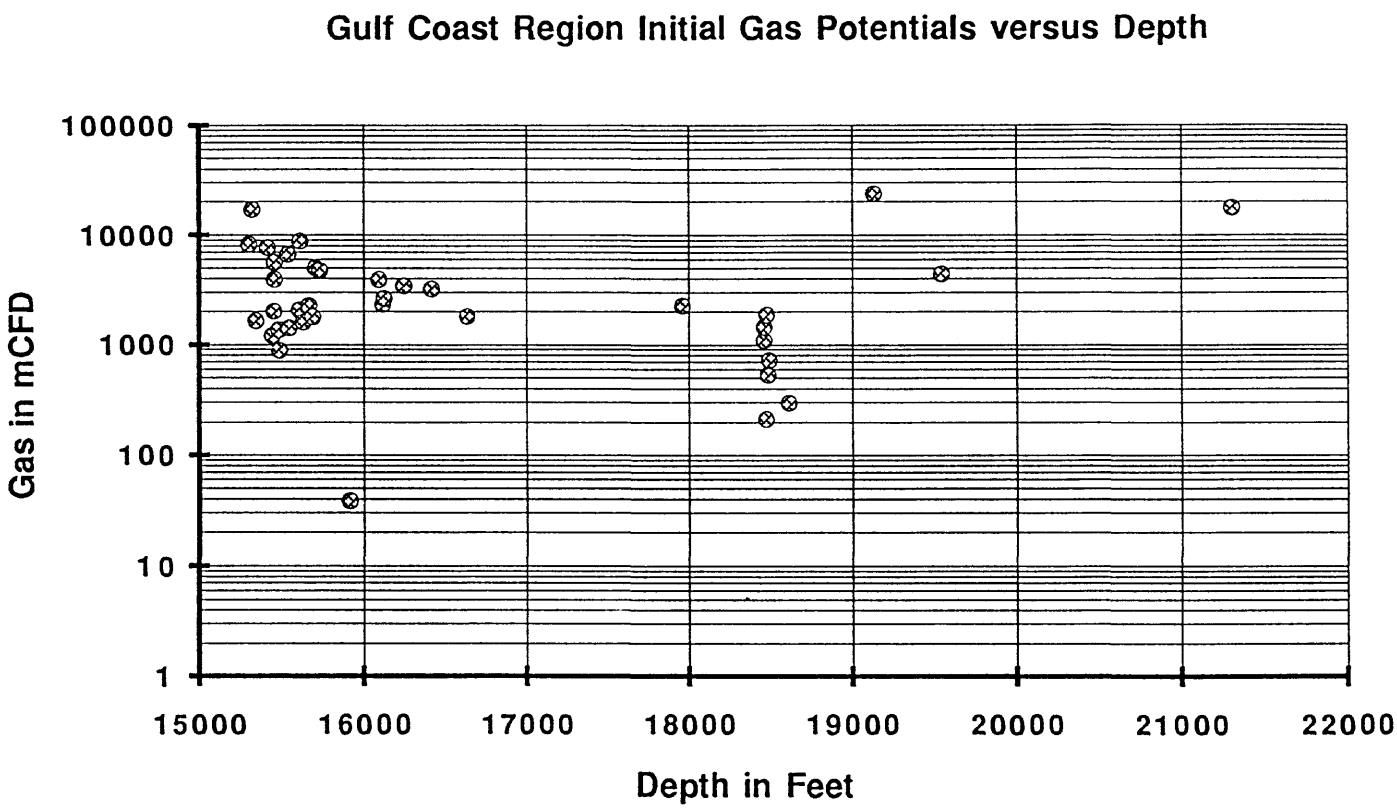

Figure 3-2D. Plot of initial-potential tests and depths for deep Smackover gas wells in Gulf Coast region excluding Texas Gas volumes presented on log scale. Data from Petroleum Information Corporation (1991).

Table 3-2. Drill-stem test summary data for deep wells in U.S. from Petroleum Information Corporation (1991). Key to abbreviations used in table:

API #	The API number is a 14 character well identification number consisting of a 2 character state code, 3 character county code, 5 character unique well number (unique within a given county), 2 character side track number, and a 2 character hole change number.
DST #	The drill stem test number indicates the number of the test for a particular well.
PROD FM	The producing formation code is an abbreviated form the formation name. The code lists are from Petroleum Informations (PI) Well History Control System files and are available through them. The codes are fairly predictable, for instance SMKV is Smackover.
WELL #	Well number assigned by the operator in most cases.
LEASE NAME	The well number should be used in conjunction with the lease name to uniquely identify a well.
DST TOP DEPTH	The drill stem top depth is the depth in feet (measured in most cases from the kelley bushing) to the top of the tested zone.
DST BASE DEPTH	The drill stem base depth is the depth in feet to the bottom of the tested zone.
FM TESTED	The formation tested is a PI formation code preceded by a 2-character system and 1 character series code. More than one formation may be included in a test but only the highest formation in the test is listed.
FLUID VOL	The fluid volume includes the units of the fluid or an abbreviated comment.
NARRATIVE	This column may contain a continuation of the previous abbreviated comments, choke size, or other comments.
BHT	The bottom hole temperature is generally displayed in degrees fahrenheit and is measured at the depth of the drill-stem test.
ISIP	The initial shut in pressure of the test is accompanied by a shut in time in hours and minutes.
FSIP	Is the final shut in pressure measured.
ACCES GAS	Accessory gases indicated where information availible.
GVTY	The gravity (density) of the fluid is indicated where that information is availible.
SALINITY	The salinity of associated waters and the units of measure are indicated where availible.

API #	DST #	PROD FM	WELL #	LEASE NAME	DST TOP DEPTH	DST BASE DEPTH	FM TESTED	FLUID VOL	NARRATIVE	BHT	ISIP	HOURS	MINS	FSIP	HR	MIN	ACCES GAS	GVTY	SALINITY
01003201370000	1	SMKV	1	WEFEL 29-2	15584	15612	553SMKV												
17009000870000	1		1	L A MOREAU	16273	16327	601CRCSL												
3001503686000020			1	JOHN N FIDEL-FE	15554	15611								2465		15			
30015108430000	2	MRRW	65	COTTON DRAW UNI	16375	16578	309DVNN	5500MCFD			5940		30	2140	1				
30015108430000	3	MRRW	65	COTTON DRAW UNI	16560	16628	309DVNN				7153	1		6859	130				
30015108430000	4	MRRW	65	COTTON DRAW UNI	16628	16681	309DVNN				7149	1		7143	1300				
30015108430000	5	MRRW	65	COTTON DRAW UNI	18745	19185	201ELBG	225MCFD			4692		30	112	1				
30015202420000	5	ATOK	1	TODD-FED	16386	16486	309DVNN	TSTM			7002	130		7002	130				
30015202720000	1	MRRW	68	COTTON DRAW UNI	16456	16548	309DVNN	TSTM			5601		5	6286	2				
30015202720000	2	MRRW	68	COTTON DRAW UNI	16456	16660	309DVNN	340MCFD			6889	1		7085		30			
30015202720000	3	MRRW	68	COTTON DRAW UNI	16456	16868	309DVNN	TSTM			6935	1		6935	310				
30015209390000	6		1	DUNES UNIT FEDE	14568	15520		35MCFD	16/64		1341	130		2869	5	9			
30015210950000	5	ATOK	42	POKER LAKE UNIT	14840	15350		280MCFD	INC 1							0			
30015234590000	1	ATOK	1	SOTOL FEDERAL	14748	15070	402MRRW												
30015234590000	2	ATOK	1	SOTOL FEDERAL	14748	15070	402MRRW	2100MCFD			7895	1		7006					
30025009600000	11		1	LITTL EDDY UNT	15325	15485	259SLLM				1540			3985		30			
30025009600000	12		1	LITTL EDDY UNT	16200	16280	201ELBG	170MCFD						6605		30		48.2	
30025009600000	13		1	LITTL EDDY UNT	16280	16330	201ELBG							2405		40			
30025009600000	14		1	LITTL EDDY UNT	16303	16415	201ELBG	354MCFD											
30025010500000	1		1	JT CAUDLE-FEDER	4301	4408	0												
30025015150000	16		6	LEA-MEX-STATE	15110	1515	7												
30025015150000	17		6	LEA-MEX-STATE	15336	1541	0												
30025015150000	18		6	LEA-MEX-STATE	15538	1566	3												
30025015150000	19		6	LEA-MEX-STATE	15790	1594	8												
30025017130000	11		1	MUSE-FEDERAL	14915	1517	0												
30025017130000	12		1	MUSE-FEDERAL	14915	1517	0							6155		30			
30025017130000	13		1	MUSE-FEDERAL	15160	1521	0309DVNN							6520		30			
30025017130000	14		1	MUSE-FEDERAL	15405	1556	0309DVNN							3880		30			
30025026080000	4		1	ETZ-FEDERAL	15560	1571	0							6065		30			
30025026080000	5		1	ETZ-FEDERAL	15710	1585	3							6760		30			
30025036370000	15		1	CROSS	15521	1555	1												
30025036700000	3		1	DANGLADE	14967	1502	5							5490		30			
30025036700000	4		1	DANGLADE	14965	1502	5							5940		30			
30025036700000	5		1	DANGLADE	14959	1511	5							6045		30			
30025083660000	1		2	STATE L	15972	1600	5							125		30			
30025083660000	2		2	STATE L	16000	1610	0							6570		30			
30025084830000	13	DVNN	6	BELL LAKE UNIT	14941	1505	6							4300	1				
30025084830000	14	DVNN	6	BELL LAKE UNIT	15318	1537	5309DVNN							80	120				
30025084830000	15	DVNN	6	BELL LAKE UNIT	15665	1574	3												
30025084910000	2	DVNN	4	BELL LAKE UNIT	15100	1530	0	TSTM						4260	1				
30025084910000	1	DVNN	4	BELL LAKE UNIT	15384	1555	4							6030	1				
30025087840000	3		17	JF JANDA NCT-F	10315	3140	7	TSTM			1595			1535		3			
30025089420000	7		1	WEST ARROWHEAD	15374	1546	8202MCKE												
30025089420000	8		1	WEST ARROWHEAD	15350	1546	8							1560					
30025203770000	11	BEND	1	NE LYNCH UNIT-F	14985	1503	5				6325		30	6325		30			
30025203770000	12	BEND	1	NE LYNCH UNIT-F	15025	1504	0				6305		30	6305		30			
30025207560000	8	MRRW	1	CUSTER MOUNTINT	15360	1559	0				2507		30	2449	1				
30025207560000	5	MRRW	1	CUSTER MOUNTINT	15886	1592	4				6091	1		3391	1				
30025207560000	6	MRRW	1	CUSTER MOUNTINT	15884	1605	0				4104	1		3780	1				

API #	DST #	PROD FM	WELL #	LEASE NAME	DST TOP DEPTH	DST BASE DEPTH	FM TESTED	FLUID VOL	NARRATIVE	BHT	ISIP	HOUR	MINS	FSIP	HR	MIN	ACCES GAS	GVTY	SALINITY
30025207560000		7MRRW	1	CUSTER MOUNTINT	16050	1628	0				7085	1		7042	4				
30025209200000		9MRRW	1	BERRY UNIT	15406	1542	0309DVNN												
300252092000001	0	MRRW	1	BERRY UNIT	15412	1547	0												
300252092000001	1	MRRW	1	BERRY UNIT	15468	1559	3												
30025210810000		6MSSP	1	BRINNINSTOOL P	15120	1538	9402MRRW				10990	1		5008		30			
30025210810000		7MSSP	1	BRINNINSTOOL P	15408	1565	8												
30025210810000		8MSSP	1	BRINNINSTOOL P	17302	1735	2309DVNN				7449	1		237	1				
30025210810000		9MSSP	1	BRINNINSTOOL P	17305	1739	7				7395		30	739	1				
300252108100001	0	MSSP	1	BRINNINSTOOL P	17408	1764	9				7268		30	746		20			
30025221530000		4WFMP	1	GULF-FEDERAL	15900	1595	3402MRRW												
30025221530000		5WFMP	1	GULF-FEDERAL	19940	2006	6252FSLM												
30025221530000		6WFMP	1	GULF-FEDERAL	19943	2006	6252FSLM				8664	1		8680	1				
30025224050000		5ATOK	1	MEXICO-FEDERA	15540	1563	0403ATOK				11191	1		10806	1	0			
30025224050000		6ATOK	1	MEXICO-FEDERA	16226	1626	6409PSLV				5898	1		5983	2				
30025224050000		7ATOK	1	MEXICO-FEDERA	16800	1688	0409PSLV				12418		30	12334		130			
300252240500001	1	ATOK	1	MEXICO-FEDERA	20393	2086	2252FSLM												
30025224050000		8ATOK	1	MEXICO-FEDERA	22199	2292	6201ELBG												
30025224050000		9ATOK	1	MEXICO-FEDERA	22199	2292	6201ELBG												
300252240500001	0	ATOK	1	MEXICO-FEDERA	22130	2292	6201ELBG							7459	3				
30025225640000		9	1Y	GOVERNMENT-CO	14998	1506	2309DVNN				6244	130		6201	130				
300252256400001	0		1Y	GOVERNMENT-CO	15062	1513	7309DVNN				6630	130		6287	130				
30025231080000		5	1	STATE H COM	14940	1503	8309DVNN				5607		30	5727	215				
30025231970000		1ELBG	1	SOUTH LEA UNIT	17710	1817	0309DVNN												
30025231970000		2ELBG	1	SOUTH LEA UNIT	17732	1817	0309DVNN				8549	1		8509	2				
30025236300000		5	1X	LOVELADY-STATE	14940	1505	1309DVNN	3500F			5987		30	5987	2				
30025239040000		1DRKD	1	VIVIAN	5070	5509	5453GLRT												
30025250460000		3FSLM	1	WEST JAL /B/ DE	18410	1849	5201ELBG												
30025250460000		1FSLM	1	WEST JAL /B/ DE	18415	1857	0201ELBG			216	7082	1		7064	2	5			
30025253180000		3PSLV	1	HAGOOD 7608 JV-	15681	1579	1409PSLV	200MCFD		195	11902			12444	8				
30025253180000		4PSLV	1	HAGOOD 7608 JV-	18910	1934	6309DVNN			260	6329	3		5422	3				
30025253180000		5PSLV	1	HAGOOD 7608 JV-	19790	1989	2252FSLM			220	8087	3		8454	6				
30025254430000		5MRRW	1	NORTHERN NATURA	15320	1537	7259SLRN												
30025256040000		3MRRW	1	GOVERNMENT /L/	15878	1597	0309DVNN				2205	120		2301	3				
30025256040000		4MRRW	1	GOVERNMENT /L/	16080	1636	1309DVNN												
30025256040000		5MRRW	1	GOVERNMENT /L/	16069	1636	1309DVNN												
30025256610000		6	1	SAND WELL COM	15772	1594	4309DVNN												
30025256610000		7	1	SAND WELL COM	15777	1594	4309DVNN				6593	1		6659	2				
30025260750000		4DVNN	1	LANGLIE GREER C	15675	1579	0201ELBG												
30025260750000		5DVNN	1	LANGLIE GREER C	15645	1579	0201ELBG												
30025260750000		6DVNN	1	LANGLIE GREER C	15718	1581	1201ELBG												
30025261580000		1ATOK	1	STATE 29 "J"	17460	1752	3309DVNN				4976	1	5	7254	4				
30025261580000		2ATOK	1	STATE 29 "J"	17585	1765	2309DVNN			250	7233	1		7363	4				
30025261750000		4DVNN	1	LANGLEY-BOREN C	15166	1529	2201ELBG			184	6219	1		6219	4				
30025261880000		1DVNN	1	7811 JV-P ROJO	17210	1742	8319WDFD				2746	130		2508	130				
30025261880000		2DVNN	1	7811 JV-P ROJO	17428	1747	5309DVNN												
30025264380000		2MRRW	1	ANDRIKOPOULOS	15547	1557	1402MRRW				9893	130		9837	2				
30025264960000		2MRRW	1	PRONGHORN UNIT	15014	1515	6402MRRW			210				7808	5				
30025272660000		2MRRW	1	FEDERAL "EBR"	14846	1527	0402MRRW				6767	1		7169	4				

API #	DST #	PROD FM	WELL #	LEASE NAME	DST TOP DEPTH	DST BASE DEPTH	FM TESTED	FLUID VOL	NARRATIVE	BHT	ISIP	HOUR	MINS	FSIP	HR	MIN	ACCES GAS	GVTY	SALINITY
30025279310000	1		1	OSUDO STATE	15355	1549	5201ELBG												
30025286510000	1ATOK		1	WILSON "C" FEDE	1523	1533	1403ATOK				21210835	3		11829	3				
30025293610000	2BSPG		1	PLATINUM "6" FE	14971	1501	6402MRRW	23MCFD											
30025293610000	3BSPG		1	PLATINUM "6" FE	15196	1535	8402MRRW												
30025304340000	3		1	NEW MEX "15" FE	16056	1606	1201ELBG												
30025304340000	2		1	NEW MEX "15" FE	16035	1614	1201ELBG												
30025304340000	4		1	NEW MEX "15" FE	16004	1628	6201ELBG				6478	1		6478	3				
35009201070000	2		1	DARRELL MACKEY	15235	1531	8				9922	130		9731	3				
35015000820000	9		1	HENRY WELLER	15095	1511	5404DEES												
35015000820000	8		1	HENRY WELLER	16020	1606	0												
35015000820000	7		1	HENRY WELLER	16225	1626	0												790GPG
35015000820000	5		1	HENRY WELLER	16320	1635	5403DKHL												
35015000820000	6		1	HENRY WELLER	16929	1770	8401SPRG												82GPG
35015203140000	2SPRG		1-21	CLANCY EST	17045	1709	3401SPRG												
35015203140000	3SPRG		1-21	CLANCY EST	17097	1709	7401SPRG												
35015203140000	4SPRG		1-21	CLANCY EST	19125	1925	0269HNTN												
35019000920001	4HNTN		1	RICHARD S BOND	12865	1500	0169ABCK				6660	015		4180	015			35.0	
35019068820000	3		1	GILL	3963	3998	2							250					
35019211280000	2GDRD		1	CITY OF ARDMORE	16180	1628	5354GDRD	12000F						14165	620				
35019211280000	3GDRD		1	CITY OF ARDMORE	16178	1628	5354GDRD				3400	1		3300	3				
35039000090000	3MRRW		1	RENE GRAFT	15147	1519	5269HNTN				6765		30	6140	1				
35039000090000	4MRRW		1	RENE GRAFT	15438	1558	0269HNTN				4840		30	540		30			
35039200140000	5		1	STATE OF OKLA S	15645	1568	0269HNTN				7350	030		7350	030				
35039200140000	6		1	STATE OF OKLA S	15685	1573	0269HNTN							7619	030				
35039200140000	7		1	STATE OF OKLA S	15735	1577	5269HNTN							7260	030				
35039200530000	4RDFK		1-15	TOUCHSTONE	17474	1760	0269HNTN												
35039200530000	5RDFK		1-15	TOUCHSTONE	17436	1760	0269HNTN												
35039200530000	6RDFK		1-15	TOUCHSTONE	17324	1760	0269HNTN												
35039200530000	7RDFK		1-15	TOUCHSTONE	17534	1780	5269HNTN				8376	1		8857	3				
35039200550000	2ATOK		1-27	WILBUR HAYES	15166	1519	6	100BWPH	F SWTR 1/2										
35039200550000	1ATOK		1-27	WILBUR HAYES	18544	1870	0269HNTN	35BWPH	SWTR					13355					
35039200560000	2MRMC		1-4	WRIGHT	15654	1590	5359MPLM	825MCFD			8153	130							
35039200560000	3MRMC		1-4	WRIGHT	15970	1601	5269HNTN	TSTM			7289			7289	130				
35039200570000	1RDFK		1-2	BEAUCHAMP	15668	1571	4												
35039200570000	2RDFK		1-2	BEAUCHAMP	16454	1661	7				12223	13		10389	2				
35039200580000	1MRRW		1	FINE	15835	1598	5269HNTN			269				7302	130				300000PPMCL
35039200580000	2MRRW		1	FINE	15603	1598	5269HNTN			269	7166	2							284000PPMCL
35039200600001	1RDFK		1	MORTON UNIT	16386	1646	0269HNTN			2640									
35039200600001	2RDFK		1	MORTON UNIT	16386	1647	4269HNTN												
35039200610000	3MRRW		1	VALENTINE UNIT	15583	1562	6269HNTN												
35039200620000	1		1-6	BREDY	19078	1926	2269HNTN												
35039200620000	2		1-6	BREDY	19033	1926	2269HNTN												
35039200620000	3		1-6	BREDY	19495	1967	3269HNTN												
35039300050000	1MRRW		1	LETTIE E ROWLAN	14939	1531	2269HNTN												
35039300120000	2HNTN		1	DIEHL ESTATE UN	15030	1504	7269HNTN	30			3913	2		3978	2				
35039300120000	1HNTN		1	DIEHL ESTATE UN	15062	1507	4269HNTN				7121	1		4130	2				
35039300120000	3HNTN		1	DIEHL ESTATE UN	14800	1507	4269HNTN				2958	2		2416	2				
35039300590000	3		1	WAGNER	15164	1523	6402PRMR												

API #	DST #	PROD FM	WELL #	LEASE NAME	DST TOP DEPTH	DST BASE DEPTH	FM TESTED	FLUID VOL	NARRATIVE	BHT	ISIP	HOUR	MINS	FSIP	HR	MIN	ACCES GAS	GVTY	SALINITY
350393005900004			1	WAGNER	15510	1552	2401SPRG	106MCFD											
350393005900005			1	WAGNER	15510	1560	6401SPRG	157MCFD											
350432009700003		HNTN	1	WALKER /A/	15580	1567	4269HNTN				7049		30	7049					
350432012800004		SKNR	1	EARNEST MARTIN	16110	1616	0269HNTN												
350432012800002		SKNR	1	EARNEST MARTIN	16162	1618	9269HNTN												
350432012800003		SKNR	1	EARNEST MARTIN	16175	1628	9269HNTN												
350432019900002		HNTN	1-10	HENRY HARREL	16468	1651	2269HNTN			273				5608	2				86000PPMCL
350432019900003		HNTN	1-10	HENRY HARREL	16520	1661	6269HNTN												
350432019900004		HNTN	1-10	HENRY HARREL	16470	1661	6269HNTN			276	6430		30	5332	1				
350432019900005		HNTN	1-10	HENRY HARREL	16472	1671	6269HNTN			276	7352	1		7228	2				91000PPMCL
350432019900006		HNTN	1-10	HENRY HARREL	16718	1684	1269HNTN	TSTM		291	7382	1		7302	1				109000PPM
350432025100001			1	F E FERRELL UT	16335	1648	5269HNTN				5510	130		6039	130				
350432025100002			1	F E FERRELL UT	16545	1675	6269HNTN				7598	1		6024	1				
350432038000001		MRRW	1	FARISS	16210	1662	8269HNTN												
350432038000002		MRRW	1	FARISS	16210	1662	8269HNTN												
350432038300001			1	WALTON	17707	1783	9269HNTN				8007	1		8007	3				
350432038300002			1	WALTON	17708	1784	9269HNTN												
350432064900001		HNTN	1-15	GAMBLE	16535	1658	5269HNTN	230MCFD											
350432064900002		HNTN	1-15	GAMBLE	16535	1660	3269HNTN	40MCFD											
350432197800001		HNTN	1-4	STOUT BENJAMIN	16700	1683	2269HNTN				7208								
350452012600001		HNTN	1	BERRYMAN UNIT	14966	1500	1269HNTN				6343	1	0	6150	155				
350452012600002		HNTN	1	BERRYMAN UNIT	14988	1502	1269HNTN												
350452013700004			1	BERRYMAN UNIT-B	14995	1506	0269HNTN												
350452013700005			1	BERRYMAN UNIT-B	14854	1506	0269HNTN				4396	1	0	4116	2	0			
350452013700003			1	BERRYMAN UNIT-B	15105	1515	8269HNTN		F LESS THA										104000PPMCL
350452013700001			1	BERRYMAN UNIT-B	15130	1530	0269HNTN				6438	1	0	6438	227				117000PPMCL
350452020700003			1-9	IMKE	14960	1505	0202VIOL							4927					
350452020700004			1-9	IMKE	15300	1539	0202SMPS			244									
350452020700006			1-9	IMKE	15302	1539	1202SMPS				6738			6567	2				
350452020800002			1-34	JACKSON	16010	1606	0269HNTN												
350452020800003			1-34	JACKSON	16017	1608	5269HNTN				3939	1		3325	2				
350452020800004			1-34	JACKSON	16085	1618	5269HNTN				3513	1		3692	3				
350452020800005			1-34	JACKSON	16185	1639	0269HNTN												
350452025800001			1-28	IDS-STATEX-HAMR	14912	1524	0269HNTN				6385	1		6363	236				
350452026100002		MRRW	1-24	BERRYMAN UNIT	16720	1706	8269HNTN				7301	1		7258	2				
350510006400001	4	SMPS	1	BRISCOE UNIT	15095	1518	4169ABCK							3700					
350510006400001	5	SMPS	1	BRISCOE UNIT	14823	1518	4202OLCK												
350510006400001	0	SMPS	1	BRISCOE UNIT	16678	1673	7202BRMD				5800			3000				48.0	
350510042900002		BRMD3	2	HARRISON	14764	1501	3202BRMD												
350510042900003		BRMD3	2	HARRISON	15080	1508	1202BRMD2												
350510042900004		BRMD3	2	HARRISON	15251	1531	0202BRMD3						5						
350512048400001		BRMD1	1	SIMMS /A/	15217	1535	0202BRMD			225	7048	1		7370	1				
350512048400002		BRMD1	1	SIMMS /A/	15666	1576	3202BRMD			222	7112	1		6726	2				
350512051500001		SPRG	1-21	LAVERTY	16408	1670	6401CNGM	6000F		234	9206	115							
350512059000001		BRMD3	1-17	FOSTER	14505	1508	0202BRMD												
350513001000002			1	MULLICAN	15638	1630	7203VIOL				9297	1		5507					
350513001000001		BRMD	1	MULLICAN	15747	1614	1202BRMD1	8500MCFD			10022		55	9932					
350513543100001		BRMD1	1	WILBUR CRADDOCK	16086	1627	0202BRMD1											56.0	

API #	DST #	PROD FM	WELL #	LEASE NAME	DST TOP DEPTH	DST BASE DEPTH	FM TESTED	FLUID VOL	NARRATIVE	BHT	ISIP	HOUR	MIN	FSIP	HR	MIN	ACCES GAS	GVTY	SALINITY
35051356290000	1	BRMD3	1	NELLIE ENGLISH	16082	1630	8202BRMD1												
35051360290000	1	BRMD2	1	W A REED	15220	1529	0202BRMD2												
35051360290000	2	BRMD2	1	W A REED	15220	1533	0202BRMD2	20MCFD	FL 3 BD 4										
35051360290000	3	BRMD2	1	W A REED	15220	1564	5202BRMD2		WTR									54.5	
35051361310000	2	SAND	7	RAY HORTON	3582	3640	0401WODS												
35051364970000	1		1	MITCHELL UNIT	16455	1657	5202BRMDL							4510	030				
35051364970000	2		1	MITCHELL UNIT	16680	1672	4202BRMDL							4695	030				
35051364970000	3		1	MITCHELL UNIT	16720	1676	9202BRMDL												
35051364970000	4		1	MITCHELL UNIT	16730	1683	6202BRMDL							9290	030				
35051364970000	5		1	MITCHELL UNIT	16812	1693	5202MCLS							6145	030				
35051365080000	2	BRMD1	1	BAKER	15183	1538	2202BRMD1		WTR CUSH					8805	130				
35051365080000	3	BRMD1	1	BAKER	15182	1541	4202BRMD1		WTR CUSH					8675	2				
35051365080000	4	BRMD1	1	BAKER	15635	1581	0202BRMD3		WTR CUSH					8720	220				
35051365780000	1	BRMD	1	W D HARRISON B	15574	1598	1202BRMD1	3540MCFD						9350	2				
35051365780000	2	BRMD	1	W D HARRISON B	16024	1609	2202BRMD3	350MCFD						9480	1			47.4	
35051365780000	3	BRMD	1	W D HARRISON B	16176	1635	1202BRMD3												
35077202850000	1		1	RETHERFORD	15200	1540	0403SPRO												
35077202850000	2		1	RETHERFORD	18515	1866	9202JONS												
35077202850000	3		1	RETHERFORD	18544	1866	9202JONS												
35077202850000	4		1	RETHERFORD	18864	1904	6169ABCK												
35079206560000	2		1	RUNESTONE	15250	1650	0169ABCK												
35079206560000	1		1	RUNESTONE	15250	1700	0169ABCK												
42003072840000	2	WFMP	1	JE PARKER	10610	1666	5				90	30		50	30				
42025004730000	13	EDRD	1	FREDDIE TOMASEK	14704	1506	0												
42025004730000	10	EDRD	1	FREDDIE TOMASEK	15170	1539	5												
42025004730000	11	EDRD	1	FREDDIE TOMASEK	15007	1539	5												
42025004730000	12	EDRD	1	FREDDIE TOMASEK	15000	1539	5												
42025004740000	7	EDRD	1	ALVIN L ONEAL	14520	1513	1		WC										
42025004740000	8	EDRD	1	ALVIN L ONEAL	15344	1536	4		WC										50000PPMCL
42039038660000	1	FRIO	1	DAVID C BINTLIF	15205	1522	5	13000F	WTR										
42039044770000	1	FRIO	1	HAYDEN MCNEILL	16877	1688	7							11750					
42039044900000	3		1	HOUSTON FARMS	15550	1557	0		FLWD PART										
42039044900000	2		1	HOUSTON FARMS	15854	1587	4												
42039044900000	1		1	HOUSTON FARMS	15986	1599	5												
42039048930000	1		3	ST TEXAS LSE 49	15862	1588	6		SURF PRESS										
42039048930000	2		3	ST TEXAS LSE 49	15862	1588	6												
42039048930000	3		3	ST TEXAS LSE 49	15762	1588	6												
42039048930000	4		3	ST TEXAS LSE 49	15762	1588	6												
42057006480000	1	FRIO	2-B	MAUDE B TRAYLOR	15126	1513	6	8000F											
42057006480000	2	FRIO	2-B	MAUDE B TRAYLOR	15147	1515	7	8000F											
42057006480000	3	FRIO	2-B	MAUDE B TRAYLOR	15076	1515	7	8000F	WTR										
42057006480000	4	FRIO	2-B	MAUDE B TRAYLOR	15076	1515	7	8000F											
42057006480000	8	FRIO	2-B	MAUDE B TRAYLOR	18662	1868	6	8000F											
42105106760000	6	WFMP	1	BLAKENEY-KRUEGE	13538	1505	0201ELBG	TSTM			2697	1		3550	4				146000PPMCL
42105107660000	8		1	HOOVER LB ETAL	14665	1509	0201ELBG	TSTM			6654	45		6484	3				
42105107660000	9		1	HOOVER LB ETAL	15100	1535	0201ELBG				3586	45		4013	3				
42105107660000	10		1	HOOVER LB ETAL	15360	1570	5201ELBG				3074	45		2677	3				
42105107870000	1		10A	MITCHELL	16065	1638	0201ELBG							2504	2				

API #	DST #	PROD FM	WELL #	LEASE NAME	DST TOP DEPTH	DST BASE DEPTH	FM TESTED	FLUID VOL	NARRATIVE	BHT	ISIP	HOUR	MINS	FSIP	HR	MIN	ACCES GAS	GVTY	SALINITY
42105311370000	2		1	WATSON RANCH 90	14667	1553	4201ELBG				2278	1		2309	3				
42105357690000	4	STRN	1	MITCHELL P Q "1	14594	1532	5309DVNN				6457	245		6115	4				
42109003360000	9		1	STATE-CULBERSON	15511	1556	0309DVNN				6772	1		6742	2				
42109308210000	3		1	SELINA STRONG	15626	1571	7				6724	1		6724	3				
42109313470000	1		1	MEEKER UNIT	15438	1557	5259SLRN				6720	130		6721	4				
42109313470000	2		1	MEEKER UNIT	15559	1558	0259SLRN				6720	130		6666	4				
42109313470000	3		1	MEEKER UNIT	15562	1561	5259SLRN			264	6824	130		6663	3				
42109313470000	4		1	MEEKER UNIT	15612	1563	6259SLRN				6609	130		6609	4				
42131057890000	2		25	WILSON J O	2285	2298	7												
42165019920000	1		1	BIRGE	12660	2179	1				5415	30		5395	30			34.4	
42167013360000	1		3	E W CRAIG	15226	1524	2		SWTR										
42167013580000	1	FRIOL	1	HOUSTON FARM DE	16132	1626	4653FRIOL							13730	26				10300PPMCL
42167013580001	1		1	HOUSTON FARM DE	15564	1557	4							13240					
42167013760000	1		1	HENCK LOWER	15255	1527	2												
42167014970000	1	JCKS	13-B	STEWART MACO	15078	1508	8												
42167014970000	4	JCKS	13-B	STEWART MACO	15078	1508	8												
42185302290000	1	WLCX	1	GARDNER WILLIAM	16660	1737	9602EDRD												
42199021250001	2		1	DISHMAN-LUCAS	15142	1516	0												
42199021250001	1		1	DISHMAN-LUCAS	15419	1543	7												
42201080150000	2		1	NO HOUSTON WILC	16255	1628	4		WTR NO GGE										
42201080150000	3		1	NO HOUSTON WILC	16255	1634	0												
42201080150000	1		1	NO HOUSTON WILC	16461	1648	1		WTR NO GGE										
42285002380001	1		1	SPANIHEL UNIT	14506	1535	0602GLRSL												
42287000910000	1		1	WILLIE MATEJCEK	16134	1618	9												
42291016840001	1		1	BOYT ETAL E W	15261	1527	3		WTR CUSH										
42291016840001	2		1	BOYT ETAL E W	15261	1527	3		WTR CUSH										
42301103130000	3		1	ANDERSON MRS OP	15819	1594	4												
42301103130000	4		1	ANDERSON MRS OP	15855	1599	4	TSTM											
42301103130000	5		1	ANDERSON MRS OP	15980	1629	3												
42301103130000	6		1	ANDERSON MRS OP	15980	1629	3									0			
42301103130000	7		1	ANDERSON MRS OP	19013	2039	9252FSLM												
42301103130000	8		1	ANDERSON MRS OP	22075	2241	9201ELBG												
42301103130000	9		1	ANDERSON MRS OP	22415	2264	3201ELBG	TSTM											
42301103170000	4	ATOK	1	WILDER	20000	2015	0252FSLM												
42301300660000	1		1	JOHNSON 87	21415	2180	5201ELBG												
42301300660000	2		1	JOHNSON 87	21415	2195	0201ELBG												
42301300660000	3		1	JOHNSON 87	21415	2205	0201ELBG												
42301300700000	1	MRRW	1	HARRISON /10/	11895	2081	0252FSLM												
42301301000000	1		1	AMARILLO-STATE	18720	2033	5359MSSP												
42301302220000	1	ATOK	1	CONTINENTAL TXL	15545	1579	5403ATOK												
42301302250000	2	WFMP	1	RED BLUFF /DEEP	16018	1620	2259SLRN												
42301302250000	3	WFMP	1	RED BLUFF /DEEP	16018	1627	7259SLRN												
42301302250000	4	WFMP	1	RED BLUFF /DEEP	16018	1705	2259SLRN												
42301302250000	5	WFMP	1	RED BLUFF /DEEP	17020	1707	7259SLRN												
42301302360000	1	ATOK	1	JOHNSON-TXL UNT	21830	2226	5201ELBG												
42301302360000	2	ATOK	1	JOHNSON-TXL UNT	21830	2226	5201ELBG												
42301303300000	1	ELBG	1-X	MENTONE GAS UNI	17726	1782	6359MPLM												
42301303300000	2	ELBG	1-X	MENTONE GAS UNI	17726	1782	6359MPLM	109MCFD											

API #	DST #	PROD FM	WELL #	LEASE NAME	DST TOP DEPTH	DST BASE DEPTH	FM TESTED	FLUID VOL	NARRATIVE	BHT	ISIP	HOUR	MIN	FSIP	HR	MIN	ACCES GAS	GVTY	SALINITY
42301303630000		1ATOK	2A-4	LINEBERY	18700	2020	0359MSSP												
42311013730000		1	1	SOUTH TEX SYNDI	14924	1500	0												
42311013730000		2	1	SOUTH TEX SYNDI	14955	1500	0												31500PPMCL
42321010380000		1	1	JANIE HAWKINS	15623	1565	4												
42339010930000		3	21	LAKE CREEK UNIT	11780	1515	4	124B	BRKW									44.5	
42353000490000		4	1	JP AYCOCK	5184	5555	0												
42355025350000		1	3	ST TR 9 C C BAY	7500	7750	4	1000F						3277					
42371003610000	10		1	KELLY STATE GAS	15979	1600	8												
42371003610000	8		1	KELLY STATE GAS	16211	1629	4												
42371003610000	9		1	KELLY STATE GAS	16211	1629	4												
42371003630000	4		1	LUCAS-STATE	16013	1611	3309DVNN												
42371003630000	5		1	LUCAS-STATE	16013	1622	5309DVNN												
42371021570000	1		11	JERUSHA ROBBIET	15130	1523	0												
42371021570000	2		11	JERUSHA ROBBIET	15147	1523	0												
42371021570000	3		11	JERUSHA ROBBIET	15250	1533	3				3825	30		2195	30				
42371021590000	12		1	FISHER-BONSACK	14860	1500	0												
42371024910000		5ELBG	1	JW ROBBINS	12620	2186	4	115MCFD											
42371028190000		7DVNN	56	ELSINORE ROYALT	16420	1646	5							4940	20				
42371028200000	2		57	ELSINORE ROYALT	14915	1501	5201ELBG							6122	1				
42371028200000	3		57	ELSINORE ROYALT	14925	1501	5	TSTM			6100	1		5986	1				
42371028200000	4		57	ELSINORE ROYALT	15015	1512	5	TSTM			6160	1		6030	1				
42371028200000	5		57	ELSINORE ROYALT	15135	1525	0	18900MCFD			6360		30	5310		30	CO2		
42371028200000	6		57	ELSINORE ROYALT	15256	1545	0201ELBG	29000MCFD			6259	115		6236		15	CO2		
42371030370000	10		1	WM EDWARDS	17239	1731	9												
42371030370000	11		1	WM EDWARDS	17241	1731	9							4040	1				
42371030370000	12		1	WM EDWARDS	17319	1752	8							3640	1				
42371030370000	13		1	WM EDWARDS	17538	1770	5							5670		56			
42371030370000	14		1	WM EDWARDS	17707	1788	0												
42371031230000	8		1	WC TYRRELL TRUS	15761	1583	1				3030		30	3290		30			
42371031230000	9		1	WC TYRRELL TRUS	15770	1588	9							3905		30			
42371031230000	10		1	WC TYRRELL TRUS	16160	1647	0							3745		15			
42371037980000	14		1	UNIVERSITY EE	16700	1688	1							4040		15			
42371037980000	15		1	UNIVERSITY EE	17190	1733	1							4050		15			
42371038110000	17		1	PUCKETT A-B	15020	1518	9							6100		15			
42371044400000	7		1	ROARK ETAL UNIT	14683	1500	5	50MCFD						5760	2				
42371048440000		9DVNN	1	PECOS FEE	15978	1600	8							2540	1				
42371048440000	10	DVNN	1	PECOS FEE	17405	1749	6												
42371048440000	11	DVNN	1	PECOS FEE	17425	1753	8							2590		45			
42371048440000	12	DVNN	1	PECOS FEE	17538	1764	5							6950	1				
42371048440000	13	DVNN	1	PECOS FEE	17648	1776	8							7400	1				
42371054110000		1PSLB	1	FRED SCHLOSSER	15494	1553	3							11260		30			
42371054110000		2PSLB	1	FRED SCHLOSSER	15125	1553	3							12990		110			
42371054110000		3PSLB	1	FRED SCHLOSSER	16300	1635	0				12810	1		12020	1				
42371100440000		2WFMP	1	STATE-MCINTYRE	21446	2177	6												
42371100450000		4ELBG	1	EFFIE POTTS SIB	15081	1528	8	190MCFD						2433	1				
42371100450000		5ELBG	1	EFFIE POTTS SIB	15289	1545	7201ELBG							6463	1				
42371100450000		6ELBG	1	EFFIE POTTS SIB	15459	1562	6							7310					
42371100450000		7ELBG	1	EFFIE POTTS SIB	15626	1583	9201ELBG							6880					

API #	DST #	PROD FM	WELL #	LEASE NAME	DST TOP DEPTH	DST BASE DEPTH	FM TESTED	FLUID VOL	NARRATIVE	BHT	ISIP	HOUR	MIN	FSIP	HR	MIN	ACCES GAS	GVTY	SALINITY
42371100450000	8	ELBG	1	EFFIE POTTS SIB	15840	1599	2	TSTM						5660	3				
42371100450000	9	ELBG	1	EFFIE POTTS SIB	15992	1628	0							7280					
42371101080000	14		1	TREES	16264	1641	2							1990	2				
42371101080000	15		1	TREES	16420	1656	2							1990	2				
42371101080000	16		1	TREES	16562	1676	2							7215	2				69000PPMCL
42371101370000	8	CSTL	1	HERSHENSON	15424	1547	2309DVNN				3515	30		3460	1				
42371101370000	9	CSTL	1	HERSHENSON	15470	1633	0	2162MCFD											
42371101370000	10	CSTL	1	HERSHENSON	15472	1633	0	2100MCFD						2346	9				
42371101370000	11	CSTL	1	HERSHENSON	18177	1822	7201ELBG												
42371101370000	12	CSTL	1	HERSHENSON	18187	1824	3201ELBG				6950	30		2770	1				
42371101370000	13	CSTL	1	HERSHENSON	18241	1830	4												
42371101370000	14	CSTL	1	HERSHENSON	18253	1834	7201ELBG				6570	1							
42371101370000	15	CSTL	1	HERSHENSON	18340	1844	2201ELBG				7685	30		7310	30				115500PPMCL
42371101390000	13	ELBG	1	WC TYRRELL	16902	1696	8	TSTM			9390	1		9180	2				
42371101390000	14	ELBG	1	WC TYRRELL	16898	1708	1												
42371101390000	15	ELBG	1	WC TYRRELL	16924	1708	1												
42371101390000	16	ELBG	1	WC TYRRELL	16940	1708	3	240MCFD			9350	30		7240	230				
42371101390000	17	ELBG	1	WC TYRRELL	19846	2002	8				10180	1		3315	1				
42371101390000	18	ELBG	1	WC TYRRELL	20028	2021	5				10835	1							
42371101390000	19	ELBG	1	WC TYRRELL	19859	2038	8201ELBG				9540	1							
42371101610000	5	DVNN	1	HOR-SUPERIOR-DS	16160	1630	9201ELBG				4460	1		2990	2				
42371101610000	6	DVNN	1	HOR-SUPERIOR-DS	16309	1653	4												
42371101610000	7	DVNN	1	HOR-SUPERIOR-DS	16292	1657	2												
42371101610000	8	DVNN	1	HOR-SUPERIOR-DS	16160	1660	1							3670	2				
42371101610000	9	DVNN	1	HOR-SUPERIOR-DS	16160	1675	1				3990								
42371101610000	10	DVNN	1	HOR-SUPERIOR-DS	16160	1686	0201ELBG				4040	2							
42371101610000	11	DVNN	1	HOR-SUPERIOR-DS	16585	1713	9201ELBG							5780	2				
42371103460000	6	ELBG	3	JO NEAL 42	14898	1535	0				6191	20		6924	30				
42371103460000	7	ELBG	3	JO NEAL 42	15571	1557	1												
42371103460000	8	ELBG	3	JO NEAL 42	14898	1557	1												
42371103460000	9	ELBG	3	JO NEAL 42	14898	1557	1												
42371103470000	15	DVNN	1	JO NEAL 55	15240	1539	0	2000F			7738	30		7350	1				
42371103470000	16	DVNN	1	JO NEAL 55	15390	1554	0	2000F			6888	30		1599	115				
42371103470000	17	DVNN	1	JO NEAL 55	15540	1569	0				5457	30		5115	1				
42371103470000	18	DVNN	1	JO NEAL 55	15690	1579	0				7956	30		7085	30				
42371103470000	19	DVNN	1	JO NEAL 55	15790	1589	0												
42371103470000	20	DVNN	1	JO NEAL 55	15770	1589	0	2000F			8164	30		7622	30				
42371103470000	21	DVNN	1	JO NEAL 55	15890	1599	0												
42371103470000	22	DVNN	1	JO NEAL 55	15851	1599	0												
42371103470000	23	DVNN	1	JO NEAL 55	15851	1599	0												
42371103470000	24	DVNN	1	JO NEAL 55	15910	1599	0	2000F			8101	30		7395	1				
42371104570000	3	DVNN	1	RAYNOLDS HF U	15320	1532	0201ELBG												
42371104570000	4	DVNN	1	RAYNOLDS HF U	15215	1532	0201ELBG				5229								
42371104570000	5	DVNN	1	RAYNOLDS HF U	15325	1543	0201ELBG				7562	1		6664	130				
42371104570000	6	DVNN	1	RAYNOLDS HF U	15434	1555	0201ELBG	8000MCFD			6986	30		6554	130				
42371104640000	1	DVNN	1	OATES GAS UNIT	16485	1670	9												
42371104640000	2	DVNN	1	OATES GAS UNIT	16700	1705	0												
42371104640000	3	DVNN	1	OATES GAS UNIT	16620	1705	0				7185	1			2				

API #	DST #	PROD FM	WELL #	LEASE NAME	DST TOP DEPTH	DST BASE DEPTH	FM TESTED	FLUID VOL	NARRATIVE	BHT	ISIP	HOUR	MIN	FSIP	HR	MIN	ACCES GAS	GVTY	SALINITY
42371104660000	2	ELBG	10	WILLBANKS HENRY	16184	1636	5				9427	1		9254	2				
42371104680000	12	DVNN	1	NEAL JO	15432	1556	7							1208	1				
42371104680000	13	DVNN	1	NEAL JO	15568	1574	6												
42371104680000	14	DVNN	1	NEAL JO	15537	1577	0												
42371104680000	15	DVNN	1	NEAL JO	15442	1577	0												
42371105060000	1	ELBG	1	TYRRELL WC UNIT	21450	2173	5201ELBG				10657	1							
42371105060000	2	ELBG	1	TYRRELL WC UNIT	21498	2205	2201ELBG												
42371105060000	3	ELBG	1	TYRRELL WC UNIT	21710	2208	1201ELBG												
42371105060000	4	ELBG	1	TYRRELL WC UNIT	22934	2296	4												
42371105200000	10	ELBG	1	WALKER CHARLES	15680	1577	8405CNYN												
42371105200000	11	ELBG	1	WALKER CHARLES	15943	1658	7405CNYN				11295	1		8910	245				
42371105200000	12	ELBG	1	WALKER CHARLES	18258	1850	2359MSSP				11500	1							
42371105200000	13	ELBG	1	WALKER CHARLES	18861	1891	7309DVNN												
42371105200000	14	ELBG	1	WALKER CHARLES	18815	1897	5309DVNN												
42371106250000	1	ELBG	1	DERRICK-WINFI U	20810	2091	0201ELBG												
42371106250000	2	ELBG	1	DERRICK-WINFI U	20950	2105	0201ELBG												
42371106420000	6	ELBG	1	BLACKSTONE-SLHT	14933	1514	5201ELBG												
42371106580000	8	ATOK	1	MENDEL M C "A"	19350	1968	5309DVNN				8745	2							
42371106580000	9	ATOK	1	MENDEL M C "A"	22330	2260	7201ELBG												
42371106580000	10	ATOK	1	MENDEL M C "A"	22350	2269	8201ELBG												
42371106580000	11	ATOK	1	MENDEL M C "A"	22705	2280	0201ELBG												
42371106580000	12	ATOK	1	MENDEL M C "A"	22718	2286	0201ELBG												
42371106580000	13	ATOK	1	MENDEL M C "A"	22705	2301	0201ELBG												
42371106580000	14	ATOK	1	MENDEL M C "A"	23024	2325	1201ELBG												
42371106580000	15	ATOK	1	MENDEL M C "A"	23251	2325	1201ELBG												
42371106580000	16	ATOK	1	MENDEL M C "A"	23027	2325	2201ELBG												
42371106580000	17	ATOK	1	MENDEL M C "A"	23258	2357	6201ELBG				9817		30	9817	2				
42371106580000	18	ATOK	1	MENDEL M C "A"	23550	2386	0201ELBG				9612		30	8758	2				
42371106590000	11	WFMP	1	PATTERSON V	22030	2223	0												
42371106590000	10	WFMP	1	PATTERSON V	22010	2223	7							9125	8				
42371106590000	7	WFMP	1	PATTERSON V	21805	2234	0				9628	1							
42371106590000	8	WFMP	1	PATTERSON V	21846	2234	0												
42371106590000	9	WFMP	1	PATTERSON V	22010	2234	0												
42371106590000	6	WFMP	1	PATTERSON V	21814	2241	7				9597	1		9552	1				
42371106600000	2		1	SCOTT M	17630	1789	5				7513	2		5888	3				
42371106600000	3		1	SCOTT M	19800	2015	0				8021	1							
42371106600000	4		1	SCOTT M	19780	2018	0							8323	2	3			
42371106600000	7		1	SCOTT M	19680	2022	5									0			87000PPMCL
42371106600000	5		1	SCOTT M	19680	2026	8												
42371106600000	6		1	SCOTT M	19680	2026	8												
42371106650000	2	ELBG	2	RAYNOLDS HF UNI	15145	1530	0	TSTM			6418	1		5069	2				180616PPMCL
42371106650000	3	ELBG	2	RAYNOLDS HF UNI	15145	1530	2201ELBG	TSTM			7012	130		6454	130				117019PPMCL
42371106770000	3	ELBG	1	GOMEZ SOUTH UNI	15818	1671	6309DVNN	TSTM			9119	1		8102	2				
42371106820000	3	ELBG	1	BLACKSTONE-SLHT	15400	1540	0201ELBG												
42371106820000	4	ELBG	1	BLACKSTONE-SLHT	14600	1540	0201ELBG	5000MCFD			6525	1		6525	3	5			
42371106820000	5	ELBG	1	BLACKSTONE-SLHT	15391	1560	0201ELBG							6789	130				
42371106820000	6	ELBG	1	BLACKSTONE-SLHT	15590	1577	2							2972	1				
42371106820000	7	ELBG	1	BLACKSTONE-SLHT	15760	1600	0							3301	130				

API #	DST #	PROD FM	WELL #	LEASE NAME	DST TOP DEPTH	DST BASE DEPTH	FM TESTED	FLUID VOL	NARRATIVE	BHT	ISIP	HOUR	MINS	FSIP	HR	MIN	ACCES GAS	GVTY	SALINITY
42371106820000	8	ELBG	1	BLACKSTONE-SLHT	15995	1621	1	8MCFD						4686	2				131000PPMCL
42371107220000	4	WFMP	1	IDOL	15066	1527	0												
42371107220000	5	WFMP	1	IDOL	15062	1527	0201ELBG	58MCFD			6578	1		6527	5				
42371107220000	6	WFMP	1	IDOL	15272	1537	0201ELBG				6781	1		6740	4				
42371107220000	7	WFMP	1	IDOL	15375	1547	0201ELBG	330MCFD			6782	1		6740	4				
42371107220000	8	WFMP	1	IDOL	15475	1557	0201ELBG	TSTM			6991	1		6085	4				
42371107220000	9	WFMP	1	IDOL	15575	1567	0201ELBG				5846	1		4031	2				
42371107220000	10	WFMP	1	IDOL	15664	1577	0201ELBG							6805	3				
42371107220000	11	WFMP	1	IDOL	15770	1592	0201ELBG				7018	1		6538	2				
42371107220000	12	WFMP	1	IDOL	15920	1607	0201ELBG				6218	1		6511	2				
42371107220000	13	WFMP	1	IDOL	16070	1627	0201ELBG				6820	1		6348	2				
42371107220000	14	WFMP	1	IDOL	16270	1650	0201ELBG												
42371107220000	15	WFMP	1	IDOL	16260	1650	0201ELBG				7565	1		6756	2				
42371107420000	1	SMPS	1	STATE OF TEXAN	16538	1703	1359MPLM				4846	1		3171	2				
42371107420000	2	SMPS	1	STATE OF TEXAN	20161	2060	4201ELBG	TSTM			7599	3		6449	230				
42371107420000	3	SMPS	1	STATE OF TEXAN	20157	2109	2201ELBG	TSTM			8520	4		8230	530				
42371107980000	1	ELBG	1	MCINTYRE CE	14480	1576	7												
42371107980000	2	ELBG	1	MCINTYRE CE	15999	1606	4201ELBG				5876		53	6146	2				
42371108200000	1	WFMP	1	WEATHERBY	17623	1842	5309DVNN				6861	1							
42371108200000	2	WFMP	1	WEATHERBY	18364	1859	5309DVNN				9771	1		9625	4				126000PPMCL
42371108200000	3	WFMP	1	WEATHERBY	21506	2219	3201ELBG				10535	1		9475	6				900000PPMCL
42371108600000	1		1	BELDING MAXWELL	15079	1514	2309DVNN												
42371108620000	2	DVNN	14	MOORE WAYNE	15485	1583	0201ELBG												
42371108620000	3	DVNN	14	MOORE WAYNE	15485	1583	0201ELBG												
42371108620000	4	DVNN	14	MOORE WAYNE	15465	1587	0201ELBG				1759	1		6878	1				
42371108660000	3	ELBG	5	HODGE JH	14950	1528	9				7619	1		7434		20			
42371108660000	4	ELBG	5	HODGE JH	14970	1533	5				7638	130		7638	3	5			
42371108660000	5	ELBG	5	HODGE JH	15335	1554	5				7675	1		7675	1				
42371108700000	2	ELBG	1	BLACKSTONE-SLHT	14583	1525	0201ELBG	15000MCFD			6977	1		6941	3	0			
42371108700000	3	ELBG	1	BLACKSTONE-SLHT	15244	1549	7201ELBG	8000MCFD			7032	1		6977	2	0			
42371108750000	1		1	SAN PEDRO RAN	16404	1699	7201ELBG				7709	1		7428	1				
42371108750000	2		1	SAN PEDRO RAN	17108	1770	8												
42371108750000	3		1	SAN PEDRO RAN	17108	1770	8												
42371108750000	4		1	SAN PEDRO RAN	17171	1770	8				8145	1		7919	2				
42371108750000	5		1	SAN PEDRO RAN	17825	1873	3												
42371108750000	6		1	SAN PEDRO RAN	17825	1873	3												
42371109440000	1	ELBG	1	DD GAS UNIT	21687	2168	7201ELBG	20MCFD											
42371109560000	1		2	COLVILLE PD EST	15855	1603	7309DVNN				8802	1		7103	1				
42371109560000	2		2	COLVILLE PD EST	16016	1626	6309DVNN				7103	1		4674					
42371110540000	11	ELBG	1	ABILENE CHRSTN	17232	1732	2201ELBG												
42371110640000	3	MNTY	1	ELSINOR CATTLE	16115	1618	0209ODVC												
42371110980000	3	DVNN	1	CONTINENTAL-LEA	15175	1539	5201ELBG				6503	1		6503	2				73000PPMCL
42371111880000	1		1	WOFFORD WR	15060	1517	5309DVNN				6323			6269	2				
42371111880000	2		1	WOFFORD WR	15240	1551	6203MNTY				7280	1		7226	2				
42371112160000	1	ELBG	1	FT STOCKTON GUN	16871	1694	9	TSTM			11499	1		11370	1300				
42371112160000	2	ELBG	1	FT STOCKTON GUN	18669	1866	9	1260MCFD											
42371112160000	3	ELBG	1	FT STOCKTON GUN	18818	1881	8	594MCFD											
42371112160000	4	ELBG	1	FT STOCKTON GUN	19240	1924	0	750MCFD											

API #	DST #	PROD FM	WELL #	LEASE NAME	DST TOP DEPTH	DST BASE DEPTH	FM TESTED	FLUID VOL	NARRATIVE	BHT	ISIP	HOUR	MIN	FSIP	HR	MIN	ACCES GAS	GVTY	SALINITY
42371112160000	5	ELBG	1	FT STOCKTON GUN	17650	1957	5				9314	2		9357	2				
42371112160000	6	ELBG	1	FT STOCKTON GUN	17650	1998	1	60BWPH			9410	2		8814	8				
42371113430000	1	ELBG	1	SIBLEY DJ	15783	1591	0				7054		30	6897	3				
42371113430000	2	ELBG	1	SIBLEY DJ	15942	1614	2203MNTY				7113		30	6975	4				
42371113430000	3	ELBG	1	SIBLEY DJ	16622	1671	4202SMPS				2895		30	4160	2				
42371113740000	1	ELBG	1	NEAL JO	15440	1576	8451CGLM				12779	13	510	263	250				
42371113740000	2	ELBG	1	NEAL JO	15910	1615	2451WFMP				8844	215		8165	210				
42371113740000	3	ELBG	1	NEAL JO	18383	1871	2309DVNN	1250MCFD			9858	218							
42371113740000	4	ELBG	1	NEAL JO	17635	1871	2	200MCFD			8081	2		515	212				
42371301690000	1	ELBG	1	GOMEZ GAS UNIT	15204	1633	4	83MCFD			10608		10	089					
42371301770000	1		1	DULANEY	15040	1507	3309DVNN				5839	2		5883	4				
42371301770000	2		1	DULANEY	15045	1512	3309DVNN				5883	2		5883	4				
42371302200000	1	ELBG	1	STOCKTON UNIT	17464	1746	4451WFMP	8200MCFD											
42371302960000	1	ELBG	1	BLACKSTONE-SLAU	16146	1625	0309DVNN	220MCFD								0			
42371302960000	2	ELBG	1	BLACKSTONE-SLAU	16345	1650	4252FSLM												
42371302980000	3	WFMP	1-26	WEST COYANOSA U	17024	1725	8309DVNN				4968	1		5228	2				
42371302980000	4	WFMP	1-26	WEST COYANOSA U	17025	1733	7309DVNN	TSTM			8235		45	823	510				
42371303150000	1	WFMP	1	SAMS-MENDEL	18216	1846	4309DVNN												
42371303150000	2	WFMP	1	SAMS-MENDEL	18464	1846	4309DVNN												
42371304480000	7	DVNN	1	SUN	15180	1553	3201ELBG												
42371304480000	8	DVNN	1	SUN	15288	1558	3201ELBG												
42371304480000	9	DVNN	1	SUN	15206	1561	9201ELBG												
42371304690000	1	ELBG	1	GOMEZ WEST GAS	22210	2282	0201ELBG												
42371304690000	2	ELBG	1	GOMEZ WEST GAS	22210	2282	0201ELBG				8922		28						
42371305730000	1	ELBG	2	LAUGHLIN-STRAUG	18186	1829	8309DVNN				5927	1		5168	1				
42371306580000	4	DVNN	1	ELSINORE CATTLE	15565	1585	0201ELBG				6345	1			2				
42371307170000	4		1	GRIFFIN GG	14710	1514	6201ELBG				6492	1		6068	2				
42371307170000	5		1	GRIFFIN GG	15016	1550	0201ELBG												
42371308150000	1	ELBG	1	REYNOLDS CATTLE	17675	1788	8				8212	1		6569	430				
42371308150000	2	ELBG	1	REYNOLDS CATTLE	21500	2169	2												
42371309970000	1		1	S PIKES PEAK	15008	1506	5309DVNN				1892	1		4470	1				79000PPMCL
42371309970000	2		1	S PIKES PEAK	15440	1601	0202SMPS												
42371311020000	1		1	R M	15326	1537	6309DVNN												
42371311020000	2		1	R M	15321	1546	0309DVNN												
42371315060000	2		1	7506 JV-S MARSH	17510	1763	0309DVNN				2452	3							
42371315090000	1		1	FAY-ELLEN	18025	1845	3319WDFD				1333	1		1266	2				
42371315260000	1	WFMP	1	ARCO-TERRAZAS	15560	1605	5309DVNN				1319	1		1265	2				
42371315260000	2	WFMP	1	ARCO-TERRAZAS	19162	2017	0201ELBG	70MCFD			4479	1		7579	4				
42371315260000	3	WFMP	1	ARCO-TERRAZAS	20085	2133	5201ELBG												
42371317800000	2		1	BELDING GAS U	19987	2008	7202CNNL												
42371317800000	3		1	BELDING GAS U	20038	2019	3201ELBG												
42371317800000	4		1	BELDING GAS U	20327	2054	0201ELBG				8439			8497	1				
42371317800000	5		1	BELDING GAS U	20340	2054	0201ELBG				7992	1		8190	230				
42371317820000	6		1	UTP MONTGOMERY	14804	1516	5201ELBG												
42371317820000	7		1	UTP MONTGOMERY	14800	1519	0201ELBG				5594			6121	4				
42371323470000	8		1	CITGO-NEAL	14580	1501	0201ELBG				6384	2		6384	4				
42371323530000	2	DVNN	1	MADDOX-STATE	15700	1585	4309DVNN	160MCFD			6165	1		6165	8				
42371323750000	1	MSSP	1	TREES J C EST "	14601	1505	0359MSSP				7140	145		717	614				

API #	DST #	PROD FM	WELL #	LEASE NAME	DST TOP DEPTH	DST BASE DEPTH	FM TESTED	FLUID VOL	NARRATIVE	BHT	ISIP	HOUR	MINS	FSIP	HR	MIN	ACCES GAS	GVTY	SALINITY
42371323750000	2	MSSP	1	TREES J C EST "	15481	1562	3309DVNN				7370	1		7486	5				
42371326820000	2		1	WHITE-STATE	15554	1576	8309DVNN				2484	1		6680	8				
42371326820000	3		1	WHITE-STATE	15665	1581	8309DVNN				3820	1		6023	8				
42371329280000	1	DVNN	1	FROST NTL BNK-S	17350	1745	8309DVNN	TSTM			7669	130		7365	8				107000PPMCL
42371331910000	4	ELBG	1	PAGE ROYALTY	17747	1796	8309DVNN	6900MCFD			8754	1		8669	3				
42371335230000	1	DVNN	3	8004 JV-P GRAND	18498	1862	7309DVNN				7117	2			5				
42373006090000	1		58	SARAH F WING	8298	8231	3	1500F	WTR					3500					
42377000010001	15		1	MITCHELL BROS-S	14890	1509	0												
42377000010001	19		1	MITCHELL BROS-S	14810	1509	0												
42377000010001	20		1	MITCHELL BROS-S	14810	1509	0												
42377000010001	21		1	MITCHELL BROS-S	14904	1509	0												
42377000010001	12		1	MITCHELL BROS-S	14920	1510	0												
42377000010001	13		1	MITCHELL BROS-S	14917	1510	0												
42377000010001	16		1	MITCHELL BROS-S	14920	1512	0												
42377000010001	17		1	MITCHELL BROS-S	14925	1513	0												
42377000010001	18		1	MITCHELL BROS-S	14810	1513	0												
42377000010001	14		1	MITCHELL BROS-S	14920	1517	5												
42377000010001	9		1	MITCHELL BROS-S	15235	1544	8												
42377000010001	10		1	MITCHELL BROS-S	15220	1544	8												
42377000010001	11		1	MITCHELL BROS-S	15238	1544	8												
42377000010001	7		1	MITCHELL BROS-S	15454	1568	4												
42377000010001	8		1	MITCHELL BROS-S	15456	1569	6												
42377000010001	5		1	MITCHELL BROS-S	15696	1599	6												
42377000010001	6		1	MITCHELL BROS-S	15683	1599	6							1900		15			
42389003100000	2		1	HOEFS	17281	1760	3												
42389003100000	3		1	HOEFS	17440	1777	7												
42389003100000	4		1	HOEFS	17457	1782	2												
42389003100000	5		1	HOEFS	17200	1782	4							7560		130			
42389003100000	6		1	HOEFS	17190	1784	0							7410		130			
42389003100000	7		1	HOEFS	17605	1786	6				7515								
42389003750000	16	ELBG	2	R CLEVELAND ETA	16700	1689	7												
42389003750000	17	ELBG	2	R CLEVELAND ETA	16897	1706	5										COZ		
42389003750000	18	ELBG	2	R CLEVELAND ETA	17068	1724	8									0			
42389003750000	19	ELBG	2	R CLEVELAND ETA	17248	1735	2									0			
42389003750000	20	ELBG	2	R CLEVELAND ETA	17352	1746	2												
42389003750000	21	ELBG	2	R CLEVELAND ETA	17462	1758	8												
42389003750000	22	ELBG	2	R CLEVELAND ETA	17588	1767	1												
42389003750000	23	ELBG	2	R CLEVELAND ETA	17608	1769	1												
42389100240000	1	ELBG	1	ZEEK GAS UNIT	17275	1740	0				6688		30	7322	1				
42389101990000	3	ELBG	1	COOK-STATE GAS	15196	1519	6	2000MCFD											
42389101990000	4	ELBG	1	COOK-STATE GAS	17310	1731	0	TSTM											
42389101990000	5	ELBG	1	COOK-STATE GAS	17341	1734	1	60MCFD											
42389101990000	6	ELBG	1	COOK-STATE GAS	17373	1737	3	213MCFD											
42389101990000	7	ELBG	1	COOK-STATE GAS	17404	1740	4	245MCFD											
42389101990000	8	ELBG	1	COOK-STATE GAS	17458	1745	8	1840MCFD											
42389101990000	9	ELBG	1	COOK-STATE GAS	17500	1750	0	1640MCFD											
42389102050000	8	ELBG	1	WAPLES-PLATTER	15303	1705	9	4300MCFD			10327		35			0			
42389102050000	9	ELBG	1	WAPLES-PLATTER	17491	1749	1												

API #	DST #	PROD FM	WELL #	LEASE NAME	DST TOP DEPTH	DST BASE DEPTH	FM TESTED	FLUID VOL	NARRATIVE	BHT	ISIP	HOUR	MIN	FSIP	HR	MIN	ACCES GAS	GVTY	SALINITY
42389102050000	10	ELBG	1	WAPLES-PLATTER	17357	1749	1	259MCFD						5008	1	2			
42389102050000	11	ELBG	1	WAPLES-PLATTER	17357	1770	0				8710	1				3			
42389102050000	21	ELBG	1	WAPLES-PLATTER	20470	2091	0	5BWPH											
42389102050000	20	ELBG	1	WAPLES-PLATTER	20930	2107	0	800MCFD								0			
42389102050000	18	ELBG	1	WAPLES-PLATTER	21100	2116	9												
42389102050000	19	ELBG	1	WAPLES-PLATTER	21100	2116	9	1490MCFD			8984	1		8743	4				
42389102050000	15	ELBG	1	WAPLES-PLATTER	21378	2146	0												
42389102050000	16	ELBG	1	WAPLES-PLATTER	21378	2146	0												
42389102050000	17	ELBG	1	WAPLES-PLATTER	21334	2146	0	2975MCFD			9057	1		8838	4	0			
42389102050000	14	ELBG	1	WAPLES-PLATTER	21500	2160	0				9144	1		8489	4				
42389102050000	12	ELBG	1	WAPLES-PLATTER	21745	2180	0												
42389102050000	13	ELBG	1	WAPLES-PLATTER	21745	2180	0	TSTM			8663	1		7004	4				
42389102510000	5	ELBG	11-1	BECKEN OP	17128	1733	9	1500MCFD											
42389102510000	9	ELBG	11-1	BECKEN OP	17140	1755	0201ELBG				7766	130		7628	115				
42389102510000	6	ELBG	11-1	BECKEN OP	17334	1758	9												
42389102510000	7	ELBG	11-1	BECKEN OP	17366	1758	9												
42389102510000	8	ELBG	11-1	BECKEN OP	17608	1780	0				8644	1		7790	130				
42389104010000	1	ELBG	1	BODKINS JD	16559	1740	0201ELBG	13300MCFD			7611	2		7576	3570				
42389104230000	4	ELBG	1	GILLISPIE EH	16448	1660	1												
42389104230000	5	ELBG	1	GILLISPIE EH	16448	1660	1353BRNT				12988	1				0			
42389104240000	4	ELBG	1	REGAN ROBERTA	17350	1779	8	7MCFD			804	1		580	1				
42389104240000	5	ELBG	1	REGAN ROBERTA	21074	2109	6	5500MCFD						9009	3				
42389104270000	2	ELBG	1	REEVES FEE	21036	2106	0	1080MCFD			8494	117		8914	3				
42389104270000	1	ELBG	1	REEVES FEE	21253	2142	8	120MCFD											
42389104280000	2	ELBG	1	REEVES TXL FEE	16629	1705	9201ELBG				3901	30		3770	45				
42389104280000	3	ELBG	1	REEVES TXL FEE	21183	2130	2201ELBG	TSTM			9313								
42389104290000	2	ELBG	1	TXL REEVES-STAT	17187	1770	4				7042	30		4885	1				
42389104290000	3	ELBG	1	TXL REEVES-STAT	20480	2063	7				7960	45							
42389104290000	6	ELBG	1	TXL REEVES-STAT	21078	2113	3	5125MCFD			9097	30		8631	3	0			
42389104290000	5	ELBG	1	TXL REEVES-STAT	21344	2147	9				8987	33		8987	3				
42389104290000	4	ELBG	1	TXL REEVES-STAT	21709	2193	4				9097	30		9097	3				
42389104750000	3	ELBG	13	MOORE WAYNE	15945	1616	4202SMPS												
42389104750000	4	ELBG	13	MOORE WAYNE	17910	1856	3201ELBG	TSTM											
42389104960000	5	DVNN	1	RAPE JM	17750	1812	9201ELBG												
42389104960000	6	DVNN	1	RAPE JM	17790	1812	9201ELBG												
42389104960000	7	DVNN	1	RAPE JM	17820	1812	9201ELBG												
42389104960000	8	DVNN	1	RAPE JM	18500	1850	0201ELBG												
42389104960000	9	DVNN	1	RAPE JM	17775	1850	0201ELBG				7983	1							
42389105040001	1	ATOK	2	WAHLENMAIER STA	17749	1802	3	80MCFD			5234	1		5400	5				
42389105080000	1	WFPD	1	MILLWEE-STATE	20966	2140	6201ELBG												
42389105100000	1	ELBG	9	TREES JC ESTAET	16895	1689	5201ELBG	2085MCFD											
42389105100000	2	ELBG	9	TREES JC ESTAET	17169	1716	9201ELBG	705MCFD											
42389105100000	3	ELBG	9	TREES JC ESTAET	17201	1720	1201ELBG	3600MCFD											
42389105140000	6	DVNN	4	REEVES TXL FEE	17234	1723	4309DVNN	2300MCFD											
42389105140000	7	DVNN	4	REEVES TXL FEE	17406	1740	6309DVNN	160MCFD											
42389105450000	1	DVNN	1	ASHLOCK UNIT	17789	1796	5201ELBG				8323	1		7514	8				
42389105450000	2	DVNN	1	ASHLOCK UNIT	17791	1810	0201ELBG	TSTM			7355	1		7355	730				
42389105540000	4	MNTY	4	FIDELITY TRUST	14724	1577	0201ELBG	75MCFD											

API #	DST #	PROD FM	WELL #	LEASE NAME	DST TOP DEPTH	DST BASE DEPTH	FM TESTED	FLUID VOL	NARRATIVE	BHT	ISIP	HOUR	MINS	FSIP	HR	MIN	ACCES GAS	GVTY	SALINITY
42389105540000		5MNTY	4	FIDELITY TRUST	14724	1626	0201ELBG	TSTM			6432	1		6144	6				
42389105550000		1ELBG	1	SOUTHERN GAS UN	17025	1724	4309DVNN				5345	1		2732	2				
42389300460000		1ELBG	9	REEVES TXL FEE	17151	1736	1309DVNN												
42389300510000		1ELBG	1	EIKEN UNIT	15650	1600	8259SLRN												
42389300510000		2ELBG	1	EIKEN UNIT	15650	1600	8259SLRN												
42389300510000		3ELBG	1	EIKEN UNIT	15650	1600	8259SLRN				4385	1		4198	1				
42389300510000		4ELBG	1	EIKEN UNIT	15990	1628	6252FSLM				7658	1		7600	2	5			
42389300560000		2ELBG	1	HUMPHREY UNIT	16490	1651	1203MNTY				7656	1		7622	4	0			
42389300630000		6	1	ARMSTRONG	15645	1586	6201ELBG				6554	1		5074	2				
42389300630000		7	1	ARMSTRONG	15876	1606	6201ELBG				7221	1		7221	130				
42389300630000		8	1	ARMSTRONG	16074	1636	3201ELBG				7450	1		7366	2				
42389300750000		1ELBG	1	CAMPBELL-STATE	16990	1831	0203MNTY	TSTM			9099	1		9214	520				
42389300810000		3ATOK	1	KIRK ETAL UNIT	16021	1611	0252FSLM	TSTM			7268		30	7268	2				
42389302220000		5ATOK	1	MONROE	20960	2141	3201ELBG												
42389302220000		6ATOK	1	MONROE	21010	2155	0201ELBG												
42389302220000		7ATOK	1	MONROE	21020	2160	0201ELBG												
42389302290000		1	1	WORSHAM	16740	1686	5252FSLM				3373	1		3718	430				
42389302290000		2	1	WORSHAM	16730	1686	5252FSLM				257	1		2104	6				
42389302310000		1FSLM	1	WIGGINS-ORLA	15380	1573	4252FSLM												
42389302390000		3FSLM	1	HERMOSA UNIT	17532	1757	6252FSLM	TSTM			7672	1		7674	6				
42389302390000		1FSLM	1	HERMOSA UNIT	16891	1758	5252FSLM												
42389302390000		2FSLM	1	HERMOSA UNIT	17514	1758	5252FSLM	36MCFD			8052	130		7921	4				
42389302390001		1	1	HERMOSA UNIT-75	14948	1754	5252FSLM				852	1		796	630				135000PPMCL
42389302390001		2	1	HERMOSA UNIT-75	14948	1756	6				7722	1		7751	5				116000PPMCL
42389302410000		1	1	TUBB	14545	1527	1309DVNN	TSTM			414	130		394	4				
42389302410000		2	1	TUBB	15586	1566	6252FSLM				7592	130		7592	2				
42389302410000		3	1	TUBB	14613	1566	6252FSLM	TSTM			610	130		610	4				
42389302410000		4	1	TUBB	14500	1585	0252FSLM	1780MCFD			4456	130		4653	330				
42389302410000		5	1	TUBB	17893	1820	0201ELBG												
42389302410000		6	1	TUBB	17893	1820	0201ELBG				5747	130		3538	4				
42389302410000		7	1	TUBB	17899	1845	0201ELBG				8084	130		6321	4				
42389302410000		8	1	TUBB	17902	1853	0201ELBG				6554	130			2				
42389302690000		2	1	J COVINGTON	17678	1787	8												
42389302690000		3	1	J COVINGTON	18275	1842	2												
42389302690000		4	1	J COVINGTON	18277	1852	5												
42389302700000		4	1	ROGENE BELL GAS	16630	1670	0	2000MCFD											
42389302700000		1	1	ROGENE BELL GAS	16750	1682	0												
42389302700000		3	1	ROGENE BELL GAS	16636	1682	2												
42389302700000		2	1	ROGENE BELL GAS	16850	1695	0												
42389302710000		2ATOK	2	HERMOSA UNIT	17131	1727	0309DVNN	TSTM											
42389302710000		3ATOK	2	HERMOSA UNIT	17131	1740	0309DVNN		DIED										
42389302750000		1DVNN	1	HARDIN-STATE	16550	1758	6309DVNN												81000PPMCL
42389302750000		2DVNN	1	HARDIN-STATE	20595	2092	8201ELBG												
42389302760000		1FSLM	1	BRENNAND-STATE	15725	1587	5												
42389302760000		2FSLM	1	BRENNAND-STATE	15725	1587	5	6000MCFD	1/2 I										
42389302800000		1DVNN	1	WORSHAM /48/	15865	1595	5359MSSP	36MCFD			11198	130	11198		6				
42389302800000		2DVNN	1	WORSHAM /48/	16525	1688	0309DVNN	385MCFD			8125	130		8125	8				
42389302800000		3DVNN	1	WORSHAM /48/	17270	1737	5252FSLM	2500MCFD			8179	1		8179	7				

API #	DST #	PROD FM	WELL #	LEASE NAME	DST TOP DEPTH	DST BASE DEPTH	FM TESTED	FLUID VOL	NARRATIVE	BHT	ISIP	HOUR	MIN	FSIP	HR	MIN	ACCES GAS	GVTY	SALINITY
42389302800000	4	DVNN	1	WORSHAM /48/	17714	1774	0203MNTY	108MCFD			573	130		1661	5				
42389302920000	3	ATOK	1	PECOS UNIT	16255	1636	0359MPLM	TSTM			7890	130		6532	130				
42389302920000	7	ATOK	1	PECOS UNIT	16940	1694	7252FSLM												
42389302920000	4	ATOK	1	PECOS UNIT	17000	1710	0252FSLM	TSTM			7404	1		7380	2				
42389302920000	6	ATOK	1	PECOS UNIT	17000	1712	5252FSLM												
42389302920000	5	ATOK	1	PECOS UNIT	17150	1730	0252FSLM	TSTM			7456	130		7456	3				
42389302920000	8	ATOK	1	PECOS UNIT	19220	1988	4201ELBG	TSTM											
42389302930000	2		1	REEVES-STATE	15515	1557	5259SLRN				6780	1		6780	1				
42389303920000	1	FSLM	1	WORSHAM /20/	16220	1658	8359MSSP	400MCFD			6426	30		7441	1				
42389303920000	2	FSLM	1	WORSHAM /20/	17517	1761	0252FSLM	TSTM			8549	130		8195	6				
42389303930000	5		1	STANFIELD GOLDA	15640	1594	0201ELBG												
42389303930000	6		1	STANFIELD GOLDA	15640	1594	0201ELBG				2534	1		6894	4				
42389304120000	2	FSLM	1	7607 JV-P ORLA	15604	1576	5252FSLM	6200MCFD			6821	4		6821	4				
42389305010000	2	ELBG	1	MEEKER "45"	15895	1632	2309DVNN												
42389305010000	3	ELBG	1	MEEKER "45"	16565	1675	8309DVNN												
42389305010000	4	ELBG	1	MEEKER "45"	16565	1675	8309DVNN	TSTM											
42389305070000	1	MRRW	1	ADAM ESTATE	19340	1945	0252FSLM												
42389305070000	2	MRRW	1	ADAM ESTATE	19335	1952	5252FSLM				8323			8323					
42389305090000	5	ELBG	7	S E LIGON	16940	1748	6201ELBG	14MCFD			6050	100		6398	300				
42389308900000	3	BSPG	1	VALLEY FARM	18328	1853	6309DVNN				6758	130		8628	6				
42389311800000	6		1	MCCARTER	18580	1878	1309DVNN					14		6409					
42389311800000	5		1	MCCARTER	22090	2235	0201ELBG												
42389312300000	6		1-6	JOBST	14918	1535	5269SLDV												
42389312300000	7		1-6	JOBST	14918	1535	5269SLDV					1		5242	4				
42389312450000	2	ELBG	2	NORTHWEST HMON	15340	1538	5451WFMP				8172	1		10408	8				320000PPMCL
42389312520000	1		1	TEXACO FEE	18525	1875	0252FSLM												
42389312520000	2		1	TEXACO FEE	20600	2144	7201ELBG												
42389313470000	4	WFMP	1	TEXACO INC-ATA	15932	1594	2201ELBG				211	2		6661	8				
42389313470000	1	WFMP	1	TEXACO INC-ATA	16070	1618	0201ELBG				7349	3		7349	4				
42389313470000	2	WFMP	1	TEXACO INC-ATA	15970	1657	5201ELBG				6459	130		4561	1				
42389313470000	3	WFMP	1	TEXACO INC-ATA	15970	1692	4201ELBG				5609	6							
42389316870000	2		1	J W MCCULLOUGH	17572	1830	0359MSSP				6934	1							
42389316870000	3		1	J W MCCULLOUGH	17572	1836	5359MSSP				6934	130							
42443000010000	1		2	BROWN-BASSETT	14910	1504	6												
42443000010000	2		2	BROWN-BASSETT	15038	1512	9	1339MCFD						6125	300				11000PPMCL
42443000540000	1		1	ETHEL CORDER	16869	1704	4												
42443000540000	2		1	ETHEL CORDER	17056	1722	5							3300	30				
42443000540000	3		1	ETHEL CORDER	17170	1732	5												
42443000540000	4		1	ETHEL CORDER	17056	1732	5							7040	30				
42443000540000	5		1	ETHEL CORDER	17218	1735	3201ELBG												
42443000540000	6		1	ETHEL CORDER	17218	1735	3												
42443000800000	1		1	JM CORDER	15220	1533	5								30				
42443100180000	3	STRN	1	GEORGE K MITCHE	15745	1574	5	50MCFD											
42443102010000	1		34-17	UNIVERSITY	16109	1639	8				3455	5		3325	52				
42443102010000	2		34-17	UNIVERSITY	16402	1669	3												
42443102010000	3		34-17	UNIVERSITY	16380	1670	0												
42443102010000	4		34-17	UNIVERSITY	16383	1670	0												
42443102010000	5		34-17	UNIVERSITY	16415	1672	0					30			1				

API #	DST #	PROD FM	WELL #	LEASE NAME	DST TOP DEPTH	DST BASE DEPTH	FM TESTED	FLUID VOL	NARRATIVE	BHT	ISIP	HOUR	MINS	FSIP	HR	MIN	ACCES GAS	GVTY	SALINITY
42443102010000	6		34-17	UNIVERSITY	16728	1692	4												
42443102010000	7		34-17	UNIVERSITY	16915	1729	0				5430	1		3842					
42443102020000	1		1	HARDGRAVE NELLI	15670	1591	4				4992	1		3387	230				
42443102040000	1	ELBG	1	MITCHELL KEITH	17410	1785	0201ELBG	6700MCFD			7895	1		7360	1	0			
42443102040000	2	ELBG	1	MITCHELL KEITH	17410	1804	9201ELBG	10000MCFD			7936	1		7894	1	0			
42443102090000	1	WFMP	1	ABILENE CHRSTOL	15098	1548	6309DVNN				8966			9022					
42443300030000	1	ELBG	1-59	MITCHELL	17930	1834	7201ELBG	750MCFD											
42443300370000	1		1	BASSETT TRUST	18854	1938	9201ELBG												
42443300370000	2		1	BASSETT TRUST	18764	1938	9201ELBG												
42443300370000	3		1	BASSETT TRUST	18764	1938	9201ELBG												
42443300370000	4		1	BASSETT TRUST	19276	1938	9201ELBG				4034	130		3729	1				
42443300370000	5		1	BASSETT TRUST	19360	1959	3201ELBG												
42443300370000	6		1	BASSETT TRUST	17156	2018	2201ELBG				3050	1		3694	4				
42443300810000	2		1	MONROE M B	15029	1548	8409PSLV												
42443303430000	1		1	BIGHORN "1"	18172	1859	6201ELBG												
42445003190000	5		123-B	PRENTICE NE UNI	5964	1610	0							1850		15			
42465000370000	4		1	MILLS MINERAL T	16415	1671	5												
42465000370000	5		1	MILLS MINERAL T	16750	1687	0												
42465000370000	6		1	MILLS MINERAL T	17164	1731	4												41800PPMCL
42465000370000	7		1	MILLS MINERAL T	17307	1746	1												
42465000390000	1		1	WARDLAW	14776	1504	5												
42465000390000	2		1	WARDLAW	14970	1529	5												142000PPMCL
4246500062000010			1	MORRISON	13761	1781	2							6340		30			
42465000950000	7		1	WW WEST	14851	1501	4							2330		15			
42465000950000	8		1	WW WEST	15013	1518	7							2385		15			
42465000950000	9		1	WW WEST	15175	1538	3							2510		15			
42465001110000	2		1X	ROBT J CAUTHORN	15726	1581	8201ELBG	2BWPH			510		30	350		30			9000PPMCL
42465001110000	3		1X	ROBT J CAUTHORN	16317	1651	7201ELBG				6250		30	4880		45			250000PPMCL
42465001110000	4		1X	ROBT J CAUTHORN	16527	1667	1201ELBG				3865		30	3020		45			86000PPMCL
42465001110000	5		1X	ROBT J CAUTHORN	16671	1689	5201ELBG				6030		30	5070		45			86000PPMCL
42465001110000	6		1X	ROBT J CAUTHORN	17087	1708	7												
42465102130000	8		1	BUNGER GL	14558	1550	0	32MCFD			4337	2		5994	455				
42465102150000	2		1	GUINN	15460	1564	4201ELBG				4409	130		6554	3				
42465102150000	3		1	GUINN	15830	1603	0201ELBG												
42465304360000	1		1	HACKBERRY FEE 8	15360	1589	5201ELBG												
42465304360000	2		1	HACKBERRY FEE 8	15865	1640	2201ELBG												
42465304360000	3		1	HACKBERRY FEE 8	15931	1640	2201ELBG				4905		50						
42465304360000	4		1	HACKBERRY FEE 8	15330	1690	8201ELBG												
42465304360000	5		1	HACKBERRY FEE 8	15303	1690	8201ELBG				2685		40						
42475107290000	1	PSLV	1	GREER-MCGINLEAS	17810	1800	0				9052	1		9182	145				
42475107290000	2	PSLV	1	GREER-MCGINLEAS	19200	1927	5				8726	1		8726	3				
42475107290000	3	PSLV	1	GREER-MCGINLEAS	21270	2144	0201ELBG				9284	1		94951639					
42475107290000	4	PSLV	1	GREER-MCGINLEAS	21436	2160	3201ELBG				10068	1		9809	2				105000PPMCL
42475107410000	1	ELBG	1	LOCKRIDGE IP	18247	1846	0201ELBG				8291	1							
42475107410000	2	ELBG	1	LOCKRIDGE IP	18344	1855	7201ELBG												
42475107410000	3	ELBG	1	LOCKRIDGE IP	18352	1855	7201ELBG							5713	1				
42475107410000	4	ELBG	1	LOCKRIDGE IP	18580	1876	0201ELBG												
42475107860000	1	ELBG	1	UNIVERSITY PYOT	15074	1529	2309DVNN				6856	130		6927	3				

API #	DST #	PROD FM	WELL #	LEASE NAME	DST TOP DEPTH	DST BASE DEPTH	FM TESTED	FLUID VOL	NARRATIVE	BHT	ISIP	HOUR	MINS	FSIP	HR	MIN	ACCES GAS	GVTY	SALINITY
42495302310000	9		1	GULF-C ETAL	19805	2092	5			266	8052	1		7288	4				
42495302360000	1	MNTY	1	7306 JV-S WINK	15590	1586	2309DVNN				4521	2		3466	2				
42495302400000	1	ELBG	1	FELMONT	16301	1662	5252FSLM	TSTM			6188		30	6402	3				
42495302400000	2	ELBG	1	FELMONT	16301	1685	2252FSLM	TSTM			6340	1		6314	2				
42495302410000	2	FSLM	1	HOWELL PAT	19600	1980	0252FSLM				8667	1		8661	2				
42495302410000	3	FSLM	1	HOWELL PAT	21660	2195	3201ELBG				10100	1		9312	2				
42495302430000	1	FSLM	1	UNIVERSITY-21-2	16150	1653	3252FSLM							6802		30			
42495302450000	1	FSLM	241	UNIV BLOCK 21 G	16602	1704	5			220				6751	1				
42495302500000	1	FSLM	1	WINK AIRPORT	15870	1615	4252FSLM				6778	3		6778	3				
42495303510000	1		1	UNIVERSITY /35-	17598	1768	9252FSLM			270	7649	1		7688	2				
42495303510000	2		1	UNIVERSITY /35-	17596	1802	2252FSLM												
42495303730000	1	FSLM	262	UNIV BLK 21 GU	17960	1880	5201ELBG							7976	2				
42495303730000	2	FSLM	262	UNIV BLK 21 GU	19000	1900	0201ELBG												
42495303730000	3	FSLM	262	UNIV BLK 21 GU	18100	1900	0201ELBG							8104	4				
42495303730000	4	FSLM	262	UNIV BLK 21 GU	18100	1900	0201ELBG				8235	1							
42495303730000	5	FSLM	262	UNIV BLK 21 GU	18100	1900	0201ELBG							7853	315				
42495303750000	1	CPTN	1	BLACK KETTLE	19696	1980	0253SLRNU				569	1		435	2				
42495303750000	2	CPTN	1	BLACK KETTLE	19815	2003	0252FSLM				8214	1		8384	515				
42495303750000	3	CPTN	1	BLACK KETTLE	21910	2222	5201ELBG				9212	1		9173	4				
42495303860000	1	SLDV	1	YELLOW WOLF	19274	1935	5269SLDV	400MCFD			8288	1		6614	5				
42495303860000	2	SLDV	1	YELLOW WOLF	19750	1983	0269SLDV				8010	6		824811					
42495303860000	3	SLDV	1	YELLOW WOLF	21900	2213	0201ELBG				9637	1		9673	6				
42495304060000	2	MRRW	1	COMANCHE UNIT	19018	1930	0309DVNN				5396	1		8753	5				
42495304060000	3	MRRW	1	COMANCHE UNIT	19240	1954	0309DVNN				826411			8225	2				
42495304060000	4	MRRW	1	COMANCHE UNIT	21424	2184	4201ELBG				8426			3888					
42495304450000	1	PSLV	1	LINEBERY /10/	18945	1917	5309DVNN			250				7623	3				
42495304450000	2	PSLV	1	LINEBERY /10/	19410	1976	0309DVNN	TSTM											
42495308650000	1		1X	UNIVERSITY /21-	18575	1905	0201ELBG	TSTM			4684	1		9254	5				
42495308650000	2		1X	UNIVERSITY /21-	18980	1915	0201ELBG												
42495308650000	3		1X	UNIVERSITY /21-	18568	1915	0201ELBG												
42495308650000	4		1X	UNIVERSITY /21-	18550	1915	0201ELBG												
42495309020000	1		1	SPOTTED HORSE	19946	2003	4359MPLM												
42495309140000	1	ATOK	1	HILL A G	19580	1964	0252FSLM				427			373					
42495309140000	2	ATOK	1	HILL A G	19568	1970	2252FSLM				8223			8223					
42495309140000	3	ATOK	1	HILL A G	19556	1974	4252FSLM				8183			8183					
42495310110000	1		2	WOLFE UNIT	19231	1935	5252FSLM			233	8093	4		8096	4				
42495310110000	2		2	WOLFE UNIT	21709	2174	0201ELBG			274	4247			3740					
42495321610000	1	STRN	3	TUBB ESTATE "22	15320	1566	0402MRRWU				12583	13		012197	8				
42495321610000	2	STRN	3	TUBB ESTATE "22	19145	1914	5259SLRN				7370	1							
42495323280000	1		1	CLIFTON	19420	1966	5259SLRN				8000	1		7968	4				

API #	DST #	PROD FM	WELL #	LEASE NAME	DST TOP DEPTH	DST BASE DEPTH	FM TESTED	FLUID VOL	NARRATIVE	BHT	ISIP	HOUR	MIN	FSIP	HR	MIN	ACCES GAS	GVTY	SALINITY
42475107860000		7ELBG	1	UNIVERSITY PYOT	17872	1787	7202JONS				4851	132		881	1				
42475107860000		2ELBG	1	UNIVERSITY PYOT	17960	1827	6201ELBG				7694	130		5646	3				
42475107860000		3ELBG	1	UNIVERSITY PYOT	18250	1852	4201ELBG				8480	132		2722		40			
42475107860000		4ELBG	1	UNIVERSITY PYOT	18327	1859	3201ELBG				8576	130							
42475107860000		5ELBG	1	UNIVERSITY PYOT	18630	1892	1201ELBG				8305								
42475107860000		6ELBG	1	UNIVERSITY PYOT	18994	1906	3201ELBG				8337	230		7335	3				108000PPMCL
42475107960000		1ELBG	1	WILLIAMS E UNIT	20146	2028	6												
42475109590000		1	1	DUGGAN	16625	1679	6309DVNN				948			4828					
42475109590000		2	1	DUGGAN	19973	2038	7201ELBG							8645	4				
42475110750000		6	1	HUTCHINGS-SEALY	14440	1544	1309DVNN	10MCFDE			6748	1		6100	1	330			
42475110930000		1FSLM	1	BARSTOW UNIT	17320	1752	8309DVNN	4000MCFD			7266	1		8409	3	0			
42475110930000		2FSLM	1	BARSTOW UNIT	17525	1775	0252FSLM												
42475110930000		3FSLM	1	BARSTOW UNIT	17315	1775	5252FSLM				8101	1							
42475110930000		4FSLM	1	BARSTOW UNIT	19798	2041	0201ELBG												
42475110930001		1	1	BARSTOW UNIT #1	17344	1739	9252FSLM					2			2				
42475111260000		3DVNN	1	CAPRITO	16930	1712	0201ELBG							7455	1	150			
42475111600001		1FSLM	1	LECROY UNIT	16230	1650	0309DVNN				3568	1		3432	1	30			
42475111600001		2FSLM	1	LECROY UNIT	16675	1689	3252FSLM				7678		30	7661	6				
42475111600001		3FSLM	1	LECROY UNIT	18815	1910	0				6018	1		2647	3				
42475111600001		4FSLM	1	LECROY UNIT	18826	1910	0				3630	1		3285	2				
42475111600001		5FSLM	1	LECROY UNIT	18843	1955	0201ELBG				8798		30	8840	1	30			
42475301560000		4ELBG	1	BLOCK 16 NO 1 U	16817	1700	0201ELBG												
42475301560000		5ELBG	1	BLOCK 16 NO 1 U	16807	1700	0201ELBG				5872		30						
42475301560000		6ELBG	1	BLOCK 16 NO 1 U	16915	1719	0201ELBG												
42475301900000		1	1	SCOTT FH	16848	1706	7309DVNN				7654	1		7234	3				
42475301960000		1FSLM	3	BARSTOW UNIT	16733	1702	3309DVNN							5185	2				
42475301960000		2FSLM	3	BARSTOW UNIT	17075	1721	8252FSLM	200MCFD						8033	6				
42475301960000		3FSLM	3	BARSTOW UNIT	19220	1970	0201ELBG												
42475301960000		4FSLM	3	BARSTOW UNIT	19224	1970	0201ELBG							7283	6	0			
42475301960000		5FSLM	3	BARSTOW UNIT	19228	1974	3201ELBG				8977			9057		0			
42475302250000		4ELBG	1	CAPRITO	16400	1700	0201ELBG							6974					
42475303050000		1FSLM	4	BARSTOW UNIT	16955	1711	8252FSLM	200MCFD											
42475303050000		2FSLM	4	BARSTOW UNIT	17360	1736	0252FSLM												
42475303050000		3FSLM	4	BARSTOW UNIT	17237	1736	0252FSLM							7521	3	0			
42475303050000		4FSLM	4	BARSTOW UNIT	19365	1986	5201ELBG	50MCFD						8983	5	2			
42475303050000		5FSLM	4	BARSTOW UNIT	19392	1989	2201ELBG												
42475303050000		6FSLM	4	BARSTOW UNIT	19347	1989	2201ELBG							8955	5	5			
42475303060000		2	1	SEALY GEO SEC 6	15050	1532	2309DVNN				4745		30	6642	6				
42475303060000		3	1	SEALY GEO SEC 6	15901	1615	0				7023		30						
42475303060000		4	1	SEALY GEO SEC 6	15878	1615	0203MNTY				6439		30	5510	5				
42475303120000		1FSLM	8	BARSTOW UNIT	17791	1779	1252FSLM												
42475303140000		2FSLM	1	AMER QUASAR-MON	17532	1753	2252FSLM												
42475303140000		3FSLM	1	AMER QUASAR-MON	17350	1753	2252FSLM				8109		30	8109	1	200			
42475303240000		2DLSD	1	WARD GRANDE	16075	1633	3309DVNN				7388	130		6990	130				
42475303240000		3DLSD	1	WARD GRANDE	16620	1695	2252FSLM	85MCFD			7400	130		7579	4				
42475303240000		4DLSD	1	WARD GRANDE	16970	1714	6203MNTY				640	130							
42475303240000		5DLSD	1	WARD GRANDE	17146	1742	0203MNTY				5813	140							
42475303240000		6DLSD	1	WARD GRANDE	18976	1924	0201ELBG				6106	130		5365	2				

API #	DST #	PROD FM	WELL #	LEASE NAME	DST TOP DEPTH	DST BASE DEPTH	FM TESTED	FLUID VOL	NARRATIVE	BHT	ISIP	HOUR	MIN	FSIP	HR	MIN	ACCES GAS	GVTY	SALINITY
42475303240000		7DLSD	1	WARD GRANDE	19204	1955	0201ELBG				8873	130		8693	3				
42475303250000		7ELBG	2	708 JV-D PYOTE	16170	1640	0201ELBG	2000MCFD			7429	1		7398	6155				104000PPMCL
42475303250000		8ELBG	2	708 JV-D PYOTE	16306	1650	0201ELBG												
42475303430000		3FSLM	1	ALVES UNIT	18428	1843	8252FSLM	10MCFD											
42475303430000		2FSLM	1	ALVES UNIT	18612	1862	2252FSLM	135MCFD								0			
42475303430000		1FSLM	1	ALVES UNIT	18410	1866	0252FSLM		E		8321	1		7965	2				
42475303500000		1FSLM	6	BARSTOW UNIT	16745	1697	0309DVNN							8373	2				
42475304230000		2	1	WILSON "73"	16915	1720	0309DVNN												
42475304230000		3	1	WILSON "73"	19839	2032	0201ELBG												
42475304230000		4	1	WILSON "73"	19842	2040	0201ELBG												
42475304230000		5	1	WILSON "73"	19842	2043	0201ELBG												
42475304230000		6	1	WILSON "73"	19865	2043	0201ELBG												
42475304250000		1FSLM	1	BARSTOW TOWNSIT	17860	1800	0							7300	230				
42475304250000		2FSLM	1	BARSTOW TOWNSIT	18243	1848	0	700MCFD			7334	1		7141	2				
42475304420000		1ELBG	1	UNIVERSITY	17065	1734	5309DVNN				4266	1		2882	2				
42475304420000		2ELBG	1	UNIVERSITY	17540	1769	6252FSLM	480MCFD			5032	3		3150	3				
42475304420000		3ELBG	1	UNIVERSITY	17655	1787	5252FSLM	TSTM			6844	1		7046	4				
42475304420000		4ELBG	1	UNIVERSITY	17810	1797	3203MNTY				2625	130		2254	2				
42475304420000		5ELBG	1	UNIVERSITY	17640	1837	0203MNTY	TSTM			7356	2		72191639					
42475304420000		6ELBG	1	UNIVERSITY	19730	2025	0201ELBG							7714	2				
42475304500000		4PSLV	1	7202 JV-S SEALY	14800	1506	8203MNTY				6616	3		5747	130				
42475304500000		5PSLV	1	7202 JV-S SEALY	16860	1720	0201ELBG	TSTM			7845	3		6821	2				
42475304500000		6PSLV	1	7202 JV-S SEALY	17190	1740	0201ELBG				7975	3		7026	5				
42475304500000		7PSLV	1	7202 JV-S SEALY	17380	1756	0201ELBG				8068	3		7938	5				
42475304500000		8PSLV	1	7202 JV-S SEALY	17570	1810	8201ELBG				8310	3		8310	4				
42475304580000		8ATOK	4	708-A JV-S PY	16740	1692	5201ELBG				2599	3		6905	215				
42475305000000		4ELBG	1	CROCKETT JEANNE	21750	2175	0201ELBG												
42475305000000		5ELBG	1	CROCKETT JEANNE	21875	2187	5201ELBG												
42475305080000		1FSLM	1	AMERICAN NAT IN	17995	1810	2252FSLM												
42475305110000		1ATOK	1	ROMONE UNIT	17040	1715	0203MNTY				7690	1		7710	2				50000PPMCL
42475305130000		4FSLM	1	UNIVERSITY 1	16970	1713	8252FSLM				7947	1		7947	2				
42475305230000		5ELBG	1	7301 JVS MOBIL	16245	1654	5201ELBG	240MCFD			8104	3		6652	2				
42475305230000		6ELBG	1	7301 JVS MOBIL	16548	1675	4201ELBG				7956	3		7247	2				
42475305230000		7ELBG	1	7301 JVS MOBIL	16767	1694	9201ELBG												
42475305230000		8ELBG	1	7301 JVS MOBIL	16712	1694	9201ELBG												
42475305510000		3ELBG	2	WEST CAPRITO UN	14938	1535	5309DVNN				7268	1		7137	230				
42475306260000		1FSLM	1	UNIVERSITY "11-	20396	2100	0201ELBG												
42475306390000		1ATOK	1	UNIVERSITY "18-	17510	1764	8												
42475306390000		2ATOK	1	UNIVERSITY "18-	17510	1764	8												
42475306390000		3ATOK	1	UNIVERSITY "18-	17286	1764	8						1	7593	4				
42475306440000		1	1	ANDERSON ETAL /	17530	1758	0252FSLM												
42475306440000		2	1	ANDERSON ETAL /	17450	1758	0252FSLM				8013	1		8097	4				
42475306440000		3	1	ANDERSON ETAL /	17420	1767	5252FSLM												
42475306440000		4	1	ANDERSON ETAL /	17445	1767	5252FSLM	TSTM			7901	1		7369	230				
42475306450000		2	1	UNIV LDS /18-32	18234	1834	0252FSLM												
42475306450000		1	1	UNIV LDS /18-32	18240	1834	6252FSLM												
42475306450000		3	1	UNIV LDS /18-32	18300	1847	5252FSLM				7750	1		7778	8				
42475306460000		1FSLM	1	UNIV 18-29 GAS	16770	1697	0				7089	1		7481	2				

API #	DST #	PROD FM	WELL #	LEASE NAME	DST TOP DEPTH	DST BASE DEPTH	FM TESTED	FLUID VOL	NARRATIVE	BHT	ISIP	HOUR	MINS	FSIP	HR	MIN	ACCES GAS	GVTY	SALINITY
42475306460000	2	FSLM	1	UNIV 18-29 GAS	19300	2060	0												
42475306590000	1		1	GOODE UNIT	18034	1814	1												
42475306590000	2		1	GOODE UNIT	18260	1835	1												
42475306590000	3		1	GOODE UNIT	18259	1835	1												
42475306590000	4		1	GOODE UNIT	18225	1841	2												
42475306730000	1	FSLM	1	ARCO-STATE /28/	16870	1727	5309DVNN	TSTM			8099	1			6				
42475306730000	2	FSLM	1	ARCO-STATE /28/	17385	1746	5252FSLM				8189	130							
42475306730000	3	FSLM	1	ARCO-STATE /28/	17382	1746	5252FSLM				2424	2		7343	8				
42475306830000	5		1	SOUTHWEST O'BRI	15330	1554	0201ELBG	575MCFD			5177	1		5268	5				
42475306830000	6		1	SOUTHWEST O'BRI	15520	1574	0201ELBG	260MCFD			4775	1		5580	5				
42475306830000	7		1	SOUTHWEST O'BRI	15725	1594	0201ELBG				6394	1		6579	4				
42475306830000	8		1	SOUTHWEST O'BRI	15965	1614	0201ELBG				7521	1		7539	6				
42475306860000	2	CRCN	1	UNIV /18-181/ G	16365	1660	0309DVNN	6MCFD			2466	1		6645	2				85000PPMCL
42475306860000	1	CRCN	1	UNIV /18-181/ G	16969	1720	0252FSLM	143MCFD			5747	4							
42475306880000	3		1	MARROW STATE /8	16624	1700	0												
42475306880000	4		1	MARROW STATE /8	16624	1704	0							7838					
42475306880000	1		1	MARROW STATE /8	19714	2015	2201ELBG	2000MCFD			5718	3							
42475306880000	2		1	MARROW STATE /8	19790	2027	5												
42475306920000	1	FSLM	1	WILLIAMS /32/	16331	1746	5359MSSP	1050MCFD			1750			7780					
42475306950000	5	ELBG	1	HNG FEE /57/	17044	1726	6201ELBG												
42475307630000	1		3	7417 JV-S WINKL	15560	1586	0309DVNN	TSTM			7060	3	5	7061	6				
42475307630000	2		3	7417 JV-S WINKL	16470	1671	6252FSLM				4210	3		3962	6				
42475307750000	1	FSLM	1	UNIV /18-30/ GA	16750	1695	0252FSLM				7227	1							
42475307880000	3	WFMP	1	HALL G T EST	16225	1652	5309DVNN	TSTM			7970	1		7645	535				
42475307910000	1	WFMP	1	UNIVERSITY /12-	18510	1871	0252FSLM				8051	130		7862	3				
42475308110000	1		2	SITTON EST /44/	17304	1768	1201ELBG				6170	340							
42475308450000	2	ELBG	1	ROBERTSON /138/	17905	1814	9252FSLM				2444	225							
42475309930000	1	ELBG	1	RODGERS	14325	1573	7309DVNN												
42475309930000	2	ELBG	1	RODGERS	15870	1624	6252FSLM	400MCFD											
42475309930000	3	ELBG	1	RODGERS	16250	1653	5203MNTY	175MCFD											
42475309930000	4	ELBG	1	RODGERS	16535	1693	1202SMPS												
42475309930000	5	ELBG	1	RODGERS	18175	1853	0201ELBG	6000MCFD											
42475315880000	4	PSLV	4	PRUET T B ET GA	19090	1919	5252FSLM	1500MCFD			8051	1		8118	6				
42475315880000	5	PSLV	4	PRUET T B ET GA	19110	1925	0252FSLM				8176	1		8176	630				
42475316350000	1	WFMP	1	UNIVERSITY /18-	16530	1694	1309DVNN	TSTM			4849	1	8	4070	4				
42475316350000	2	WFMP	1	UNIVERSITY /18-	17160	1732	2201ELBG				7863	1		7970	4				
42475316350000	3	WFMP	1	UNIVERSITY /18-	17150	1737	5201ELBG	TSTM			2706	1		3928	8				
42475316680000	1	WFMP	1	UNIVERSITY /17-	14529	1609	3319WDFD												
42475316680000	2	WFMP	1	UNIVERSITY /17-	18248	1955	0201ELBG				4925	315		4478	915				
42475316690000	1	ATOK	1	KELTON	19220	1957	5201ELBG				462								
42475316690000	2	ATOK	1	KELTON	19518	1987	0201ELBG												
42475318360000	2		1	1 HTCHNGS-SEALY	15895	1602	5203MNTY				1907	1		1826	1				
42475318360000	3		1	1 HTCHNGS-SEALY	17578	1825	9201ELBG	50MCFD			6241	2		6298	2				
42475318560000	1		1-8	STATE GAS UNIT	17790	1807	2252FSLM				4358								
42475319550000	3		1	SEALY EST /60/	15930	1624	0201ELBG												
42475319550000	4		1	SEALY EST /60/	15920	1624	0201ELBG												
42475319550000	2		1	SEALY EST /60/	15970	1625	0201ELBG												
42489000490000	3		10-A	YTURRIA	15030	1522	0												

API #	DST #	PROD FM	WELL #	LEASE NAME	DST TOP DEPTH	DST BASE DEPTH	FM TESTED	FLUID VOL	NARRATIVE	BHT	ISIP	HOUR	MINS	FSIP	HR	MIN	ACCES GAS	GVTY	SALINITY
424890004900000	1		10-A	YTURRIA	15592	1561	0												
424890004900000	2		10-A	YTURRIA	15600	1561	0												
4249510256000010		ELBG	1	UNIV H	17612	1779	5				4035		45	3773	1				
4249510256000011		ELBG	1	UNIV H	17964	1815	2												
4249510256000012		ELBG	1	UNIV H	18011	1815	2				4520		45	4191	1				
4249510256000013		ELBG	1	UNIV H	20100	2030	0				8873	1		8025	1				20000PPMCL
4249510256000014		ELBG	1	UNIV H	20295	2049	8				9318	1		8096	1				
42495107440001		1ATOK	1	WOLFE UNIT	15374	1539	1403ATOK							12499					
42495107440001		2ATOK	1	WOLFE UNIT	15374	1539	1403ATOK	7900MCFD						11570	6			48.0	
42495107840000		2PSLV	880	OBRIEN GW ETAL	16150	1623	6201ELBG				3958								
42495107840000		3PSLV	880	OBRIEN GW ETAL	16100	1633	8201ELBG				5855	1							
42495107840000		4PSLV	880	OBRIEN GW ETAL	16006	1636	8201ELBG				5265	1		2500	3				
42495107840000		5PSLV	880	OBRIEN GW ETAL	16352	1652	0201ELBG												
42495107840000		6PSLV	880	OBRIEN GW ETAL	16000	1662	9201ELBG				7255		30						
42495107840000		7PSLV	880	OBRIEN GW ETAL	16527	1672	0201ELBG				7389	1		5081	3				
42495107840000		8PSLV	880	OBRIEN GW ETAL	16529	1697	0201ELBG												
42495110330000		2	1	UNIVERSITY 2	15580	1558	0												
42495110350000		1ELBG	1	HUTCHINGS-SEALY	15582	1575	1309DVNN				5375	2		6868	2				
42495110350000		2ELBG	1	HUTCHINGS-SEALY	16300	1657	1203MNTY	25MCFD			3986	2		6915	5	0			
42495110350000		3ELBG	1	HUTCHINGS-SEALY	16551	1690	2203MNTY				3341	140							
42495300320000		1SLRN	1	HALEY UNIT NO 1	17810	1814	0259SLRN	5000MCFD			8350	1		8346	3	5			
42495300460000		2ELBG	2	HUTCHINGS-SEALY	16060	1633	5252FSLM				7734	1		7734	2				
42495300460000		3ELBG	2	HUTCHINGS-SEALY	16390	1662	5203MNTY				6751	1		7024	2				
42495300460000		4ELBG	2	HUTCHINGS-SEALY	16620	1690	2203MNTY				7262	130		7389	4				
42495300460000		5ELBG	2	HUTCHINGS-SEALY	16630	1693	0203MNTY	TSTM											
42495300460000		6ELBG	2	HUTCHINGS-SEALY	18330	1851	4201ELBG												
42495300460000		7ELBG	2	HUTCHINGS-SEALY	18282	1866	1201ELBG	TSTM			9123	1		9039	2				
42495300460000		8ELBG	2	HUTCHINGS-SEALY	18582	1895	3201ELBG	1600MCFD			8523	1							
42495301410000		4MRRW	1	LINEBERRY EVELY	21155	2160	0201ELBG	TSTM											
42495301410000		5MRRW	1	LINEBERRY EVELY	21158	2180	0201ELBG												
42495301410000		6MRRW	1	LINEBERRY EVELY	21158	2180	0201ELBG	TSTM						9354		20			
42495301440000		1MSSP	1	HALEY JOHN JR	16910	1718	4359MSSP				12382	1		1228116		0			
42495301500000		1PSLV	2	MITCHELL GP	18472	1868	7259SLRN				8401	1		8401	1				
42495301510000		3ELBG	1	UNIVERSITY GU 2	16648	1679	0252FSLM												
42495301510000		4ELBG	1	UNIVERSITY GU 2	16579	1679	0252FSLM				7235	1		7178	230				
42495301510000		5ELBG	1	UNIVERSITY GU 2	16582	1709	0203MNTY				7063	2		7523	230				
42495301510000		6ELBG	1	UNIVERSITY GU 2	16585	1709	0203MNTY							7310					
42495301510000		7ELBG	1	UNIVERSITY GU 2	18980	1950	0201ELBG												
42495301510000		8ELBG	1	UNIVERSITY GU 2	19150	1950	0201ELBG												
42495301510000		9ELBG	1	UNIVERSITY GU 2	18948	1950	0201ELBG							7763	4				
42495302310000		3	1	GULF-C ETAL	17600	1765	0			242	2258	1		8222	4				
42495302310000		1	1	GULF-C ETAL	17540	1769	0			244	7899	1		7927	330				
42495302310000		2	1	GULF-C ETAL	17760	1792	1				8113			8113					
42495302310000		4	1	GULF-C ETAL	19810	2007	8			272	6704	1		2877	310				
42495302310000		5	1	GULF-C ETAL	20120	2042	8			262									
42495302310000		6	1	GULF-C ETAL	19820	2042	8	75MCFD	1/2 I	266	7810	1		0	2				
42495302310000		7	1	GULF-C ETAL	20460	2092	5												
42495302310000		8	1	GULF-C ETAL	20499	2092	5												

Appendix 4: Deep gas-prone basins of the Rocky Mountain region, by W.J. Perry, Jr.

INTRODUCTION

The goals of Task 4 include identifying the structural settings and trapping mechanisms of deep gas accumulations in different sedimentary basins in order to relate these factors to undiscovered resources. This effort involves studying selected deep basins in the Rocky Mountain region in detail and using them as models from which to compare the structural characteristics of other deep basins. Also, the timing and structural style of many Rocky Mountain basins will be identified in order to determine the evolution of deformation and subsequent generation, migration, and entrapment of oil and gas. Some results of structural studies are presented in the Task 3 (Dyman and others, Appendix 3) discussion section.

Perry, 1989 summarized the structural settings of deep natural gas occurrences in the conterminous U.S. and showed that such occurrences are associated primarily with (1) passive continental margin basins and (2) basins associated with and inland from active continental margins. This latter group of basins (Type 2 basins of Perry, 1989) were subdivided into forearc basins, seaward of the magmatic arc above a continentward-dipping subduction zone, foreland basins, beneath and cratonward of the frontal zone of fold and thrust belts, and extensional or transtensional basins, associated chiefly with transform margins. In this report, deep gas-prone Late Cretaceous and early Tertiary Laramide basins of the Rocky Mountain foreland will be explored.

Several sedimentary basins in the central Rocky Mountains have substantial volumes of sedimentary rock at depths greater than 15,000 ft; the largest being the Green River and Uinta basins, respectively north and south of the Uinta uplift (Fig. 4-1). These initially developed during Cretaceous time, as foredeeps in front of the eastward prograding Wyoming and Utah salients of the Cordilleran thrust belt. A southeastward progression of major uplift and consequent basin development in the Rocky Mountain foreland began in extreme southwestern Montana west of the Neogene Yellowstone Volcanic area (Fig. 4-1) during Cenomanian-Turonian time (Haley and others, 1991; Perry and others, 1990). Investigation of the sequence of Laramide deformation and relative timing of Rocky Mountain foreland basin development (Perry and others, 1990, 1991 and in press) has begun to revolutionize our understanding of the Late Cretaceous and early Tertiary history of the Rocky Mountain region (Flores and others, 1991; Keighin and others, 1991; Nichols and others, 1991; Roberts and others, 1991).

The Late Cretaceous eastward progradation of the Laramide deformation front reached the Colorado Front Range by 69 Ma (Kluth and Nelson, 1988; Wallace, 1988). No evidence of Campanian or older Cretaceous Laramide-style deformation is present in the Rocky Mountain foreland east or southeast of the Blacktail-Snowcrest and Wind River uplifts, based on available palynostratigraphic dating of preorogenic and synorogenic sediments, with the exception of gravels of unknown origin in the Frontier Formation in the northwestern Bighorn basin. Such dating reveals that growth of the Front Range uplift culminated in exposure of the crystalline basement by early Paleocene time (Kluth and Nelson, 1988; D.J. Nichols, oral communication, 1991). Subsequent Laramide deformation spread northeastward from the Granite Mountains-Shirley Mountains uplift (Fig. 4-1) in south-central Wyoming. The Laramide deformation front reached the Black Hills by late Paleocene time, creating first the Wind River and then the Powder River basins, partitioning these basins from an earlier continuous foreland basin with minor welts

(Merewether and Cobban, 1986). These broad structural welts of low relief, such as the San Rafael swell in eastern Utah, had begun to grow in the Rocky Mountain foreland by mid-Cretaceous time (about 90 Ma).

A major east-west crustal discontinuity along the Wyoming-Colorado border separates Archean basement rocks on the north from Proterozoic basement rocks to the south. South of this discontinuity, Laramide deformation appears to have proceeded from east to west, culminating along and defining the eastern boundary of the Colorado Plateau in late Eocene, chiefly Green River time (Fig. 4-2).

Economic implications of this new model of deformation of the Rocky Mountain foreland include progressive opening and subsequent blockage of migration paths for HC's generated from Paleozoic source rocks in southeastern Idaho, southwestern Montana, Wyoming, Colorado, and eastern Utah. Deep natural gas, generated during the Tertiary, has likely migrated from the deeper parts of these foreland basins into structural traps formed during Laramide deformation.

DISCUSSION

Within the Rocky Mountain foreland, the Laramide Green River and Uinta basins are followed in order of size of area deeper than 4,572 m (15,000 ft) by the Wind River basin, the Great Divide and Washakie basins, and perhaps the deepest of all, the Hanna basin, all in Wyoming (Fig. 4-1). These latter four basins began to subside in Late Cretaceous time as part of the Hanna trough (Thomas, 1949; LeFebre, 1988). This trough extended from the front of the Cordilleran thrust belt, in northeastern Utah and southeastern Idaho, eastward across southern Wyoming. Southward thinning of the upper Maastrichtian siliciclastic sequence along the southern margin of this trough along the eastern flank of the late Laramide Washakie basin is shown in great detail by Hettinger and others (1991). The region of the Great Divide, Hanna, and Washakie basins were partitioned from the Green River basin to the west in latest Cretaceous time by growth of the Rock Springs uplift (Kirschbaum and Nelson, 1988; Hettinger and Kirschbaum, 1991) following Late Cretaceous development of the Wind River-ancestral Teton-Granite Mountains uplift (Perry and others, 1990). The Rawlins uplift finally isolated the Hanna basin from the rest most likely in latest Paleocene to Eocene time, subsequent to deposition of early Paleocene coals (of P2 age according to R.D. Hettinger, oral commun., 1992).

HANNA BASIN

The Hanna basin (Fig. 4-3) contains more than 9,150 m (30,000 ft) of Phanerozoic sedimentary rocks of which more than 4,572 m (15,000 ft) are Upper Cretaceous and predominantly marine origin. Less than 760 m (2,500 ft) of pre-Cretaceous Phanerozoic sedimentary rocks are present (from sections by Blackstone, 1983). Latest Cretaceous (?) and Paleocene nonmarine rocks (the Ferris and Hanna Formations) are more than 4,270 m (14,000 ft) thick. The nonmarine formations penetrated are gas-prone, and these more shallowly buried rocks are being exploited for coal-bed methane.

The major compressional structural framework along the southern margin of the basin was defined by Beckwith (1941). Gill and others (1970) discuss the stratigraphy and nomenclature of Upper Cretaceous and Lower Tertiary rocks in the area, and they indicate that a major unconformity is present between the Upper Paleocene and Eocene(?) Hanna Formation and Cretaceous rocks in the northern Hanna basin, although a deep drill hole to the south of the surface

expression of this major unconformity shows that at least 1,980 m (6,500 ft) of intervening rocks are present within the basin (Fig. 4-3). The basin contains numerous Late Cretaceous(?) to Paleocene coals (Glass, 1975, 1984) for which precise palynologic dates have not been previously reported. Eight carefully selected samples from these formations, provided by Dr. G.B. Glass, State Geologist of Wyoming, have been processed for pollen by D.J. Nichols, U.S Geological Survey. The results indicate that virtually the entire coal-bearing section of the Hanna basin, a more than 2,480 m (8,150 ft) thick sequence primarily composed of nonmarine siliciclastics, is Paleocene in age (Table 4-1).

Twenty-five vitrinite samples have been analysed by Ben Law, U.S. Geological Survey from the #1 Hanna Unit well (Fig. 4-3). This dry hole was drilled to a depth of 3,809 m (12,496 ft), but did not reach the base of the Ferris Formation. To a depth of nearly 3,048 m (10,000 ft), vitrinite reflectance values were less than 0.7 R_O. Below 3,048 m (10,000 ft) the vitrinite values rose rapidly to a value of 1.23 R_O near the bottom of the hole 3,805 m (12,485 ft). Because of the high reflectance values near the base of the #1 Hanna Unit drill hole, the more deeply buried marine Cretaceous rocks should yield thermogenic natural gas. However, only one small gas field has been developed -- on the northwest flank of the basin.

Structural and economic implications

The Hanna basin is surrounded by Laramide thrust faults which are imprecisely dated. The coal-bearing nonmarine sequence represented by the Hanna and Ferris Formations may represent the time of maximum thrust-related subsidence. This more than 8,150 ft thick sequence (Glass, 1975, 1976) now appears to be entirely Paleocene (palynologic results summarized in Table 4-1). Assuming an original mean porosity of 45% and a present mean porosity of 25% (both ball-park estimates), results in a simple decompaction coefficient of 1.36. Using this coefficient to expand the presently known conservative thickness of at least 2,484 m (8,150 ft), more than 3,353 m (11,000 ft) of subsidence may have occurred during the Paleocene in the north-central part of the Hanna basin over a period of about 8.6 m.y., or roughly 1.3 ft/10^3 years decompacted, or 0.95 ft/10^3 years uncorrected for compaction. This is a minimum estimate. These data compare to Cenozoic subsidence rates in southern California of 2.3 ft/10^3 year in the Eocene-Miocene and 3.3 ft/10^3 post-Miocene in small pull-apart basins (Yeats, 1978), in which the extreme subsidence rates are driven by major strike-slip faulting. Representative tectonic subsidence histories are given for various types of basins by Angevine and others (1990, Fig. 6.1). They show that maximum subsidence rates for foreland basins range from 0.085 to 0.57 ft/10^3 years (0.02 to 0.17 m/10^3 years), whereas strike-slip basins range from 0.5 to 2.18 ft/10^3 years (0.15 to 0.66 m/10^3 years). Clearly anomalously high subsidence rates occurred in the Hanna basin, well outside the norm for foreland basins, but well within the range of rates typical of strike-slip related basins. The northern margin of the Hanna basin is interpreted to represent the locus of a significant zone of latest Cretaceous to Paleocene strike slip/accommodation faulting as the northern boundary of the zone of Colorado Front Range-Laramie Range Laramide shortening.

The sequence of structural events in the Hanna basin region are: **first,** development of the Hanna trough sequence of thick marine Upper Cretaceous rocks which trends east-west across southern Wyoming; **second,** partial isolation of the Hanna basin as a subarea of the Greater Green River basin by early Paleocene growth of the Granite Mountains-Shirley Mountains

transpressive zone to the north; **third,** southward tilting, probably in mid-Paleocene time concurrent with growth of the Sweetwater uplift and initial development of the Shirley thrust along the northern margin of the basin. The last phase of structural growth, uplift of the Medicine Bow Mountains and Rawlins uplift concurrent with development of the Arlington thrust appears to have been initiated in late Paleocene time. The geometry (Fig. 4-4) of the northern margin of the basin, suggests major gas possibilities in the undrilled northern part of the basin beneath the Shirley thrust provided that gas generation continued during and after thrusting. Published seismic data (Kaplan and Skeen, 1985) do not adequately define the structure of the northern margin of the Hanna basin. It would appear that much deep gas remains to be found in deep Rocky Mountain foreland basins if the scenario shown here is found to be correct and this type of tilting prior to thrusting can be demonstrated in other areas. Because of the high vitrinite reflectance values at depths of greater than 3,048 m (10,000 ft), the deeper Cretaceous units should also yield natural gas. However, only one small gas field has been developed -- on the northwest flank of the basin. Very little deep drilling has been conducted in the Hanna basin, unlike other basins to the west and north, a substantial amounts of deep gas may yet be found in this basin.

WIND RIVER BASIN

The Wind River basin, northwest of the Hanna basin, is separated from the latter by the Granite Mountains-Sweetwater uplift which may have begun to grow in mid-Cretaceous time (Merewether and Cobban, 1986) and was a positive element in Campanian time (Reynolds, 1976). Late Cretaceous rocks thicken southeastward in the Wind River basin to greater than 5,486 m (18,000 ft). The Bull Frog field developed in Cretaceous Frontier sandstones in this part of the basin contains the deepest producing Cretaceous gas reservoir in the Rocky Mountain region (more than 5,700 m--18,700 ft deep). Other significant nearby fields include West Poison Spider, and Tepee Flats, the latter beneath the lip of the Casper arch, from which it is separated by a major blind basement-involved thrust system which dips northeastward beneath and is responsible for the arch.

The deep Madden gas field, in the northern part of the Wind River basin, (with Madison and Big Horn gas reservoirs as deep as 7,162 to 7,284 m--23,500 to 23,900 ft) lies in front of (south of) the Owl Creek thrust which bounds the northern margin of the basin and is likely continuous with that under the lip of the Casper arch. The Madden anticline, the locus of this growing giant gas field, is cored by a thrust wedge and the north-bounding Owl Creek thrust has more than 10,668 m (35,000 ft) of structural relief (Dunleavy and Gilbertson, 1986), comparable to the Wichita frontal fault system along the southern margin of the Anadarko basin (Perry, 1989). The Wind River basin is thus bounded on two sides by thrust faults whereas the Hanna basin is nearly surrounded by thrust faults (Fig. 4-3).

The Wind River basin was partitioned from the remainder of the Rocky Mountain foreland in late Paleocene time by growth of the Casper arch which led to internal drainage as represented by Lake Walton (Keefer, 1965) and isolation from long-distance migration of HC's from previously down-dip areas to the west and southwest.

The Wind River basin occupies a critical position with respect to the sequential development of Laramide structure in Wyoming. Conglomerate in the Late Cretaceous Lance Formation in the northwestern part of the Wind River basin, nearest the Wind River uplift, contains granule-size fragments and

scattered pebbles of chert, silicious shale, and porcellanite (Keefer, 1965). Here the Lance is about 351 m (1,150 ft) thick (Keefer, 1965, p. A17), and only the lower part is conglomeratic. Keefer found no definite evidence for uplift of the Wind River Range during Cretaceous time, but his control was inadequate along the southwestern margin of the basin (contours dashed, no control points within 50 km (30 mi) of the northeast flank of the Wind River Mountains, see his Fig. 9). The above described conglomerate in the lower part of the Lance was probably eroded from Frontier and older Mesozoic rocks exposed on the growing Wind River uplift.

Murphy and Love (1958) inferred that a broad, domal uplift occurred in latest Cretaceous time on the southeastern flank of the Wind River basin in the area of the present Granite Mountains. Keefer (1965) reached similar conclusions. In a summary of the Laramide history of the Granite Mountains area, Love (1971) indicated that uplift of this area did not begin until latest Cretaceous time and culminated in the earliest Eocene time. He suggested that the early phase of this uplift may have been coextensive with that of the south-central part of the Wind River Range.

Keefer (1965) concluded that the Cretaceous-Tertiary boundary in the Wind River basin is generally conformable, but that extensive downwarping occurred at this time along the present-day northern margin of the basin. Along the northeastern margin of the Wind River basin, Keefer (1965) observed that the oldest conglomerate zones are in the lower Eocene Indian Meadows Formation. The oldest arkosic conglomerate in this part of the basin is at the base of the Lost Cabin Member of the overlying Eocene Wind River Formation. The presence of extensive lacustrine sediments, which first appeared in the Wind River Basin in late Paleocene time (Nichols and Ott, 1978; Phillips, 1983), is indicative of internal drainage that likely reflects initial growth of the Casper arch and Owl Creek uplift (Fig. 4-1) that closed the outlets of the basin.

Keefer (1965) estimated more than 2,682 m (8,800 ft) of middle to late Paleocene uplift in the Owl Creek Mountains and nearly 3,200 m (10,500 ft) of subsidence in the adjacent Wind River basin; these amounts indicate a cumulative vertical separation (uplift + subsidence) rate of slightly more than 1.2 m/10^3 years (4 ft/10^3 years). Keefer estimated an additional 2,591 m (8,500 ft) of uplift and an additional 1,707 m (5,600 ft) of subsidence in the early Eocene, a cumulative vertical separation rate of about nearly 1.2 m/10^3 years (4 ft/10^3 years). He showed that Casper arch thrust faults cut the lower Eocene Indian Meadows Formation and that the rocks deformed by this thrusting are erosionally truncated by the overlying lower Eocene Wind River Formation. These relations date the cessation of major Laramide deformation in the area as early Eocene. These rates are consistent with relatively late Laramide strike-slip dominated transpressional deformation along the northern margin of the Wind River basin, similar to the earlier Laramide transpressional boundary along the northern margin of the Hanna basin to the south. Undiscovered structurally trapped deep gas may still be found north and northwest of the Madden anticline in the northern part of the Wind River basin.

REFERENCES CITED

Angevine, C.L., Heller, P.L., and Paola, C., 1990, Quantitative basin modelling: American Association of Petroleum Geologists, Continuing Education Course Note Series #32, 133 p.

Bayley, R.W., and Muehlberger, 1968, Basement rock map of the United States: U.S. Geological Survey, scale 1:2,500,000.

Beckwith, R.H., 1941, Structure of the Elk Mountain district, Carbon County, Wyoming: Geological Society of America Bulletin, v. 52, 1445-1486.

Blackstone, D.L., Jr., 1983, Laramide Compressional tectonics, southeastern Wyoming: Contributions to Geology, University of Wyoming, v. 22, p. 1-38.

Blackstone, D.L., Jr., 1990, Precambrian basement map of Wyoming: outcrop and structural configuration, revised, 1990: Geological Survey of Wyoming Map Series 27, scale 1:1,000,000.

Dobbin, C.E., Bowen, C.F., and Hoots, H.W., 1929, Geology and coal and oil resources of the Hanna and Carbon basins, Carbon County, Wyoming: U.S. Geological Survey Bulletin 804, 88 p., 27 plates.

Dunleavy, J. M., and R. L. Gilbertson, 1986, Madden anticline: growing giant, *in* Noll, J. H., and K. M. Doyle, eds., Rocky Mountain oil and gas fields: Wyoming Geological Association 1986 Symposium, p. 107-157.

Flores, R.M., Roberts, S.B., Perry, W.J., Jr., and Nichols, D.J., Evolution of Paleocene depositional systems and coal basins in a tectonic continuum, Rocky Mountain region: Geological Society of America Abstracts with Programs, v. 23, no. 4, p. 22.

Gill, J.R., Merewether, E.A., and Cobban, W.A., 1970, Stratigraphy and nomenclature of some Upper Cretaceous and Lower Tertiary rocks in south central Wyoming: U.S. Geological Survey Professional Paper 667, 53 p.

Glass, G.B., 1975, Analyses and measured sections of 54 Wyoming coal samples (collected in 1974): Geological Survey of Wyoming Report of Investigations no. 11, 219 p.

Glass, G.B., and Roberts, J.T., 1984, Analyses and measured sections of 25 coal samples from the Hanna Coal Field of south central Wyoming (collected between 1975 and 1979): The Geological Survey of Wyoming, Report of Investigations n. 27, 104 p.

Haley, J.C., Dyman, T.S., and Perry, W.J., Jr., 1991, The Frontier Formation -- A record of mid-Cretaceous foreland uplift in southwestern Montana [abs.]: Geological Society of America Abstracts with Programs, v. 23, no. 4, p. 29.

Hansen, D.E., 1986, Laramide tectonics and deposition of the Ferris and Hanna Formations, south-central Wyoming, *in* Peterson, J.A., Paleotectonics and sedimentation: American Association of Petroleum Geologists Memoir 41, p. 481-495.

Hettinger, R.D., Honey, J.G., and Nichols, D.J., 1991, Chart showing correlations of Upper Cretaceous Fox Hills Sandstone and Lance Formation, and lower Tertiary Fort Union, Wasatch, and Green River Formations, from the eastern flank of the Washakie Basin to the southeastern part of the Great Divide Basin, Wyoming: U.S. Geological Survey Miscellaneous Investigations Series I-2151, 1 sheet with chart, map, and text.

Hettinger, R.D., and Kirschbaum, M.A., 1991, Chart showing correlations of some Upper Cretaceous and lower Tertiary rocks, from the east flank of the Washakie Basin to the east flank of the Rock Springs uplift: U.S. Geological Survey Miscellaneous Investigations Series I-2152, 1 sheet with chart, map, and text.

Kaplan, S.S., and Skeen, R.C., 1985, North-south regional seismic profile of the Hanna basin, Wyoming, *in* Gries, R.R., and Dyer, R.C., eds., Seismic exploration of the Rocky Mountain region: Rocky Mountain Association of Geologists and Denver Geophysical Society, p. 219-224.

Keefer, W.R., 1965, Stratigraphy and geologic history of the uppermost Cretaceous, Paleocene, and lower Eocene rocks in the Wind River basin, Wyoming: U.S. Geological Survey Professional Paper 495-A, 77 p.

Keighin, C.W., Flores, R.M., and Perry, W.J., Jr., 1991, Provenance tectonism and petrofacies in Paleocene sediments, northern Rocky Mountains: Geological Society of America Abstracts with Programs, v. 23, no. 5, p. A68.

Kirschbaum, M.A., and Nelson, S.N., 1988, Geologic history and palynologic dating of Paleocene deposits, western Rock Springs uplift, Sweetwater County, Wyoming: Contributions to Geology, University of Wyoming, v. 26, no. 1, p. 21-28.

Kluth, C.F., and Nelson, S.N., 1988, Age of the Dawson Arkose, southwestern Air Force Academy, Colorado, and implications for the uplift history of the Front Range: The Mountain Geologist, v. 25, p. 29-35.

LeFebre, G.B., 1988, Tectonic evolution of Hanna Basin, Wyoming: Laramide block rotation in the Rocky Mountain foreland: PhD dissertation, University of Wyoming, 240 p.

Love, J.D., 1971, Relation of Cenozoic geologic events in the Granite Mountains area, central Wyoming, to economic deposits, *in* Renfro, A. R., ed., Symposium on Wyoming tectonics and their economic significance: Casper, Wyoming Geological Association 23rd Annual Field Conference Guidebook, p. 74-80.

Merewether, E.A., and Cobban, W.A., 1986, Biostratigraphic units and tectonism in the mid-Cretaceous foreland of Wyoming, Colorado, and adjoining areas, *in* Peterson, J.A., ed., Paleotectonics and sedimentation: American Association of Petroleum Geologists Memoir 41, p. 443-468.

Murphy, J.F., and Love, J.D., 1958, Tectonic development of the Wind River Basin, central Wyoming [abs.] *in* American Association of Petroleum Geologists Rocky Mountain Section, Geologists rec., 1958, p. 126-127.

Nichols, D.J., Perry, W.J., Jr., and Brown, J.L., 1991, Palynostratigraphy in reconstruction of tectonic history and basin evolution, western North America [abs]: International Symposium on Origin, Sedimentation, and Tectonics of Late Mesozoic to Early Cenozoic Sedimentary Basins at the Eastern Margin of the Asian Continent and Workshop of IGCP 245 -- Nonmarine Cretaceous correlations, Fukuoka, Japan, Program and Abstracts, p. 56.

Perry, W.J., Jr., 1989, Structural settings of deep natural gas accumulations in the conterminous United States, Appendix B., *in* Rice, D.D., Distribution of natural gas and reservoir properties in the continental crust of the United States: Final Report for GRI Contract no. 5087-260-1607, Department of Commerce NTIS Report #89/0188, p. 62-72.

Perry, W.J., Jr., Dyman, T.S., and Nichols, D.J., 1990, Sequential Laramide deformation of the Rocky Mountain foreland, *in* Thorman, C.H., ed., Workshop on application of structural geology to mineral and energy resources of the Central Region: U.S. Geological Survey Open-File Report 90-0508, p. 11-12.

Perry, W.J., Jr., Nichols, D.J., Dyman, T.S., and Haley, C.J., in press, Sequential Larmide deformation in Montana and Wyoming, *in* Thorman, C.H., ed., Application of structural geology to mineral and energy resources of the central and western United States: U.S. Geological Survey Bulletin 2012, 23 manuscript pages, 6 figs.

Perry, W.J., Jr., Weaver, J.N., Flores, R.M., Roberts, S.B., and Nichols, D.J., 1991, Sequential Laramide deformation in Montana and Wyoming: Geological Society of America Abstracts with Programs, v. 23, no. 4, p. 56.

Phillips, S.T., 1983, Tectonic influence on sedimentation, Waltman Member, Fort Union Formation, Wind River Basin, Wyoming, *in* Lowell, J.D., and Gries, R., eds., Rocky Mountain foreland basins and uplifts: Rocky Mountain Association of Geologists, Denver, Colorado, p. 149-160.

Reynolds, M.W., 1976, Influence of recurrent Laramide structural growth on sedimentation and petroleum accumulation, Lost Soldier area, Wyoming: American Association of Petroleum Geologists Bulletin, v. 60, p. 12-33.

Roberts, S.B., Flores, R.M., Perry, W.J., Jr., and Nichols, D.J., 1991, Preliminary paleogeographic interpretations of Paleocene coal basins, Rocky Mountain region: Geological Society of America Abstracts with Programs, v. 23, no. 4, p. 87.

Thomas, H.D., 1949, The geological history and geological structure of Wyoming: Wyoming Geological Survey Bulletin 42, 28 p.

Wallace, A.R., 1988, Comment on "Age of the Dawson Arkose, southwestern Air Force Academy, Colorado, and implications for the uplift history of the Front Range": The Mountain Geologist, v. 25, p. 37-38.

Yeats, R.S., 1978, Neogene acceleration of subsidence rates in southern California: Geology, v. 6, p. 456-460.

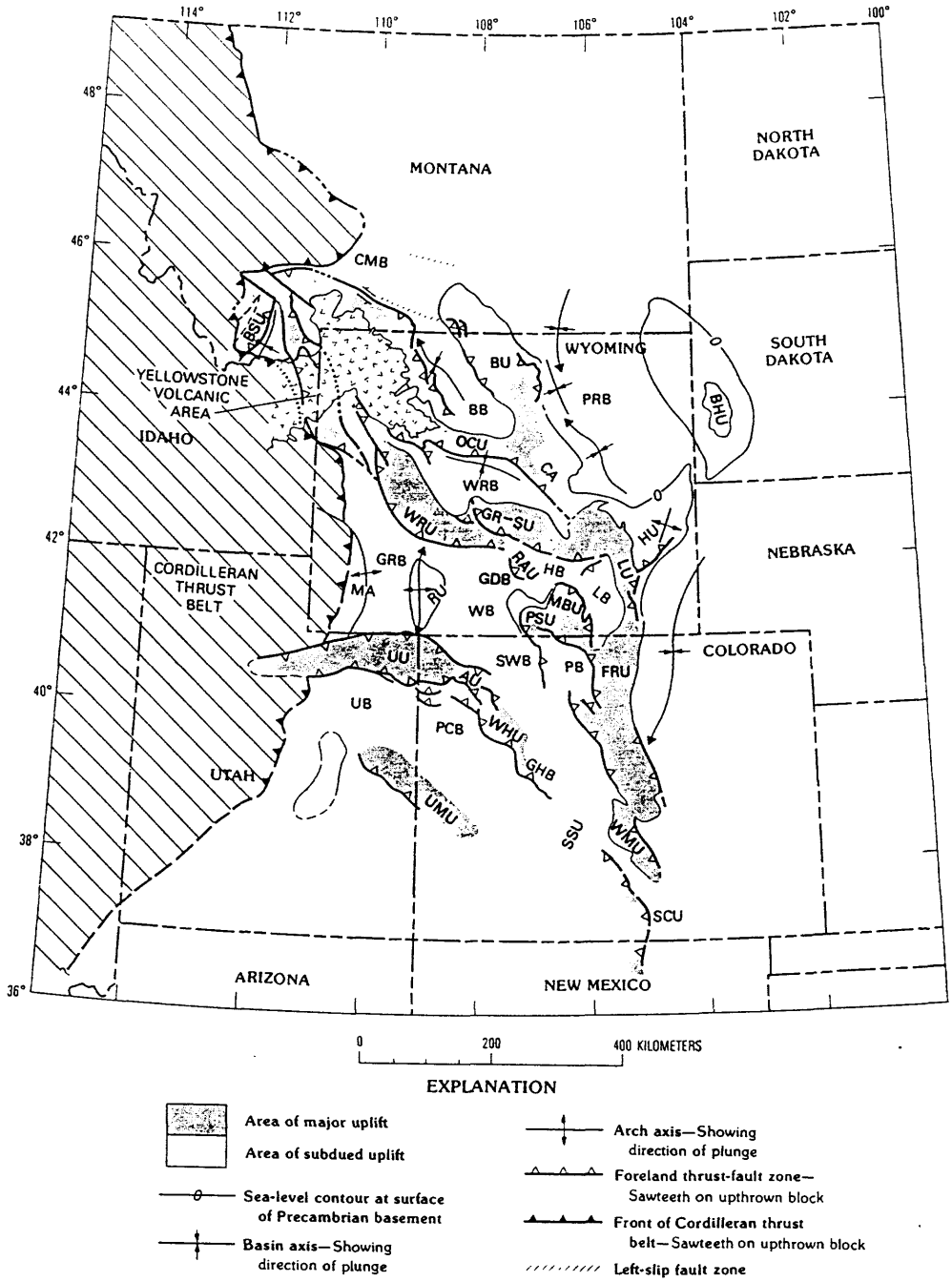

Figure 4-1. Map of Rocky Mountain foreland province showing principal Laramide basins and uplifts. Major uplifts are shown in closely spaced dot pattern; broad positive areas in more widely spaced dot pattern. Sawteeth on thrust faults point into upper plates. AU, Axial uplift; BB, Bighorn Basin; BHU, Black Hills uplift; BSU, Blacktail-Snowcrest uplift; BU, Bighorn uplift; CA, Casper arch; CMB, Crazy Mountains basin; FRU, Front Range uplift; GDB, Great Divide basin; GHB, Grand Hogback uplift; GRB, Green River Basin; GR-SU, Granite Mountains-Shirley Mountains (Sweetwater) uplift; HB, Hanna Basin; HU, Hartville uplift; LB, Laramie Basin; LU, Laramie uplift; MA, Moxa arch; MBU, Medicine Bow uplift; OCU, Owl Creek uplift; PB, North and Middle Parks basin; PCB, Piceance Creek basin; PRB, Powder River basin; PSU, Park-Sierra Madre uplift; RAU, Rawlins uplift; RU, Rock Springs uplift; SCU, Sangre de Cristo uplift; SSU, Sawatch-San Luis uplift; SWB, Sand Wash basin; UB, Uinta basin; UMU, Uncompagre uplift; UU, Uinta Mountains uplift; WB, Washakie basin; WHU, White River uplift; WMU, Wet Mountains uplift; WRB, Wind River Basin, and WRU, Wind River uplift. Modified from Bayley and Muehlberger (1968).

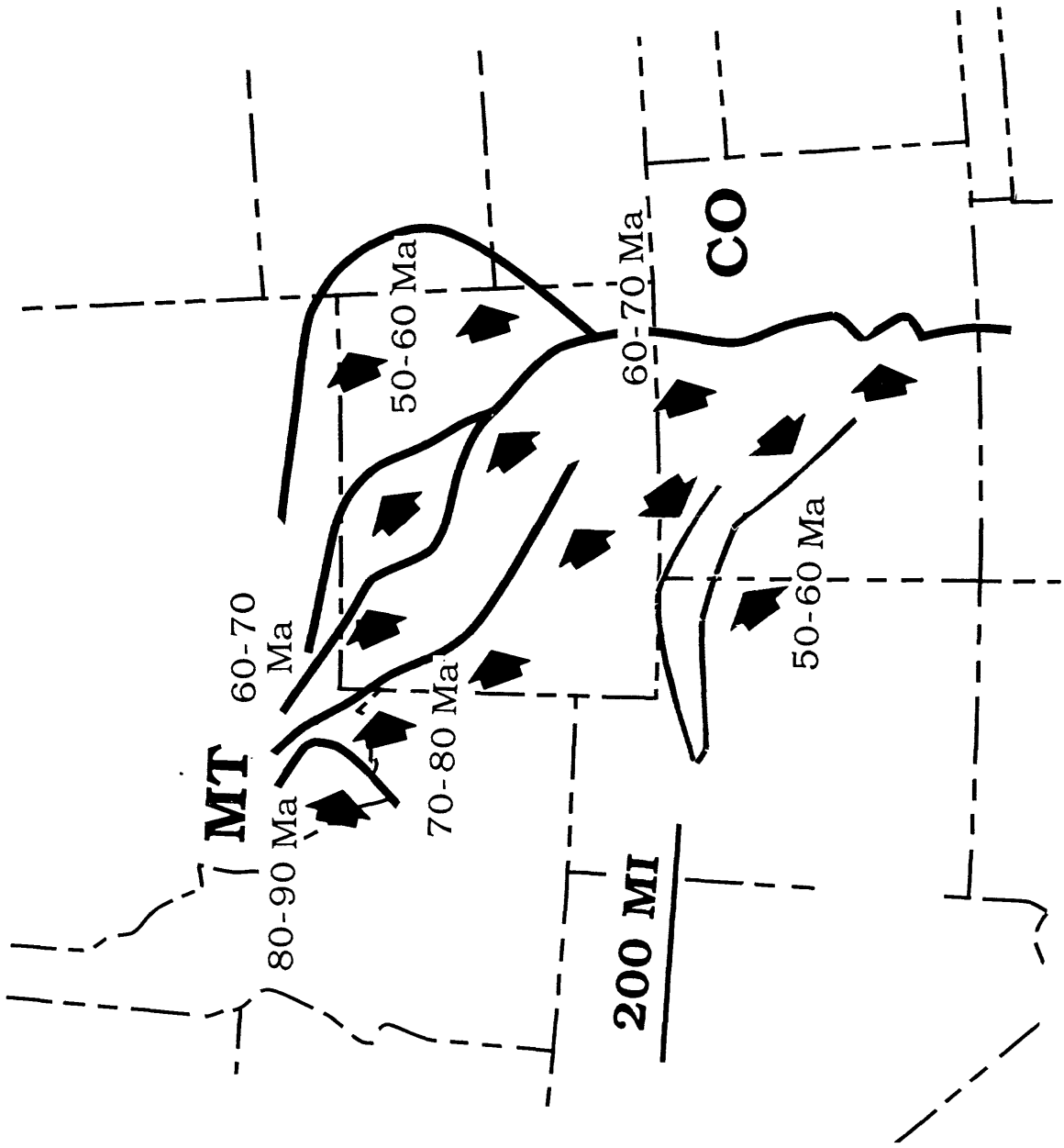

Figure 4-2. Sequence of inception of Laramide deformation in millions of years before present (Ma). Arrows indicate migration of Laramide deformation front.

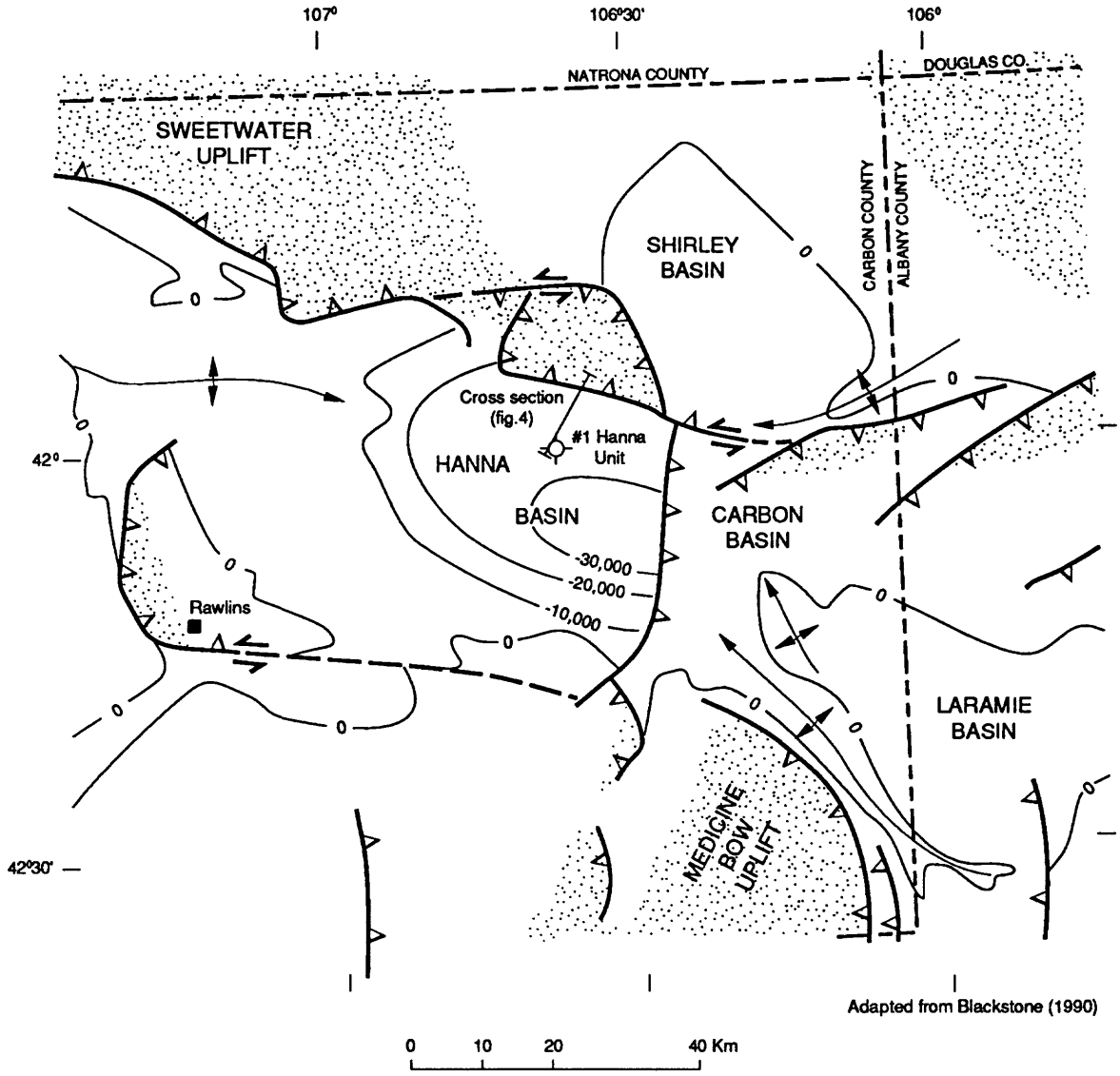

Figure 4-3. Tectonic map of the Hanna basin region (from Blackstone, 1990), showing the location of the No. 1 Hanna Unit well and cross section (Fig. 3). Stippled areas are structurally elevated, with Precambrian basement significantly above sea level. Contours on elevation of top of Precambrian basement are from Blackstone (1990).

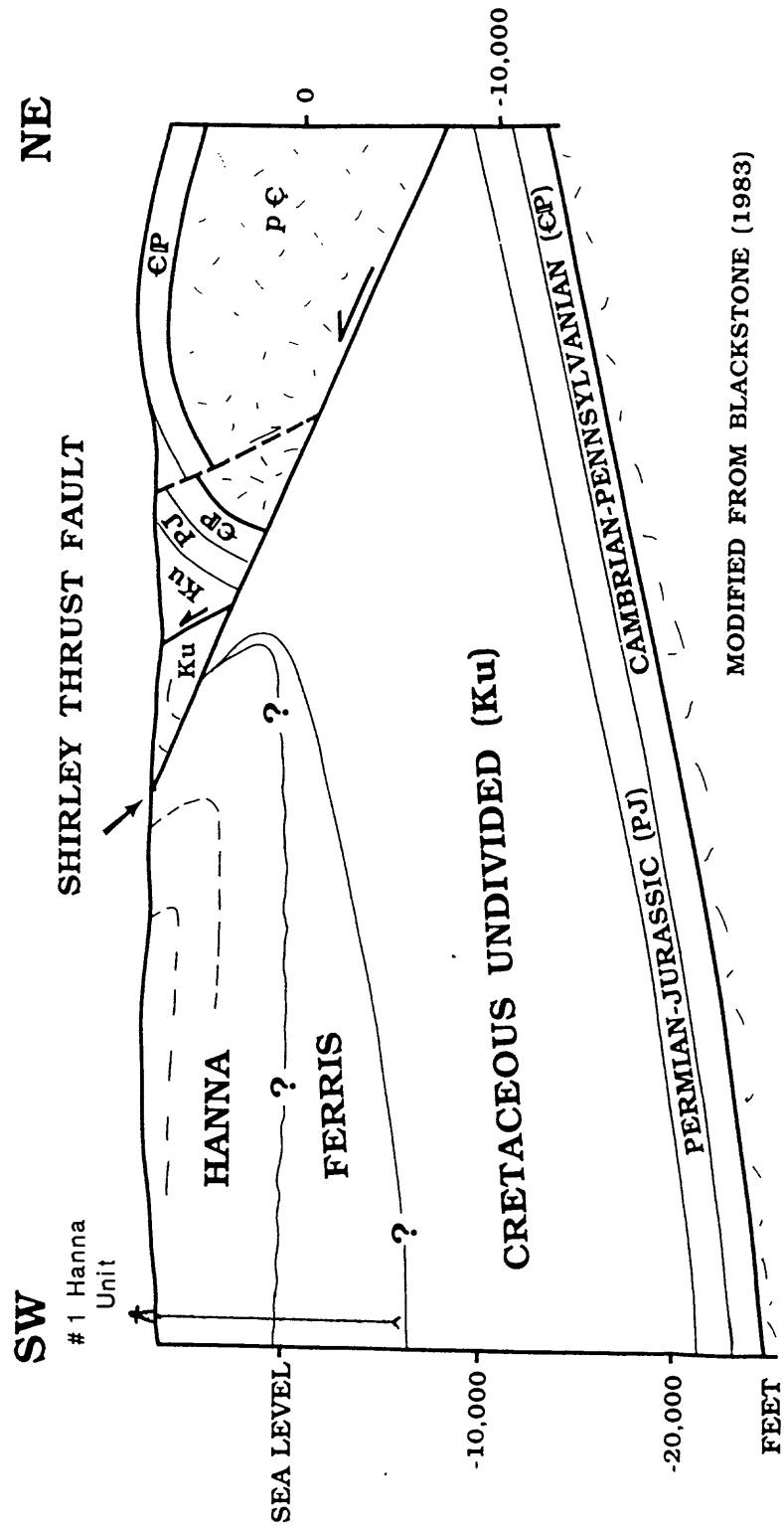

Figure 4-4. Cross-sectional model through the northern part of the Hanna basin.

Table 4-1. Summary of results of palynologic studies of coal samples from the Ferris and Hanna Formations by D.J. Nichols; samples provided by Dr. Gary Glass, State Geologist, Wyoming Geological Survey. Bed designations are given, sampled intervals described, and relative positions in the sequence shown in Glass (1975) and Glass and Roberts (1984).

Hanna Formation	Bed 80	Sample 74-24	late Paleocene, probably zone P5
Hanna Formation	Bed 76	Sample 75-14	late Paleocene, probably zone P5
The above are not latest Paleocene (D.J. Nichols, written communication)			
Hanna Fm., Brooks Rider		Sample 75-14	middle Paleocene, zone P3
Ferris Formation	Bed 65	Sample 75-16	early Paleocene, probably zone P2
Ferris Formation	Bed 60	Sample 77-6	early Paleocene, probably zone P2
Ferris Formation	Bed 25	Sample 77-14	early Paleocene, possibly zone P1
Ferris Formation	Bed 24	Sample 74-24	early Paleocene, possibly zone P1

Appendix 5--Source-rock potential of Precambrian rocks in selected basins of the U.S., by J.G. Palacas

INTRODUCTION

The goal of this task is to determine the source-rock potential of Precambrian (Proterozoic) unmetamorphosed sedimentary rocks in selected basins of the U.S. The Proterozoic rocks are widely distributed in the U.S. and commonly occur in the deeper parts of basins. Their petroleum source-rock potential, however, is poorly known. These rocks may have generated and expelled petroleum which was subsequently trapped in Precambrian and/or younger overlying Phanerozoic rocks.

The impetus for ascribing a viable petroleum potential to Precambrian rocks in the U.S. is provided by the actual production of commercial oil and gas derived from Precambrian rocks in other parts of the world. For example, in Oman the upper Proterozoic Huqf Group carbonate-evaporite rocks are believed to be the source of about 12 billion barrels of oil and undetermined amounts of gas accumulated in Precambrian and overlying Paleozoic and Mesozoic reservoirs (Grantham and others, 1987; Brett Mattes, reported in Fritz, 1989; and Edgell, 1991). In the Lena-Tunguska petroleum province of Eastern Siberia, major and giant fields produce gas, gas condensate and oil from Proterozoic (Riphean and Vendian age) and Lower Cambrian strata (Meyerhoff, 1980; Clarke, 1985). Meyerhoff (1980) reported that one of the largest fields discovered, the Verkhnevilyuy field, had proved plus probable reserves of 10.5 Tcf of gas and about 260 million bbl of condensate. Both Meyerhoff (1980) and Clarke (1985) indicated that the predominant source beds are of Proterozoic age. According to Clarke (1985), the undiscovered petroleum resources of the Lena-Tunguska basin may be as high as 189 Tcf of gas and about 11 billion bbls of oil. Interestingly, in an earlier assessment, Meyerhoff (1980, p. 225) estimated an ultimate recovery of "200 Tcf of gas together with condensate".

In the Sichuan basin, southwest China, giant accumulations of natural gas have been shown to be derived from Late Proterozoic (Sinian) carbonate rocks (Korsch and others, 1991). One of the gas fields in the basin, the Weiyuan Gas Field, is estimated to have a total reserve of as much as 1.41 Tcf of gas (Korsch and others, 1991).

This report focuses on the source rock evaluation of Proterozoic rocks in two regions of the U.S., the Midcontinent Rift System (MRS) and the Grand Canyon area, northern Arizona and vicinity. Other promising areas exhibiting Precambrian petroleum potential are in the Uinta Mountains and vicinity, wherein the relatively organic-rich Upper Proterozoic Red Pine Shale and equivalent rocks are widely distributed both in the surface and subsurface (M. W. Reynolds, personal communication, 1990; R. Raynolds, Amoco Production Company, unpublished data), and in the Rocky Mountain Overthrust Belt, northwestern Montana, where gas shows were encountered in 1.43 billion-year-old rocks to depths of 5,418 m (17,774 ft) in the Atlantic-Richfield No. 1 Gibbs well (Shirley, 1985).

MIDCONTINENT RIFT SYSTEM

Rocks of the Midcontinent Rift System, delineated by strong gravimetric and magnetic anomalies, are exposed in the Lake Superior district of Michigan, northern Wisconsin, and Minnesota and extend in the subsurface through Minnesota, Iowa, Nebraska and into northeastern Kansas (Fig. 5-1). Based on gravity measurements, a related arm can also be traced in the subsurface from the Lake Superior district southeastward into the lower peninsula of Michigan

(Fig. 5-1) (Dickas, 1986). This easterly extension of the rift, however, is not discussed in this report. The 1,567-m-long (940-mile-long) MRS is a failed rift characterized by a series of asymmetric basins filled with clastic rocks, in places up to 9,754 m (32,000 ft) in thickness (Anderson, 1989). The rocks belong to the Middle Proterozoic, Keweenawan Supergroup, comprised of the Bayfield Group above and the Oronto Group below. Since the MRS is conveniently divided into four geographically identifiable segments -- Lake Superior, Minnesota, Iowa, and Kansas -- each segment will be assessed separately. The assessment will be based largely on geologic and/or geochemical data derived from examination of Middle Proterozoic rocks from specific localities within each segment (Fig. 5-1).

Lake Superior Segment

The potential for petroleum reserves in the Midcontinent Rift System has long been recognized because of the active crude oil seeps emanating from the ~1.1 billion-year-old Nonesuch Formation at the White Pine Mine locality, Lake Superior region (Fig. 5-1). In this region, the Nonesuch Formation, the middle unit of the Oronto Group, ranging in thickness from about 76 to 213 m (250 to 700 ft) and averaging 183 m (600 ft), consists of interbedded dark grayish to greenish sandstones, siltstones and silty shales. Combined analyses of nearly 400 outcrop and shallow core samples by Imbus and others (1987) and Pratt and others (1989) indicate that the total organic carbon (TOC) contents for all Nonesuch rocks are generally less than 0.3%. However, for the finely laminated calcareous and noncalcareous silty shales that occur in thin intervals, TOC contents range from 0.25 to 2.8% and average 0.6% (Table 1) (Hieshima and others, 1989). It is these finely laminated silty shales that show promise of potential HC source beds. Surprisingly, these 1.1-billion-year-old shales along the outcrop belt have never experienced severe thermal stress. Rock-Eval T_{max} data (Table 1) and biological marker distributions suggest that these fine-grained source rocks are marginally mature to mature with respect to the principal zone of oil generation (Hieshima and others, 1989; Pratt and others, 1989).

It would seem that if thicker sections of these finely laminated, HC-generating shales occur downdip from the outcrop belt and if they were subjected to higher levels of thermal maturation in the geologic past, the gas source potential for the Lake Superior and the adjoining area in northern Wisconsin would be considered fair to good. This evaluation, of course, would be contingent also upon the presence of adequate reservoir rocks and seals.

Minnesota Segment

The source rock potential of the Minnesota segment of the MRS is evaluated from examination of Keweenawan Solor Church Formation rocks as sampled in the Lonsdale 65-1 borehole, in the Saint Croix horst, Rice County, Minnesota (Hatch and Morey, 1985). The Lonsdale borehole penetrated 579 m (1,898 ft) of the Solor Church Formation but seismic evidence indicates at least a 975-m (3,200-ft) sequence of the formation is present at this locality. The formation consists principally of interbedded conglomerate, sandstone, siltstone, and shale or mudstone, similar in lithology and hence broadly correlative to the Oronto Group of Michigan and Wisconsin.

Analyses of 25 core samples, mainly from the lower 20% of the 578-m (1,898-ft) core, show TOC contents ranging from 0.01 to 1.77% and averaging 0.24%, indicating an overall poor source rock potential for oil or gas for the entire formation. However, darker gray mudstones which make up about half of the samples analyzed, are characterized by slightly higher TOC contents

ranging from 0.13 to 1.77% and averaging 0.4%. Under certain circumstances, average TOC values of 0.4% and even 0.3% have been considered by some geochemists as the minimum necessary to form a HC source rock (Dow, 1977; Palacas, 1978; Tissot and Welte, 1984, p. 497). Thus from the standpoint of TOC alone, the shales could be considered as having some petroleum source rock potential. However, the average genetic potential ($S_1 + S_2$) is less than 0.1 mg HC/g rock, strongly indicating that these rocks are now poor in HC-generating organic matter both for oil and gas. The very low average genetic potential is largely attributed to the advanced level of thermal maturation. This is corroborated by the only realistic T_{max} value (494°C) obtained from the richest mudstone sample analyzed (TOC = 1.77%). Based on previous maturity evaluations of basins worldwide, the T_{max} value of 494°C suggests that the Solor Church organic matter at the Lonsdale 65-1 locality has advanced to the transition stage between the wet gas and dry gas generating zones (Hatch and Morey, 1985).

From the above considerations, it is clear that at the present time the gas source potential of the Precambrian Solor Church Formation rocks is poor in the region of the Saint Croix horst and particularly at the Lonsdale well locality. Perhaps in the geologic past, economic quantities of gas were generated. However, Hatch and Morey (1985) suggested that if HC's were generated during Solor Church time (i.e., when the formation experienced maximum burial depth and high geothermal gradients), the generated HC's were lost as a consequence of subsequent uplift and erosion that produced clastic sediments included in the overlying Fond du Lac Formation (Bayfield Group).

Iowa Segment

The Iowa segment of the MRS is unique in that the HC source rock assessment has been made of the thickest section (4,540 m--14,898 ft) of Precambrian sedimentary rock sampled by drilling from anywhere throughout the 940-mile-long structure. Assessment is based on analysis of 40 core and cuttings samples from the 5,440-m (17,851-ft) deep Amoco M. G. Eischeid #1 well, drilled in 1987 in an asymmetric half-graben-like basin northwest of the medial horst (Iowa Horst), Carroll County, Iowa (Figs. 5-1, 5-2) (Palacas and others, 1990). The Eischeid well penetrated 854 m (2,802 ft) of Phanerozoic (mostly Paleozoic) strata, 4,541 m (14,898 ft) of Middle Proterozoic (Keweenawan) unmetamorphosed sedimentary rocks, and 46 m (151 ft) of Middle Proterozoic gabbroic intrusive rocks. The Keweenawan Supergroup rocks are comprised of 2,349 m (7,708 ft) of an Upper "Red Clastic" sequence, resembling the Bayfield Group of Wisconsin, and 2,191 m (7,190 ft) of a Lower "Red Clastic' sequence, broadly correlative to the Oronto Group of Wisconsin.

Most of the Keweenawan sedimentary rocks, composed of red and red-brown sandstones, siltstones, and silty shales, are oxidized and have no source rock potential. These oxidized rocks have TOC contents <0.1% and genetic potentials <0.1 mg HC/g rock. However, in the Lower "Red Clastic" sequence, at depths between 4,572 and 5,006 m (15,000 and 16,425 ft), a conspicuous darker colored section of rock, possibly equivalent to the Nonesuch Formation of the Lake Superior region, contains a cumulative thickness of 61 to 91 m (200 to 300 ft) of gray to black, pyrite-bearing, laminated shales. In these shales, TOC contents average 0.6% and are as high as 1.4% (Table 5-1) and genetic potentials range from 0.1 to 0.4 mg HC/g rock. T_{max} values average 503°C, strongly indicating that the shales are thermally overmature and in the transitional zone between wet gas and dry gas, similar to the findings for the Solor Church Formation in southeastern Minnesota.

The above data indicate that the laminated shales have little remaining capacity for HC generation but may have generated significant amounts of gas in the geologic past, most likely during Proterozoic time. Support for this is shown by the on-site chromatographic detection of minor occurrences of methane and ethane throughout most of the darker colored shaley interval 4,572 and 5,006 m (15,000 to 16,425 ft). If indeed commercial volumes of gas were generated and expelled, we speculate that the most plausible pathway of migration would not have been vertical because of constraints imposed by very low porosities (avg. 2.3%) and permeabilities (Schmoker and Palacas, 1990) but rather updip along bedding structures toward the shallower portions of the basin. This direction of movement would be in harmony with the probable hydrodynamic flow from the deeper, central parts of the basin toward the updip margins of the basin (Ludvigson and Spry, 1990). We further speculate that equivalent laminated shale facies, as those observed in the Eischeid well, might have fair to good HC source potential if present at shallower depths of burial, under lower levels of thermal stress, along basin flanks, away from the frontal fault zone of the medial horst.

Kansas Segment

The Kansas segment of the MRS is tentatively evaluated on the basis of examination of cuttings samples form two boreholes in northeastern Kansas: the Texas Poersche #1 well, sec 31, T5S, R5E, Washington County and the Producers Engineering Finn #1 well, sec 4, T4S, R7E, Marshall County (Berendsen and others, 1988; Newell and others, 1989). The two wells exhibit remarkably different lithologies, probably reflecting different structural, stratigraphic, and/or depositional regimes. Hence, the two sections of rock may belong to two different subbasins. This is commensurate with the findings provided by geophysical and borehole data that the MRS segment in northeastern Kansas is divided into small subbasins that probably are only a few tens of square miles in areal extent (K. D. Newell, personal communication, 1991).

The Poersche well, drilled to total depth of 3,444 m (11,300 ft), penetrated 867 m (2,846 ft) of Phanerozoic rock and 2,576 m (8,454 ft) of Precambrian (Keweenawan) rock, the latter of which is comprised of nearly equal successions of highly oxidized arkosic sandstones and siltstones and mafic volcanic and intrusive rocks. No organic matter was noted in any of the oxidized sedimentary rocks, unequivocally indicating no source rock potential.

On the other hand, the Producers Engineering Finn #1 well, which encountered 563 m (1,848 ft) of Precambrian rock, consisting mostly of arkosic sandstones, siltstones and shales, showed some minor gas source potential in a 300-ft section of gray siltstones directly beneath the Paleozoic-Precambrian unconformity. The upper 40 m (130 ft) of this section is the richest zone, characterized by TOC contents reaching as high as about 0.8% and averaging 0.6% and genetic potentials ranging from 0.16 to 0.67 mg HC/g rock and averaging 0.5 mg HC/rock (K.D. Newell, personal communication, 1991). The lower 52-m (170-ft) section is much leaner in organic matter, having TOC contents averaging about 0.15 to 0.2%. The Tmax values are mostly in the range of 445° to 450°C, well within the oil generation window (435-465°C). These maturity values contrast dramatically with the decidely higher maturity values observed in the Minnesota and Iowa segments of the MRS (Table 1).

In summary, although the deepest penetration of Precambrian rock (Poersch well) indicated no HC source rock potential, the Finn #1 well, only 30 km (18 mi) northeast of the Poersch well demonstrated that some gas source potential is present. Because of the structural complexity and abrupt facies changes, it appears that individual subbasins need to be examined before

complete source rock evaluation be made of the Kansas portion of the rift system.

GRAND CANYON AREA, NORTHERN ARIZONA

Exposed in the eastern portion of the Grand Canyon is the Late Proterozoic Chuar Group, a 1,636-m-thick (5,370-ft-thick) succession of predominantly very fine grained siliciclastic rocks that contains thin sequences of sandstone and stromatolitic and cryptalgal carbonate rocks (Fig. 5-3) (Reynolds and others, 1988). More than half the succession consists of organic-rich gray to black mudstone (or shale) and siltstone. Fossil microorganisms, such as *Chuaria* (discoidal megaplanktonic algae), tear and flask-shaped chitinozoa(?), filamentous algae, and individual and clusters of spheroidal, cyst-like planktonic organisms, are abundant to common throughout successions of dark mudstone and siltstone (Vidal and Ford, 1985).

Geochemical analyses indicate that the 281-m-thick (922-ft-thick) Walcott Member, the uppermost unit of the Kwagunt (Fig. 5-3), has good to excellent petroleum source rock potential. The lower half of the Walcott is characterized by total organic carbon (TOC) contents as much as 8.0 to 10.0%, (averaging ~3.0%), hydrogen indices as much as 204 mgHC/g TOC (averaging 1335 mgHC/g TOC), genetic potentials ($S_1 + S_2$) of nearly 16,000 ppm (averaging ~6,000 ppm), and extractable organic matter (EOM) as much as 4,000 ppm (Palacas and Reynolds, 1989; Palacas and Reynolds, unpublished data). Data for the upper Walcott are incomplete but suggest that these rocks are as rich or richer than the lower Walcott. Maturity assessment indicates that source rocks of the Walcott are within the oil generation window.

Strata of the underlying thermally mature Awatubi Member of the Kwagunt and the thermally mature to overmature Galeros Formation are, in general, rated as poor oil sources with genetic potentials generally less than 1,000 ppm, but they appear to be acceptable to good source rocks for gas generation. Chuar Group strata may be potential sources for economic accumulations of gas and oil in upper Proterozoic or lower Paleozoic reservoir rocks in northwest Arizona and Utah. The relative proportion of gas or oil in any one area will depend in large part upon the degree of thermal maturation that the rocks have undergone.

A preliminary map indicating the geographic extent of the Chuar Group or equivalent rocks is shown in Figure 5-4.

REFERENCES

Anderson, R. R., 1989, Gravity and magnetic modeling of central segment of Mid-Continent Rift in Iowa: New insights into its stratigraphy, structure, and geologic history (abs.): American Association of Petroleum Geologists Bulletin, v. 73, no. 8, p. 1043.

Berendsen, P., Borcherding, R. M., Doveton, J., Gerhard, L., Newell, K. D., Steeples, D., and Watney, W. L., 1988, Texaco Poersch #1, Washington County, Kansas--preliminary geologic report of the pre-Phanerozoic rocks: Kansas Geological Survey Open-File Report 88-22, 116 p.

Clarke, J. W., 1985, Petroleum geology of East Siberia, U.S. Geological Survey Open-File Report 85-267, 123p.

Dickas, A. B., 1986, Comparative Precambrian stratigraphy and structure along the Mid-Continent Rift: American Association of Petroleum Geologisits Bulletin, v. 70, no. 3, p. 225-238.

Dow, W. G., 1977, Kerogen studies and geological interpretations: Journal of Geochemical Exploration, v. 7, p. 79-99.

Edgell, H. S., 1991, Proterozoic salt basins of the Persian Gulf area and their role in hydrocarbon generation: Precambrian Research, v. 54, p. 1-14.

Fritz, M., 1989, An old source surfaces in Oman: American Association of Petroleum Geologists Explorer, v. 10, no. 9, p. 1, 14-15.

Grantham, P. J., Lijmbach, G. W. M., Posthuma, J., Hughes Clark, M. W., and Willink, R. J., 1987, Origin of crude oils in Oman: Journal of Petroleum Geology, v. 11, no. 1, p. 61-80.

Hatch, J R., and Morey, G. B., 1985, Hydrocarbon source rock evaluation of Middle Proterozoic Solor Church Formation, North American Mid-Continent rift system, Rice County, Minnesota: American Association of Petroleum Geologists Bulletin, v. 69, no. 8, p. 1208-1216.

Hieshima, G. B ., Zaback, D. A., and Pratt, L. M., 1989, Petroleum potential of Precambrian Nonesuch Formation, Mid-Continent rift systm (abs.): American Association of Petroleum Geologists Bulletin, v. 73, no. 3, p. 363.

Imbus, S. W., Engel, M. H., Elmore, R. D., and Zumberge, J. E., 1988, The origin, distribution and hydrocarbon generation potential of organic-rich facies in the Nonesuch Formation, central North American rift system: A regional study: *in* Matttavelli, L., and Novelli, L., eds., Advances in organic geochemistry 1987: Organic Geochemistry, v. 13, p. 207-219.

Korch, R. J., Mai Huazhao, Sun Zhaocai, and Gorter, J. D., 1991, The Sichuan Basin, southwest China: a Late Proterozoic (Sinian) petroleum province: Precambrian Research, v. 54, p. 45-63.

Ludvigson, G. A., and Spry, P. G., 1990, Tectonic and paleohydrologic significance of carbonate veinlets in the Keweenewan sedimentary rocks of the Amoco M. G. Eischeid #1 drillhole, *in* Anderson, R. R., ed., The Amoco M. G. Eischeid Deep Petroleum Test Carroll County, Iowa: Iowa Department of Natural Resources, Special Report Series No. 2, p. 153-167.

Meyerhoff, A. A., 1980, Geology and petroleum fields in Proterozoic and Lower Cambrian strata, Lena-Tunguska petroleum province, Eastern Siberia, USSR, *in* Halbouty, M. T., ed., Giant Oil and Gas Fields of the Decade 1968-78: American Association of Petroleum Geologists Memoir 30, p. 225-252.

Newell, K. D., Berendsen, P., Doveton, J. H., and Watney, W. L., 1989, Correlation and implications of results from recent wildcat wells in Mid-Continent Rift in northeastern Kansas (abs.), American Association of Petroleum Geologists Bulletin, v. 73, no. 8, p. 1049.

Palacas, J. G., 1978, Preliminary assessment of organic carbon content and petroleum source rock potential of Cretaceous and lower Tertiary carbonates, South Florida Basin: Transaction Gulf Coast Assoc. Geological Societies, v. 28, p. 357-381.

Palacas, J. G., and Reynolds, M. W., 1989, Preliminary petroleum source rock assessment of the Late Proterozoic Chuar Group, Grand Canyon, Arizona (abs.): American Association of Petroleum Geologists Bulletin, v. 73, no. 3, p. 397.

Palacas, J. G., Schmoker, J. W., Daws, T. A., Pawlewicz, M. J., and Anderson, R. R., 1990, Petroleum source-rock assessment of Middle Proterozoic (Keweenawan) sedimentary rocks, Eischeid #1 well, Carroll County, Iowa, *in* Anderson, R. R., ed., The Amoco M. G. Eischeid #1 Deep Petroleum Test Carroll County, Iowa: Iowa Department of Natural Resources, Special Report Series No. 2, p. 119-134.

Pratt, L. M., Hieshima, G. B., Hayes, J. M., and Summons, R. E., 1989, Lithofacies and biomarkers in Precambrian Nonesuch Formation: petroleum source potential of Midcontinent Rift System, North America, *in* Abstracts, 28th International Geological Congress, Washington, D.C., v. 2, p. 2-637 to 2-638.

Rauzi, S. L., 1990, Distribution of Proterozoic hydrocarbon source rock in northern Arizona and southern Utah: Arizona Oil and Gas Conservation Commission Publication 5, 38p.

Reynolds, M. W., Palacas, J. G., and Elston, D. P., 1988, Potential petroleum source rocks in the Late Proterozoic Chuar Group, Grand Canyon, Airzona (abs.) *in* Carter, L. M. H., ed., V. E. McKelvey Forum on Mineral and Energy Resources: U.S. Geological Survey Circular 1025, p. 49-50.

Schmoker, J. W., and Palacas, J. G., 1990, Porosity of Precambrian sandstones in lower portion of the Eischeid #1 well, Carroll County, Iowa, *in* Anderson, R. R., ed., The Amoco M. G. Eischeid #1 Deep Petroleum Test, Carroll County, Iowa: Iowa Department of Natural Resources, Special Report Series No. 2, p. 135-142.

Shirley, K., 1985, Wildcat tests Precambrian gas: American Association of Petroleum Geologists Explorer, v. 6, no. 8, p. 1, 12-13.

Tissot, B. P. and Welte, D. H., 1984, Petroleum Formation Occurrence: Springer-Verlag, New York, 699p.

Utah Geological and Mineral Survey, 1990, Survey Notes, v. 20, No. 2, p. 18.

Vidal, G., and Ford, T. D., 1985, Microbiotas from the Late Proterozoic Chuar Group (Northern Arizona) and Uinta Mountain Group (Utah) and their chronostratigraphic implications: Precambrian Research, v. 28, p. 349-389.

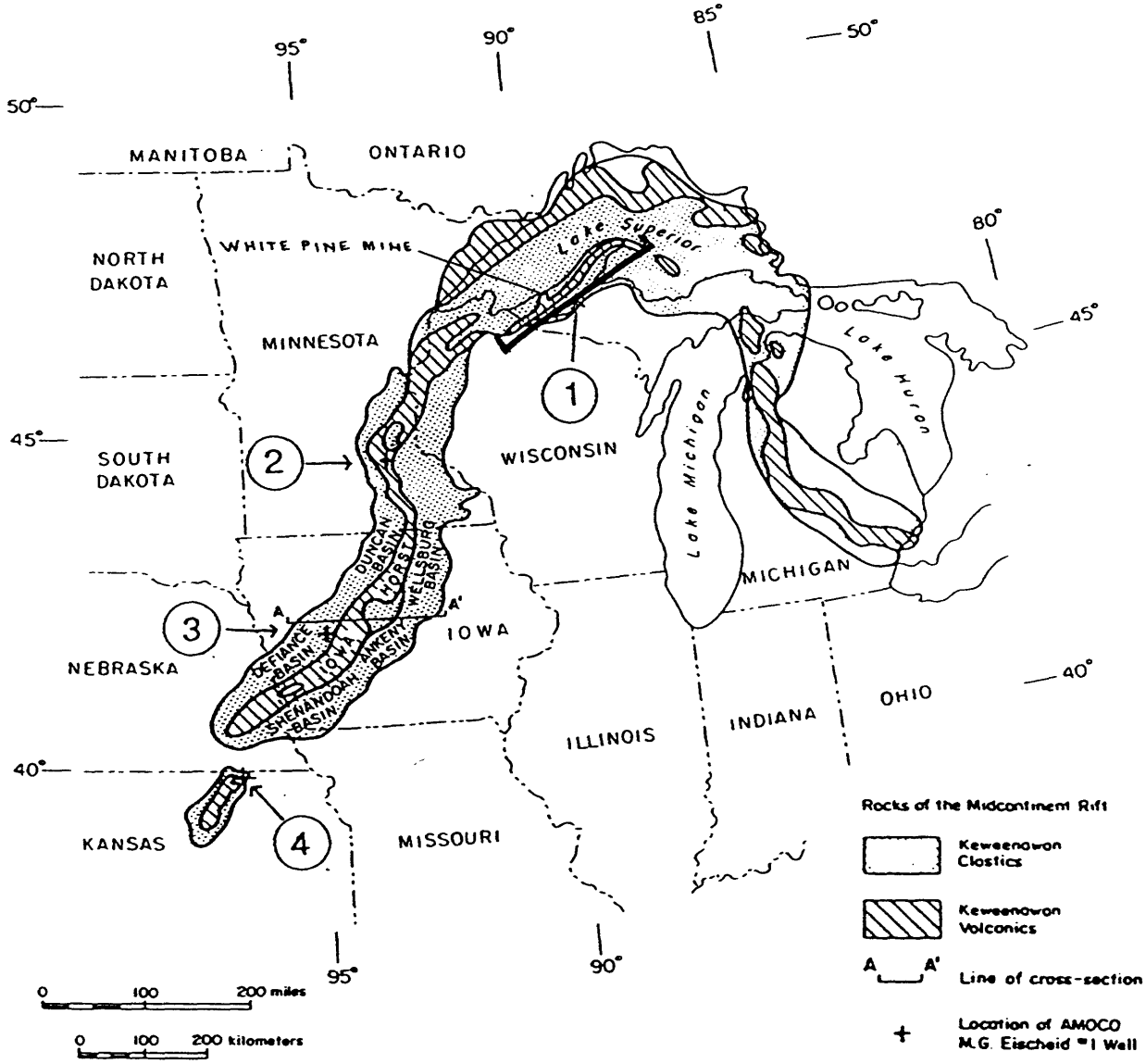

Figure 5-1. Map showing the general location and major rock types of the Midcontinent Rift System and the location of the four sites in which Precambrian sedimentary rocks were studied. (1) Lake Superior segment outcrop belt; (2) Minnesota segment, Lonsdale 65-1 well, Rice County; (3) Iowa segment, Amoco Eischeid #1 well, Carroll County; (4) Kansas segment, Texaco Poersch #1, Washington County, and Producers Finn #1, Marshall County. (From Palacas and others, 1990).

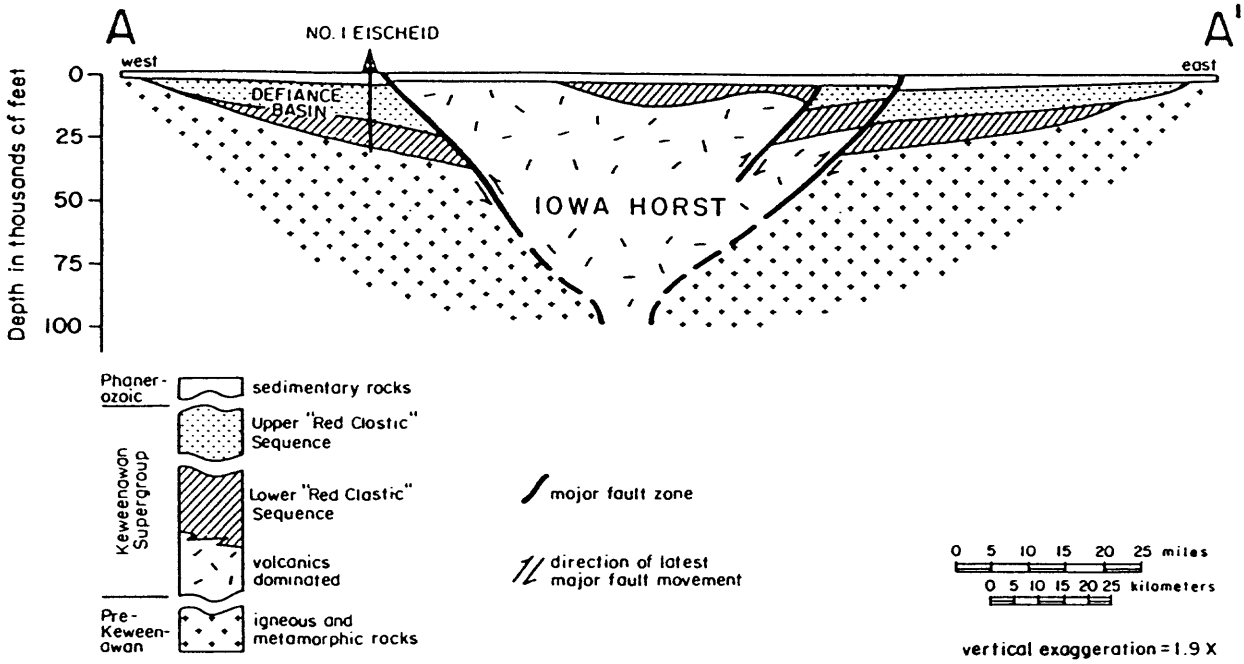

Figure 5-2. Schematic geologic cross section of the Midcontinent Rift System, central Iowa. Note approximate location of Amoco M. G. Eischeid #1 well with respect to Iowa horst. Location of cross section is shown in Figure 5-1. (From Palacas and others, 1990).

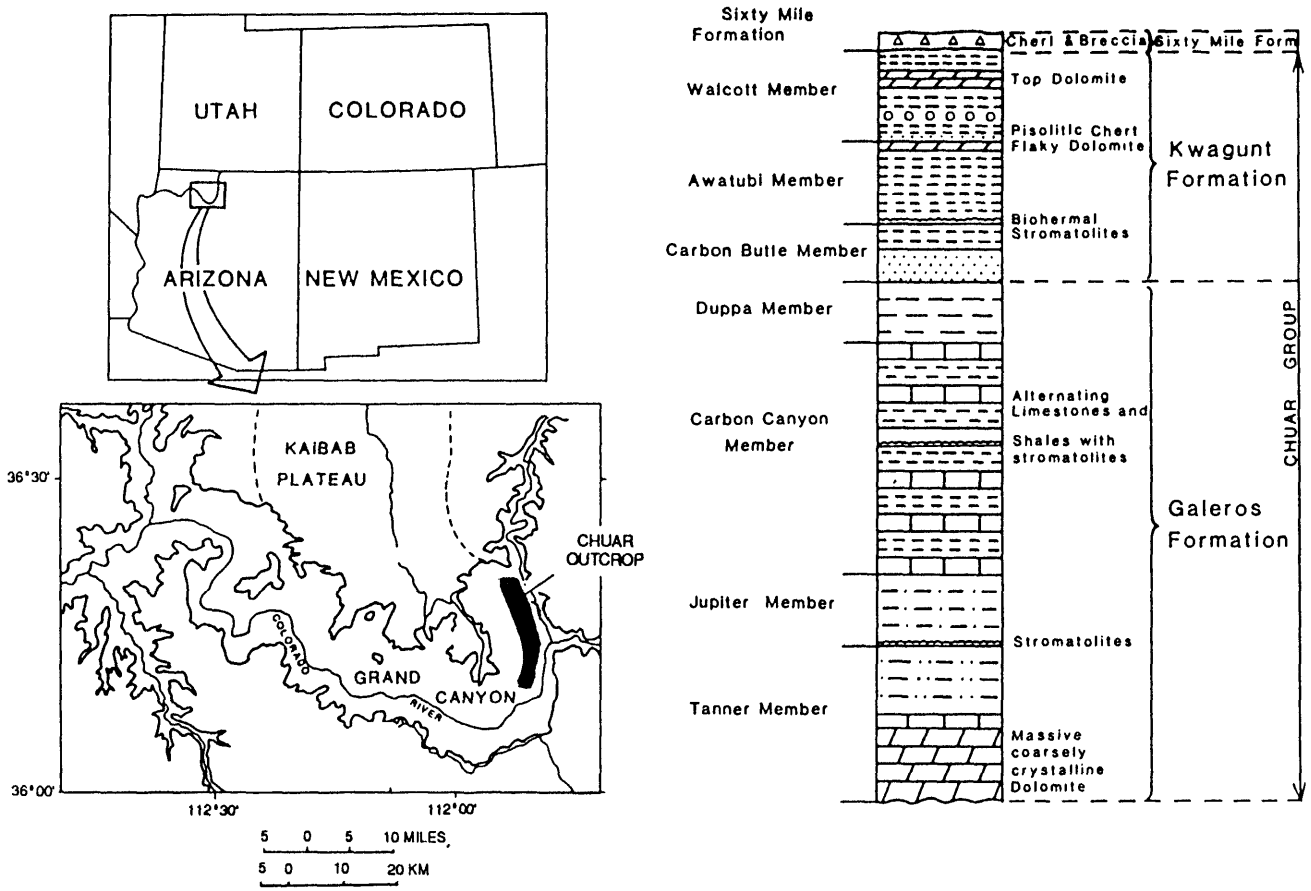

Figure 5-3. Sketch-map of the eastern Grand Canyon in northern Arizona showing sampling locality (solid black pattern), and simplified geological section of the Chuar Group. (Modified from Vidal and Ford, 1985).

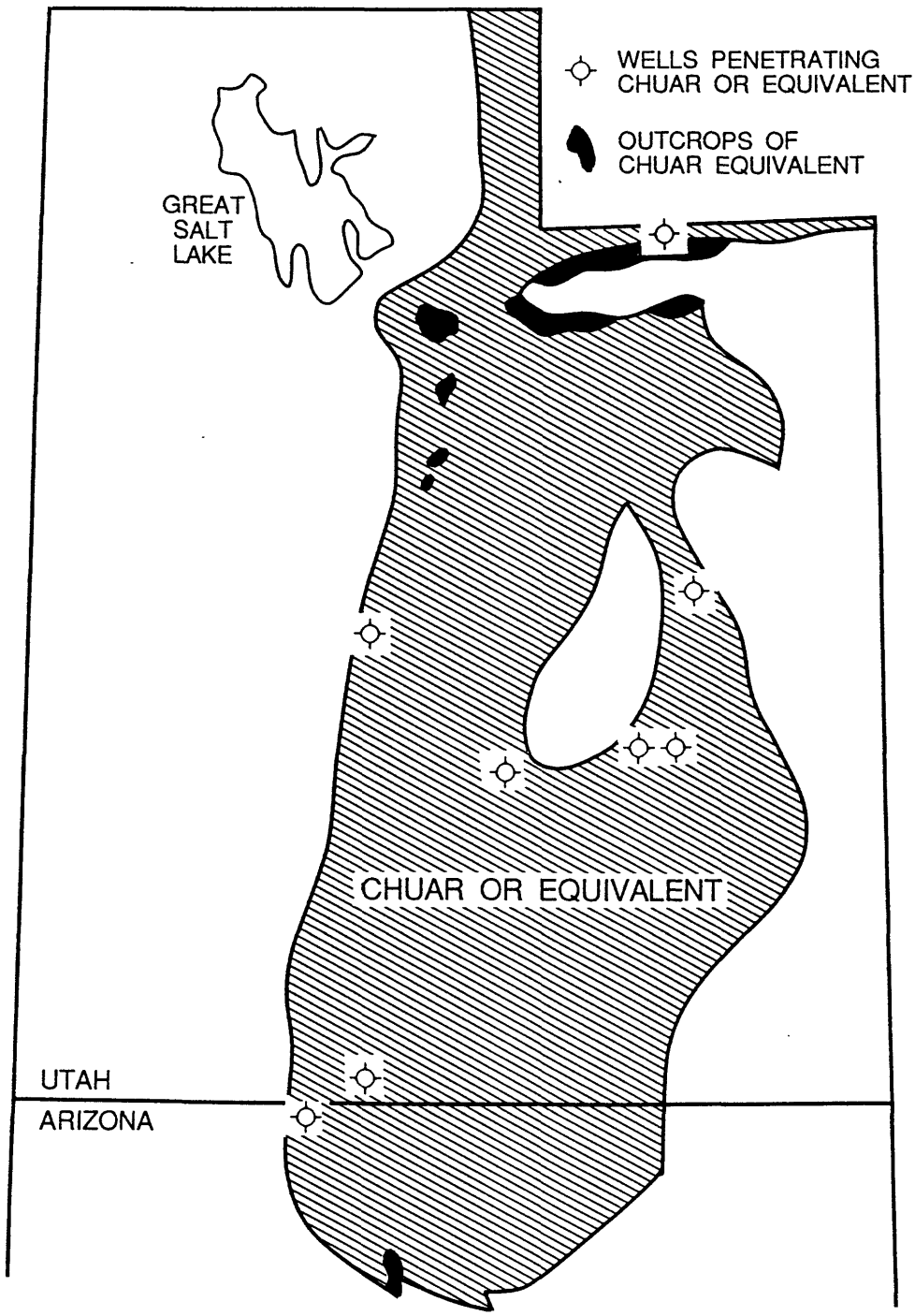

Figure 5-4. Map indicating possible distribution of Proterozoic Chuar Group or equivalent rocks in northern Arizona and Utah. (Modified form Utah Geological and Mineral Survey (1990); and Rauzi (1990).

Table 5-1. Geochemical Data of Possible Precambrian Source Rocks, Midcontinent Rift System (MRS) and Grand Canyon, Northern Arizona

Location	Stratigraphic Unit (Lithology)	TOC (wt. %) Range	Avg.	T_{max} °C	Level of Maturity
		Midcontinent Rift System			
Lake Superior Segment	Nonesuch Fm.	0.25-2.8	0.6	418-427	Marginally mature to mature
Minnesota Segment	Solor Church Fm. (mudstones)	0.13-1.77	0.4	494	Overmature
Iowa Segment	Nonesuch Shale equivalent (dark shales)	0.1-1.4	0.6	497-508	Overmature
Kansas Segment (Producers Finn #1 well)	Keweenawan (undifferentiated) (siltstones)	0.1-0.8	0.6	445-450	Mature
		Grand Canyon Area, Northern Arizona			
Eastern Grand Canyon	Walcott Member[1] (dark mudstones)	1.0-9.0	~3.0	424-452	Mature

[1]Walcott Member is the uppermost stratigraphic unit in the Chuar Group. See Figure 5-3 for stratigraphic position.

Task 6--C15+ Hydrocarbon Thermal Destruction as Related to High-Rank, Deep-Basin Gas Resource Bases, by Leigh C. Price

ABSTRACT

To correctly assess the potential of deep-basin gas resource bases, the thermal stability of C_{15+} hydrocarbons (HC's) and the generation (origin) and migration of deep-basin gas must be understood. It is taken as petroleum-geochemical law that C_{15+} HC's are thermally destroyed by vitrinite reflectance (R_o) values of 1.35% and that C_2-C_4 HC's are destroyed by R_o = 2.00%, with rock (greenschist) metamorphism commencing at R_o = 4.00%. The data of this study lead to the conclusion that these petroleum-geochemical "laws" must be in error. C_{15+} HC's, in reality, are thermally stable to R_o = 7.0-8.0% in the natural system, dependent on several variables in deep petroleum basins. The C_2-C_4 HC's are probably thermally stable well into greenschist metamorphism, and methane very possibly persists to mantle conditions. The proposed (but erroneous) thermal destruction of C_{15+} HC's by R_o = 1.35 % strongly contradicts long-standing physical-chemical thermodynamic principles, because of the extreme bond strengths (82.6-117 kcal/mole) which must be broken for HC destruction. These bond strengths require extreme maturation ranks for disruption.

Evidence for a significantly greater thermal stability of C_{15+} HC's than that portrayed by present-day petroleum-geochemical paradigms comes from a large petroleum-geochemical data base which demonstrates that high to moderate concentrations of indigenous C_{15+} HC's and bitumen persist in deeply-buried rocks at present-day R_o values of 1.35-5.0%. Furthermore, moderate to low concentrations of C_{15+} HC's and bitumen persist in rocks with R_o values of 5.0-7.0%.

Qualitative analyses of: 1) bitumen from high-rank rocks (R_o = 2.0-7.6%), 2) high-rank gases and gas condensates, and 3) bitumen from aqueous-pyrolysis experiments in the HC-thermal-destructive phase, all provide significant insight to C_{15+} HC thermal destruction. Very characteristic carbon-isotopic and chemical assemblages occur both in HC gases and C_{5+} HC's in the approach to, and during, C_{15+} HC thermal destruction. These high-rank HC assemblages are discussed in detail in the report.

Part of the reason for the contradiction between actual C_{15+} HC thermal stability (as outlined in this report) and the predicted petroleum-geochemical paradigm of C_{15+} HC thermal stability lies in the controlling parameters of organic matter (OM) metamorphism. (In this report, OM metamorphism is defined as all the reactions involving generation, maturation, and thermal destruction of methane and all C_{2+} HC's (and bitumen), and maturation of kerogen). By present-day petroleum geochemistry, OM metamorphism is hypothesized to occur by a parallel series of first-order reactions and thus to be controlled primarily by burial temperature and geologic time. A large body of petroleum-geochemical data from long-term U.S. Geological Survey investigations, and much published data, all dictate that OM metamorphic reactions can not be first-order, but must be higher-ordered reactions. If this is the case, then geologic time would play no, or only a minimal, role in OM metamorphism.

Furthermore, possible generally-unrecognized, but important, controlling parameters of OM metamorphism have been suggested by U.S. Geological Survey research. These parameters have direct bearing on the genesis and persistence of deeply-buried, high-rank gas deposits and are: 1) The *absence or presence of water in the system,* because C_{15+} HC thermal destruction is significantly

promoted in water-barren systems and is significantly suppressed in water-bearing systems. 2) *Increasing fluid pressure* strongly suppresses all aspects of OM metamorphism, including C_{15+} HC generation and thermal destruction. 3) Product escape from reaction sites (*whether the reaction takes place in an open or closed system*) also is a controlling parameter. Lack of product escape (closed systems) retards OM metamorphism, and product escape (open systems) promotes OM metamorphism. 4) *Increasing temperature* is the principal drive for OM metamorphic reactions, which is in agreement with present-day petroleum-geochemical paradigms.

A strong zonation of oil and gas deposits exists in many petroleum basins, with only "dry" gas in deep-basin reservoirs and increasing amounts of oil at shallower basinal depths. Also, both API gravity and gas-oil ratios of oil deposits decrease as one moves to shallower depths on the basin shelves away from the deep basin. Previously this basinal-HC zonation has been taken as prima facie evidence that dry gas (methane) was being formed from the thermal destruction of C_{15+} HC's in the deep basin. However: 1) the persistence of C_{15+} HC's to great depths (7-10 km) and extreme maturation ranks (R_o = 5.0-7.0 km) in petroleum basins, and 2) methane carbon-isotopic compositions in the Anadarko basin (discussed in text below) both strongly argue against the above hypothesis of deep-basin methane resulting from C_{15+} HC thermal destruction. Instead, a model is favored in this report where most deep-basin methane has simply been generated from kerogen during the C_{15+} HC generative phase. The invariably-observed basinal zonation of HC's, discussed above, is hypothesized to result from condensation, buoyancy, and separation-migration processes.

In the deep-basin, due to high fluid pressures only methane remains in the gas phase. The C_2-C_4 HC gases are condensed into, and behave as, a liquid phase. With continued C_{15+} HC (and methane) generation in the deep basin, eventually all (or most) deep-basinal traps are filled to the spill point with methane and all other fluids (crude oil, condensed C_2-C_4 HC gases, and water) are displaced out of the deep basin to shallower traps on the stable shelves of petroleum basins by Gussow's (1954) principal of differential entrapment. These processes are driven by buoyancy differences within the fluids and the fact that methane "rides over"or is found on top of, all other fluids in the deep basin.

Evidence exists that water may have been flushed from some (many?) deep-basinal traps by methane as hypothesized above. Both carbon dioxide and hydrogen sulphide are found in abundance in some deep-basin gas reservoirs and would have existed in those reservoirs for tens to hundreds of millions of years. Because those gases are highly soluble in water, their presence dictates that water is not in contact with such gas reservoirs. The absence of water in some deep-basinal gas reservoirs carries implications for the deep-basin gas resource base, two of the more important of which are that: 1) HC thermal cracking reactions will be promoted in these water-free environments. 2) When water is introduced into such reservoirs during drilling and completion operations, in some cases significant reservoir damage could occur in a skin around the wellbore from the principles of two phase fluid flow and the Jamin effect. If it occurs, such reservoir damage could greatly harm gas productivities, which could lead to an underestimation of the recoverability and economic viability of the deep-basin gas resource bases and the condemnation of individual wells.

As stated, it is hypothesized here that most deep-basinal gas deposits have originated from methane generation which accompanies C_{15+} HC generation, combined with condensation-buoyancy-separation-migration processes. However,

carbon isotopic values of methane and carbon dioxide in some deep-basinal gas deposits demonstrate that high-rank dry-gas deposits do exist which have originated from C_{15+} HC thermal destruction. Such deposits do appear to be unusual, however.

It is hypothesized here that primary gas migration from the source rock, like primary oil migration, is significantly less efficient than generally perceived. It is also hypothesized that primary gas migration would be greatly facilitated by major faulting (with accompanying large-scale fracturing). Such faulting would greatly disrupt source rocks (and the rocks adjacent to them) to allow gas to escape in significant volumes. Therefore, a "rule of thumb" for this report concerning deep-gas deposits, is that "conventional" deep-gas deposits (not tight gas, basin-centered gas, etc.) should always be associated with major faults.

One of the hypotheses serving as a foundation for the above rule of thumb is that deep petroleum basins are more of a "closed system", with regards to fluid flow and fluid expulsion, than generally envisioned. Current petroleum-geologic/geochemical thought largely models deep petroleum basins as open systems which allow efficient primary HC migration and expulsion of deep-basin fluids to proceed largely unabated through geologic time. However, there is strong evidence against this viewpoint, evidence which supports the proposition that deep basins are largely closed systems regarding fluid flow. If this latter viewpoint more closely approximates the natural system, then much more of the gas generated in the deep basin would have been retained in the deep basin than previously perceived. This possibility carries the implication that much larger and much higher-grade deep-basin gas-resource bases may exist than previously envisioned . In point of fact, monstrous in-place gas-resource bases have already been proven, such as coal-gas, tight-gas, basin-centered gas, Gulf Coast geopressured-geothermal gas, etc.). The very existence of these various gas-resource bases validates the proposition that deep basins are much more of a closed system with regards to fluid flow than as portrayed by some basinal models.

It is the principal recommendation of this paper that geologic-based engineering studies be instituted to ascertain if wider-spread commercially-viable production of such in-place unconventional gas-resource bases is possible. Significant production of such unconventional in-place gas (and oil) resource bases at this point appears to be the only possible avenue by which the United States may significantly curtail a certain, and dangerous, ever-increasing dependence on the Middle East for our energy needs.

INTRODUCTION

The data from this study clearly demonstrate that C_{15}+ hydrocarbons (HC's) are thermally stable to *much* higher maturation ranks than called for by popularized present-day petroleum-geochemical models. Because the degree of disagreement between data from nature and the expected behavior of these models is so great, it is not enough just to present the data. The reasons for the disagreement must also be examined, and these reasons are the possible parameters which control organic matter (OM) metamorphism. (In this paper, OM metamorphism is defined as HC generation, maturation, and thermal destruction, and kerogen diagenesis and maturation.) Thus, before the data on both C_{15}+ HC thermal stability and compositional changes within the C_{15}+ HC's at their destruction are presented, the different controlling parameters of OM metamorphism will be discussed as viewed by both conventional wisdom and newer, alternate models. A detailed discussion then follows on C_{15}+ HC thermal stability and the compositional changes which occur in both saturated and aromatic HC's in their approach to, and during, C_{15}+ HC thermal destruction. A number of different petroleum-geological and petroleum-geochemical topics are then discussed. These topics, although diverse, are all interrelated in that they help delineate both possible huge in-place gas resource bases in deep-basinal settings and some "rules of thumb" governing different facets of these resource bases. An index with page numbers listed for the different topics discussed as an aid to the reader follows this introduction. Major conclusions are given at the end of the article, before the bibliography.

PARADIGMS OF PETROLEUM GEOCHEMISTRY

According to present-day petroleum-geochemistry, OM metamorphic reactions are first order with burial temperature and geologic time being the principal controls. As such, it is accepted that geologic time can be substituted for burial temperature in Arrhenius equations describing first-order reactions. HC generation begins at a vitrinite reflectance (R_o) of 0.6% +/- 0.15% (Fig. 6-1) and maximizes in intensity at R_o = 0.9%. OM type can affect these R_o values; however, agreement does not exist among petroleum geochemists on the magnitude or direction of the effect for the different OM types. At R_o = 0.9%, C_{15}+ HC thermal destruction commences. By R_o = 1.35%, all C_{15}+ HC's have been destroyed. (Some investigators maintain that all C_5+ HC's are destroyed by this point). By R_o = 2.0%, only methane is stable, and by R_o= 4.0% methane is destroyed and rock metamorphism begins.

OM METAMORPHISM - ALTERNATE HYPOTHESES

A large published petroleum-geochemical data base does not wholly conform to the above paradigms. Furthermore, interpretation of this data base strongly suggests that alternate petroleum-geochemical models are possible with regards to OM metamorphism.

REACTION ORDER

Increasing burial temperature indeed appears to be the principal drive for OM metamorphic reactions. However, laboratory OM metamorphic experiments carried out in closed, pressurized, water-wet systems which are thought to simulate nature, are not first- order reactions, but are higher-ordered reactions (Rogers and others, 1962; Bostick, 1979; Brooks, 1971; McIntyre, 1972; Hesp and Rigby, 1973; Ishwatari and others, 1977; Goodarzi and Murchison, 1977; Chung and Sackett, 1978; Pearson, 1981; Price, 1983, and Fig.

6-2). It must bve stressed that first-order reactions plot as straight lines on plots such as Figure 6-2, while higher-ordered reactions do not. The experiments referenced directly above lead to the conclusion that the effect of geologic time on OM metamorphism may have been overestimated. Furthermore, there is ample geologic evidence which supports this conclusion (Price, 1983; Quigley and MacKenzie, 1988; Barker, 1991). As discussed in Price (1983), the original evidence (Karweil,1955; Lopatin, 1971; and Connan, 1974) for the hypothesis of geologic time being a controlling parameter in OM metamorphism came from geologically-older sedimentary basins. In these basins, rocks at high maturation rank are at low present-day burial temperatures. Thus it was concluded in these studies that the same extent of OM metamorphism would take place over long geologic times at low burial temperatures as would take place in short geologic times at higher burial temperatures. However, as discussed in Price (1983) in *all* the basins studied by Karweil (1955), Lopatin (1971) and Connan (1974), compelling geologic evidence exists, apparently not originally observed, that high, to extreme, paleo-heat flows existed in these basins, heat flows which had later decayed to the low, present-day values. Thus, the original data base for the hypothesis of geologic time being a controlling parameter in OM metamorphism was highly flawed. It appears that the principal influence geologic time has on OM metamorphic reactions is simply that the longer rocks exist in sedimentary basins, the better the chance they have to be affected by high heat flows from different geologic processes.

THE EFFECT OF WATER

Hesp and Rigby (1973) demonstrated that water significantly retarded the thermal destruction of HC's (Fig. 6-3). M.D. Lewan has documented the same effect in his hydrous-pyrolysis experiments (M.D. Lewan, personal communication, 1992). U.S.G.S. aqueous-pyrolysis experiments (Wenger and Price, 1991; Price and Wenger, 1992) and aqueous crude oil solubility measurements of Price (1981) also support this conclusion. Hoering and Ableson (1964) reacted kerogen with D_2O at 100°C for seven days, dried the kerogen, and then heated it under vacuum at 200°C, and found that the HC's cracked from the kerogen were deuterated. Those authors thus demonstrated that during mild catagenesis, kerogen exchanges, and perhaps incorporates, water into its structure. This phenomenon has also been observed (Wenger and Price, 1991; and Price and Wenger, 1992) in aqueous-pyrolysis experiments on six rocks with different OM types. In the lower temperature (pre-HC generation) experiments of those authors, ROCK EVAL hydrogen indices (HI's) significantly increased over the values for the unreacted rocks. Furthermore, the same phenomenon is evident in natural samples. The significant increase in HI's for the coals of Figure 6-4 over $R_o \geq 0.3\%$ to $R_o = 0.7\%$, a trend also present in Bertrand's (1984) coal set (Fig. 6-5), has previously been attributed to loss of volatiles, especially CO_2, with increasing rank. Aqueous-pyrolysis experiments carried out on a hydrogen-poor lignite (Price, 1989a, his Figs. 7-10; and Wenger and Price, 1991) demonstrate the copius amounts of CO_2 that coals generate at low maturation ranks (Fig. 6-6) even before intense C_{15+} HC generation (Fig. 6-7). Such CO_2 loss would increase coal (and kerogen) hydrogen content, and thus ROCK EVAL HI's. For example, in the above-mentioned aqueous-pyrolysis experiments with the lignite, HI's increase from 55 in the original unreacted sample to maximal values of 78-84 at experimental temperatures of 175°-250°. However, mass-balance calculations for these experiments suggest that CO_2 loss alone cannot account for the increase in HI's. The shortfall appears to be made up by incorporation of water into the lignite. This would also increase the hydrogen content, and thus the HI's, of the lignite, which confirms the earlier results of Hoering and Abelson (1964). Given this proposed interaction of water with the lignite, excess oxygen should be present in the system from the oxygen in H_2O.

This is the case, because the lignite at higher aqueous-pyrolysis temperatures generates over five times more CO_2 than possible (Fig. 6-6) given the original ROCK EVAL oxygen indices (72) of the lignite.

SYSTEM OPENNESS

By Le Chatelier's principle (Sienko and Plane, 1961), lack of reaction product removal during a chemical reaction can create a stress on a system, a stress which can impede or halt the reaction. This especially applies to systems where the reactants are liquid or solid and one or more of the products are gas, which is the case in both HC-generation and HC-thermal-destruction reactions. It is possible, but has not been demonstrated, that intermediate species in HC thermal destruction reactions may exist in equilibrium situations. If this is the case, then one might expect Le Chatelier's principle to apply to these reactions in closed chemical systems, and experimental results (discussed below) suggest that this may be the case. Previously petroleum geochemists (including this author) have considered primary petroleum from organic-rich rocks to be very efficient, largely removing HC's from their generation sites (Price and others, 1984; Cooles and others, 1986; Leythaueser and others, 1987, 1988; Mackenzie and others, 1987; Talukdar and others, 1987; Ungerer and others, 1987; Espitalié and others, 1988). Efficient primary migration implies an open chemical system. However, other considerations (Price, 1992; Price and LeFever, 1992) suggest that in reality most generated HC's: (1) remain locked in source rocks, (2) escape only when such rocks are disrupted by faulting, and (3) are lost to drilling muds during the rock trip up the well bore in drilling operations (discussed below) and thus are not measured in the laboratory. By these considerations, HC-generation and thermal-destruction reactions would often occur in closed chemical systems with little or no meaningful product escape. Experiments, discussed below, demonstrate that HC destruction reactions are impeded or halted in closed chemical systems. Thus in my opinion, the openness of OM metamorphic reaction sites in nature may be a pivotal, and generally unrecognized, controlling parameter in OM metamorphism. The important consequences of this point, as related to deep-basin, high-rank gas deposits, are discussed below.

It must be stressed that regional shearing of fine-grained rocks opens up closed chemical systems and relieves high fluid pressures, and thus strongly promotes both OM and inorganic (rock) metamorphism at much lower burial temperatures than would be the case in unsheared rocks. The results of Goffé and Villey's (1984) study corroborate this point. Thus, regional shearing would be highly unfavorable for the possible existence of HC accumulations of any type.

FLUID PRESSURE

Some investigators believe that fluid pressure plays no role in OM metamorphism (Hunt, 1979), or plays a role subordinate to temperature (Tissot and Welte, 1984), or promotes HC thermal destruction (Braun and Burnham, 1990). Different investigators have provided data from the laboratory and/or nature which demonstrate that increasing fluid pressures retards many aspects of OM metamorphism, including HC thermal destruction (Hesp and Rigby, 1973; McTavish, 1978; Cecil and others, 1979; Goffé and Villey, 1984; Dominé, 1991; Dominé and Enguehard 1992; Price and Wenger, 1992; and Connan and others, 1992). Contrasting experimental results of Monthioux and others (1986), who found pressure to have no effect on OM metamorphism, were attributed to experimental technique by Price and Wenger (1992). Monthioux and others (1986) carried out their experiments in small gold bags which became totally flattened with no dead volume in their experiments. Such a lack of dead volume precludes product escape from reaction sites. Such lack of product

escape could so strongly retard OM metamorphism that the effects of pressure would not be observed. Larger pressure vessels, with dead volumes for product removal from the reaction sites, give different experimental results.

Fluid pressures in sedimentary basins can fluctuate significantly over geologic time. Thus, understanding the effect of increasing static-fluid pressure on HC generation and maturation is difficult using natural samples. Consequently, the effect of increasing fluid pressure on OM metamorphism has been debated. A series of aqueous-pyrolysis experiments were performed by the U.S.G.S. on different organic-rich rocks (Table 6-1). under a wide range of conditions, among which were experiments on the Retort Shale Member of the Permian Phosphoria Formation (Type II-S OM) at three different constant temperatures, as a function of increasing static-fluid pressure. The degree to which these laboratory experiments replicated natural OM metamorphism was addressed by comparing the compositions of different aqueous-pyrolysis bitumens to natural products: crude oils, gas-condensates, and rock extracts, at equivalent maturities. Close correlations were found, and the lack of any laboratory artifacts (compounds not found in abundance in natural samples) in the aqueous-pyrolysis bitumens indicated that these experiments had closely replicated nature.

Variable-temperature and constant-pressure experiments were among the experiments performed on the Phosphoria shale. Qualitative analyses of the products from these constant-pressure, variable-temperature experiments (immature to post super-mature maturation ranks) delineated changes in both the generation products and reacted rocks due to increasing maturation rank (increasing experimental temperatures). By comparing results of these analyses to the results of the same analyses for the constant-temperature, variable-pressure experiments, it was evident that increasing static-fluid pressure strongly retarded HC generation, maturation, and thermal destruction. For example, at 287°C and 31 bars pressure, the Phosphoria shale is in the middle of mainstage HC generation (Fig. 6-8). With increase in system pressure to 965 bars at 287°C, HC generation was suppressed (Fig. 6-9), and the quantitative reaction extent became equivalent to that of the threshold of intense HC generation at an experimental temperature of 225°C (Fig. 6-8). Concurrently, the hydrogen index (HI) of the reacted and Soxhlet-extracted rock also greatly increased, from 209 at 287°C and 31 bars to 371 at 287°C and 965 bars, as the amount of generated products decreased due to the pressure increase. Likewise, qualitative aspects of the extracted bitumen (i.e., maturation indices) shifted from moderately-mature to immature values. Thus, at 287°C and 31 bars, the gas chromatograms (not shown) of the C_{8+} saturated HC's had moderately mature characteristics: 1) n-paraffin concentrations generally greater than that of both adjacent isoprenoid HC's and of biomarker peaks; and 2) a regular n-paraffin profile (Price and Wenger, 1992, their Fig. 7. However, at 287°C with increasing pressure, C_{8+} saturated HC distributions become increasingly immature, with that of the 287°C and 865 bar sample being quite immature (n-paraffin concentrations equal to or less than that of adjacent isoprenoid HC's and biomarker peaks; an irregular n-paraffin profile; and a bimodal distribution in the naphthene envelope). These, and much other data (Price and Wenger, 1992), demonstrate that increasing static-fluid pressure retards HC generation.

With increasing temperature, by 350°C and 118 bars, the aqueous-pyrolysis experimental system for the Phosphoria shale was strongly into the thermal cracking phase for C_{5+} generation products because the sum of the C_{5+} products decreased from a maximum value (versus temperature) of over 160 mg/g of rock at 333°C to 31 mg/g rock at 350°C (Fig. 6-8). However, at 350°C with

increasing pressure, by 1,077 bars, thermal cracking was retarded, such that the sum of the C_{5+} products increased from 31 to 88 mg/g rock (Fig. 6-10). Furthermore, whereas the C_1-C_4 HC gases made up 58.0% normalized percent of all the products by weight at 350°C and 118 bars, these gases made up only 16.9% of the total product by weight at 350°C and 1,077 bars. At 350°C with increasing pressures, qualitative aspects (maturation indices) of the bitumen and reacted rock also took on less mature characteristics and/or values, as was true in the 287°C experiments. Thus, the data from the 350°C experiments demonstrate that increasing static-fluid pressure also strongly retards the thermal destruction of C_{15+} HC's at a given temperature.

These experiments have implications regarding both HC generation and thermal destruction in nature. Consider two situations, all other things being equal, but one with a high geothermal gradient and the other with a low geothermal gradient. HC generation may be expected to occur at lower burial temperatures in the high geothermal gradient case compared to the low geothermal gradient case due to shallower burial depths and thus the lower static-fluid pressures. The retardation of C_{15+} HC thermal destruction at high static-fluid pressures helps explain the presence of moderate to high C_{15+} HC concentrations from deep (7-10 km) high-rank rocks of deep wellbores where the existence of such HC's would not otherwise be expected (discussed below).

Abnormal-fluid pressures would accompany maximum heat flow in deep basins. Thus with increasing burial, the tendency of higher burial temperatures to destroy C_{15+} HC's would be offset by concurrent increasing static-fluid pressures, which inhibit C_{15+} HC thermal destruction. Light oil, condensate, and especially gas deposits may be expected at higher burial temperatures than predicted by some organic-geochemical models, because of the suppression of C_{15+} HC thermal destruction by high static-fluid pressures. Computerized models of HC generation and maturation do not employ static-fluid pressure as a variable. Inclusion of this controlling parameter of organic metamorphism in such models, may allow nature to be more closely represented.

OM TYPE

OM Type, in my opinion, plays a dominant and generally unappreciated role in HC generation and to a lesser extent in the generation of high-rank methane. Different OM Types have different distributions of bond strengths, and thus different activation energies, and as such require significantly different burial temperatures for HC generation. Although it is recognized that some differences exist in the reactivities of the different OM types, in my opinion the magnitude of these differences has gone unappreciated. Also, there is not uniform agreement among petroleum geochemists as to the direction of the effect for any given OM type. Type II-S (sulfur-rich, marine) OM has weak, sulfur-bearing bonds and begins HC generation first, at low (R_o = 0.4%?), but yet undefined, maturation ranks, yielding a very heavy, sulfur-rich oil (Lewan, 1985; Orr, 1986; and Wenger and Price, 1991). However, Type II-S OM retains significant HC generation potential to high ranks, and oil quality dramatically improves with rank. Type III OM, with oxygen-bearing bonds, some of which are relatively weak, begins HC generation next at R_o = 0.6% and suffers loss of all HC generation potential by R_o = 2.00% (Figs. 6-4, 6-5, 6-14, 6-18). Types I and II OM, with relatively strong bonds, generate last, and the higher the original hydrogen content on the kerogen, the higher the burial temperature needed to initiate HC generation (Price, 1988, 1991). This scenario contrasts with models which have been presented by some investigators (see Tissot and others, 1987, their Fig. 26, for example) wherein Type II OM is held to begin HC generation substantially before Type

III OM. Ungerer (1990) also has proposed that Type II OM generates before Type I OM, which generates before Type III OM. However, such HC generation models are derived from ROCK EVAL kinetics, where thermal kerogen degradation occurs in open, low-pressure, water-free systems, and significant percentages of reaction products are chemical artifacts not found in nature. In contrast, natural HC generation occurs in high-pressure, water-bearing, closed systems. ROCK EVAL is a convenient method to examine kerogen thermal degradation. However, it is tenuous to extrapolate to nature results from experiments carried out under conditions unlike those found in nature where some products from those experiments are unlike HC generation products in nature.

Hydrous-pyrolysis (Lewan, 1983, 1985, 1992) and aqueous-pyrolysis (Wenger and Price, 1991; Price and Wenger, 1992) experiments carried out in closed, water-bearing, pressurized systems yield products which are very similar and often identical to those found in nature and thus these experimental techniques clearly simulate natural OM metamorphism much closer than ROCK EVAL pyrolysis. Results from such experiments yield a significantly different scheme of reaction kinetics for the different OM Types than the results from ROCK EVAL pyrolysis.

In aqueous-pyrolysis experiments of Wenger and Price (1991) and Price and Wenger (1992) carried out by L.C. Price and L.M. Wenger at the U.S. Geological Survey, six different rocks (Table 6-1) with widely different OM types were run under the same experimental conditions (different reaction temperatures, 150°-450°C, in 25°C intervals, at constant pressures, for 30 days, see Price and Wenger (1992) for a description of experimental conditions and techniques). Because all experimental conditions were held constant except for OM type, the reaction extent of the different OM types (and thus OM type reactivity) can be directly compared to one another at each experimental temperature (Fig. 6-11). In Fig. 6-11, C_{8+} saturated HC gas chromatograms for the starting rock ("Raw Rock") and two experimental temperatures are presented for three of the rocks of Table 6-1. Comparison of the gas chromatogram of the 200°C experiment to that of the raw (starting) sample for the carbonaceous Anna shale (moderately hydrogen-poor Type III/II OM, HI = 320) shows that distinct differences are present between the two chromatograms. In the 200°C Anna chromatogram: 1) there are noticeably greater concentrations of n-paraffins; 2) ratios of different compounds to each other have changed, e.g. - n-C_{18}/phytane (an especially useful maturity index which can be used to track HC generation), n-C_{17}/pristane, n-C_{16}/i-C_{18}; and 3) noticeable differences occur in the peak distribution of the biomarker range compounds (n-C_{26} to n-C_{35}). The chromatogram for the 275°C Anna shale experiment has extreme differences compared to that of the raw sample, because by 275°C this rock is well into intense HC generation.

In contrast, the C_{8+} saturated HC gas chromatograms for the raw and 200°C sample of the mid-Miocene shale from the Los Angeles basin (moderately hydrogen rich, Type II OM, HI = 500) demonstrate only minor differences from one another because only insignificant HC generation has taken place at 200°C. Although noticeable HC generation has occurred in this rock by 275°C, the 275°C Los Angeles sample still exhibits pronounced immature characteristics compared to the 275°C Anna sample: 1) an irregular n-paraffin distribution; 2) lower ratios of n-C_{17} and n-C_{18} to their adjacent isoprenoid HC's pristane and phytane; 3) a bimodal naphthenic envelope (especially noticeable in the C_{15+} saturated HC gas chromatogram, not shown); 4) noticeable biomarker peaks; and 5) a lower concentration of C_{14}-HC's.

C_{8+} saturated HC gas chromatograms for the raw and 200°C samples from the Eocene Green River Shale are identical because no HC generation has occurred in the very hydrogen-rich OM (Type I, HI = 805) of this rock at 200°C. Furthermore, the reaction extent in the OM of the Green River shale is minimal at 275°C, compared to that of the other two rocks at 275°C. The data of Figure 6-11 clearly demonstrate that significantly greater burial temperatures are required to initiate mainstage HC generation in hydrogen-rich OM compared to hydrogen-poor OM. These differences are probably caused by higher activation energies in hydrogen-rich OM compared to hydrogen-poor OM. In sulfur-poor, hydrogen-rich OM, activation energies are believed to increase with increase in the original hydrogen content of the kerogen.

The control that OM type has on kerogen reactivity can also be seen in samples from the natural system, if such control is carefully looked for. Based on a large unpublished U.S. Geological Survey petroleum-geochemical data base for the Los Angeles, Ventura, and Southern San Joaquin Valley Basins, intense HC generation does commence at burial temperatures of 120°-125°C (R_O ~0.6%) as reported by Phillipi (1965), in rocks with Type III OM (HI ≤250) in those basins. However, concurrently in these basins, in rocks with high HI's (and thus hydrogen-rich OM), commencement of HC generation is not detected at highly elevated burial temperatures, for example not by 200°C in the Wilmington field, Los Angeles Basin (Price, 1983, Figs. 3 and 4) and not by 210°C in the Shell Taylor 653 well bore, Ventura Basin Price, 1988, p. 31). In fact, all organic maturation indices are suppressed in rocks with high HI's, and the higher the HI, the greater the degree of suppression of reaction extent for any given burial temperature range (Figs. 6-12 and 6-13). R_O is perhaps the most widely used organic maturation index, and increases in the values of the ROCK EVAL S_1 pyrolysis peak, and the transformation ratio, are easily measurable, direct consequences of C_{15+} HC generation. In Figures 12 and 13 , as sample HI's increase, the values of the three parameters discussed directly above strongly decrease. In the California petroleum basins, rocks with high HI's retain very immature characteristics to highly elevated burial temperatures, and give no indication that they have commenced intense HC generation at these burial temperatures.

Differences in reaction kinetics between different OM Types are also demonstrated by data from organic-geochemical studies of deep well bores (Price, and others, 1979, 1981; Sagjó, 1980; Price, 1982, 1988; and Price and Clayton, 1990). In these wells, an orderly progression of organic maturation proceeds with depth in thick sequences of rocks with Type III OM, often with kerogen burnout (loss of all HC generation potential) being reached in Type III OM by R_O = 2.0%, as shown by zero or near zero HI's or by kerogen elemental hydrogen to carbon (H/C) ratios of 0.29-0.32 or lower. With further increase in depth and passage into rocks which were deposited under different conditions and which contain a marine-derived, more hydrogen-rich OM, HI's and kerogen HC ratios increase to moderate or even high values. Furthermore, an entirely different maturation progression takes place in these rocks, as demonstrated by the data of the Foerster-1 wellbore (Price and Clayton, 1990). Thus various maturation indices (whether measured from whole rocks, extracted bitumen, or macerated kerogen) after continuously increasing with depth in rock sequences with Type III OM, strongly reverse themselves to more immature values in passing into deeper rocks with more hydrogen-rich OM. Double HC generation zones have been reported in some deep wells (Kontorovich and Trofimuk, 1976; Sagjó, 1980; and Price and Clayton, 1990), the shallower zone being due to Type III OM, and the deeper zone presumably being due to hydrogen-rich OM. Lastly, the deep rocks in these well bores retain

measurable to moderate HC generation capacity (HI's) to extreme maturation ranks, far past R_O = 2.0%, the thermal burnout for Type III OM.

The Ralph Lowe-1 wellbore serves as an example (Fig. 6-14). The kerogen in rocks shallower than 7,010 m (23,000 ft) in this well is dominated by vitrinite and inertinite (Type III OM). However, the deepest rocks of this wellbore contain an overmature, hydrogen-rich OM made up largely of amorphous kerogen (column A, Fig. 6-14). HI's approached and reached values of zero at Ro ≥ 2.0% in this wellbore (column C, Fig. 6-14) as is typical for Type III OM (Figs. 6-4 and 6-5). However, with the shift in OM Type at well bottom to a more hydrogen-rich OM, HI's dramatically increased. The behavior in the HI's was mirrored by parallel changes in the kerogen atomic H/C ratios (column B, Fig. 6-14). Dramatic increases in both C_{15}+ bitumen and C_{15}+ HC concentrations accompanied this shift in OM type at depth in the Ralph Lowe-1 wellbore (columns E and F, Fig. 6-14).

Petroleum-geochemical data from another deep wellbore, the 9,590 m (31,464 ft) Bertha Rogers-1, Washita Co., Oklahoma, also demonstrate the control that OM Type has on HC generation reactions. The rocks from 0 to 5,338 m (17,514 ft) in this well contain Type III OM. As such, both HI's and the kerogen H/C ratio progressively decrease with depth (Fig. 6-15), with the HI's projecting to zero values at about R_O = 2.0% (dashed line, column D, Fig. 6-15), again typical behavior for Type III OM. However, the Pennsylvanian Morrowan and older rocks (5,338 m--17,514 ft and deeper) were deposited under more marine conditions and as such contain a more hydrogen-rich OM than the shallower rocks. Hence, both HI's and kerogen atomic HC ratios exhibit dramatic increases in the deeper rocks (columns B and D, Fig. 6-15). With further increase in depth, kerogen H/C ratios again continuously decrease to low values (0.25-0.30) at well bottom. The behavior of the HI in the deeper rocks is clouded by a large scale expulsion of bitumen generated by the organic-rich Woodford shales at depth into the adjacent organic-poor rocks. The ROCK EVAL analysis includes the resins and asphaltenes in this migrated bitumen in the S_2 pyrolysis peak. Thus the elevated HI's at depth do not reflect the true HC generation capacity (which would be low) of these organic-poor rocks, if the rocks were Soxhlet extracted.

Accurate cross comparisons of reaction kinetics for the different OM Types from natural samples have previously been obfuscated by the fact that it is very difficult to obtain valid maturation-rank estimates which can be directly related to R_O and/or paleo-burial temperatures, from natural samples which contain Types I and II OM. It is recognized that R_O in Types I and II OM is suppressed at any rank compared to what would be read in Type III OM (Price and Barker, 1985). However, all maturation reactions, including R_O, proceed at slower rates for any given thermal history in sulfur-poor, hydrogen-rich OM, compared to Type III OM buried under the same conditions (Price, 1991). Thus, it is currently not possible to assign accurate maturation ranks to sections of rocks which do not contain Type III OM, such as the Jurassic section of the Paris basin, the Lower Cretaceous through the Jurassic section of the Greater Gulf Coast, and the Eocene to the uppermost Cretaceous section in the Uinta basin. The true maturity of carbonate-evaporiate sections presently cannot be estimated with any confidence.

The above discussion demonstrates that OM Type has a dominant control on HC generation. Hydrogen-rich Types I and II OM both require higher burial temperatures than Type III OM to commence HC generation and also retain measurable (and sometimes moderate to high) HC generation potential to much higher ranks than Type III OM. The bearing that these conclusions have on high-rank gas deposits is discussed below.

ALTERNATE RANKS FOR SOME PETROLEUM-GEOCHEMICAL EVENTS

The R_o-event pairs of Figure 6-1 are accepted as geochemical law. However, that a large body of published data do not fall within the constraints of Figure 6-1 suggests that significant problems may exist with Figure 6-1. Figure 6-4 provides insight to this point. The S_1 pyrolysis peak is a measure of C_{15+} HC generation. Thus the increase in the S_1 pyrolysis peak values (Fig. 6-4) at R_o = 0.6% (due to an increase in Soxhlet-extractable HC's) results from the commencement of HC generation. This increase in C_{15+} HC's at R_o = 0.6% has been equated to the first possibility of commercial-oil deposits. The maximum in the S_1 pyrolysis peak at R_o = 0.9% has been equated to the maximum in HC generation, with C_{15+} HC thermal destruction occurring at higher R_o values, and being complete by R_o = 1.35%. However, the coals at R_o ≥1.35% still retain high HI's and thus significant HC generation capacity. Furthermore, pyrolysis-gas chromatography (Teichmüller and Durand, 1983) on some of the high rank coals of Figure 6-4 demonstrated that part of this generation capacity was for C_{15+} HC's (approximately 37% for coals at R_o = 1.35%, Fig. 6-16). Clearly the bonds broken in HC generation are weaker than those broken in HC thermal destruction. Thermodynamic or kinetic models are simply not possible wherein C_{15+} HC's can be thermally destroyed before they are generated. Thus the data of Figures 6-4, 6-5, and 6-16 demonstrate that the low S_1 pyrolysis peak values at R_o ≥1.35% must be due to causes other than HC thermal destruction.

Those causes are most probably primary migration by gaseous solution and loss of generated HC's to the drilling mud during the rock trip up the well bore in drilling operations. In Figure 6-4, HC concentrations (the S_1 pyrolysis peak) increase at R_o = 0.6% from commencement of HC generation. However, *intense* HC generation commences with the first noticeable decrease in maximal HI values of the coals, which occurs at R_o = 0.8%. Aqueous-pyrolysis experiments of Wenger and Price (1991) demonstrate that with commencement of intense HC generation, intense generation of HC gases also commences, and thus intense primary migration by gaseous solution (Price, 1989a,b). Such a migration contributes to the decrease in HC concentrations observed in Type III OM at R_o ≥0.8% to 0.9%.

However, the greatest loss of generated HC's results from the large pressure decreases which occur during the rock trip up the wellbore in drilling operations, especially when rocks contain gas prone Type III OM. This HC loss has been discussed in some detail in Price and LeFever (1992) in detail but will be reviewed here. Price and Clayton (1992) have demonstrated that a crude-oil like phase is prefractionated from the whole bitumen in organic-rich source rocks and concentrated in cracks and parting laminae in such rocks ready for expulsion. As conventional core and cuttings chips ascend the well bore during drilling operations, the rocks undergo large fluid pressure decreases, from high formation pressures at depth to atmospheric pressure at the wellhead. Deep (7,620 m--25,000 ft) Gulf Coast shales, for example, would suffer pressure decreases of 20,000-24,000 psi at depth, to less than 15 psi at wellhead. Gases present both in the rocks, and in the bitumen in the rocks, greatly expand in volume as pressure decreases in partial response to the ideal gas law PV=nRT, and almost totally exit from the rocks to the drilling muds. Such gases, moving from interior rock volumes, blow out oil-like bitumen concentrated in parting laminae and fractures into the drilling mud. Sokolov and others (1971) provided insight into the magnitude of this HC gas loss (Table 6-2). They took rock samples at depth and at formation pressure in what they termed the "KC lifter" (a pressure core barrel sampler) and brought the samples to the surface, sealed and at formation pressure, with no gas loss. Sokolov and others (1971) compared the

amount of gas recovered in this manner to that recovered during an open-hole rock trip up the wellbore, where only 0.11-2.13% of the gas originally in the rock was recovered.

Observations by wellsite geologists and drilling personnel corroborate the results of Sokolov and others (1971). Cuttings chips of organically-mature, fine-grained rocks violently spin and fizz at wellhead from outgassing of only the gas remaining in the rocks at wellhead, which is a small fraction of the gas originally present in the rock, before the trip up the wellbore. When drilling through mature organic-rich rocks, mud gas-logging values always dramatically increase from the outgassing of these rocks into the drilling mud. Occasionally, the logging results from such shales are deleted, as the shale values can be so large as to overshadow values from possible gas-bearing, coarse-grained rocks. While drilling through organic-rich, mature, fine-grained rocks, mud-fluoresncence values also always dramatically increase due to the effusion of oil-like bitumen from these rocks into the drilling mud. When mature Bakken shales in the Williston basin are drilled with a water-based drilling mud, an oil film always covers the mud pit. Source rock cores crackle in the core barrel from gas loss at wellhead, or bleed oil while being held at wellhead, and can continue to bleed oil long after while sitting in the laboratory. This HC loss is enhanced during drilling operations when cores, and especially cuttings chips, are highly disrupted by the drill bit. Although many petroleum geochemists do not appreciate the magnitude of this HC loss from mature source rocks during the rock trip uphole, this large HC loss from mature source rocks has been well known to well-site geologists for over 40 years (C.W. Spencer, written communication 7/7/91).

It is maintained here that the hypothesized thermal deadline of C_{15+} HC's at R_o = 1.35%: 1) is incorrect, and 2) originated from an assignation of the decrease of C_{15+} HC concentrations in Type III OM at R_o ≥0.9% to HC thermal destruction, when this decrease was most probably due to primary migration and loss to drilling mud during the rock trip uphole in drilling operations.

The data of Figure 6-4 suggest alternate ranks to those of Figure 6-1 for important petroleum-geochemical events in Type III OM. HC generation does commence by R_o = 0.6%. However, intense HC generation and primary migration commence at R_o = 0.8%, and largely occur over R_o = 0.9%-1.6%, over which the greatest loss of HI's occur (Figs.6-4 and 6-5). HC's cannot form oil deposits until they leave the source rocks (expulsion), which commences at R_o = 0.9% and corresponds to the significant decrease in the S_1 pyrolysis peak values at that rank. Thus R_o = 0.9% would be a better estimate than R_o = 0.6% for the first possibility of commercial-oil deposits. Type III OM loses most or all HC generation potential by R_o = 2.0% (zero or near zero HI's, Fig. 6-4 and 6-5). However, this is not equivalent to C_{15+} HC thermal destruction, because Types I and II OM retain remnant to moderate HC generation potential to much higher ranks (discussed above and below).

HC THERMAL STABILITY LIMITS

There are three possible approaches to determine HC thermal-stability limits: (1) Quantitative and qualitative changes, versus maturation rank, can be examined in HC's from rocks which have been at high paleo burial temperatures in deep well bores. (2) Aqueous-pyrolysis experiments can be performed at temperatures high enough to result in HC thermal destruction. (3) Qualitative changes can be examined in HC compositions of gas condensates or light oils which have previously been exposed to high paleo burial temperatures.

DEEP WELLBORE DATA

Detailed petroleum geochemistry of high-rank rocks (Table 6-3) from deep (7-10 km) well bores (Price and others, 1979, 1981; Price, 1982, 1988; Price and Clayton, 1990) demonstrates that moderate to high concentrations of both C_{15+} HC's and C_{15+} bitumen (Fig. 6-17) can persist to elevated maturation ranks (R_O = 2.0%-7.0%). Furthermore, other investigators have reported similar results (Kontorovich and Trofimuk, 1976; Sagjó, 1980; Guthrie and others, 1986). Such data do not conform to the hypothesis of a thermal destruction of C_{15+} HC's by R_O = 1.35%. Some investigators have attributed the data of Figure 6-17 as simply due to caving or contamination by organic-based drilling fluids. These possibilities were thoroughly discussed (and dismissed) in each of the above publications. Singular compositional characteristics of the high-rank HC's, or of the rocks from which they were derived, for all the wells of Table 6-3 demonstrate that the measured high-rank HC's were indigenous. The data from the Ralph Lowe-1 (discussed above, Fig. 6-14) serve as an example, and data from Chevron R. G. Jacobs-1, Goliad Co., Texas (Fig. 6-18), serve as another example.

In Figure 6-18, the Tertiary rocks shallower than 4,270 m (14,000 ft) all contain Type III OM, and the usual increase in C_{15+} bitumen for Type III OM is evident at R_O = 0.6%, with a maximum in the bitumen coefficient at R_O = 0.9% and decreasing values at higher ranks. As characteristic of Type III OM, by R_O = 2.00%, the Tertiary rocks have lost all HC generation capacity as shown by the low and decreasing HI values at those ranks. (The low HI value for the sample at 914 m (3,000 ft) (R_O = 0.5%) is from original depositional conditions and is not a result of OM metamorphism). At the top of the Lower Cretaceous section (wavy lines in TOC & HI plots, Fig. 6-18), different depositional conditions than those of the Tertiary rocks resulted in a marine Type II OM in the deeper rocks. This is demonstrated by the elevated HI's in the five Gulfian Series samples (dots below the wavy line, HI plot Fig. 6-18). These elevated HI's at R_O = 1.7-3.0% are: (1) from ground shales which had been Soxhlet extracted for 48 hours prior to ROCK EVAL analysis, (2) representative of HC generation potential indigneous only to the rock, and (3) clearly do not conform to the hypothesis of a thermal destruction of C_{15+} HC's by R_O = 1.35%.

The crosses at depths of 6,400 m (21,000 ft) and greater (Fig. 6-18) represent core samples from a low porosity-low permeability carbonate rock which had heavy oil staining as shown by residual oil saturation analyses (Fig. 6-19) performed by Core Labs. This oil staining: 1) causes the high bitumen coefficients (Fig. 6-18) in rocks at R_O = 4.25-6.5% and at present-day burial temperatures of 250° to 282°C; and 2) provide incontrovertible evidence of the thermal stability of C_{15+} HC's to extreme maturation ranks in highly-pressurized, tight, fine-grained (closed-system) rocks. The data of Figures 6-18 and 6-19 have been replicated by several laboratories other than those of the U.S. Geological Survey, Core Labs, and Chevron Oil Field Research.

The high concentrations of both C_{15+} HC's and C_{15+} bitumen (Fig. 6-14, columns E and F), found in the deep, high-rank rocks with hydrogen-rich OM in the Ralph Lowe-1 are other data which demonstrate that C_{15+} HC's are thermally stable to much higher maturation ranks than represented by the paradigm of Figure 6-1. It should be noted that the deep rocks from the Ralph Lowe-1 wellbore also retain significant HC generation potential (as reflected by their HI values) even to these extreme ranks which again demonstrates that Types I and II OM can retain significant remnant HC generation potential to much higher maturation ranks than Type III OM.

COMPOSITIONAL CHANGES IN SATURATED HC'S AT DESTRUCTION

Compositional changes in the saturated HC's during their thermal destruction are better appreciated by briefly reviewing gross compositional changes in the saturated HC's during HC generation. The gas chromatograms of Figure 6-20 are from aqueous-pyrolysis experiments performed on the carbonaceous Pennsylvanian Anna shale. The unreacted rock has total organic carbon (TOC) contents of 23-25% and contains Type III/II OM (HI = 320). Typically, immature (pre-HC generation) saturated HC's (with some variance due to OM Type) have (Fig. 6-20): (1) bimodal distributions in large naphthenic envelopes, (2) low concentrations of n-paraffins relative to adjacent isoprenoid HC's, (3) large biomarker peaks (over the carbon number range 26-32) relative to adjacent n-paraffins, (4) an irregular n- paraffin profile (distribution), and (5) low concentrations of C_{15}-HC's. During HC generation, these characteristics progressively change (Fig. 6-20) and gas chromatograms of mature saturated HC's have: (1) small naphthenic envelopes with unimodal distributions, (2) n-paraffins with a regular profile and in high concentrations relative to both adjacent isoprenoid HC's and biomarker peaks, and (3) high concentrations of C_{14}- HC's.

Changes in saturated HC's during thermal destruction are demonstrated by the gas chromatograms of Figure 6-21 from aqueous-pyrolysis experiments on the shale of the Retort member of the Permian Phosphoria Formation and on a hydrogen-poor lignite. The Phosphoria shale sample run at 350°C and 1,077 bars is in the middle of mainstage saturated HC thermal destruction. As such, total C_{5+} extractables have decreased to 83 mg/g rock from 161 mg/g of rock at the next lowest experimental temperature (333°C, 80.8 bars). In the gas chromatogram of the 350°C and 1,077 bar sample, the thermally-labile isoprenoid HC's, especially pristane and phytane, are in greatly reduced concentrations relative to their adjacent n-paraffins (compare to the 333°C Anna shale chromatogram Figure 6-20). Furthermore, the concentration of each isoprenoid HC decreases with increase in isoprenoid HC carbon number. Also, the naphthenic envelope is quite small, and the smooth logarithmic n-paraffin distribution suggests that a kinetic or thermodynamic (metastable?) equilibrium has been established within the n-paraffins. In another 350°C Phosphoria shale experiment, system pressure was decreased from 1,077 bars to 119 bars, which illustrates the effect of increasing fluid pressure on retarding OM metamorphism. The 119 bar sample is near the end of saturated HC thermal destruction and C_{5+} extractables have decreased to 31 mg/g rock from 83 mg/g rock in the 350°C and 1,077 bar sample. The isoprenoid HC peaks are in reduced concentrations, note the absence of pristane and phytane. The isoprenoid HC's, and all other peaks between the n-paraffins, decrease in concentration with increasing carbon number. The concentrations of the C_{25+} n-paraffins are also reduced in the 119 bar sample, compared to those in the gas chromatogram from the 1,077 bar sample, and there is almost no naphthenic envelope.

The lignite run at 350°C and 125 bars is at the end of C_{15+} saturated HC thermal destruction. Comparison of the gas chromatogram of this sample with the chromatogram of the Phosphoria 350°C and 119 bar experiment demonstrates the effect of product escape on OM metamorphism. The hydrogen-poor lignite (HI's = 55 for the unreacted rock) has a low HC-generating capacity compared to the hydrogen-rich OM in the Phosphoria shale (HI's = 450 in the unreacted rock). The 350°C and 125 bar lignite and 350° and 119 bar Phosphoria shale experiments were run essentially under the same conditions. However, the C_{15+} saturated HC concentration in the lignite experiment was 0.19 mg/g rock versus 3.85 mg/g rock in the Phosphoria shale experiment. The low concentration of

saturated HC's (and total bitumen) in the lignite experiment allowed saturated HC thermal destruction to proceed further compared to similar experiments with more organic-rich rocks. As such, in the lignite chromatogram: (1) All C_{27+} saturated HC's have been thermally destroyed. (2) Peaks other than the n-paraffins are in very small concentrations. (3) No naphthenic envelope is present. (4) The n-paraffins make up 95-99% of the sample. In the 375°C and 132 bar experiment, the thermal deadline for C_{15+} saturated HC's has been passed, and all C_{14+} saturated HC's have been destroyed.

Saturated HC's have the following characteristics during their thermal destruction as delineated by U.S. Geological Survey aqueous-pyrolysis experiments (Wenger and Price, 1991; Price and Wenger, 1992). The thermally-unstable 4 and 5 ringed naphthenic HC's crack first, followed by the isoprenoid HC's, and then the iso-alkanes. The n-paraffins are the most stable of the common saturated HC's. This fact was also noted by Sassen and Moore (1988) in their study of high rank gas condensates from Jurassic Smackover Limestone reservoirs. Within any one compound group, as carbon number, or length of side chain, increases, compound stability decreases with increasing temperature. *Thermally-stressed saturated HC's are readily characterized by low or zero concentrations of pristane and phytane.*

These observations regarding the relative thermal stability of the different saturated-HC compound classes in the aqueous-pyrolysis experiments require discussion. Firstly, the naphthenes might be expected to undergo aromatization rather than simply thermally crack, and to a limited extent this may have occurred. However, C_{15+} aromatic HC concentrations also strongly decreased in going from the maximum of C_{15+} HC generation (333°C) to HC thermal destruction (350°C) in the aqueous-pyrolysis experiments for all rocks. For example, with the Phosphoria shale, C_{15+} aromatic HC's decreased from 27.3 mg/g rock at 333°C to 7.93 mg/g rock at 350°C. Hence, a wholesale aromatization of naphthenes would appear unlikely. Secondly, the observations about the relative thermal stability of the different saturated-HC compound classes contradicts Mango's (1990) conclusions that the naphthenes are the most stable saturated-HC class. However, Mango's (1990) conclusions and discussion are based principally on the C_5-C_9 cyclo-alkanes, and Mango's (1990) principal conclusions in this regard are in agreement with other data of this study. Namely: 1) The single ring cyclo-alkanes are remarkably thermally-stable. 2) There is no evidence that the high concentrations of C_5-C_9 cyclo-alkanes in oils are derived from the decomposition of 4-5-ringed naphthenes.

Mango (1990) actually provided no conclusive evidence for enhanced thermal stability of 4-5 ringed naphthenes. The one multi-ring (bicyclic) compound he discusses, decahydronaphthalene (decalin), is not found in abundance in nature. A thermal cracking experiment he carried out (cholestane and octadecane at 330°C, dry?, four weeks) if anything showed that the naphthene was less thermally stable than the n-paraffin (17% destruction versus 2.3% destruction, respectively). However, a more meaningful experiment would be in a wet system at 345°-350°C with cholestane and a higher molecular weight n-paraffin (e.g. - C_{27}-C_{30}). Furthermore: 1) As will be discussed, natural samples also exhibit greatly reduced concentrations of 4-5 ringed naphthenes relative to equivalent carbon-numbered n-paraffins during thermal destruction. 2) As stated, Sassen and Moore (1988) also concluded that the n-paraffins were the most stable higher molecular weight species within the saturated HC's in their study of thermally-stressed gas condensates.

C_{8+} saturated HC gas chromatograms from highly-mature gas condensates from Jurassic Smackover Limestone reservoirs in Alabama from the Chatom and Big Escambia Creek fields are shown in Figure 6-22. The marked similarity of these two chromatograms to the C_{8+} saturated HC chromatogram from the Phosphoria shale 350°C and 119 bars experiment (Fig. 6-22) strongly suggests that the two gas condensates were derived from, or exposed to, conditions equivalent to mainstage saturated HC thermal destruction.

Gas chromatograms of C_{15+} saturated HC's (Fig. 6-23) from high-rank rocks of deep well bores are quite mature. Nonetheless, comparison to the C_{15+} saturated HC chromatogram from the Phosphoria shale 350°C and 119 bar experiment suggests that, except for the Foerster-1 sample, none of the other samples have entered mainstage HC destruction. Four of these chromatograms (Rogers-1, Lowe-1, and two Jacobs-1), in spite of their extreme maturation ranks have large pristane and phytane peaks and significant naphthenic envelopes. The reduced pristane and phytane peaks in the chromatogram from the Foerster-1 sample, and other data discussed in Price and Clayton (1990) which will not be discussed here, show that the Foerster-1 sample has just entered C_{15+} saturated HC thermal destruction. The apparent large naphthenic envelope of the Foerster-1 sample is an analytical artifact caused by laboratory evaporative loss of C_{18-} HC's.

Differences between the Foerster-1 and Rogers-1 chromatograms can be ascribed to differences in paleo fluid pressures. The deeper Rogers-1 sample has an extrapolated R_o value of 7.6% versus an extrapolated R_o value of 7.0% for the Foerster-1 sample. However, the saturated HC's from the Foerster-1 sample have attained slightly higher levels of OM metamorphism than those from the Rogers-1 sample. The 2,750 m deeper Rogers-1 sample would have experienced substantially (25 to 50%) higher paleo fluid pressures than the Foerster-1 sample, assuming near lithostatic abnormal fluid pressure gradients at the time of maximum heat flow for the two wells. Thus the Foerster-1 sample could have achieved a higher level of OM metamorphism than the Rogers-1 sample because of lower paleo fluid pressures.

Data from high-rank rocks from deep well bores demonstrate that C_{15+} saturated HC's persist to extrapolated R_o values of around, or above, 7.6% in situations with normal or low paleo geothermal gradients, and probably to values slightly below 7.0% in situations with very high paleo-geothermal gradients, because of the suppression effect that increasing fluid pressures have on OM metamorphism. Furthermore, high concentrations of bitumen and C_{15+} HC's (Fig. 6-17) can persist to reflectances of 3.0 to 5.0%. However, these conclusions relate only to the high-rank persistence of HC's in highly-pressurized, fine-grained rocks (closed chemical systems) which do not allow product escape. These conclusions have no bearing to either HC-generation reactions, which occur at much lower ranks, or to the possible existence of commercial-oil deposits at high maturation ranks.

COMPOSITIONAL CHANGES IN AROMATIC HC'S DURING DESTRUCTION

The aromatic HC's, like the saturated HC's, compositionally evolve through mainstage HC generation as demonstrated by C_{8+} aromatic HC gas chromatograms from aqueous-pyrolysis experiments on the Anna shale (Fig. 6-24). The chromatogram of the immature sample is dominated by one large peak (which elutes in the range of the alkylated benzenes) and has an unresolved naphtheno-aromatic hump with few peaks of significant size on it. The chromatogram from the sample at commencement of HC generation (250°C) has significant differences, with a series of well defined peaks on a large

naphtheno-aromatic hump. Aromatic HC's from mature (Anna shale, 333°C) samples: (1) are biased towards lighter compounds, (2) have a greatly reduced unresolved (naphtheno-aromatic) hump, (3) have reduced peak heights of higher-molecular weight aromatic HC's, and (4) are characterized by large concentrations of alkylated benzenes, alkylated naphthalenes, and alkylated phenanthrenes with the principal sulfur-bearing aromatic compounds being alkylated benzo- and dibenzothiophenes.

Throughout HC thermal destruction, the aromatic HC's are both more complex and thermally stable than the saturated HC's, as shown by C_{8+} aromatic HC gas chromatograms from aqueous-pyrolysis experiments carried out on the Phosphoria shale (Fig. 6-25). In these experiments, C_{8+} aromatic HC concentrations decreased from a maximum value of 33.8 mg/g rock at the maximum of HC generation (333°C and 80.8 bars) to 11.7 mg/g rock in the 350°C and 119 bar experiment (middle of mainstage HC thermal destruction). In the 350°C and 119 bar chromatogram, the unresolved naphtheno-aromatic hump is small, and the chromatogram is dominated by large peaks of alkylated: benzenes, naphthalenes, benzothiophenes, dibenzothiophenes, and phenanthrenes. In the 375°C and 132 bar Phosphoria experiment, C_{15+} saturated HC's were thermally destroyed (Fig. 6-21). However, a suite of C_{15+} aromatic HC's persists both in this experiment and in the 400°C and 144 bar experiment. These experimental data demonstrate that aromatic HC's are much more thermally stable than saturated HC's. The 375°C and 132 bar chromatogram of Figure 6-25 has become simpler compared to that of the 350°C and 119 bar experiment. This is in part due to the thermal destruction of the methylated benzothiophenes whose peaks no longer interfere with those of the methylated naphthalenes. The aromatic hump has also completely disappeared in the 375°C sample. The 400°C and 144 bar experiment (Fig. 6-25) would be equivalent to conditions of true rock metamorphism, yet a moderately complex distribution of aromatic HC's persists even to these conditions. In the 400°C experiment, aromatic HC's are dominated by both: 1) parent compounds (e.g., naphthalene, fluorene, phenanthrene, and dibenzothiophene), and 2) methyl variants of the parent compounds. Furthermore, dimethyl- and trimethyl-variants are in reduced concentrations and more highly alkylated species have been destroyed (Fig. 6-25, Tables 6-5 and 6-6).

Several points of qualification should be discussed. First, the aqueous-pyrolysis data of Figure 6-25 and Tables 6-5 and 6-6 are for aromatic HC's generated by the very sulfur-rich OM of the Retort member of the Phosphoria shale. The OM in almost all other rocks in nature contains far less sulfur than that of the Phosphoria shale, and therefore generates far lower quantities of sulfur-bearing aromatic HC's. The high concentrations of sulfur-bearing aromatic HC's in Figure 6-25 and Tables 6-5 and 6-6 are also present in lower-temperature aqueous-pyrolysis experiments on the Phosphoria shale. As such, pure aromatic HC peaks (e.g., the naphthalenes) are in smaller concentrations, and even sometimes drawfed by the sulfur-bearing aromatic HC's. Although sulfur-rich OM is present in nature, it is not the norm. Thus, the high-rank aromatic HC compositions of the Phosphoria shale (Fig. 6-25) should not be considered representative. For example, with OM of lower sulfur contents, the high concentrations of the alkylated benzothiophenes would be lower at experimental temperatures lower than 375°C (Table 6-5), and the high concentrations of dibenzothiophene and the methyldibenzothiophenes would be lower at all experimental temperatures (Table 6-6).

A second point to consider with high concentrations of sulfur-bearing aromatic HC's is that the utility of gas chromatography as an analytical tool is greatly diminished. This is because sulfur-bearing aromatic HC's coelute with the "normal" aromatic HC's beginning with the methyldibenzothiophenes coeluting with the methylnaphthalenes and proceeding through the methyldibenzothiophenes coeluting with the methylphenanthrenes. Thus quantitative, and even qualitative, gas chromatography is impossible with the aromatic HC's from samples with sulfur-rich OM, such as those from the aqueous-pyrolysis experiments on the Phosphoria shale, and mass spectrometry becomes necessary. Also, flame-ionization detection gas chromatography largely measures carbon-hydrogen bonds. Thus, the same concentration of a highly-alkylated species will give a much higher response than an equal weight of the parent compound (e.g. - pentamethylnaphthalene will give a much higher response than naphthalene in equal concentrations). Therefore, overall, mass spectrometry is a better analytical tool for aromatic HC analyses than gas chromatography.

The data of Tables 6-5 and 6-6 (and Fig. 6-25) demonstrate that unusual suites of aromatic-HC distributions are present in experiments even beyond 400°C. These data strongly suggest that low concentrations of such simple aromatic HC distributions: (1) should extend well into some high-pressure, high-temperature rock-metamorphic facies; (2) should be found in inclusions in some of the minerals of these regimes; and (3) may be utilitarian as geothermic-geobaric research tools.

The U.S. Geological Survey aqueous-pyrolysis experiments of Wenger and Price (1991) and Price and Wenger (1992) have shown that irrespective of the starting OM Type, in the thermal destructive phase, repetitive exact, or very similar, aromatic-HC distributions result, no doubt from response to thermodynamic and kinetic dictums on the systems. Such aromatic-HC distributions should be present and observable from many different high-pressure, high-temperature geologic regimes, including high-rank deeply buried sedimentary rocks. An example of very similar aromatic-HC distributions is given in Figure 6-26 for aqueous-pyrolysis experiments performed in the C_{15+} HC thermal destructive phase, on rocks with two different OM types (Table 6-1): a Los Angeles Basin mid-Miocene shale (Type II-S/III-S OM) and the Eocene Green River Shale (Type I OM). In spite of the large differences in OM types, the two sets of chromatograms are very similar. The 350°C chromatograms: 1) are dominated by the methyl-, dimethyl-, and trimethylnaphthalenes, and the methyl and dimethylphenanthrenes; 2) have reduced naphtheno-aromatic unresolved envelopes ("humps"); and 3) have a pronounced absence of higher-molecular weight compounds which are present in lower-rank samples (e.g., - Fig. 6-24, Anna Shale 250° and 333°C samples). The 375°C chromatograms (Fig. 6-26): 1) have essentially no unresolved "hump"; 2) have increased concentrations of methylated-naphthalenes relative to methylated-phenanthrenes; and 3) have become simpler with a significantly reduced number of prominent peaks.

The same, or very similar, aromatic-HC distributions present in high-temperature aqueous-pyrolysis experiments (333°-375°C) are also present in high-rank natural samples. For example, flame-photometric detection (FPD; specific for sulfur-bearing compounds) gas chromatograms are shown for C_{8+} aromatic HC fractions from two natural samples and from two samples from aqueous-pyrolysis experiments of equivalent maturities (Fig. 6-27). The Phosphoria 275°C and Orcutt oil field samples: 1) are both immature; 2) have large unresolved humps; and 3) have significant concentrations of alkylated-thiopenes (molecular weights 112, 126, 140, 154, 168, 182, 196, 210, etc., not

labeled Figure 6-27 but range from the first eluting peaks to about dibenzothiophene -184 DBT). The Phosphoria 350°C and Big Escambia Creek samples: 1) are both highly mature; 2) have no alkylated thiophenes, which have been thermally destroyed at lower ranks (only traces of 112-154 molecular weight alkylated thiophenes persist to 333°C, and no 168+ molecular weight thiophenes persist past 333°C in the aqueous-pyrolysis experiments, Table 6-5); 3) have become much simpler with the methyl-, dimethyl-, and trimethyl-benzothiophenes and dibenzothiophenes making up almost all of the sulfur-bearing aromatic HC's.

Details of changes within the higher molecular weight (methyldibenzothiophenes and heavier compounds) sulfur-bearing aromatic HC's versus maturity are shown in the FPD gas chromatograms of Figure 6-28 for three natural samples and for three aqueous-pyrolysis samples of equivalent maturities. The Cottonwood Creek oil sample and Phosphoria 287°C sample are both moderately mature and have large unresolved envelopes of high-molecular compounds which make up most of the sample, with only a limited number of well-resolved peaks on top of this envelope. The "M-DBT's" peaks in both samples are made up by the 1-, 2-, 3- and 4-methyldibenzothiophenes and by a yet unidentified series of methylnaphthenothiophenes, with the latter group of compounds being in larger concentrations in the Phosphoria sample. Dimethyl-, trimethyl-, and tetramethyl-naphthenothiophenes also coelute with the respective different classes of alkylated-dibenzothiophenes. The Pollard oil and 333°C Phosphoria samples: 1) are both mature; 2) have greatly reduced unresolved envelopes; and 3) a significant percentage of the sample is made up by the methyl-, dimethyl-, and trimethyl-dibenzothiophenes and naphthenothiophenes (198, 212, and 226 molecular weight compounds) Although no obvious alkylated-naphthenothiophenes are present in the Pollard sample, this may be due more to facies control of the original OM from which the Pollard oil was derived than a maturity control. The Phosphoria 375°C and Flomaton samples: 1) are both ultra mature and well into the C_{15}+ HC thermal destructive phase; 2) have no unresolved hump of higher-molecular weight sulfur-bearing aromatic HC's; and 3) are made up almost entirely of the (198) methyl-, (212) dimethyl-, and (226) trimethyldibenzothiophenes. A series of higher-molecular weight compounds (possibly naphthenobenzothiophenes?) is present in higher concentrations in the Phosphoria 375°C sample compared to the Flomaton sample. Note the similar distribution of methyl-, and dimethyl-dibenzothiophenes in both samples.

C_{15}+ non-sulfur bearing aromatic HC distributions from deeply-buried high-rank rocks from nature have the same trends as are present in aqueous-pyrolysis experiments at equivalent ranks as C_{15}+ HC thermal destruction is approached (Fig. 6-29). Because of the rank (R_o = 0.97%), the Ralph Lowe 2,709.5-2,712.6 m sample would be considered "mature" by many petroleum geochemists. However, it is far less mature than the other chromatograms of Figure 6-29. Among other characteristics, the Ralph Lowe chromatogram: 1) has a pronounced unresolved hump which extends to high-molecular weight compounds; 2) and has a significant percentage of higher-molecular weight compounds. The 8,210.9-8,357.2 m (R_o = 4.8%) Bertha Rogers C_{15}+ aromatic HC gas chromatogram has a reduced unresolved envelope, significantly reduced concentrations of higher-molecular weight compounds, and an increasing bias towards methyl-, dimethyl-, and trimethylnaphthalenes and phenanthrenes, and these trends strengthen through the Bertha Rogers 9,125.3-9,189.3 m (Ro = 6.9%) and 9,305.1-9,518.4 (R_o = 7.4%) samples. As discussed above, C_{15}+ HC thermal destruction was probably suppressed in the deep Bertha Rogers samples from high fluid pressures (2,150 bars and greater?) most likely present in the rocks at the time of maximum paleo heat flow in the basin. Thus, even though

the HC's of the deeper rocks in this well are at R_o ≤7.0%, they have not yet begun C_{15+} HC thermal destruction. However, the deepest samples from the Foerster-1 well bore were at lower fluid pressures which apparently allowed C_{15+} HC thermal destruction to commence in the Foerster-1 at equivalent ranks. Thus the 6,613.8-6,703.7 m (R_o = 7.0%) Foerster-1 samples (Fig. 6-29): 1) are largely made up of methyl-, dimethyl-, and trimethylnaphthalenes; 2) have moderate concentrations of phenanthrene and the methyl- and dimethylphenanthrenes; 3) have very small unresolved envelopes; and 4) have only minute concentrations of higher-molecular weight compounds. These compositional changes are the same as those observed in the U.S Geological Survey aqueous-pyrolysis experiments in the approach to, and in, C_{15+} HC thermal destruction (Figs. 6-24, 6-25, 6-26, and Tables 6-5 and 6-6). For example, note that the two deepest Rogers-1 samples (Fig. 6-29) resemble the 350°C C_{15+} aromatic HC gas chromatograms of Figure 6-26, whereas the two Foerster-1 chromatograms have characteristics intermediate between those of the 350° and 375°C chromatograms of Figure 6-26.

The above discussion demonstrates that like the saturated HC's, during C_{15+} HC thermal destruction, the aromatic HC's also follow distinct compositional trends. For example at high ranks, the sulfur-bearing aromatic HC's are made up principally of the methyl-, dimethyl-, and trimethyl-benzothiophenes and dibenzothiophenes and the parent compounds, benzothiophene and dibenzothiophene (Figs. 6-27 and 6-28). The lower molecular weight thiophenes, and the higher molecular weight sulfur-bearing compounds making up the unresolved hump in gas chromatograms of more immature samples are all thermally destroyed at high ranks. Non sulfur-bearing aromatic HC's at high ranks are made up largely by the methyl-, dimethyl-, and trimethyl-naphthalenes and phenanthrenes and by the parent compounds naphthalene and phenanthrene. Like the saturated HC's, within any one compound group (e.g., the naphthalenes), as molecular weight or length of side chain increases, thermal stability greatly decreases. Thus, during C_{15+} HC thermal destruction, ethyl, propyl, butyl (etc.) side chains are highly unstable compared to methyl groups. Also, during C_{15+} HC thermal destruction, all naphtheno-aromatic HC's which results in are destroyed, due to the relative thermal instability of the saturated HC's, which results in the disappearance of the aromatic hump at elevated maturation ranks. Thermally-stressed aromatic HC's are characterized by (Fig. 6-30): 1) high concentrations of alkylated benzenes (especially in oils and condensates; 2) an absence of alkylated thiophenes; 3) high concentrations of methyl-, dimethyl-, and trimethyl-naphthalenes, benzothiophenes, phenanthrenes, and dibenzothiophenes; 4) a small or no unresolved hump; 5) a lack of higher-molecular weight compounds; and 6) relatively simple peak distribution patterns.

C_{15+} HC THERMAL STABILITY-DISCUSSION

Although the hypothesis of the thermal instability of C_{15+} HC's at moderate burial temperatures (150°-200°C) is generally accepted as a law in petroleum geochemistry, other investigators have questioned the validity of this hypothesis. Shock (1990), Mango (1991), and Helgeson (1992) have addressed HC thermal stability from theoretical considerations, and have all concluded that HC's have significantly greater thermal stability than called for by current petroleum-geochemical paradigms. Hayes (1991) pointed out that current petroleum geochemical paradigms regarding C_{15+} HC thermal stability required serious reconsideration.

The theoretical considerations of the above workers are supported by the very high activation energies must be overcome for carbon-carbon bond breakage during HC thermal destruction. The average activation energy for carbon-

carbon bond breakage in saturated HC's is 82.6 kcal/mole (Cottrell, 1958; Pauling, 1960; Roberts and Caserio, 1964; Klotz, 1964; Eggers and Halsey; 1964). The activation energy for carbon-carbon bond breakage of the benzene ring is 117 kcal/mole (Gould, 1959). These differences in bond strengths between saturated and aromatic HC's explain the much greater thermal stabilities of aromatic HC's observed in the aqueous-pyrolysis experiments discussed above. Activation energies for HC generation reactions (from kerogen) have been experimentally estimated from both open and closed system pyrolysis to be in the range of 42-58 kcal/mole, varying as a function of OM type or experimental method (Akihisa 1978; Lewan 1985; Ungerer and others, 1986; Burnham and others, 1987; Novelli and others, 1987; Tissot and others, 1987; Espitalié and others, 1988; Zumberge and others, 1988, Burnham 1989; Castelli and others, 1990). From Figure 6-4, most HC generation (and loss of HI's) occurs over R_o = 0.8-1.6% in Type III OM. Thus HC thermal destruction, which must overcome activation energies of 82.6-117 kcal/mole, would be expected to occur only at extreme maturation ranks.

In addition to the data discussed above for high-rank rocks at high burial temperatures from deep well bores, C_{15+} HC's have been reported by different investigators from a variety of high-temperature geologic settings. Baker and Claypool (1970) found measurable concentrations of Soxhlet-extractable HC's in various metamorphic rocks. Forsman and Hunt (1958) reported remnant HC generation capacity, as determined by hydrogenolysis, on some kerogens in metamorphic rocks they studied. Hoering and Hart (1964) reported on a graphite schist, whose kerogen still retained remnant generation potential for both methane and heavier HC's. Shepeleva and others (1990) described aromatic HC suites they found in kimberlite pipes, hydrothermal ore deposits, and crystalline bedrock in the Daldyn-Alakit region, Siberia, USSR. Goffé and Villey (1984) reported crude-oil like HC distributions in mineral inclusions in metamorphic rocks they studied in the French Alps. High temperature (300°-350°C) petroleum in the hydrothermal vent water of the Guaymas basin spreading center is well known (Simoneit 1983, 1984, 1985; Simoneit and others, 1984; Simoneit and Kawka, 1987; Kawka and Simoneit, 1987). Other examples could be given.

The above data allow the conclusion that not only methane but also C_{15+} HC's are thermally stable in fine-grained rocks to much higher maturation ranks than called for by current petroleum geochemical paradigms (Fig. 6-1). C_{15+} HC's apparently approach thermal destruction in the range of R_o = 7.0-8.0% depending on basin variables. Methane clearly would be thermally stable to far higher temperatures and ranks than R_o = 7.0-8.0%. For example, it is well known among metamorphic petrologists that methane is thermally stable within the graphite-methane-water-carbon dioxide system to at least 800°C (Fig. 6-31), and it is likely that methane survives to far higher temperatures than this, probably extending well into the mantle (Hal Helgeson, written communication, 1991).

Lastly it must be noted that the existence of high to moderate concentrations of C_{15+} HC's at extreme maturation ranks (R_o = 2.0-6.0%) and high burial temperatures (200°-300°C or higher) for geologic time periods as long as 300 million years would not be possible if OM metamorphic reactions proceeded by first-order reaction kinetics. Thus, the very existence of such high-rank C_{15+} HC's over long periods of geologic time would seem to preclude the possibility that C_{15+} HC destruction reactions could be first-order reactions.

DISCUSSION

BASINAL OIL AND GAS ZONATION

A paucity of oil deposits in high-rank coarse-grained rocks is another persausive and primary line of evidence, besides reduced HC concentrations in fine-grained rocks with Type III OM at $R_o \geq 0.9\%$, cited to support C_{15+} HC thermal instability. As discussed in Price (1991), this sparsity of oil deposits in high-rank rocks can alternatively be explained by two other processes. First, during vertical oil migration and emplacement, abnormal fluid pressures of deep-basin rocks would prevent oil from entering such rocks. As such, oil is vertically bypassed to shallower, hydrostatically-pressured rocks, during compaction, oil-expulsion, and emplacement processes. Second, increasing amounts of methane are cogenerated with C_{15+} HC's through all stages of HC generation (Figs. 6-6 and 6-7), with significant amounts of methane being generated during the end stages of C_{15+} HC generation.. Also in some cases, true high-rank methane ("dry gas") is generated at great depths in some sedimentary basins by thermal destruction of C_{15+} HC's (discussed below). Such methane streaming out of the deep basin will displace oil from any deep-basin, high-rank reservoirs to shallower basinal depths, by Gussow's (1954) principle of differential entrapment (buoyancy). It must be stressed that water will also be displaced from deep-basin reservoirs (even before oil, because of the buoyancy differences between water and oil) by Gussow's (1954) principle. Furthermore, methane gas has the ability to dissolve and transport water (Fig. 6-32), an ability which dramatically increases with increasing temperature. Thus, some (many?) deep-basin gas reservoirs can be expected to be water-free reservoirs. Any entry of gas into deep-basin oil reservoirs also causes asphaltene precipitation ("desasphaltening" from the oil onto the reservoir rock. The asphaltenes, in such a water-free environment, would undergo enhanced maturation reactions, from the lack of water in the system, resulting in a pyrobitumen char. The end result of these processes would be a strong basinal-segregation of HC fluids. Oil would be in reservoirs at shallow and moderate depths on the stable shelves of petroleum basins, and dry gas would be in deep-basin reservoirs, some of which would contain a charred pyrobitumen. Furthermore, as discussed in Price (1980a), the oil deposits would also exhibit a zonation, with a strong decrease in both gas-oil ratios and API gravities with increasing distance from the basin center. Such decreases would be due to two causes: First with increasing distance of secondary migration, lighter fractions (including HC gases) are progressively lost from oils. Second, the most distant oils from the deep basin would be the oils generated first by any given source rock. Oils generated later by the same source rock will be more mature (higher percentages of lighter fractions) than the first-generated oils, and would be found closer to the basin deeps than the first-generated oils. The end HC distribution (Fig. 6-33) would clearly appear to be due to thermal destruction of oil at high maturation ranks. However, this HC distribution can also be explained by other processes operative in petroleum basins, with fluid buoyancy playing a key role. Furthermore, the HC distribution of Figure 6-33 will independently result from these processes irrespective of any contributions from C_{15+} HC thermal destruction.

It must be stressed that not only oils but also the C_2-C_4 HC gases would be flushed from the deep-basin reservoirs in some basins by methane. Salisbury (1968) discussed the strong zonation of oil and gas in Silurian and Devonian reservoirs of the West Texas Permian Basin. He noted that methane has a very low critical temperature compared to the other (C_2-C_4) HC gases. Whereas methane is always in the gas phase under the pressure-temperature conditions of the West Texas Permian basin deep-basin gas reservoirs, *the C_2-C_4 HC gases will be condensed in the liquid phase.* As such, the C_2-C_4 HC gases in deep-basin reservoirs will be subject to the same separation-

migration phenomena as crude oil by Gussow's (1954) principle of differential entrapment. It is important to realize that such condensation-buoyancy-driven HC gas migrations will cause the zonation of "dry gas" deposits (high concentrations (98%+) of methane in the gas, normalized to the other HC gases) observed in many deep petroleum basins irrespective of any contribution from the thermal destruction of C_2+ HC's. *A high concentration of methane (≥98%) in a gas deposit by itself cannot be taken as absolute evidence of a high-rank origin for the methane.* In fact, data discussed below strongly suggest that much (most?) dry gas in deep- basin reservoirs could have originated from condensation-separation-migration processes with no or little contribution from HC thermal destruction reactions.

The proposition is easily tested if the lack of deep-basin, high-rank oil is due to buoyancy displacement by methane or to in-reservoir conversion of oil to "high-rank" methane. Methane gas has the capacity to dissolve C_5+ HC's in solution (Price and others, 1983). Buoyancy displacement of oil by methane would still leave small, but measurable, concentrations of C_{15}+ HC's dissolved in dry gas deposits. In-reservoir conversion of oil to high-rank methane, on the other hand, should result in the total destruction of C_{15}+ HC's. Cold trapping or filtration of a pressurized gas stream from a high-rank gas deposit would isolate any C_{15}+ HC's dissolved in the methane, such that they could be quantitatively and qualitatively analyzed.

In point of fact such an investigation has already been carried out. A senior petroleum-geochemist, recently retired from a major oil company, informed this author of a study he helped carry out wherein "dry gases" from around 20 different high-rank "gas deposits" from Texas and Oklahoma were analyzed by mass spectrometry for C_5+ HC's filtered from the gas deposit. A full suite of crude oil components was found in all these gases. Analysis of the biomarkers showed all entrained oils to be "normal" of only moderate maturity, with one exception which showed slight thermal stress. The principal conclusion from that study was that only one of the "high-rank" gas deposits analyzed had any possible contribution of methane from the thermal destruction of higher molecular weight HC's.

Compaction, migration, emplacement processes, and gas flushing by buoyancy differences, all displace oil (and sometimes C_2-C_4 HC gases) from the deep basin. Thus it is unlikely that large, high-rank oil deposits will be routinely discovered. However, isolated cases of high-rank oil do exist. Stahl (1974) describes oil produced at 7,300 m (R_o = 3.50%) by the Lonestar Baden-1 well bore, Anadarko Basin, USA. Horsfield and others (1992) describe an oil field discovered by the Saga Petroleum 2/4-14 well bore at 4,300 m in the North Sea, an oil field which lies beyond the postulated thermal deadline for C_{15}+ HC's. R_o profiles can be extrapolated from Tertiary-Upper Cretaceous rocks bearing Type III OM in the Williston basin, to the deeper oil-bearing carbonate reservoir rocks (Price and others, 1986; their Figs. 19-21). Such extrapolations lead to the conclusion that oil is produced in reservoirs on the American side of the Williston basin at R_o values significantly above 1.35%.

HIGH RANK GAS COMPOSITION

Data from both nature and U.S. Geological Survey aqueous-pyrolysis experiments provide insight to the relative control of HC cracking versus condensation-buoyancy-migration processes on high-rank gas composition. In the U.S. Geological Survey experiments, different "rates" of methane generation take place at experimental temperatures below about 320°C compared to temperatures above 320°C (Fig. 6-34), with *the rate* of methane generation

(slope of the curve versus temperature) decreasing at higher experimental temperatures, in the C_{15+} HC thermal destructive phase. The lower rate at higher experimental temperatures is because the Phosphoria shale kerogen has lost almost all its capacity for HC generation at higher experimental temperatures, as reflected by the kerogen's low atomic hydrogen to carbon ratios at high experimental temperatures (Table 6-7). Thus in the thermal destructive phase, any hydrogen which is used to make methane, the most hydrogen-rich of all HC's, must be "scavenged" from previously generated products, which results in the charring process (formation of "pyrobitumen") during HC thermal destruction. From Figure 6-34, the first detectable onset of thermal destruction (break in slopes of the curve at 320°C) clearly overlies the maximum in HC generation for the rock (Fig. 6-8), and by 350°C the experimental system is well into HC thermal destruction.

Changes in both the carbon isotopic values of methane and the gas wetness values for the generated gases accompany HC thermal destruction (Fig. 6-35). The carbon isotopic value which progressively became slightly more negative during progressive HC generation, strongly reversed itself and progressively became much less negative (enriched in the carbon-13 isotope) during HC thermal destruction. The HC gases progressively became wetter (enriched in C_2-C_4 HC gases) during HC generation. This trend reverses itself during HC thermal destruction and the HC gases progressively became enriched in methane as hydrogen is scavenged from all other entities in the system. The trend of HC gases becoming both "drier" (enriched in methane) and enriched in the carbon-13 isotope with increasing rank has been long recognized (Tissot and Welte, 1984). Previously, this trend has been attributed solely to thermal destruction of the C_{2+} HC's.

Rice and others (1988) provided a large data base for natural gases from different areas of the Anadarko basin; and although some scatter is present, a clear trend exists of increasing methane content in the gases with increasing enrichment in the carbon-13 isotope in the methane (Fig. 6-36), especially for fields from the central basin. However, when similar data from the U.S. Geological Survey aqueous-pyrolysis experiments are plotted with the data of Rice and others (1988), the two data sets plot in distinctly different fields (Fig. 6-37); although the data do trend in the same direction in the HC thermal destructive phase (experimental temperatures ≥320°C).

Qualifications exist to direct comparison of gas data from nature and from aqueous-pyrolysis experiments. It has been conclusively demonstrated that large percentages of conventional gas deposits in basins worldwide wide consist of contributions from dry (methane-rich) bacterial gases with carbon-13 isotopic values of -80 to -60 (Rice, 1980; Rice and Claypool, 1981; and Mattavelli and others, 1983). Thus methane carbon-13 isotopic variations of gas deposits in nature are strongly influenced by the amount of biogenic gas incorporated into the deposit. However, gas from the U.S. Geological Survey aqueous-pyrolysis experiments is only thermogenic gas with no contribution from biogenic gas in the system. Also in nature, a significant degree of mixing of thermogenic gases from different sources may occur during gas migration. Such mixing is clearly not present in the U.S. Geological Survey aqueous-pyrolysis experiments. Thus direct comparison of experimental gas data with natural gas data has limitations. However, even with these qualifications, certain insights arise from such a comparison. For example, the HC gas data from the U.S. Geological Survey aqueous-pyrolysis experiments suggest that C_2-C_4 HC gases are thermally stable at experimental temperatures which would be greater to those of true greenschist metamorphism (temperature ≥375°C). The U.S. Geological Survey data also supports the proposition that

in most cases the high methane content of "dry gases" from nature is not necessarily related to HC thermal stability (destruction of C_2+ HC's, discussed below). The data of Rice and others (1988) when plotted versus depth, also support this proposition.

On a detailed scale, distinctly different paleo-geothermal gradients may exist within the Greater Anadarko basin. However, the R_o data of Cardott and Lambert (1985) demonstrate that on a gross scale, maturation-rank profiles (and thus paleo-geothermal gradients and paleo-heat flows) are remarkedly uniform throughout the Anadarko basin (Fig. 6-38), because their data exhibit a strong correlation to increasing depth ($r = 0.958$) despite the fact that their samples are from widely geographically separated localities throughout the Anadarko basin. Thus, in the Anadarko basin *on a gross scale*, depth may be taken as a measure of maturation rank.

If high concentrations of methane in deep-basin gas deposits in the Anadarko basin were due to HC thermal destruction, then both percentage of methane in the gas deposits and the amount of the carbon-13 isotope in the methane molecules would both: 1) increase versus depth, and 2) exhibit decreasing scatter versus depth. However, if the "dryness" (high methane contents) of deep-basin gas deposits were principally due to condensation-buoyancy-migration processes, then only methane percentages (and not $d^{13}C$ values) in the gas deposits should demonstrate a significant increase versus depth. This is because increasing fluid pressures versus depth would cause condensation of C_2+ HC gases into a liquid phase. That liquid phase would then be displaced to shallower traps by Gussow's (1954) principle of differential entrapment, as more methane passed through the deeper reservoir. From Figure 6-39 at depths of 3,657 m (12,000 ft) and deeper (and especially beyond 4,270 m--14,000 ft), there is a pronounced trend of increasing methane content in the gases whether one chooses the dashed or solid envelope. Furthermore, below 4,270 m (14,000 ft), the amount of scatter in the data significantly increases versus depth. However, the $d^{13}C$ value for methane exhibits significant scatter at 3,657 m (12,000 ft) and deeper and does not demonstrate a pronounced trend of becoming less negative with increase in depth. Thus, the data of Figure 6-39 suggest that the characteristics of "high-rank" gas deposits in the deep Anadarko basin are not significantly related to HC thermal destruction. Furthermore, the trends in the methane compositional data (C_1/C_1-C_4 plot) of Figure 6-39 (with the exception of a few data points - shown by arrows) behave as would be expected if condensation-buoyancy-migration processes were largely responsible for the compositional characteristics of the deeply buried "high-rank" gases.

The three deep sample points shown by arrows are exceptions to the trend of increasing methane content with increasing depth, and these three data points offer significant insight into the natural system. First, the elevated amounts of C_2+HC's and highly negative $d^{13}C$ values both argue against an origin of these gas deposits from HC thermal destruction. Secondly, the model of condensation, separation by buoyancy, and migration for gases as discussed above a priori assumes laterally continuous migration paths for the HC's to follow. In such cases, after a trap is filled with methane, the displaced oil (including C_2+HC's condensed in the liquid phase) would migrate to a shallower trap, updip from the original trap. However, if the original trap becomes isolated from a lateral migration path (a closed system) and has no updip outlet, then the trap would quickly become overpressured, could not accept more fluid migration into it, and could not expel fluids from it, thus retaining abnormally high concentrations of C_2+ gases for the trap depth. If the sample set compiled by Rice and others (1988) is a valid representation of all gas deposits in the Anadarko basin, then most gas deposits there would

belong to laterally-continuous migration paths (relatively open systems) and only a minority of gas deposits would be isolated closed systems. The deep (7300 m, R_o = 3.50%) oil deposit which the Lonestar Baden-1 wellbore found (Stahl, 1974; discussed above) is clearly another example of a closed or isolated trap which prevented gas flushing of reservoired C_2+ HC's.

The lack of methane enriched in the carbon-13 isotope ($d^{13}C$ values of -38 to -20 in the data of Rice and others (1988) is significant. Only four gas samples have $d^{13}C$ methane values less negative than -38 (Fig. 6-39). Increasingly less negative $d^{13}C$ methane values are a product of C_{15}+ HC thermal destruction. That so few gas samples have such values strongly suggests that only small percentages of the gas sample base of Rice and others (1988) could have originated from C_{15}+ HC thermal destruction. This conclusion is also supported by the moderate to measurable concentrations of C_{15}+ HC's found in the deepest rocks of the Bertha Rogers-1 wellbore of the Anadarko Basin (Price, and others, 1981; Figs. 6-17, 6-23, 6-29).

FRACTURES VERSUS POROSITY

This study has provided evidence that methane will be thermally stable to depths (maturation ranks) even beyond those which can be reached by current drilling technology in most basins. Thus the question as to the possible existence of conventional, or non-conventional, deep-basin, high-rank gas deposits centers on whether or not adequate porosity and permeability can persist at great depths and high ranks to hold such gas. Examples of abnormally high porosities and permeabilities (20-25%, 1-2 darcies) exist in the Tuscaloosa sandstones of the Tuscaloosa trend gas fields (Smith, 1985), even though these sandstones are at measured R_o values of 2.0-2.2% (Price, 1991). Furthermore, a similar example apparently exists in the "Flex Trend" gas fields offshore Texas. The possible controlling parameters and characteristics of deep-basin, high-rank sandstone porosities are being examined by other investigators on this project. However, it is unlikely that our understanding of the deep-basinal processes that preserve or destroy porosity will reach the point in the near future where pre-drill, site-specific predictions can routinely be correctly made concerning high-rank porosity preservation.

On the other hand, the question of porosity preservation to great depths and high-ranks may be in part academic, depending on the role played by fractures, cracks, and the space between parting laminae of bedding. As noted by Price and LeFever (1992), the Bakken shales and adjacent rocks apparently contain between 100-250 billion barrels of generated oil. Yet the porosities of those rocks range between 0-4%. It has been established that most of this Bakken-generated oil exists in cracks, fractures, and parting laminae in the Bakken shales and adjacent rocks. It is possible that an analogous situation may exist with deep-basin gas, in that the bulk of the deep-basin gas may be stored in a "non-classical" manner in fractures, parting laminae, etc. All rocks are fractured to some extent, and many different processes lead to fractures and cracks in rocks. For example, all onshore basins have been uplifted and cooled somewhat, because all these basins are now above sea level. Furthermore, some of these basins have suffered very large declines in heat flow, for example the northern rim of the San Juan basin. During such cooling, pronounced thermal contraction of both rocks and pore fluids would occur, a contraction which would likely lead to tensional fractures being developed in the uplifted rocks. Once a deep-basin fracture or void were formed by any such process, it might be quickly filled with gas, and this gas might keep the fracture open during subsequent geologic history. If deep-basin, high-rank gas is stored in significant volumes in fractures, parting laminae, and other non-classical void volumes, rather than in rock

porosity, then possible economic recovery of this gas-resource base might hinge on geologic-engineering studies related to such non-classical void volumes.

THE SIGNIFICANCE OF NON-HC GASES

Carbon dioxide, hydrogen-sulfide, and nitrogen are occasionally found in abundance in some gas fields in different basins. Furthermore, high concentrations of these non-HC gases have existed in some fields for long periods of geologic time. For example, such gases in deep traps of Western Canada would have been in those traps since Laramide (Cretaceous-Tertiary boundary) deformation. Such gases in traps in the West Texas Permian and Anadarko basins would have been in those traps since at least the Permian. Both carbon dioxide and hydrogen sulfide strongly undergo association-dissociation reactions to ionic species (HS^-, HCO_3^-, $CO_2^=$) which are *extremely* soluble in water. Both CO_2 and H_2S in gas traps with a water leg will quickly be leached out of the gas and dissolved into the water phase over geologic time, probably on the order of 10,000 to 100,000 years. Thus the existence of CO_2 or H_2S in traps for tens to hundreds of millions of years absolutely dictates that: 1) water is neither in the trap as a mobile phase nor is in contact with the trap at the edge of the gas deposit, and 2) that such traps are closed systems with regards to fluid migration.

The absence of water in some (and possibly many) deep-basin gas traps carries two important implications. First as discussed above, the absence of water greatly promotes HC thermal-destruction reactions at lower temperatures than those under which such reactions would normally take place with water in the system. Thus HC destruction and conversion to high-rank methane would be promoted in deep, water-free reservoirs. Second, when water is introduced to deep-basin, water-free gas reservoirs during drilling, completion, or maintenance operations the principals of two phase fluid flow and the Jamin effect come into play (Price and LeFever, 1992) and *gas-productivity of the reservoir could possibly be damaged or totally destroyed.* Such an introduction of bubbles of pore-throat plugging water (from the Jamin effect) would occur during drilling operations with a water-based (or even oil-based) drilling mud, during a water-based frac job, or during acidization. These concepts have been fully discussed in Price and LeFever (1992) as related to the introduction of water to the oil-productive capabilities of the oil-wet Bakken shales, and will not be further discussed in this report. However, it is a major recommendation of this paper that it is critical to determine: 1) if some (many?) deep-basin reservoirs are water-free systems; and 2) if this is the case, whether or not extensive formation (skin) damage can occur around the well bore in some water-free deep-basin gas reservoirs from introduction of water to them. If the latter is the case, production economics could be severely negatively affected, which would lead to a significant underestimate of deep-basin, high-rank gas resource bases.

Thermochemical sulfate reduction has been invoked to explain both high CO_2 and H_2S concentrations in some gas deposits and also the origin of some of the high-rank gas-condensates of the Alabama-Florida panhandle area (Sassen and Moore, 1988; Claypool and Mancini, 1989). However, close examination of the origin of the hypothesis of thermochemical sulfate reduction, of the evidence for the hypothesis, and of the geographic areas where it has been invoked to be operative all strongly suggest that the hypothesis actually has little basis in fact.

The hypothesis of thermochemical sulfate reduction was first advanced by Orr (1974) in an elegant, well-documented, and detailed discussion to explain the presence of H_2S and CO_2, the sulfur content, and the sulfur isotopic

ratios (becoming heavier or enriched in S^{34} with maturity) of Big Horn Basin oils. To help both explain the observed variations in oil composition, and support his hypothesis, Orr (1974) called upon : 1) in-reservoir maturation of the oils (extensive thermal cracking of C_{15+} HC's) occurring throughout the basin at reservoir temperatures of 80°-120°C, 2) no or minimal water washing or bacterial degradation occurring in the oil reservoirs of the basin, and 3) a long-distance migration of an originally uniform oil from a source to the west with the oil ending up in traps completely ringing the Big Horn Basin depocenter.

The data of this study strongly suggest that in-reservoir maturation of oils (thermal destruction of C_{15+} HC's) at burial temperatures of 80°-120°C is simply not possible. Furthermore the hypothesis of widespread, low-temperature (≥120°C) in-reservoir maturation of oil has been fully discussed and dismissed by both Phillipi (1979) and Price (1980b), the principal conclusions of those studies being that: 1) Extreme variations in the characteristics of crude oils are explained by crude-oil degradation (bacterial attack and water washing). 2) There is no firm evidence that in-reservoir maturation of oil actually exists. 3) Variation of maturity characteristics in undegraded oils are better explained as due to original variation inherited from generation at different maturation ranks in the source rocks than by in-reservoir maturation.

Orr's (1974) second contention that crude-oil degradation is at best minimal in the Big Horn Basin is, in my opinion, erroneous. Crude-oil degradation of many Big Horn Basin oils has been documented by a number of investigators including Todd (1963). Analysis of a number of Big Horn oils by the U.S. Geological Survey has demonstrated decreased concentrations of n-paraffins in some oils compared to other "normal" Big Horn Basin oils. These decreases are due to bacterial attack of crude oils. Orr (1974) noted that the Pennsylvanian Tensleep Sandstone oil-reservoirs in the Big Horn Basin outcrop in the Big Horn Mountains where they are subject to strong meteoric water recharge and that these reservoirs have over 6,096 m (20,000 ft) of hydrodynamic head driving this meteoric water into the deep basin. The well-known inclined oil-water contacts in some of the Paleozoic reservoirs of the Big Horn Basin (Todd, 1963) are most probably due to the strong meteoric water flow occurring throughout the basin. Orr's (1974) assumption of no, or a minimum amount of, crude-oil degradation occurring in the Big Horn Basin simply must be considered flawed given the optimum conditions for oil degradation which occur in the basin and the fact that crude-oil degradation is well-documented there. His subsequent assumption (Orr, 1974, P. 2297) that, "Most of the oils are black asphaltic oils classed as chemically immature", which are then cracked to lighter oils would also be flawed. Although not widely recognized in 1974, it is now well known that most "immature oils" are actually degraded oils which were originally "mature" oils.

The third assumption of a long-distance migration of a "common-pool", compositionally-uniform oil to the traps in the Big Horn Basin strongly contradicts actual oil distribution in the basin. As discussed in Price (1980a), Gussow (1954) and Partridge (1958) both noted that only the anticlines immediately adjacent to the depocenter of the Big Horn Basin contain oil. Anticlines nearer the mountains and removed from the depocenter, both in easterly and westerly directions, are oil barren, yet all the basinal anticlines have equivalent geologic histories. A west to east long-distance migration of oil would absolutely dictate that the westernmost anticlines removed from the basin deep would be oil-bearing, which they are not. On the other hand, a local origin of oil from the Big Horn Basin deep, would dictate

that the oil would be found primarily in the anticlines ringing and immediately adjacent to the basin deep, which is the case.

Thus although Orr (1974) elegantly presented his hypothesis of thermochemical sulfate reduction using the Big Horn Basin as a model, he appears to have put unrealistic constraints on the Big Horn Basin to fit the requirements of his model. These constraints contradict known geologic and petroleum-geochemical features in this basin. Thus in my opinion, the original type model (the Big Horn Basin) for thermochemical sulfate reduction is a poor example.

Orr (1974) specifically detailed reaction schemes and expected products for thermochemical sulfate reduction. However later investigations invoking the mechanism have called for reaction schemes and products which are antithetic to Orr's (1974) original scheme. Furthermore, different subsequent investigators working in the same area have reached different conclusions regarding the mechanism and its reaction products. For example, the sulfur-bearing HC's Orr (1974) detailed as the reaction products from thermochemical sulfate reduction are low maturity compounds: mercaptans, thiaalkanes, cyclothiaalkanes, and thiophenes. As Orr (1974) p. 2315) noted, "A major conclusion from this type of mechanism is that the organic-sulfur compounds in a high-temperature reservoir are not predominantly the thermally stable compounds which have survived the original oil." Also Orr (1974, p. 2316) noted that the enrichments in S^{34} and C^{13} he observed in the Big Horn Basin oils would be due to different processes, only increases in S^{34} would be due to thermochemical sulfate reduction: "The most likely mechanism for S^{34} enrichment requires sulfate, but sulfate availability presumably would have no direct effect on C^{13} enrichment."

Claypool and Mancini (1989, p. 920) called upon thermochemical sulfate reduction to explain the gas and gas-condensate compositions they observed in Jurassic Smackover production of southwestern Alabama, "The products of the oxidation reactions, coupled with the reduction of sulfate, include CO_2, aromatic HC's, and thiophenes (Orr, 1974)." Two facts should be noted here: 1) Orr (1974) did not call for aromatic HC's as products of thermochemical sulfate reduction. 2) The full suite of samples Claypool and Mancini (1989) reported on exist, and many have been analyzed, at the U.S. Geological Survey, and no thiophenes (or thiaalkanes, or cyclothiaalkanes, or mercaptans) are present in any of these samples. In fact the highest-rank samples which Claypool and Mancini (1989) call upon as products of thermochemical sulfate reduction contain only methyl-, dimethyl-, and trimethyl- benzothiophenes and dibenzothiophenes as sulfur-bearing compounds, which in point of fact are the most thermally-stable, sulfur-bearing compounds. Thus the composition of the sulfur-rich gas condensates of southern Alabama clearly fall far outside of the original contraints proposed by Orr (1974).

Claypool and Mancini (1989) noted a significant decrease in the ratio of C_{15+} saturated HC's to C_{15+} aromatic HC's and a noticeable increase in the carbon 13 isotope (less negative $d^{13}C$ values) for the saturated HC's in the highest rank gas condensates they studied. They attributed the decrease they observed in the saturated HC/aromatic HC ratio to preferential destruction of saturated HC's. They also called for a preferential destruction of n-paraffins over all other saturated HC compound classes. However this conclusion was based on a saturated HC gas chromatogram (their Fig. 10) from the Flomaton field, which due to inefficient silica gel-alumina column chromatography actually had high contents or aromatic HC's and sulfur-bearing aromatic HC's eluted with the saturated HC's. Flomaton field saturated HC's

when isolated by properly performed silica gel-alumina chromatography are actually n-paraffin rich, all the other saturated HC's having been preferentially destroyed. A significant part of Claypool and Mancini's (1989) evidence for thermochemical sulfate reduction in the gas condensation of southwestern Alabama arose from their perception of the unusual character of the Flomaton field saturated HC's. However the "unusual characteristics" of these samples are only a laboratory artifact, and the Flomaton field saturated HC's are in reality quite similar to those from other gas condensates studies by Claypool and Mancini (1989) such as Perdido, Chunchula, Chatom, Copeland, and Big Escambia Creek.

An earlier study by Sassen and Moore (1988) in the same area and using some of the same samples as that of Claypool and Mancini (1989) reached significantly different conclusions than those of the Claypool and Mancini (1989) study. Sassen and Moore (1988) believed their data indicated that aromatic HC's were destroyed preferentially to saturated HC's with increasing maturation. Furthermore within the saturated HC's, the n-paraffins were interpreted as the most thermally-stable compound group. It should be noted that the two studies reported on four of the same samples, and reported significantly different percentages of C_{15+} saturated (and aromatic) HC's making up the C_{15+} fraction. Thus any conclusions regarding changes in saturated or aromatic HC abundances in the gas condensates and oils examined by either study would seem tenuous.

Thermochemical sulfate reduction and in-reservoir thermal cracking of C_{15+} HC's were proposed, and have been invoked, to explain high concentrations of CO_2 and H_2S in reservoir gases, and heavier sulfur and carbon isotopes in the saturated HC's with increasing maturation rank. However all these features are also explained by other processes. For example Lewan (1983) demonstrated with hydrous-pyrolysis experiments on the Mississippian-Devoinian Woodford shale that the saturated HC fraction of the generated-expelled oil became isotopically heavier (less negative $d^{13}C$ values) with increasing experimental temperature. This feature has also been observed in U.S. Geological Survey aqueous-pyrolysis experiments. It is well known, in point of fact, that all different maturity indices of oils, generated either in hydrous-pyrolysis experiments or from source rocks in nature, increase in maturity with increase in maturation rank from either increasing experimental or burial temperatures. Thus, there is no apparent reason why sulfur in crude oil would not also become isotopically heavier with increasing maturation rank in oils generated from source rocks at increasing maturation ranks.

With some exceptions, gas reservoirs which contain high concentrations of H_2S and/or especially CO_2 are most usually in reservoirs at high maturation ranks in basin deeps. This fact suggests that high concentrations of either or both CO_2 and H_2S could be related to processes which occur in deep basins at high maturation rank. For example, a review by Petroleum Information Corporation (1984) discusses how CO_2 in sedimentary basins is released from volcanic intrusions into sedimentary rocks or how CO_2 is generated from volcanic, plutonic, or metamorphic intrusions or processes on carbonate rocks. Le Tran et al (1974) demonstrated that high concentrations of H_2S are generated at elevated maturation ranks from the sulfur-rich OM in the fine-grained rocks of carbonate sequences.

The strongest argument against the widespread existence of thermochemical sulfate reduction is in the presence of the principal products from the proposed reaction, CO_2 and H_2S. As stated above, CO_2 and H_2S are both extremely soluable in water. Therefore their presence in high

concentrations in gas reservoirs over any length of geologic time absolutely dictates that the reservoir in which they reside be either an absolutely closed hydrogeologic system, where no water movement or diffusion through water can occur, or be water free, or be both. Thermochemical sulfate reduction on the other hand, absolutely requires an outside source of the SO_4= ion to be transported via water into the HC reservoir in an open hydrogeologic system. Therefore because of the need for an open system, if thermochemical sulfate reduction were occurring, CO_2 and H_2S could not possibly accumulate as products of the reaction in high concentrations. In point of fact, the presence of these species in high concentrations actually dictates that thermochemical sulfate reduction cannot be responsible for their origin.

THE DATA OF WEISMAN

Weisman (1971) carried out a study wherein he examined isotopic compositions of methane and carbon dioxide from Sacramento and West Texas Permian-Val Verde Basin gas fields which had been affected by igneous or volcanic activity. He recorded data which supported his hypothesis that at very high temperatures (500°1200°C) carbon dioxide and methane equilibrate to each other (Fig. 6-40) with respect to the carbon-13 isotope. Weisman's (1971) hypothesis also receives support from data from U.S. Geological Survey aqueous-pyrolysis experiments (Fig. 6-35), as even at lower temperatures than those considered by Weisman (1971), values for both methane and carbon dioxide are trending towards one-another with increase in temperature. However this feature could simply be a strong control of the original OM in the Phosphoria shale. By measuring $d^{13}C$ values in associated methane and carbon dioxide and employing his $d^{13}C$ thermometer, Weisman (1971) was able to document strong increases in estimated paleotemperatures of a number of gas fields towards intrusive and extrusive plutonic or volcanic features in both the Sacramento and West Texas Permian-Val Verde Basins. Wiesman (1971) also found a strong vertical and lateral zonation of $d^{13}C$ values for methane in several West Texas Permian-Val Verde Basin fields he studied. He also noted a strong zonation of increasing carbon dioxide concentrations in Cambro-Ordovician Ellenburger limestone West Texas Permian Basin gas fields to the south and southwest which he attributed to deep-seated igneous activity. Weisman (1971) measured methane $d^{13}C$ values of several gas fields, values which strongly suggest a methane origin from HC thermal destruction ($d^{13}C$ for methane of -35 at Puckett and -28 at Brown-Bassett in West Texas). If the extreme paleotemperatures Weisman (1971) calculated are valid, then the gas in the fields he studied would be true high-rank methane which had at least partially originated from true C_2+ HC thermal destruction. A reexamination of the gas fields studied by Weisman (1971) would be most appropriate. If his original work and conclusions are found to be valid, an extension of his work to other possible high-rank gas fields would also be in order.

PRIMARY MIGRATION OF GASES

It is a principal hypothesis of this paper that in-reservoir thermal destruction of C_2+ HC's has resulted in only a small percentage of the methane in deep-basin, "high-rank" gas deposits. Instead, most of the methane in these deposits appears to originate by processes involving HC condensation, buoyancy, and migration which result from mainstage HC generation in source rocks. If this indeed is the case, then understanding primary migration of HC gases could play a major role in understanding the distribution of high-rank gas deposits in deep basins. Clearly HC gases, especially methane, are much more mobile than crude oil. Thus many constraints applicable to primary oil migration will not directly apply to primary gas migration. However, some of the same rules may at least partially apply.

Previously, most petroleum geochemists, including this author, have considered primary petroleum migration to be a very efficient process with the result that most generated HC's (75-95% in organic-rich rocks) were thought to migrate from their source rocks. These conclusions had previously been reached because of the large decrease in the HC generation capacity of source rocks, as reflected by decreasing ROCK EVAL HI values, as a given source rock was progressively buried deeper in a basin. However, these HI decreases are never matched by numerically-equivalent increases in either Soxhlet-extractable HC's or the ROCK EVAL S_1 pyrolysis peak, both of which exhibit rather constant values versus depth. Thus we petroleum geochemists had concluded that primary petroleum migration is very efficient, because almost all generated HC's clearly leave the source rocks. However, as discussed by Price and LeFever (1992) and Price (1992), an almost total lack of oil generated from the Bakken shales in the conventional reservoirs of the Williston basin leads to the conclusion that primary petroleum migration is actually quite inefficient. Furthermore as discussed above, most generated HC's appear to be lost to the drilling mud during the cutting chip or core trip up the wellbore during drilling operations. Thus the high apparent efficiencies of primary petroleum migration previously called for in reality are due to efficient loss of generated HC's to drilling muds. A strong association of increasing basin richness regarding conventional oil deposits versus intensity of faulting in the HC kitchens of deep basins was noted by Price (1992), Table 6-8). Price (1992) attributed this association to major faulting (with accompanying major fracturing) physically disrupting organic-rich source rocks and freeing generated HC's for primary migration, such that these generated HC's could form conventional oil deposits.

Even though gas is significantly more mobile than oil, it is possible and perhaps probable, that significant faulting of mature and post mature source rocks is necessary before highly efficient expulsion of generated HC gases can occur. Thus it is a hypothesis of this paper that a rule of thumb may exist regarding location and occurrence of deep, high-rank "conventional" gas deposits. Such deposits, by the models developed in this paper, should always be associated with a major fault which has disrupted mature and post mature source rocks to allow HC, and HC gas, expulsion. Structures not associated with such faulting should not contain deep, high-rank conventional gas deposits.

Normal and extensional faulting are much more favorable for expulsion of oil into fault zones for upward migration, compared to high-angle compressional reverse faulting (Price, 1992). This is because the voids created along normal and extensional faults allow fluid migration along faults compared to compressional reverse faults which restrict fluid movement because of their "tightness". However, the much greater mobility of gas compared to oil may cancel out this difference between the different fault classes somewhat.

Basinal structural styles evolve through geologic time. For example, the depocenter and southernmost margin of the Anadarko basin, although previously an extensional wrench fault regime, later evolved into a compressional tectonic regime, characterized by numerous, large, high-angle reverse faults. Migration of HC fluids could occur during periods of normal or extensional faulting and later evolution to a compressional tectonic regime might be quite favorable to preserving deep, high-rank gas deposits over geologic time by minimizing loss by leakage up these "tight" compressional systems.

EVIDENCE FOR HUGE IN-PLACE UNCONVENTIONAL GAS RESOURCE BASES

Based on the results of: 1) the horizontal Bakken-shale drilling program in the Williston basin; 2) ongoing detailed petroleum-geochemical analyses of the conventionally and non-conventionally produced oils in the Williston basin; 3) the apparent high *inefficiency* of primary petroleum migration; and 4) other considerations discussed in Price and LeFever (1992), those authors proposed the possible existence of an in-place oil resource base in fractured, mature, organic-rich source rocks in many different petroleum basins of the lower 48 United States in the range of tens to hundreds of trillions of barrels of oil. Clearly much more gas than oil will escape from mature unstructured source rocks because of the much greater mobility of gas compared to oil. Indeed as discussed in Price (1986), C_1-C_4 thermogenic HC gases can be detected in very low concentrations at any surface location in all petroleum-bearing basins (and even in many petroleum-barren basins) by a variety of surface geochemical exploration methods. Such thermogenic HC gases at the earth's surface both: 1) result from the much greater mobility of HC gases compared to oil, and 2) result in a substantial loss of generated HC gases over geologic time. Source rocks are certainly more chemically-open systems (easier product escape) with respect to HC gases than to oils. However, it appears probable that monstrous, non-conventional, in-place gas resource bases also exist in different forms in different basins. These non-conventional in-place gas resource bases may parallel the non-conventional oil resource base proposed by Price (1992).

Examples of such large, non-conventional, in-place gas-resource bases are: 1) the basin-centered gas deposits of the San Juan, Denver, and Western Canadian sedimentary basins; 2) known tight gas deposits in various American onshore basins; 3) coal-gas deposits actively being exploited in different American basins, especially the San Juan basin; and 4) the (currently non-economic) geopressured-geothermal gas resource base of the Gulf Coast (and other basins. The fact that mud gas logging values *always* dramatically increase when organic-rich rocks, and the rocks immediately adjacent to them, are penetrated by the drill bit is also strong evidence of the ubiquity of such gas resource bases. These in-place gas resource base exist in different forms: 1) gas dissolved in high temperature pore-water in sands and shales; 2) free gas bubbles in concentrations below (or above) the critical gas saturation levels for the stratigraphic units in which the gas bubbles reside; 3) (small) non-economic traces or pockets (shows) of free gas dispersed throughout the rocks of sedimentary basins; 4) gases absorbed in coals; and 5) gases absorbed on the kerogen of shales or dissolved in free bitumen in mature source rocks. Furthermore the sizes of the different in-place gas-resource bases are, to say the least, very large. For example, Law and others (1989) estimated that the in-place gas-resource base of only the coarse-grained rocks in the Greater Green River Basin as between 3,611 to 6,837 TCF. Masters (1984a) estimated 3,600 TCF of in-place gas in the Canadian Alberta Basin (deep basin and adjacent foothills belt).

Although dispersed in-place HC gas resource bases in all probability exist, and their size is beyond imaginable calculations, unless at least a small fraction of a resource base can be recovered, then its existence and size are of little more than academic interest. It is the opinion here that successful recovery of such unconventional gas-resource bases is not solely a geologic problem, but more largely depends on the development of new drilling, stimulation, production, and maintenance techniques which are applicable to the non-classical characteristics of the particular non-conventional gas-resource base under consideration. For example, experience with attempted economic recovery of the non-conventional oil resource base of the self-sourced, fractured Bakken shales has clearly demonstrated that application of conventional drilling-production techniques to that resource base has not been

successful. As another example, economic recovery of coal gas is made possible by first producing substantial volumes of water from coals (and adjacent rocks). This greatly lowers formation pressures and allows a free gas phase to either form or increase in volume (or both). As such, the critical gas saturation level of the coal is exceeded to a point that the permeability of the formation with respect to gas is significantly increased. This allows the coal gas to flow towards the wellbore in meaningful (economic) amounts. Hundreds of millions of dollars have been spent to demonstrate that geopressured-geothermal gas in the Gulf Cost *cannot be* economically produced by producing sandstone brines from moderate depths 3,048 to 4,572 m (10,000-15,000 ft) and bringing those brines to the earth's surface for surface extraction of dissolved methane. It was predicted (Paul Jones, unpublished research and Price 1978 a,b) that such a recovery technique would not be economic. However, economic recovery of an essentially infinite geopressured-geothermal resource base appears possible in the Gulf Coast from rocks at greater depths than those being utilized by the current geopressured-geothermal research effort. Deeper rocks: 1) carry greater levels of immobile free gas bubbles at or below critical gas saturation levels for those formations; 2) carry much higher concentrations of HC gases dissolved in sandstone and shale pore water from the higher burial temperatures and higher (abnormal) fluid pressures at depth; and 3) are much further into intense HC (and HC gas) generation than the shallower rocks, thus providing more gas to be recovered. Economic recovery of the deep geopressured-geothermal gas resource base can likely be accomplished by production techniques similar to those being used to recover the dispersed gas resource base from coals: removal of sufficient volumes of deep formation waters to greatly lower reservoir pressure and therefore greatly increase free gas mobility leading to an *in situ* recovery, as opposed to surface extraction, of the resource base (L.C. Price and P. Jones, unpublished research).

As a last example of the non-classical characteristics of the non-conventional gas resource base, let us assume that many deep, high-rank gas deposits are in water-free reservoirs. If this is the case, then introduction of any water to those rocks would greatly decrease, and perhaps totally destroy, the gas-productive capabilities of the deep reservoir rocks.

It is a conclusion of this study that essentially infinite, in-place, unconventional, gas-resource bases can be proven from further geologic and geochemical research. However, enough evidence exists such that perhaps we can take these in-place HC gas resource bases as a given. Much more potentially rewarding effort would be in research to determine if appropriate drilling, completion, stimulation, and maintenance techniques can be developed, techniques which are applicable to the different facets of unconventional, in-place gas-resource bases.

DEEP PETROLEUM BASINS: OPEN OR CLOSED SYSTEMS?

The existence of the very large, in-place, nonconventional gas-resource bases discussed above very probably are due to the nature of fluid flow in sedimentary basins. For the purpose of discussion, two opposite views can be taken regarding fluid flow in sedimentary basins: 1) The depocenters of these basins are "open systems" which allow continuous product escape from HC generation (primary migration) and essentially unrestricted, or only slightly restricted, fluid flow between different stratigraphic units in basins. 2) The depocenters of these basins are closed systems where primary petroleum migration is difficult (inefficient) unless source rocks are physically disrupted by faulting or fracturing or (in uncommon cases) are bounded by a continuously laterally hydraulically transmissive unit. Furthermore,

significant fluid flow between stratigraphically- separate units in a basin is greatly restricted or impossible.

As discussed above, most petroleum geochemists call for efficient primary petroleum from source rocks (Price and LeFever, 1992), and therefore subscribe to the first model. Furthermore, many investigators, including Meissner (1978) and Spencer (1987), view slight to moderately-high overpressures in source rocks to be proof of present-day HC generation taking place in such rocks. Products from such generation are thought to continuously escape through "leaky" systems to replenish either conventional deposits or unconventional resource bases which are assumed to be losing HC's via leakage also. This view is best summed by Masters (1984a, p. 25-26) who described present-day gas generation, from presumed HC thermal destruction, occurring in the deep rocks of the paleo-depocenter of the Western Canadian basin (the disturbed belt):

"West of the updip edge of the Deep basin, the entire Mesozoic section generated gas and the deeper part of it continues today to explode gas out of the organic material. This active thermal area is called the 'gas furnace.'

Our understanding of the trapping conditions which created the vast and thick gas-saturated section downdip from water in the Deep basin has been substantially enlarged. Previously, the updip seal had been tentatively ascribed to 'water block' caused by lower relative permeability to gas in the high-water saturation on the updip side (Masters, 1979). Now, Leythaeuser and others (1982), Welte and others (1984), and Gies (1984) have recognized that the trap is 'dynamic' in the sense that the tight sand (much of it with the permeability of a silty shale) slows down the passage of gas into the more porous, water-wet sand updip. There is not actually a seal. Gas is continually leaking out updip. But gas is still being generated fast enough that the trap stays filled. A catchy term would be to call it a 'bottleneck trap.' In Welte's words 'the gas saturation of the rock column depends on a dynamic equilibrium between gas generation and gas losses. The low permeabilities and low porosities of the gas saturated part of the rock column are essential for the existence of this unconventional gas deposit. Migration and losses of gas seem to be mainly controlled by diffusion.' The coincidence of the Deep basin gas trap and the gas window is explained by this bottleneck concept which requires that the trap be continually fed."

The second view that primary migration is a very inefficient process is a minority viewpoint recently advanced by Price and LeFever (1992) and Price (1992). However: 1) the major documented loss of both HC's and HC gases from mature source rocks during the trip up the well bore, 2) petroleum geochemistry of the Williston basin, and 3) Table 6-6 through 6-8 all strongly support this view. The proposal that general fluid flow is highly restricted in some deep portions of sedimentary basins has only recently been advanced by the work of Powley (1990), Tigert and Al-Shaieb (1990), Ghaith and others (1990), and Al-Shaieb (1991). These investigators have documented "compartmentation" in basins worldwide, wherein nested compartments of rocks whose fluids are significantly underpressured or overpressured exist in the depocenters of most petroleum basins. As noted by Powley (1990, p. 219-220),

> "The compartmented hydraulic systems in currently sinking basins are almost universally overpressured and are underpressured in many onshore basins undergoing erosion. The principal source of overpressures appears to be thermal expansion of confined fluids and the generation of petroleum during continued sinking, and the

> principal source of underpressures appears to be thermal contraction of confined fluids as buried rocks cool during continued uplift and erosion at the surface. Thus, it appears that the compartments have an amazing longevity as they undergo a continuum from overpressures through normal appearing pressures to underpressures as their host basins progress from deposition to quiescence, to basin uplift and erosion."

This author is in agreement with Powley (1990) regarding both the origins of overpressures and underpressures and their "amazing longevity" over geologic time. As noted by Dickey and Cox (1977), subnormal pressure gradients exist in the shallower rocks of all onshore United States petroleum basins; and as Dickey and Cox (1977) also noted, *such gradients can only originate from a decrease in rock burial temperatures* which causes a thermal contraction of both rocks and fluids. Such a decrease in rock burial temperature can only arise from: 1) uplift and erosion, 2) a decrease in the heat flow (and thus in the geothermal gradient), or 3) both processes in combination. Clearly, all onshore basins have been uplifted and eroded somewhat, as they are all currently above sea level.

Al-Shaieb (1991) discussed "compartmentation" in the Paleozoic rocks of the deep Anadarko basin where nested compartments of rocks with very high fluid pressure gradients are adjacent to rock volumes with normal or only slightly overpressured pressure gradients. Pressure gradients within Lower Pennsylvanian Morrowan rocks as high as 0.987 psi/ft have been recorded. The high fluid-pressure gradients found in the deep Anadarko basin were probably formed before basin evolution ceased in the Permian. Thus it appears that extreme fluid pressure gradients can persist in hydraulically isolated volumes of rocks for long periods of geologic time. Such restriction of fluid flow for periods of hundreds of millions of years also supports the concept of inefficient primary migration as hypothesized above.

Let us return to Powley's (1990) comment above regarding the origin of overpressures from either: 1) HC generation, or 2) the thermal expansion of confined fluids (as best stated by Barker's (1972) model of aquathermal pressuring, which is thermal expansion of a fixed amount of fluid (usually pore water) in a fixed pore volume).

Abnormal fluid pressures first came to prominence from oil exploration in the Gulf Coast in the late 1960's and were originally attributed to restricted compaction processes such that the sediments retained more water than they should for a given burial depth. However, as an aside, it should be noted that the mechanism for Gulf Coast shales retaining excess pore water in many cases likely also indirectly involves HC generation. As HC generation proceeds, more and more HC gas is generated, and eventually methane dissolved in shale pore waters reaches saturation levels and a gas phase (bubble) exsolves. This gas bubble will be below the critical gas saturation level for the shale. If the bubble becomes locked in a shale-pore throat, the Jamin effect (Hedberg, 1980) comes into play, triggering Barker's (1972) aquathermal pressuring mechanism.

As overpressures were discovered in other basins, they were also (incorrectly in some cases) attributed to the thermal expansion of confined fluids. However, exploration geologists, first Meissner (1978) and later Spencer (1987) and others, noted that HC generation involved a volume increase as kerogen degraded to various products. This proposal was verified by petroleum geochemists, and Ungerer and others (1983) who calculated that HC generation involves a 15% volume increase. However, at this point in time,

overpressures in any organic-rich rock are almost always taken as an indication that present-day HC-generation is occurring, and this can be an erroneous assessment, in this author's opinion.

For example, many investigators, including Meissner (1978) and Spencer (1987), have attributed the overpressures in the Bakken shales of the Williston basin in mature basinal areas to present-day HC generation taking place in the shales. By this hypothesis, some of these generated HC's constantly move out of the shales to either form conventional oil deposits or to be lost as seepage at the earth's surface through geologic time. While these interpretations are possible, they are not favored here. Even though the Bakken shales are overpressured, all the other units in the basin are underpressured (Fig. 6-41), and significantly so. As discussed, a decline in rock burial temperatures which causes thermal contraction of both rocks and pore fluids, is the only mechanism which can result in basin-wide sub-normal fluid pressures. Low surface intercepts (0.25-0.29) of ten different vitrinite reflectance (R_o) profiles compiled by this author throughout the North Dakota portion of the Williston basin show that there has not been significant erosion in the basin. Thus only a decline in heat flow and hence geothermal gradients can explain the subnormal pressures observed basinwide in all units except the Bakken shales. Such declines are supported by the extreme R_o gradients versus depth reported by Price and others (1984) in the Type III OM of the Tertiary and Upper Cretaceous rocks in basinal areas where the Bakken shales are mature. Furthermore, the original four R_o profiles of Price and others, 1984 have been corroborated by six newer, unpublished R_o profiles. Although the Williston basin still is quite warm, present-day geothermal gradients would have to be *at least* doubled to account for the observed R_o gradients. If paleogeothermal gradients have been at least halved, all ongoing HC generation would immediately stop, by any time-temperature dependent HC-generation model. Although the Bakken shales are overpressured, the pressure gradients in those shales are usually lower than others reported on by Spencer (1987) for other Rocky Mountain basins, and are lower still than those found in coastal or offshore petroleum basins which are clearly at their maximal geothermal gradients. It is the interpretation here that the current overpressures in the Bakken shales are lower than what they once were before basin cooling occurred. Furthermore, the current overpressures would have been retained in the Bakken shales through geologic time because of the model advocated here of restricted fluid movement and inefficient primary petroleum migration in the depocenters of petroleum basins, a model which is supported by the investigations of Powley and co-workers.

The basin-centered gas deposit of the Western Canadian basin depocenter is another case where investigators have called for present-day HC generation and concurrent migration through an "open" HC generation system (Masters, 1984; Gies, 1984; and Welte and others, 1984). This HC generation has been proposed in spite of the fact that the gas deposit is at *sub-normal* pressures. Various other investigators, including Hacquebard and Donaldson (1974), Hacquebard (1975), Magara (1986), Hutcheon and others (1980), Kalkreuth and McMechan (1988), and Tilley and others (1989), have provided evidence for, and/or discussed, the extensive erosion which has taken place in the Western Canadian sedimentary basin. The amount of erosion increases on a one trend southwestward from the Canadian plains, past the disturbed belt, into the present-day deep basin, and lastly into the ancestral deep basin (present-day Rocky Mountains). Evidence for this erosion comes from studies of fluid inclusions, coal rank, shale and sandstone diagenesis and metamorphism, and vitrinite reflectance. Estimates of erosion range from 1,000 m of sediment or less from the Canadian plains to up to 6,000 m of

sediment from the Rocky Mountains. As an example, Hutcheon and others (1980) calculated that rocks in the Elk Valley and Mount Allan areas (southeastern British Columbia and southwestern Alberta), at present-day depths of 0-1,000 m, had paleo temperatures of 180°-250°C.

R_o profiles from the Elmworth gas field and other areas of the present-day deep Alberta basin have surface intercepts of R_o = 0.7 ±0.1%. In the absence of erosion, irregardless of time-temperature burial history considerations, R_o profiles should have surface intercepts of R_o = 0.25-0.29%. Whether one uses the R_o paleothermometer of Price (1983) or of Barker and Pawlewicz (1986), surface R_o intercepts of 0.7 ±0.1% imply decreases in sediment burial temperatures of at least 100°C. No current functional petroleum-geochemical model of HC generation allows significant continued HC generation after decreases in burial temperatures of 100°C or more.

HC generation, by all published models of present-day petroleum geochemistry known to this author, is principally driven by increases in burial temperatures, with lesser contributions from other controlling parameters (such as geologic time) depending on the model. The dominant control of burial temperature is due to the progressively stronger bonds in kerogen which must be broken by increasingly higher burial temperatures for HC generation to proceed. Thus, burial temperature decreases of ≥100°C would preclude any possibility of HC generation continuing; because once bonds are broken at a given burial temperature, the bonds cannot be rejuvenated, they have been destroyed.

In my opinion, two other major flaws exist with the conclusion of Welte and others (1984) that present-day dry gas generation is occurring in the deep Alberta basin. First, I am not aware of any investigators, outside of Welte and others (1984), who call for significant HC generation from underpressured rocks. Second, the very evidence which Welte and others (1984) call upon to support their model of present-day methane generation and loss via updip diffusion to the surface is the evidence which conclusively demonstrates that their proposed model is erroneous. Welte and others (1984) found rocks at 2,350-2,450 m of burial whether coals (~80% TOC) or shales (~1.0% TOC) had the same ethane concentration as normalized to rock TOC (5-6 x 10^4 nanograms of ethane/gram rock organic carbon). They interpreted these "equal concentrations" of ethane as due to diffusion to support their model. However, diffusion of HC gases occurs in water-saturated rock porosity, and has nothing to do with the organic carbon content of the rocks in which diffusion is occurring. If active present-day gas generation were occurring, ethane (and methane) should be diffusing away from the coals into the shales, because the coals have at least an 80 fold higher generation capacity for methane than the shales (80% TOC versus 1.0% TOC). Thus, active present-day gas generation and diffusion would manifest itself by equal concentrations of methane as normalized to *rock weight*, or *rock volume*, or *rock pore space* . That the coals have rock-normalized ethane concentrations, some 80 fold higher than interbedded and adjacent shales demonstrates that neither active gas diffusion or generation can possibly be taking place.

Clearly current petroleum-geochemical thought is more oriented towards HC generation models which call for present-day HC generation coupled with leaky deep-basins (efficient primary petroleum migration) than oriented towards models of limited primary migration coupled with detailed consideration of a basin's geologic history as a controlling parameter of HC generation. The latter model of HC generation and migration is favored by this author. Basins are not viewed here as constants through geologic time,

but instead are viewed as entities which evolve through time. HC generation and primary migration (and basinal fluid flow in general) are held as tightly linked to basinal heat flow and structuring. Maximal HC generation and migration are thought to occur in a basin's youthful stage when heat flow, sedimentation, and structuring are all also at a maximum . Decrease in heat flow and structural activity should lead to basinal quiescence at mature stages. It is maintained here that with decrease in heat flow, significant HC generation and migration cease as does meaningful fluid flow in, and out of, the deep basin. Continued significant uplift and erosion can lead to total basin destruction. If basinal uplift and erosion are halted, basinal hydrodynamic patterns can be established wherein significant meteoric water recharge in the uplift areas of basins can lead to basin-wide hydrostatic-pressure water flows, at shallow depths, driven by such recharge. If giant or super-giant oil accumulations are not breached by basinal uplift and erosion (and subsequently degraded), water washing and bacterial attack driven by such meteoric water recharge may well degrade such deposits (tar sands of the Alberta basin).

Whether or not petroleum basins (and petroleum and gas generating systems) are open or closed systems is more than academic. Assume that they are leaky systems and that most of the gas generated through geologic time is bled off and eventually lost to surface leakage. This would leave only a fraction of the total gas generated trapped in the deep basin. However, if deep-petroleum basins are closed or semi-closed systems with only limited fluid flow, then the majority of the gas generated by rocks in the deep basin may remain in-situ. The latter case results in much larger in-place gas resource bases which would also have a distinctly higher concentration (grade) then the former "leaky" case. Whether a resource base under consideration be energy, water, or heavy metals, higher-grade resource bases are always easier to recover than lower-grade resource bases.

A model favored here wherein deep-basin fluid flow occurs in closed or semi-closed systems. It is expected that organic-rich rocks with good gas generation potential (and the rocks adjacent to them) will retain most (70-90%?) of the gas that they have generated if such rocks are not highly faulted or fractured or bounded by hydraulically-transmissive units. Fine-grained rocks which are in the deep-basin and which are highly to moderately structured, would be expected to retain much smaller percentages of the total gas which they have generated, as many routes would be available to allow escape of the highly mobile methane molecule. If the model favored here is a reasonable representation of nature, then we may expect in- place *wet-gas* resource bases of the largest possible imaginable magnitudes. However, these wet-gas resource bases will largely be in the form of non-conventional gas deposits and will not be recoverable by the present-day drilling, completion, production, and maintenance operations which are used to recover gas from conventional gas deposits. Examples of known, in-place, deep-basin nonconventional gas deposits are coal gas, basin-centered gas, , tight gas, deep (>4,572 m-->15,000 ft) Gulf Coast geopressured-geothermal gas, "black-shale" gas (Mississippian-Devonian black shale, Appalachian basin). Other types or classes of deep-basin gas deposits no doubt exist which we have not yet recognized. Furthermore, some of these deposits also exist in what are now shallow rocks (from uplift and erosion) but were once more deeply buried.

It is the principal and final recommendation of this paper that research be instituted to determine if such large in-place wet-gas resource bases do exist and accurately determine the grade (concentration) of the various resource bases. If high-grade, in-place, gas-resource bases do exist, then economic recovery of the resource should become a research focus, by joint

geologic-engineering studies. Such recovery will clearly depend on the development of non-conventional drilling, completion, stimulation, production, and maintenance techniques which are uniquely applicable to the non-classical characteristics of each of the different resource bases.

THE NEED FOR RESEARCH INTO U.S. UNCONVENTIONAL RESOURCE BASES

It is clear that no matter which resource assessment model or published study one uses, one only may conclude that most of the large American oil fields to be discovered, have already been discovered (with possible exceptions of undiscovered North Slope (coastal), Santa Barbara Channel, and deep-water Gulf Coast, e.g., - Green Canyon, fields). Furthermore, it is well established that the Persian Gulf Basin holds the bulk of the world's conventionally producible oil. Even if another American Prudhoe Bay were discovered, it would only be forestalling the inevitable, which is an ever-increasing and dangerous dependence on the Middle East for American energy requirements. In my opinion, the only currently foreseeable chance the United States has to avoid this undesirable outcome, is definitive research into the possible commercial productivities of our *known, in-place* nonconventional mobile gas (and oil, Price and LeFever, 1992) resource bases. Examples already exist of non-conventional gas-resource bases which are both commercially viable and provide significant contributions to the U.S. energy needs: the basin-centered gas deposits of the San Juan, Denver, and Western Canadian Basins; and coal-gas from numerous basins, but especially the San Juan Basin. There is no apparent reason why properly-designed research would not delineate appropriate techniques which must be utilized for commercially viable recovery of , other non-conventional, gas and oil resource bases. However, such research designed and carried out from a conventional mind set will only fail because exploitation of unconventional gas and oil resource bases will be difficult or impossible to achieve by conventional thought patterns. As Masters (1984b, P. ix) noted discussing the basin-centered Elmworth gas field of the Western Canadian Basin,

"Finding a giant Deep basin-type gas field is technologically relatively simple, although statistically very rare. Exploiting such a field, however, calls upon some of the most advanced reservoir technology available and requires an unusual amount of coordination between the geological and engineering arms of a company. It is virtually impossible for one man to have all the skills required to analyze, measure, and produce these low-permeability, high-damage reservoirs, so a chain-link team of specialists must be available. Few companies have built, or can hold together, such teams. Perhaps the most significant contribution of this memoir, in fact, is its description of the several areas of expertise that must necessarily bond together in the exploitation of a major Deep basin-type gas field."

It must be stressed that with the large-scale departure of the American major oil companies from domestic onshore exploration, that funding of such research into unconventional-energy-resource bases, if such research is even carried out, will have to come from the Federal Government (which is currently significantly cutting back energy funding) and/or from institutions such as the Gas Research Institute (GRI) which have a vested interest in the production of United States energy resource bases. The American major oil companies are corporations which have a minimal, if any, interest in American energy self sufficiency. Nor should they have such an interest, as corporations, by their very nature, exist only to achieve favorable profit margins for stockholders.

The United States still has a strong industry base of domestic independent oil-exploration companies, although with time this industry base

also will erode. These companies historically have been the last true onshore "wildcatters". These companies often are comprised of explorationists who are always ready to aggressively pursue new exploration concepts or plays. For example, these companies have played the key role in development of the coal-gas resource base (along with an "independent-minded" American major-Amoco oil) and have also played the key roles in the attempted commercial recovery of the fractured-shale oil resource base of the Bakken shales in the Williston basin. There is no doubt that if research were successful into optimum recovery techniques for unconventional gas and oil resource bases, that the American independent oil companies would agressively pursue the development of respective HC resource bases. However, favorable tax statuses may be necessary to aid initial research into, and production of, unconventional HC resource bases. It would clearly be the responsibility of the Federal Government to establish these statuses if they are necessary to abate the domestic energy problem.

CONCLUSIONS

The principal conclusions of this study may occasionally be annotated as either facts or hypotheses to aid the reader.

1) By accepted paradigms in petroleum geochemistry, C_{15+} HC's are destroyed by R_o = 1.35%, C_{2+} HC's by R_o = 2.00%, and methane by R_o = 4.00%. It is fact that: 1) C_{15+} HC's are thermally stable to ranks as high as R_o = 7.0-8.0% in deep, unsheared, petroleum basins. 2) C_{2+} HC's are thermally stable to even higher ranks, well into true rock metamorphism. 3) Methane is stable probably into mantle conditions. However, these HC thermal stabilities carry no connotations for the existence of conventional oil or gas deposits extending to those respective ranks, and such deposits may not necessarily be expected at those ranks.

2) The evidence for such C_{15+} HC thermal stability comes from: A) petroleum-geochemical analyses of ultra-deep (7-10 km), high-rank (R_o = 2.0-8.0%), fine-grained rocks, analyses which demonstrate that moderate to high concentrations of C_{15+} HC's survive to these ranks; B) compositional changes in both the saturated and aromatic HC's in the approach to and during C_{15+} HC thermal destruction, changes which have been only occasionally observed in the deepest rocks of sedimentary basins; c) long-established physical-chemical laws which demonstrate that C_{15+} saturated, and especially aromatic, HC's are thermally stable species with high bond energies; D) published data which demonstrates that low concentrations of C_{15+} HC's persist into conditions of true rock metamorphism and other high temperature settings; E) "oils" of normal (moderate) maturities (as determined by biomarker analyses) entrained in very low concentrations (by gas solution) in dry "high-rank" gas deposits; F) a lack of high-temperature assemblages of saturated and aromatic HC's in "high-rank" gas deposits; 6) the rare occurrences of high-rank oil deposits that do exist, and H) the lack of the expected methane carbon-isotopic compositions versus depth in the high-rank, dry gas deposits of the Anadarko Basin, if such gas deposits indeed originated by thermal destruction of C_{15+} HC's.

3) According to paradigms of present-day petroleum geochemistry, the controlling parameters of OM metamorphism are burial temperature and geologic time (e.g. - first-order reaction kinetics). These controlling parameters predict C_{15+} HC thermal destruction by R_o = 1.35%. This prediction is in strong contrast with observed C_{15+} HC thermal stability to R_o = 7.0-8.0%. Furthermore, it is maintained here that no *solid* evidence exists which allows

the conclusion that OM metamorphism follows first-order reaction kinetics. Thus it is concluded that the controlling parameters of OM metamorphism, according to present-day petroleum-geochemical paradigms, must be at least partially in error.

Alternate controlling parameters of OM metamorphism are hypothesized here based on long-term research on the topic. Increases in burial temperature are the principal drive for the reactions, a conclusion in agreement with accepted models. Other controlling parameters and characteristics of OM metamorphic reactions are hypothesized to be: A) Increases in static fluid pressures retard all aspects of OM metamorphism. B) The presence of water enriches (hydrogenates) kerogen and suppresses HC thermal destruction. C) Open or closed reaction sites: open reaction sites (product escape) promotes OM metamorphism, closed reaction sites (product retention) retards OM metamorphism. D) OM metamorphic reactions are not first-order reactions, but are higher-ordered reactions. E) The reactivities of the different kerogen (OM) types vary, increasing with increase in sulphur content and decreasing with increase in hydrogen content. Thus Type II-S OM reacts before Type III OM which reacts before Type II OM which reacts before Type I OM.

4) Evidence for deep-basin HC destruction has classically been attributed to the lack of deep-basin oil deposits and strong basinal HC zonations: dry gas only in the deep basin, oil on the shelves with both gas-oil-ratios and API gravities decreasing with decreasing burial. However, these two HC distribution patterns (no deep-basin oil and strong basinal HC zonations) can also be explained by: 1) emplacement processes during migration (oil emplaced mostly at shallow depths during vertical migration); and 2) condensation, buoyancy, migration, and "flushing" processes (Gussow's (1954) principle of differential entrapment) which also applies to the C_2-C_4 HC gases in the deep basin).

5) It is fact that because of their high aqueous solubilities, both CO_2 and H_2S would quickly (10^4-10^5 years) be leached out of water-bearing deep gas deposits. Thus the presence of either of these two gases in deep-basin gas deposits dictates that such gas deposits: 1) contain no water; and 2) are closed systems with regard to fluid migration. The probability of water-free, deep-basin gas reservoirs carry strong implications for: 1)enhanced thermal destruction of C_{15+} HC's; and 2) possible formation (skin) damage around the wellbore during drilling, completion, and stimulation procedures.

6) It is fact that some gas deposits show by methane-isotopic, compositional, and geologic evidence that they have had a high temperature (400°-1200°C?) origin, involving C_{15+} HC thermal destruction. However, such gas deposits appear to be unusual, based on existing data. It is hypothesized that most high-rank, deep-basin, dry gas deposits have not originated by an in-reservoir thermal destruction of C_{15+} HC's. Such methane deposits instead are believed to largely be made up of methane cogenerated with C_{15+} HC's during both the intense and late stages of C_{15+} HC generation from kerogen. Condensation and buoyancy processes combined with Gussow's (1954) principal of differential entrapment, are believed to lead to an expulsion of all C_{2+} HC's (and perhaps water) from deep-basin gas traps.

7) It is hypothesized that intense faulting and fracturing are necessary for highly efficient primary migration of gases from source rocks. Thus "conventional" deep-basin gas deposits should nearly always be associated with major faulting. Normal and extensional faulting would be most favorable for

migration because of voids along the fault zones. Later evolution to compressional (high-angle reverse) faulting (such as occurred in the Anadarko Basin in Southern Oklahoma) would be favorable for preservation of deep-basin gas deposits over geologic time.

8) The existence of cracks, fractures, parting laminae and other such "non-classical" voids in deep-basin rocks may help offset a general trend of decreasing porosity with increase in maturation rank (depth) in deep petroleum basins.

9) It is fact that very large, in-place, non-conventional gas-resource bases have been proven, among which are: basin-centered gas deposits, coal-gas, tight-gas, black-shale gas, and Gulf Coast geopressured-geothermal gas. It is hypothesized that the existence of such unconventional gas-resource bases are primarily due to, and are direct evidence of, highly restricted fluid flow and inefficient primary HC migration in deep sedimentary basins. Much of the rock volume of deep sedimentary basins is perceived to be an essentially closed system with respect to significant fluid flow once basinal evolution goes beyond the youthful stage to the mature stage with a corresponding decline in geothermal gradients.

It is further hypothesized that some parts of these different non-conventional gas-resource bases may be both larger and of a higher grade than previously perceived.

10) It is concluded here that (with some exceptions) further geologic-geochemical studies attempting to document the existence and characteristics of such non-conventional gas-resource bases may to some extent be counter-productive. Much more beneficial research might be geologic-based engineering studies to determine the appropriate techniques, applicable to the non-classical characteristics of each of these different gas-resource bases, so that viable economic recovery of these energy bases may possibly be carried out by American independent oil companies.

It is further concluded here, that with our present knowledge, America's only viable hope of abating an increasing and dangerous dependence on Middle East energy are aggressive research programs on possible economic recovery of these very large, in-place, non-conventional gas (and oil) resource bases.

REFERENCES CITED

Akihisa, K., 1978, Etude cinétique des roches méres de pétrole (rapport n°4): Formation de produits pétroliers par pyrollyse du kérogene á basse température: Journal Japanese Association Petroleum Technology 44, p. 26-33.

Al-Shaieb, Z., 1991, Compartmentation, fluid pressure important in Anadarko exploration: Oil and Gas Journal, July 8, p. 52-55.

Baker, D.R., and Claypool, G.E., 1970, Effects of incipient metamorphism on organic matter in mudrock: American Association Petroleum Geologists Bulletin, v. 54, p. 456-468.

Barker, C., 1972, Aquathermal pressuring - Role of temperature in development of abnormal-pressure zones: American Association Petroleum Geologists Bulletin, v. 56, p. 2068-2071.

Barker, C.E., 1991, Implications for organic maturation studies of evidence for a geologically rapid increase and stabilization of vitrinite reflectance at peak temperature: Cerro Prieto geothermal system, Mexico. American Association Petroleum Geologists Bulletin, v. 75, p. 1852-1863.

Barker, C.E., and Pawlewicz, M.J., 1986, The correlation of vitrinite reflectance with maximum temperature in organic matter, *in* Paleogeothermics, Lecture Notes in Earth Sciences, v. 5, (eds. G. Buntebarth, and L. Stegna), Springer-Verlag, p. 79-93.

Bertrand, P., 1984, Geochemical and petrographic characterization of humic coals considered as possible source rocks: Organic Geochemistry, v. 6, p. 481-488.

Bostick, N., 1970, Thermal alteration of clastic organic particles (phytoclasts) as an indicator of contact and burial metamorphism in sedimentary rocks: Ph.D. Thesis, Stanford University.

Braun, R.L., and Burnham, A.K., 1990, Mathematical model of oil generation, degradation, and expulsion: Energy and Fuels, v. 4, p. 132-146.

Brooks, T.D., 1971, Some chemical and geochemical studies on sporopollenin, *in* Sporopollenin (eds. J. Brooks, P.R. Grant, M. Muir, P. Gijzel, and G. Shaw), Academic Press, London, p. 351-407.

Burnham, A.K., 1989, A simple model of petroleum formation and cracking: Lawerence Livermore Laboratory Report UCID 21665, March 1989.

Burnham, A.K., Braun, R.L., and Gregg, H.R., 1987, Comparison of methods for measuring kerogen pyrolysis rates and fitting kinetic parameters: Journal of Energy Fuels 1, p. 452-458.

Cardott, B.J., and Lambert, M.W., 1985, Thermal maturation by vitrinite reflectance of Woodford Shale, Anadarko Basin, Oklahoma: American Association Petroleum Geologists Bulletin, v. 69, p. 1982-1988.

Castelli, A., Chiaramonte, M. A., Bettrame, P.L., Carniti, P., Delbianco, A., and Stroppa, F., 1990, Thermal degradation of kerogen by hydrous pyrolysis: a kinetic study, *in* Advances in Organic Geochemistry 1989 (eds: B. Durand and F: Behar): Organic Geochemistry, v. 16, p: 75-82.

Cecil, B., Stanton, R., Allshouse, S., and Cohen, M.A., 1979, Effects of pressure on coalification: Ninth International Congress of Carboniferous Stratigraphy and Geology, Univ. of Illinois, Urbana, Illinois, May 19-267, Abstracts of Papers, p. 32.

Chung, M., and Sackett, W., 1978, Carbon isotope fractionation during coal pyrolysis, Fuel, v. 57, p. 734-735.

Claypool, G.E., and Mancini, E.A., 1989, Geochemical relationships of petroleum in Mesozoic reservoirs to carbonate source rocks of Jurassic Smackover Formation, southwestern Alabama: Bulletin of the American Association of Petroleum Geologists, v. 73, p. 904-924.

Connan, J., 1974, Time-temperature relation in oil genesis: American Association Petroleum Geologists Bulletin, v. 58, p. 2516-2521.

Connan, J., Montel, F., Blanc, P.H., Sahuquet, B., Jouhannel, R., 1992, Experimental study of expulsion of HC's from shaley source rocks-Importance of pressure on expulsion efficiencies: in Advances in Organic Geochemistry 1991 (in press).

Cooles, G.P., Mackenzie, A.S., and Quigley, T.M., 1986, Calculation of petroleum masses generated and expelled from source rocks, *in* Advances in Organic Geochemistry 1985 (eds. D. Leythaeuser and J. Rullkötter): Organic Geochemistry, v. 10, p. 235-245.

Cottrell, T.L., 1958, The Strengths of Chemical Bonds: Butterworths.

Davis, J.B., 1967, Petroleum Microbiology: Elsevier.

Dickey, P.A., and Cox, W.C., 1977, Oil and gas reservoirs with subnormal pressures: American Association Petroleum Geologists Bulletin, v. 61, p. 2134-2142.

Dominé, F., 1991, High pressure pyrolysis of n-hexane, 2-4 dimethylpentane and 1-phenylbutane. Is pressure an important geochemical parameter? Organic Geochemistry, v. 17, p. 619-634.

Dominé, F., and Enguehard, F., 1992, Kinetics of hexane pyrolysis at very high pressures. Application to geochemical modeling: Organic Geochemistry (in press).

Eggers, D.F., Gregory, N.W., Halsey, G.D., and Rabinovitch, B.S., 1964, Physical Chemistry: Wiley and Sons.

Espitalié, J., Maxwell, J. R., Chenet, Y., and Marquis, F., 1988, Aspects of hydrocarbon migration in the Mesozoic in the Paris Basin as deduced from an organic geochemical survey, *in* Advances in Organic Geochemistrty 1987 (eds. L. Mattavelli and L. Novelli): Organic Geochemistry, v. 13, p. 457-481.

Espitalié, J., Ungerer, P., Irwin, I., and Marquis, F., 1988, Primary cracking of kerogens. Experimenting and modeling C_1, C_2-C_5, C_1-C_{15} and C_{15+} classes of hydrocarbons formed: Organic Geochemistry, v. 13, p. 893-899.

Forsman, J.P., and Hunt, J.M., 1958, Insoluble organic matter (kerogen) in sedimentary rock of marine origin, *in* Habitat of Oil (ed. L.G. Weeks), American Association Petroleum Geologists, p. 747-778.

Ghaith, A., Chen, W., Ortoleva, P., 1990, Oscillatory methane release from shale source rock: Earth Science Reviews, v. 29, p. 241-248.

Gies, R.M., 1984, Case history for a major Alberta deep basin gas trap: The Cadomin Formation, in Elmworth-Case study of a deep basin gas field (ed. J. A. Masters): American Association Petroleum Geologists Memoir 38, p. 35-47.

Goffé, and Villey, M., 1984, Texture d'un matériel carboné impliqué-dans un metamoprhisme haute pression-basse température (Alpes Francaises). Les hautes pressions influenant--elles la carbonification? Bulletin Minéral. 107, p. 81-91.

Goodarzi, F., and Murchison, D., 1977, Effect of prolonged heating on the optical properties of vitrinite: Fuel, v. 56, p. 89-96.

Gould, E.S., 1959, Mechanism and Structure in Organic Chemistry: Henry Holt and Co.

Gussow, W.C., 1954, Differential entrapment of oil and gas.- A fundamental principle: American Association Petroleum Geologists Bulletin, v. 38, p. 816-853.

Guthrie, J.M., Houseknecht, D.W., and Johns, W.D., 1986, Relationships among vitrinite reflectance, illite crystallinity, and organic geochemistry in Carboniferous strata, Ouachita Mountains, Oklahoma and Kansas: Bulletin American Association Petroleum Geologists, v. 70, p. 26-33.

Hacquebard, P.A., 1975, Correlation between coal rank, paleotemperature and petroleum occurrences in Alberta: Canadian Geological Survey, Paper 75-1, Part B, 5-8.

Hacquebard, P.A., and Donaldson, J.R., 1974, Rank studies of coals in the Rocky Mountains and Inner Foothills Belt, Canada: Geological Society of American Special Paper Paper 153, p. 75-94.

Hamill, W.H., Williams, R.R., 1959, Principles of physical chemistry: Prentice-Hall.

Hayes, J.M., 1991, Stability of petroleum: Nature, v. 352, July 11, p. 108-109.

Hedberg, H.D., 1980, Methane generation and petroleum migration, *in* Problems of petroleum migration (eds. W.H. Roberts and R.J. Cordell): American Association of petroleum Geologists Studies in Geology 10, p. 179-206.

Helgeson, H., 1992, Organic/inorganic reactions in metamorphic processes: Canadian Mineralogy Greenwood Symposium Issue (in press).

Hesp, W., and Rigby, D., 1973, The geochemical alteration of hydrocarbons in the presence of water: Erdöl und Kohle-Erdgas, v. 26, p. 70-76.

Hoering, T.C., and Abelson, P.H., 1964, Hydrocarbons from the low-temperature heating of a kerogen: Carnegie Institute Yearbook 1963-1964, v. 1440, p. 256-258.

Hoering, T.C., and Hart, R., 1964, A geochemical study of some Adirondack graphites: Carnegie Institute Yearbook 1963-1964, v. 1440, p. 265-267.

Horsfield, B., Schenk, H.J., Mills, N., and Welte, D.H., 1992, Closed-system programmed temperature pyrolysis for simulating the conversion of oil to gas in a deep petroleum reservoir, compositional and kinetic findings: in Advances in Organic Geochemistry 1991 (in press).

Hunt, J.M., 1979, Petroleum Geochemistry and Geology: Freeman and Company.

Hutcheon, I., Oldershaw, A., and Ghent, E.D., 1980, Diagenesis of Cretaceous sandstones of the Kootenay Formation at Elk Valley (southeastern British Columbia) and Mt. Allan (southwestern Alberta): Geochimica et Cosmochimica Acta, v. 44, p. 1425-1435.

Ishiwatari, R., Ishiwatari, M., Rohrback, B.G., and Kaplan, I.R., 1977, Thermal alteration experiments on organic matter from recent marine sediments in relation to petroleum genesis: Geochim. et Cosmochim. Acta, v. 41, p. 815-828.

Kalkreuth, W., and McMechan, M., 1988, Burial history and thermal maturity, Rocky Mountain Front Ranges, Foothills, and Foreland, East Central British Columbia and adjacent Alberta, Canada: Bulletin of the American Association of Petroleum Geologists, v. 72, p. 1395-1410.

Karweil, J., 1955, The metamorphasis of coals from the standpoint of physical chemistry: Z. Deut. Geol. 107, p. 132-139.

Kawka, O.E., and Simoneit, B.R.T., 1987, Survey of hydrothermally-generated petroleums from the Guaymas Basin spreading center: Organic Geochemistry, v. 11, p. 311-328.

Klotz, I.M., 1964, Introduction to Chemical Thermodynamics: W. A. Benjamin.

Kontorovich, A.E., and Trofimuk, A.A., 1976, Lithogenezi neftegazoobrazoveniye (Lithogenesis and formation of oil and gas), *in* Goryuchiye Iskopayeme-Problemy Geoloii i Geokhiii Noftidov i Bituminoznykh Porod, Mezhdunarodnyy Geologicheskiy Kongress XXV Sessiya Doklady Sovetskikh Geologov (eds. N.B. Vassoyevich and others): Nauka Press, p. 19-36.

Law, B.E., Spencer, C.W., Charpentier, R.A., Crovelli, R.A., Mast, R.F., Dolton, G.L., and Wandrey, C.J., 1989, Estimates of gas resources in overpressured low-permeability Cretaceous and Tertiary sandstone reservoirs, Greater Green River Basin, Wyoming, Colorado, and Utah: in Gas resources of Wyoming, Wyoming Geological Association Guidebook, Fourtieth Field Conference, p. 36-62.

Lewan, M.D., 1983, Effects of thermal maturation on stable organic carbon isotopes as determined by hydrous pyrolysis of Woodford Shale: Geochim. Cosmochim. Acta, v. 47, p. 1471-1479.

Lewan, M.D., 1985, Evaluation of petroleum generation by hydrous pyrolysis experimetnation: Phil. Trans. R. Soc. Lond., v. 315, p. 123-134.

Lewan, M.D., 1992, Laboratory simulation of petroleum formation: Hydrous pyrolysis, *in* Organic Geochemistry (eds. M.H. Engel and S.A. Macko), Plenum Publishing (in press).

Leythaeuser, D., Schaefer, R.G., and Yukler, A., 1980, Diffusion of light hydrocarbons through near-surface rocks: Nature, v. 284, p. 522-525.

Leythaeuser, D., Littke, R., Radke, M., and Schaefer, R.G., 1983, Geochemical effects of petroleum migration and expulsion from Toarcian source rocks in the Hills syncline area, NW Germany, *in* Advances in Organic Geochemistry 1987 (eds. L. Mattavelli and L. Novelli), Organic Geochem. 13, p. 489-502.

Leythaeuser, D., Miller, P.J., Radke, M., and Schaefer, R.G., 1987, Geochemistrty can trace primary migration of petroleum: Recognition and quantification of expulsion effects, *in* Migration of Hydrocarbons in Sedimentary Basins (ed. B. Doligez): Editions Technip. p. 197-222.

Lopatin, N.V., 1971, Temperature and geologic time as factors in coalification: Akademiya Nauk SSSR Ser. Geologicheskaya, Izvestiya 3, p. 95-106.

Mackenzie, A.S., Price, I., Leythaeuser, D., Muller, P., Radke, M., and Schaefer, R.G., 1987, The expulsion of petroleum from Kimmeridge clay source rocks in the area of the Brae Oilfield, UK Continental Shelf, *in* Petroleum Geology of Northwest Europe (eds. J. Brooks and K. Glennie), Graham and Trotman, p. 865-877.

Magara, K., 1986, Thickness of removed sedimentary rocks, Paleopore pressure, and Paleotemperature, Southwestern part of Western Canada basin: American Association Petroleum Geologists Bulletin, v. 60, p. 554-565.

Mango, F.D., 1990, The origin of light cycloalkanes in petroleum: Geochim. Cosmochim. Acta, v. 54, p. 23-27.

Mango, F., 1991, The stability of hydrocarbons under time-temperature conditions of petroleum genesis: Nature, v. 352, p. 146-148.

Masters, J.A., 1979, Deep basin gas trap, Western Canada: Bulletin of the American Association Petroleum Geology, v. 63, p. 152-181.

Masters, J.A., 1984, Lower Cretaceous oil and gas in western Canada: in Elmworth-Case study of a deep basin gas field (ed. J.A. Masters), American Association Petroleum Geologists Memoir 38, p. 1-33.

Masters, J.A., 1984b, Elmworth-Case study of a deep basin gas field, *in* Elmworth-çase study of a deep basin gas field (ed. J.A. Masters), American Association Petroleum Geologists Memoir 38.

Mattavelli, L., Ricchiuto, T., Grignani, D., and Schoell, M., 1983, Geochemistry and habitat of natural gases in Po basin, northern Italy: American Association Petroleum Geologists Bulletin, v. 67, p. 2239-2254.

McIntyre, D.J., 1972, Effect of experimental metamorphism on pollen in a lignite: Geoscience and Man, v. 4, p. 111-117.

Meissner, F.F., 1978, Petroleum geology of the Bakken Formation, Williston basin, North Dakota and Montana, *in* 1978 Williston basin Symposium: Billings, Montana Geological Society (ed: D. Rehrig), p: 207-227.

McTavish, R.A., 1978, Pressure retardation of vitrinite diagenesis, offshore northwest Europe: Nature 271, 648-650.

Monthioux, M., Landais, P., and Durand, B., 1986, Comparison between extracts from natural and artificial maturation series of Mahakam delta coals, *in* Advances in Organic Geochemistry 1985 (eds. D. Leythaeuser and J. Rullkötter): Organic Geochemistry, v. 10, p. 299-311.

Novelli, L., Chiaramonte, M.A., Mattavelli, L., Pizzi, G., Satori, L., and Scotti, P., 1987, Oil habitat in the Northwestern Po basin: *in* Migration of Hydrocarbons in Sedimentary Basins (ed. B. Doligez), Editions Technip., p. 27-58.

Orr, W.L., 1974, Changes in sulfur content and isotopic ratios of sulfur during petroleum maturation-- study of Big Horn basin Paleozoic oils: Bulletin of the American Association of petroleum Geologists, v. 58, p. 2295-2318.

Orr, W.L., 1986, Kerogen/asphaltene/sulfer relationships in sulfur-rich Monterey oils, in Advances in Organic Geochemistry 1985: Organic Geochemistry, v. 10, p. 499-516.

Patridge, J.F., 1958, Oil occurrence in Permian, Pennsylvanian and Mississippian rocks, Big Horn Basin, Wyoming: *in* L.G. Weeks, ed., Habitat of oil: American Association of Petroleum Geologists, p. 293-306.

Pauling, L., 1960, The Nature of the Chemical Bond: Cornell Unviersity Press.

Pearson, D.B., 1981, Experimental simulation of thermal maturation in sedimentary organic matter: Ph.D. Thesis, Rice University.

Petroleum Information Corporation, 1984, Carbon dioxide and its application to enhanced oil recovery: Petroleum Frontiers, v. 2, no. 1, p. 1-63.

Phillipi, G.T., 1965, On the depth, time, and mechanism of petroleum generation: Geochimica et Cosmochimica Acta, v. 29, p. 1021-1051.

Phillipi, G.T., 1977, On the depth, time and mechanism of petroleum generation: Geochim. Cosmochim. Acta, v. 29, p. 1021-1051.

Powley, D.E., 1990, Pressures and hydrogeology in petroleum basins: Earth Science Reviews, v. 29, p. 215-226.

Price, L.C., 1978a, Crude oil and natural gas dissolved in deep, hot geothermal waters of petroleum basins--a possible significant new energy source: *in* Proceedings of the Third Conference on Geopressured-Geothermal Energy (ed. J. Meriwether), Lafayette, Louisiana, Nov. 16-18, 1977, 1, p. G1167-G1249.

Price, L.C., 1978b, Crude oil and natural gas dissolved in deep, hot, geothermal waters of petroleum basins--a possible significant new energy source: American Association Petroleum Geologists Bulletin, v. 62, p. 555-556.

Price, L.C., 1980a, Shelf and shallow basin as related to hot-deep origin of petroleum: Journal of Petroleum Geology, v. 3, p. 91-116.

Price, L.C., 1980b, Crude oil degradation as an explanation of the depth rule: Chemical Geology, v. 28, p. 1-30.

Price, L.C., 1981, Aqueous solubility of crude oil to 400°C, 2000 bars pressure in the presence of gas: Journal of Petroleum Geology, v. 4, p. 195-223.

Price, L.C., 1982, Organic geochemistry of 300°C, 7-km core samples, South Texas: Chemical Geology, v. 37, p. 205-214.

Price, L.C., 1983, Geologic time as a parameter in organic metamorphism and vitrinite reflectance as an absolute paleogeothermometer: Journal of Petroleum Geology, v. 6, p. 5-38.

Price, L.C., 1985, Geologic time as a parameter in organic metamorphism and vitrinite reflectance as an absolute paleogeothermometer: Reply. Journal of Petroleum Geology, v. 8, p. 233-240.

Price, L.C., 1986, A critical overview and proposed working model of surface geochemical exploration, *in* Unconventional methods in exploration for petroleum and natural gas, IV (ed. M.J. Davidson): Dallas, Tex., Southern Methodist University Press, p. 245-304.

Price, L.C., 1988, The organic geochemistry (and causes thereof) of high-rank rocks from the Ralph Lowe-1 and other well bores: U.S.Geological Survey Open-File Report 91-307, 55 p.

Price, L.C., 1989a, Primary petroleum migration from shales with oxygen-rich organic matter: Journal of petroleum Geology, v. 12, p. 289-324.

Price, L.C., 1989b, Hydrocarbon generation and migration from Type III kerogen as related to the oil window: U.S. Geological Survey Open-File Report 89-194.

Price, L.C., 1991, Considerations of oil origin, migration, and accumulation at Caillou Island and elsewhere in the Gulf Coast: U.S. Geological Survey Open-File Report 91-307, 55 p.

Price, L.C., 1992, Basin richness versus faulting and source rock disruption--a fundamental relationship: in prep.

Price, L.C., Clayton, J.L., and Rumen, L.L., 1979, Organic geochemistry of a 6.90 kilometer-deep well, Hinds County, Mississippi: Transactions Gulf Coast Geological Society, v. 29, p. 352-370.

Price, L.C., Clayton, J.L., and Rumen, L.L., 1981, Organic geochemistry of the 9.6 km Bertha Rogers #1, Oklahoma: Journal Organic Geochemistry, v. 3, p. 59-77.

Price, L.C., Wenger, L.M., Ging, T. G., and Blount, C. W., 1983, Solubility of crude oil in methane as a function of pressure and temperature: Organic Geochemistry, v. 4, p. 201-221.

Price, L.C., Ging, T.G., Daws, T.A., Love, A.H., Pawlewicz, M.J., and Anders, D.E., 1984, Organic metamorphism in the Mississippian-Devonian Bakken

shale North Dakota portion of the Williston basin, *in* Hydrocarbon Source Rocks of the Greater Rocky Mountain Region (eds. J. Woodward, F.F. Meissner, and J.L. Clayton): Rocky Mountain Association of Geologists, p. 83-113.

Price, L.C., and Barker, C.E., 1985, Suppression of vitrinite reflectance in amorphous rich kerogen--A major unrecognized problem: Journal of Petroleum Geology, v. 8, p. 59-84.

Price, L.C., Daws, T., and Pawlewicz, M., 1986, Organic metamorphism in the Lower Mississippian-Upper Devonian Bakken Shales. Part I: Rock-Eval pyrolysis and vitrinite reflectance: Journal of Petroleum Geology, v. 9, p. 125-162.

Price, L.C. and Clayton, J.L., 1990, Reasons for and significance of deep, high-rank hydrocarbon generation in the South Texas Gulf Coast: in Gulf Coast Oils and Gases (eds. D. Schumacher and B. F. Perkins), Proceedings Ninth Annual Research Conference Gulf Coast Section, SEPM, p. 105-137.

Price, L.C., and Le Fever, J.A., 1992, Does Bakken horizontal drilling imply huge oil-resource bases in fractured shales? *in* Geological Studies Relavent to Horizontal Drilling, Western North America, ed. J. Schmoker), Rocky Mountain Association of Geologist (in press).

Price, L.C., and Wenger, L.M., 1992, The influence of pressure on petroleum generation and maturation as suggested by aqueous pyrolysis: in Advances in Organic Geochemistry 1991 (in press).

Rice, D.D., 1980, Chemical and isotopic evidence of the origins of natural gases in offshore Gulf of Mexico: Gulf Coast Geological Society Transactions, v.30, p. 203-213.

Rice, D.D., and Claypool, G.E., 1981, Generation, accumulation, and resource potential of biogenic gas: American Association Petroleum Geologists Bulletin, v. 65, p. 5-25.

Rice, D.D., Threlkeld, C.N., and Vuletich, A. K., 1988, Analyses of natural gases from Anadarko basin, southwestern Kansas, Western Oklahoma, and Texas Panhandle: U.S. Geological Survey Open-File Report 88-391.

Roberts, J.D., and Caserio, M.C., 1964, Basic Principles of Organic Chemistry: W.A. Benjamin.

Rogers, J., Suggate, R., Elphick, J., and Ross, J., 1962, Metamorphism of a lignite: Nature, v. 195, p. 1078-1080.

Sagjó, Cs., 1980, Hydrocarbon generation in a super-thick Neogene sequence in south-east Hungary. A study of the extractable organic matter: *in* Advances in Organic Geochemistry 1979 (eds. A.G. Douglas and J.R. Maxwell), Pergamon, p. 103-113.

Salisbury, G.P., 1968, Natural gas in Devonian and Silurian rocks of Permian Basin, West Texas and Southeast New Mexico. *in* Natural gases of North America (eds. B.W. Beebe, and B.F. Curtis): American Association Petroleum Geologists Memoir 9, p. 1433-1445.

Sassen, R., and Moore, C.H., 1988, Framework of hydrocarbon generation and destruction in eastern Smackover trend: Bulletin of the American Association of Petroleum Geologists, v. 72, p. 649-663.

Schock, E., 1990, Geochemical considerations of the origin of organic compounds in hydrothermal systems: Origins of Life and Evolution of the Biosphere, v. 20, p. 331-367.

Shepeleva, N.N., Ogloblina, A.I., and Pikovskiy, Yu I., 1990, Polycyclic aromatic hydrocarbons in carbonaceous material from the Daldyn-Alakit region, Siberian Platform: Geochem. Int., v. 28, 4, p. 98-107.

Sienko, M.J., and Plane, R.A., 1961, Chemistry: McGraw-Hill.

Simoneit, B.R.T., 1983, Organic matter maturation and petroleum genesis: Geothermal versus hydrothermal, in The Role of Heat in the Development of Energy and Mineral Resources in the Northern Basin and Range Province: Geothermal Resources Council, Davis, CA, Special Report No. 13, p. 215-241.

Simoneit, B.R.T., 1984, Hydrothermal effects on organic matter. High versus low temperature components, *in* Advances in Organic Geochemistry 1983 (eds. P.A. Schenck, J.N. de Leuw, and G.W.M. Lijmbach): Organic Geochemistry, v. 6, p. 857-864.

Simoneit, B.R.T., 1985, Hydrothermal petroleum: Genesis, migration and deposition in Guaymas basin, Gulf of California: Canadian Journal of Earth Sciences, v. 22, p. 1919-1929.

Simoneit, B.R.T., Philp, R.P., Jenden, P.D., and Galimov, E.M., 1984, Organic geochemistry of Deep Sea Drilling Project sediments from the Gulf of California - Hyrothermal effects on unconsolidated diatomooze: Organic Geochemistry, v. 7, p. 173-205.

Simoneit, B.R.T. and Kawka, O.E., 1987, Hydrothermal petroleum from diatomites in the Gulf of California, *in* Marine Petroleum source Rocks (eds. J. Brooks and A. Fleet): Geological Society of London Special Publication No. 26, p. 217-228.

Smith, G.W., 1985, Geology of the deep Tuscaloosa (Upper Cretaceous) gas trend in Louisiana, *in* Proceedings Fourth Annual Research Conference Gulf Coast Section SEPM (eds. B.F. Perkins, and G.B. Martin, p. 153-190

Sokolov, V.A., Geodekyan, A.A., Grigoryev, C.G., Krems, A.Ya., Stroganov, V. A., Zorkin, L.M., Zeidelson, M.I., and Vainbaum, S. Ja., 1971, The new methods of gas surveys, gas investigations of wells and some practical results: *in* Geochemical Exploration, Special Volume 11 Canadian Institute of Mining and Metallurgy (ed. R.W. Boyle), p. 538-544.

Spencer, C.W., 1987, Hydrocarbon generation as a mechanism for overpressuring in Rocky Mountain region: \ American Association Petroleum Geologists Bulletin, v. 71, p. 368-388.

Stahl, W., 1974, Carbon isotopic ratios of German natural gases in comparison with isotope data of gaseous hydrocarbons from other parts of the world: *in* Advances in Organic Geochemistry 1973 (eds. B. Tissot and F. Biennier), p. 453-462.

Stanier, R.Y., Doudoroff, M., and Adelberg, E.A., 1963, The Microbial World. Second Edition: Prentice-Hall.

Talukdar, S., Gallango, O., Vallejos, C., and Ruggiero, A., 1987, Observations on the primary migration of La Luna source rocks of the Maracaibo Basin, Venezuela: *in* Migration of Hydrocarbons in Sedimentary Basins (ed. B. Doligez, Editions Technip, p. 59-77.

Teichmüller, M., and Durand, B., 1983, Fluorescence microscopial rank studies on liptinites and vitrinites in peats and coals and comparison with results of the ROCK EVAL pyrolysis: International Journal of Coal Geology, v. 2, p. 197-230.

Tigert, V., and Al-Shaieb, Z., 1990, Pressure seals their diagenetic banding patterns, 29, p. 227-240.

Tilley, B.J., Nesbitt, B.E., and Longstaffe, F.J., 1989, Thermal history of Alberta deep basin: Comparative study of fluid inclusion and vitrinite reflectance data: American Association Petroleum Geologists Bulletin, v. 73, p. 1206-1222.

Tissot, B.P., and Welte, D.H., 1984, Petroleum Formation and Occurence: Springer Verlag.

Tissot, B.P., Pelet, R., and Ungerer, P.H., 1987, Thermal history of sedimentary basins, maturation indices, and kinetics of oil and gas generation: Bulletin American Association of Petroleum Geology, v. 71, p. 1445-1466.

Todd, T.W., 1963, Post-depositional history of Tensleep Sandstone (Pennsylvanian), Big Horn basin, Wyoming: Bulletin of the American Association of Petroleum geologists, v. 47, p. 599-616.

Ungerer, P., Behar, E., and Discamps, D.,1983, Tentative calculation of the overall volume expansion of organic matter during hydrocarbon genesis from geochemistry data: Implications for primary migration: *in* Advances in Organic Geochemistry 1981, eds. M. Bjoray and others), 129-135, Wiley, Chichester.

Ungerer, P., and Pelet, R., 1987, Extrapolation of the kinetics of oil and gas formation from laboratory experiments to sedimentary basins: Nature, v. 327, p. 52-54.

Ungerer, P., 1990, State of the art reserarch in kinetic modeling of oil formation and expulsion: *in* Advances in Organic Geochemistry 1989 (eds. B. Durand and F. Behar). Organic Geochemistry, v. 16, p. 1-25.

Ungerer, P., Chenet, P.Y., Moretti, I., Chiarelli, A., and Oudin, J.L., 1986, Modeling oil formation and migration in the southern part of the Suez rift, Egypt: Organic Geochemistry, v. 10, p. 247-260.

Ungerer, P., Doligez, B., Chenet, P.Y., Burrus, J., Bessis, F., Lefargue, E., Giroir, G., Heurn, O., and Eggen, S., 1987, A 2-D model of basin scale petroleum migration by two-phase fluid flow appliciation to some case studies: *in* Migration of Hydrocarbons in Sedimentary Basins (ed. B. Doligez), Editions Technip p. 415-456.

Weismann, T.J., 1971, Stable carbon isotope investigation of natural gases from Sacramento and Delaware-Val Verde basins--Possible igneous origins: American Association of Petroleum Geologists Bulletin, v. 55, p. 369.

Welte, D.H., Stoessinger, W., Schaefer, R.G., Radke, M., 1984, Gas generation and migration in the deep basin of Western Canada: *in* Elmworth-Case Study of a deep basin gas field (ed. J.A. Masters), American Association Petroleum Geologists Memoir 38, p. 1-33.

Wenger, L.M., and Price, L.C., 1992, Differential petroleum generation and maturation paths of the different organic matter types as determined by hydrous pyrolysis over a wide range of experimental temperatures: Advances in Organic Geochemistry 1991 (in press).

Winkler, H.G.F., 1976, Petrogenesis of metamorphic rocks: Springer Verlag, New York.

Zumberge, J.E., Sutton, C., Martin, S.J., and Worden, R.D., 1988, Determining oil generation kinetic parameters by using a fused quartz pyrolysis system: Energy and Fuels, v. 2, p. 264-266.

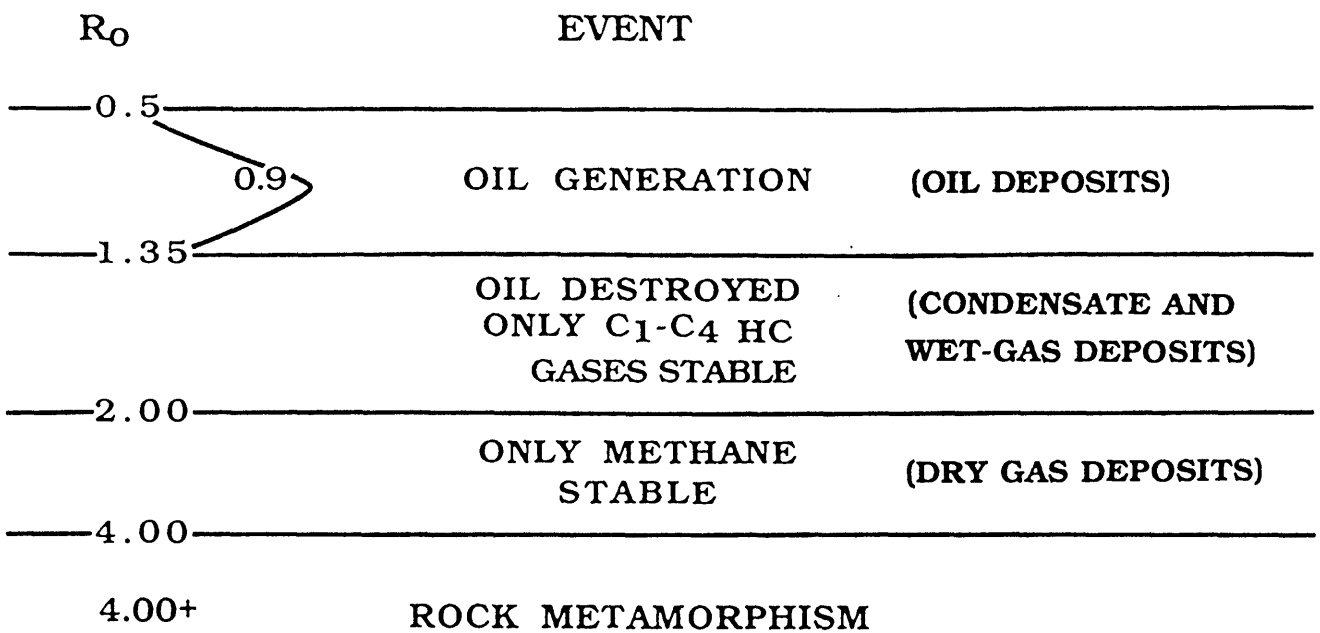

Figure 6-1. Accepted convention regarding occurrence of principal petroleum-geochemical events and HC thermal stability.

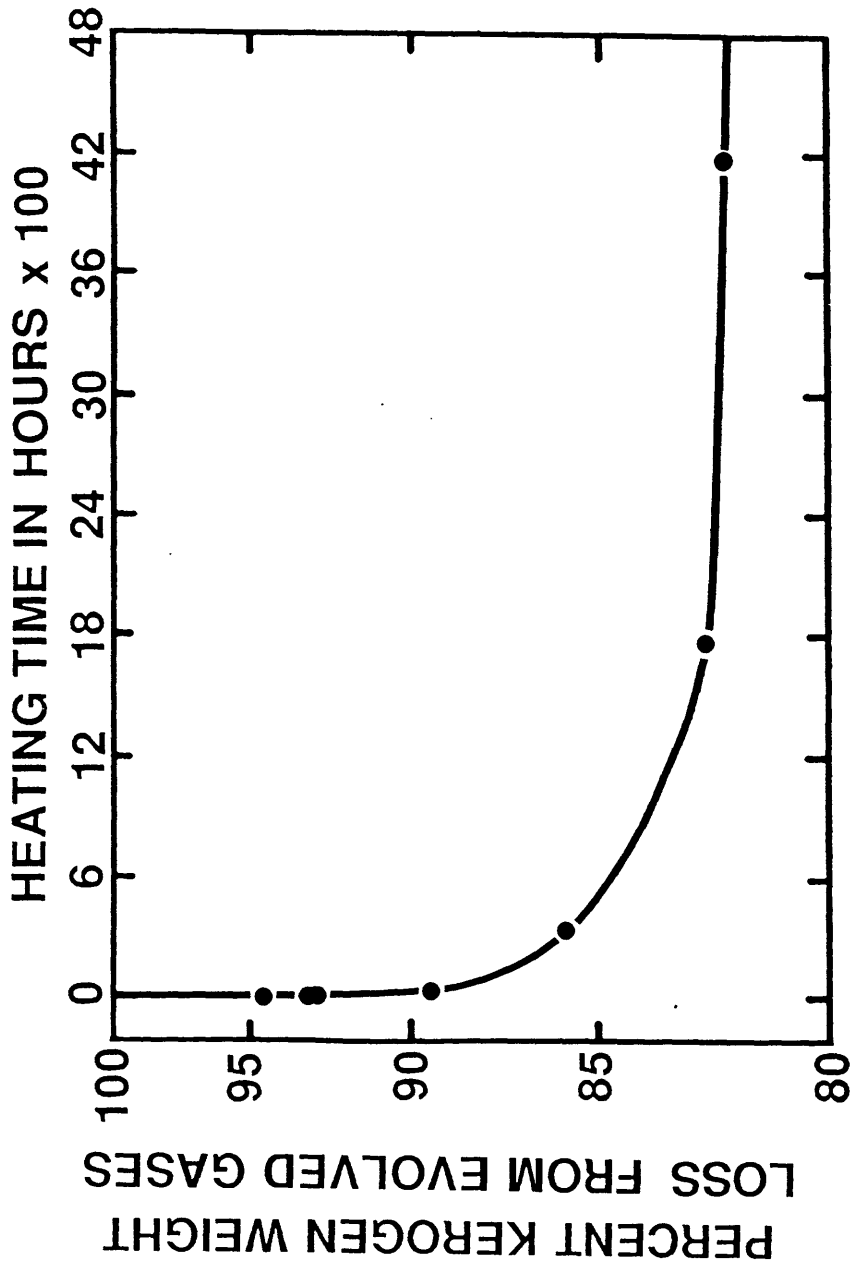

Figure 6-2. Plot of reaction extent (kerogen weight loss in weight percent from the evolved gases: carbon dioxide, methane, ethane, and propane) versus time for aqueous-pyrolysis experiments on the Pennsylvanian Anna shale (TOC = 29.6%, type II/III organic matter). Short time experiments were 4, 12, 24, and 48 hours.

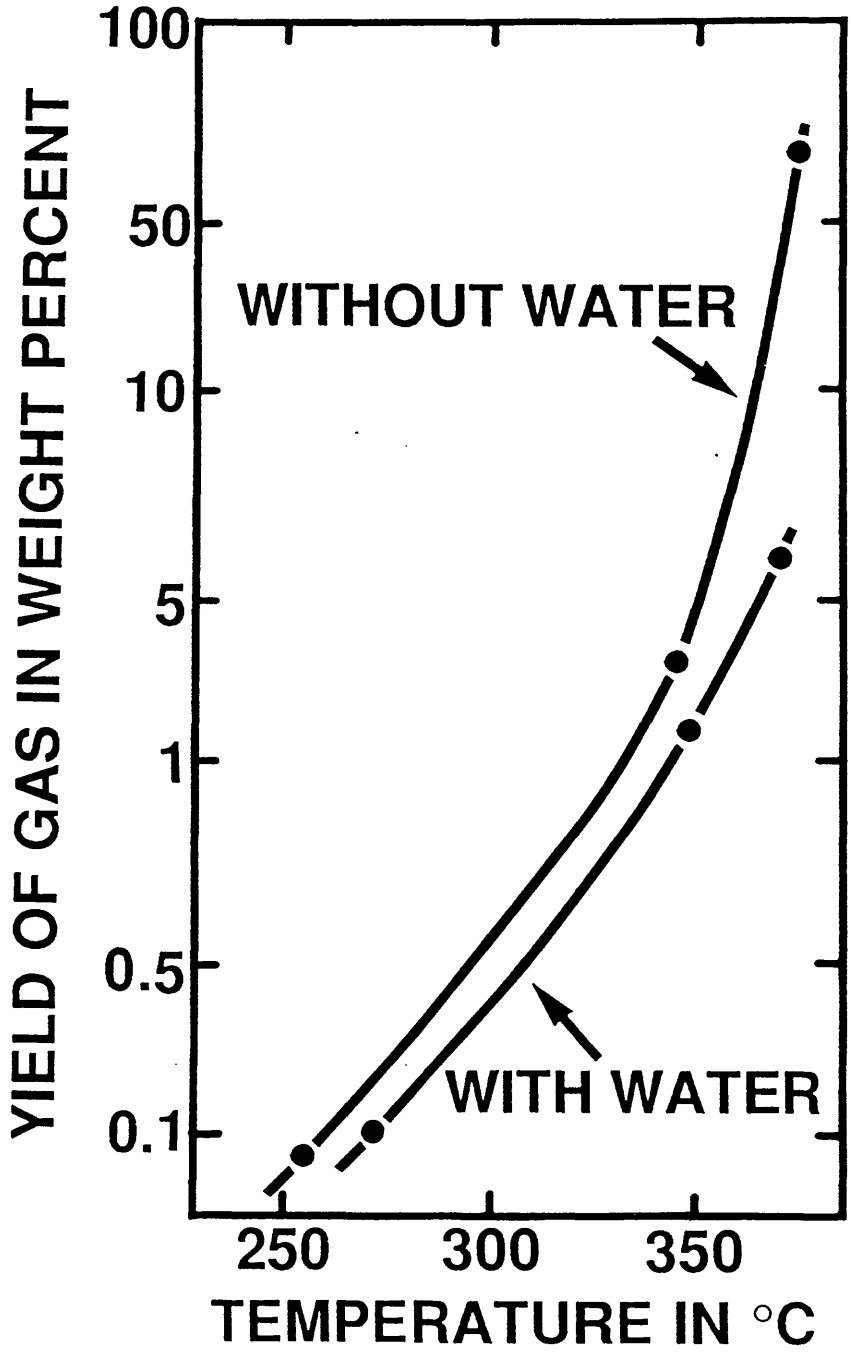

Figure 6-3. Effect of water on thermal cracking to gas of a middle oil distillate fraction from Kingfish oil field, Gippsland basin at different experimental temperatures. After Hesp and Rigby (1973).

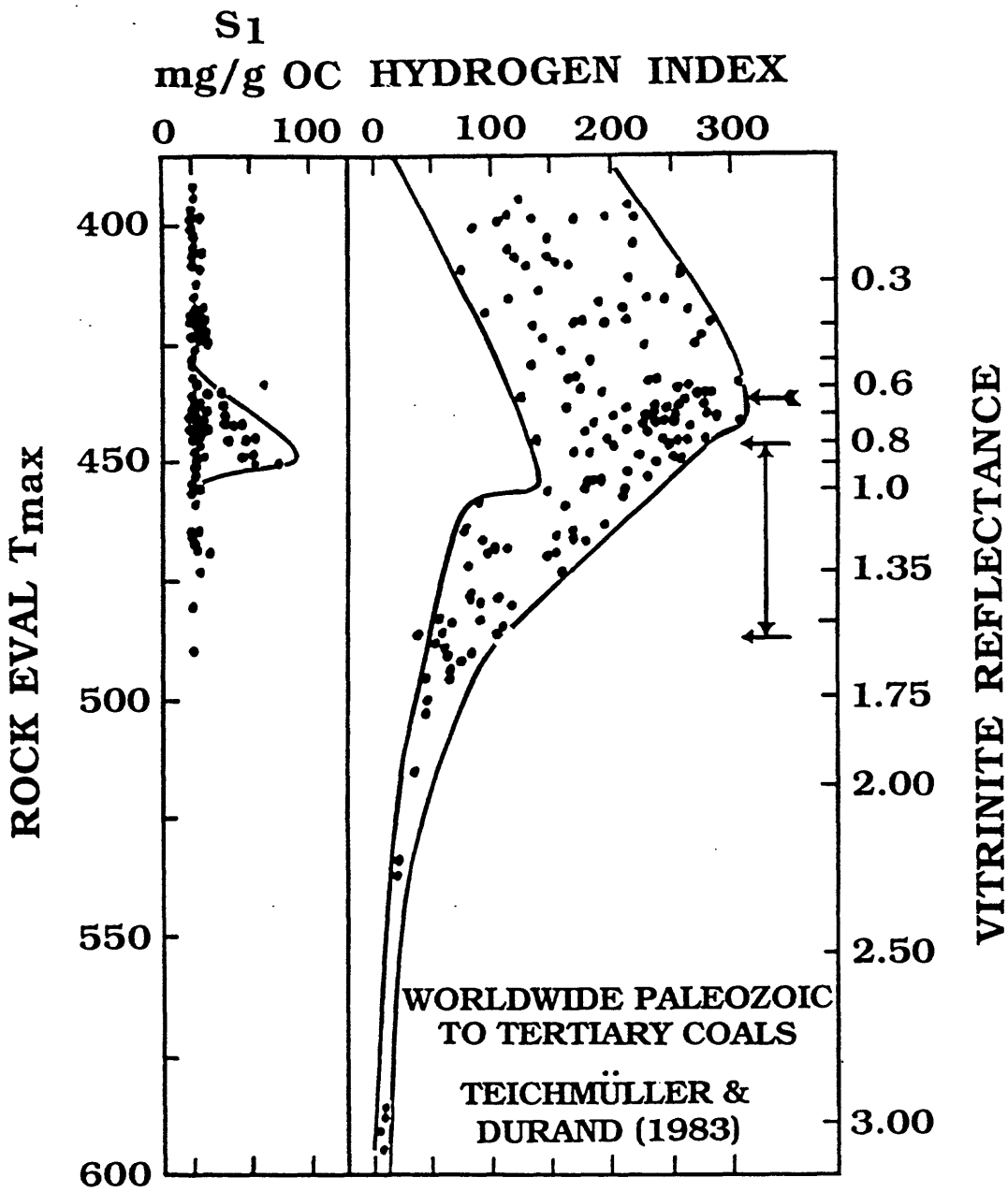

Figure 6-4. Plot of ROCK EVAL T_{max} and R_o versus the ROCK EVAL S_1 and S_2 pyrolysis peaks (normalized to organic carbon-mg/g O.C.) for worldwide Paleozoic to Tertiary coals. The feathered arrow indicates the maximum in the HI data. The vertical arrow indicates the maximum loss in the HI's. Data from Teichmüller and Durand (1983), whose original vitrinite reflectance data was given in R_m values; R_m was converted to R_o by $R_m = 1.066(R_o)$.

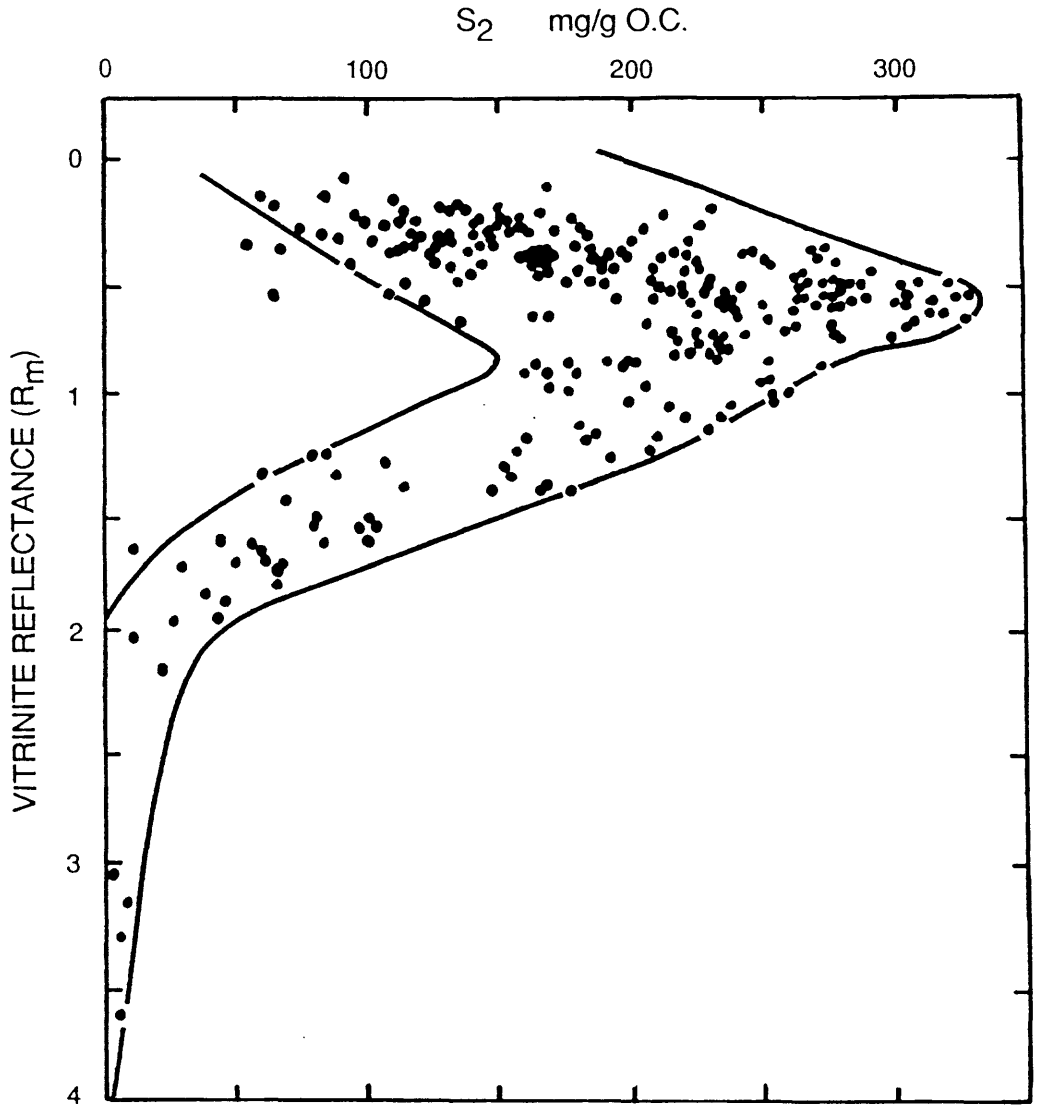

Figure 6-5. Plot of mean vitrinite reflectance (R_m) versus the ROCK EVAL HI in milligrams per gram of organic carbon (S_2 mg/g O.C.) for coals of worldwide distribution and all geologic ages. After Bertrand (1984).

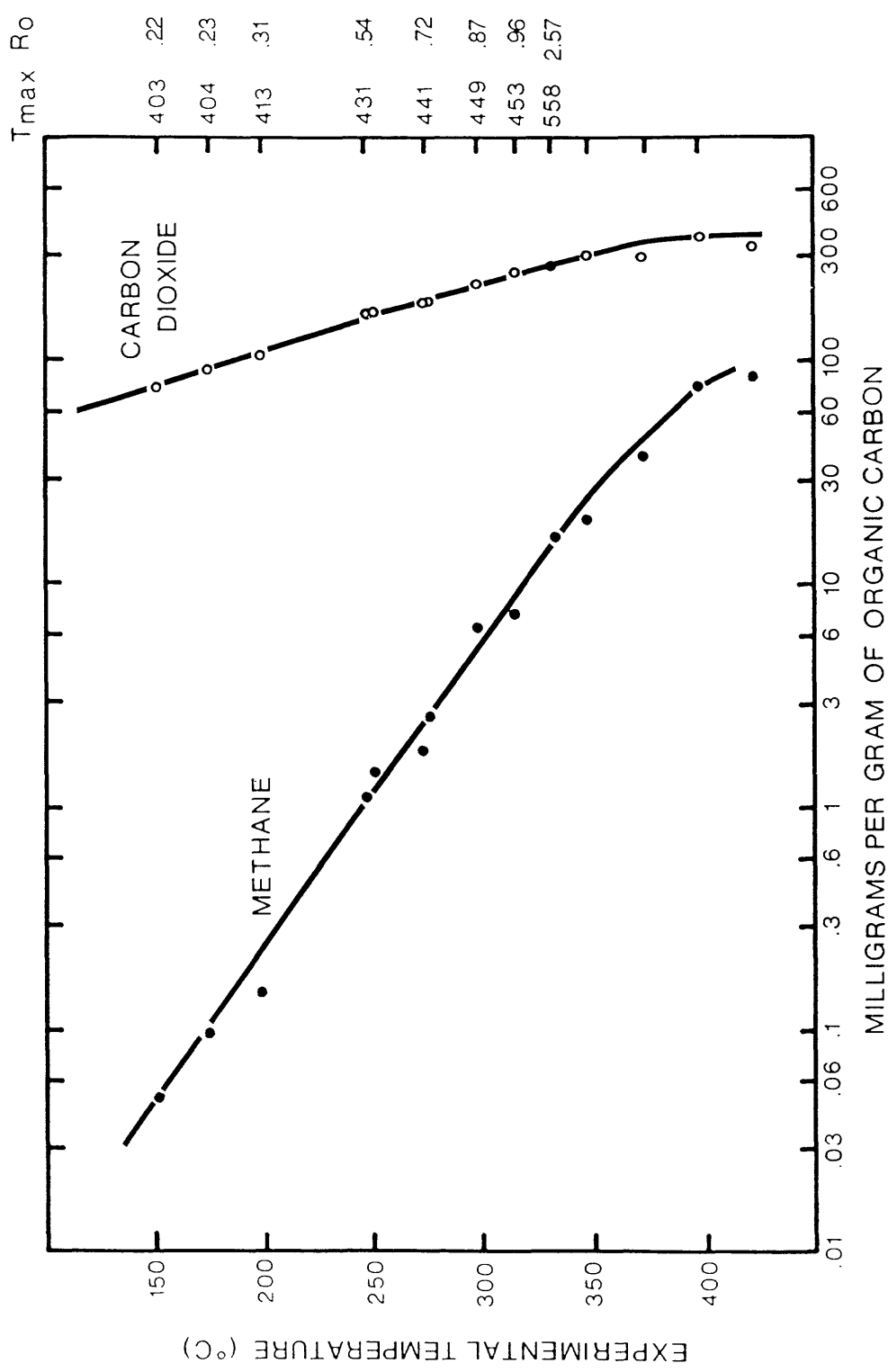

Figure 6-6. Composition of products from thermal vaporization of coals (ROCK EVAL pyrolysis, product trapping, and gas chromatography). R_o values derived from T_{max} values by use of table 1. Data from Teichmüller and Durand (1983). The original vitrinite reflectance data of those authors was given in R_m values; R_m was converted to R_o by $R_m = 1.0666\ (R_o)$.

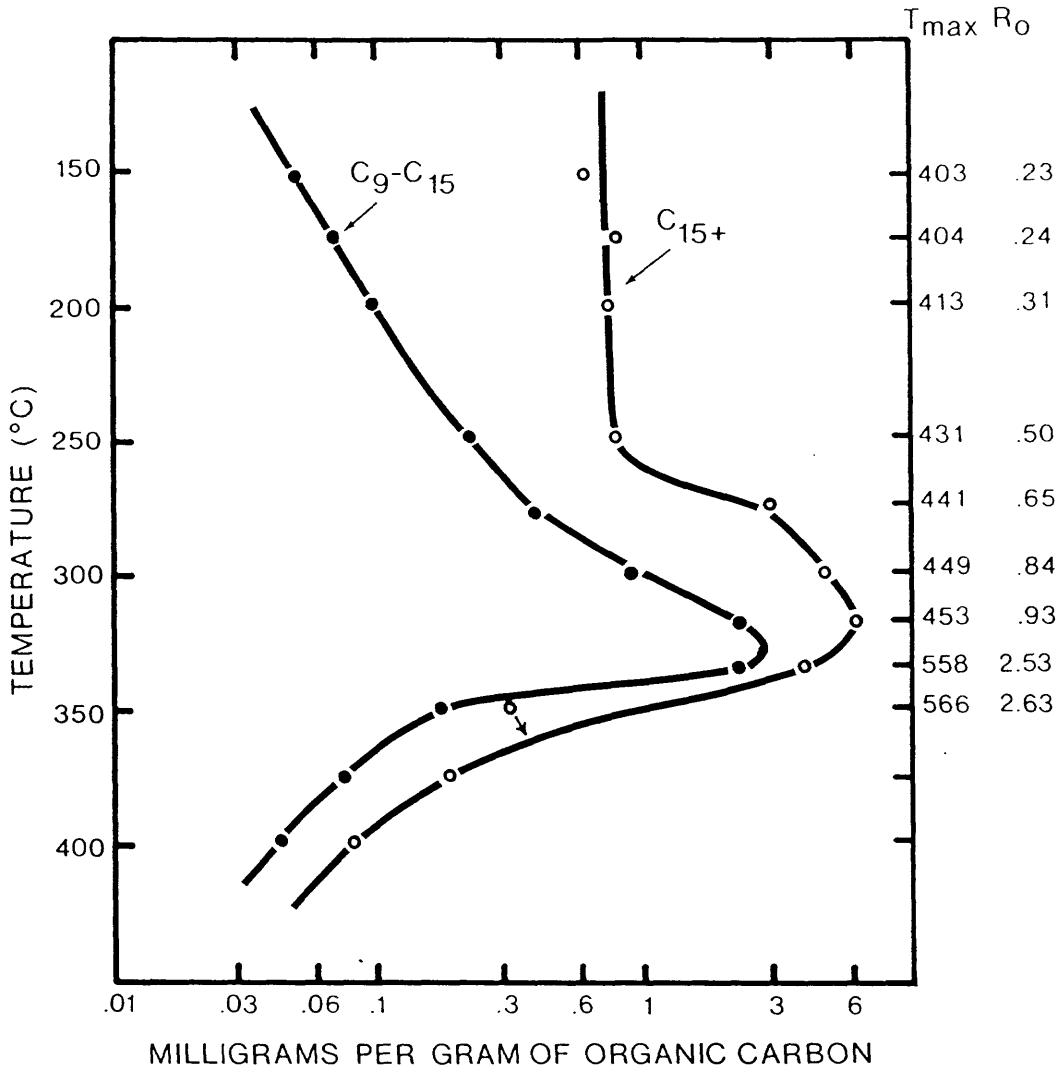

Figure 6-7. Amounts of C_9 to C_{15} and $C_{15}+$ saturated HCs in mg/g OC generated by aqueous pyrolysis of the Eocene Rattlesnake Butte Lignite *versus* experimental temperature, measured T_{max}, and estimated R_o.

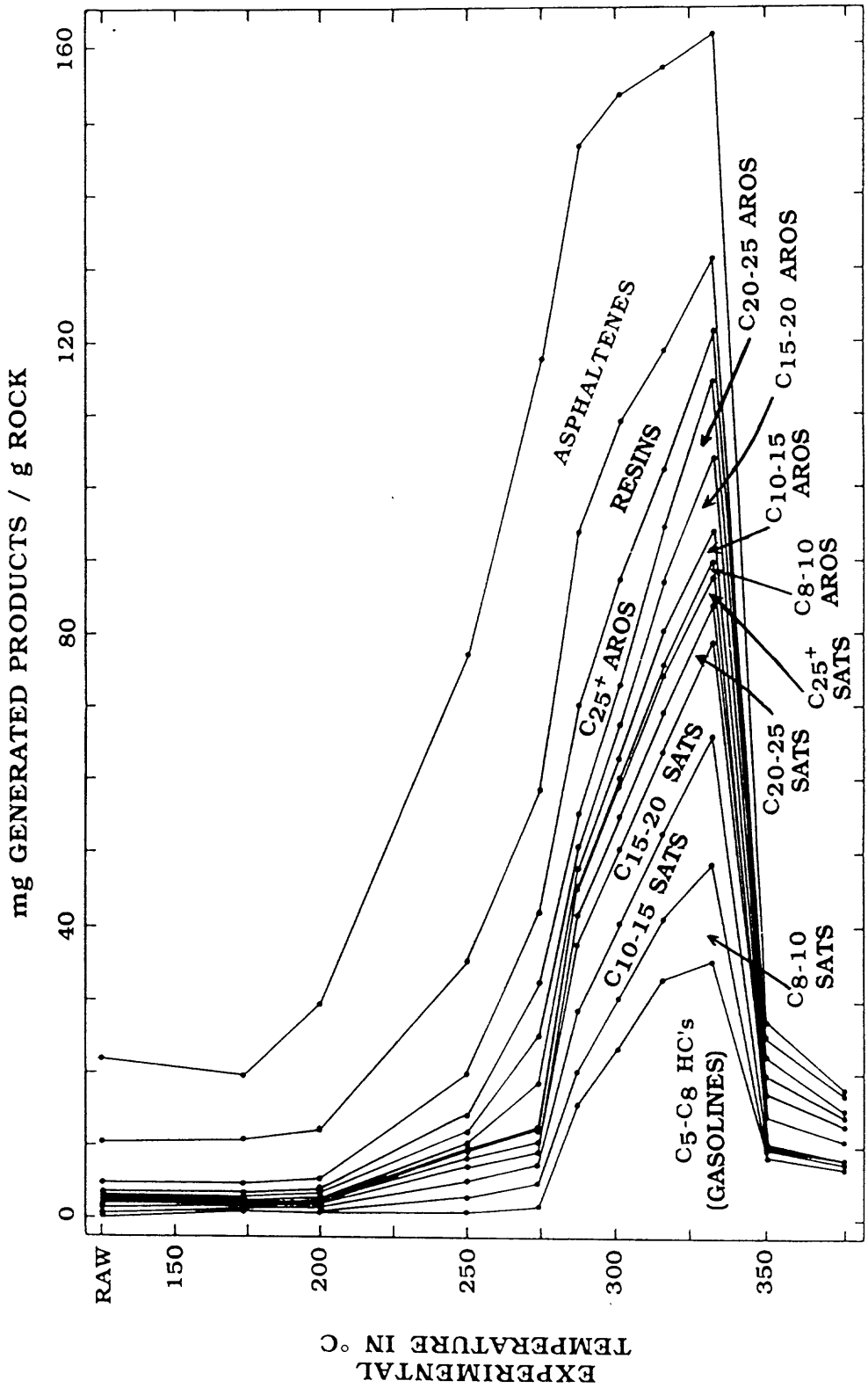

Figure 6-8. Plot of the concentration (in mg of generated products per gram of unreacted (starting) rock) of various products from aqueous-pyrolysis experiments with the Phosphoria shale, as a function of increasing experimental temperature. "RAW" signifies the original unaltered rocks, SATS are saturated hydrocarbons, and AROS are aromatic HC's.

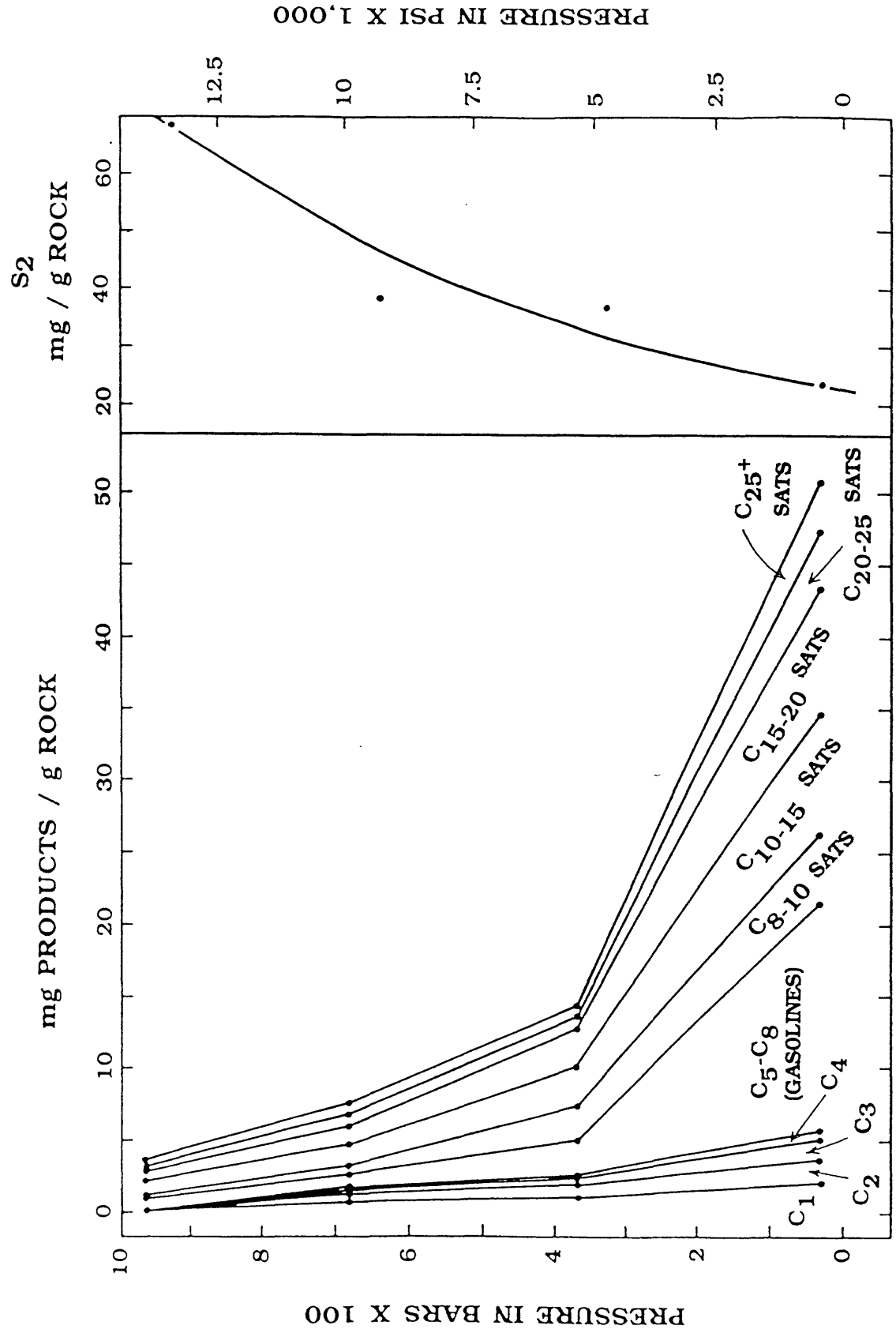

Figure 6-9. Plot of amounts of hydrocarbon gases, gasoline-range hydrocarbons (C_5-C_8), the different carbon number ranges of the saturated (SATS) hydrocarbon's (C_8-C_{10} to C_{25}+) and the ROCK EVAL S2 peak in milligrams per gram of rock (mg/g ROCK) of the Soxhlet-extracted, reacted rock, all versus increasing system static fluid pressure at a reaction temperature of 287°C.

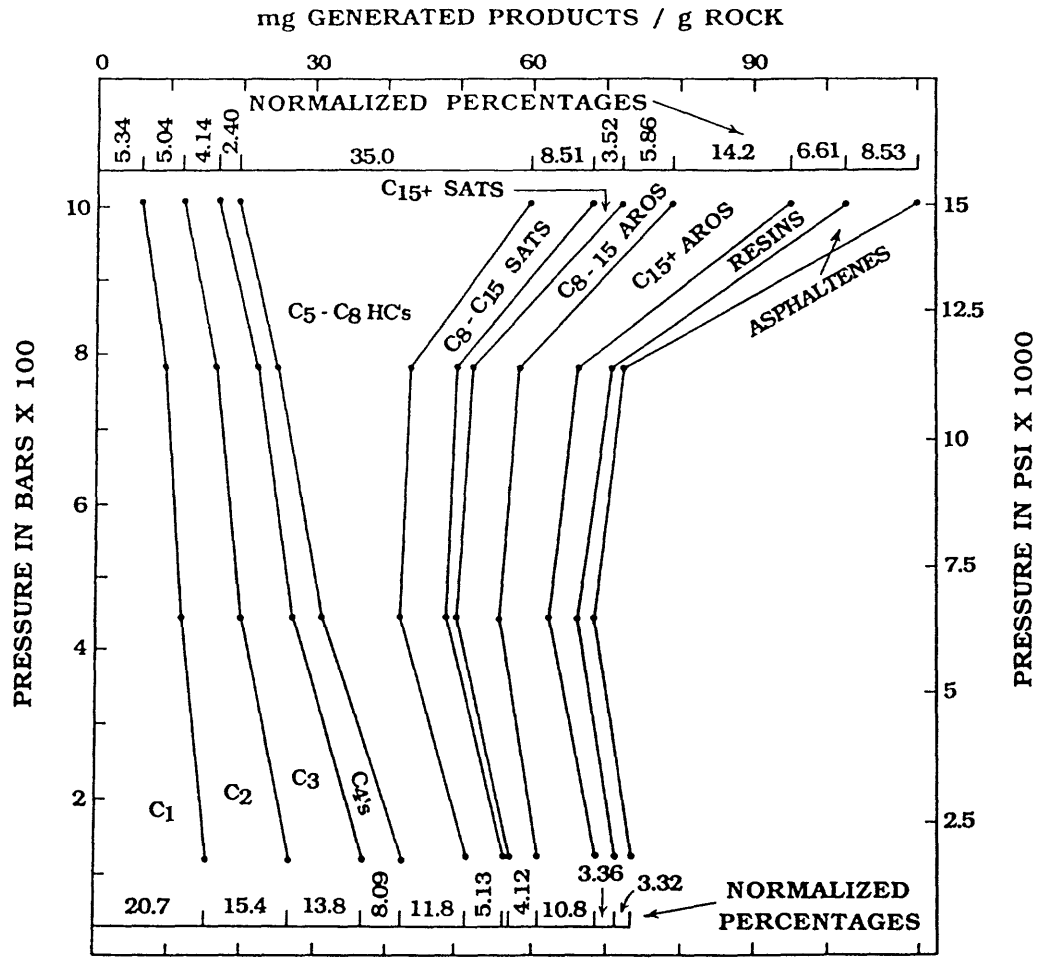

Figure 6-10. Plot of the concentration (in milligrams of generated products per gram of starting rock from aqueous-pyrolysis reactions with the Phosphoria Shale at 350°C as a function of increasing static fluid pressure. Normalized percentages which each component or compound group make up of the total product are shown for the 350°C 118 bar and 350°C 1,077 bar experiments. C_1 to C_4's are the hydrocarbon gases methane through the butanes. SATS are saturated hydrocarbons and AROS are aromatic hydrocarbons. C_{15+} saturated hydrocarbon-gas chromatograms from aqueous-pyrolysis.

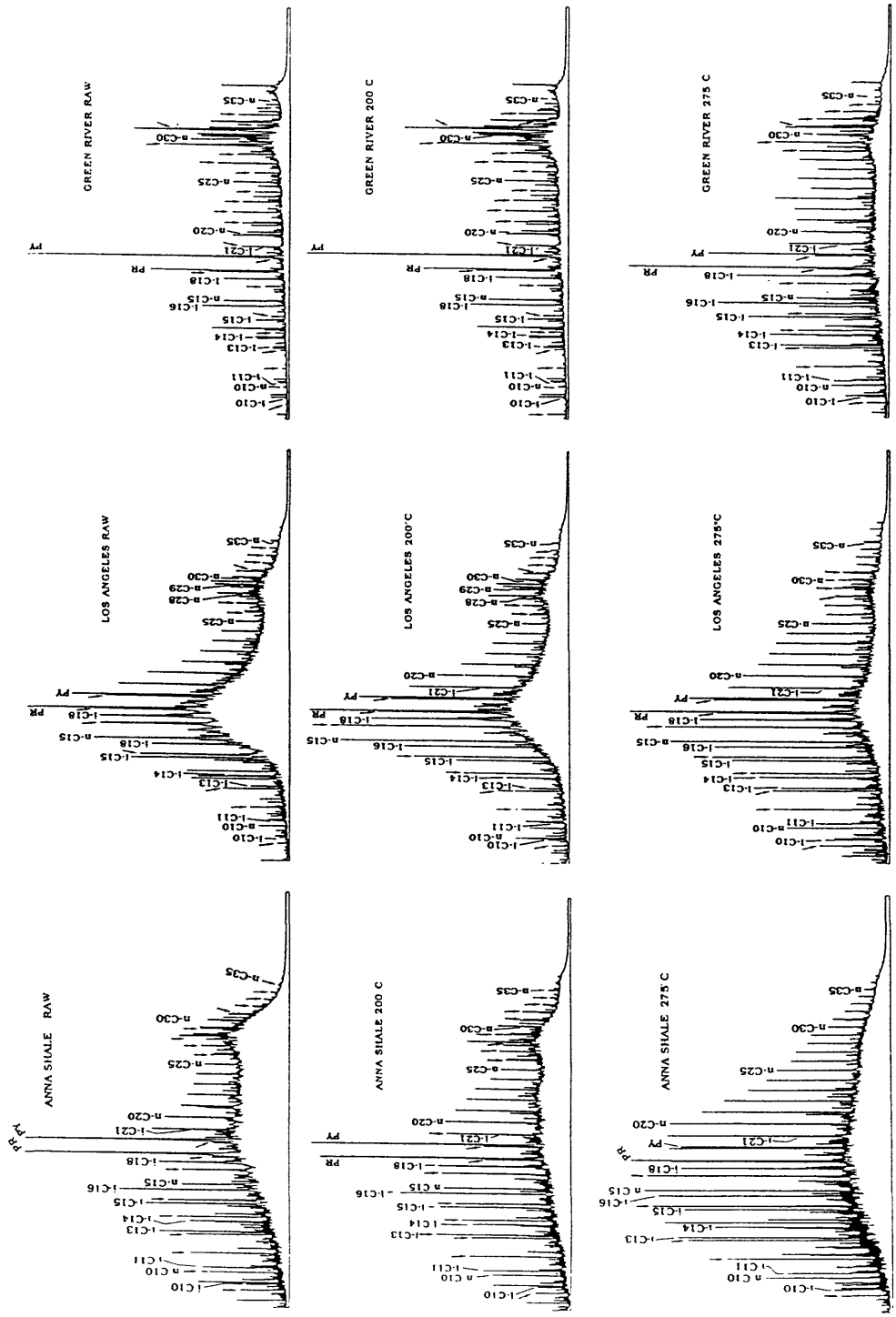

Figure 6-11. Gas chromatograms of C8+ saturated HC's from the Pennsylvanian Anna Shale, a mid-Miocene shale from the Los Angeles basin, and the Eocene Green River shale from the raw (starting) rocks and from aqueous-pyrolysis experiments carried out on the rocks at 200° and 275 C. Isoprenoid HC's are designated by i-c and the respective carbon number. PR is pristane. PY is phytane. N-paraffins are designated by n-c and the respective carbon numbers are by arrows.

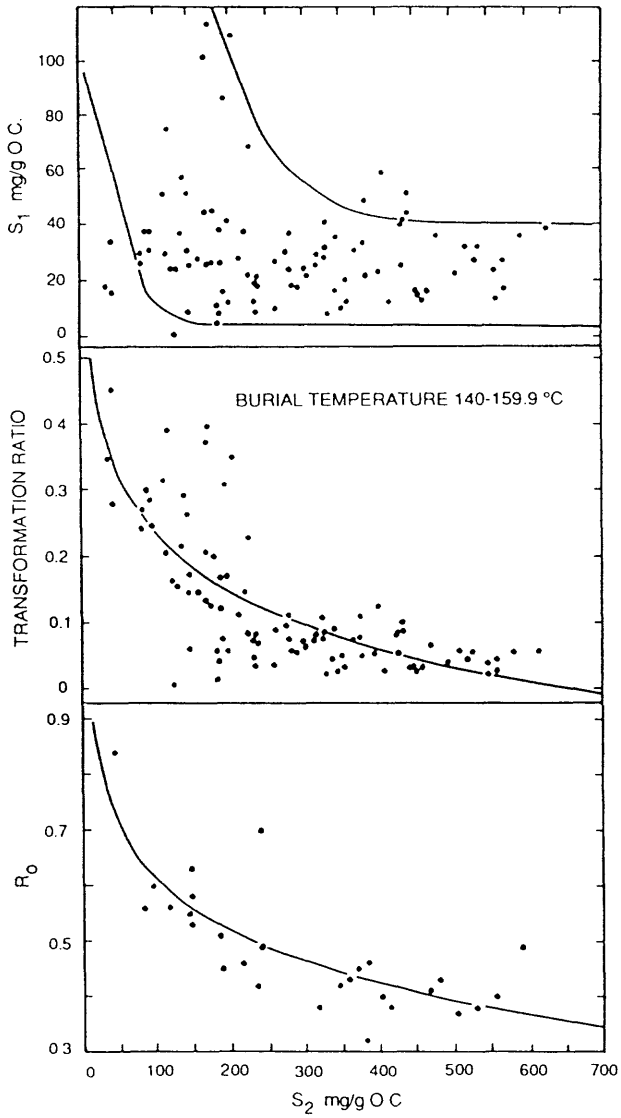

Figure 6-12. Plot of R_o, the ROCK EVAL Transformation Ratio (S_1/S_1+S_2, also termed the Production Index), and the ROCK EVAL S_1 pyrolysis peak normalized to organic carbon (S_1 mg/g O.C.) all versus the ROCK EVAL S_2 pyrolysis peak (HI) normalized to organic carbon (S_1 mg/g O.C.) for rocks which are from the California petroleum basins and are at equilibrium burial temperatures of 140°-159.9°C. Samples are from the Ventura central syncline, and Ventura Avenue field of the Ventura basin; from the Whittier, Long Beach, Wilmington, Santa Fe Springs, and Seal Beach fields of the Los Angeles basin; from the Baldwin Springs field), the American Petrofina "Central C. H. -2" (central syncline, Los Angeles basin) and the Long Beach Airport-1 (NE of the various wells in the Anahiem nose and northeast flank areas of the Los Angeles basin; from various wells in the Paloma field, Southern San Joaquin Valley basin; and from a well in the Santa Maria Valley basin. All samples except for the American Petrofina and Santa Maria Valley basin samples (cuttings chips) are core samples. The curved line in the R_o plot results from logarithmic regression analysis of the data and has a correlation coefficient of $r = 0.805$ to the data. The line in the transformation ratio plot results from logarithmic regression analysis of the data and has a correlation coefficient of $r = 0.744$ to the data. The lines in the S_1 pyrolysis peak plot define the principal sample population.

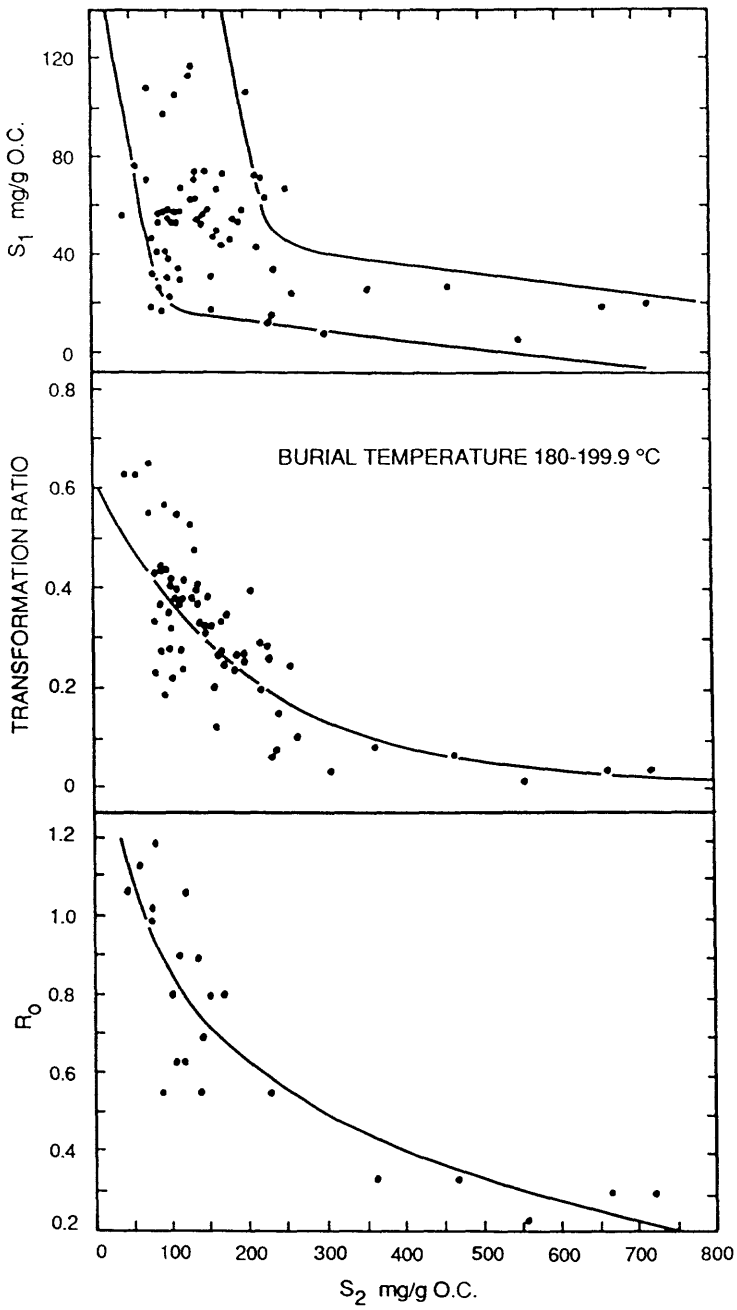

Figure 6-13. Plot of R_o, the ROCK EVAL Transformation Ratio (S_1/S_2+S_2, also termed the Production Index), and the ROCK EVAL S_1 pyrolysis peak normalized to organic carbon (S_1 mg/g O.C.) all versus the ROCK EVAL S_2 pyrolysis peak (HI) normalized to organic carbon (S_2 mg/g O.C.), for rocks which are from the California petroleum basins and are at equilibrium burial temperatures of 180°-199.09°C. Samples are from the Wilmington field, Los Angeles basin; the Houghton Community-1 (NW plunge Santa Fe Springs field); the American Petrofina "Central C.H.-2" (central syncline Los Angeles basin; and from the Paloma field, Southern San Joaquin Valley basin. The curved line in the R_o plot results from logarithmic regression analysis of the data and has a correlation coefficient of r = 0.867 to the data. The lines in the S_1 pyrolysis peak plot define the principal sample population.

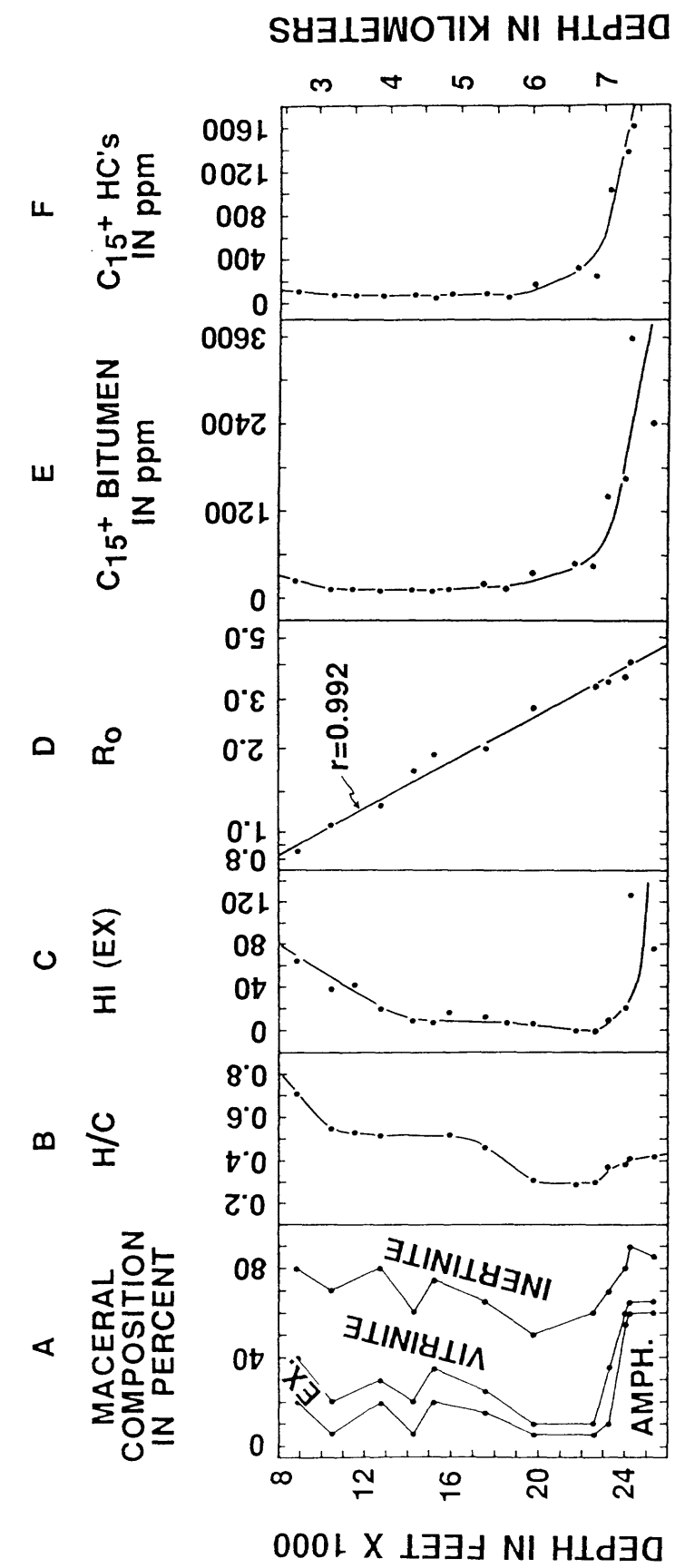

Figure 6-14. Petroleum-geochemical data from the Ralph Lowe-1 wellbore, Pecos County, Texas versus depth in feet x1,000 and kilometers. Maceral analyses of isolated kerogen (column A) by Robertson Research, EX. is exinite, AMPH. is amorphous. H/C (column B) is atomic hydrogen to carbon ratio for isolated kerogen. HI (EX) are ROCK EVAL hydrogen indices for Soxhlet-extracted powdered rock (column C). R_o (column D) is vitrinite reflectance in percent, the straight line in this plot has a correlation coefficient (r) of 0.992 to the data. C_{15}^+ BITUMEN IN ppm (column E) is C_{15}^+ bitumen in parts per million by rock weight. C_{15}^+ HC's IN ppm (column F) is C_{15}^+ HC's in parts per million by rock weight.

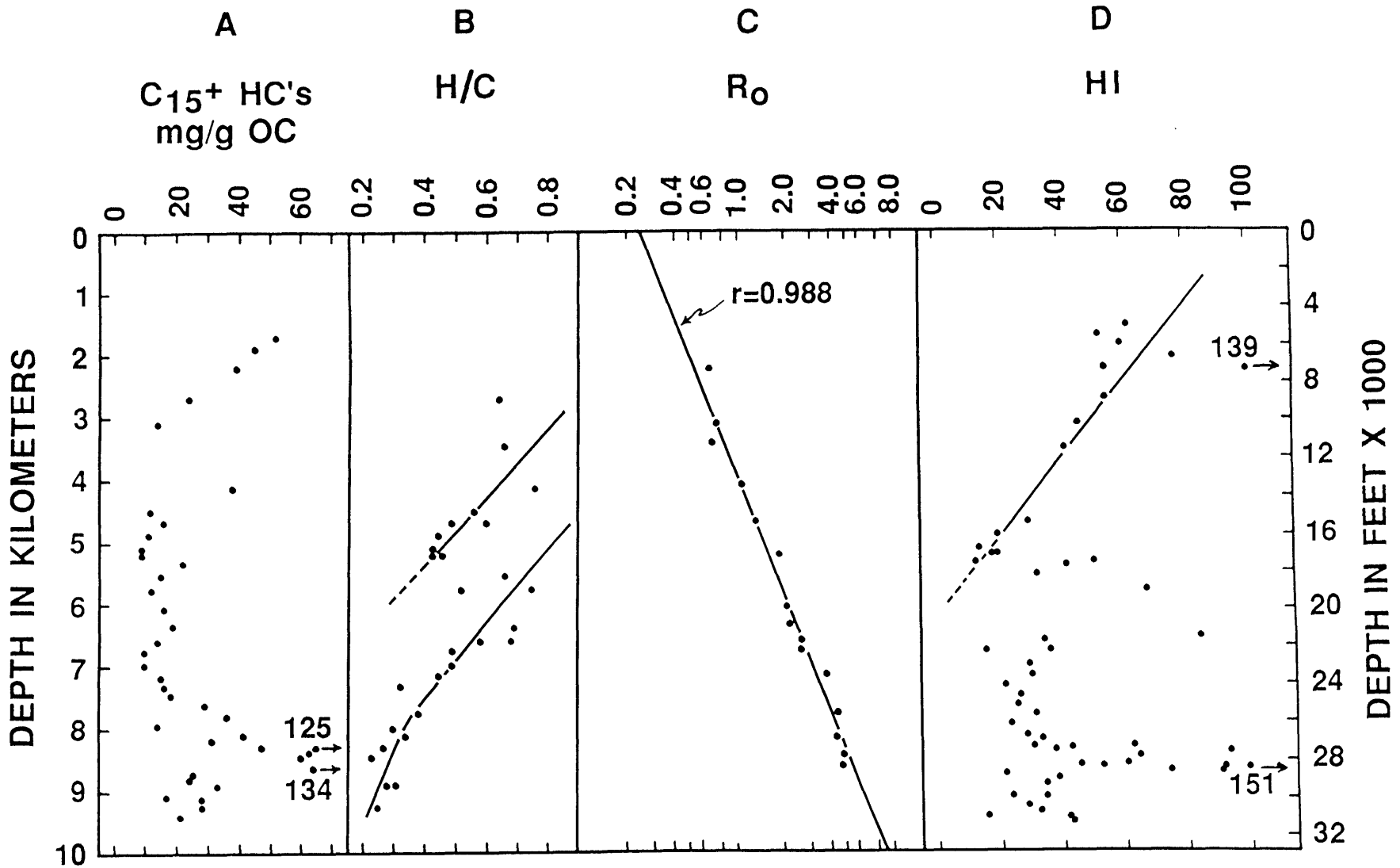

Figure 6-15. Petroleum-geochemical data from the Bertha Rogers-1 wellbore, Washita County, Oklahoma versus depth in kilometers and feet x1,000. C_{15+} HC's mg/g OC (column A) are milligrams of C_{15+} HC's per gram of organic carbon. H/C (column B) is the atomic hydrogen to carbon ratio for isolated kerogen. R_o (column C) is vitrinite reflectance in percent, the straight line in this plot has a correlation coefficient (r) of 0.988 to the data. HI (column D) are ROCK EVAL hydrogen indices.

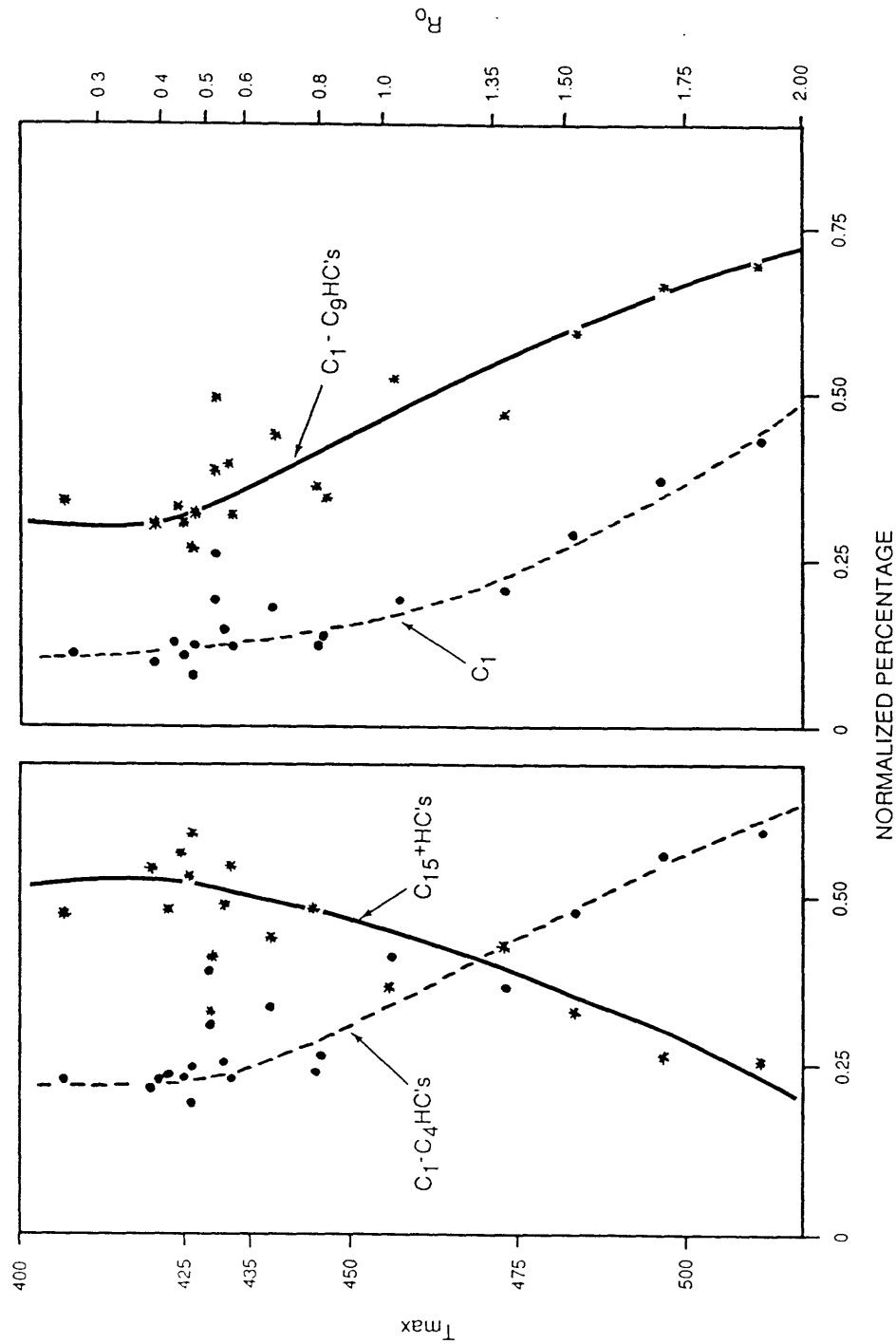

Figure 6-16. Composition of products from thermal vaporization of coals (ROCK EVAL pyrolysis, product trapping, and gas chromatography). R_o values derived from T_{max} values by use of table 1. Data from Teichmüller and Durand (1983). The original vitrinite reflectance data of those authors was given in R_m values; R_m was converted to R_o by $R_m = 1.066\ (R_o)$.

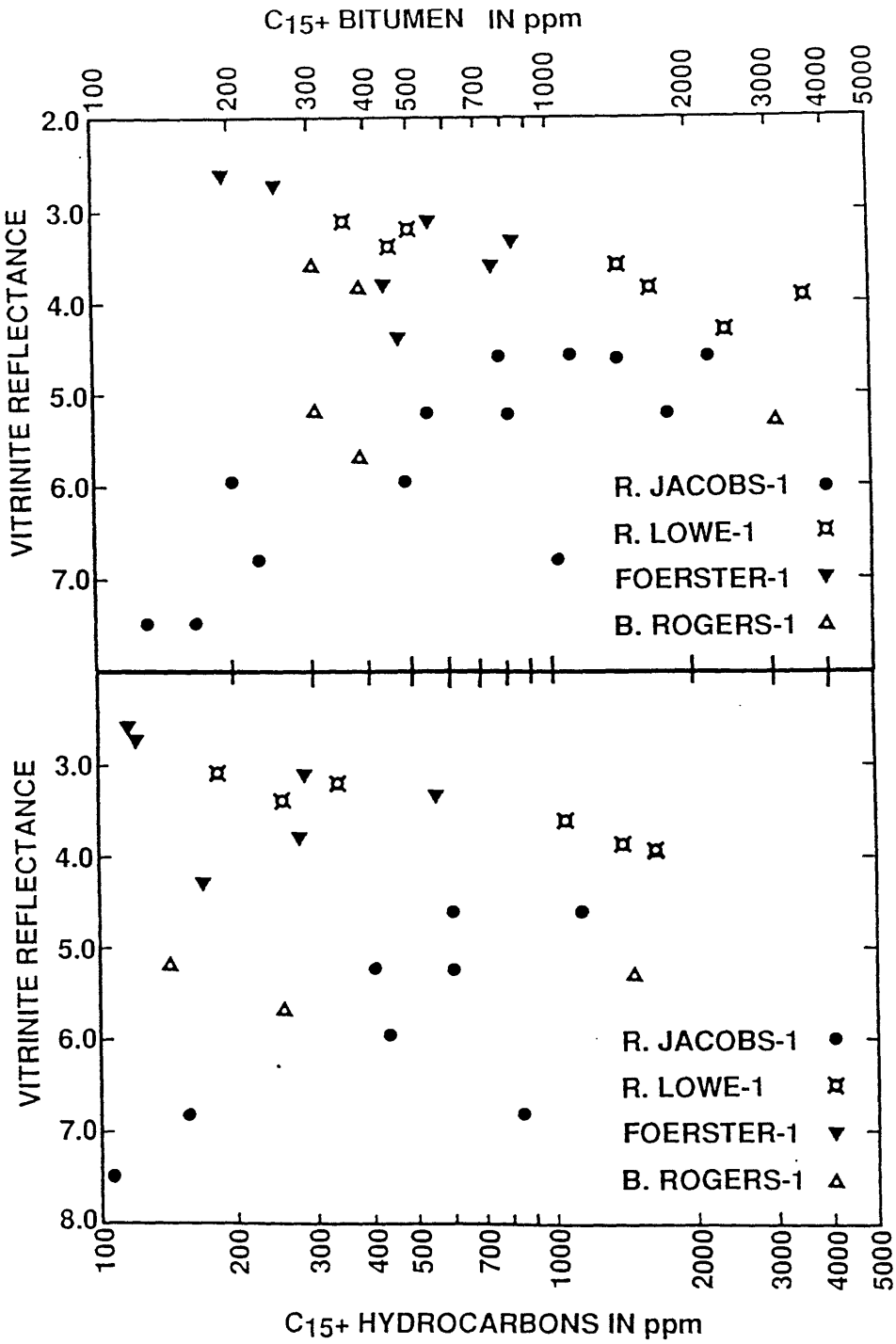

Figure 6-17. Plots, versus R_O, of C_{15+} bitumen and C_{15+} saturated plus aromatic HC's Soxhlet extracted from deep rocks of the (Table 6-1): Bertha Rogers 1, R. G. Jacobs-1, Ralph Lowe-1, and A. M. Foerster-1.

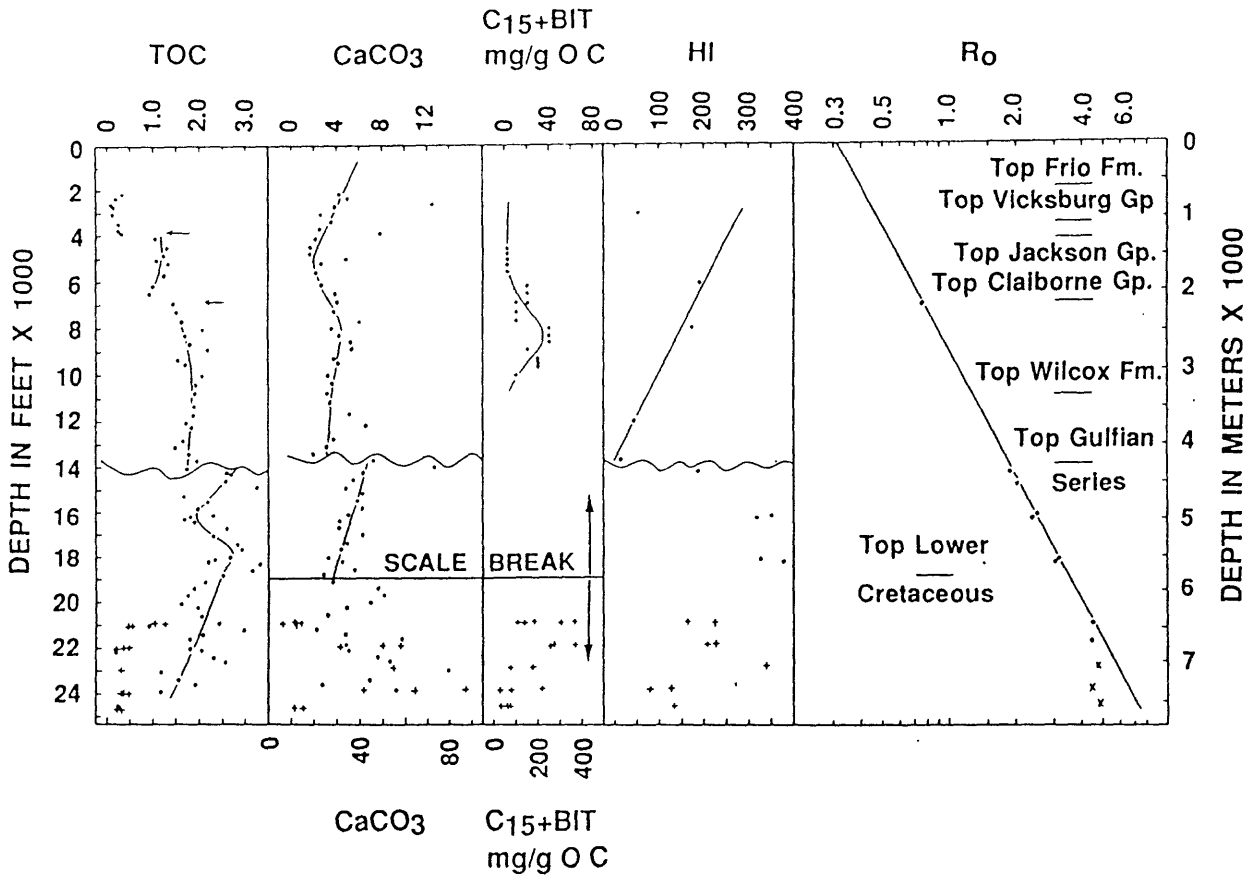

Figure 6-18. Total organic carbon (TOC) and calcium carbonate ($CaCO_3$) contents in weight percent; C_{15+} bitumen (by Soxhlet extraction) in milligrams per gram of organic carbon (C_{15+} BIT mg/g OC); HI's by ROCK EVAL pyrolysis (mg/g OC) and R_O, all versus depth for the Chevron R. G. Jacobs-1, Goliad Co. Texas. Arrows in the TOC plot delineate sharp increases in TOC at stratigraphic boundaries. Wavy lines signify a lithologic depositional break at the Tertiary-Cretaceous boundary. The solid line in the $CaCO_3$ and C_{15+} bitumen plots signifies a scale break (at the Upper Cretaceous-Lower Cretaceous boundary) for these two plots; the $CaCO_3$ and bitumen scales on top of the figure serve for samples above this line and the scales on the bottom of the figure serve for samples below this line. The "X's" in the R_O plot represent R_O values which probably have some degree of R_O suppression. Fm. is Formation; Gp. is Group.

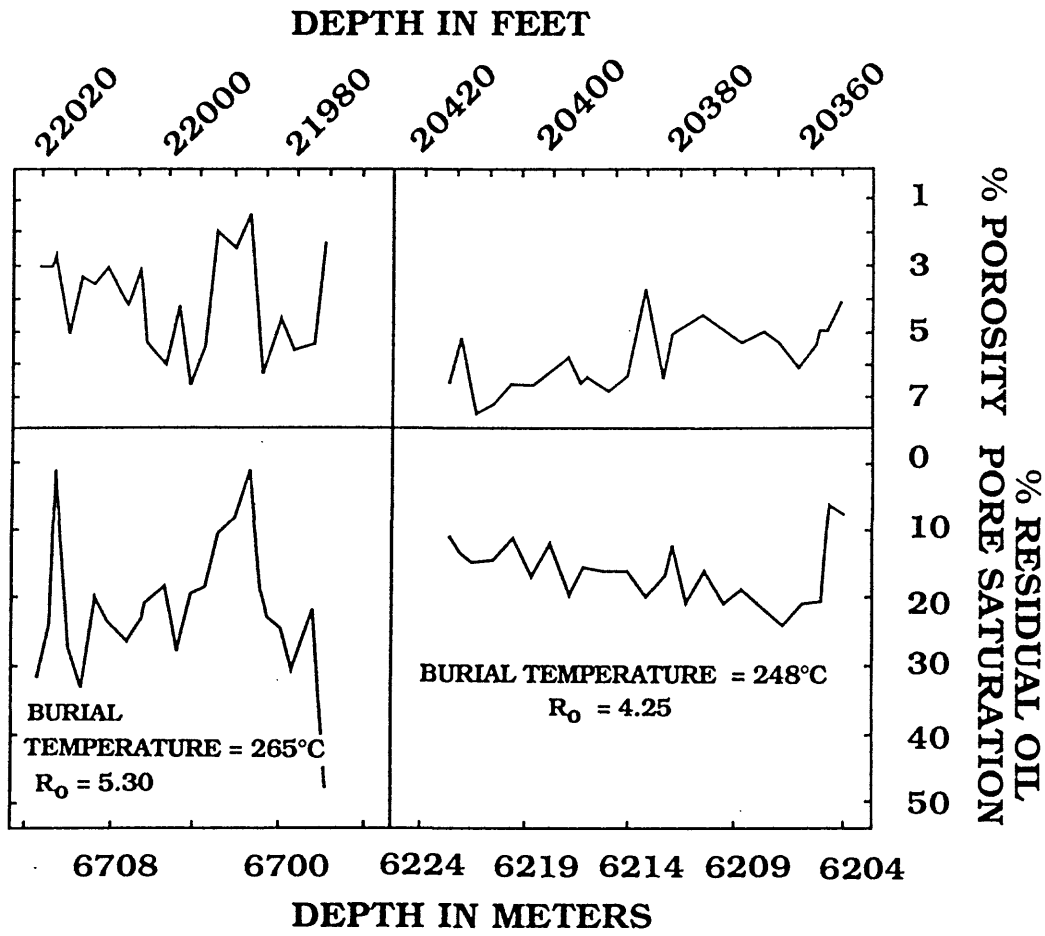

Figure 6-19. Percent porosity and percent residual oil pore saturation versus depth for two of the deep cored intervals of the R. G. Jacobs-1. Analyses by Core Labs. Data supplied by Chevron Oil Field Research Company.

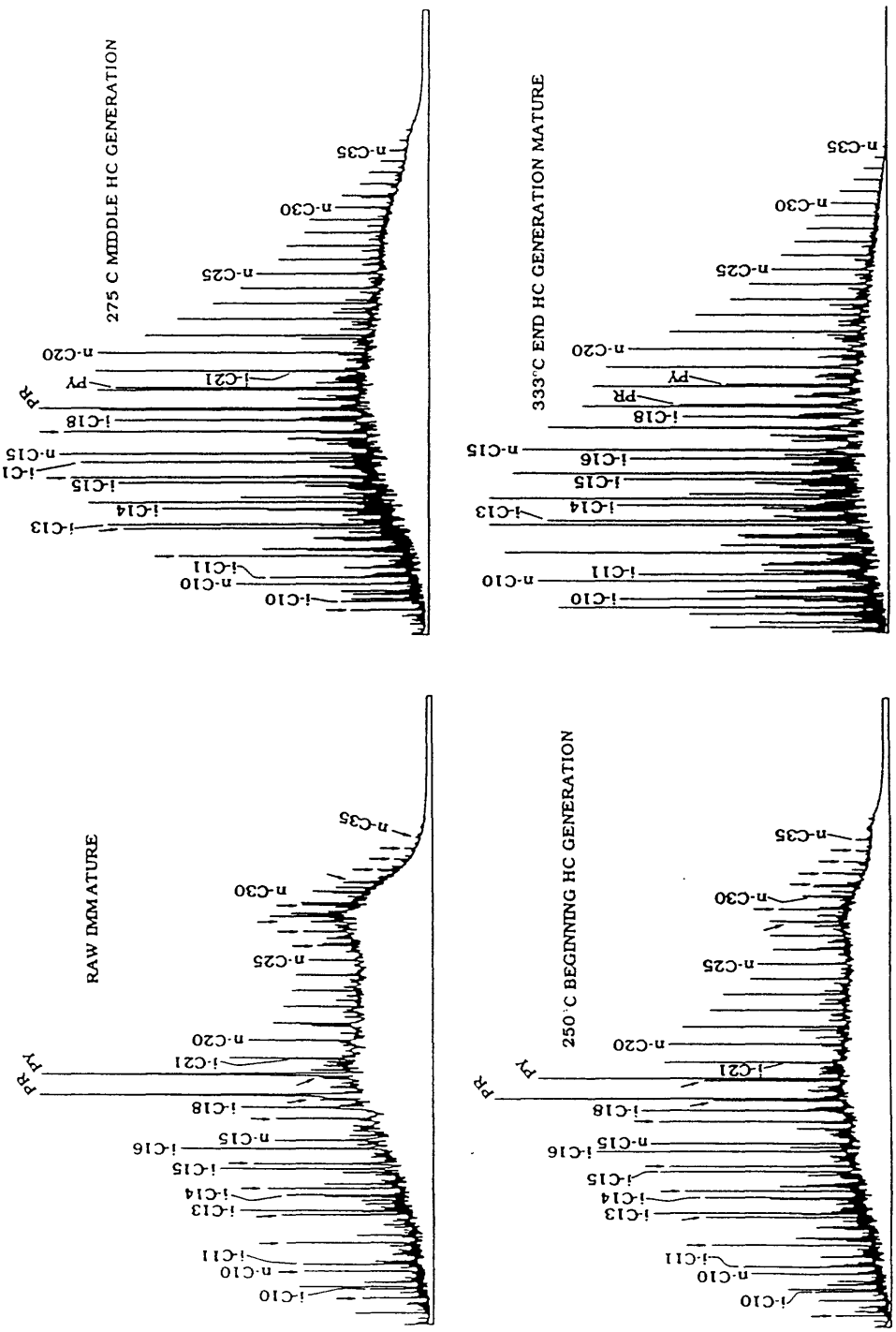

Figure 6-20. C_{8+} saturated HC gas chromatograms from aqueous-pyrolysis experiments performed on the carbonaceous Pennsylvanian Anna shale. Every fifth n-paraffin is labeled by n-C with its respective carbon number. N-paraffins are also labeled by arrows when necessary. Isoprenoid HC's are labeled by i-C with their respective carbon number. PR is pristane, PY is phytane.

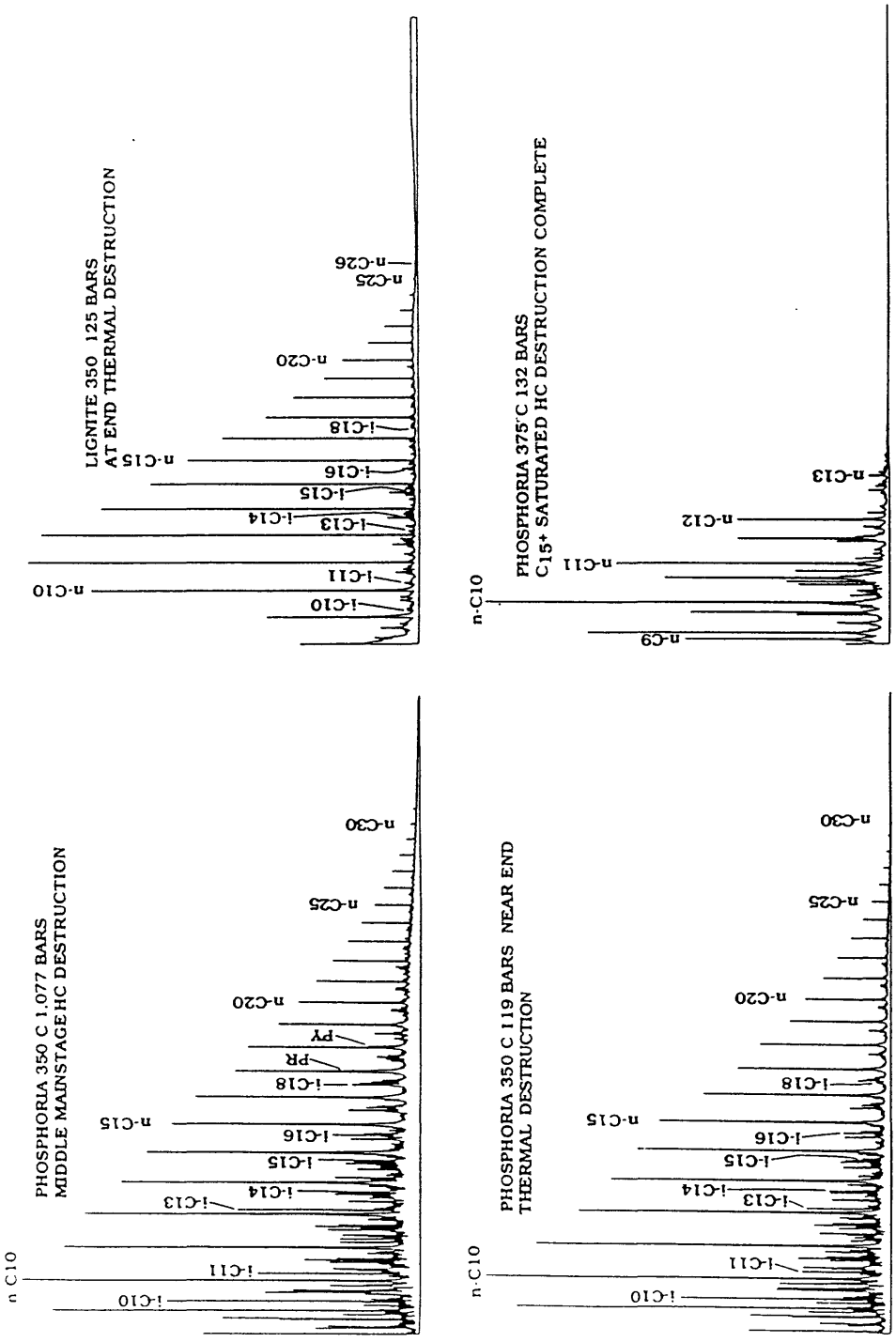

Figure 6-21. C_8+ saturated HC gas chromatograms from aqueous-pyrolysis experiments performed on the Phosphoria shale and a lignite. Compound labeling as in Figure 6-7 caption.

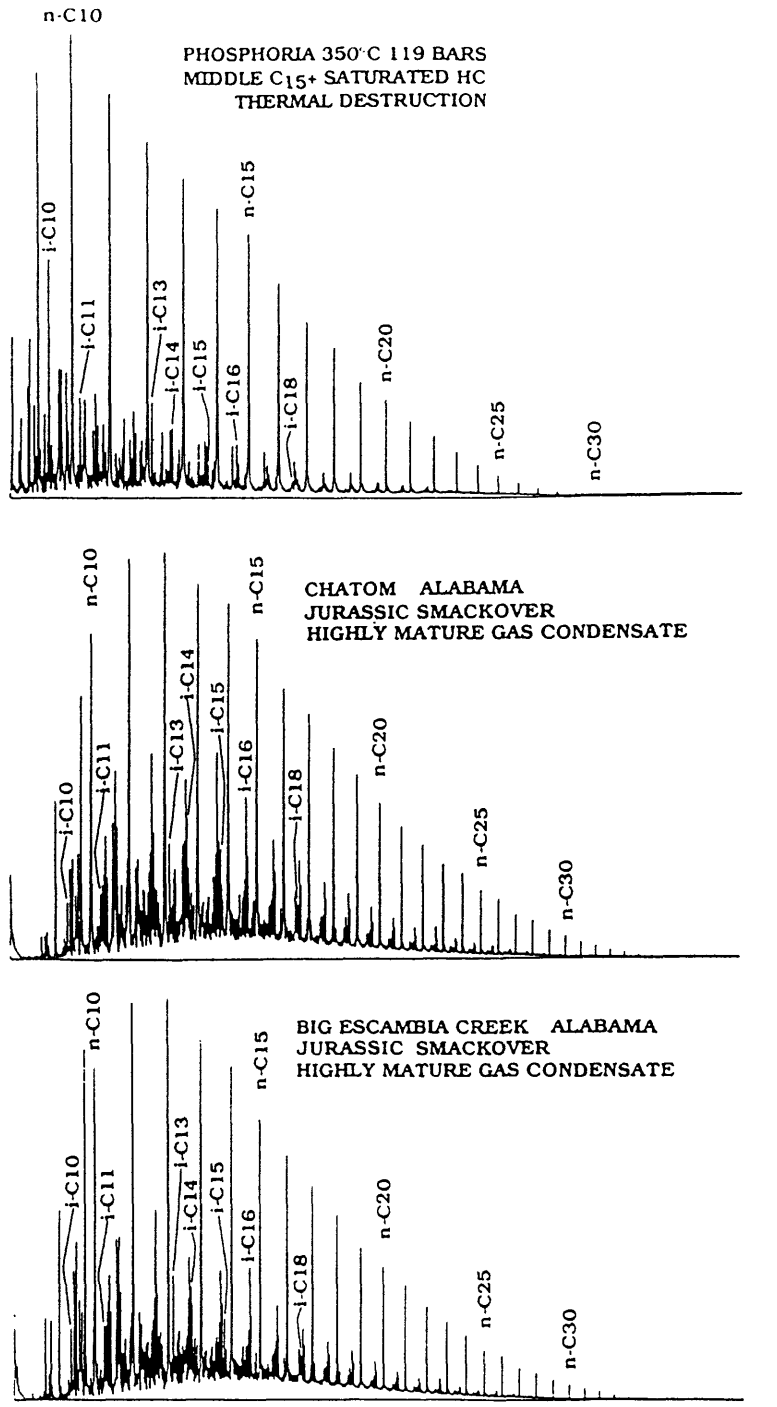

Figure 6-22. C8+ saturated HC gas chromatograms from two highly-mature Jurassic Smackover gas condensates from the Chatom and Big Escambia Creek fields, Alabama and from an aqueous-pyrolysis experiment performed on the Phosphoria shale. Compound labeling as in Figure 6-7 caption.

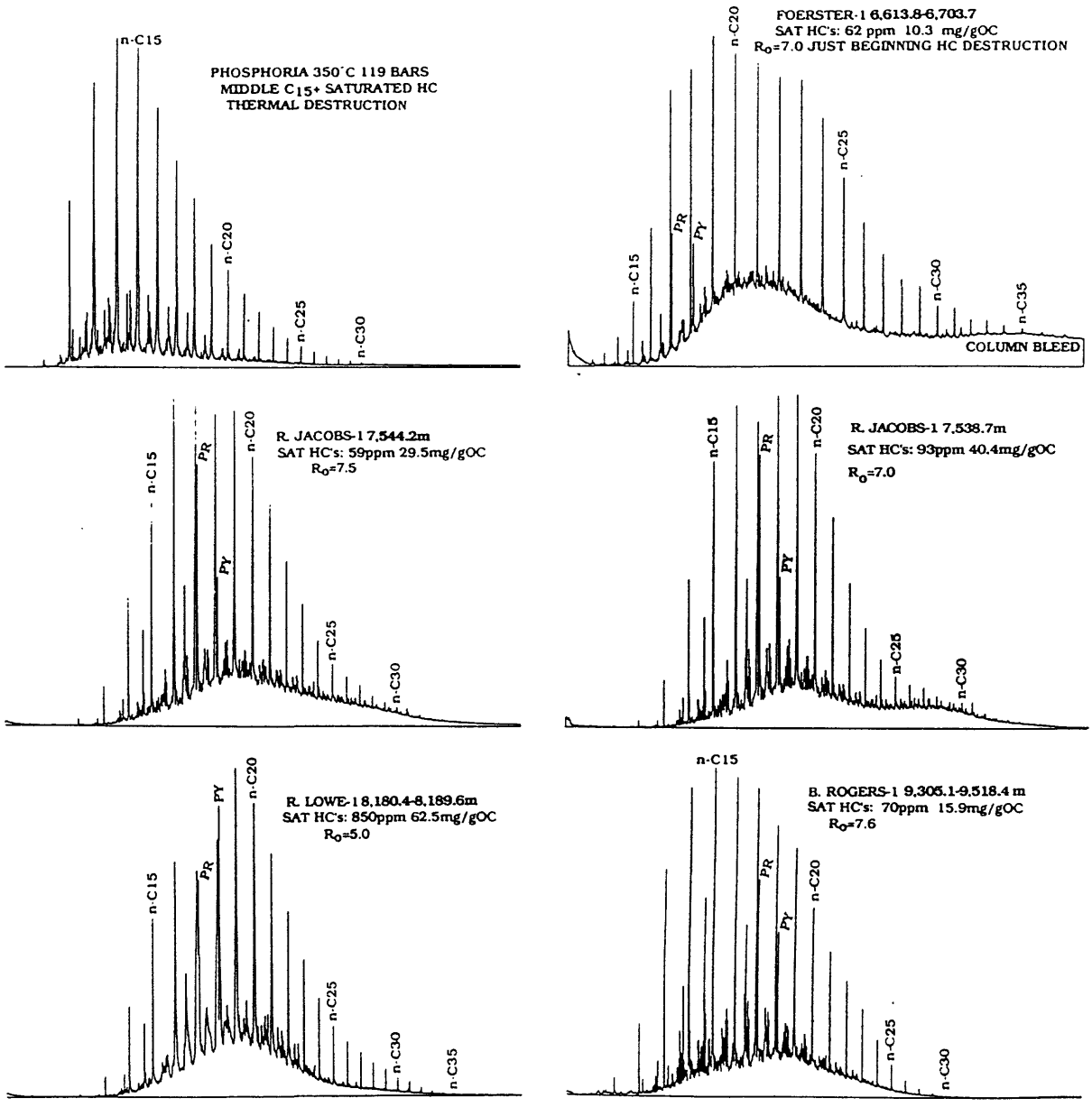

Figure 6-23. C_{15}+ saturated HC's from deep rocks of the Rogers-1, Foerster-1, Lowe-1, and Jacobs-1 wellbores (Table 6-1) and from an aqueous-pyrolysis experiment performed on the Phosphoria shale. Sample depths in meters (m), C_{15}+ saturated HC concentrations in parts per million (ppm), and normalized to rock TOC, mg/gOC) and R_O values (extrapolated or read) are given for each rock sample above the respective chromatogram. Compound labeling as in Fig.ure 6-7 caption.

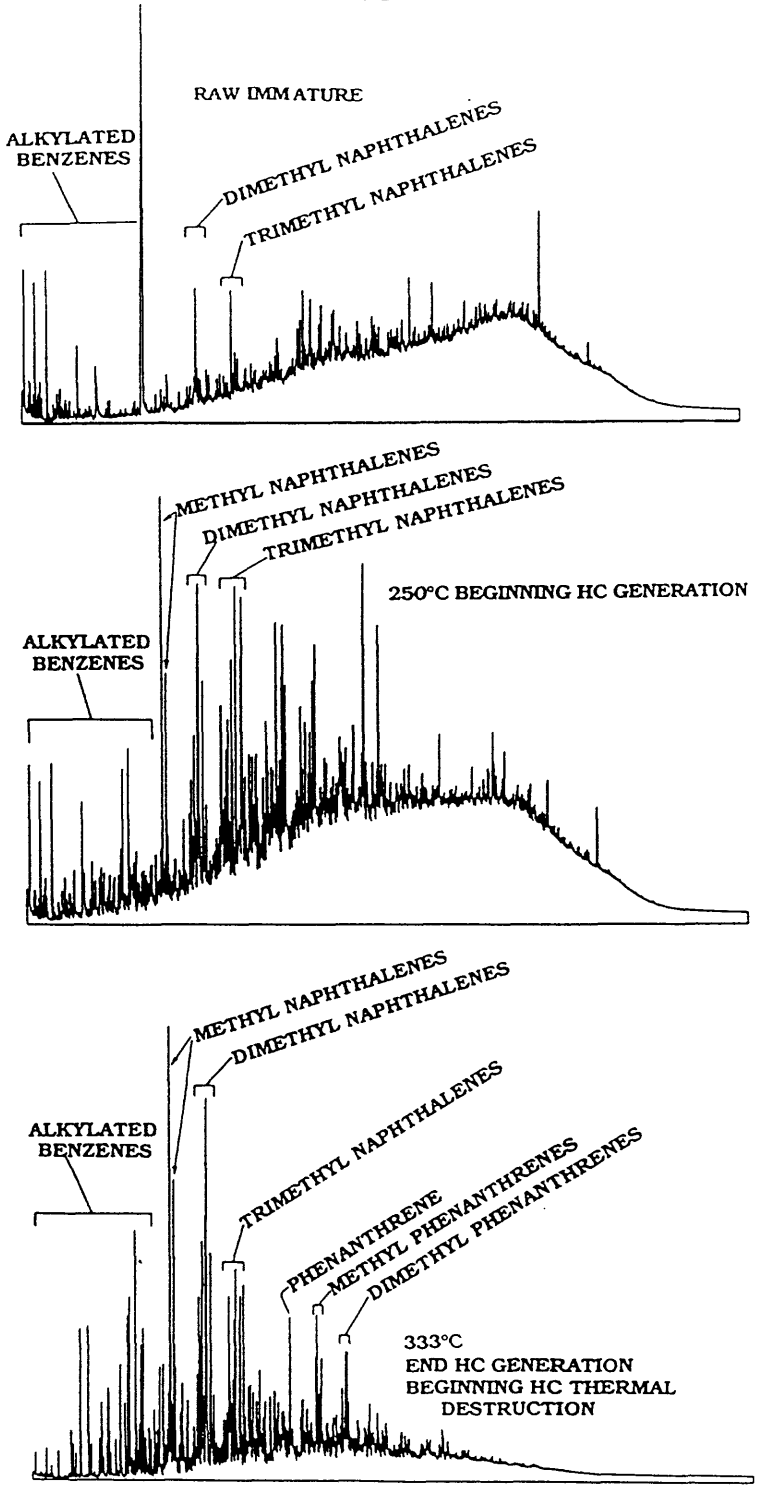

Figure 6-24. C_{8+} aromatic HC chromatograms from aqueous-pyrolysis experiments performed on the carbonaceous Anna shale and from the unreacted (immature, R_O = 0.25%) rock.

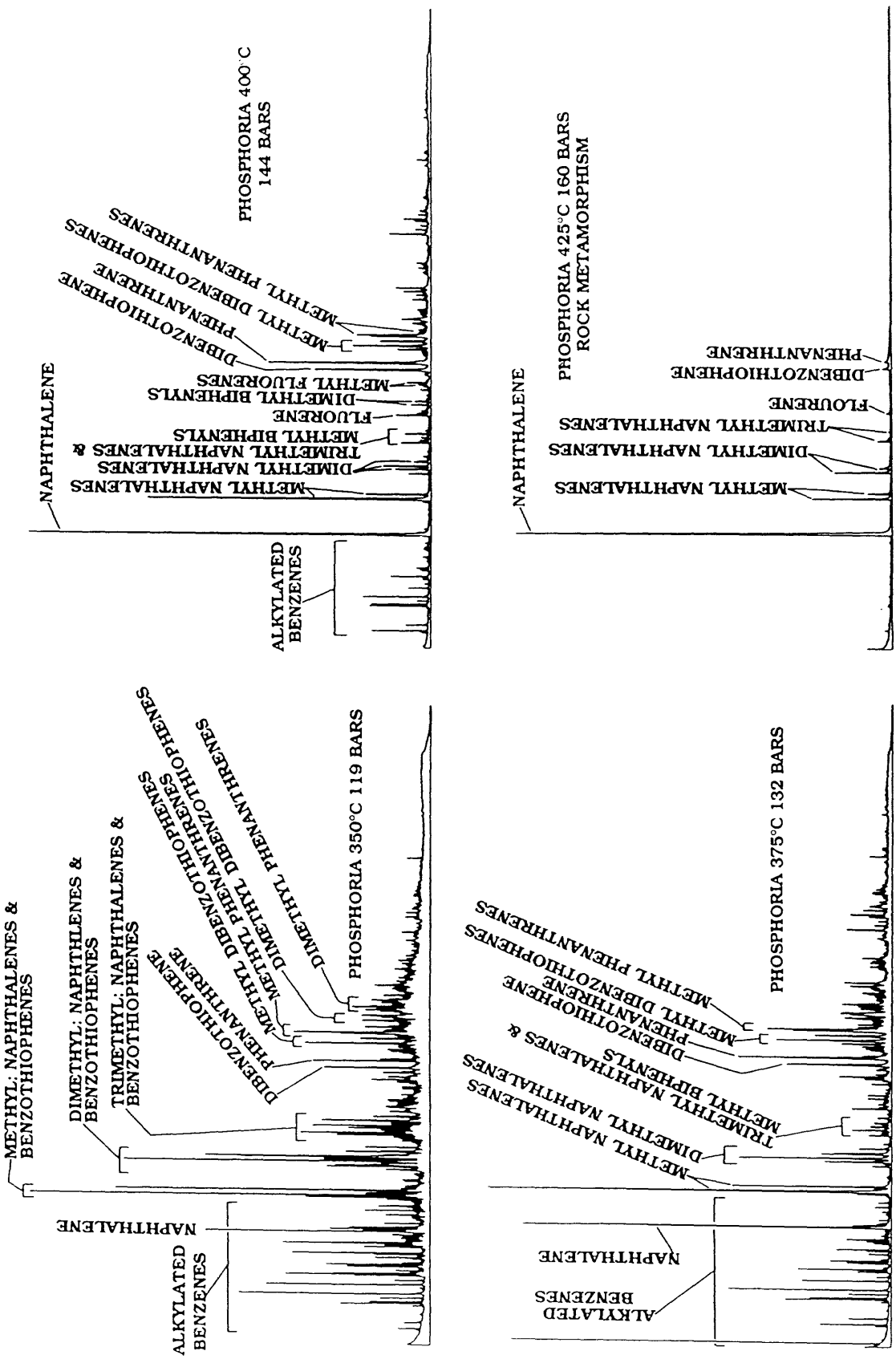

Figure 6-25. C8+ aromatic HC gas chromatograms from aqueous-pyrolysis experiments performed on the Phosphoria shale, experiments which are in the HC thermal destructive phase.

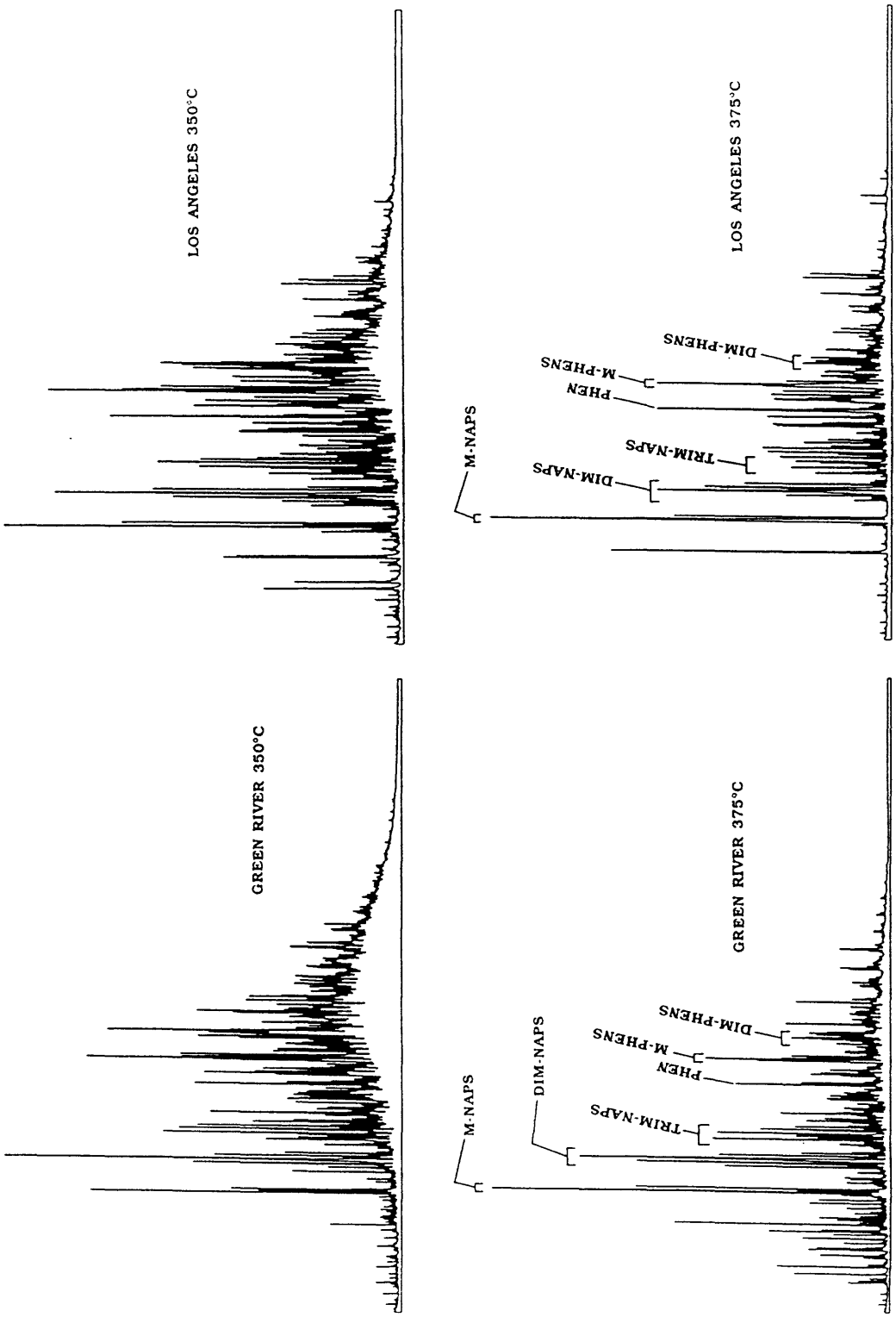

Figure 6-26. C8+ aromatic HC gas chromatograms from aqueous pyrolysis experiments carried out on the Eocene Green River Shale and on a mid-miocene shale from the Los Angeles Basin, California. Experimental temperatures are given in °C. M-NAPS are methyl-naphthalenes; DM-NAPS are dimethyl-naphthalenes; TRIM-NAPS are trimethylOnaphthalenes; M-PHENS are methyl-phenanthrenes; and DIM-PHENS are dimethyl-phenanthrenes.

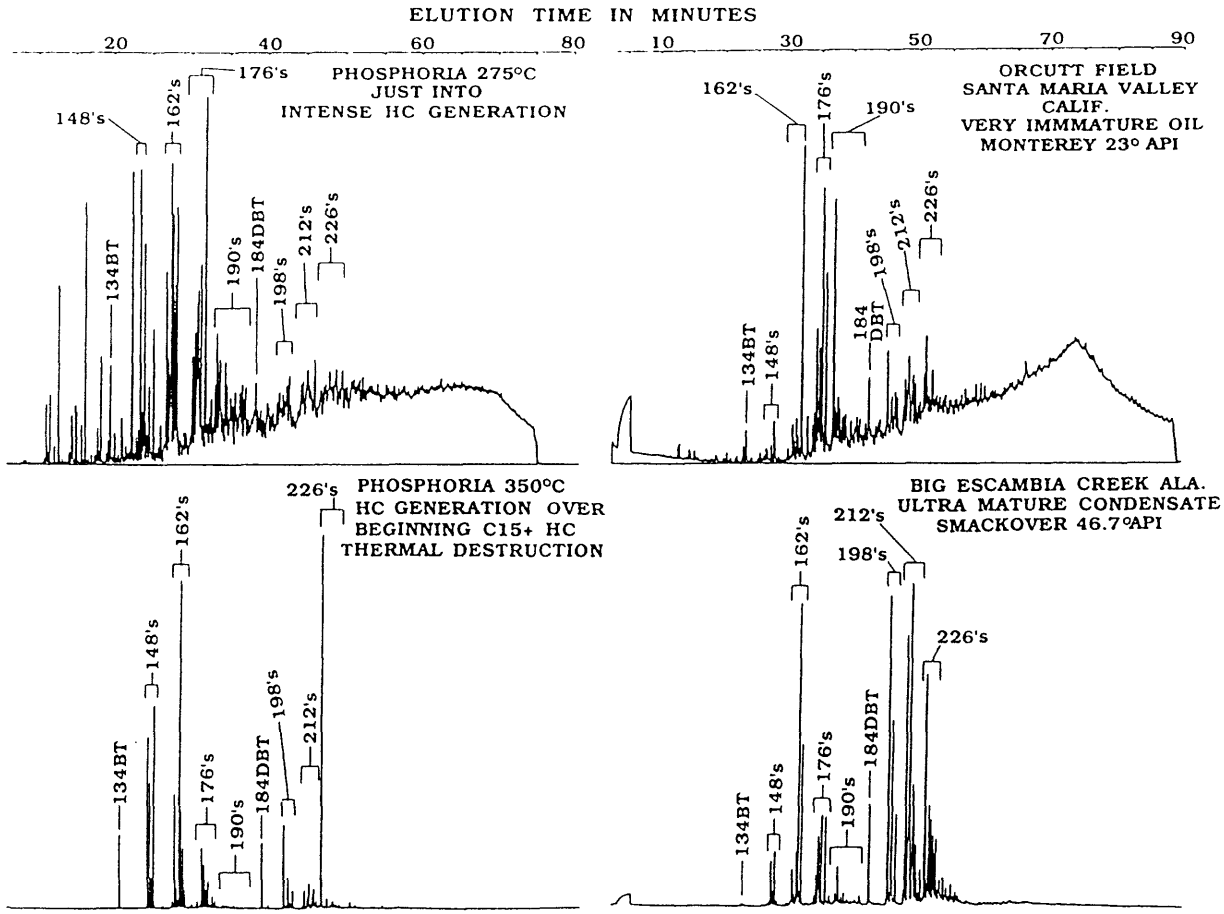

Figure 6-27. C_8+ (flame-photometric detection) gas chromatograms of sulfur-bearing aromatic HC's from an immature oil from the Orcutt field, Santa Maria Valley, California, Miocene Monterey Formation (0.916 gm/cc specific gravity); from a mature gas-condensate from the Big Escambia Creek field, Escambia Co., Alabama, Jurassic Smackover (0.794 gm/cc specific gravity); and from two aqueous-pyrolysis experiments performed on the Phosphoria shale with comparable maturities to the oil and gas condensate samples. Unlabeled peaks in the front third of the Orcutt field and Phosphoria 275°C chromatograms are series of alkylated thiophenes. Numbers (and letters) above the peaks refer to molecular weights and compound classes. 134BT is benzothiophene, 148's are methylbenzothiophenes, 162's are dimethylbenzothiophenes, 176's are trimethylbenzothiophenes, 190's are tetramethylbenzothiophenes, 184BT is dibenzothiophene, 198's are methyldibenzothiophenes, 212's are dimethyldibenzothiophenes, and 226's are trimethyldibenzothiophenes.

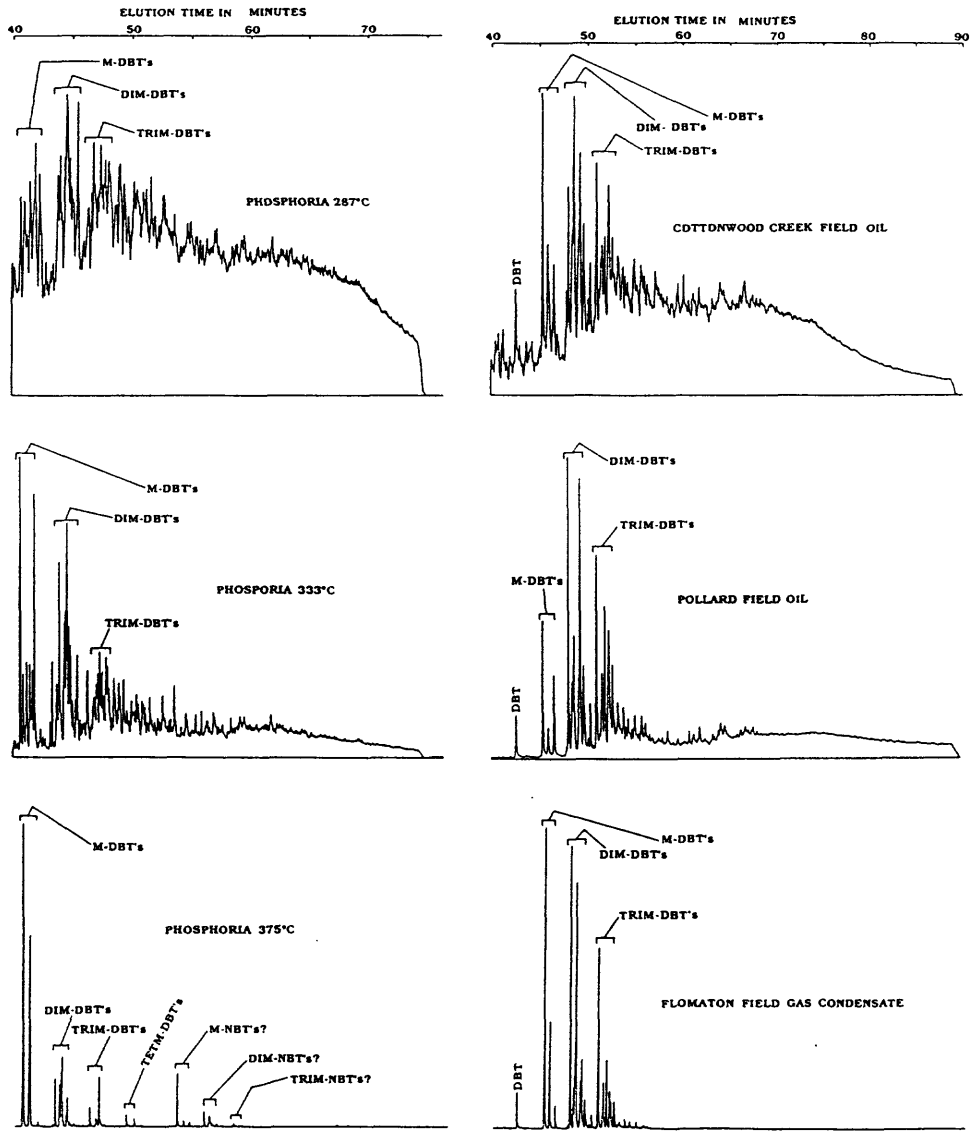

Figure 6-28. FPD (flame-photometric detection gas chromatograms of high-molecular weight sulphur-bearing aromatic HC's (roughly dibenzo-thiophene and higher eluting HC's) for three aqueous-pyrolysis experiments performed on the Phosphoria shale and two oils and one gas condensate of equivalent maturities to the aqueous-pyrolysis experiments. The Cottonwood Creek oil, Washakie County, Wyoming, Big Horn Basin, is produced from the Permian Phosphoria Formation. The Pollard oil, Escambia County, Alabama, is produced from the Lower Cretaceous Tuscaloosa Formation. The Flomaton gas condensate, Escambia County, Alabama, is produced from the Jurassic Norphlet Formation.

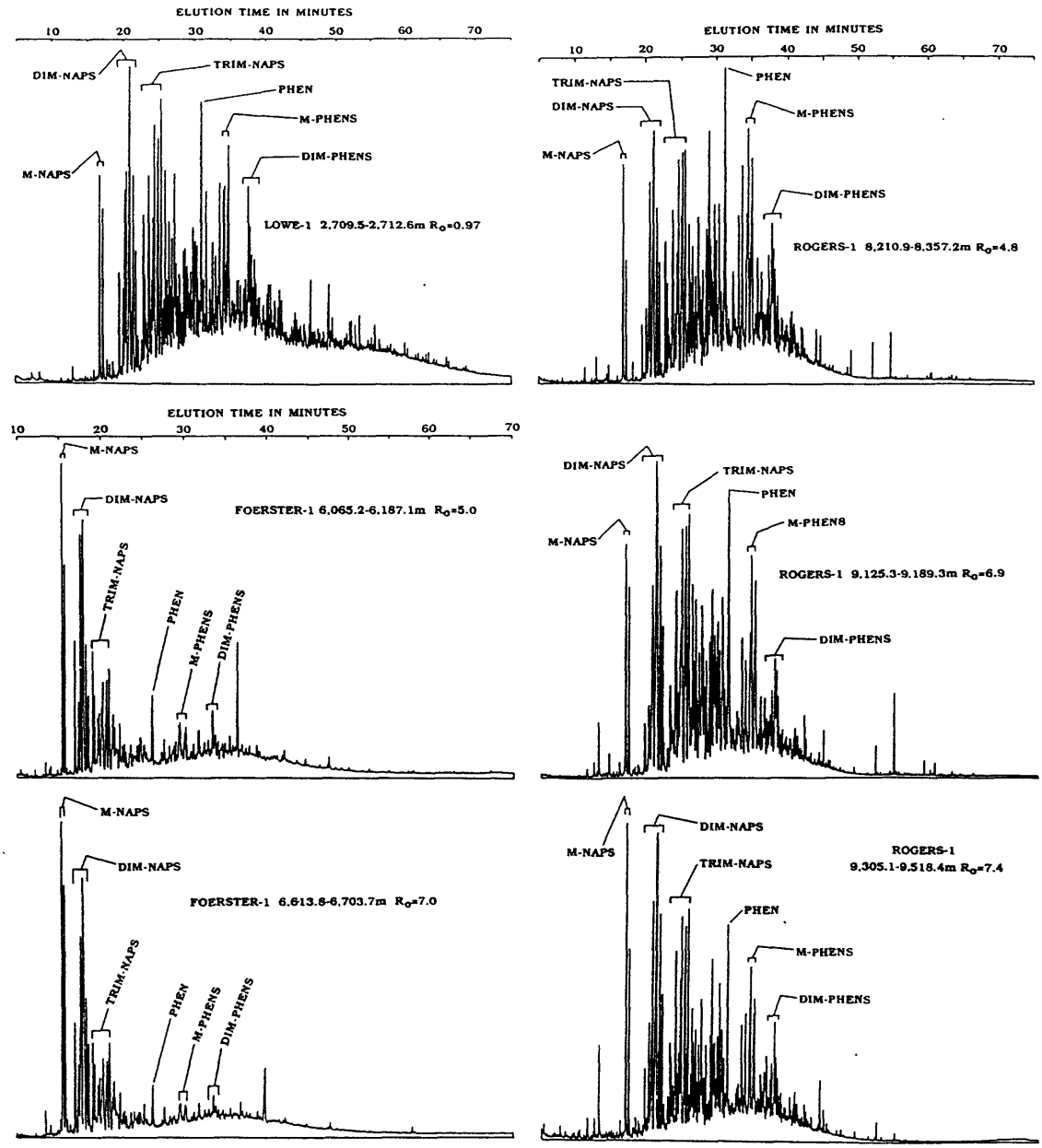

Figure 6-29. C_{15+} aromatic HC gas chromatograms from bitumen extracted from deep rocks of three deep wells of Table 6-3 (Bertha Rogers-1, Ralph Lowe-1, and Foerster-1). Sample depth and measured, or interpolated, or extrapolated R_O values are given for each chromatogram. M-NAPS are methyl-naphlthalenes, DIM-NAPS are dimethyl-naphthalenes, TRIM-NAPS are trimethyl-naphthalenes, PHEN is phenanthrene, M-PHENS are methyl-phenanthrenes, and DIM-PHENS are dimethyl-phenanthrenes, and DIM-PHENS are dimethyl-phenanthrenes. The Rogers-1 and Lowe-1 samples were analyzed under the same gas chromatographic conditions, which were different than those used for the Foerster-1 samples.

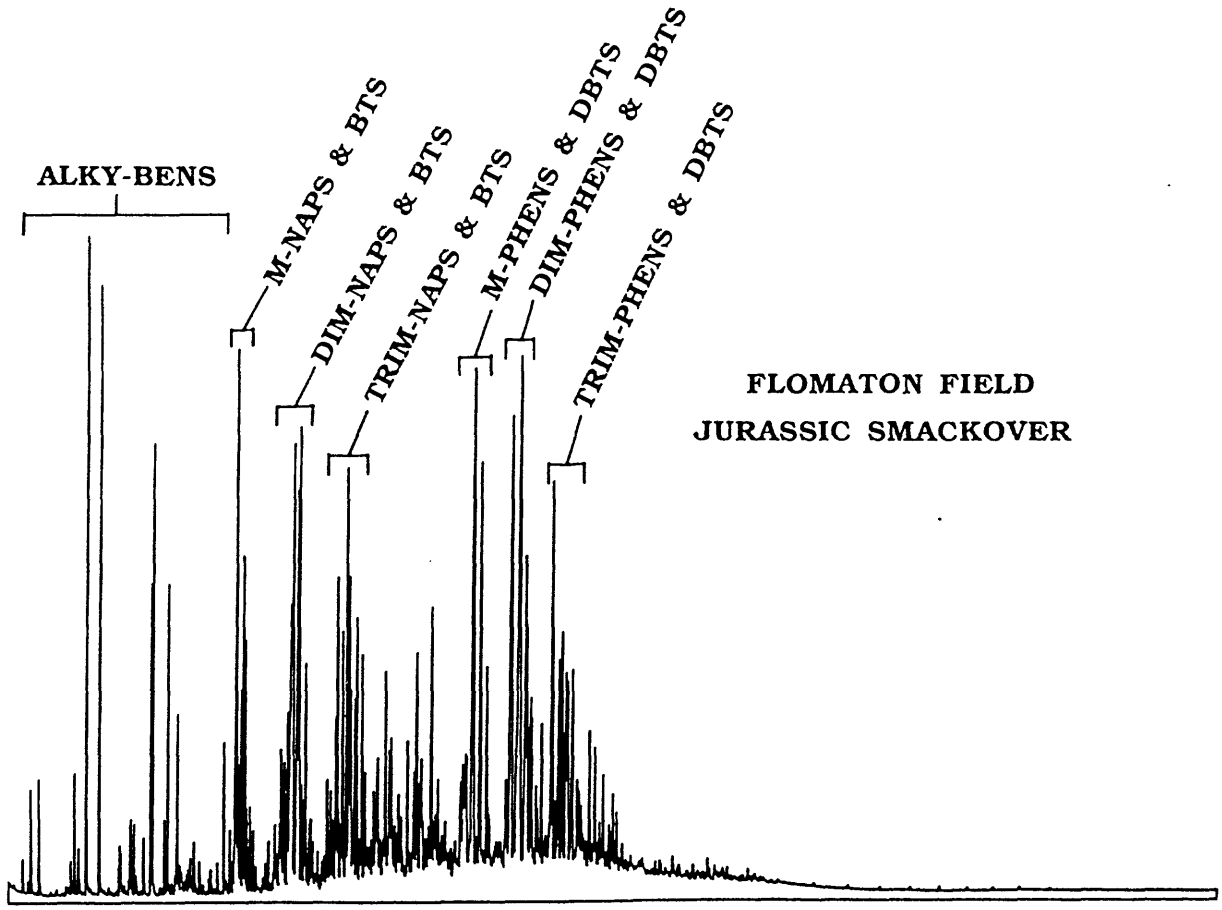

Figure 6-30. Gas chromatogram (flame-ionization detection) of C_8+ aromatic HC's of the Flomaton field gas condensate (see Fig. 6-28 caption for vita). ALKY-BENS are alkylated - Benzenes. M-NAPS & BTS are methyl-naphthalenes and methyl-benzothiophenes, DIM-NAPS & BTS are dimethyl-naphthalenes and dimethyl-benzothiophenes, TRIM-NAPS & BTS are trimethyl-naphthalenes and trimethyl-benzothiophenes, M-PHENS & DBTS are methyul-phenanthrenes and methyl-dibenzothiophenes, DIM-PHENS & DBTS are dimethyl-phenanthrenes and dimethyl-dibenzothiophenes, and TRIM-PHENS & DBTS are trimethyl-phenanthrenes and trimethyl-dibenzothiophenes.

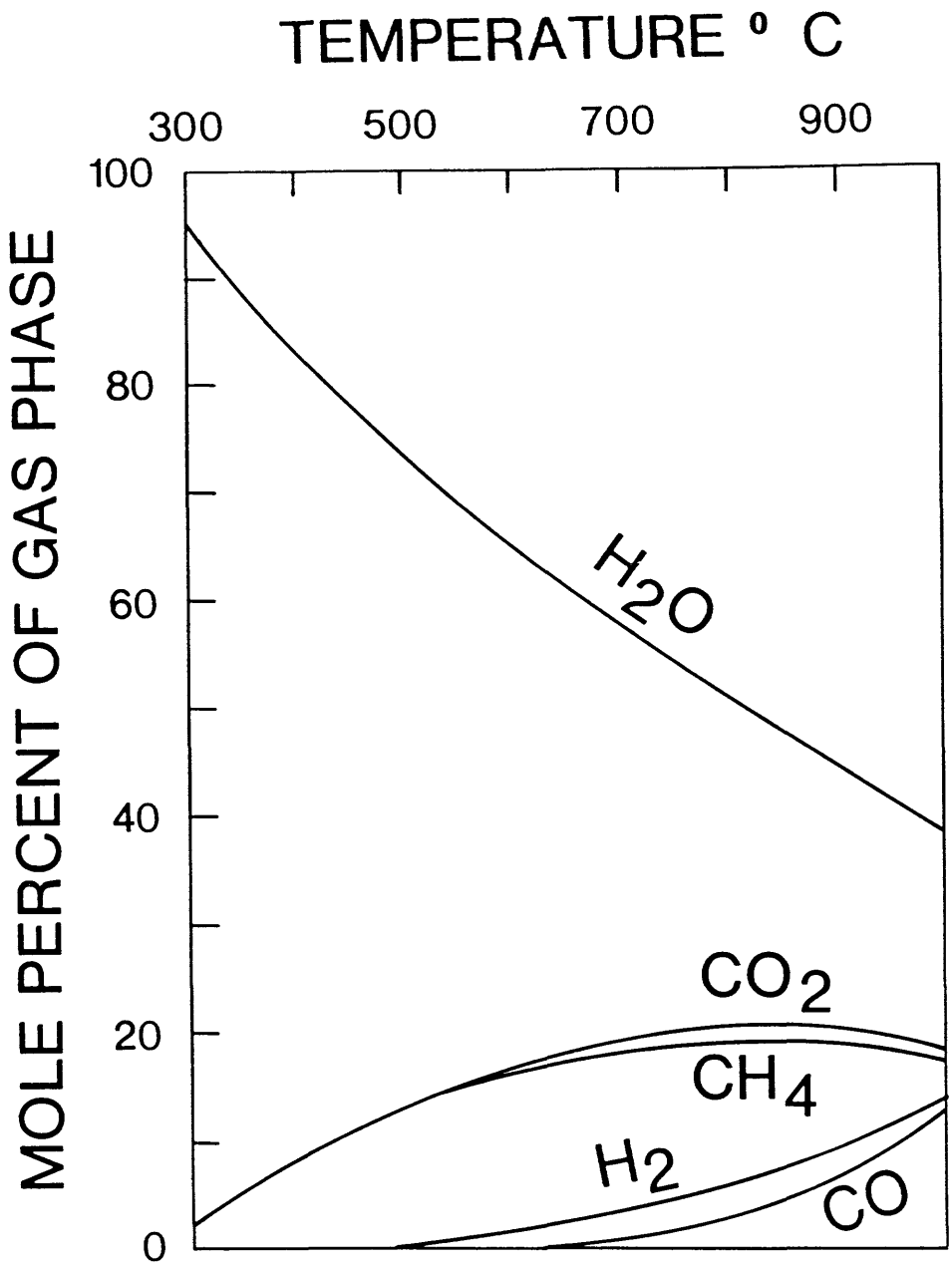

Figure 6-31. Phase diagram of gas species in equilibrium with graphite at a pressure of 1,000 bars. After Winkler (1976).

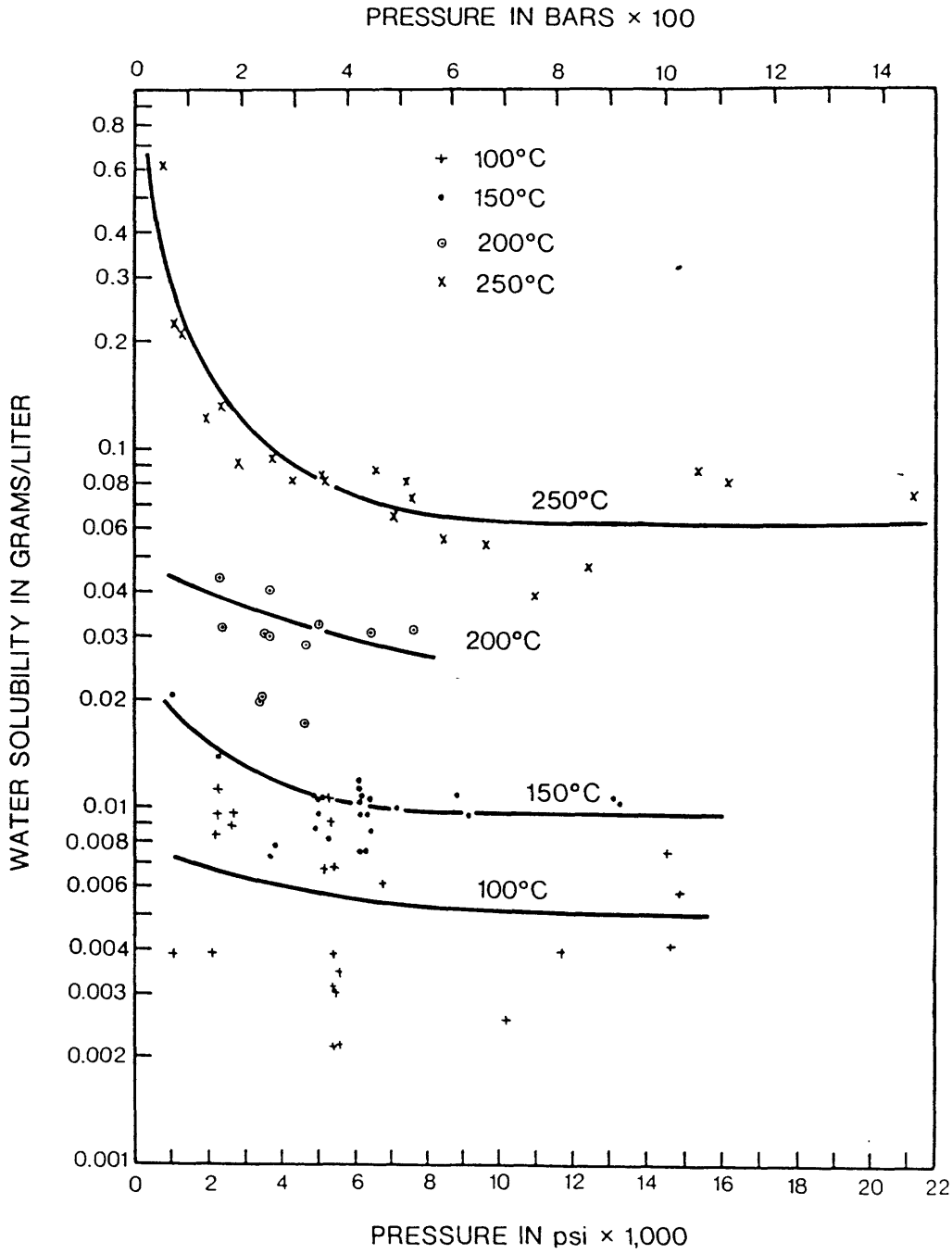

Figure 6-32. Solubility of water in pure methane at four different isotherms as a function of pressure. The solubility scales on both sides of the figure are accurate. (Water has a constant density of 1.00 g/cc.) Data from Price et al. (1983).

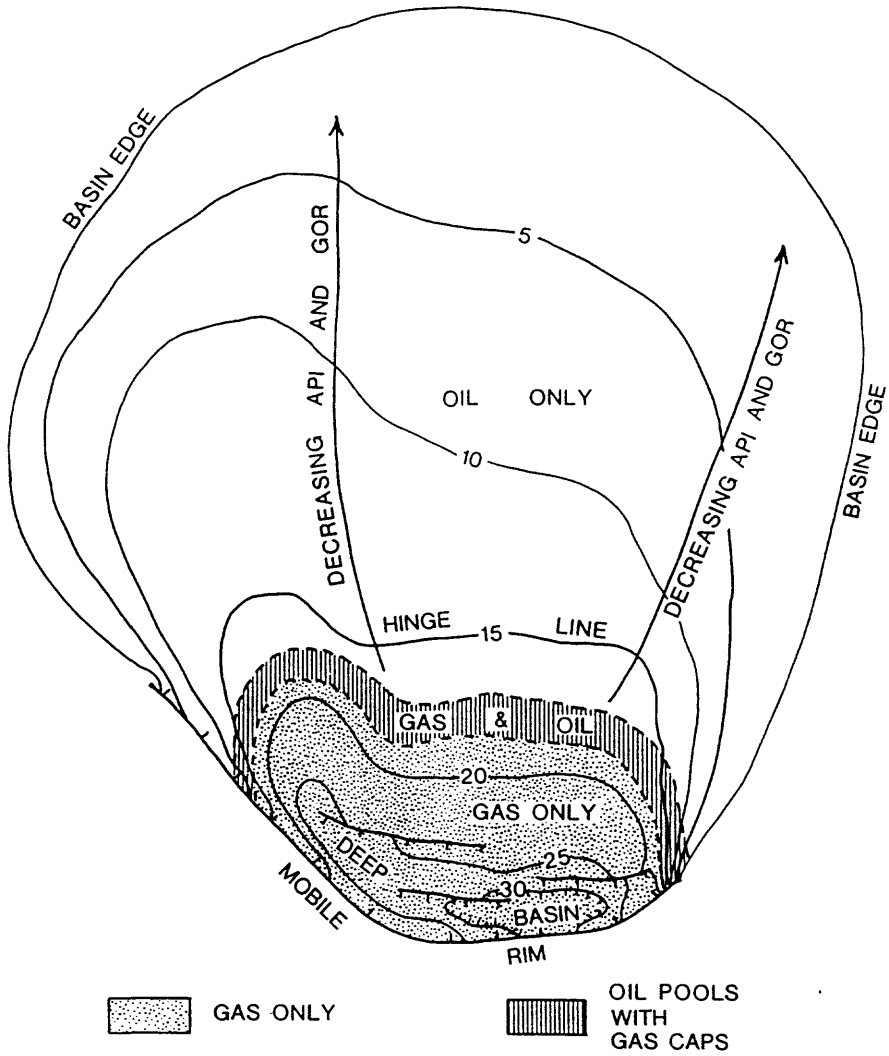

Figure 6-33. Hypothetical basins in plan view, showing oil and gas distribution in any one formation expected from the application of the present model. Contours are total sediment thickness in thousands of feet. Faults (which are shown by hachured lines) dip back into the deep basin and transport hydrocarbons from this area. Hydrocarbons move from the faults into carrier beds. The hydrocarbon distribution shown in the figure results and dashed boundaries signify approximate nature of this distribution. API stands for API oil gravity and GOR stands for gas-oil ratio.

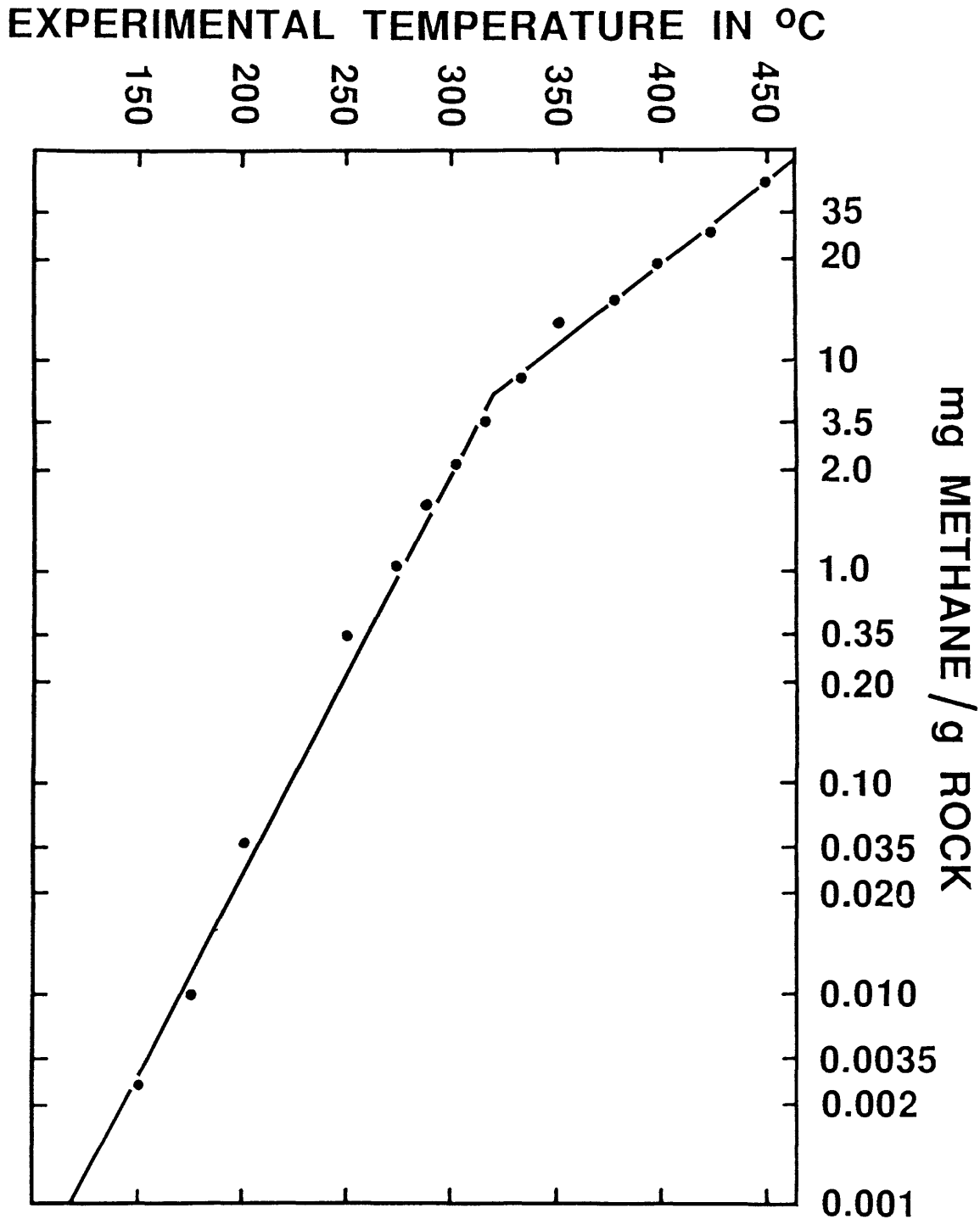

Figure 6-34. Milligrams of methane generated per gram of rock (mg METHANE/g ROCK) versus experimental temperature in °C for aqueous-pyrolysis.

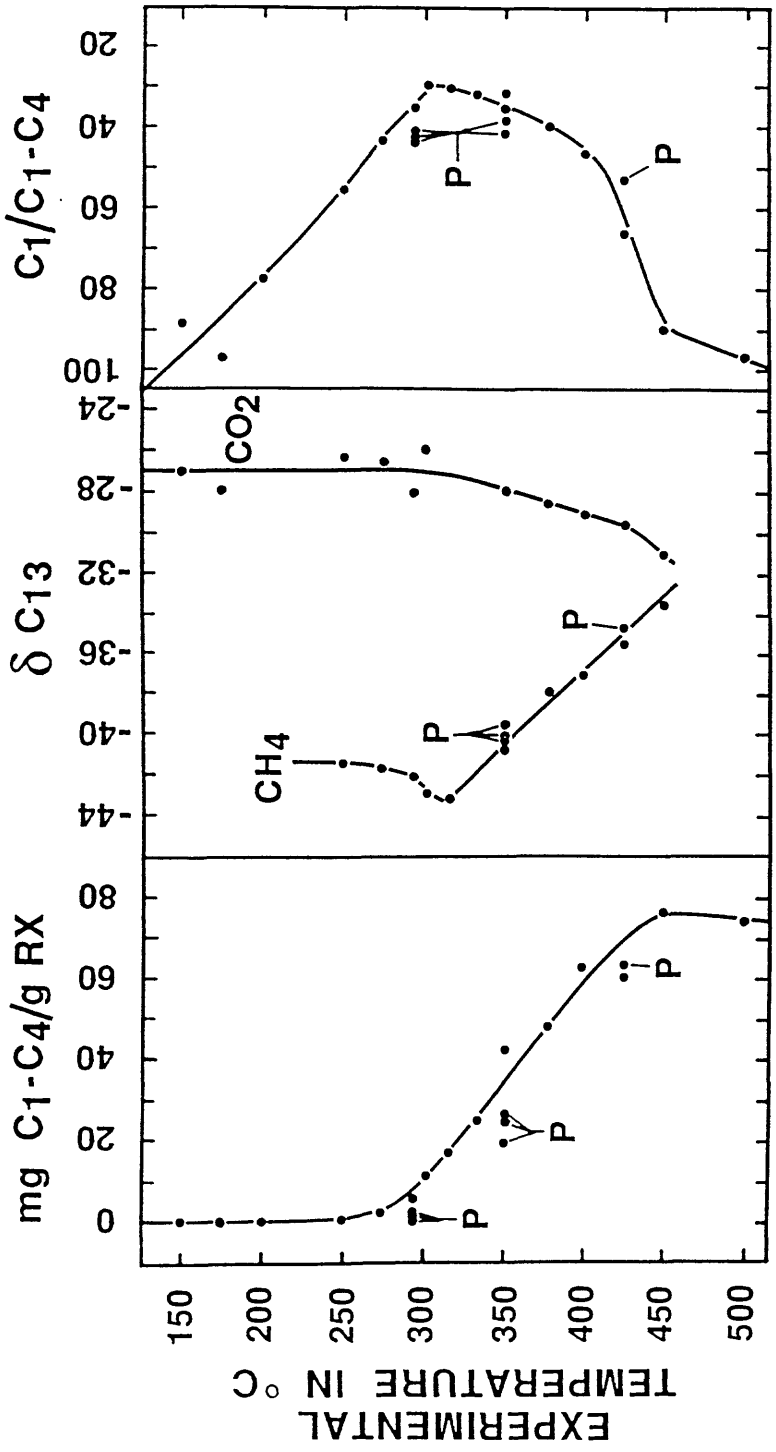

Figure 6-35. Plots of milligrams of the C_1 through C_4 HC gases generated per gram of rock (mg C_1-C_4/g RX), carbon-isotopic dC13 values for methane and carbon dioxide, and the ratio of methane to the sum of methane through the butanes (C_1/C_1-4) versus experimental temperature in °C for aqueous-pyrolysis experiments performed on the Phosphoria shale. Refers to data points from pressurized experiments

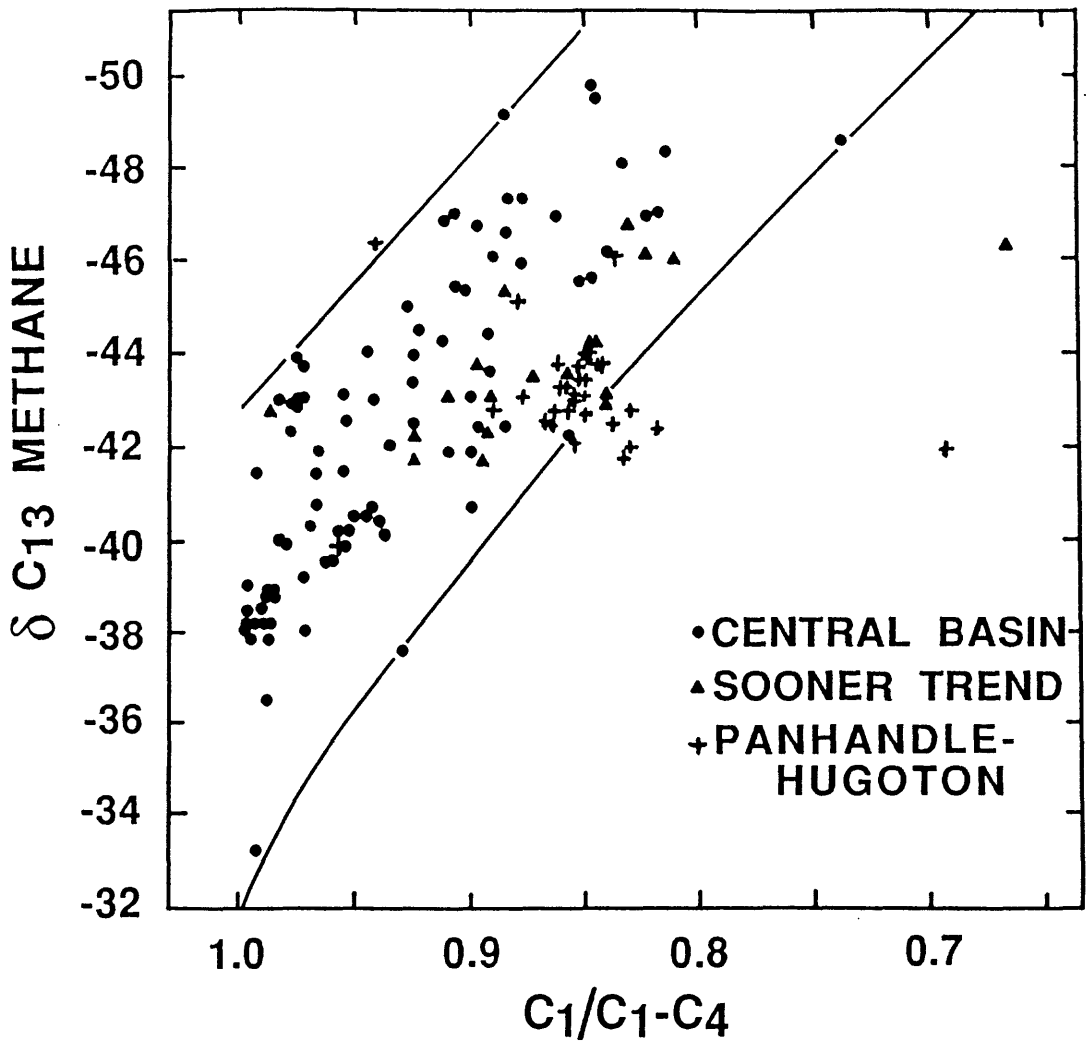

Figure 6-36. Plot of dC_{13} for methane versus the ratio of methane to methane + ethane + propane + the butanes (C_1/C_1-C_4) for produced natural gases of the Anadarko basin. Data from Rice et al. (1988).

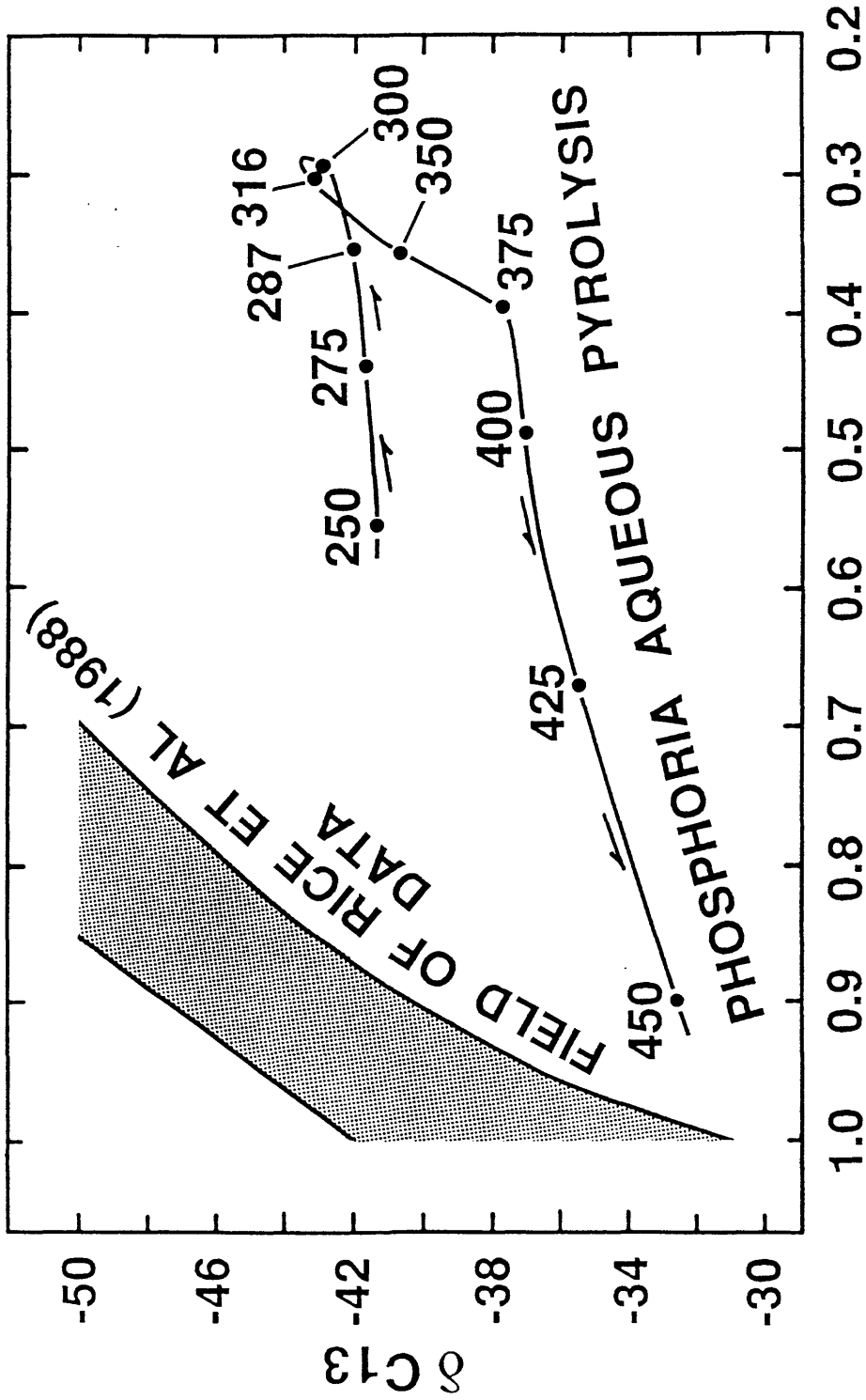

Figure 6-37. Plot of dC_{13} for methane versus the ratio of methane to methane + ethane + propane + the butanes (C_1/C_1-C_4) for produced natural gases of the Anadarko basin (stipled pattern, data from Rice et al., 1988) and for HC gases generated in aqueous-pyrolysis experiments performed on the Phosphoria shale. Numbers of experimental temperatures, arrows signify trends in the experimental data.

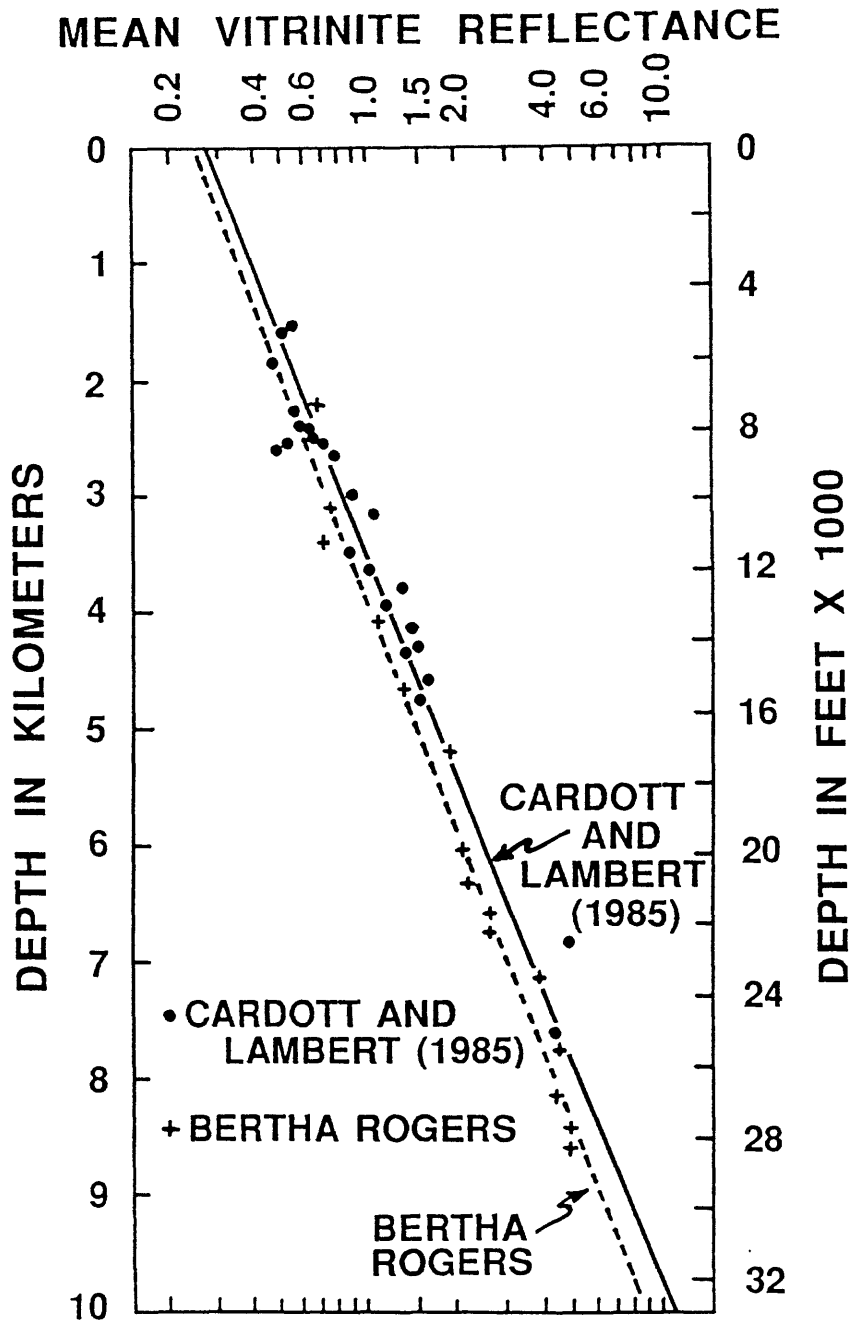

Figure 6-38. Plots of R_O versus depth for the Mississippian-Devonian Woodford shale versus depth for different sample locations of the Anadarko Basin (dots and solid line) from the data of Cardott and Lambert (1985). R_O data from the Bertha Rogers-1 (crosses and dashed line) are also given for comparison. The dashed line has a correlation coefficient of r = 0.989 to the crosses. The solid line has a correlation coefficient of r = 0 to the dots.

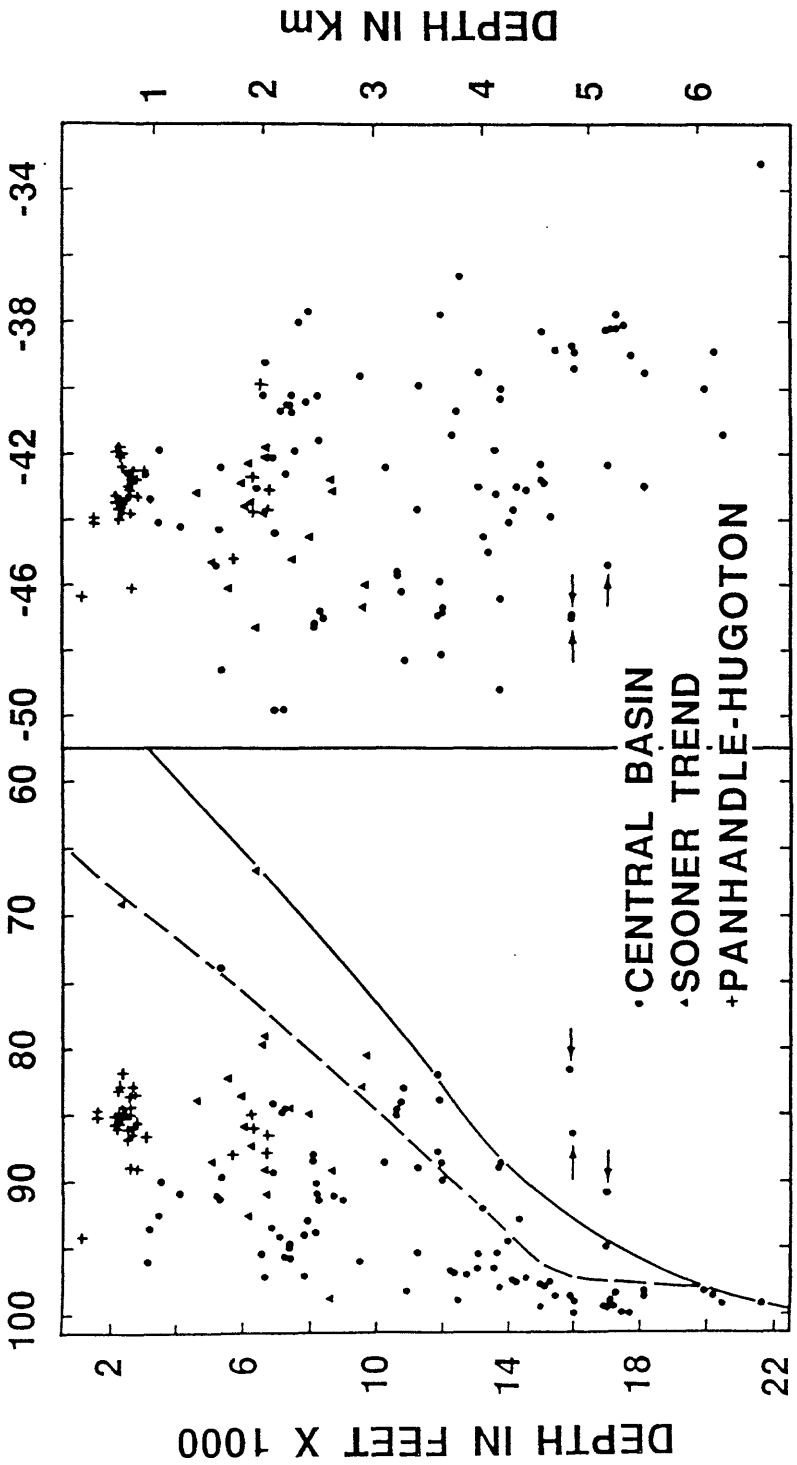

Figure 6-39. Plots of percent methane of the C_1-C_4 HC gases and the methane carbon isotopic value (dC13) versus depth for gas deposits of the Anadarko Basin. Percent methane values calculated from original data of Rice et al. (1988). Arrows designate samples discussed in the text. Dashed and solid line sin percent methane plot represents arbitrary sample envelopes (discussed in text).

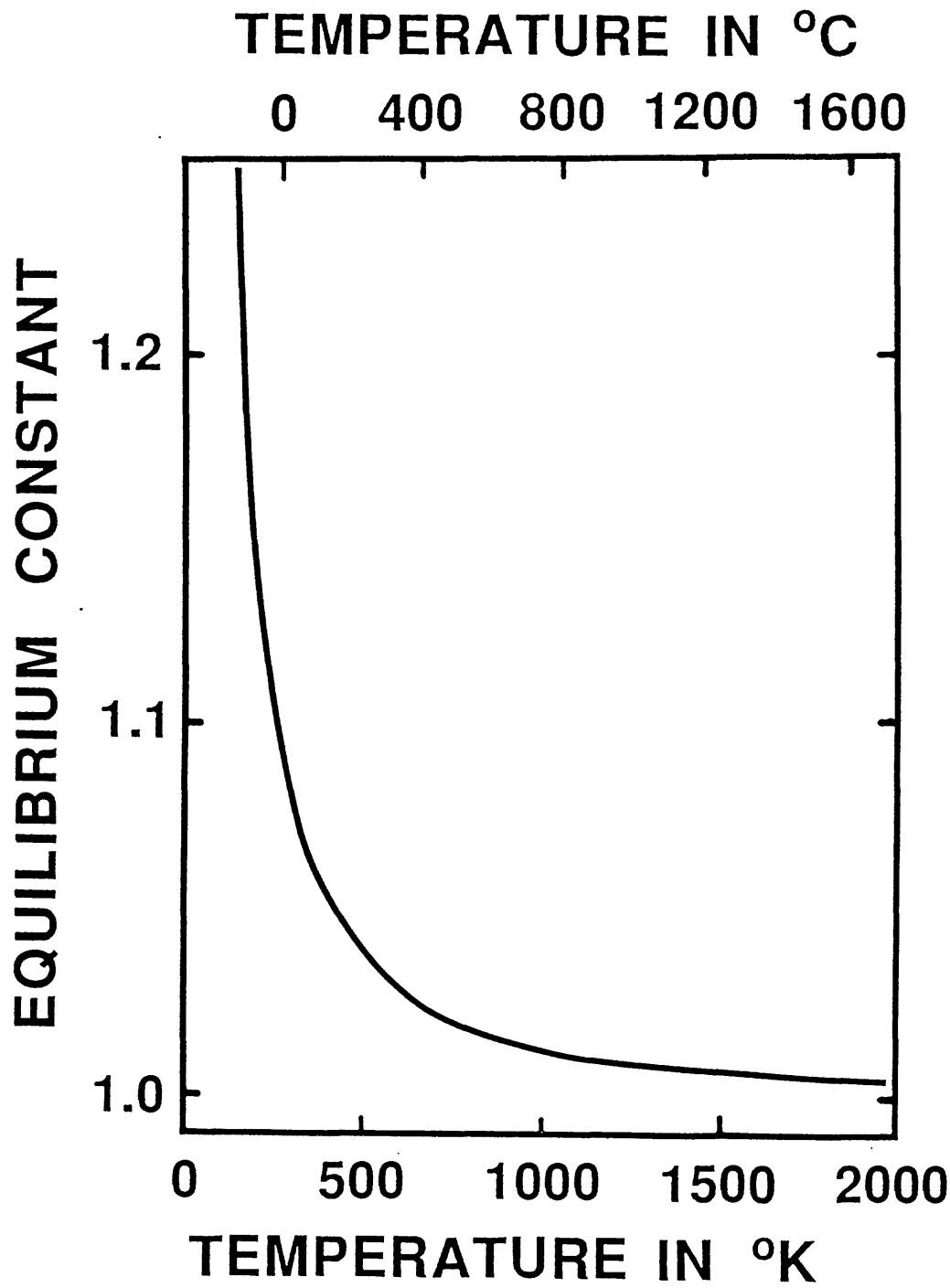

Figure 6-40. Plot of equilibrium constant for the exchange of the carbon-13 isotope between methane and carbon dioxide. After Weisman (1971).

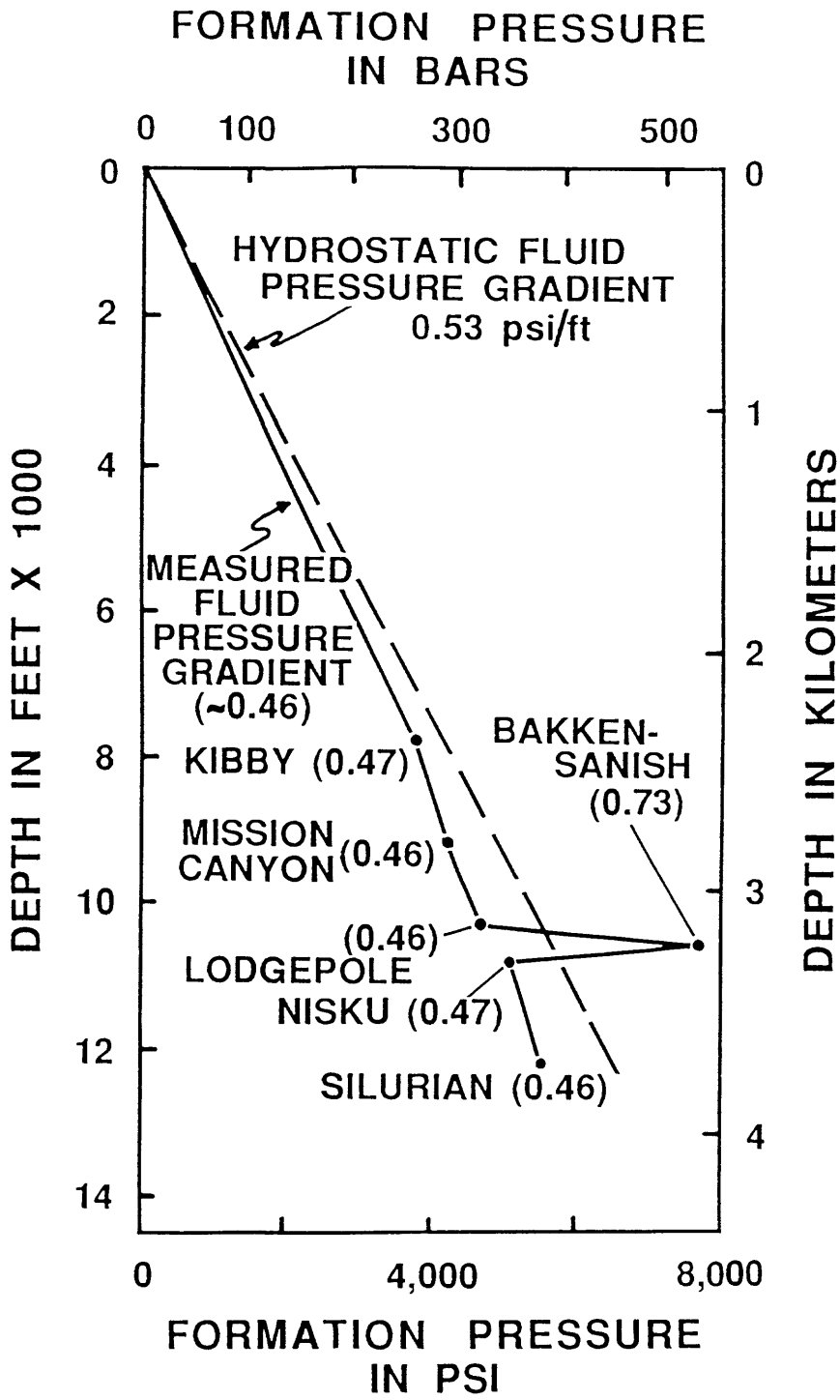

Figure 6-41. Plot of formation fluid pressure in bars and pounds per square inch (PSI) versus depth in feet and kilometers for wells in the Antelope field, McKenzie Co., North Dakota. Numbers in parenthesis are fluid pressure gradients at the stratigraphic units shown. After Meissner (1978).

Table 6-1. List of rocks with starting total organic carbon (TOC) values in weight percent of rock, hydrogen indices (HI, after enrichment from hydrogenation), and OM type, on which USGS aqueous-pyrolysis experiments were carried out.

Rock	TOC	HI	OM Type
Pennsylvanian Anna Shale	25	320	II/II
Mississippian-Devonian Bakken Shale	14	570	II
Eocene Green River Shale	14	805	I
Eocene Rattlesnake Butte Lignite	50	70	III/II
Permian Phosphoria Shale	22	620	II-S
Los Angeles Basin mid-Miocene shale	5	500	II

Table 6-2. HC gas concentration and relative loss from equivalent core samples using "KC core lifter" and normal "open" method. After Sokov and others (1971).

Rock Type	Sample Depth (ft)	Sample Mode	Gas Concentration $10^{-4}cm^3$/ kg ROCK	Gas Relative Loss KC/OPEN
Sand	1263	KC	106,243	893
		OPEN	119	
Shale	1887	KC	2,431	47
		OPEN	52	
Shale	2034	KC	36,473	529
		OPEN	69	

Table 6-3. List of wells used for Fig. 4 R_O in % is extrapolated R_O at well bottom based on depth versus R_O plots, all of which have correlation coefficients <0.99. Sediment age is range of rock ages penetrated in the wellbore. Reference is published petroleum geochemical study on each wellbore.

Well	Location in m	Depth in m	R_O in %	Sediment Age	Reference
Lone Star Bertha Rogers-1	Washita Co., Okla.	9,583.7	8.0	Permian-Cambrian	Price et al. (1981)
Ralph-Lowe-1	Pecos Co., Texas	8,686.4	5.8	Permian-Ordovician	Price (1988)
Shell McNair-1	Hinds Co., Miss.	6,911.0	2.8	Lower Tertiary-Jurassic	Price et al. (1979)
Chevron Jacobs-1	Goliad Co., Texas	7,546.8	7.5	Miocene-Lower Cretaceous	Price (1982)
Pan Am Foester-1	La Salle Co., Texas	6,703.7	7.0	Lower Tertiary-Jurassic	Price and Clayton (1990)

Table 6-4. Depths in meters (m); vitrinite reflectance (R_o) values; C_{15+} bitumen (C_{15+} BIT) in parts per million by rock weight (ppm), and normalized to organic carbon (mg/g OC); C_{15+} hydrocarbons (C_{15+} HC's) in parts per million by rock weight (ppm), and normalized to organic carbon (mg/g OC); total organic carbon (T.O.C.) in percent; present-day burial temperature in °C; and rock geologic age for four of the five wells of Table 3. Burial temperatures for the Foerster-1 are based on an estimated regional geothermal gradient for La Salle County, Texas, of 36.7° km.

Depth in (m)	Ro	C15+ BIT		C15+ HC's		T.O.C	Present Day Burial Temp. °C	Geologic Age
		ppm	mg/gOC	ppm	mg/gOC			
Foerster-1								
4602-4724	2.58	193	80.4	114	47.7	0.24	196	Lower Cretaceous
4724-4846	2.73	252	105	118	49.2	0.24	201	"
4968-5151	3.10	556	132	280	67.0	0.42	211	"
5151-5334	3.36	828	172	545	114	0.48	218	Jurassic
5334-5456	3.60	740	154	476	99.1	0.48	224	"
5456-5578	3.80	442	108	271	56.1	0.41	228	"
5761-5882	4.37	467	31	165	10.8	1.51	238	"
Ralph Lowe-1								
6026-6032	3.08	358	26	179	13	1.39	187	Pennsylvanian
6629-6635	3.20	500	37	332	25	1.34	204	"
6882-6888	3.38	451	14	251	8	3.08	211	"
7080-7087	3.57	1,410	41	1,030	30	3.46	216	Mississippian
7324-7330	3.86	1,650	38	1,380	32	4.32	223	"
7391-7398	3.93	3,590	151	1,610	68	2.87	225	"
7718-7724	4.30	2,420	90	NA	NA	2.68	234	Devonian
R. G. Jacobs-1								
6400.8	4.60	2,200	176			1.25	254	Lower Cretaceous
6401.7	4.60	1,400	303	1,100	239	0.46	254	"
6407.7	4.61	1,100	105			1.05	255	"
6418.3	4.61	776	141	588	107	0.55	255	"
6698.7	5.22	1,800	367			0.49	265	"
6705.8	5.22	805	267	590	174	0.34	266	"
6711.2	5.23	548	261	398	189	0.21	266	"
7000.0	5.95	200	74			0.27	276	"
7005.7	5.95	483	172	365	130	0.28	276	"
7297.7	6.80	1,025	214	844	176	0.48	286	"
7313.8	6.81	230	74	153	49.0	0.31	288	"
7539.1	7.50	165	72	104	45.0	0.23	296	"
7544.6	7.51	129	64	65	32.5	0.20	296	"
Bertha Rogers-1								
8357-8378	5.20	306	278	140	145	0.11	224	Mississippian
8442-8470	5.30	3,010	84	1,450	60	3.59	226	Mississippian-Devonian
8558-8723	5.70	389	162	252	134	0.24	230	Devonian

Table 6-5. Normalized percentages for aromatic HC compound classes eluting roughly between the dimethylbenzenes and the trimethylnaphthalenes as determined by full-scan mass spectrometry, for aqueous-pyrolysis experiments on the Phosphoria shale. Each vertical column are normalized percentages which add up to 100%±1%. Numbers after each compound class are approximate molecular weights. Temperature (Temp.) in °C and pressure (Press.) in bars (B) are shown at the top of each column and represent experimental conditions. Bottom line in the total of the C8+ aromatic HC's determined for each experimental run by a combination of gas chromatography and gravimetrics on an analytical balance in milligrams of HC's per gram of reacted rock (mg/g RX). ND (for the 500°C sample) is none detected. Mass spectrometry, being very sensitive, will determine the presence of compounds not recognized by gas chromatography and gravimetrics.

Compound Class	Normalized Percentages								
Sample Temp. Press.	500°C 226.5	450°C 192B	425°C 160B	425°C 551B	440°C 144B	375°C 132B	350°C 118B	350°C 1,077B	333°C 80.8B
Dimethylbenzenes (106)	0.68	0.83	2.31	8.39	7.81	12.50	4.80	1.12	0.81
Alkylated Benzenes (120)	0	0.15	0.58	4.70	4.75	7.02	19.41	24.14	1.06
" " (134)	0	0.02	0.02	0.30	0.46	1.87	3.59	3.62	0.28
" " (148)	0	0	0	0.01	0.03	0.23	1.43	2.49	0.34
" " (162)	0	0	0	0	0.003	0.03	0.42	0.69	0.08
' ' (176)	0	0	0	0	0	0	0.10	0.85	0.06
" " (190)	0	0	0	0	0	0	0	0.07	0.05
Naphthalene (128)	28.55	77.79	87.08	70.43	62.37	48.02	8.56	1.78	0.41
Methylnaphthalene(142)	0.18	1.49	5.94	13.94	22.12	23.00	22.91	20.33	10.82
Dimethylnaphthalene (156)	0	0.17	0.14	0.50	1.14	4.10	11.12	11.02	11.36
Trimethylnaphthalene(170)	0	0	0.04	0.57	0.03	0.76	5.83	6.97	15.80
Biphenyl (154)	70.14	19.46	3.75	0.33	0.03	0.02	0.03	0.02	0.07
Methylbiphenyl (168)	0.45	0.07	0.86	0.86	0.41	0.27	0.36	0.11	0.54
Benzofuran (118)	0	0.01	0.04	0.20	0.04	0.04	0.05	0.11	0.01
Methylbenzofuran (132)	0	0.02	0.01	0.11	0.30	0.35	1.79	1.11	0.31

Dimethylbenzothiophene(146)	0	0	0	0.10	0.01	0.08	0.37	1.44	0.21
Trimethylbenzofuran(160)	0	0	0	0	0	0.02	0.24	0.53	0.24
Benzothiophene (134)	0	0.01	0.003	0.01	0.06	0.30	1.17	0.27	0.44
Methylbenzothiophene(148)	0	0	0	0.01	0.08	0.71	6.16	5.64	15.35
Dimethylbenzothiophene(162)	0	0	0	0.01	0.05	0.61	8.14	7.76	16.25
Trimethylbenzothiophene(176)	0	0	0	0	0.01	0.05	3.53	10.89	25.11
Alkylated Thiophene(112)	0	0	0	0	0	0	0.01	0.01	0.04
" " (126)	0	0	0	0	0	0	0	0.24	0.07
" " (140)	0	0	0	0	0	0	0	0.24	0.23
" " (154)	0	0	0	0	0	0	0	0.03	0.01
" " (168)	0	0	0	0	0	0	0	0.004	0
" " (182)	0	0	0	0	0	0	0	0	0
" " (196)	0	0	0	0	0	0	0	0	0
" " (210)	0	0	0	0	0	0	0	0	0
ΣC8+ Aromatic HC's mg/g RX	ND	2.214	6.22	6.76	6.37	7.02	11.70	23.06	33.78

Table 6-6. Normalized percentages for aromatic HC compound classes eluting roughly between the trimethylnaphthalenes and the methylphenanthrenes as determined by full-scan mass spectrometry, for aqueous-pyrolysis experiments on the Phosphoria shale. Each vertical column are normalized percentages which add up to 100%±1%. Numbers after each compound class are approximate molecular weights. Temperatures (Temp.) in °C) and pressure (Press.) in bars (B) are shown at the top of each column and represent experimental conditions.

Compound Class	Normalized Percentages								
Sample									
Temp.	500°C	450°C	425øC	425°C	440°C	375°C	350°C	350°C	333°C
Press.	226.5	192B	160B	551B	144B	132B	118B	1,077B	80.8B
Trimethylnaphthalenes (170)	0	0.05?	0	0.02	0.03	0.23	12.88	24.06	20.70
Tetramethylnaphthalenes (184)	0	0	0	0.03	0.10	0.95	8.82	11.68	15.75
Pentamethylnaphthalenes (198)	0	0	0	0	0.01	0.08	3.09	8.72	5.60
Fluorene (166)	25.62	2.80	2.25	0.64	0.56	0.69	2.45	0.068	0.13
Methylfluorenes (180)	0	0.16	0.16	0.20	0.35	1.45	1.38	0.45	0.50
Dimethylfluorenes (194)	0	0	0.02	0.06	0.16	1.19	1.91	1.04	0.86
Dibenzothlophene (184)	10.89	69.52	42.14	36.43	31.18	25.29	8.96	3.63	4.61
Methyldibenzothiophenes & Methylnapthobenzothiophenes (198)	0	0.18	1.87	7.62	8.99	17.94	24.01	21.32	22.58
Methylbipheoryk (182)	0	0.03	0.26	0.19	0.74	1.35	1.35	0.87	1.18
Dimethylbiphenyls (196)	0	0	0.02	0.23	0.55	1.24	1.67	1.87	2.02
Phenanthrene (178)	63.49	26.84	52.45	47.43	47.64	31.42	9.09	1.10	1.19
Methylphenanthrenes (192)	0	0.13	0.79	6.11	0.86	17.19	19.71	8.835	6.14
Methyldibenzofurans (182)	0	0.08	0.04	0.26	0.23	0.49	1.36	1.52	2.21
Dimethyldibenzofurans (196)	0	0.08	0.01	0.08	0.17	0.28	1.12	1.58	2.52
Trimethylbenzothiophenes (176)	0	0	0	0	TR	0	1.52	2.74	2.80
Tetramethylbenzothiophenes (190)	0	0	0	0	0	0	1.83	9.49	9.93
Methylacenaphthenes (166)	0	0.13	0.02	0.70	0.10	0.19	1.03	0.95	1.26
Alkylbenzenes (106-190)	0	0	0	0	0	0	0.03	0.08	TR

Table 6-7. Geochemical data from Soxhlet-extracted rock samples of the Phosphoris S after aqueous pyrolysis and from kerogens isolated from those rocks. H/C is kerogen atomic H/C ratio. HI and OI are ROCK-EVAL hydrogen and oxygen indices, respectively, of the reacted rock. TOC is total organic carbon of the r in weight percent. S_2 and S_3 mg/gRX are the ROCK-EVAL S_2 and S_3 pyroly peaks in milligrams per gram of Soxhlet-extracted rock. Tmax °C is the maximum of the ROCK EVAL S_2 pyrolysis peak in °C.

Table 7

	H/C	HI	OI	TOC	S_2	S_3	T_{max}
RAW	1.29	451	30	21.41	96.58	6.44	418
175°C, 4.32 bars	1.23	507	21	20.12	102.06	4.21	418
200°C, 6.36 bars	1.24	481	18	20.28	97.56	3.55	418
250°C, 14.5 bars	1.16	485	14	15.39	74.66	2.13	429
275°C, 22.3 bars	1.04	330	17	15.18	50.03	2.57	433
287°C, 31.0 bars	0.67	209	12	11.45	23.98	1.35	430
287°C, 366 bars	0.99	248	13	14.83	36.72	2.00	428
287°C, 681 bars	0.99	279	15	13.76	38.37	2.07	427
287°C, 965 bars	1.19	371	22	18.52	68.62	4.08	421
300°C, 41.4 bars	0.78	165	9	11.32	18.69	1.06	437
316°C, 58.2 bars	0.63	108	8	11.66	12.64	0.92	450
333°C, 80.8 bars	0.63	69	5	12.70	8.77	0.64	463
350°C, 118 bars	0.52	25	4	15.54	3.91	0.65	582
350°C, 442 bars	0.51	27	2	15.34	4.18	0.29	575
350°C, 782 bars	0.48	29	3	14.98	4.31	0.41	578
350°C, 1077 bars	0.59	62	3	13.76	8.49	0.38	466
375°C, 132 bars	0.45	10	2	16.57	1.67	0.27	585
400°C, 144 bars	0.41	6	1	17.58	1.12	0.21	598
425°C, 160 bars	0.36	3	2	18.00	0.46	0.34	599
425°C, 551 bars	0.36	6	2	17.21	1.05	0.26	598
450°C, 190 bars	0.31	2	1	16.62	0.26	0.17	--

Table 6-8. Average basin productivity in millions of barrels of producible oil and oil-equivalent gas per thousand square miles (10^6 Bbls/1000 mi^2) and total estimated ultimate recovery (EUR) in billions of barrels (10^9 Bbls) for the different major basinal structural classes discussed by Price in a manuscript in preparation. Examples of each class are given in parentheses. Structural intensity over and adjacent to the basin deep increases from Class I through Class VIII. EUR and productivity data in Table 2 results from data compiled from 62 of the world's major basins based on work by D. Klemme.

Class	Basin Type	EUR 10^9 Bbls	Productivity 10^6Bbls/ 1000 mi^2
I	Shallow cratonic (Williston, Paris)	12.48	17.4
II	Moderately deep to deep cratonic basins with slight to moderate mobile rims (Uinta, Fort Worth)	22.67	88.4
III	Pull aparts (Gabon, NW Shelf Australia)	7.58	74.9
IV	Block fault - Aborted rift (North Sea, West Texas Permian)	317.6	265
V	Mobile Foredeeps (Anadarko, Persian Gulf)	930.5	299
VI	Downwarps (Greater Gulf Coast, Tampico-Reforma)	269	472.5
VII	Deltas (Niger, Mississippi Fan)	85	555
VIII	Wrench (Los Angeles, Eastern Venezuela)	132.6	969.3

Appendix 7: Migration of 10's to 100's of TCF of Hydrocarbon and non-Hydrocarbon Gases from the Deep Crust: Composition, Flux, and Tectonic Setting, by R.C. Burruss

INTRODUCTION

The purpose of Task 7 was to investigate the composition of non hydrocarbon gases (NHCG) and HC's in deep (>4,270 m-->14,000 ft.) natural gas reservoirs in order to yield evidence of migration of gases from deep crustal levels (>9,144 m-->30,000 ft.). Any indication of migration of gases from great depth to drillable depths in sedimentary basins will be significant for two reasons. First it will expand our knowledge of the source of gases beyond "conventional" concepts of gas generation, and second, the presence of non-HC gases can have a significant impact on the economics of gas production from deep reservoirs.

Comparison of gas compositions in deep reservoirs with the compositions of gases generated in the deep crust yields three types of information. First, information will demonstrate whether there are similarities between the gases in the two crustal regimes. Second, the evidence for volumetric fluxes of NHCG and HC gases in metamorphic rocks presently exposed at the surface can be used to estimate the potential flux of gases to shallow crustal levels that are currently accessible to the drill. Third, identification of crustal environments (tectonic and metamorphic terranes) that generate significant quantitities of gas can be coupled with analysis of structural style and setting (W.J. Perry, Jr., this volume) to identify basins where deep crustal sources may have contributed to the HC resource base.

GASES IN DEEP RESERVOIRS AND METAMORPHIC ROCKS

A. Reservoirs greater than 4,270 m (14,000 ft)

Initial analysis of trends in gas composition versus depth and reservoir lithology were performed on all the available gas data in the NRG Associates Significant Field File (NRG Associates, 1991) for reservoirs at depths equal to or greater than 4,270 m (14,000 ft). This file contains gas data for 120 reservoirs: 44 from the Permian basin, 38 from the Midcontinent (mostly Anadarko basin), 15 from the Gulf Coast North, 14 from the Gulf Coast South, and 9 from the basins in the Rocky Mountains region. When the fraction of total NHCG is plotted (Fig. 7-1) as a function of reservoir temperature (to eliminate significant variations in geothermal gradient), two trends are apparent. Trend A consists of gradually increasing NHCG with depth up to about 10% and is common to both carbonate and sandstone reservoirs from all basins. Trend B consists of rapidly increasing NHCG with depth and is present in a small number of reservoirs in carbonate rocks with the exception of two cases. Trend A is due to fluid-rock interactions involving organic matter and dissolution and reprecipitation of carbonate cements. Trend B occurs in carbonate reservoirs of the Permian basin (Ellenberger Formation) and carbonate and sandstone reservoirs in the Smackover Formation and related strata (Norphlet Formation) of the Gulf Coast. Although the dominant NHCG in these reservoirs is CO_2, H_2S is also important (up to 25%). The occurrence of these high NHCG gases in carbonate reservoirs and the presence of H_2S indicates that thermochemical sulfate reduction and simultaneous oxidation of HC's to CO_2 may be the dominant control on gas composition in these reservoirs.

There is some danger in overinterpreting the trends in the data from the NRG Associates field file. Because this file only contains data on reservoirs with greater than one million barrels of equivalent (BOE) or 6 Bcf of gas ultimate production, the range of compositions represented is limited by the economics of production.

B. Fluids in Deep Crustal Rocks

Most of the evidence for the composition of fluids in the deep crust comes from observations on fluid inclusions in metamorphic and igneous rocks. Extensive reviews were published by Hollister and Crawford (1981) and Roedder (1984). Most of the information that is relevent to gas generation is related to metasedimentary rocks which contain graphitic carbon and carbonate minerals which can act as a source of carbon bearing gas components, CH_4 and CO_2 (Hollister and Burruss, 1976; Burruss, 1977; Duke and Rumble, 1986). Although igneous rocks can be important sources of CO_2 (Murck, and others, 1978; Roedder, 1984), they will not be considered further in this discussion. An additional source of information on fluids in crustal rocks is fluid inclusions in quartz veins associated with ore mineralization. The information from ore deposits was recently reviewed by Landis and Hofstra (1991) and Kerrich and Feng (1992), and related observations from a non-mineralized setting were presented by Ferry (1992). This information is important because it records the flux of fluids from deep to shallower levels of the crust and provides a basis for quantitative estimates of the flux of gases to shallow crustal levels as discussed in the following section.

The trends in NHCG content of natural gases shown in Figure 7-1 can be extended to deeper crustal levels by including data from fluid inclusions in rocks of well constrained depth of burial. Figure 7-2 shows the data of Figure 7-1 together with fluid inclusion compositions in metasedimentary rocks from three different terranes, two with different temperatures of equilibration at different sample localities. Although an individual locality may show a significant range in composition, it is obvious that even the highest temperature rocks still contain some methane and the compositions tend to lie along the extension of trend A, for sandstone reservoirs, from Figure 7-1. Clearly, the "early burnout" of HC gases that one would predict from trend B, for carbonate reservoirs, does not occur in all crustal rocks. In fact, work by van den Kerkhof (1991) on a siliceous marble that equilibrated at 800°C documents the occurrence of about 1 mole % methane in carbon dioxide at this temperature. Although not shown on Figure 7-2, this occurrence would plot much closer to trend A than to trend B, clearly showing that methane is stable to great depths in the crust.

The metamorphic rocks that contain more than about 10 mole percent methane in fluid inclusions tend to be graphite bearing. The compositions of the inclusions tend to be generally consistent with calculated compositions of aqueous fluids in equilibrium with graphite (Ohmoto and Kerrick, 1977; Duke and Rumble, 1986), especially when the possibility of hydrogen diffusion (loss) from inclusions is taken into account (Burruss, 1977). This observation plus the textural evidence for precipitation of graphite from fluids (Duke and Rumble, 1986) clearly documents the generation and migration of methane and carbon dioxide bearing fluids in the deep crust. This also suggests that identification of geologic environments where carbon-rich sediments have

been incorporated into metamorphic rocks will help define areas where there is the greatest probability of deep crustal sources contributing to shallower natural gas resources.

Gas flux from deep crustal level

Estimates of the flux of gases from the deep crust are based on the measured solubility of quartz in water as a function of temperature, pressure, and salinity which can be translated into a quantity of quartz precipitated per volume of water in a vein system at a given depth in the crust. From the volume of quartz veins that can be measured in the field, we can estimate the volume of water necessary to form the vein system. The ratio of HC and non-HC gases to water can be determined from fluid inclusion measurements (Burruss, 1981, van den Kerkof, 1988; Landis and Hofstra, 1991). Therefore we can estimate the volume of gases that are transported with the water that is necessary to form quartz veins at depth in a given tectonic setting.

An extensive series of studies by R. Kerrich and his students (see review paper, Kerrich and Feng, 1992, and references therein) have documented the geochemical processes and tectonic setting of formation of "giant quartz vein systems" which in many cases have associated gold mineralization (see Goldfarb, and others, 1991). In one example of a giant vein system, Kerrich, and others (1987) estimated that 6 X 10^{18} g of aqueous fluid (6 X10^3 km^3) deposited about 6 X 10^{15} g of quartz and in the process transported 3 X 10^{15} g of CO_2. This is 1500 trillion cubic ft (TCF) of CO_2. Based on the range of methane/carbon dioxide ratios observed in fluid inclusions in quartz from one of these giant vein systems (1:3 to 1:40, Landis and Hofstra, 1991, "southern Alaska mesothermal veins" which are part of Kerrich's example "Cretaceous-Tertiary Coast Range Megalineament, Juneau belt, Alaska" which extents south into British Columbia with similar observations made by Hollister and Burruss, 1976), a single giant vein system may transport on the order of 50 to 500 TCF of CH_4 to shallow crustal levels. Twelve giant vein systems have been documented by Kerrich and Feng (1992) and they range in age and location from Archean (2700-2600 Ma) in the Canadian and Australian shields to Tertiary (38-27 Ma) in the Alps. These twelve are only the systems that are documented in the literature and are biased by the fact that they are now exhumed and exposed at the surface where they can be readily studied. Fluid fluxes of similar magnitude have documented in recent work by Ferry (1992) in giant vein systems of more common dynamo-thermal metamorphic terranes.

Discussion and Significance

Kerrich's giant quartz vein systems are an important component of any consideration of deep crustal sources of HC and non-HC gases for several reasons. First quartz veins are direct evidence of focused flow of fluids from deep to shallow crustal levels. Second, giant vein systems occur at convergent plate margins, especially those associated with transpressive tectonic regimes (Kerrich and Feng, 1992), a geologic environment with major HC accumulations. In fact, the giant vein systems may be the best evidence to support earlier suggestions of natural gas accumulations in "accretionary" terranes (Gwilliam and Cohen, 1986).

The association of giant vein systems with convergent, transpressive plate margins may have both positive and negative aspects

for potential HC gas accumulations. On the positive side, there are major gas accumulations associated with such tectonic settings, for example the deep Anadarko basin of Oklahoma and Texas, and the Arkoma basin of Arkansas. On the negative side, convergent, transpressive tectonic regimes tend to have a component of very active vertical tectonics. This can lead to rapid erosional exhumation of potential reservoir rocks and loss of accumulations. For example, there is a large amount of fluid inclusion evidence for methane generation and transport through the Alpine quartz veins, but any sedimentary cover that could have provided reservoirs has been stripped off this young terrane.

REFERENCES CITED

Burruss, R.C., 1977, Analysis of fluid inclusions in graphitic metamorphic rocks from Bryant Pond, Maine, and Khtada Lake, British Columbia: Thermodynamic basis and geologic interpretation of observed fluid compositions and molar volumes, unpublished Ph.D. dissertation, Princeton University.

Burruss, R.C., 1981, Analysis of phase equilibria in C-O-H-S fluid inclusions, Chap. 3, *in* Hollister, L. S., and Crawford, M. L., eds., Fluid inclusions: Applications to petrology: Mineralogical Association of Canada, Short Course Notes, v. 6, p. 39-74, Calgary.

Duke, E.F., and Rumble, D., III, 1986, Textural and isotopic variations in graphite from plutonic rocks, South-Central New Hampshire, Contributions to Mineralogy and Petrology, v. 93, p. 409-419.

Ferry, J.M., 1992, Regional metamorphism of the Waits River Formation, Eastern Vermont: Delineation of a new type of giant metamorphic hydrothermal system, Journal of Petrology, v. 33, p. 45-94.

Goldfarb, R.J., Snee, L.W., Miller, L.D., and Newberry, R.J., 1991, Rapid dewatering of the crust deduced from ages of mesothermal gold deposits, Nature, v. 354, p. 296-298.

Gwilliam, W.J., and Cohen, K.K., 1986, Deep source gas potential along west coast of North America [abs.], American Association of Petroleum Geologists Bulletin, v. 70, p. 924.

Hollister, L.S., and Burruss, R.C., 1976, Phase equilibria in fluid inclusions from the Khtada Lake metamorphic complex: Geochimica et Cosmochimica Acta, v. 40, p. 163-175.

Hollister, L.S., and Crawford, M.L., eds., 1981, Fluid inclusions: Applications to petrology: Mineralogical Association of Canada, Short Course Notes, v. 6, Calgary.

Kerrich, R., and Feng, R., 1992, Achean geodynamics and the Abitibi-Pontiac collision: implications for advection of fluids at transpressive collisional boundaries and the origin of giant quartz vein systems, Earth-Science Reviews, v. 32, p. 33-60.

Kisch, H.J., and van den Kerkhof, A.M., 1991, CH4-rich inclusions form quartz veins in the Valley-and-Ridge province and the anthracite fields of the Pennsylvania Appalachians, American Mineralogist, v. 76, p. 230-240.

Landis, G.P., and Hofstra, A.H., 1991, Fluid inclusion gas chemistry as a potential minerals exploration tool: Case studies from Creede, CO, Jerritt Canyon, NV, Coeur d'Alene district, ID and MT, southern Alaska mesothermal veins, and mid-continent MVT's, Journal of Geochemical Exploration, v. 42, pp. 25-59.

Murck, B.W., Burruss, R.C., and Hollister, L.S., 1978, Phase equilibria in fluid inclusions in ultramafic xenoliths: American Mineralogist, v. 63, p. 40-46.

NRG Associates Inc., 1988, The significant oil and gas fields of the United states (through December 31, 1988): Available from Nehring Associates, Inc., P.O. Box 1655, Colorado Springs, CO 80901.

Ohmoto, H., and Kerrick, D., 1977, Devolatilization equilibria in graphitic systems, American Journal of Science, v. 227, p. 1013-1044.

Roedder, E.,1984, Fluid Inclusions, Reviews in Mineralogy, v. 12, P. H. Ribbe, ed., Mineralogical Society of America, 644 p.

Van den Kerkhof, A.M.,1988, The system CO_2-CH_4-N_2 in fluid inclusions: Theoretical modelling and geological applications, Amsterdam, Free University Press, 206 p.

Van den Kerkhof, A.M., 1991, Heterogeneous fluids in high-grade siliceous marbles of Pusula (SW Finland), Geologische Rundschau, v. 80, p. 249-258.

Van den Kerkhof, A.M., Touret, J.L.R., Maijer, C., and Jansen, J.B.H., 1991, Retrograde methane-dominated fluid inclusions from high-temperature granulites of Rogaland, southwestern Norway, Geochimica et Cosmochimica Acta, v. 55, p. 2533-2544.

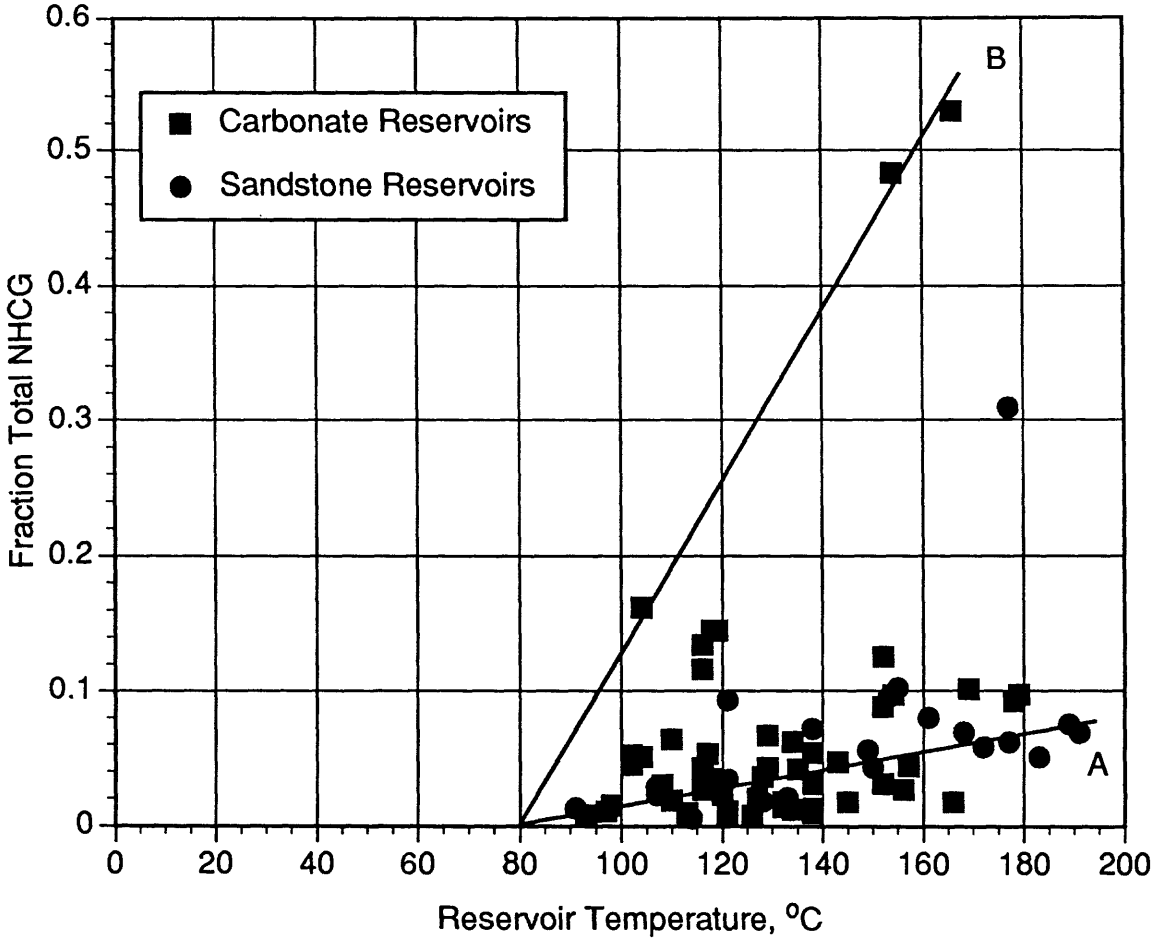

Figure 7-1. Plot of the fraction of total non-hydrocarbon gases (NHCG, as $(N_2+CO_2+H_2S+He)/(\text{Sum of all gases})$ versus reservoir temperature for all production from depths greater than 14,000 ft. that are available in the Nehring database. Fields are separated by sandstone and carbonate reservoir lithologies. Lines A and B define general trends in the data and are not mathematical fits to the data.

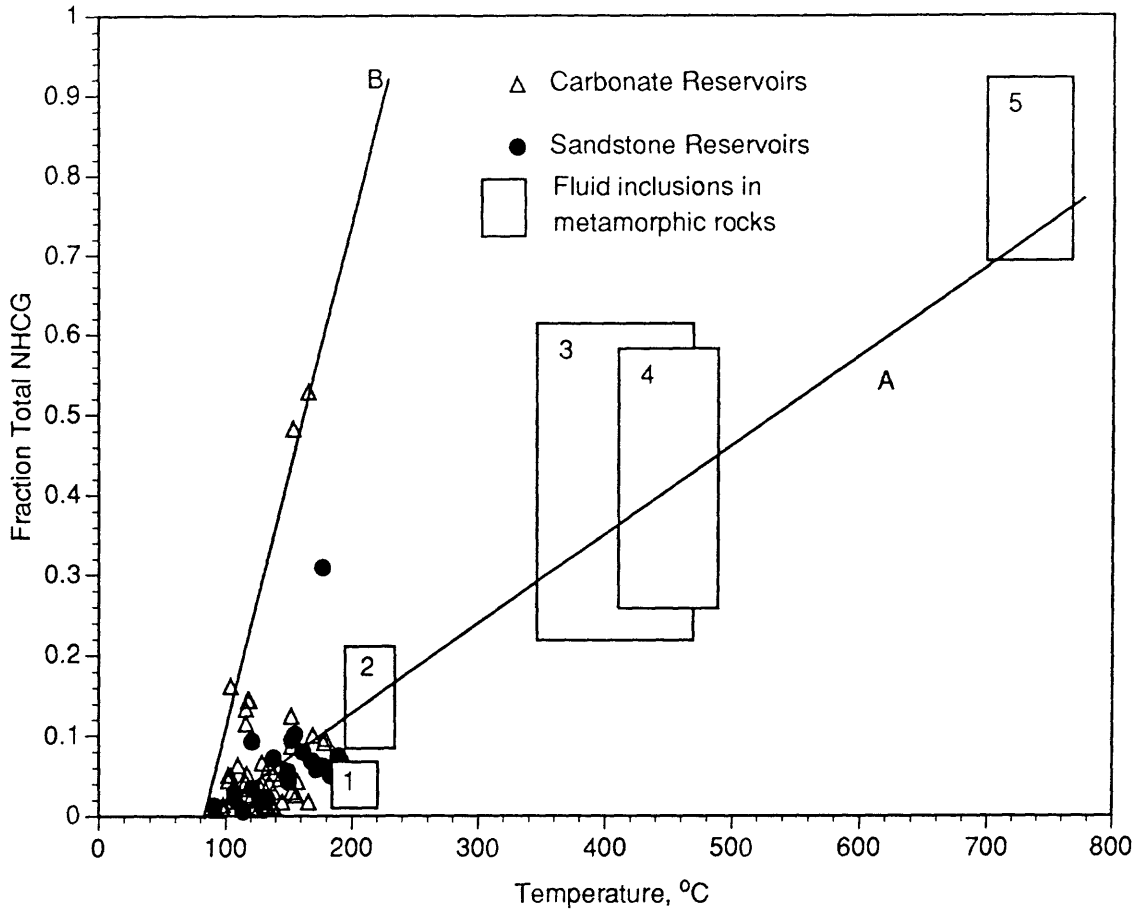

Figure 7-2. Data from Figure 7-1 plotted over a wider range of composition and subsurface temperature for comparison with the composition of fluid inclusions in metamorphic rocks. The numbered boxes define the range of temperature and composition of inclusions from five sample localities. The references are as follows: #1 and #2: anthracite belt of the Valley-and-Ridge province, Pennsylvania, USA, Kisch and van den Kerkhof, 1991; #3 and #4: retrograded rocks in the granulites of Rogaland, Norway, van den Kerkhof, et al., 1991; #5: prograde granulite rocks of Khtada Lake, British Columbia, Canada, Hollister and Burruss, 1976, and Burruss, 1977. Lines A and B are approximate extensions of the same lines in Figure 7-1.

Appendix 8--Resource assessment methodology for deep natural gas resources

by G.D. Dolton and R.A. Crovelli

The primary goal of Task 8 was to (1) identify and develop quantitative resource assessment methods and models for evaluation of undiscovered deep gas resources, based on geologic models of occurrence and information developed by Tasks 1-7 of this project; and (2) present a modelled assessment of a hypothetical deep gas play in order to better understand the wide range of resources resulting when geologic variables change.

Review and analysis of resource appraisal methodologies and approaches have been completed and allow identification of methodologies for dealing with some of the more common types of deep gas occurrences. These methods are ultimately dependent upon the level of geologic and engineering data available and an understanding of the geologic model for specific deep gas occurrences. One or more may be appropriate in a given case, and multiple approaches are desirable as independent checks. In general we feel that methods which lead to assessment of accumulation size and number are preferable because they allow satisfactory modelling for economic and supply purposes. As indicated by Baker and others (1984),

> "assessments of undiscovered oil and gas potentials from a group of geologically-related, untested prospects can be effectively made from an estimate of the possible ranges in number and size of potential fields, assuming that the play exists, coupled with an evaluation of geologic risks that it might not exist. Field-size distributions are constructed from known field reserves in geologically similar plays from assessments of representative prospects in the play or, from simulations of distributions of the play's prospect areas, reservoir parameters and potential HC relations.... The possible range of numbers of potential fields is estimated from counted and postulated numbers of untested prospects in conjunction with the success ratio, or from look-alike field densities."

Several of these underlying methods are discussed separately in the following section, as well as more general approaches.

The methods of assessment which appear most appropriate to assessment of undiscovered resources of deep gas are: (1) deposit simulation, (2) reservoir performance, (3) analog, (4) discovery process and finding rate models, (5) mass balance calculations, and (6) volumetric and areal yield determinations. For a general review of overall methodologies and their characteristics, the reader is referred to White (1978), Dolton (1984), and Charpentier (1986).

These methods meet the criterion for evaluation of deep gas resources and the specific assessment methodology employed depends to a large extent upon the intended use of the assessment, time and manpower constraints, and the geologic and engineering data which are available for synthesis and analysis. The geologic model of gas occurrence also indicates the level of assessment that is appropriate, that is, whether it is at the basin, play, petroleum system or at some other level. Geologic information in our companion studies

(Appendices 1 through 7) indicate that many deep gas occurrences should be treated at a play level and with a method that will provide information on the size of the deposits and their geologic characteristics, as well as a total resource value, so that economic and supply studies can be made.

The following methods for quantification of undiscovered or poorly known occurrences of deep gas are discussed in order of preference. Availability of data for them ultimately determine methods of assessment and adequacy of results.

DEPOSIT SIMULATION

This method is a volumetric calculation of resources based on measurement or estimation of physical properties of the traps, reservoir rocks and fluids, and of the host environment in terms of temperatures, pressures and fluid dynamics. This method has the advantage of working directly with the basic geologic properties of the accumulations and dealing with them in a rigorous, quantitative manner. It allows for simulation of the HC deposit(s) through modeling their geologic properties. Consequently, subjectivity is introduced and uncertain parameters are represented as estimates expressed as ranges of values, accompanied by probabilities of occurrence (probability distributions). The approach therefore uses stochastic and probabilistic methods, as well as statistical methods. An example of input for this type of approach is shown in Fig 8-1. A general resource assessment model using these inputs has been described by Energy, Mines and Resources Canada (1977), U.S. Department of Interior (1979), Dolton and others (1987), and has been published by Crovelli and Balay (1986, 1988, 1990).

The calculation of gas volume of a deposit is based on a fundamental reservoir engineering formula. Basic to calculation, therefore, is the determination of reservoir volume. The dimension of the gas container is critical, whether it be a single homogeneous reservoir rock in a conventional trap, a compartment of lesser size within a larger reservoir, or a heterogeneous reservoir of great size associated with an unconventional basin-center gas occurrence.

The modelling of gas-saturated reservoir volumes is affected by various geometric constraints. White (1987) and Abrahamsen (1989) discuss some of these geometric considerations as they may be applied when dealing with reservoir thicknesses within closures. For example, in a conventional deep gas trap, reservoir thickness is a function not only of the available stratigraphic thickness of the reservoir unit and effective porosity within it, but of the position of the gas-water contact and the configuration and size of the trap and its fractional fill. The problem becomes a particular issue when available reservoir thickness is great relative to closure area (as in many fields in the gas-productive Ellenberger Group of the deep Permian basin) or where dealing with small vertical closures, small fractional fill, or small areal trap sizes. Where sufficiently mapped, thickness can be measured or, alternatively, gross HC-bearing reservoir volume may be calculated directly from planimetered areas (Pirson, 1950), thereby collapsing the variables of reservoir thickness, area and trap fill.

The internal physical characteristics of the reservoir, which determine contained HC volumes, are porosity and water saturation. Porosity values used must meet an assigned threshold value to qualify as "effective porosity". It is important that this same minimum value be adhered to in terms of measurement of reservoir thickness and risking of attributes. Water saturation can be estimated directly (as in the input example), or based on an algorithm which relates water saturation to the average porosity of the reservoir.

Adjustment for non-HC gas volumes which may occupy pore space is simply made through introduction of an estimate of the fractional percent of HC gas. This is an especially important element in such deep gas areas as the Delaware-Val Verde basin of West Texas and deep gas reservoirs of southwestern Wyoming, and probably is an issue in many other deep gas basins.

It is essential to deal with engineering factors, including estimation of the thermal and pressure conditions of the simulated reservoir and trap. In addition, it is necessary to calculate the compressibility factor of the gas (Z), based on known or estimated gas composition.

Adequate framing of the basic geologic model or models of occurrence is absolutely essential to assessment, both in terms of assignment of risk to the variables controlling the occurrence of gas and to the assessment of volume parameters. The rock and fluid characteristics identified and investigated in companion studies are critical and include physical properties of reservoirs such as thickness, distribution, porosity amount and variation, pore geometries and dimensions; trap types and dimensions; effectiveness of seals; physical environments of accumulations, including depths, present and past thermal conditions, pressure regimes, and fluid dynamics; and saturations and properties of the involved fluids, their composition and physical state. Availability of data for them and their sufficient quantification ultimately determine the adequacy of results. Development of relevant databases is a requirement for assessment.

The simulation method provides not only an overall resource assessment, but a description of the individual accumulations in terms of their geologic characteristics and their contained gas, and affords an easily updatable assessment record. It estimates resources in situ, and does not tell the user directly about their recoverability or producing characteristics, although permitting use of known or estimated recovery factor. The method is flexible in that it allows the geologist to model the geologic conditions controlling the resource. This allows for a wide range of resource values for a wide range of geologic conditions.

The actual production characteristics of reservoirs which lead to recoverability are best determined by engineering studies of the reservoir rock and fluids themselves, including reservoir drive and pressure characteristics, reservoir rock permeability, and fluid composition and properties, and is especially critical with reference to "tight" gas reservoirs.

RESERVOIR PERFORMANCE

This somewhat empirical method relies on production data which are extrapolated to permit a calculation of ultimately recoverable resources, based upon certain economic and technologic assumptions and well spacing. The method, including variously, production decline curve methods, cumulative production curve methods, material balance and others, relies heavily on a careful engineering approach, beyond the scope of this analysis. It is useful in a reservoir that has seen some development, as locally may be the case in a tight-gas reservoir, or for reserve calculations within a developed field. It deals not only with the basic physical characteristics of the reservoirs and fluids, but measures, over time, how production and reservoirs respond to development controlled by both technologic and economic factors. This can be a very effective method in areas where there has been a sufficient history of production. However, the assessor often does not have sufficient information to satisfy the method, except on an analog basis.

ANALOG

A fundamental approach to assessment is that of geologic analogy and, in fact, this method underlies elements of several of the other methods. As a explicit assessment method, it relies upon identification of an appropriate and adequately documented analog model for use in a subject assessment area and scaling it to that area. Where well understood models of deep gas occurrences are adequately documented, analog comparisons and calculations can be used to approximate resource values of subject areas. The method is relatively unsophisticated, although flexible in the sense that it an be readily modified to incorporate adjustments for geologic differences between analog and subject areas. It is particularly useful in areas lacking detail information other than that of a broad geologic setting. In somewhat more sophisticated forms it is used to model not only geologic properties but to model HC accumulations and populations for use in resource procedures dealing with evaluation of field sizes and numbers (White and Gehman, 1978; Mast and others, 1989). We feel that it is particularly useful for deep gas in basins where reasonable analogs can be established.

DISCOVERY PROCESS AND FINDING RATES

Where there is a sufficient exploration history, an effective assessment approach is that of extrapolating from the sequence of field discoveries to derive what remains to be discovered, both in terms of field sizes and their aggregate resource value. These approaches are variously termed discovery process models or finding rate models, and, in their more sophisticated forms, were pioneered by Arps and Roberts (1958), Drew (1974), and Barouch and Kaufman (1975). At their best, they are done at a play level, that is, by identifying and using natural populations of fields, which are identifiable by common geologic characteristics of trap, reservoir, seal and source (Energy, Mines, and Resources Canada, 1977; Lee and Wang, 1986; Podruski and others, 1988). In a subjective format, it was part of the analysis of field sizes employed in the U.S. Geological Survey national assessment (Mast and others, 1989; Houghton and others, 1989). Various specific methodologic approaches can be used, and are often highly statistical in nature. The reader is referred to White (1978) and Miller (1986) for further discussion of methods of this class. Because development of deep gas in most areas is relatively new and has not yet proceeded to a point to allow this kind of analysis, the method has been limited, although successfully employed in the Permian basin,

West Texas and southeast New Mexico, by Drew and others (1979). Sufficient data are needed concerning exploration effort and discovery.

The more basic models of this class of historical extrapolations deal simply with overall resources discovered as a function of exploratory footage or exploration wells drilled, without reference to the underlying field size population, and are not considered appropriate for deep gas assessment.

MASS BALANCE

Mass balance calculations have been used by various workers as a tool for estimation of resources. The method deals with the amount of HC generated, based on geochemical data, the amount which is expelled and migrated, and the amount which is finally retained in traps. Because of the difficulty and uncertainty in quantitatively assessing several of these variables, the method has been useful mostly in a qualitative sense, identifying the probable HC composition, the migration history and adequacy of charge, and the general resource potential. The method is particularly useful in identifying critical geologic elements and processes needed for resource evaluation. In very well-studied areas containing the requisite information, it may be applied as an estimation method.

YIELD METHODS

These methods use basic geologic data, and areas or volumes of rock for calculation of resources. Yields of HCs per unit of rock, obtained from analog areas, are used as the basis for calculation of resources in a subject area. The method can be used on a basin, play, or stratigraphic scale. The result is only as good as the analogy, which can be either internal or external, and the information regarding its HC's. Factors are often used in modifying the yield factors to more closely model the subject area. Providing that a strong analogy can be established, a useful estimate can be obtained in areas where detailed geologic data may be lacking. It appears useful in deep gas assessment in some areas of the Rocky Mountains.

APPLICATION OF A DEPOSIT SIMULATION MODEL--HYPOTHETICAL PLAY EXAMPLE

Several of the preceding methods meet criterion for evaluation of undiscovered deep gas resources. Where sufficient information is available concerning the geologic characteristics of known or suspected deposits of deep gas, we believe that a **deposit simulation based on a geologic model of reservoir volume,** as as discussed previously. This method is based on measurement of known or estimated physical properties of the traps, reservoir rocks and fluids and of the host environment in terms of temperatures, pressures and fluid dynamics. It has the advantage of working with the basic geologic properties of the accumulations and dealing with them in a rigorous, quantitative manner and allows for simulation of the HC deposit(s) through estimation of properties where data are lacking or incomplete.

The calculation of gas resources is based on a fundamental reservoir engineering formula, expressed as follows:

$$\text{Gas volume } (ft^3) = 43{,}560\ A\ F\ H\ Por\ (1-Sw)(Pr/Tr)(1/Z)(Tsc/Psc)$$

where A = area of closure (acres)
F = trap fill (decimal fraction)
H = reservoir thickness (ft)
Por = porosity (decimal fraction)
Sw = water saturation
Pr = original reservoir pressure
Tr = reservoir temperature (degrees Rankine)
Psc = pressure, standard conditions
Tsc = temperature (degrees Rankine)
Z = gas compressibility factor

Simulation of properties of the accumulation or an aggregate of accumulations requires that the parameters are represented as estimates expressed as ranges of values, accompanied by probabilities of occurrence (probability distributions), representing the natural geologic variability of geologic characteristics and our uncertainty about them. Hence, the values shown represent the range of possibilities which might be encountered at a randomly selected prospect within a population. The model can be used both at the scale of a single prospect or for an aggregate of prospects within a common geologic setting or play.

We present an example of a case of deep gas occurrence in a hypothetical basin and use of this model. Several U.S. basins meet the requirements for the conditions for this model such as the Anadarko basin, the Gulf Coast basin, and several deep Rocky Mountain basins. This exercise is only intended to demonstrate the use and flexibility of this model rather than providing an actual assessment of recoverable resources.

In this case, we assume a population of drillable prospects, which have been identified geologically or geophysically or are hypothesized to exist, and which we believe bear common geologic characteristics. We estimate that we are dealing with a sandstone reservoir lying in structural traps at depths ranging from 5,486 to 6,706 m (18,000 to 22,000 ft).

The input used for this example is shown in Figure 8-1. In this case, we assume that the various play attributes for HC occurrence have been met, hence no risk has been assigned. If questionable, then a probability of occurrence of less than one would be assigned.

In the case of the prospect attributes, we believe that there is a possibility that they may not be present or favorable at a randomly selected prospect. For instance, we consider that on an individual prospect basis or at a randomly selected prospect, the trapping mechanism or trapping configuration we envision has a 6 in 10 chance of existence (Probability of Trapping Mechanism = .6) and also that the necessary migration paths from source rocks to the trap have a 7 in 10 chance of existence (Probability of Hydrocarbon Accumulation = .7). Each attribute is assessed conditioned on the other attributes being favorable and also on the basis of being sufficient to

meet the minimum values for HC volume parameters of the deposits to be considered (indicated in the lower part of the form, Fig. 8-1).

For the HC volume parameters, we have used the general characteristics and properties of deep gas deposits or occurrences which have been documented elsewhere in the companion studies. In this case, we have required minimum values to be: area of closure = 300 Ac; reservoir thickness = 10 ft; effective porosity = 5%; trap fill = 10%; and HC saturation = 60%. The program FASPU was used to calculate the estimates (Crovelli and Balay, 1990).

Results from calculation of the modelled play are shown in Table 8-1. Several interesting relationships emerge from this calculation. First, is the relatively modest amount of gas calculated, given the given prospect areal sizes. This result is largely the function of small amounts of effective matrix porosity assumed. Should porosity of less than 5% contribute gas to the reservoir, then such volumes should be included and the porosity cut-off adjusted. Porosity loss is viewed as a significant factor in many deep gas reservoirs. It effects not only the amount of resource but producibility, as a consequence of associated low permeability. In many cases, the presence of natural fractures is necessary for economic production. In such reservoirs, adjustment of reservoir porosity values must be made to include fracture porosity for volume calculations. Situations in which porosity is retained at great depth, as in some geopressured reservoirs need to be considered in exploration, development and assessment scenarios.

Note that in this calculation, we have assumed independence of volume parameters, other than a positive correlation between porosity and gas saturation. However, dependencies may exist and may be dealt with. For instance, one might assume that a positive correlation or dependency exists between trap size and fill, effectively collapsing the container size parameters into a single variable; in that case the field size possible at the 5th fractile (the largest reported field size) increases from about 160 billion cubic ft to approximately 200 billion cubic ft. This recoverable resource represents the conservative case.

Alternatively, if we assume overpressured reservoir mode, in which better reservoir conditions occur as in some of the clastic reservoirs of the Gulf Coast basin (e.g. Norphlet and Tuscaloosa), resources increase significantly. overpressuring, and use these variables in place of the original data set Table 8-2 shows the recoverable gas estimated for the improved reservoir conditions. For this case, we assumed a average reservoir porosity of 18%, and a pressure gradient of 0.75 psi/ft (clearly an overpressured reservoir as is commonly associated with deep natural gas accumulations). In the original case (Table 8-1), the mean resource value in these prospects contained 298 Bcf. In the second, more optimistic case, the prospects contained 1,017 Bcf of gas, a three-fold increase due entirely to the increase in porosity and pressure. Other variables which particularly affect the overall reservoir volume include reservoir thickness and size of prospects. In both calculations, we have assumed that pore space is occupied by non-HC gas, then this may be accommodated by a percentage reduction of the gas calculated or incorporated as part of the input recovery factor. This flexibility of the assessment method allows the geologist to model the geologic conditions controlling the resource values to reflect a wide range of geologic conditions.

REFERENCES CITED

Abrahamsen, K.A., 1989, Application of the resource estimation program FASPUM; experiences from offshore Norway, *in* Symposium of the 6th Meeting of the Working Group on Resource Assessment, Committee for Co-ordination of Joint Prospecting for Mineral Resources in Asian Offshore Areas (CCOP), Bangkok, Thailand, August 28- September 2, 1989, unpaged.

Arps, J.J., and Roberts, T.J., 1958, Economics of drilling for Cretaceous oil on east flank of Denver-Julesburg basin: American Association of Petroleum Geologists Bulletin V. 42, No. 11, p. 2549-2566.

Baker, R.A., Gehman, H.M., James, W.R., and White, D.A., 1984, Geologic field number and size assessments of oil and gas plays: American Association of Petroleum Geologists Bulletin, v. 68, no. 4, p. 426-437.

Barouch, E., and Kaufman, G.M., 1975, Predicting undiscovered oil and gas in a play using a stochastic model of discovery, *in* Davis, J.C., Doveton, J.H., and Harbaugh, J.W., convenors, Probability methods in oil exploration, American Association of Petroleum Geologists Research Symposium, Stanford, California: Kansas Geological Survey, 7 p.

Canada Department of Energy, Mines, and Resources, 1977, Oil and natural gas resources of Canada, 1976: Ottawa, Ontario, Canada Department of Energy, Mines, and Resources Report EP 7-1, 76 p.

Charpentier, R.C., and Wesley, J.S., 1986, Annotated Bibliography of methodology for assessment of undiscovered oil and gas resources, *in* Rice, D.,D., Oil and gas assessment, methods and applications, American Association of Petroleum Geologists Studies in Geology No. 21, p. 247-264.

Crovelli, R.A., and Balay, R.H., 1986, FASP, an analytic resource appraisal program for petroleum play analysis: Computers and Geosciences, v. 12, No. 4B, p. 423-475.

Crovelli, R.A., and Balay, R.H., 1988, FASPUM metric version: Analytic petroleum resource appraisal microcomputer programs for play analysis using a reservoir-engineering model, U.S. Geological Survey Open File Report 87-414A, 14 p.

Crovelli, R.A., and Balay, R.H., 1990, FASPU English and Metric Version: Analytic petroleum resource appraisal microcomputer programs for play analysis using a reservoir -engineering model: U.S. Geological Survey Open File Report 90-509B, 23 p.

Crovelli, R.A., Mast, R.F., Dolton, G.L., and Balay, R.H., 1989, Assessment methodology for estimation of undiscovered petroleum resources in play analysis of the United States and aggregation methods, *in* National Assessment of Undiscovered conventional oil and gas resources, USGS-MMS Working Paper, USGS Open File Report 88-373, p. 34-46.

Dolton. G.L., 1984, Basin assessment methods and approaches in the U.S. Geological Survey, *in* Masters, C.D., ed, Petroleum Resource Assessment, International Union of Geological Sciences Publication No. 17, p. 4-23.

Dolton, G.L., Bird, K.J., and Crovelli, R.A., 1987, Assessment of in-place oil and gas resources, *in* Bird, K.J. and Magoon, L.B., eds., Petroleum Geology of the northern part of the Arctic National Wildlife Refuge, Northeastern Alaska: U.S. Geological Survey Bulletin 1778, p. 277-298.

Drew L.J., 1974, Estimation of petroleum exploration success and the effects of resource base exhaustion via a simulation model: U.S. Geological Survey Bulletin 1328, 25 p.

Drew, L.J., Root, D.H., and Bawiec, W.J., 1979, Estimating future rates of petroleum discoveries in the Permian basin, *in* Hydrocarbon Economics and Evaluation Symposium, 8th, Dallas, Texas, 1979, Proceedings of Petroleum Engineers-AIME p. 101-109.

Houghton, J.C., Dolton, G.L., Mast, R.F., Masters, C.D., and Root, D.H., The estimation procedure for field size distributions in the U.S. Geological Survey's National oil and gas resource assessment, *in* National Assessment of Undiscovered conventional oil and gas resources, USGS-MMS Working Paper, U.S. Geological Survey Open File Report 88-373, p. 51-86.

Lee, P.J. , 1986, Evaluation of petroleum resources from pool size distributions, *in* Rice, D.D., ed, Oil and Gas Assessment, Methods and Applications, American Association of Petroleum Geologists, Studies in Geology No. 21, p. 33-42.

Mast, R.F., Dolton, G.L., Crovelli, R.A., Root, D.H., and Attanasi, E.D., Martin, P.E., Cooke, L.W., Carpenter, G.B., Pecora, W.C., and Rose M.B., 1989, Estimates of undiscovered conventional oil and gas resources in the United States-A part of the Nation's energy endowment: U.S. Geological Survey and Minerals Management Service special publication, 44 p.

Miller, B.M., 1986, Resource Appraisal Methods: choice and outcome, *in* Rice, D.D., Oil and gas assessment, methods and applications, American Association of Petroleum Geologists Studies in Geology No. 21, p. 1-24.

Pirson S.J., 1950, Elements of Reservoir Engineering, McGraw-Hill Book Company, 441 p.

Podruski, J.A., Barclay, J.E., Hamblin, A.P., Lee, P.J., Osadetz, K.G., Procter, R.M., and Taylor, G.C., 1988, Part 1: Resource Endowment, *in* Conventional oil resources of western Canada, Geological Survey of Canada Paper 87-26, p. 7-14.

White, D.A, and Gehman H.M., 1978, Methods of estimating oil and gas resources, American Association of Petroleum Geologists Bulletin v. 63, No. 12, p. 2183-2192.

White, D.A., 1987, Methods of oil and gas prospect and play assessment course manual, Oil & Gas Consultants International.

Oil and Gas Appraisal Data Form

Evaluator : _____ Play Name _____

Date Evaluated: _____

	Attribute		Probability of Favorable or Present	Comments
Play Attributes	Hydrocarbon Source		1.0	
	Timing		1.0	
	Migration		1.0	
	Potential Reservoir Facies		1.0	
	Marginal Play Probability		1.0	
Prospect Attributes	Trapping Mechanism		0.6	
	Effective Porosity (>3%)		1.0	
	Hydrocarbon Accumulation		0.7	
	Conditional Deposit Probability		0.42	
Hydrocarbon Volume Parameters	Reservoir Lithology	Sand	X	
		Carbonate		
	Hydrocarbon	Gas	1.0	
		Oil	0	

Attribute \ Fractiles	Probability of equal to or greater than						
	100	95	75	50	25	5	0
Area of Closure (Km^2)	0.3	0.4	0.9	1.7	3.0	4.6	6.2
Reservoir Thickness/vertical closure (meters)	10	20	35	50	70	100	120
Effective Porosity %	5	5.2	6	8	10	14	20
Trap Fill (%)	10	25	45	60	75	90	100
Reservoir Depth (m)	18	18.75	19.5	20	20.5	21.25	22
HC Saturation (%)	60	65	70	75	80	85	90
No. of drillable prospects (a play characteristic)	[illegible]						

Figure 8-1. Oil and gas appraisal data form (from Crovelli and Balay, 1988) completed for hypothetical deep natural gas play. Reservoir variables as follows: Pe: original reservoir pressure (PSL)= 0.46 psi/ft (depth in ft) + 14.7 PSI; T: reservoir temperature (^{o} Rankine)= 0.013 ^{o} ft (depth in ft) + 515^{o}; Z= gas compressibility factor (= 1.2); gas recovery factor= 0.80.

Table 8-1. Results of calculation of modelled deep natural gas play based on input in this report. See Figure 8-1 for input.

Estimated recoverable gas (billions of cubic feet--Bcf)

	Mean	F95	F75	F50	F25	F05
Number of acumulations	6.3	3	5	6	8	10
Accumulation size (Bcf)	55	8	19	35	66	164
Unconditional play potential	345	122	207	298	430	726

Table 8-2. Results of calculation of modelled deep natural gas play based on input in this report. Figure 8-1 modified to increased porosity (mean value 18 percent) and pressure (0.75 psi per foot); all other variables constant.

Estimated recoverable gas (billions of cubic feet--Bcf)

	Mean	F95	F75	F50	F25	F05
Number of acumulations	6.3	3	5	6	8	10
Accumulation size (Bcf)	185	27	66	122	226	547
Unconditional play potential	1169	425	712	1017	1454	2431